



# MARINE BIODIVERSITY OBSERVATION NETWORK (MBON)

EDITED BY: Frank Edgar Muller-Karger, Enrique Montes, Dominique Pelletier,  
Juan Carlos Azofeifa-Solano and James Hendee  
PUBLISHED IN: Frontiers in Marine Science



# frontiers

## Frontiers eBook Copyright Statement

The copyright in the text of individual articles in this eBook is the property of their respective authors or their respective institutions or funders. The copyright in graphics and images within each article may be subject to copyright of other parties. In both cases this is subject to a license granted to Frontiers.

The compilation of articles constituting this eBook is the property of Frontiers.

Each article within this eBook, and the eBook itself, are published under the most recent version of the Creative Commons CC-BY licence.

The version current at the date of publication of this eBook is CC-BY 4.0. If the CC-BY licence is updated, the licence granted by Frontiers is automatically updated to the new version.

When exercising any right under the CC-BY licence, Frontiers must be attributed as the original publisher of the article or eBook, as applicable.

Authors have the responsibility of ensuring that any graphics or other materials which are the property of others may be included in the CC-BY licence, but this should be checked before relying on the CC-BY licence to reproduce those materials. Any copyright notices relating to those materials must be complied with.

Copyright and source acknowledgement notices may not be removed and must be displayed in any copy, derivative work or partial copy which includes the elements in question.

All copyright, and all rights therein, are protected by national and international copyright laws. The above represents a summary only. For further information please read Frontiers' Conditions for Website Use and Copyright Statement, and the applicable CC-BY licence.

ISSN 1664-8714

ISBN 978-2-88974-521-0

DOI 10.3389/978-2-88974-521-0

## About Frontiers

Frontiers is more than just an open-access publisher of scholarly articles: it is a pioneering approach to the world of academia, radically improving the way scholarly research is managed. The grand vision of Frontiers is a world where all people have an equal opportunity to seek, share and generate knowledge. Frontiers provides immediate and permanent online open access to all its publications, but this alone is not enough to realize our grand goals.

## Frontiers Journal Series

The Frontiers Journal Series is a multi-tier and interdisciplinary set of open-access, online journals, promising a paradigm shift from the current review, selection and dissemination processes in academic publishing. All Frontiers journals are driven by researchers for researchers; therefore, they constitute a service to the scholarly community. At the same time, the Frontiers Journal Series operates on a revolutionary invention, the tiered publishing system, initially addressing specific communities of scholars, and gradually climbing up to broader public understanding, thus serving the interests of the lay society, too.

## Dedication to Quality

Each Frontiers article is a landmark of the highest quality, thanks to genuinely collaborative interactions between authors and review editors, who include some of the world's best academicians. Research must be certified by peers before entering a stream of knowledge that may eventually reach the public - and shape society; therefore, Frontiers only applies the most rigorous and unbiased reviews. Frontiers revolutionizes research publishing by freely delivering the most outstanding research, evaluated with no bias from both the academic and social point of view. By applying the most advanced information technologies, Frontiers is catapulting scholarly publishing into a new generation.

## What are Frontiers Research Topics?

Frontiers Research Topics are very popular trademarks of the Frontiers Journals Series: they are collections of at least ten articles, all centered on a particular subject. With their unique mix of varied contributions from Original Research to Review Articles, Frontiers Research Topics unify the most influential researchers, the latest key findings and historical advances in a hot research area! Find out more on how to host your own Frontiers Research Topic or contribute to one as an author by contacting the Frontiers Editorial Office: [frontiersin.org/about/contact](https://frontiersin.org/about/contact)



# MARINE BIODIVERSITY OBSERVATION NETWORK (MBON)

Topic Editors:

**Frank Edgar Muller-Karger**, University of South Florida, United States

**Enrique Montes**, University of South Florida, United States

**Dominique Pelletier**, Institut Français de Recherche pour l'Exploitation de la Mer (IFREMER), France

**Juan Carlos Azofeifa-Solano**, Universidad de Costa Rica, Costa Rica

**James Hendee**, National Oceanic and Atmospheric Administration (NOAA), United States

**Citation:** Muller-Karger, F. E., Montes, E., Pelletier, D., Azofeifa-Solano, J. C., Hendee, J., eds. (2022). Marine Biodiversity Observation Network (MBON). Lausanne: Frontiers Media SA. doi: 10.3389/978-2-88974-521-0

# Table of Contents

- 05 Editorial: Marine Biodiversity Observation Network (MBON)**  
Dominique Pelletier, Juan Carlos Azofeifa-Solano, Enrique Montes and Frank Edgar Muller-Karger
- 08 Dynamic Satellite Seascapes as a Biogeographic Framework for Understanding Phytoplankton Assemblages in the Florida Keys National Marine Sanctuary, United States**  
Enrique Montes, Anni Djurhuus, Frank E. Muller-Karger, Daniel Otis, Christopher R. Kelble and Maria T. Kavanaugh
- 27 Sandy Beach Macrofauna of Yucatán State (Mexico) and Oil Industry Development in the Gulf of Mexico: First Approach for Detecting Environmental Impacts**  
Edlin Guerra-Castro, Gema Hidalgo, Raúl E. Castillo-Cupul, María Muciño-Reyes, Elsa Noreña-Barroso, Jaime Quiroz-Deaquino, Maite Mascaró and Nuno Simoes
- 44 A Marine Biodiversity Observation Network for Genetic Monitoring of Hard-Bottom Communities (ARMS-MBON)**  
Matthias Obst, Katrina Exter, A. Louise Allcock, Christos Arvanitidis, Alizz Axberg, Maria Bustamante, Ibon Cancio, Diego Carreira-Flores, Eva Chatzinikolaou, Giorgos Chatzigeorgiou, Nathan Christmas, Melody S. Clark, Thierry Comtet, Thanos Dailianis, Neil Davies, Klaas Deneudt, Oihane Diaz de Cerio, Ana Fortič, Vasilis Gerovasileiou, Pascal I. Hablützel, Kleoniki Keklikoglou, Georgios Kotoulas, Rafal Lasota, Barbara R. Leite, Stéphane Loisel, Laurent Lévêque, Liraz Levy, Magdalena Malachowicz, Borut Mavrič, Christopher Meyer, Jonas Mortelmans, Joanna Norkko, Nicolas Pade, Anne Marie Power, Andreja Ramšak, Henning Reiss, Jostein Solbakken, Peter A. Staehr, Per Sundberg, Jakob Thyrring, Jesus S. Troncoso, Frédérique Viard, Roman Wenne, Eleni Ioanna Yperifanou, Malgorzata Zbawicka and Christina Pavludi
- 53 The Importance of Surface Orientation in Biodiversity Monitoring Protocols: The Case of Patagonian Rocky Reefs**  
Gonzalo Bravo, Juan Pablo Livore and Gregorio Bigatti
- 65 The National Geographic Society Deep-Sea Camera System: A Low-Cost Remote Video Survey Instrument to Advance Biodiversity Observation in the Deep Ocean**  
Jonatha Giddens, Alan Turchik, Whitney Goodell, Michelle Rodriguez and Denley Delaney
- 78 Mass Mortality of Foundation Species on Rocky Shores: Testing a Methodology for a Continental Monitoring Program**  
María M. Mendez, Juan P. Livore, Federico Márquez and Gregorio Bigatti
- 85 Time-Varying Epipelagic Community Seascapes: Assessing and Predicting Species Composition in the Northeastern Pacific Ocean**  
Caren Barceló, Richard D. Brodeur, Lorenzo Ciannelli, Elizabeth A. Daly, Craig M. Risien, Gonzalo S. Saldías and Jameal F. Samhour

- 103** *Low Densities of the Ghost Crab *Ocypode quadrata* Related to Large Scale Human Modification of Sandy Shores*  
Carlos A. M. Barboza, Gustavo Mattos, Abílio Soares-Gomes, Ilana Rosental Zalmon and Leonardo Lopes Costa
- 114** *Metabarcoding Analysis of Ichthyoplankton in the East/Japan Sea Using the Novel Fish-Specific Universal Primer Set*  
Ah Ran Kim, Tae-Ho Yoon, Chung Il Lee, Chang-Keun Kang and Hyun-Woo Kim
- 129** *Application of a Simple, Low-Cost, Low-Tech Method to Monitor Intertidal Rocky Shore Assemblages on a Broad Geographic Scale*  
Juan Pablo Livore, María M. Mendez, Eduardo Klein, Lorena Arribas and Gregorio Bigatti
- 139** *Beyond Post-release Mortality: Inferences on Recovery Periods and Natural Mortality From Electronic Tagging Data for Discarded Lamnid Sharks*  
Heather D. Bowlby, Hugues P. Benoît, Warren Joyce, James Sulikowski, Rui Coelho, Andrés Domingo, Enric Cortés, Fabio Hazin, David Macias, Gérard Biaïs, Catarina Santos and Brooke Anderson
- 153** *Fieldable Environmental DNA Sequencing to Assess Jellyfish Biodiversity in Nearshore Waters of the Florida Keys, United States*  
Cheryl Lewis Ames, Aki H. Ohdera, Sophie M. Colston, Allen G. Collins, William K. Fitt, André C. Morandini, Jeffrey S. Erickson and Gary J. Vora
- 170** *Distribution, Temporal Change, and Conservation Status of Tropical Seagrass Beds in Southeast Asia: 2000–2020*  
Kenji Sudo, T. E. Angela L. Quiros, Anchana Prathep, Cao Van Luong, Hsing-Juh Lin, Japar Sidik Bujang, Jillian Lean Sim Ooi, Miguel D. Fortes, Muta Harah Zakaria, Siti Maryam Yaakub, Yi Mei Tan, Xiaoping Huang and Masahiro Nakaoka
- 181** *A Standardized Workflow Based on the STAVIRO Unbaited Underwater Video System for Monitoring Fish and Habitat Essential Biodiversity Variables in Coastal Areas*  
Dominique Pelletier, David Roos, Marc Bouchoucha, Thomas Schohn, William Roman, Charles Gonson, Thomas Bockel, Liliane Carpentier, Bastien Preuss, Abigail Powell, Jessica Garcia, Matthias Gaboriau, Florent Cadé, Coline Royaux, Yvan Le Bras and Yves Reecht
- 198** *Robots Versus Humans: Automated Annotation Accurately Quantifies Essential Ocean Variables of Rocky Intertidal Functional Groups and Habitat State*  
Gonzalo Bravo, Nicolas Moity, Edgardo Londoño-Cruz, Frank Muller-Karger, Gregorio Bigatti, Eduardo Klein, Francis Choi, Lark Parmalee, Brian Helmuth and Enrique Montes



# Editorial: Marine Biodiversity Observation Network (MBON)

**Dominique Pelletier<sup>1\*</sup>, Juan Carlos Azofeifa-Solano<sup>2</sup>, Enrique Montes<sup>3</sup> and Frank Edgar Muller-Karger<sup>4</sup>**

<sup>1</sup> Unité Ecologie et Modèles pour l'Halieutique, Département Ressources Biologiques et Environnement, Institut Français de Recherche pour l'Exploitation de la Mer, Nantes, France, <sup>2</sup> Centro de Investigación en Ciencias del Mar y Limnología (CIMAR), Universidad de Costa Rica, San José, Costa Rica, <sup>3</sup> Ocean Chemistry and Ecosystems Division, National Oceanic and Atmospheric Administration Atlantic Oceanographic and Meteorological Laboratory, Miami, FL, United States, <sup>4</sup> College of Marine Science, University of South Florida, St Petersburg, FL, United States

**Keywords:** MBON, ocean observing, marine essential biodiversity variables (EBV), ecosystem-based management, species distribution, marine monitoring

## Editorial on the Research Topic

### Marine Biodiversity Observation Network (MBON)

A growing human population depends on healthy ocean ecosystems for economic and social benefits including high quality food, pharmaceuticals and other materials, coastal protection, recreation, transportation, and renewable energy. Governments and scientists around the world have recognized the need for information on changes in marine biodiversity that are relevant to these ecosystem services. This includes practical information to implement conservation and sustainable development targets such as those agreed to under the Convention on Biological Diversity (CBD) and the U.N. Sustainable Development Goals (SDG). Biodiversity observations are fundamental to enable global assessments such as those by the Intergovernmental Platform on Biodiversity and Ecosystem Services (IPBES) and the UN World Ocean Assessment.

Important questions are where particular species populations and hotspots of multiple marine species occur at any time and how their distributions are changing. Standardized data sets and products are needed to answer questions on whether present place-based conservation measures are suitable for a particular location. Standardized approaches are also needed for adaptive management strategies given climate change scenarios and projected ocean uses. These factors have confounding effects on changes in life in the ocean that affect phenology, distribution of species including invasives and alien species, and decreases in the abundance of specific organisms or groups of organisms. Understanding how this affects the ecology and benefits that people and other forms of life may derive (or lose) from such changes requires monitoring and studying the abundance and distribution of species from the coast to the deep sea.

The Marine Biodiversity Observation Network (MBON) is a global community of practice for the sustained collection, curation, and analysis of marine biodiversity data for information on the status and trends of life in the sea. MBON operates within the framework of the Group on Earth Observations (GEO) Biodiversity Observation Network (GEO BON) to inform society of changes on ecosystem services. The role of the MBON is to broker relationships and activities. MBON members benefit from learning emerging and best practices, new collaborations, and co-authored publications.

The Frontiers MBON Research Topic invited a broader set of actors to contribute to this community of practice. A total of fifteen articles were published under the Research Topic.

## OPEN ACCESS

### Edited and reviewed by:

Hervé Claustre,  
Centre National de la Recherche  
Scientifique (CNRS), France

### \*Correspondence:

Dominique Pelletier  
dominique.pelletier@ifremer.fr

### Specialty section:

This article was submitted to  
Ocean Observation,  
a section of the journal  
Frontiers in Marine Science

**Received:** 09 December 2021

**Accepted:** 29 December 2021

**Published:** 24 January 2022

### Citation:

Pelletier D, Azofeifa-Solano JC,  
Montes E and Muller-Karger FE (2022)  
Editorial: Marine Biodiversity  
Observation Network (MBON).  
Front. Mar. Sci. 8:832328.  
doi: 10.3389/fmars.2021.832328



They showcase different facets of marine biodiversity research in polar, temperate and tropical ecosystems, in coastal and deep waters. Emerging technologies are providing new insights into marine life and enhancing our capacity to gather high-quality observations faster and over larger spatial domains. The use of molecular methods including environmental DNA (eDNA) is exploding around the world, with applications to evaluate presence and function from viruses to top predators and to explore human impacts on the ocean. One example published under the Research Topic is a survey of biodiversity of ichthyoplankton around Japan (Kim et al.). Another study provided the first assessment of jellyfish biodiversity in the Florida Keys, USA (Ames et al.).

Several articles feature protocols for processing imagery to quantify biodiversity. Obst et al. use molecular methods and image-based identification methods in comparative studies of benthic diversity, as well as for detecting non-indigenous species, working with Autonomous Reef Monitoring Structures (ARMS). They proposed an ARMS-MBON to advance standard protocols for monitoring hard-bottom environments. Bravo et al. used artificial intelligence to evaluate macroalgae and sessile organisms on rocky shores across the American continent, from Patagonia (Argentina) to Canada, including the Galapagos Islands (Ecuador). Livore et al. expanded a study of rocky shore biodiversity to include satellite-derived assessments of biogeography or “*Seascapes*” of Kavanaugh et al. (2021).

Much progress is being made with imaging devices including autonomous video landers to quantify biodiversity and behavior of organisms in the water column and on the ocean bottom. Giddens et al. describes an autonomous benthic lander platform with a baited camera system to conduct stationary video surveys of deep-sea megafauna, sponsored by the National Geographic Society Exploration Technology Lab. Pelletier et al. describe a standardized workflow for remote underwater video to assess fishes and habitats in coastal areas, using unbaited video cameras.

Two articles combine remote sensing data with *in situ* physical and biological measurements. Montes et al. also uses the satellite-derived “*Seascapes*” to illustrate how phytoplankton communities coincide with biogeographic provinces that can be mapped quickly with satellites using a case study of the Florida Keys National Marine Sanctuary (FKNMS, USA). Barceló et al. use satellite images to evaluate oceanographic predictor variables of epipelagic fish communities in the Northeast Pacific Ocean.

Other studies use more traditional methods to evaluate the status of specific organisms and communities. Bowlby et al. address the issue of natural and post-release mortality for particularly vulnerable shark species through archival satellite tags. Sudo et al. evaluate seagrass area cover in 9 countries in Southeast Asia and find that more than half of the seagrass beds declined at rates of over 10% per year since the late 1990s due to coastal development,

fisheries and aquaculture, and natural factors such as typhoons and tsunamis. They make recommendations for large-scale, regional management strategies. Barboza et al. highlight the relevance of ghost crabs as indicator species to reflect response to anthropogenic stressors and changes in environmental conditions.

In summary, these papers emphasize the utility and applications of biodiversity information. They show scalability and the importance of standardized protocols to enable large-scale, regional assessments. Communities of practice like MBON and regional efforts such as the MBON Pole to Pole of the Americas (MBON P2P) showcase the value of collaborations and sharing protocols for data collection, processing, curation, and publication (Bravo et al.; Guerra-Castro et al.; Livore et al.; Mendez et al.). The studies show how collaborations can be established across large geographies and different countries to lower the cost of methods and generate syntheses that have a greater scope than possible otherwise (Giddens et al.; Kim et al.; Livore et al.; Pelletier et al.). Overall, the articles document many approaches to evaluate Essential Biodiversity Variables (EOV: phytoplankton, zooplankton, benthic invertebrates, fishes, macroalgae, sea grass, and coral cover), and show that this is a necessary step to construct Essential Biodiversity Variables including time series of maps of biodiversity.

It is encouraging to see the community come together under networking frameworks like MBON. This effort continues as MBON is a core partner in the Marine Life 2030 Programme endorsed by the UN Decade of Ocean Science for Sustainable Development, providing evidence-based science in support of marine conservation, sustainable development, and improving human health everywhere.

We thank the authors of these papers, the many people involved in such studies for their contributions and their willingness to share them broadly, and the staff at Frontiers for their advice and support through this process.

## AUTHOR CONTRIBUTIONS

DP and FM-K wrote the draft. EM and JA-S revised the editorial. All authors contributed to the article and approved the submitted version.

## FUNDING

This is a contribution to the Marine Biodiversity Observation Network (MBON) of the Group on Earth Observations Biodiversity Observation Network. The MBON work was funded under the US National Ocean Partnership Program (NASA, NOAA, U.S. IOOS, BOEM, and ONR) through NASA grants NNX14AP62A, 80NSSC20K0017, and 80NSSC18K0318; and NOAA IOOS Award NA19NOS0120199. Additional support was provided by NSF Grant No. 1728913 (the OceanObs RCN).

## REFERENCES

Kavanaugh, M. T., Bell, T., Catlett, D., Cimino, M. A., Doney, S. C., Klajbor, W., et al. (2021). Satellite remote sensing and the marine biodiversity observation network: current science and future steps. *Oceanography* 34, 62–79. doi: 10.5670/oceanog.2021.215

**Conflict of Interest:** The authors declare that the research was conducted in the absence of any commercial or financial relationships that could be construed as a potential conflict of interest.

**Publisher's Note:** All claims expressed in this article are solely those of the authors and do not necessarily represent those of their affiliated

organizations, or those of the publisher, the editors and the reviewers. Any product that may be evaluated in this article, or claim that may be made by its manufacturer, is not guaranteed or endorsed by the publisher.

Copyright © 2022 Pelletier, Azofeifa-Solano, Montes and Muller-Karger. This is an open-access article distributed under the terms of the Creative Commons Attribution License (CC BY). The use, distribution or reproduction in other forums is permitted, provided the original author(s) and the copyright owner(s) are credited and that the original publication in this journal is cited, in accordance with accepted academic practice. No use, distribution or reproduction is permitted which does not comply with these terms.



# Dynamic Satellite Seascapes as a Biogeographic Framework for Understanding Phytoplankton Assemblages in the Florida Keys National Marine Sanctuary, United States

Enrique Montes<sup>1\*</sup>, Anni Djurhuus<sup>2</sup>, Frank E. Muller-Karger<sup>1</sup>, Daniel Otis<sup>1</sup>, Christopher R. Kelble<sup>3</sup> and Maria T. Kavanaugh<sup>4</sup>

<sup>1</sup> College of Marine Science, University of South Florida, St. Petersburg, FL, United States, <sup>2</sup> Department of Science and Technology, University of the Faroe Islands, Tórshavn, Faroe Islands, <sup>3</sup> Ocean Chemistry and Ecosystems Division, Atlantic Oceanographic and Meteorological Laboratory, National Oceanic and Atmospheric Administration, Miami, FL, United States, <sup>4</sup> College of Earth, Ocean, and Atmospheric Sciences, Oregon State University, Corvallis, OR, United States

## OPEN ACCESS

### Edited by:

Angel Borja,  
Technological Center Expert in Marine  
and Food Innovation (AZTI), Spain

### Reviewed by:

Tomonori Isada,  
Hokkaido University, Japan  
Gabriel Navarro,  
Institute of Marine Sciences  
of Andalusia (ICMAN), Spain

### \*Correspondence:

Enrique Montes  
emontesh@usf.edu

### Specialty section:

This article was submitted to  
Marine Ecosystem Ecology,  
a section of the journal  
Frontiers in Marine Science

**Received:** 18 December 2019

**Accepted:** 22 June 2020

**Published:** 15 July 2020

### Citation:

Montes E, Djurhuus A,  
Muller-Karger FE, Otis D, Kelble CR  
and Kavanaugh MT (2020) Dynamic  
Satellite Seascapes as  
a Biogeographic Framework  
for Understanding Phytoplankton  
Assemblages in the Florida Keys  
National Marine Sanctuary,  
United States. *Front. Mar. Sci.* 7:575.  
doi: 10.3389/fmars.2020.00575

Physical, chemical, geological, and biological factors interact in marine environments to shape complex but recurrent patterns of organization of life on multiple spatial and temporal scales. These factors define biogeographic regions in surface waters that we refer to as seascapes. We characterize seascapes for the Florida Keys National Marine Sanctuary (FKNMS) and southwest Florida shelf nearshore environment using multivariate satellite and *in situ* measurements of Essential Ocean Variables (EOVs) and Essential Biodiversity Variables (EBVs). The study focuses on three periods that cover separate oceanographic expeditions (March 11–18, May 9–13, and September 12–19, 2016). We collected observations on bio-optical parameters (particulate and dissolved spectral absorption coefficients), phytoplankton community composition, and hydrography from a ship. Phytoplankton community composition was evaluated using (1) chemotaxonomic analysis (CHEMTAX) based on high-performance liquid chromatography (HPLC) pigment measurements, and (2) analysis of spectral phytoplankton absorption coefficients ( $a_{phy}$ ). Dynamic seascapes were derived by combining satellite time series of sea surface temperature, chlorophyll-*a* concentration, and normalized fluorescent line height (nFLH) using a supervised thematic classification. The seascapes identified areas of different salinity and nutrient concentrations where different phytoplankton communities were present as determined by hierarchical cluster analyses of HPLC pigments and  $a_{phy}$  spectra. Oligotrophic, Mesotrophic, and Transition seascape classes of deeper offshore waters were dominated by small phytoplankton ( $<2 \mu m$ ;  $\sim 40$ – $60\%$  of total cell abundance). In eutrophic, optically shallow coastal seascapes influenced by fresh water discharge, the phytoplankton was dominated by larger taxa ( $>60\%$ ). Spectral analysis of  $a_{phy}$  indicated higher absorption levels at 492 and 550 nm wavelengths in seascapes carrying predominantly small phytoplankton than

in classes dominated by larger taxa. Seascapes carrying large phytoplankton showed absorption peaks at the 673 nm wavelength. The seascape framework promises to be a tool to detect different biogeographic domains quickly, providing information about the changing environmental conditions experienced by coral reef organisms including coral, sponges, fish, and higher trophic levels. The effort illustrates best practices developed under the Marine Biodiversity Observation Network (MBON) demonstration project, in collaboration with the South Florida Ecosystem Restoration Research (SFER) project managed by the Atlantic Oceanographic and Meteorological Laboratory of NOAA (AOML-NOAA).

**Keywords:** Marine Biodiversity Observation Network, Florida Keys National Marine Sanctuary, biogeographic seascapes, phytoplankton functional types, phytoplankton pigment analysis, HPLC, CHEMTAX, bio-optics

## INTRODUCTION

Phytoplankton, a diverse group of prokaryotic and eukaryotic micro-organisms, are primary producers that support extensive food webs and are involved in various biogeochemical cycles in aquatic environments. Phytoplankton communities shift in composition with environmental changes over timeframes of days to years (Boyce et al., 2010). Such changes can propagate throughout the food web and thus affect the biodiversity of the ocean, and the abundance and productivity of other organisms, including fish assemblages (Boyd and Doney, 2002; Hays et al., 2005; Mutshinda et al., 2013; Irwin et al., 2015; Pinckney et al., 2015). The ability to evaluate such changes in different parts of the ocean quickly and effectively is of interest to gain a basic ecological understanding and for practical purposes to support ecosystem-based management and decision-making (Turner et al., 2003; Game et al., 2009; Hazen et al., 2013; Lewison et al., 2015).

Phytoplankton phenology and distribution patterns have been assessed synoptically by combining satellite remote sensing reflectance ( $R_{rs}$ ) observations with *in situ* pigment and bio-optical measurements throughout the world's oceans (Friedland et al., 2018). These studies have relied on empirical relationships between phytoplankton biomass (as chlorophyll-a concentration) and relative abundances of broad phytoplankton functional types (PFT; e.g., silicifiers, calcifiers, and nitrogen fixers) and size classes (Uitz et al., 2006; Hardman-Mountford et al., 2008; Brewin et al., 2010; Hirata et al., 2011). More recently, empirical orthogonal functions and machine learning methods have been applied to *in situ* pigment data and satellite retrievals to examine the biogeography and succession of taxonomic groups (e.g., diatoms, cyanobacteria, and nanoeucaryotes) within regional domains and globally (Alvain et al., 2008; Taylor et al., 2011; Réve-Lamarche et al., 2017; Catlett and Siegel, 2018; El Hourany et al., 2019a; Xi et al., 2020). These efforts have improved our understanding of the affinity of phytoplankton groups to static biogeographic provinces and phytoplankton responses to climate forcings (Alvain et al., 2008; Catlett and Siegel, 2018). This study complements this toolbox by characterizing phytoplankton communities within dynamic seascapes (Kavanaugh et al., 2014, 2016) derived from a machine

learning classification of satellite ocean color and thermal data in south Florida waters.

Pioneering studies of the typical physical and biogeochemical characteristics of different parts of the ocean led to maps of oceanic biogeographic provinces (Longhurst, 1998; Platt and Sathyendranath, 1999). More recently, ecological seascapes that change with time have been outlined based on satellite remote sensing and model results (Saraceno et al., 2006; Oliver and Irwin, 2008; Reygondeau et al., 2013; Kavanaugh et al., 2016). These dynamic seascape maps allow scaling of habitat characteristics inferred from a few *in situ* measurements to larger areas (Devred et al., 2007; Hales et al., 2012). They account for the fluid and changing dynamics of the ocean. The seascapes can be generated at the native spatial and temporal resolution of satellite data, and therefore resolve potential habitat for different species and how these habitats change daily, with season and over the years (Hales et al., 2012; Duffy et al., 2013; Kavanaugh et al., 2014; Muller-Karger et al., 2014).

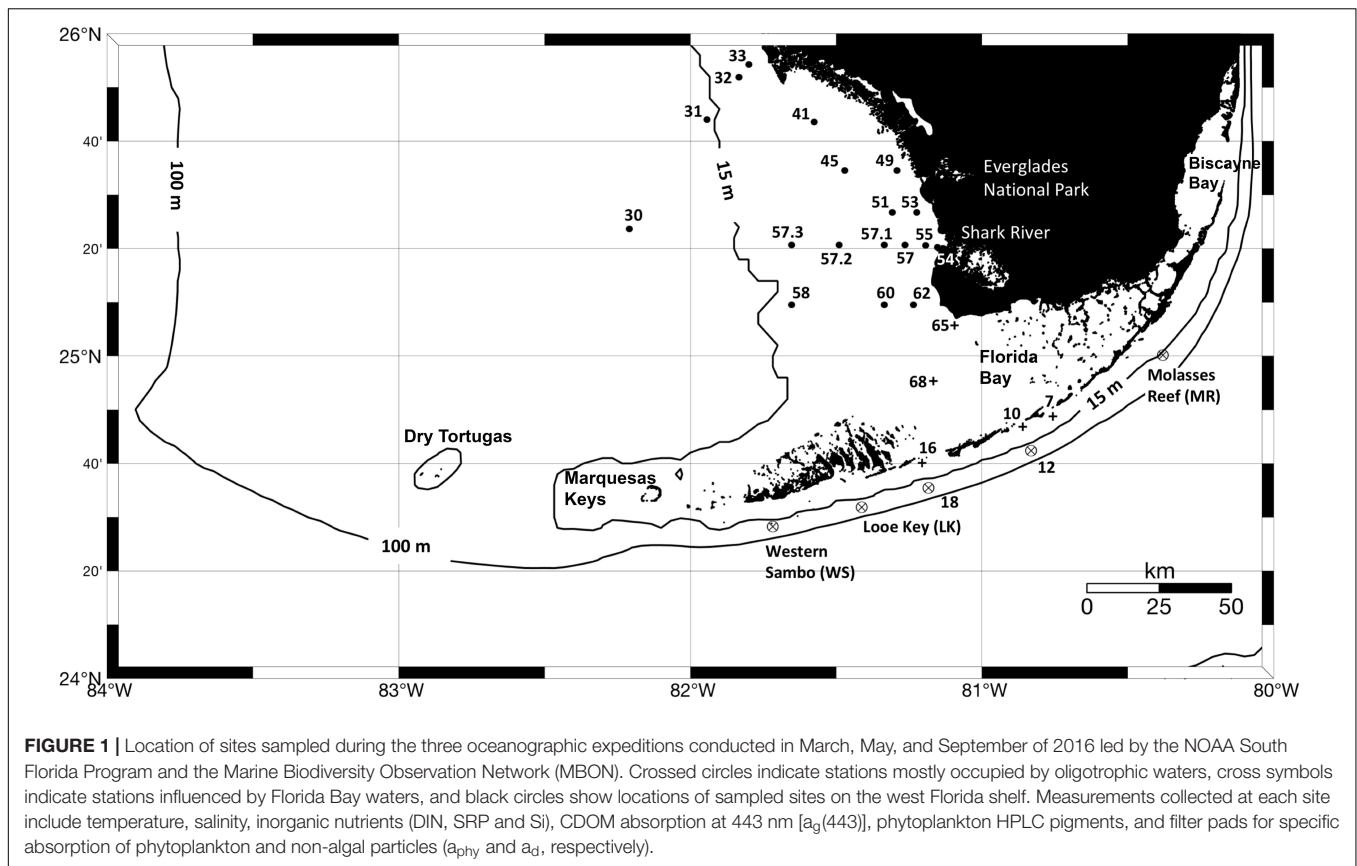
Here we describe an analysis of phytoplankton community structure, size classes, bio-optical properties, inorganic nutrient concentrations and hydrographic conditions in the context of satellite-derived seascapes of shelf and oceanic waters off southwest Florida, United States, including part of the eastern Gulf of Mexico. The goals were to understand changes in the diversity of phytoplankton in the region around the Florida Keys National Marine Sanctuary (FKNMS), and to validate the applicability of the satellite-derived seascapes for rapid assessment of water quality and habitat status in and around the FKNMS.

## MATERIALS AND METHODS

### Satellite Data and Seascape Classification

Seascapes are classified using a suite of synoptic time series observations from satellites. Specifically, we used as inputs concurrent observations of sea surface temperature (SST), chlorophyll-a (chl-a) concentration, and normalized fluorescence line height (nFLH; a metric of phytoplankton biomass, health, and nutrient status). nFLH is used in the seascape classification





as a proxy for phytoplankton bloom conditions in Case II waters, which are typically found in our region; conventional blue-green ratio algorithms tend to significantly overestimate chl-*a* concentration in shallow coastal areas due to bottom reflectance contamination or sensitivity of the blue spectral region to CDOM absorption (Hu et al., 2005). Nonetheless, the nFLH signal can be affected by, for example, non-photochemical quenching (NPQ) from photo-inhibition of phytoplankton under high irradiance conditions (Kiefer, 1973; Falkowski and Kiefer, 1985; Xing et al., 2007). While the combined effects of these processes on the classification are outside the scope of this study we recognize that seascape distributions could be affected by nFLH variations associated with drivers of NPQ.

Data from the Moderate Resolution Imaging Spectroradiometer (MODIS on the Aqua satellite) were obtained from the Ocean Biology Processing Group (OBPG) at NASA's Goddard Space Flight Center<sup>1</sup> at 4-km (monthly means) and 1-km (daily) resolution for waters around Florida (24° to 26° N, 80° to 84° W; **Figure 1**). These data were obtained in 2016 and consisted of files from the R2014.0 reprocessing at the OBPG. Daily SST, chl-*a*, and nFLH were mapped to an equidistant cylindrical projection, combined into daily mosaics, and binned to 8-day periods. SST scenes were collected at night and used the 4  $\mu$ m channel. We used the 1 km daily mosaics to generate seascapes maps during our oceanographic expeditions

conducted in the study site on March 11–18, May 9–13, and September 12–19, 2016.

To compute the seascapes, we followed the classification approach of Kavanaugh et al. (2014). Briefly, climatological monthly means of SST, chl-*a*, and nFLH (2003–2010) were used as inputs to derive probabilistic self-organizing maps (PrSOM) (Anouar et al., 1998). The three variable spatio-temporal vectors led to 15 × 15 neuronal maps (i.e., 225 classes), each with its own 3-dimensional weight based on maximum likelihood estimation (3-D MLEs). The 3-D MLEs were reduced using a hierarchical agglomerative clustering (HAC) with Ward linkages (Ward, 1963). This method uses combinatorial, Euclidian distances that conserve the original data space with sequential linkages (McCune et al., 2002). The seascapes were then successively grouped until 90% of the variance was explained. This led to a total of 18 unique classes.

The 18 seascapes were numerically ordered according to the trophic state of each class. They increase from deep, offshore, oligotrophic conditions (class 1) to optically shallow, near-shore, eutrophic conditions (class 18; see **Table 1**). For example, seascape classes 1 through 3 correspond to water masses with *very high* SST (> 27°C) and *very low* chl-*a* values (<0.1 mg m<sup>-3</sup>). Classes 16 through 18 are indicative of water masses with the highest chl-*a* (> 1.8 mg m<sup>-3</sup>) and nFLH (>0.15 mW cm<sup>-2</sup>  $\mu$ m<sup>-1</sup> sr<sup>-1</sup>) values.

Once the spatial-temporal vectors were classified, the means, covariances, and proportion of total pixels classified within

<sup>1</sup><http://oceancolor.gsfc.nasa.gov>

**TABLE 1** | Mean and variance values of satellite input data for each seascape class with corresponding qualitative description.

Seascape class	<sup>1</sup> Log10 [Chl-a]	<sup>2</sup> Log10 [nFLH]	<sup>3</sup> SST	<sup>1</sup> Chl-a	<sup>2</sup> nFLH	nFLH/Chl-a	Log10 Chl-a variance	Log10 nFLH variance	SST variance	Qualitative description
1	-1.16	-1.58	28.18	0.07	0.03	0.38	0.01	0.01	0.81	Very warm, Very oligotrophic 1
2	-1.07	-1.49	29.25	0.09	0.03	0.38	0.01	0.02	0.56	Very warm, very oligotrophic 2
3	-1.05	-1.93	27.23	0.09	0.01	0.13	0.01	0.03	1.06	Very warm, very oligotrophic 3
4	-0.93	-1.87	25.00	0.12	0.01	0.11	0.02	0.02	1.54	Moderate oligotrophic 1
5	-0.93	-1.51	29.06	0.12	0.03	0.26	0.06	0.02	1.01	Warm, oligotrophic
6	-0.93	-1.80	23.81	0.12	0.02	0.13	0.03	0.03	2.50	Winter oligotrophic
7	-0.80	-1.45	26.60	0.16	0.04	0.23	0.02	0.03	1.32	Moderate oligotrophic 2
8	-0.76	-1.29	24.23	0.17	0.05	0.30	0.01	0.02	2.51	Mesotrophic winter 1
9	-0.70	-1.36	23.79	0.20	0.04	0.22	0.02	0.04	1.77	Mesotrophic winter 2
10	-0.49	-1.25	27.11	0.32	0.06	0.18	0.04	0.03	4.62	Mesotrophic summer
11	-0.40	-1.35	24.16	0.40	0.04	0.11	0.13	0.05	1.44	Transition summer
12	-0.21	-1.08	20.26	0.62	0.08	0.13	0.04	0.04	3.07	Transition winter
13	0.09	-0.85	23.04	1.23	0.14	0.12	0.14	0.03	3.09	Florida Bay Cool
14	0.17	-1.17	28.63	1.47	0.07	0.05	0.14	0.05	3.46	Florida Bay Warm
15	0.22	-2.12	26.27	1.66	0.01	0.00	0.21	0.08	7.09	Nearshore
16	0.26	-0.78	27.65	1.84	0.17	0.09	0.08	0.05	3.92	Warm, eutrophic, optically shallow
17	0.59	-0.64	28.57	3.90	0.23	0.06	0.10	0.03	3.96	Summer, nearshore, optically shallow
18	0.67	-0.57	18.49	4.63	0.27	0.06	0.07	0.04	7.15	Winter, nearshore high chla, optically shallow

<sup>1</sup> (mg m<sup>-3</sup>), <sup>2</sup> (mW cm<sup>-2</sup> μm<sup>-1</sup> sr<sup>-1</sup>), <sup>3</sup> (°C).

each seascape informed a multivariate Gaussian mixture model. Class assignments based on satellite data collected over each cruise duration were then determined by their maximum posterior probabilities.

To examine relationships between seascape classes and *in situ* observations, the dominant seascape class at each site sampled by ship was identified. Seascape values within a 3-pixel radius around each station were extracted using the *Distance* function of the Matlab software (Mathworks®), yielding ~ 32 class values at each site depending on cloud cover or other possible masking. Therefore, a seascape class array could be composed by a particular combination of the 18 possible categories. In order to identify a predominant seascape category occupying each sampled site, a unique seascape value per station was obtained by calculating the distance-weighted geometric mean value ( $\bar{x}$ ) of the corresponding 32 class array, using the equation:

$$\bar{x} = \exp \left( \frac{\sum_{i=1}^n D_i \ln x_i}{\sum_{i=1}^n D_i} \right)$$

where  $x$  is the seascape value of the extracted pixel, and  $D$  is the inverse of the distance (geodetic arc length) between the center of the extracted pixel and the station location. Inverse distance values  $D$  were used to proportionally assign more weight to pixels closer to the stations. Weighted geometric means were employed to normalize differences in minimum and maximum seascape values amongst stations; some sites showed only one

or two classes whereas other stations were surrounded by a higher number of seascape categories and thus showed more mixed conditions. The  $\bar{x}$  values were then rounded to the nearest unit for a final seascape classification assigned to each particular ship station.

## In situ Measurements

Measurements of phytoplankton pigment concentration, hydrography, nutrient concentration, and inherent optical properties (light absorption coefficient by particulate and dissolved substances) were made from the *R/V Walton Smith* (University of Miami). Three expeditions were conducted in 2016: March 14–18 (WS16074), May 5–12 (WS16130), and September 19–23 (WS16263). A total of 24 stations were sampled for pigment concentration using High Performance Liquid Chromatography (HPLC) and bio-optical properties in March, 23 stations in May, and 27 stations in September. All cruises sampled waters around the Florida Keys, Florida Bay, and the west Florida shelf (**Figure 1**). The expeditions were conducted as part of the NOAA South Florida Ecosystem Restoration project [SFER; Atlantic Oceanographic and Atmospheric Laboratory (AOML)] and the Sanctuaries Marine Biodiversity Observation Network (MBON) field program.

Hydrographic data were collected using a Conductivity-Temperature-Depth (CTD) Sea Bird 911plus CTD system mounted on a rosette with twelve Teflon-coated 10-L Niskin

bottles. The CTD was also equipped with Seapoint chlorophyll-a and colored dissolved organic matter (CDOM) fluorometers, a Biospherical Instruments 4-Pi Photosynthetically Available Radiation (PAR) sensor, and a WetLabs 25 cm transmissometer. Only the surface (1 m) data were used in this study to compare with satellite observations.

Surface concentrations of dissolved inorganic nitrogen (DIN, i.e., nitrate, nitrite and ammonia), soluble reactive phosphorus (SRP), and silicate (Si) were measured from samples collected directly from Niskin bottles. Nutrient samples were filtered through a 0.45  $\mu\text{m}$  filter into 8-ml polystyrene test tubes that had been rinsed three times with the seawater to be sampled. The samples were stored frozen at  $-20^{\circ}\text{C}$  until analysis at the Ocean Chemistry and Ecosystems Division of the AOML. Nutrients were measured on a SEAL Analytical autoanalyzer using standard gas-segment continuous flow colorimetric methods (Zhang and Berberian, 1997; Zhang et al., 1997, 2000; Zhang, 2000).

## HPLC Pigment and CHEMTAX Analyses

Separate samples for HPLC, chlorophyll-a, and accessory pigment concentration measurements were collected by vacuum-filtering  $\sim 0.1 - 2$  L of seawater (depending on biomass concentration present) through a 25 mm glass fiber filter (Whatman GF/F, 0.7  $\mu\text{m}$  pore size) on board ship. Filters were wrapped in aluminum foil and stored in liquid nitrogen. Once on land, HPLC samples were kept at  $-80^{\circ}\text{C}$  until analyzed. HPLC analyses were conducted at the NASA Goddard Space Flight Center (GSFC), Maryland, following Van Heukelem and Thomas (2001) and Hooker et al. (2005). A total of 13 diagnostic HPLC pigments were recorded (**Supplementary Table S1**). All pigment data are available online at the NASA SeaWiFS Bio-optical Archive and Storage System (SeaBASS)<sup>2</sup>.

Of the pigment suite collected, seven diagnostic pigments (DP) were used to calculate the proportion of micro-, nano-, and pico-phytoplankton in a sample per Uitz et al. (2006):

$$\begin{aligned} \text{Micro-phytoplankton } (>20 \mu\text{m}) \\ &= (1.41[\text{Fuco}] + 1.41[\text{Perid}])/\text{DP} \\ \text{Nano-phytoplankton } (2 \text{ to } 20 \mu\text{m}) \\ &= (0.60[\text{Allo}] + 0.35[\text{But-fuco}] + 1.27[\text{Hex-fuco}])/\text{DP} \\ \text{Pico-phytoplankton } (<2 \mu\text{m}) \\ &= (0.86[\text{Zea}] + 1.01[\text{TChlb}])/\text{DP} \\ \text{DP} &= 1.41[\text{Fuco}] + 1.41[\text{Peri}] + 0.60[\text{Allo}] + 0.35[\text{But-fuco}] \\ &\quad + 1.27[\text{Hex-fuco}] + 0.86[\text{Zea}] + 1.01[\text{TChlb}] \end{aligned}$$

Several diagnostic pigments in **Supplementary Table S1** are unique to specific types of phytoplankton. For example, alloxanthin marks the presence of cryptophytes, and peridinin marks dinoflagellates. Most of the other pigments are present in more than one phytoplankton group (e.g., zeaxanthin is shared by cyanobacteria and chlorophytes). Since many algal groups

have characteristic proportions of maker pigments, the relative abundance of specific taxa in a mixed phytoplankton population can be estimated using the ratio of individual diagnostic pigments (IP) to the sum of all diagnostic pigments ( $\sum \text{DP}$ ) or to total Chl-a (Mackey et al., 1996; Vidussi et al., 2001; Pinckney et al., 2015).

The relative abundances of chlorophytes, cryptophytes, cyanobacteria, diatoms, dinoflagellates, haptophytes, and prasinophytes were computed from pigment distributions using CHEMTAX v.1.95 chemical taxonomy software (Mackey et al., 1996; Wright et al., 1996). Specifically, relative abundances of two nominal sub-groups of cyanobacteria (Type 2 and 4), diatoms (Type 1 and 2) and haptophytes (Type 6 and 8), and of all remaining groups were derived following Pinckney et al. (2001, 2015) and Higgins et al. (2011) (**Supplementary Table S2**). Therefore, a total of ten phytoplankton groups were analyzed. CHEMTAX seeks to achieve an optimal fit to a matrix of phytoplankton taxa based on an initial IP:TChl-a ratio matrix (**Supplementary Table S2**). An initial limit matrix determines the extent to which each pigment ratio can be adjusted. We used the initial pigment ratio described in Higgins et al. (2011) with the default limit matrix included in CHEMTAX (Mackey et al., 1996) (see **Supplementary Tables S2, S3**). In this study we used the new CHEMTAX software (version 1.95), which runs multiple trials from randomized starting points that in turn generate 60 pigment ratio tables as described in Wright et al. (2009). To minimize errors resulting from inaccurate pigment ratio seed values, we separated the pigment data from each cruise into four bins using hierarchical cluster analysis (HAC; see section “Data Clustering and Statistical Analysis” and **Supplementary Figure S1**), and each sample group was run separately in CHEMTAX.

## Inherent Optical Properties

### Particulate Matter Light Absorption Coefficients

Samples were collected at each station for determinations of spectral absorption coefficients of total particulate matter and detritus [ $a_p(\lambda)$  and  $a_d(\lambda)$ , respectively; in  $\text{m}^{-1}$ ]. We used the filter pad method of Mitchell and Kiefer (1988). Surface samples (0.1 to 2 L of seawater) from each station were vacuum-filtered through a 25 mm glass fiber filter (Whatman GF/F, 0.7  $\mu\text{m}$  pore size) on board ship. After collection, filter pads were placed in Histoprep capsules and flash-frozen in liquid nitrogen until arrival to the laboratory, where they were transferred to a  $-80^{\circ}\text{C}$  freezer. Filter pads were processed within 6 months of collection.

Spectral optical density [ $\text{OD}(\lambda)$ ] was measured on the filters from 330 to 880 nm at  $\sim 2$  nm resolution using a custom-built, 512-channel spectrometer at the Optical Oceanography Laboratory of the College of Marine Science at University of South Florida. Initial OD measurements were used to estimate  $a_p(\lambda)$  following the methods of Bricaud and Stramski (1990) and Mitchell and Kiefer (1988). After collection of  $a_p(\lambda)$  spectra, filters were rinsed with hot ( $\sim 60^{\circ}\text{C}$ ) methanol for  $\sim 20$  min under low light conditions to extract phytoplankton pigments (Kishino et al., 1985; Roesler et al., 1989). Filters were then re-scanned for  $a_d(\lambda)$  (non-algal particles; NAP)

<sup>2</sup>seabass.gsfc.nasa.gov

determinations. For each sample the difference between  $a_p(\lambda)$  and  $a_d(\lambda)$  was calculated to obtain the absorption coefficient of phytoplankton,  $a_{phy}(\lambda)$ .

Derivative analysis of phytoplankton absorption spectra was used to examine the relative dominance of diagnostic pigments in these mixed algal populations (Bidigare, 1989). This technique identifies absorption peaks of individual pigments using the second or fourth derivative of  $a_{phy}$ . We computed vectors of the second derivative of  $a_{phy}$  spectra ( $a_{phy}''$ ) using differences among consecutive waveband elements over the entire spectral range of the data. Spectral noise was removed from each  $a_{phy}$  vector before computations of second derivative spectra by applying a least-squares smoothing filter (i.e., Savitzky-Golay) following Lorenzoni et al. (2015). Prior to calculating second derivative spectra  $a_{phy}''$ , vectors were normalized by the corresponding  $a_{phy}$  value at 440 nm [i.e.,  $a_{phy}(\lambda)/a_{phy}(440)$ ]. This helps to remove some effects of Chl-a variability among samples (Nair et al., 2008).

We used the “finite approximation” technique to detect subtle changes in the spectral curvature between waveband elements or band separation (BS) (Torrecilla et al., 2009). BS between 5 and 10 nm yielded identical results. Thus, cluster analyses were constructed using a BS value of 9 nm as in Torrecilla et al. (2011). Matrices containing arrays of normalized  $a_{phy}''$  spectra were then used in the cluster analysis to classify sampled stations.

Observations of phytoplankton light absorption at 492, 512, 550, and 673 nm and the concentration of photo-synthetic and photo-protective carotenoids provide information about phytoplankton community structure (Chase et al., 2013; Pinckney et al., 2015). We conducted least-square correlation analyses between these parameters using relative pigment concentrations values. Specifically, photosynthetic and photoprotective carotenoids [(PSC = but-fuco + fuco + hex-fuco + perid; PPC = allo + diadinoxanthin + diato + zea + alpha-carotenoid + beta-carotenoid)], as well as individual diagnostic pigments (e.g., zeaxanthin and fucoxanthin), were compared against  $a_{phy}''$  minima centered at 492, 550 nm and 673 nm, and maxima centered at 512 with a linear regression model using the “fitlm” function in Matlab®. Negative correlation between  $a_{phy}''$  values and pigment concentrations denote higher phytoplankton absorption with increasing pigment content, whereas positive correlations indicate lower phytoplankton absorption as a result of lower concentration of these pigments.

### Dissolved Organic Matter Light Absorption Coefficients

Samples for colored dissolved organic matter (CDOM) absorption coefficient measurements were collected at each site by filtering 200 mL of seawater through a 47 mm Millipore membrane filter (0.2  $\mu$ m pore size) using vacuum filtration. Samples were kept at  $\sim 4^\circ\text{C}$  until analysis within 2 weeks after collection. CDOM absorbance spectra,  $A(\lambda)$ , were determined between 200 and 800 nm at  $\sim 1$  nm resolution using a Perkin Elmer Lambda 25 spectrophotometer equipped with 10-cm pathlength cells. Recently distilled Milli-Q water was used as a blank. The CDOM absorption coefficient ( $a_g$  in  $\text{m}^{-1}$ ) was

calculated with the following equation:

$$a_g(\lambda) = \ln(10) A(\lambda)/r$$

where  $r$  is the pathlength (10 cm). CDOM absorption values at 443 nm were used for analysis.

### Data Clustering and Statistical Analysis

Hierarchical agglomerative cluster (HAC) analysis was employed for the classification of sampled stations based on HPLC diagnostic pigment and  $a_{phy}''$  measurements (Figure 2). The HAC analysis uses an unsupervised algorithm that generates cluster trees (dendrograms) that group objects hierarchically according to pairwise distances between these objects. We utilized the *Linkage* function of the Matlab software (Mathworks®) to group stations occupied during each cruise. Specifically, we employed “Euclidian” distance as a metric to group objects (stations). The “average” method computes unweighted average distance between clusters. Dendrogram clusters were used to assess how station groupings during a field campaign related to seascape classes identified at each site (Figure 2). Input data to the HAC analysis consisted of matrices containing one numerical array per station. For example, the pigment matrix for the HAC analysis using data collected in the March cruise had 24 rows (stations) and 12 columns (pigment ratios).

Canonical correspondence analysis (CCA) were employed to identify relationships between pigment-derived phytoplankton taxa, environmental conditions (i.e., temperature, salinity,  $a_g(443)$ , and nutrients), and seascape classes. To facilitate interpretation of results we reduced the ten algal groups to seven classes by merging Diatoms Type 1 and 2, Cyanobacteria Type 2 and 4, and Haptophytes Type 6 and 8 into single corresponding groups. The CCA was performed using the statistical R software.

To examine relationships between the spatial distribution of phytoplankton based on pigment analyses and patterns in bio-optical data, we compared dendrograms constructed with  $a_{phy}''$  vectors and those generated from HPLC pigment data using the cophenetic index as in Torrecilla et al. (2011) (Figure 2). This index represents correlation coefficient between cophenetic matrices of analyzed dendrograms and is proportional to the level of similarity of pairwise distances between data objects in each dendrogram. A cophenetic correlation coefficient of 1 means that dendrograms are identical.

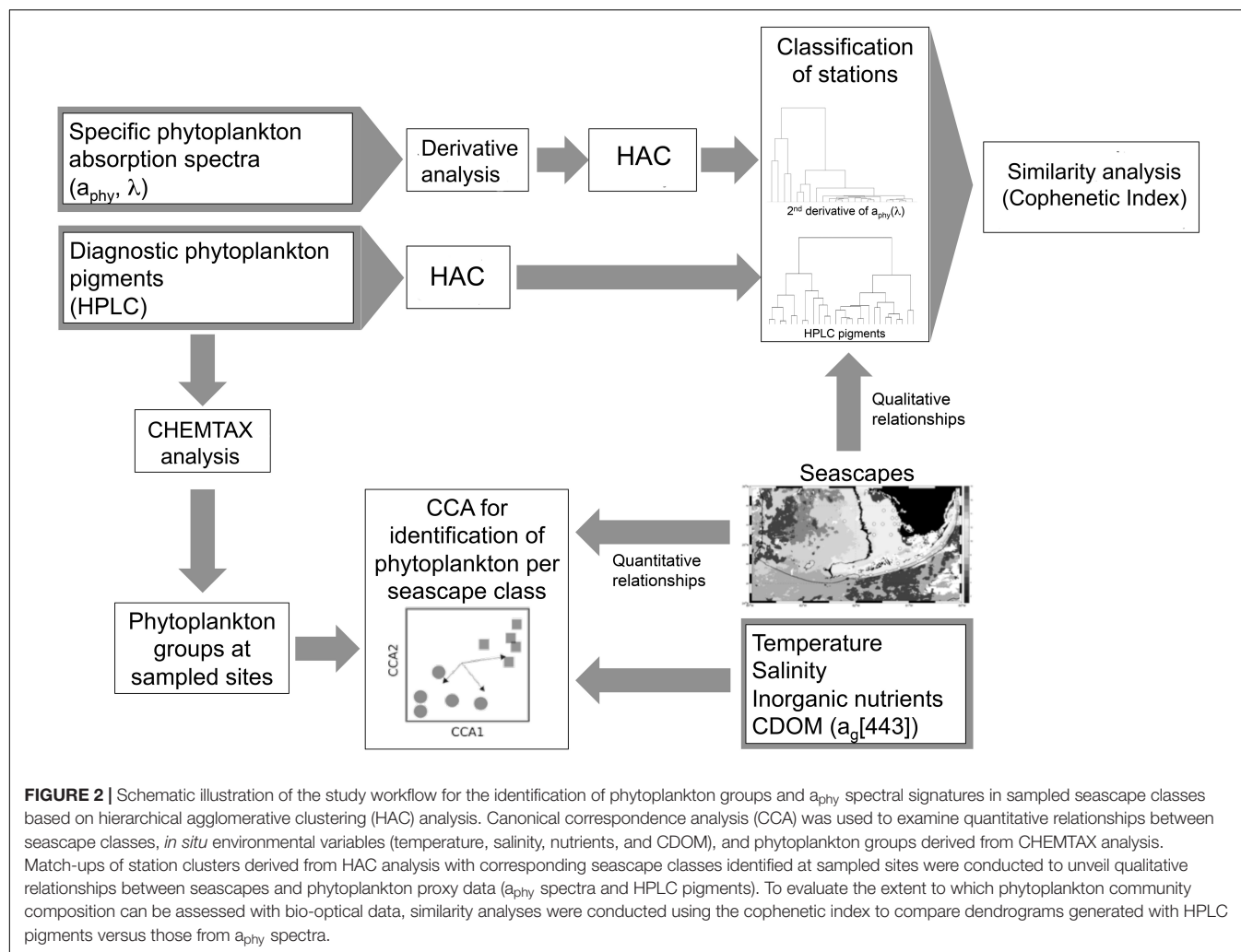
## RESULTS

### Seascape Classes

Seascape class values were derived for all stations that had complete datasets for all parameters of interest during the three cruises (Figure 3; see Figure 1 for station location). The lone exception was the pixel at Station 12 in March, 2016, which was obscured; therefore, the seascape value was assumed to be that of neighboring stations with similar oceanographic properties [i.e., Looe Key (LK) and Station 18].

During the March 2016 cruise, six dominant seascape classes were identified across the 24 sampled stations (Table 2). The





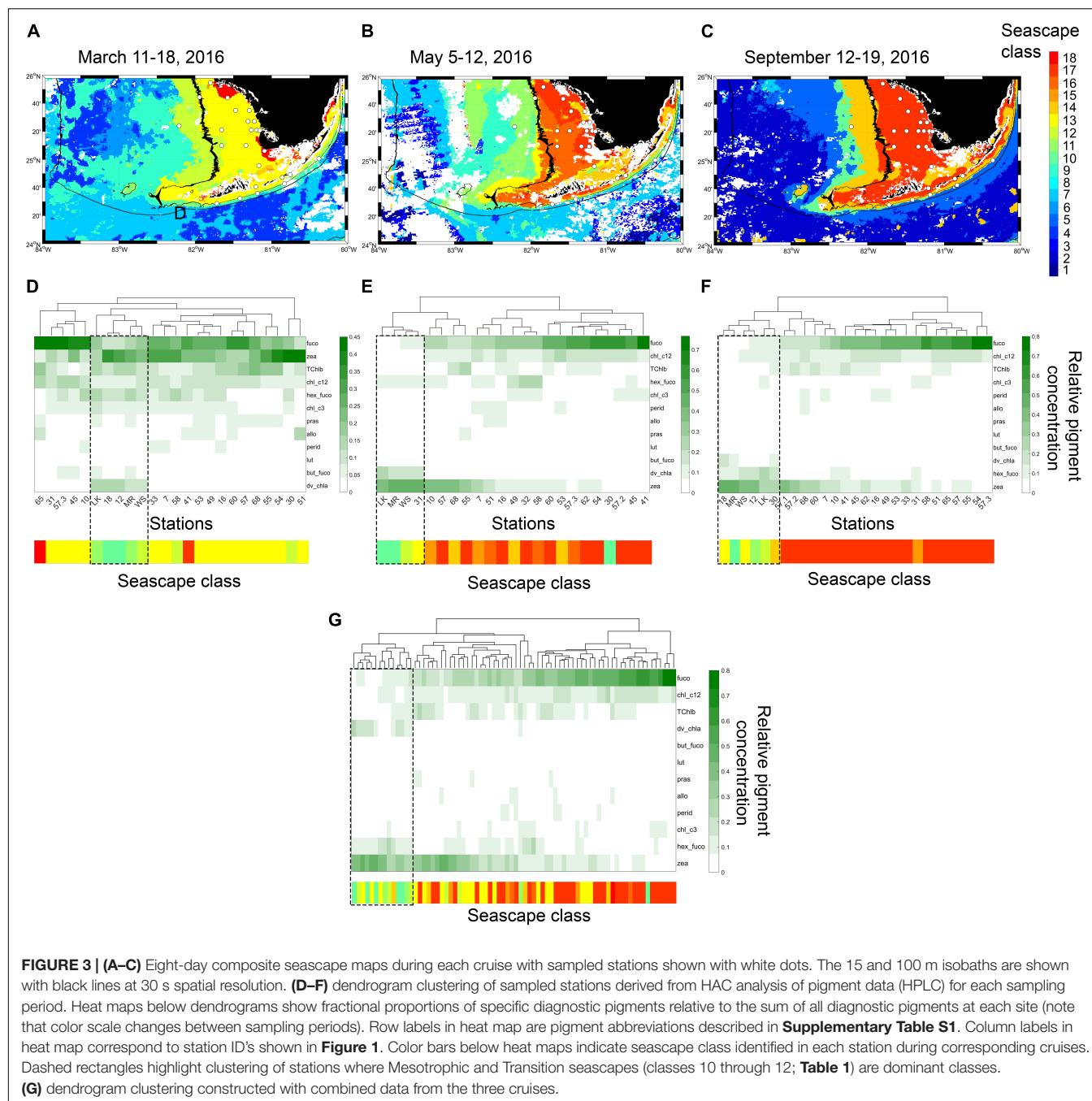
**TABLE 2 |** Seascape classes identified across all sampled stations during the three field campaigns.

Cruise date (cruise identifier)	Number of stations sampled	Total number of pixels analyzed	No-data pixels (%)	Seascape classes within the 3-pixel radius (% pixels)	Dominant seascape classes identified
March 14–18, 2016 (WS16074)	24	754	82 (11)	7 (1), 9 (2), 10 (0.6), 11 (10), 12 (10), 13 (68), 18 (8)	10, 11, 12, 13, 17, and 18
May 5–12, 2016 (WS16130)	23	753	155 (21)	4 (0.7), 7 (2), 9 (2), 10 (2), 11 (9), 13 (10), 14 (7), 16 (19), 17 (48)	10, 12, 13, 14, 15, 16, and 17
September 19–23, 2016 (WS16263)	27	847	64 (8)	5 (4), 10 (2), 14 (20), 16 (1), 17 (73)	10, 11, 12, 13, 14, 15, and 17

*Pixels were extracted from seascape maps within a 3-pixel radius around each site, thus yielding ~32 pixels per site.*

Florida Bay Cool seascape (class 13) was the dominant class in ~ 63% of stations, most of which were located within the 15 m isobath across the west Florida Shelf (**Figure 3**). Moderate Oligotrophic 1 through Transition Winter seascapes (i.e., seascapes with values < 13; see **Table 1** for seascape description) were detected in ~ 30% of stations, mostly in deeper waters of the west Florida Shelf and along the reef track. During

the May and September cruises, mean seascape conditions at sampled stations corresponded to eight classes between class 10 and 17. In May, ~ 65% of stations occupied were optically shallow seascape classes 16 and 17 mostly over the Florida Bay and west Florida shelf waters with depths <15 m. All other sites in May exhibited more mixed seascape conditions. In September, 74% of stations had optically shallow seascape class



17 over the west Florida shelf, while Mesotrophic, Transition and Florida Bay seascapes (classes 10 through 14) were observed at all other stations.

The dominant seascape classes detected at stations near the 100 m isobath along the southern side of the Florida Keys (gray squares in **Figure 1**) during the three sampling periods varied between Mesotrophic Summer and Florida Bay Cool (classes 10 and 13, respectively; see **Table 2**). Florida Bay stations (crosses in **Figure 1**) typically had seascapes classes ranging from Florida Bay Cool (class 13) to Winter, Nearshore High Chla, Optically Shallow (class 18) over the same period. The west Florida shelf

stations (black circles in **Figure 1**) exhibited higher seascape variability (Transition Summer [class 11] through to Summer, Nearshore, Optically Shallow [class 17]; see **Table 2**).

### Types of Phytoplankton Pigments in Different Seascapes

On average, Fucoxanthin (Fuco), Zeaxanthin (Zea), Chlorophyll c1 + c2 (Chl\_c12), total chlorophyll b (TChlb) and 19'-hexanoyloxyfucoxanthin (Hex-fuco) represented 82% of the total pigment pool in all samples collected during the three

cruises. Fucoxanthin and zeaxanthin accounted for 54% of the total pigment assemblage. Hex-fuco was generally the fifth most abundant pigment in all sampling periods. Relative contributions of chlorophyll c3, prasinoxanthin, alloxanthin, 19'-butanoyloxyfucoxanthin and lutein to the total pigment pool did not show a clear relationship with seascape class.

Stations grouped based on similar HPLC pigment composition (HAC analysis) allowed inferences to be drawn about phytoplankton community composition in different seascapes (**Figure 3**). During the three field campaigns, stations occupied by Mesotrophic Summer through Transition Winter seascapes (classes 10 – 12) typically grouped within the same pigment clusters, an indication that they had similar phytoplankton communities (see section “Phytoplankton Assemblages in Sampled Seascapes” for description of phytoplankton communities). The exceptions were stations 58 and 30 in March, and station 30 in May. These did not cluster with those also occupied by the same seascape classes (10 through 12) possibly because these sites were located at or near the boundary of higher category seascapes.

High-performance liquid chromatography groupings in Florida Bay and Nearshore seascapes (classes 13 – 15) displayed a weaker correlation; these pigment clusters often spanned different seascapes (e.g., see May cruise; **Figure 3**). Pigment composition of stations in optically shallow seascapes (classes 16 – 18), here defined as seascapes with the highest chl-a and nFLH values (see **Table 1**) that were typically present over shallow areas, generally showed consistent differences with respect to stations in Mesotrophic and Transition seascapes (classes 10 – 12). The HAC algorithm identified typical pigment groups in Eutrophic, Optically Shallow seascapes.

In general, the lowest relative fucoxanthin and chlorophyll c1 + c2 concentrations were observed in Mesotrophic Summer through Transition Winter seascape (classes 10 – 12; **Figure 3**). Fucoxanthin in Nearshore to Optically Shallow seascapes (classes  $\geq 15$ ) was nearly three-fold higher than in Mesotrophic and Transition seascapes, and two-fold higher than in Florida Bay seascapes (classes 13 and 14; **Figure 3**). Chlorophyll c1 + c2 showed a similar pattern. TChlb was  $\sim 28\%$  higher in seascapes  $\geq 13$  than lower seascape classes. Hex-fuco fractions were between 8 and 48% lower in samples collected in seascapes  $\geq 13$  than lower seascapes classes. Zeaxanthin values were nearly two-fold higher in seascapes  $\leq 13$  than seascape classes 14 to 18 (Florida Bay Cool to Optically Shallow).

Divinyl chlorophyll a (DVChl-a), a diagnostic pigment of the cyanobacteria *Prochlorococcus* spp. (Cyanobacteria Type 4), was undetected in stations occupied by Nearshore through Optically Shallow seascapes throughout the study period (**Figure 3**). DVChl-a values observed in seascapes  $< 13$  during March and May cruises were three to 79-fold higher than in seascapes 13 and 14. During the September cruise, however, DVChl-a was  $\sim 40\%$  higher in seascapes 13 and 14 than seascapes classes 12 and lower.

Peridinin, a pigment diagnostic of dinoflagellates, was generally observed at low concentrations across all seascape classes. Relative pigment concentration values of peridinin  $\geq 0.1$  were only measured in Nearshore and Optically Shallow seascapes in May (stations 7 and 16), and only in Optically

Shallow seascapes in September (stations 7 and 49; **Figure 3**). Peridinin in seascape classes  $\geq 14$  were, on average,  $\sim 40\%$  higher than in lower seascape classes.

## Phytoplankton Assemblages in Sampled Seascapes

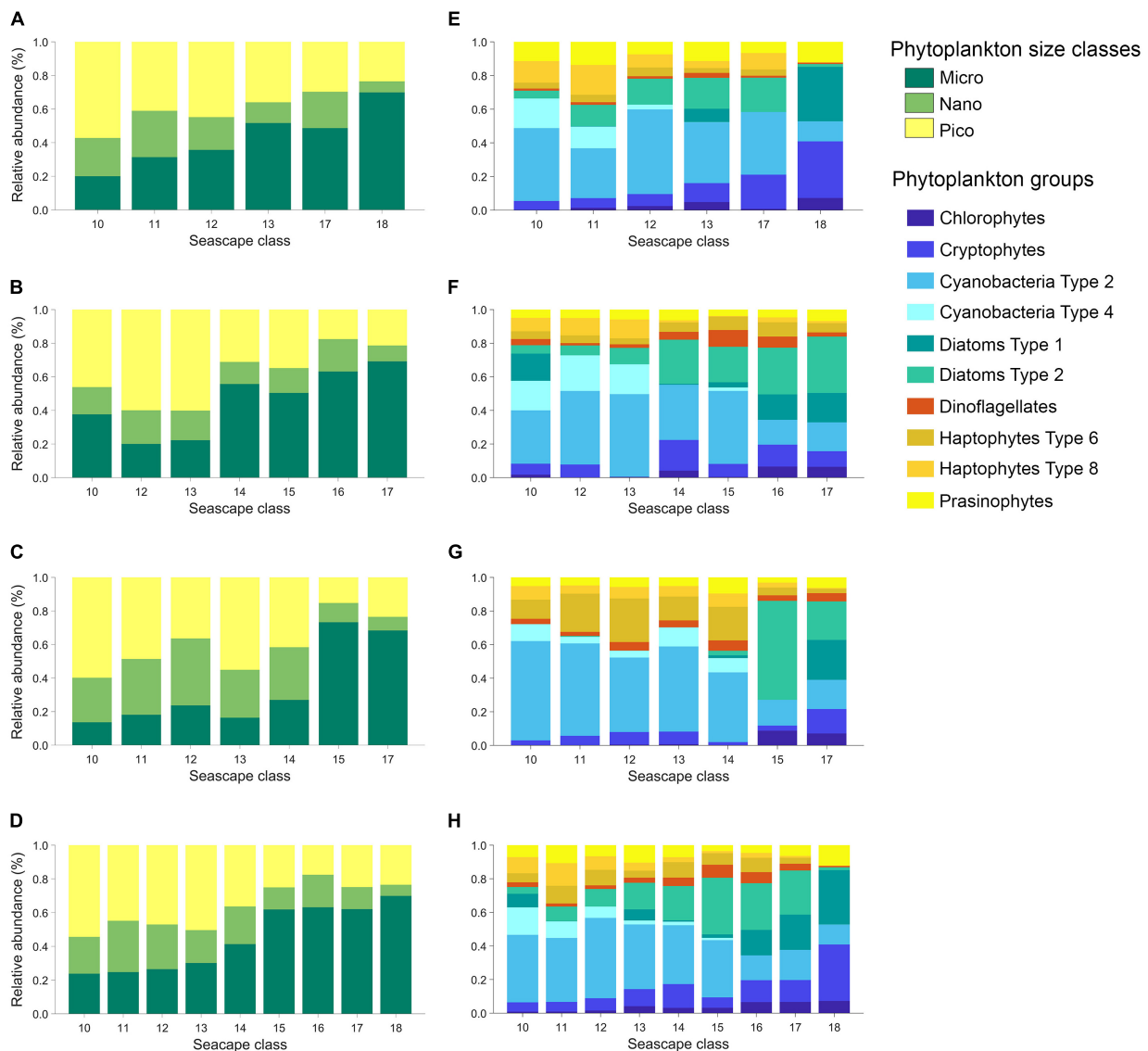
There were consistent relationships between seascapes, phytoplankton size classes, and taxa observed in the three expeditions (**Supplementary Figure S2**). The relative contributions to total Chla [(TChla)] of micro-phytoplankton ( $> 20 \mu\text{m}$  size class) increased from  $\sim 24\%$  in Mesotrophic Summer seascapes (class 10) to  $\sim 70\%$  in Winter, Nearshore High Chla, Optically Shallow seascape (class 18; **Figure 4**).

The opposite was observed with pico-phytoplankton ( $< 2 \mu\text{m}$ ). They showed  $\sim 55\%$  relative chl-a biomass in Mesotrophic Summer seascape (low chl-a; see **Table 1**) and steadily decreasing to  $\sim 24\%$  in Optically Shallow seascapes (high chl-a). Minimum and maximum pico-phytoplankton relative biomass were observed in Optically Shallow seascapes ( $\sim 18\%$  in class 16) and Mesotrophic Summer ( $\sim 55\%$  in class 10), respectively. Similar results, but with greater uncertainty, were obtained with relative biomass of nano-phytoplankton ( $2 - 20 \mu\text{m}$ ). Nano-phytoplankton was lowest in Optically Shallow seascapes ( $\sim 7\%$  in class 18) and highest in mesotrophic and Transition seascapes ( $\sim 30\%$  in class 11).

Cyanobacteria dominated in Mesotrophic Summer through Florida Bay Cool seascapes (classes 10 – 13) with mean relative contributions to TChla ranging from  $\sim 57\%$  to over 60% (**Figure 4** and **Supplementary Figure S2**). Cyanobacteria also dominated in Florida Bay Warm seascape (class 14) but their contribution to TChla dropped to  $\sim 38\%$  in this class. Specifically, Cyanobacteria Type 4 as indicative of *Prochlorococcus* spp. was only present in Mesotrophic Summer through Florida Bay Cool seascapes. The exception was observed at Station 30 where *Prochlorococcus* was detected during the September cruise when the site was occupied by Florida Bay Warm (class 14). The relative biomass contribution of this phytoplankton group decreased steadily in higher seascape classes to a minimum of about  $\sim 11\%$  (Optically Shallow class 18). Haptophyte relative biomass also appeared to be higher in the lower seascape classes (10 – 12) than in higher ones, and their contributions to TChla never exceeded  $\sim 24\%$ .

Diatoms showed lower contributions to TChla in Mesotrophic and Florida Bay seascapes ( $< 10\%$  in classes 10 to 13) and significantly increased in Florida Bay Warm and Optically Shallow ( $\sim 36\%$  in classes 14 to 18; **Figure 4**). Cryptophytes and chlorophytes showed a similar distribution, with higher relative biomass with increasing seascape class. Cryptophytes contributed  $\sim 5$  to 29% to total chl-a pool (seascapes 10 and 18, respectively). Minimum and maximum relative biomass of chlorophytes were  $\sim 3$  and 10% observed in seascapes 11 and 18, respectively.

The relative biomass of dinoflagellates and prasinophytes did not show a clear relationship with seascape class. These organisms were present at low concentrations in every class (**Figure 4** and **Supplementary Figure S2**). For example, the relative biomass of dinoflagellates ranged between  $\sim 2\%$  in



**FIGURE 4 |** Left: Average contribution of phytoplankton functional types (PFT: micro-, nano-, and pico-phytoplankton) to total chl-a (TChla) derived from diagnostic HPLC pigments using equations described in Uitz et al. (2006) estimated for each seascape class during March, May, and November 2016 cruises (**A–C**), and for all the data combined (**D**). Right: Average community composition of ten phytoplankton groups estimated for each seascape class derived from CHEMTAX analysis during March, May and November 2016 cruises (**E–G**), and for all the data combined (**H**).

Mesotrophic and Transition Summer seascapes (classes 10 and 11) and ~ 6% in Florida Bay Warm seascapes (class 14), and those of prasinophytes oscillated between ~ 3% in Nearshore seascapes (class 15) and ~ 11% in all higher seascape categories.

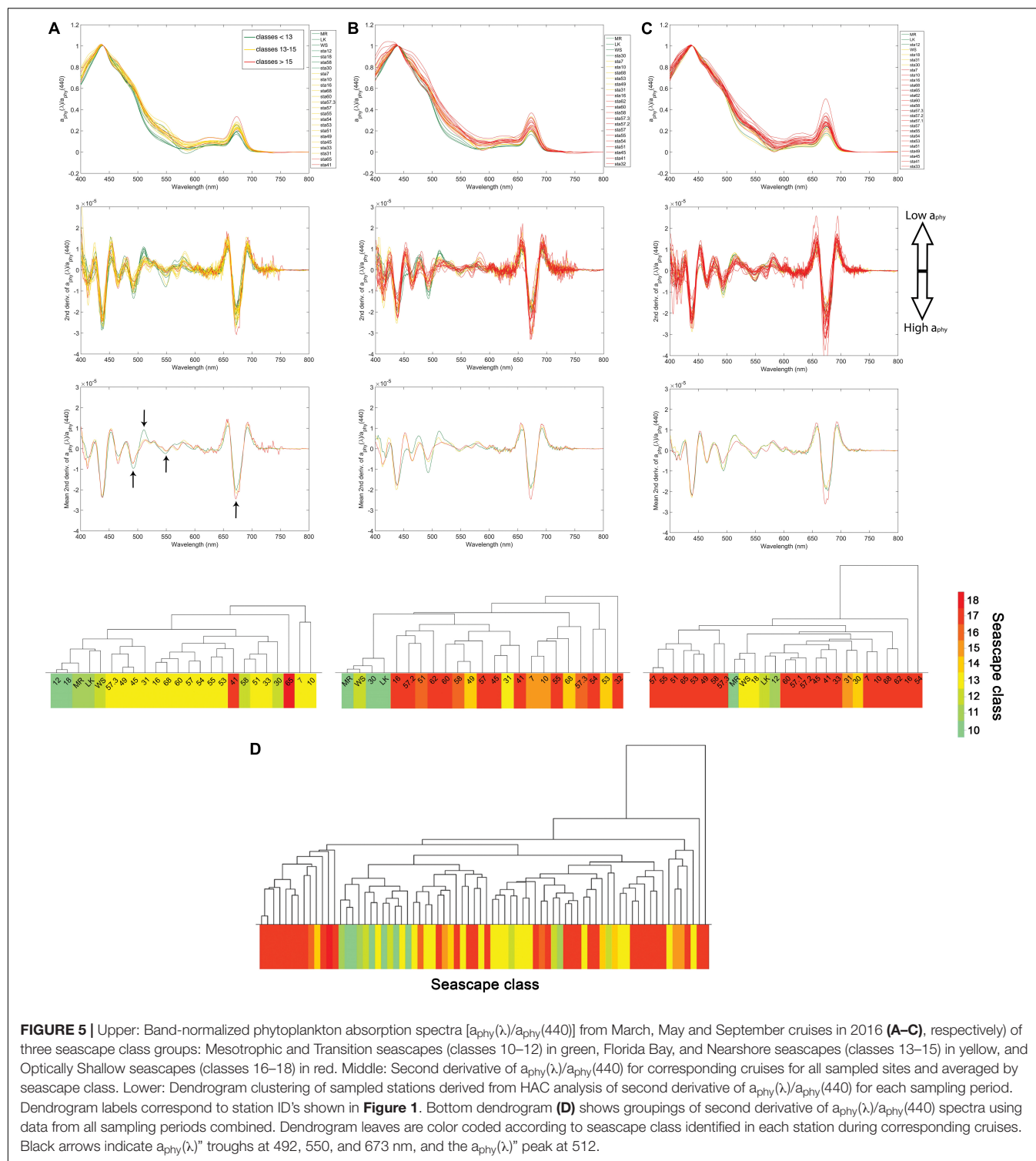
## Seascapes and Inherent Optical Properties

Analysis of the derivative of the absorption coefficient of phytoplankton ( $a_{phy}$ ) spectra (see section “Inherent Optical Properties”) allowed us to identify dominant phytoplankton in different seascapes. Differences in the shape of the second derivative of  $a_{phy}$  (here denoted as  $a_{phy}''$ ) between 450 and

550 nm, and also at 673 nm (**Figure 5**), were especially apparent between seascapes. The lowest minima in  $a_{phy}''$  were observed at ~492 nm and the highest maxima at ~512 nm in Mesotrophic and Transition seascapes (classes 10 – 12). A statistically significant inverse relationship between PPC and  $a_{phy}(492)''$  ( $r_{ppc-492} = 0.53$ ;  $p < 0.001$ ;  $n = 74$ ) was also found. A weaker correlation was observed between zeaxanthin levels and  $a_{phy}(492)''$  values ( $r_{zea-492} = 0.44$ ;  $p < 0.001$ ;  $n = 74$ ). Zeaxanthin and PPC showed a significant positively correlation to a peak in  $a_{phy}(512)''$  ( $r_{zea-512} = 0.62$  and  $r_{ppc-512} = 0.63$ ;  $p < 0.001$ ;  $n = 74$ ).

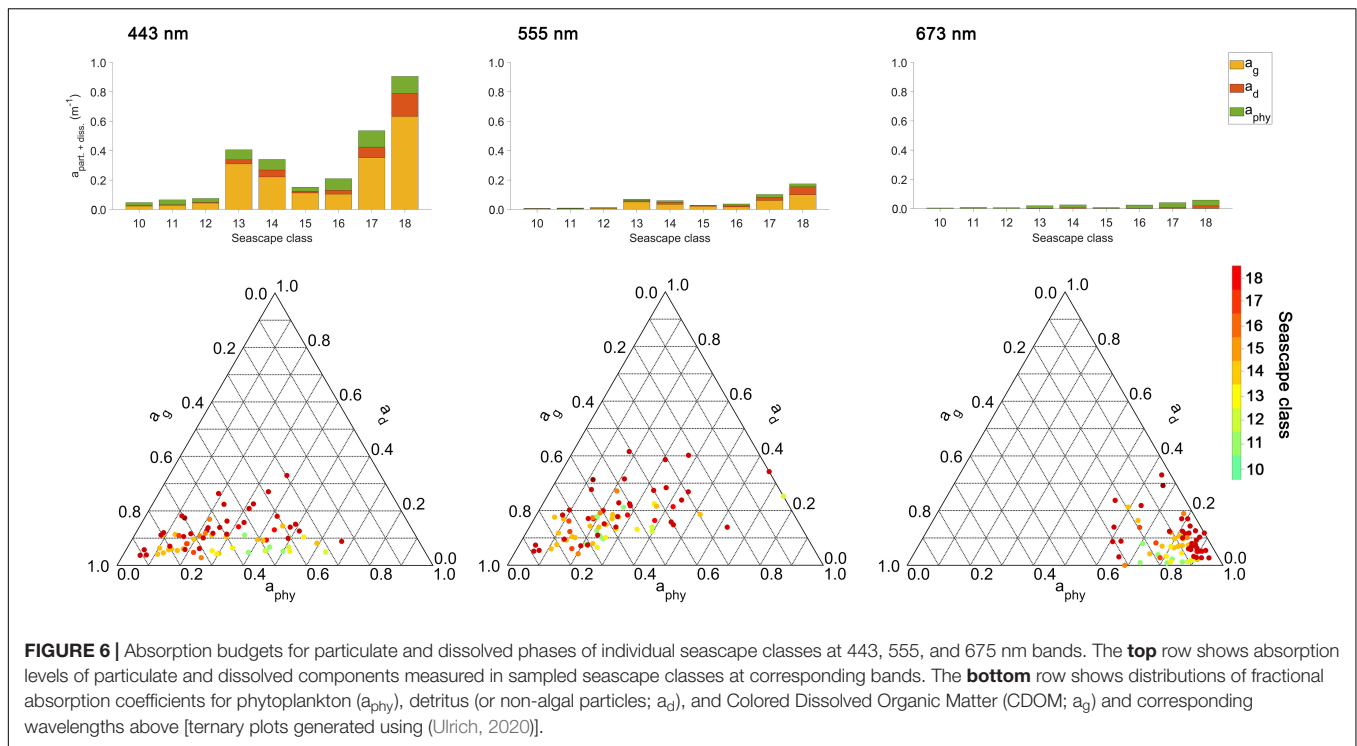
PPC and zeaxanthin relative concentrations tended to be higher in Mesotrophic Summer through Transition Winter seascapes (class 10 – 12) than in higher seascape categories. Both





minima at 492 nm and maxima at 512 nm became progressively smaller with increasing seascapes value, from Florida Bay through Optically Shallow seascapes. The  $a_{phy}$  values in Nearshore seascapes (class 15) or higher were consistently less variable within the 450 and 550 nm region than those of lower classes during the three cruises (Figure 5). Differences in  $a_{phy}$  minima

between seascapes classes were also found in the 600 – 700 nm region, which is strongly affected by the chl-a red absorption peak. Large minima around 673 nm were typically observed in samples collected in Optically Shallow seascapes. Seascapes classes of lower trophic state (e.g., Mesotrophic classes) showed less pronounced troughs; the lowest minima of  $a_{phy}$  at 673 nm



were observed in Mesotrophic Summer through Transition Winter seascapes.

Our results indicate distinct phytoplankton spectral absorption signatures across seascape classes. HAC cluster analysis using  $a_{phy}$  spectra revealed groupings of seascape classes similar to those obtained with HPLC pigment data. Mesotrophic and Transition seascapes (classes 10 – 12) along the Florida Keys reef tract and some offshore stations (i.e., stations 58 and 30; **Figure 1**) generally matched pigment-based HAC clusters (**Figure 5**). Stations occupied by Florida Bay and Nearshore seascapes (classes 13 – 15) were also generally clustered together by the HAC algorithm. The largest linkage distances were observed between groups represented by Mesotrophic and Transition seascapes (<13) and those of Optically Shallow classes (>15).

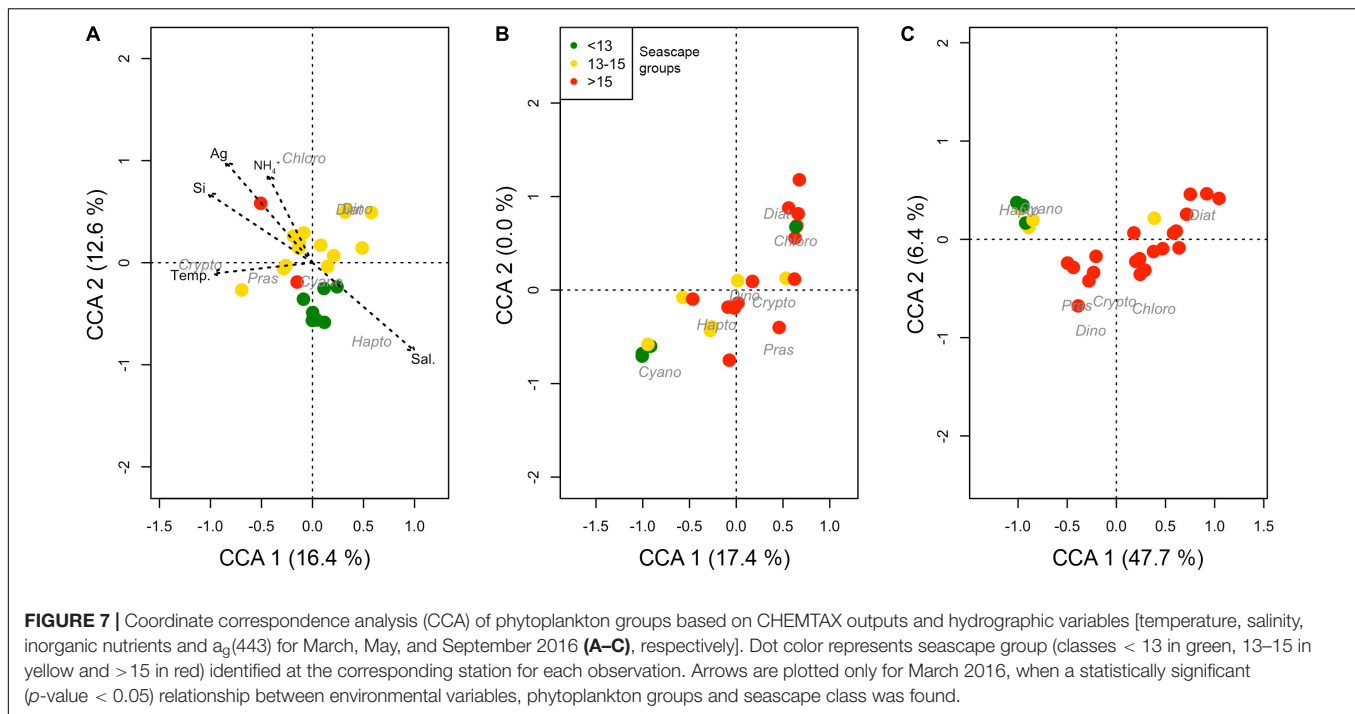
Seascapes also showed clear differences in CDOM spectral absorption ( $a_g$ ) curves (**Supplementary Figure S3**). The  $a_g$  at 443 nm (blue) generally increased progressively with increasing seascape number (i.e., moving toward the coast and in river-influenced areas).  $a_g(443)$  values measured in Florida Bay, Nearshore and Optically Shallow seascapes (classes 13 through 18) typically observed on the coastal zone of Florida Bay and west Florida shelf and around areas affected by freshwater discharge from the Everglades were ~ 2 to 20-fold higher than in Mesotrophic and Transition seascapes (classes 10 – 12) along the Florida Keys reef tract, Florida Straits, and in deeper offshore waters.

**Figure 6** shows total absorption values of particulate and dissolved phases, namely phytoplankton absorption ( $a_{phy}$ ), non-algal particles ( $a_d$ ) and CDOM ( $a_g$ ), and the fractional contributions of these individual constituents to total absorption

at 443, 555, and 673 nm wavelengths for sampled seascape classes. Light absorption at 443 nm observed in Mesotrophic and Transition seascapes (classes < 13) was mainly affected by phytoplankton and CDOM. The contribution of non-algal particles to the absorption budget in these classes was negligible (< 10%), except at 555 nm where  $a_d$  reached maximum fraction of ~ 25%. In Florida Bay and Nearshore seascapes (classes 13 – 15), CDOM showed the highest contribution to total absorption in the 443 and 555 nm bands, followed by  $a_{phy}$ . The same was observed in Optically Shallow seascapes (classes > 15), where also the highest contributions from non-algal particles were measured with values of up to ~ 40% (at 555 nm). Phytoplankton was the dominant constituent affecting ~ 50 – 100% of the absorption budget at 673 nm in all seascape classes.

Canonical correspondence analysis indicate that the lower Mesotrophic through Transition seascape classes showed distinct phytoplankton communities compared to higher categories (**Figure 7**). Except for May, these classes formed statistically significant clusters generally associated with cyanobacteria and haptophytes, and larger taxa like diatoms and chlorophytes (ANOSIM  $r_{March} = 0.4$  and  $r_{September} = 0.48$ ; both with  $p < 0.01$ ). In March these classes also showed a consistent affinity with higher salinity and lower CDOM values indicative of oceanic conditions; statistical relationships between Mesotrophic through Transition seascape, and SST, salinity and nutrients were significant at  $p < 0.01$  (**Figure 7**). These seascapes (classes 10–13) were generally associated with high relative proportions of *Prochlorococcus* spp. (Cyanobacteria Type 4) almost exclusively, and haptophytes (**Supplementary Figure S2**).

Similarity among cluster trees obtained from  $a_{phy}$  coefficients versus pigment measurements varied depending on the spectral



region examined. Cophenetic correlation analysis revealed high similarity levels (>0.5) in pairwise comparisons between dendrograms constructed with  $a_{phy}$  arrays and reference HPLC-derived dendrograms within narrow spectral bands (5 – 10 nm), notably in the violet through yellow and orange regions (440 – 540 and 640 nm, respectively; **Supplementary Figure S4**). The highest cophenetic correlation indices ( $\sim 0.9$ ) were observed in May when comparing cluster trees derived from seascape class distributions and  $a_{phy}$  dendrogram trees as reference, in similar spectral regions covering blue through yellow bands (450–540 nm, respectively).

## DISCUSSION

### Phytoplankton Pigments and Inherent Optical Properties of Seascapes

CHEMTAX and bio-optical results agree and show that: 1) nano- and pico-phytoplankton dominate in more oceanic and clear waters (lower seascape classes, < 13), that 2) larger taxa dominate in nearshore areas (higher seascape classes, > 15), and that 3) intermediate seascapes contain mixed communities (classes 13 – 15; **Figure 4**). Mixed phytoplankton assemblages were found in Florida Bay Cool and Warm, and Nearshore seascapes with balanced relative proportions of pico-, nano- and micro-phytoplankton taxa (**Figure 4**). Comparable proportions of pico- and micro-phytoplankton (41% and 36%, respectively) were measured in Florida Bay Warm seascape (class 14), with similar relative abundances of cyanobacteria, diatoms, and dinoflagellates.

As expected, the Optically Shallow seascape categories (classes > 15) appeared to cluster around communities

dominated by larger taxa like diatoms, dinoflagellates and chlorophytes. Fast-growing large phytoplankton can be expected in these classes since these typically occupy very shallow areas likely exposed to higher runoff and nutrient inputs (Nunes et al., 2018). Furthermore, we found that *Synechococcus* spp. and *Prochlorococcus* spp. (Cyanobacteria Type 2 and 4, respectively) are well represented, or dominate, assemblages of oceanic Mesotrophic and Transition (classes 10–12) and Florida Bay Cool (class 13) seascapes. *Prochlorococcus* spp. in particular was observed in these seascapes almost exclusively (**Figure 4** and **Supplementary Figure S2**); Mesotrophic and Transition classes are characterized by high salinity and low nutrient conditions under which cyanobacteria typically thrive (Mojica et al., 2015; Nunes et al., 2018). Vaillancourt et al. (2018) also found positive correlations between the cyanobacterium *Prochlorococcus* spp. and high salinity and nutrient-poor waters, whereas eukaryotic phytoplankton typically dominate in cooler and nutrient-rich areas. As in this study, they observed that cyanobacteria tend to cluster separately from eukaryotic phytoplankton in response to nutrient levels driven by temperature gradients and water column stratification. These findings are also consistent with results from previous studies describing HPLC-based phytoplankton assemblages across hydrographic or biogeochemical provinces in the Atlantic Basin (Gibb et al., 2000; Aiken et al., 2009; Torrecilla et al., 2011; Lorenzoni et al., 2015; Barlow et al., 2016; Araujo et al., 2017).

Results from spectral analyses confirmed phytoplankton assemblages derived from pigment observations. We identified a significant correlation between  $a_{phy}(492)$  minima and PPC relative concentrations, including zeaxanthin, possibly as a result of increasing dominance of small phytoplankton, i.e., *Synechococcus* spp. and *Prochlorococcus* spp., in lower seascape

classes (Mesotrophic Summer through Transition Winter), which identify more offshore waters with lower nutrient and CDOM loads (**Figure 5**). Previous studies in this region have shown that high PPC concentrations associated with cyanobacterial blooms of *Synechococcus* spp. dominate the phytoplankton absorption budget at the 490 nm spectral band (Cannizzaro et al., 2019). A similar statistical relationship between  $a_{\text{phy}}(492)$  and DVChl-a was also observed in these classes, indicating dominance of the cyanobacteria *Prochlorococcus* spp specifically in these classes.

Higher  $a_{\text{phy}}$  (thus lower phytoplankton absorption) at 512 nm were observed with increasing relative concentrations of these pigments in Mesotrophic Summer through Transition Winter seascapes. In Optically Shallow seascapes (classes > 15), where zeaxanthin and PPC had lower relative concentrations,  $a_{\text{phy}}$  spectra tended to be flatter around the 512 nm band (**Figure 5**). This spectral band is in the vicinity of the  $a_{\text{phy}}$  peak of PSC centered at 523 reported by Chase et al. (2013) and thus higher phytoplankton absorption at 512 nm can be expected when the abundance of diagnostic pigments of large taxa such as diatoms (fucoxanthin) or dinoflagellates (peridinin), increases. These results are further supported by significant negative correlations observed between PSC and  $a_{\text{phy}}(512)$  ( $r = 0.62$ ;  $p < 0.001$ ).

Comparable high correlations between PPC and  $a_{\text{phy}}(550)$  peak values were also observed, providing further evidence of increased dominance of small phytoplankton in Mesotrophic Summer through Transition Winter seascapes (**Figure 5**). This is consistent with findings by Chase et al. (2013, 2017) using data from the Atlantic, Pacific and Indian ocean basins, and results by Lorenzoni et al. (2015) from the Cariaco Basin, Venezuela, collected by the CARIACO Ocean Time Series program (Muller-Karger et al., 2019), and Cannizzaro et al. (2019) from observations in Florida Bay.

Inverse correlations were observed between fucoxanthin and  $a_{\text{phy}}(673)$  ( $r = 0.46$ ;  $p < 0.001$ ), likely driven by dominance of large taxa with increasing seascape class (**Figure 5**); fucoxanthin is a diagnostic pigment of large phytoplankton groups such as diatoms. Several other studies have found a consistent effects of diatom concentrations on  $a_{\text{phy}}$  spectra at this wavelength or in its close vicinity across different ocean regions (Werdell et al., 2014; Lorenzoni et al., 2015; Catlett and Siegel, 2018; Reynolds and Stramski, 2019).

## Phytoplankton Spectral Characterization of Seascapes

Light absorption in sampled seascapes was mostly affected CDOM concentration and phytoplankton at spectral bands known to capture information about diagnostic pigments, i.e., 443, 555 and 673 nm wavelengths (**Figure 6**). In all three bands  $a_{\text{phy}}$  accounted for a significant portion of the absorption budget across all seascapes, and most notably at the 673 nm band where phytoplankton ( $a_{\text{phy}}$ ) often dominated > 90% of the light absorption. Similar results were found in studies carried out in the western Arctic Ocean (Reynolds and Stramski, 2019), Mediterranean Sea (El Hourany et al., 2019b) and the tropical

and subtropical eastern Atlantic Ocean (Taylor et al., 2011; Torrecilla et al., 2011).

To determine the degree to which phytoplankton absorption properties and phytoplankton communities can be represented by seascapes, we compared dendrograms generated from pigment data and  $a_{\text{phy}}$  spectra using the cophenetic correlation coefficient, a similarity metric (Taylor et al., 2011; Torrecilla et al., 2011). This pairwise comparison was carried out using HPLC-derived dendrograms as a reference versus those constructed with varying combinations of spectral ranges of  $a_{\text{phy}}$  curves (Methods). The rationale is that PSC and PPC affect  $a_{\text{phy}}$  peaks computed across narrow ( $\sim 5$ – $10$  nm) spectral bands, e.g., PPC in the 490 – 500 nm region and PSC in the 510 – 520 nm region (Chase et al., 2013). Thus, dendrogram trees constructed with data from more constrained spectral bands should have a higher similarity to corresponding reference HPLC trees than those using the entire spectral range (400 – 800 nm).

Although the degree of similarity between pigment and  $a_{\text{phy}}$  dendrogram clusters varied among cruises, the highest cophenetic index ( $\sim 0.5$  –  $0.6$  in March and September cruises, and  $\sim 0.3$  in the May cruise) was generally found in the 440 (violet) and 640 nm (orange) spectral regions (**Supplementary Figures S4A–C**). The highest similarity between pigment-based and  $a_{\text{phy}}$  dendrogram trees was observed in the  $\sim 480$  –  $570$  nm spectral range, consistent with results from the eastern Atlantic Ocean (Taylor et al., 2011). These are somewhat modest cophenetic index values, but they are likely a result of statistical biases from relative oversampling of Florida Bay Warm and Summer, Nearshore, Optically Shallow seascapes classes (13 and 17, respectively) with respect to lower trophic state Mesotrophic and Transition seascapes (classes 10 – 12). Indeed, 66% of our samples came from seascapes classes 13 and 17 versus 19% in seascape classes 10 through 12.

Low cophenetic correlation between pigment and  $a_{\text{phy}}$  dendrogram trees could be attributed to high similarity among spectra collected in Florida Bay seascapes (13 and 14), and those of lower and higher seascape classes. For example,  $a_{\text{phy}}$  spectral curves from seascapes 13 – 15 were often indistinguishable from those collected in seascapes classes 16 – 18 during the March cruise and classes 10 – 12 during the September (**Figure 5**). This further supports the notion that Florida Bay seascapes carry a mixture of phytoplankton taxa also present in lower and higher seascapes. These actually have similar bio-optical characteristics with similar  $a_{\text{phy}}$  spectral curves, therefore affecting the performance of the clustering algorithm. Higher similarity among  $a_{\text{phy}}$  and pigment cluster trees could be expected if data collected over a wider range of seascape classes with a more balanced sampling distribution is used.

A similarity analysis using  $a_{\text{phy}}$  dendrogram trees as reference and dendrogram trees based on seascape classes was also applied. The goal was to identify spectral regions with  $a_{\text{phy}}$  signals dominated by phytoplankton assemblages in particular seascapes. Dendrogram trees constructed with seascape class data matched those derived from  $a_{\text{phy}}$  measurements to varying degrees (**Supplementary Figures S4D–F**). As with HPLC reference dendrograms, seascape groupings appeared to have the highest similarity to  $a_{\text{phy}}$  clusters in the blue through yellow region



(450 – 540 nm), reaching cophenetic correlation index values up to  $\sim 0.9$ , likely due to absorption effects from relative contributions of PPC and PSC to the total pigment pool within this spectral region.

## Seascapes as Integrated Water Quality Proxies in the FKNMS

We observed major shifts in seascape occupancy within the FKNMS boundaries throughout the study period that likely affected water quality and thermal conditions of benthic habitats of the Sanctuary. Changing seascape distributions were driven by seasonal shifts in ocean circulation, surface heat content and primary producer biomass measured as chl-a and nFLH. Seascape conditions in the study area could have also been affected by runoff from the Everglades into Florida Bay, the west Florida shelf, and deeper waters along the reef track of the Florida Straits.

Seascape dominance within the FKNMS varied significantly from March through September 2016 (**Figure 8**). During the March cruise  $\sim 30\%$  of FKNMS was occupied by the Florida Bay Cool seascape, which is characterized by water temperature of  $\sim 23^\circ\text{C}$ , moderate chl-a concentrations ( $< 1.5 \text{ mg m}^{-3}$ ), and elevated CDOM values ( $a_g \approx 0.3 \text{ m}^{-1}$ ) suggesting some level of freshwater input. However, discharge from the Everglades was low during this time, suggesting that CDOM in Florida Bay Cool seascape is possibly of autochthonous origin (**Figure 8**). The observed high CDOM concentrations could also be a lagged response from high discharge during January and February months in 2016. This class carries a mixture of phytoplankton of various size ranges, mostly cyanobacteria and some diatoms (**Figure 4**). This seascape covered seagrasses in nearshore areas and some portion of deeper waters, possibly affecting light and nutrient conditions of patch and fringe coral reefs on the southern edge of the FKNMS and around the Marquesas Keys.

In May, several classes were present in the FKNMS with comparable areal extent (**Figure 8**). Over 15% of the Sanctuary was bathed by Warm, Eutrophic, Optically Shallow seascape (class 16), which is largely dominated by diatoms. This class also has a high nFLH signal ( $\sim 0.2 \text{ mW cm}^{-2} \mu\text{m}^{-1} \text{ sr}^{-1}$ ; **Table 1**) indicative of bloom conditions in this region (Hu et al., 2005). Other seascapes with over 10% coverages also showed intermediate to high CDOM concentrations ( $a_g \approx 0.1\text{--}0.3 \text{ m}^{-1}$ ; **Supplementary Figure S3**), especially Florida Bay classes (14 and 15), suggesting a strong freshwater influence from the Everglades. Average discharge was slightly higher during this time compared to the previous cruise. Under these conditions optical depth and overall water quality conditions are likely sub-optimal for benthic organisms, with curtailed light availability during this time. Mixed seascape conditions also suggest exposure of benthic habitats to high variability of thermal conditions with possible impacts to metabolic performance of fishes and coral reefs in these areas. For example, a shift in seascapes from Florida Bay Cool to Florida Bay Warm (13 and 14) could lead to a temperature drop of as much as  $\sim 5^\circ\text{C}$ .

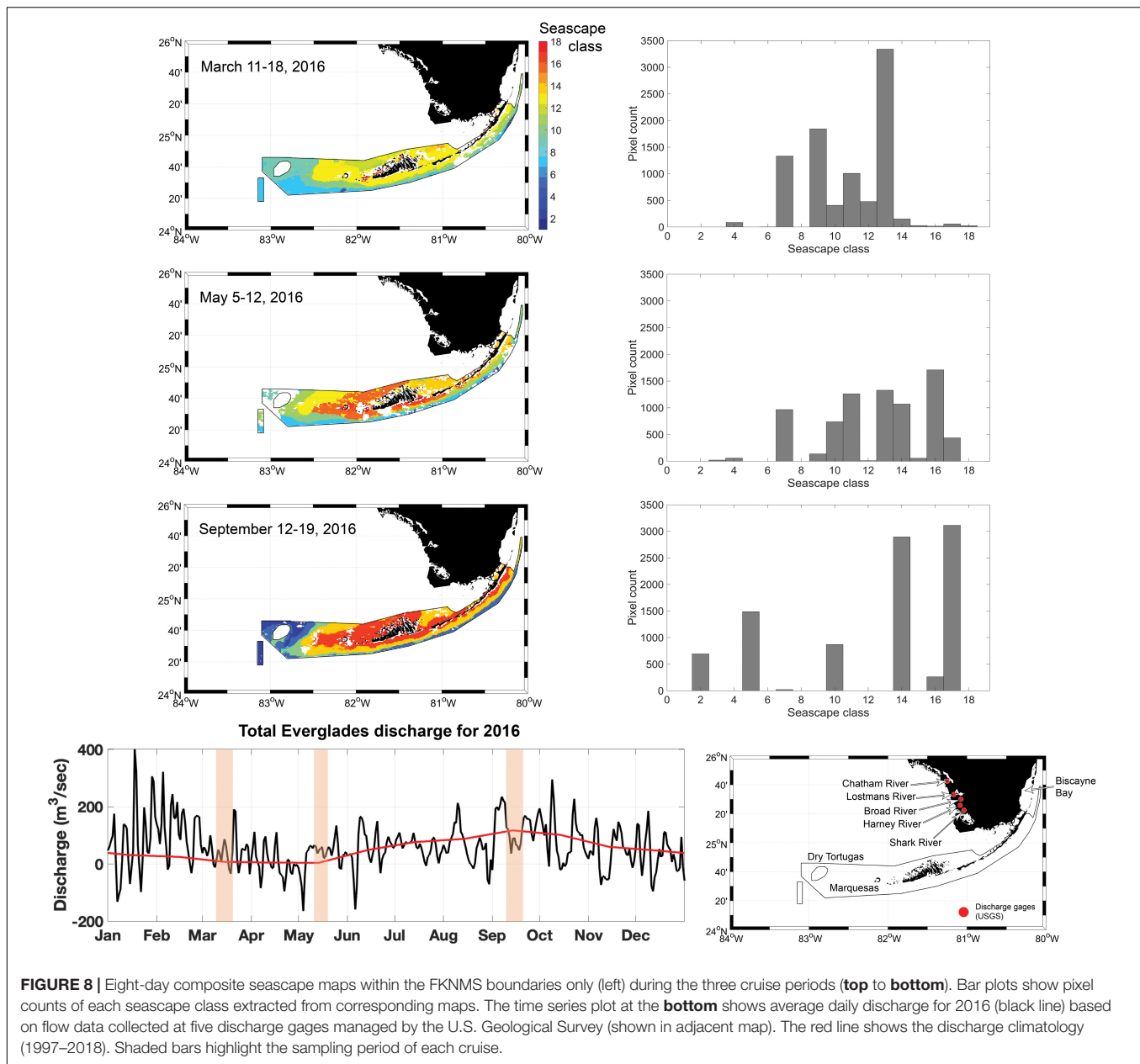
In September, over 50% of the Sanctuary was bathed by Summer, Nearshore, Optically Shallow (class 17) and Florida Bay Warm (class 14) seascapes, from the Upper Keys south

of Biscayne Bay through west of Marquesas Keys toward Dry Tortugas (**Figure 8**). These are very warm classes almost reaching  $29^\circ\text{C}$  and thus some level of thermal stress can be expected in shallow benthic habitats under sustained occupancy of these seascapes. Water quality conditions of these classes could also affect photosynthetic performance of benthic organisms due to high light attenuation by phytoplankton mainly dominated by micro- and nano-phytoplankton size classes ( $\sim 60\text{--}70\%$ ). These classes also carry high concentrations of non-algal particles that further attenuate light penetration through the water column (**Figure 6**). Furthermore, high levels of chl-a, nFLH, non-algal particles and CDOM in seascapes 14 and 17 are consistent with increased Everglades runoff during the 2 weeks prior to the cruise (**Figures 6, 8**). In deeper waters along the southern edge of the FKNMS, however, seascape conditions were indicative of low phytoplankton concentrations and thus high water clarity conditions. We observed significantly higher dominance of Very Warm, Very Oligotrophic (class 2) and Warm, Oligotrophic (class 5) seascapes not detected during the March or May cruises within the Sanctuary. When these classes occur over coral reefs and seagrasses, light availability may be higher but so is thermal stress with temperatures exceeding  $29^\circ\text{C}$ .

Penetration of Florida Bay, Nearshore, and Optically Shallow seascapes (classes 13 through 18) carrying elevated CDOM, non-algal particles and phytoplankton loads over the reef track and the Marquesas Keys likely results from the transfer of waters from Florida Bay and the West Florida Shelf through connecting channels. Outflow of these seascapes into the southern portion of the FKNMS makes benthic habitats particularly sensitive to intermittent sub-optimal water quality conditions. Based on satellite diffuse attenuation coefficient ( $K_d$ ) and remote sensing reflectance ( $R_{rs}$ ) anomalies Barnes et al. (2013, 2014) reported large shifts in water clarity in the Middle and Lower Keys possibly due to discharge from Florida Bay and the West Florida Shelf. Other studies suggest that degradation of seagrass beds and coral reefs in the FKNMS is likely driven by nutrient inputs from these areas, which in turn stimulate phytoplankton growth and thus poor light conditions over the reef track (Hu et al., 2004; Lapointe et al., 2004). However, long-term trends in nutrient concentration in waters bathing these benthic habitats are yet not clear due to observational limitations related to low sampling frequent and spatial coverage. Sediment resuspension and associated turbidity is possibly a major driver of water column light attenuation in the very shallow areas of Florida Bay and West Florida Shelf (Hall et al., 1999; Barnes et al., 2014). Therefore, dominance of lower water clarity seascapes can be expected along the western FKNMS during outflow events of water masses with high concentrations of non-algal particles from the northern portion of the Sanctuary (Stumpf et al., 1999).

Our results demonstrate that the seascape framework can be used to rapidly evaluate seasonal and high-frequency changes in water quality within a marine protected area (MPA) and its surroundings to examine their possible impacts on benthic habitats providing critical ecosystem services. Seascapes can help evaluate the extent to which water quality conditions change over time and space within and around MPAs, investigate why these are changing, and implement effective strategies for





conservation and management of living resources based on a coherent, spatially explicit and temporally dynamic, standardized synoptic approach.

## CONCLUSION

Seascapes serve as integrated environmental proxy indicators to examine impacts of various water quality conditions on benthic habitats and species populations, and therefore on fisheries and other relevant ecosystem services. Real-time tracking of seascape occupancy (e.g., shifts or persistence) can inform on the evolution of water quality and thermal properties in critical habitats in support of conservation and

management efforts. Seascape data can aid in establishing baseline oceanographic conditions at local to regional scales, including optically shallow areas, and determine how these change over time and space to better gauge the responses of species populations, ecosystem health, and overall biodiversity to environmental change. Seascape observations can also provide insights into dominant phytoplankton groups within water masses of different oceanographic conditions. In this study we found that phytoplankton communities characterized by *in situ* pigments and bio-optical measurements have a consistent association pattern with seascape classes. Our results indicate that oceanic seascapes are mainly occupied by small phytoplankton taxa such as *Synechococcus* spp. and *Prochlorococcus* sp. whereas more coastal seascapes are dominated larger groups like

diatoms and dinoflagellates. These observations can help track phytoplankton phenology, ecological connectivity, land-ocean interactions, and areas with transient or persistent exposure to runoff or circulation patterns to guide policy and marine spatial planning more effectively, better protect marine habitats, and sustainably use natural living resources.

## DATA AVAILABILITY STATEMENT

All pigment and bio-optical data are available on the NASA SeaWiFS Bio-optical Archive and Storage System (SeaBASS).

## AUTHOR CONTRIBUTIONS

AD contributed to statistical analysis for identifying relationships between seascape classes and phytoplankton communities. FM-K and CK contributed to field data, knowledge on underlying process controlling water quality in the Florida Keys, and ideas on conceptual framework for validation of seascapes. MK provided the seascape classification data for the study region and technical approaches for the seascape validation. All authors contributed to ideas and knowledge on experimental design, methodological approach, and interpretation of results.

## ACKNOWLEDGMENTS

This manuscript is a contribution to the Marine Biodiversity Observation Network (MBON) of the Group on Earth Observations Biodiversity Observation Network. The work was funded under the US National Ocean Partnership Program (NASA, NOAA, U.S. IOOS, BOEM, and ONR) through NASA grant NNX14AP62A [“National Marine Sanctuaries as Sentinel Sites for a Demonstration Marine Biodiversity Observation Network (MBON)”] and Department of the Navy Award NA19NOS0120199 [“Implementing a Marine Biodiversity Observation Network (MBON) in South Florida to Advance Ecosystem-Based Management”]. Additional support was provided by NSF Grant Number 1728913 [“Research

Coordination Networks (RCN): Sustained Multidisciplinary Ocean Observations” – the OceanObs RCN]. The manuscript is also a contribution to the Integrated Marine Biosphere Research (IMBeR) project, which is supported by the Scientific Committee on Oceanic Research (SCOR) and Future Earth. Mention of trade names or commercial products does not constitute endorsement or recommendation for use by the US Government. The views expressed in this article are those of the authors and do not necessarily reflect the views or policies of US Government Agencies.

## SUPPLEMENTARY MATERIAL

The Supplementary Material for this article can be found online at: <https://www.frontiersin.org/articles/10.3389/fmars.2020.00575/full#supplementary-material>

**FIGURE S1 |** Hierarchical cluster analysis derived from HPLC pigment ratios calculated as described in section “HPLC Pigment and CHEMTAX Analyses” of the Methods for the March, May, and September 2016 cruises (A–C), respectively. Main clusters are indicated with colors. Binning of the pigment data for CHEMTAX analysis was carried out according to the corresponding colored cluster. Dendrogram labels correspond to station ID’s shown in **Figure 1**.

**FIGURE S2 |** Relative abundance of phytoplankton groups derived from CHEMTAX analysis at sampled stations during March, May, and September 2016 cruises (A–C), respectively, and combined data (D). Dendrograms above stack plots are the same as in **Figure 3** for reference. Seascape class observed at each station is shown with color bars below stack plots. Station ID’s are as in **Figure 1**. Dashed rectangles highlight clustering of stations where Mesotrophic and Transition seascapes (classes 10 through 12; **Table 1**) are dominant classes.

**FIGURE S3 |** CDOM absorption ( $a_g$ ) at 443 nm measured at sampled sites during the March, May, and September 2016 cruises (A–C), respectively. Bar plot shows average  $a_g(443)$  in seascape classes 10 through 18 derived from combined data collected during these cruises. Error bars show standard error.

**FIGURE S4 |** Similarity matrices showing cophenetic correlation coefficients between dendrogram clusters derived from the second derivative of band-normalized phytoplankton absorption spectra [ $a_{phy}(\lambda)/a_{phy}(440)$ ] versus HPLC pigments (A–C) and seascape class (D–F). Absorption-based dendrograms were constructed using different combinations of spectral range and then compared to dendrograms derived from HPLC pigments or seascape class data. Lower and upper limits of spectral ranges are indicated in the Y and X axis, respectively, within 10 nm bins. Left, middle, and right panels correspond to data collected during March, May, and September 2016 cruises, respectively.

## REFERENCES

- Aiken, J., Pradhan, Y., Barlow, R., Lavender, S., Poulton, A., Holligan, P., et al. (2009). Phytoplankton pigments and functional types in the Atlantic Ocean: a decadal assessment, 1995–2005. *Deep Sea Res. Part II* 56, 899–917. doi: 10.1016/j.dsr.2008.09.017
- Alvain, S., Moulin, C., Dandonneau, Y., and Loisel, H. (2008). Seasonal distribution and succession of dominant phytoplankton groups in the global ocean: a satellite view. *Glob. Biogeochem. Cycles* 22. doi: 10.1029/2007GB003154
- Anouar, F., Badran, F., and Thiria, S. (1998). Probabilistic self-organizing map and radial basis function networks. *Neurocomputing* 20, 83–96. doi: 10.1016/S0925-2312(98)00026-25
- Araujo, M. L. V., Mendes, C. R. B., Tavano, V. M., Garcia, C. A. E., and Baringer, M. O. (2017). Contrasting patterns of phytoplankton pigments and chemotaxonomic groups along 30°S in the subtropical South Atlantic Ocean. *Deep Sea Res. Part I* 120, 112–121. doi: 10.1016/j.dsr.2016.12.004
- Barlow, R., Gibberd, M.-J., Lamont, T., Aiken, J., and Holligan, P. (2016). Chemotaxonomic phytoplankton patterns on the eastern boundary of the Atlantic Ocean. *Deep Sea Res. Part I* 111, 73–78. doi: 10.1016/j.dsr.2016.02.011
- Barnes, B. B., Hu, C., Holekamp, K. L., Blonski, S., Spiering, B. A., Palandro, D., et al. (2014). Use of Landsat data to track historical water quality changes in Florida Keys marine environments. *Remote Sens. Environ.* 140, 485–496. doi: 10.1016/j.rse.2013.09.020
- Barnes, B. B., Hu, C., Schaeffer, B. A., Lee, Z., Palandro, D. A., and Lehrter, J. C. (2013). MODIS-derived spatiotemporal water clarity patterns in optically shallow Florida Keys waters: a new approach to remove bottom contamination. *Remote Sens. Environ.* 134, 377–391. doi: 10.1016/j.rse.2013.03.016
- Bidigare, R. R. (1989). “Photosynthetic pigment composition of the brown tide alga: unique chlorophyll and carotenoid derivatives,” in *Novel Phytoplankton Blooms*, eds E. M. Cosper, V. M. Brice, and E. J. Carpenter (Berlin: Springer), 57–75. doi: 10.1007/978-3-642-75280-3\_4
- Boyce, D. G., Lewis, M. R., and Worm, B. (2010). Global phytoplankton decline over the past century. *Nature* 466, 591–596. doi: 10.1038/nature09268

- Boyd, P. W., and Doney, S. C. (2002). Modelling regional responses by marine pelagic ecosystems to global climate change. *Geophys. Res. Lett.* 29:53. doi: 10.1029/2001GL014130
- Brewin, R. J. W., Sathyendranath, S., Hirata, T., Lavender, S. J., Barciela, R. M., and Hardman-Mountford, N. J. (2010). A three-component model of phytoplankton size class for the Atlantic Ocean. *Ecol. Model.* 221, 1472–1483. doi: 10.1016/j.ecolmodel.2010.02.014
- Bricaud, A., and Stramski, D. (1990). Spectral absorption coefficients of living phytoplankton and nonalgal biogenous matter: a comparison between the Peru upwelling area and the Sargasso Sea. *Limnol. Oceanogr.* 35, 562–582. doi: 10.4319/lo.1990.35.3.0562
- Cannizzaro, J. P., Barnes, B. B., Hu, C., Corcoran, A. A., Hubbard, K. A., Muhlbach, E., et al. (2019). Remote detection of cyanobacteria blooms in an optically shallow subtropical lagoonal estuary using MODIS data. *Remote Sens. Environ.* 231:111227. doi: 10.1016/j.rse.2019.111227
- Catlett, D., and Siegel, D. A. (2018). Phytoplankton pigment communities can be modeled using unique relationships with spectral absorption signatures in a dynamic coastal environment: modeling pigment communities. *J. Geophys. Res. Oceans* 123, 246–264. doi: 10.1002/2017JC013195
- Chase, A., Boss, E., Zaneveld, R., Bricaud, A., Claustre, H., Ras, J., et al. (2013). Decomposition of in situ particulate absorption spectra. *Methods Oceanogr.* 7, 110–124. doi: 10.1016/j.mio.2014.02.002
- Chase, A. P., Boss, E., Cetinić, I., and Slade, W. (2017). Estimation of phytoplankton accessory pigments from hyperspectral reflectance spectra: toward a global algorithm. *J. Geophys. Res. Oceans* 122, 9725–9743. doi: 10.1002/2017JC012859
- Devred, E., Sathyendranath, S., and Platt, T. (2007). Delineation of ecological provinces using ocean colour radiometry. *Mar. Ecol. Prog. Ser.* 346, 1–13. doi: 10.3354/meps07149
- Duffy, J. E., Amaral-Zettler, L. A., Fautin, D. G., Paulay, G., Ryneerson, T. A., Sosik, H. M., et al. (2013). Envisioning a marine biodiversity observation network. *Bioscience* 63, 350–361. doi: 10.1525/bio.2013.63.5.8
- El Hourany, R., Abboud-Abi Saab, M., Faour, G., Aumont, O., Crépon, M., and Thiria, S. (2019a). Estimation of secondary phytoplankton pigments from satellite observations using self-organizing maps (SOMs). *J. Geophys. Res. Oceans* 124, 1357–1378. doi: 10.1029/2018JC014450
- El Hourany, R., Abboud-Abi Saab, M., Faour, G., Mejia, C., Crépon, M., and Thiria, S. (2019b). Phytoplankton diversity in the mediterranean sea from satellite data using self-organizing maps. *J. Geophys. Res. Oceans* 124, 5827–5843. doi: 10.1029/2019JC015131
- Falkowski, P., and Kiefer, D. A. (1985). Chlorophyll a fluorescence in phytoplankton: relationship to photosynthesis and biomass. *J. Plankton Res.* 7, 715–731. doi: 10.1093/plankt/7.5.715
- Friedland, K. D., Mouw, C. B., Asch, R. G., Ferreira, A. S. A., Henson, S., Hyde, K. J. W., et al. (2018). Phenology and time series trends of the dominant seasonal phytoplankton bloom across global scales. *Glob. Ecol. Biogeogr.* 27, 551–569. doi: 10.1111/geb.12717
- Game, E. T., Grantham, H. S., Hobday, A. J., Pressey, R. L., Lombard, A. T., Beckley, L. E., et al. (2009). Pelagic protected areas: the missing dimension in ocean conservation. *Trends Ecol. Evol.* 24, 360–369. doi: 10.1016/j.tree.2009.01.011
- Gibb, S. W., Barlow, R. G., Cummings, D. G., Rees, N. W., Trees, C. C., Holligan, P., et al. (2000). Surface phytoplankton pigment distributions in the Atlantic Ocean: an assessment of basin scale variability between 50°N and 50°S. *Prog. Oceanogr.* 45, 339–368. doi: 10.1016/S0079-6611(00)00007-0
- Hales, B., Strutton, P. G., Saraceno, M., Letelier, R., Takahashi, T., Feely, R., et al. (2012). Satellite-based prediction of pCO<sub>2</sub> in coastal waters of the eastern North Pacific. *Prog. Oceanogr.* 103, 1–15. doi: 10.1016/j.pocean.2012.03.001
- Hall, M. O., Durako, M. J., Fourqurean, J. W., and Ziemann, J. C. (1999). Decadal changes in seagrass distribution and abundance in Florida Bay. *Estuaries* 22, 445–459. doi: 10.2307/1353210
- Hardman-Mountford, N. J., Hirata, T., Richardson, K. A., and Aiken, J. (2008). An objective methodology for the classification of ecological pattern into biomes and provinces for the pelagic ocean. *Remote Sens. Environ.* 112, 3341–3352. doi: 10.1016/j.rse.2008.02.016
- Hays, G., Richardson, A., and Robinson, C. (2005). Climate change and marine plankton. *Trends Ecol. Evol.* 20, 337–344. doi: 10.1016/j.tree.2005.03.004
- Hazen, E. L., Jorgensen, S., Rykaczewski, R. R., Bograd, S. J., Foley, D. G., Jonsen, I. D., et al. (2013). Predicted habitat shifts of Pacific top predators in a changing climate. *Nat. Clim. Chang.* 3, 234–238. doi: 10.1038/nclimate1686
- Higgins, H. W., Wright, S. W., and Schlüter, L. (2011). “Quantitative interpretation of chemotaxonomic pigment data,” in *Phytoplankton Pigments*, eds S. Roy, C. Llewellyn, E. S. Egeland, and G. Johnsen (Cambridge: Cambridge University Press), 257–313. doi: 10.1017/CBO9780511732263.010
- Hirata, T., Hardman-Mountford, N. J., Brewin, R. J. W., Aiken, J., Barlow, R., Suzuki, K., et al. (2011). Synoptic relationships between surface Chlorophyll-a and diagnostic pigments specific to phytoplankton functional types. *Biogeosciences* 8, 311–327. doi: 10.5194/bg-8-311-2011
- Hooker, S. B., Van Heukelem, L., Thomas, C. S., Claustre, H., Ras, J., Barlow, R., et al. (2005). *The Second SeaWiFS HPLC Analysis Round-Robin Experiment (SeaHARRE-2)*. Washington, DC: NASA.
- Hu, C., Muller-Karger, F. E., Taylor, C., Carder, K. L., Kelble, C., Johns, E., et al. (2005). Red tide detection and tracing using MODIS fluorescence data: a regional example in SW Florida coastal waters. *Remote Sens. Environ.* 97, 311–321. doi: 10.1016/j.rse.2005.05.013
- Hu, C., Muller-Karger, F. E., Vargo, G. A., Neely, M. B., and Johns, E. (2004). Linkages between coastal runoff and the Florida Keys ecosystem: a study of a dark plume event. *Geophys. Res. Lett.* 31. doi: 10.1029/2004GL020382
- Irwin, A. J., Finkel, Z. V., Müller-Karger, F. E., and Troccoli Ghinaglia, L. (2015). Phytoplankton adapt to changing ocean environments. *Proc. Natl. Acad. Sci. U.S.A.* 112, 5762–5766. doi: 10.1073/pnas.1414752112
- Kavanaugh, M. T., Hales, B., Saraceno, M., Spitz, Y. H., White, A. E., and Letelier, R. M. (2014). Hierarchical and dynamic seascapes: a quantitative framework for scaling pelagic biogeochemistry and ecology. *Prog. Oceanogr.* 120, 291–304. doi: 10.1016/j.pocean.2013.10.013
- Kavanaugh, M. T., Oliver, M. J., Chavez, F. P., Letelier, R. M., Muller-Karger, F. E., and Doney, S. C. (2016). Seascapes as a new vernacular for pelagic ocean monitoring, management and conservation. *ICES J. Mar. Sci.* 73, 1839–1850. doi: 10.1093/icesjms/fsw086
- Kiefer, D. A. (1973). Fluorescence properties of natural phytoplankton populations. *Mar. Biol.* 22, 263–269. doi: 10.1007/BF00389180
- Kishino, M., Takahashi, M., Okami, N., and Ichimura, S. (1985). Estimation of the spectral absorption coefficients of phytoplankton in the sea. *Bull. Mar. Sci.* 37:9.
- Lapointe, B. E., Barile, P. J., and Matzie, W. R. (2004). Anthropogenic nutrient enrichment of seagrass and coral reef communities in the Lower Florida Keys: discrimination of local versus regional nitrogen sources. *J. Exp. Mar. Biol. Ecol.* 308, 23–58. doi: 10.1016/j.jembe.2004.01.019
- Lewis, R., Hobday, A. J., Maxwell, S., Hazen, E., Hartog, J. R., Dunn, D. C., et al. (2015). Dynamic ocean management: Identifying the critical ingredients of dynamic approaches to ocean resource management. *Bioscience* 65, 486–498. doi: 10.1093/biosci/biv018
- Longhurst, A. R. (1998). *Ecological Geography of the Sea*. Cambridge, MA: Academic Press.
- Lorenzoni, L., Toro-Farmer, G., Varela, R., Guzman, L., Rojas, J., Montes, E., et al. (2015). Characterization of phytoplankton variability in the Cariaco Basin using spectral absorption, taxonomic and pigment data. *Remote Sens. Environ.* 167, 259–268. doi: 10.1016/j.rse.2015.05.002
- Mackey, M., Mackey, D., Higgins, H., and Wright, S. (1996). CHEMTAX - a program for estimating class abundances from chemical markers: application to HPLC measurements of phytoplankton. *Mar. Ecol. Prog. Ser.* 144, 265–283. doi: 10.3354/meps144265
- McCune, B., Grace, J. B., and Urban, D. L. (2002). *Analysis of Ecological Communities*. Gleneden Beach, Oregon: MjM Software Design. Available online at: <https://trove.nla.gov.au/version/27016941> (accessed May 1, 2019).
- Mitchell, G., and Kiefer, D. A. (1988). Chlorophyll a specific absorption and fluorescence excitation spectra for light-limited phytoplankton. *Deep Sea Res.* 35, 639–663. doi: 10.1016/0198-0149(88)90024-6
- Mojica, K. D. A., Poll, W. H., van de Kehoe, M., Huisman, J., Timmermans, K. R., Buma, A. G. J., et al. (2015). Phytoplankton community structure in relation to vertical stratification along a north-south gradient in the Northeast Atlantic Ocean. *Limnol. Oceanogr.* 60, 1498–1521. doi: 10.1002/lno.10113
- Muller-Karger, F. E., Astor, Y. M., Benitez-Nelson, C. R., Buck, K. N., Fanning, K. A., Lorenzoni, L., et al. (2019). The scientific legacy of the CARIACO Ocean time-series program. *Annu. Rev. Mar. Sci.* 11, 413–437. doi: 10.1146/annurev-marine-010318-095150

- Muller-Karger, F. E., Kavanaugh, M. T., Montes, E., Balch, W. M., Breitbart, M., Chavez, F. P., et al. (2014). A framework for a marine biodiversity observing network within changing continental shelf seascapes. *Oceanography* 27, 18–23. doi: 10.5670/oceanog.2014.56
- Mutshinda, C. M., Troccoli-Ghinaglia, L., Finkel, Z. V., Müller-Karger, F. E., and Irwin, A. J. (2013). Environmental control of the dominant phytoplankton in the Cariaco Basin: a hierarchical Bayesian approach. *Mar. Biol. Res.* 9, 246–260. doi: 10.1080/17451000.2012.731693
- Nair, A., Sathyendranath, S., Platt, T., Morales, J., Stuart, V., Forget, M.-H., et al. (2008). Remote sensing of phytoplankton functional types. *Remote Sens. Environ.* 112, 3366–3375. doi: 10.1016/j.rse.2008.01.021
- Nunes, S., Latasa, M., Gasol, J. M., and Estrada, M. (2018). Seasonal and interannual variability of phytoplankton community structure in a Mediterranean coastal site. *Mar. Ecol. Prog. Ser.* 592, 57–75. doi: 10.3354/meps12493
- Oliver, M. J., and Irwin, A. J. (2008). Objective global ocean biogeographic provinces. *Geophys. Res. Lett.* 35:L15601. doi: 10.1029/2008GL034238
- Pinckney, J. L., Benitez-Nelson, C. R., Thunell, R. C., Muller-Karger, F., Lorenzoni, L., Troccoli, L., et al. (2015). Phytoplankton community structure and depth distribution changes in the Cariaco basin between 1996 and 2010. *Deep Sea Res. Part I* 101, 27–37. doi: 10.1016/j.dsr.2015.03.004
- Pinckney, J. L., Richardson, T. L., Millie, D. F., and Paerl, H. W. (2001). Application of photopigment biomarkers for quantifying microalgal community composition and in situ growth rates. *Org. Geochem.* 32, 585–595. doi: 10.1016/S0146-6380(00)00196-190
- Platt, T., and Sathyendranath, S. (1999). Spatial structure of pelagic ecosystem processes in the global ocean. *Ecosystems* 2, 384–394. doi: 10.1007/s100219900088
- Réve-Lamarche, A.-H., Alvain, S., Racault, M.-F., Dessailly, D., Guiselin, N., Jamet, C., et al. (2017). Estimation of the potential detection of diatom assemblages based on ocean color radiance anomalies in the north sea. *Front. Mar. Sci.* 4:408. doi: 10.3389/fmars.2017.00408
- Reygondeau, G., Longhurst, A., Martinez, E., Beaugrand, G., Antoine, D., and Maury, O. (2013). Dynamic biogeochemical provinces in the global ocean. *Glob. Biogeochem. Cycles* 27, 1046–1058. doi: 10.1002/gbc.20089
- Reynolds, R. A., and Stramski, D. (2019). Optical characterization of marine phytoplankton assemblages within surface waters of the western Arctic Ocean. *Limnol. Oceanogr.* 64, 2478–2496. doi: 10.1002/lno.11199
- Roesler, C. S., Perry, M. J., and Carder, K. L. (1989). Modeling in situ phytoplankton absorption from total absorption spectra in productive inland marine waters: modeling in situ absorption. *Limnol. Oceanogr.* 34, 1510–1523. doi: 10.4319/lo.1989.34.8.1510
- Saraceno, M., Provost, C., and Lebbah, M. (2006). Biophysical regions identification using an artificial neuronal network: a case study in the South Western Atlantic. *Adv. Space Res.* 37, 793–805. doi: 10.1016/j.asr.2005.11.005
- Stumpf, R. P., Frayer, M. L., Durako, M. J., and Brock, J. C. (1999). Variations in water clarity and bottom albedo in Florida Bay from 1985 to 1997. *Estuaries* 22:431. doi: 10.2307/1353209
- Taylor, B. B., Torrecilla, E., Bernhardt, A., Taylor, M. H., Peeken, I., Röttgers, R., et al. (2011). Bio-optical provinces in the eastern Atlantic Ocean and their biogeographical relevance. *Biogeosciences* 8, 3609–3629. doi: 10.5194/bg-8-3609-2011
- Torrecilla, E., Piera, J., and Vilaseca, M. (2009). “Derivative analysis of hyperspectral oceanographic data,” in *Advances in Geoscience and Remote Sensing*, ed. G. Jedlovec (London: IntechOpen), doi: 10.5772/8316
- Torrecilla, E., Stramski, D., Reynolds, R. A., Millán-Núñez, E., and Piera, J. (2011). Cluster analysis of hyperspectral optical data for discriminating phytoplankton pigment assemblages in the open ocean. *Remote Sens. Environ.* 115, 2578–2593. doi: 10.1016/j.rse.2011.05.014
- Turner, W., Spector, S., Gardiner, N., Fladeland, M., Sterling, E., and Steininger, M. (2003). Remote sensing for biodiversity science and conservation. *Trends Ecol. Evol.* 18, 306–314. doi: 10.1016/S0169-5347(03)00070-73
- Uitz, J., Claustre, H., Morel, A., and Hooker, S. B. (2006). Vertical distribution of phytoplankton communities in open ocean: an assessment based on surface chlorophyll. *J. Geophys. Res.* 111. doi: 10.1029/2005JC003207
- Ulrich, T. (2020). *Ternary Plots*. Available online at: <https://www.mathworks.com/matlabcentral/fileexchange/7210-ternary-plots> (accessed May 16, 2020).
- Vaillancourt, R. D., Lance, V. P., and Marra, J. F. (2018). Phytoplankton chemotaxonomy within contiguous optical layers across the western North Atlantic Ocean and its relationship to environmental parameters. *Deep Sea Res. Part I* 139, 14–26. doi: 10.1016/j.dsr.2018.05.007
- Van Heukelem, L., and Thomas, C. S. (2001). Computer-assisted high-performance liquid chromatography method development with applications to the isolation and analysis of phytoplankton pigments. *J. Chromatogr. A* 910, 31–49. doi: 10.1016/S0378-4347(00)00603-604
- Vidussi, F., Claustre, H., Manca, B. B., Luchetta, A., and Marty, J.-C. (2001). Phytoplankton pigment distribution in relation to upper thermocline circulation in the eastern Mediterranean Sea during winter. *J. Geophys. Res. Oceans* 106, 19939–19956. doi: 10.1029/1999JC000308
- Ward, J. H. (1963). Hierarchical grouping to optimize an objective function. *J. Am. Stat. Assoc.* 58, 236–244. doi: 10.1080/01621459.1963.10500845
- Werdell, P. J., Roesler, C. S., and Goes, J. I. (2014). Discrimination of phytoplankton functional groups using an ocean reflectance inversion model. *Appl. Opt.* 53, 4833–4849. doi: 10.1364/AO.53.004833
- Wright, S., Thomas, D., Marchant, H., Higgins, H., Mackey, M., and Mackey, D. (1996). Analysis of phytoplankton of the Australian sector of the Southern Ocean: comparisons of microscopy and size frequency data with interpretations of pigment HPLC data using the “CHEMTAX” matrix factorisation program. *Mar. Ecol. Prog. Ser.* 144, 285–298. doi: 10.3354/meps144285
- Wright, S. W., Ishikawa, A., Marchant, H. J., Davidson, A. T., van den Enden, R. L., and Nash, G. V. (2009). Composition and significance of picophytoplankton in Antarctic waters. *Polar Biol.* 32, 797–808. doi: 10.1007/s00300-009-0582-589
- Xi, H., Losa, S. N., Mangin, A., Soppa, M. A., Garnesson, P., Demaria, J., et al. (2020). Global retrieval of phytoplankton functional types based on empirical orthogonal functions using CMEMS GlobColour merged products and further extension to OLCI data. *Remote Sens. Environ.* 240:111704. doi: 10.1016/j.rse.2020.111704
- Xing, X.-G., Zhao, D.-Z., Liu, Y.-G., Yang, J.-H., Xiu, P., and Wang, L. (2007). An overview of remote sensing of chlorophyll fluorescence. *Ocean Sci. J.* 42, 49–59. doi: 10.1007/BF03020910
- Zhang, J.-Z. (2000). Shipboard automated determination of trace concentrations of nitrite and nitrate in oligotrophic water by gas-segmented continuous flow analysis with a liquid waveguide capillary flow cell. *Deep Sea Res. Part I* 47, 1157–1171. doi: 10.1016/S0967-0637(99)00085-80
- Zhang, J.-Z., and Berberian, G. A. (1997). Determination of Dissolved Silicate in Estuarine and Coastal Waters by Gas Segmented Continuous Flow Colorimetric Analysis. EPA Method 366.0. National Exposure Research Laboratory Office of Research and Development. Cincinnati, OH: U.S. Environmental Protection Agency.
- Zhang, J.-Z., Fischer, C. J., and Ortner, P. B. (2000). Continuous flow analysis of phosphate in natural waters using hydrazine as a reductant. *Intern. J. Environ. Anal. Chem.* 80, 61–73. doi: 10.1080/03067310108044386
- Zhang, J.-Z., Ortner, P. B., Fischer, C. J., and Moore, L. D. (1997). *Determination of Ammonia in Estuarine and Coastal Waters by Gas Segmented Continuous Flow Colorimetric Analysis. EPA Method 349.0. National Exposure Research Laboratory Office of Research and Development. Cincinnati, OH: U.S. Environmental Protection Agency.*

**Conflict of Interest:** The authors declare that the research was conducted in the absence of any commercial or financial relationships that could be construed as a potential conflict of interest.

Copyright © 2020 Montes, Djurhuus, Muller-Karger, Otis, Kelble and Kavanaugh. This is an open-access article distributed under the terms of the Creative Commons Attribution License (CC BY). The use, distribution or reproduction in other forums is permitted, provided the original author(s) and the copyright owner(s) are credited and that the original publication in this journal is cited, in accordance with accepted academic practice. No use, distribution or reproduction is permitted which does not comply with these terms.





## OPEN ACCESS

### Edited by:

Dominique Pelletier,  
Institut Français de Recherche pour  
l'Exploitation de la Mer (IFREMER),  
France

### Reviewed by:

Jan Marcin Weslawski,  
Polish Academy of Sciences, Poland  
Rodrigo Riera,  
University of Las Palmas de Gran  
Canaria, Spain

### \*Correspondence:

Edlin Guerra-Castro  
edlin.guerra@enesmerida.unam.mx  
Nuno Simoes  
ns@ciencias.unam.mx

### †ORCID:

Edlin Guerra-Castro  
orcid.org/0000-0003-3529-4507  
Gema Hidalgo  
orcid.org/0000-0002-3680-8410  
Raúl E. Castillo-Cupul  
orcid.org/0000-0002-9152-7988  
María Muciño-Reyes  
orcid.org/0000-0002-2343-8027  
Elsa Noreña-Barroso  
orcid.org/0000-0002-0800-1222  
Maite Mascaro  
orcid.org/0000-0003-3614-4383  
Nuno Simoes  
orcid.org/0000-0001-7490-3147

### Specialty section:

This article was submitted to  
Marine Ecosystem Ecology,  
a section of the journal  
Frontiers in Marine Science

**Received:** 31 July 2020

**Accepted:** 08 October 2020

**Published:** 29 October 2020

### Citation:

Guerra-Castro E, Hidalgo G,  
Castillo-Cupul RE, Muciño-Reyes M,  
Noreña-Barroso E,  
Quiroz-Deaquino J, Mascaro M and  
Simoes N (2020) Sandy Beach  
Macrofauna of Yucatán State (Mexico)  
and Oil Industry Development  
in the Gulf of Mexico: First Approach  
for Detecting Environmental Impacts.  
*Front. Mar. Sci.* 7:589656.  
doi: 10.3389/fmars.2020.589656

# Sandy Beach Macrofauna of Yucatán State (Mexico) and Oil Industry Development in the Gulf of Mexico: First Approach for Detecting Environmental Impacts

Edlin Guerra-Castro<sup>1,2\*†</sup>, Gema Hidalgo<sup>2,3†</sup>, Raúl E. Castillo-Cupul<sup>4†</sup>,  
María Muciño-Reyes<sup>5,6†</sup>, Elsa Noreña-Barroso<sup>2,7†</sup>, Jaime Quiroz-Deaquino<sup>5</sup>,  
Maite Mascaro<sup>2,5†</sup> and Nuno Simoes<sup>2,5,8\*†</sup>

<sup>1</sup> Escuela Nacional de Estudios Superiores Unidad Mérida, Universidad Nacional Autónoma de México, Mérida, Mexico,

<sup>2</sup> Laboratorio Nacional de Resiliencia Costera, Laboratorios Nacionales, CONACYT, Mexico City, Mexico, <sup>3</sup> Centro del Cambio Global y la Sustentabilidad A.C., Villahermosa, Mexico, <sup>4</sup> Kalanbio A.C., Mérida, Mexico, <sup>5</sup> Unidad Multidisciplinaria de Docencia e Investigación Sisal (UMDI-SISAL), Facultad de Ciencias, Universidad Nacional Autónoma de México, Sisal, Mexico, <sup>6</sup> Posgrado en Ciencias Biológicas, Universidad Nacional Autónoma de México, Ciudad de México, Mexico,

<sup>7</sup> Unidad de Química Sisal, Facultad de Química, Universidad Nacional Autónoma de México, Sisal, Mexico, <sup>8</sup> International Chair for Coastal and Marine Studies in Mexico, Harte Research Institute for Gulf of Mexico Studies, Texas A&M University-Corpus Christi, Corpus Christi, TX, United States

The biodiversity of the coastal ecosystems in the Gulf of Mexico is threatened by anthropogenic activities of various kinds. The predominant portion of the land-sea margin in the State of Yucatán consists of exposed sandy beaches. This ecosystem is threatened by several activities that vary in spatial scales, at a local: cargo/fishing ports, touristic facilities, maritime traffic, and domestic pollution; and at a larger scale: the forthcoming development of the oil industry. In the absence of information about the biodiversity of the beaches of Yucatán, we implement the Marine Biodiversity Observation Network (MBON) Pole to Pole sampling protocol to (1) Quantify the spatial patterns of diversity of macrofauna along the beaches; (2) quantify current levels of pollution by hydrocarbons (aromatic and aliphatic); (3) estimate sampling effort for future environmental impact assessments. During November 2018, six localities along the coastline of Yucatán State were sampled following a spatial hierarchical design that included three sites at each locality, and 9–18 core samples in the intertidal strata of each site. As a result, 31 species of invertebrates were registered. The patterns of distribution and abundance of species showed that there was a base community structure along the entire coast dominated by four species. In general, the density of species was relatively low (2–4 species/0.01 m<sup>3</sup>) and the density of individuals was high (20–200 ind./0.01 m<sup>3</sup>). The beta diversity was higher between localities with good environmental health, but the estimated alpha diversities did not show a pattern regarding the health of the coast. Lastly, the overall number of species reported suggest that gamma diversity of the macrofauna in the beaches of Yucatán is within the highest known worldwide. Levels of hydrocarbons detected in this study are exceptionally low compared to those reported for other coastal areas of the Gulf of Mexico and are several orders of magnitude lower



than those considered as lower-threshold values for marine sediments. The biological and chemical patterns reported here indicated that it is an appropriate moment to start long-term monitoring. The sampling design we suggest is based on statistical precision and internationally recognized protocols for assessment of marine diversity on sandy beaches.

**Keywords:** sandy beaches, macrobenthos sampling, hydrocarbon pollution, sampling design, environmental impact assessment, Gulf of Mexico, oil spill, Marine Biodiversity Observation Network

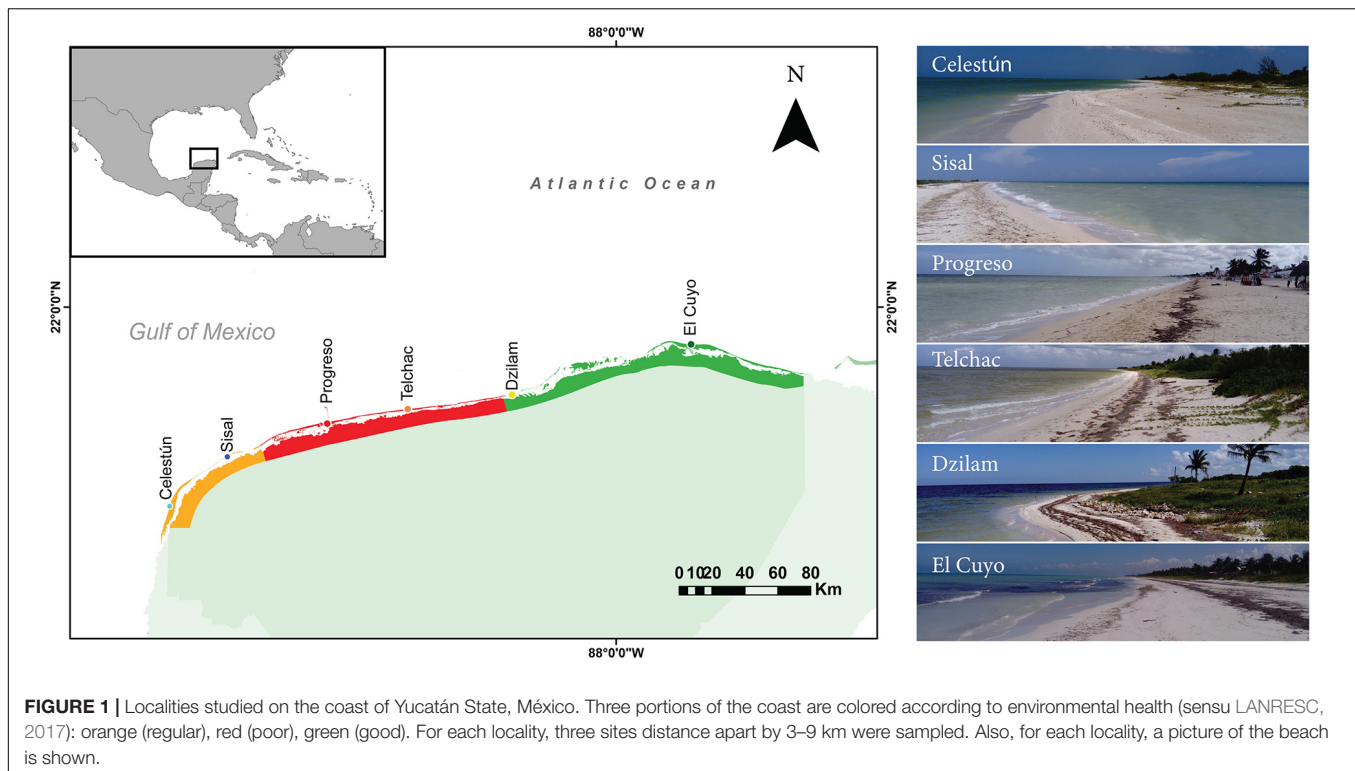
## INTRODUCTION

Biodiversity of the coastal ecosystems in the Gulf of Mexico is threatened by anthropic activities of various kinds (Peterson et al., 1996; Andrade, 2010; Joye, 2016). Especially on the Southern and North-western coast, the environmental impacts of oil exploitation and marine traffic stand out. In 2013, the Gulf of Mexico contributed with 54% of oil and 47% of the US production, whilst 75% of Mexico oil production comes from this area (National Ocean Service NOAA, 2011; Yoskowitz et al., 2013). In the same year, there were 3,095 oil & gas related offshore platforms in the northern GMx coast (United States), and 183 in the southern GMx coast (Mexico), with many more expected to be built due to the exploration of deeper fields within the US jurisdiction, and new areas in Mexico as a result of the recent energy reform in Mexico (SENER, 2015). Therefore, there is a historic track with many oil spill accidents, including two very large ones with enormous environmental consequences: the Ixtoc I by PEMEX (Bay of Campeche, 1979; see Sun et al., 2015), and the Deepwater Horizon (Delta of the Mississippi, 2010) by BP (Jernelov and Linden, 1981; Jernelov, 2010). Currently, no oil is extracted from the Yucatán platform, but that condition will change as foreseen in the 5-year Mexican plan for the exploration and extraction of hydrocarbons 2015–2019 (SENER, 2015). Of the 12 Oil Mexican Provinces recognized by the Mexican Hydrocarbons Commission, two are prone to generate environmental impacts on the coasts of the State of Yucatán. The first is the shallow water exploration area AS1012, with a coverage of 461 km<sup>2</sup>, located on the Yucatán platform, and whose reserves are estimated at 13.5 MMbpce (SENER, 2015). The second is the Deep Gulf of Mexico, which is the province with the greatest potential for exploitation of conventional resources, estimated at 27.8 MMbpce (SENER, 2015). Besides, it was recently announced the construction of a fuel terminal in the Puerto de Altura in Progreso (**Figure 1**), with a capacity to store 70 million liters of fuel. While all these activities will contribute to the economic development of the nation, they will also greatly increase the potential of environmental impacts of different magnitudes on regional marine biodiversity (Andrade, 2010; Pech Pool et al., 2010).

The coast of the Yucatán is characterized by its calcareous origin, without surface drainage, and consists mostly of dissipative beaches of low slope (Ramos, 1975). The coastal ecosystems include sandy beaches, mangrove forests, seagrass meadows, and reef archipelagos that increase the physiographic complexity and importance of the natural capital of the region. There has been an important scientific descriptive effort of

biodiversity and environmental characteristics of mangrove forests and coastal lagoons (Herrera-Silveira et al., 1998; Tapia González et al., 2008), as well as reef archipelagos of this region (González-Muñoz et al., 2013; Ortigosa et al., 2015; Ugalde et al., 2015; Mendoza-Becerril et al., 2018; Palomino-Alvarez et al., 2019; Paz-Ríos et al., 2019, 2020; Robertson et al., 2019); however, the biodiversity of the beaches has been little studied. Sandy beaches represent around 286 km (86%) of coastline in the State of Yucatán. These beaches are critical habitats for shorebirds (Arturo Lopez et al., 1989), turtles (Cuevas et al., 2010), as well as dune vegetation along the entire coast (Espejel, 1984; Islebe et al., 2015). They also support diverse touristic activities, especially important for the local economy (Meyer-Arendt, 2001; Cuevas Jiménez et al., 2016). Due to its extension, it is the one that presents the greatest probability of being negatively impacted by the potential accidents of the oil & gas industry in the Yucatán platform.

In general, impacts generated by the oil & gas industry in coastal ecosystems imply loss and long-term modification of local biodiversity (Teal and Howarth, 1984; Kingston, 2002). The effects of oil spills on the biodiversity of sandy beaches have strongly depended on the magnitude of the spill, on the granulometric properties of the beaches and the persistence of oil in the sediment (Bejarano and Michel, 2016). Estimating these effects requires a good understanding of the patterns of spatial and temporal variation that naturally occur on sandy beaches. Likewise, to identify the level of resilience of the ecosystem (i.e., biological recovery), it will be essential to know the system well before the disturbance, and this implies estimating the spatiotemporal variation of its ecological components at different spatial and temporal scales (Underwood, 1991; Cruz-Motta et al., 2007; Bejarano and Michel, 2016). The information necessary to detect environmental impacts of this nature arises from the so-called “Baseline Studies,” framed within the “Environmental Impact Assessment approach” (Mareddy, 2017). However, the vast majority of these studies have transcendental failures in the sampling designs, some of them are: (a) the measured impact indicator variables are inadequate (e.g., Shannon index of diversity), (b) the sampling start shortly before the project execution process (e.g., few weeks before the start of the operations), (c) there are not reference localities and, (d) the sample size is not representative of the natural variability (e.g., usually three-five samples per site), resulting in statistical tests of low power (Underwood and Chapman, 2003). Consequently, there is rarely enough solid information to unequivocally indicate the existence of an environmental impact (Bulleri et al., 2007; Cruz-Motta et al., 2007), this is particularly remarkable



in post-impact environmental assessments on polluted sandy beaches (Schlacher et al., 2008; Bejarano and Michel, 2016).

Sandy beaches provide several ecosystem services to society, but they are threatened by various human activities (Schlacher et al., 2008; Defeo et al., 2009; Rodríguez-Revelo et al., 2018; Martínez et al., 2020). In general, some of the recognized anthropogenic threats with the greatest risk on beaches are surface physiographic removal, microbial biohazards, introduced technological hazards, chronic chemical hazards, and chronic geopolitical hazards (Fanini et al., 2020). The risk associated with oil spills is considered lower than those mentioned (Fanini et al., 2020), although they have the potential to generate mass mortalities and drastically reduce the quality of habitats for several years (Bejarano and Michel, 2016). Unfortunately, this habitat has been ignored in long term ecological surveys. There is a global need to measure beaches' resilience to short (pulse) and long (press) term perturbations and increased demand for information from less-represented areas, including beach morphodynamics, pollution, ecological and socio-economic indicators, to undertake comprehensive and long-term impact assessments (Fanini et al., 2020; Thom, 2020).

Although there are significant efforts to compare spatiotemporal patterns of diversity in these ecosystems on a global scale (Defeo and McLachlan, 2005, 2013; McLachlan and Dorvlo, 2005; Rodil et al., 2014; Barboza and Defeo, 2015), a lack of standardized methodologies for this very dynamic environment, with huge variation in geological history, tide range, sediment texture, slope, and exposition to waves, make comparisons of spatial patterns a big challenge, compromising the forecasting of future ecological scenarios and management

activities. To overcome this limitation, some workshops have been held to develop sampling protocols that allow the comparison of results in regional contexts (Schlacher et al., 2008; Canonico et al., 2019). To attend this, the Marine Biodiversity Observation Network - Pole to Pole of the Americas (MBON Pole to Pole) promoted the design of a standardized sampling protocol for sandy beaches that allows obtaining comparable information on all continental coasts (MBON Pole to Pole, Pole, 2019). This protocol was recognized as an *OceanBestPractice* initiative of UNESCO/IODE<sup>1</sup>.

Considering the imminent development of oil and gas exploration and production activities on the Yucatán platform, as well as the background of environmental impact in other nearby regions of the Gulf of Mexico, it is predictable the potential generation of negative impacts on the biodiversity of the coastal ecosystems of the State of Yucatán, mainly its beaches. In this sense, a baseline study with biological indicators at different spatial scales, which allows detecting non-natural changes in the biological component, as well as the potential chemical mechanisms that may cause any loss or alteration of biodiversity, are required. To help address this need, this study presents an extensive pilot data, with biological and chemical variables, as a first baseline data set of the region, as well as a quantitative description of the patterns of diversity of macrofauna and pollutants in the Yucatán Peninsula, using the MBON Pole to Pole sampling protocol. Finally, we make recommendations regarding the sampling effort necessary for future environmental assessment.

<sup>1</sup><https://repository.oceanbestpractices.org/handle/11329/1142>

## MATERIALS AND METHODS

### Study Area

Sampling was carried out in November 2018 on six localities (distance apart by 50 km or more) of the windward side of the Yucatán peninsula; from west to east: Celestún, Sisal, Progreso, Telchac, Dzilam and El Cuyo (**Table 1** and **Figure 1**). The entire littoral is characterized by being microtidal, sea breeze dominated with a dissipative profile, low slopes, and medium to coarse sands (Appendini et al., 2012; Medellín and Torres-Freyermuth, 2019). In general, the region is karstic, with no superficial rivers or estuaries, but with well-developed mangrove forests surrounding coastal lagoons that are strongly influenced by groundwater discharges (Herrera-Silveira et al., 1998; Tapia González et al., 2008). These coastal lagoons are connected with the sea in several zones along the littoral, being the source of hipohaline waters with a high concentration of dissolved inorganic nutrients, especially in the rainy season. Trade winds tend to dominate in spring and summer, but in autumn and winter, the pattern changes with recurrent cold fronts from the north, with increased macrophyte wrack deposition (Enriquez et al., 2010; Medellín and Torres-Freyermuth, 2019). The current environmental health of the coast was assessed in 2017 by an interdisciplinary panel (LANRESC, 2017), resulting in three heterogeneous coastal segments. The portion of the coast between Celestún and Sisal is recognized as an area with regular environmental health; then, beyond Sisal until Dzilam, including Progreso and Telchac, it is a region classified with areas with poor environmental health; finally, Dzilam and El Cuyo stand out for presenting good environmental health (**Table 1** and **Figure 1**).

### Sampling Protocol

The sampling design included three spatial scales: tens of kilometers (localities), few kilometers (sites), few meters (cores). At each locality, three sites (separated by 3–9 kilometers) were sampled. None of the sites was less than 2 km from the mouth of any coastal lagoon or estuary. We applied the first version of the MBON P2P sampling methodology for sandy beaches, inspired in recommendations by Schlacher et al. (2008). At each site (a.k.a. sampling station), three transects (separated by 10 m) were displayed perpendicularly to the coastline. Along each transect, a sample of sand was collected each meter, starting from the waterline to the drift line (measured in all cases with a tape measure), this protocol ensures collecting samples from the infra, meso, and supralittoral. The fauna was collected with a core of 22 cm in diameter, which was inserted between 20 and 25 cm inside the sediment, representing 0.038 m<sup>2</sup> of area or 0.01 m<sup>3</sup> of volume. The tidal strata (infra, meso, supra), as well as the depth of the core, were annotated for each sample core. The samples were transferred fresh to the laboratory for immediate processing. In addition to biological samples, four sediment samples were taken at one randomly chosen site of each locality to estimate the concentration of aliphatic and aromatic hydrocarbons, as well as for granulometric analysis. These samples were taken at the meso littoral zone using the same core used for biological sampling.

### Laboratory Protocols

#### Biological Samples

Samples were sieved with a 0.5 mm mesh opening, and the retained organisms were photographed alive and subsequently fixed in a 4% solution of neutralized formaldehyde with sodium tetraborate. Organisms were identified to the lowest possible

**TABLE 1** | Names of localities sampled along the coast of Yucatán.

Locality	Site	Latitude	Longitude	Environmental health	Beach width (m)	Intertidal zone width (m)
Celestún	1	20°51'44	90°23'45	Regular	50	4
Celestún	2	20°53'45	90°23'16	Regular	11	5
Celestún	3	20°56'02	90°22'30	Regular	16	4
Sisal	1	21°9'34	90°4'23	Regular	24	4
Sisal	2	21°10'23	90°1'52	Regular	24	4
Sisal	3	21°11'4	89°58'44	Regular	10	5
Progreso	1	21°17'05	89°40'33	Poor	10	5
Progreso	2	21°17'19	89°39'27	Poor	18	4
Progreso	3	21°17'39	89°37'02	Poor	7	3
Telchac Puerto	1	21°20'32	89°16'48	Poor	14	6
Telchac Puerto	2	21°20'41	89°15'09	Poor	10	5
Telchac Puerto	3	21°20'54	89°13'15	Poor	9	5
Dzilam	1	21°32'47	88°29'01	Good	2	1
Dzilam	2	21°25'14	88°46'57	Good	6	3
Dzilam	3	21°22'53	88°57'35	Good	4	2
El Cuyo	1	21°33'02	87°48'36	Good	47	7
El Cuyo	2	21°30'55	87°40'08	Good	18	8
El Cuyo	3	21°29'23	87°32'36	Good	6	5

Geographical coordinates, current environmental health status (*sensu* LANRESC, 2017), beach width (Distance in meters between dune crest and the lower limit of swash on beach face), and intertidal zone width (distance between the drift line and the swash lower limit) of each site.



taxonomic level and counted. The specimens were deposited in the biological collection of the UMDI-Sisal, UNAM. Also, a database was built using the standard Darwin Core (Darwin Core Task Group, 2009)<sup>2</sup>. This database is available from the Global Biodiversity Information Facility<sup>3</sup> and visible on the Ocean Biodiversity Observation Network<sup>4</sup>. Alternatively, all the data can be accessed at Zenodo (DOI: 10.5281/zenodo.3771828) (Guerra-Castro et al., 2019).

## Sand Samples

Sediment samples collected for hydrocarbon determination were kept frozen at  $-20^{\circ}\text{C}$  and then freeze-dried and passed through a 500  $\mu\text{m}$  sieve. Concentrations of aliphatic and aromatic hydrocarbons in sediment (15 of the 16 PAHs considered as priorities by the US Environmental Protection Agency, EPA) were determined based on modifications of EPA methods 3550C, 3535 and 8270D (US EPA, 2007a,b,c). For each sample, 6 g of lyophilized sediment were extracted twice by ultrasound-assisted extraction (USE) with 12 mL hexane:acetone (1:1, v/v) using an ultrasonic processor (Cole Palmer CPX500) at 60% amplitude over 2 min. After each extraction, the organic phase was separated by centrifugation (5,000 rpm for 10 min). Extracts were mixed, treated with activated copper to remove sulfur, and concentrated using a rotary-evaporator. Hydrocarbon fractions were obtained from extracts by solid-phase extraction (SPE) using C-18 500 mg/6mL cartridges (Supelclean ENVI-18, 57064, Supelco). Cartridges were conditioned with 10 mL of hexane, sample extracts were passed by gravity flow and then eluted with 10 mL of hexane to obtain the aliphatic fraction, and 5 mL of hexane:dichloromethane (7:3, v/v) followed by 5 mL of dichloromethane to recover the PAH fraction. Fractions were evaporated using a gentle nitrogen flow and individual hydrocarbons were determined by gas chromatography/mass spectrometry (GC-MS), using a gas chromatograph coupled to a mass selective detector operated in electron impact (EI) ionization mode and equipped with an automatic liquid sampler (Agilent Technologies 7890B Series GC; 5977B MSD and 7693A Autoinjector, respectively). The injection was carried out in split-less mode (1 min) at  $280^{\circ}\text{C}$ . Chromatographic separation was performed using a J&W HP-5MS capillary column (30 m  $\times$  0.25 mm I.D. and 0.25  $\mu\text{m}$  of film thickness). Carrier gas was He (ultra-pure grade) with a flow rate of 0.8 mL/min; oven temperature was initially set at  $60^{\circ}\text{C}$ , then increased  $6^{\circ}\text{C}/\text{min}$  to  $290^{\circ}\text{C}$  (hold time 11.67 min). Mass spectra ( $m/z$  50–550) were recorded at a rate of five scans per second at 70 eV. Mass spectrometric analysis for quantitative determination was performed by selected ion monitoring (SIM Mode) of two characteristic fragment ions for each analyte (Supplementary Table 1). Analytical quality control included procedural blanks, calibration curves, and internal standards. The aliphatic hydrocarbon detection limit was 0.5 ng/g and PAH detection limits ranged from 0.09 to 0.79 ng/g. Particle

size analyzes were done with conventional sieving methods (Keith, 1996).

## Analyses of Data

### Patterns of Species Diversity

We evaluated patterns of spatial variation for four features of intertidal macrofauna diversity: (1) structure of the assemblages, (2) patterns of density of species and abundance of organisms (3) beta diversity, and (4) alpha and gamma diversity. For the structure of the assemblages, the counts of each species were arranged in an  $N \times P$  matrix, with  $N$  being the total number of samples and  $P$  being the number of species. This matrix was transformed into the natural logarithms (plus 1) to downweigh the effect of highly abundant species. Then, the Bray-Curtis coefficient of dissimilarity was estimated between each pair of samples, generating a matrix of dissimilarities that was used for statistical analyses and ordination. The total variation of this matrix was decomposed with a multifactorial linear model using Permutational Multivariate Analysis of Variance (Anderson, 2017). In the model, the main sources of variation were: Localities (fixed factor with six levels: Celestún, Sisal, Progreso, Telchac, Dzilam, and El Cuyo), Sites (random factor, nested in localities, three levels: site 1, site 2, site 3) and Strata (fixed factor, three levels: infra, meso, supra). The null hypotheses were generated using 9,999 permutations of residuals under the reduced model (Anderson and Ter Braak, 2003). The relative importance of each spatial scale (tens of km, few km, few m) were identified as the relativized square root of the *pseudo*-component of variation of Localities, Sites, and residuals in the model. Then, to visualize the pattern of similarity among localities, centroids for each locality-site-strata were estimated and projected with a non-metric MDS. Patterns of distribution and abundance of species along the coast were identified with an ordered shade plot using constrained seriation of most similar species in its spatial distribution regarding the locality (Clarke et al., 2014b). Variability in the density of species and abundance (i.e., number of species per sampling core, and the number of individuals per sample core, respectively), were analyzed using the same linear model for the structure of the assemblage but with univariate analysis of variance based on permutations. Both variables were analyzed without any transformation and using 9,999 permutations of residuals under the reduced model. Patterns of spatial trends in the density of species and abundance were summarized and represented using mean ( $\pm\text{SD}$ ) plots. All these analyses were done using the software PRIMER v7 & PERMANOVA (Clarke et al., 2014a).

For beta diversity, we explore the relationship between the Jaccard dissimilarities in species composition along the coast of Yucatán (approach T3 sensu Anderson et al., 2010) and the partitioning proposed by Baselga (2010). To identify the proportion of species replacement and species loss along the coast, the Jaccard dissimilarities among sites were estimated and partitioned in their components of turnover/nestedness and correlated with the geographic distances among sites using the rank-based Spearman coefficient of correlation. The null hypothesis of no spatial autocorrelation was tested using 9,999

<sup>2</sup><https://dwc.tdwg.org/>

<sup>3</sup><https://www.gbif.org/en/>

<sup>4</sup><https://obis.org/dataset/5700fdc3-956f-4e33-903b-e66ba38d980c>

permutations. These analyses were done with the statistical software R (R Core Team, 2013) using the packages betapart (Baselga and Orme, 2012) and vegan (Oksanen et al., 2015).

Alfa diversity was associated with the potential number of species per locality, while gamma diversity as the potential number of species along the coast of Yucatán. In both cases, we use species accumulation curves with interpolation-extrapolation of Hill Numbers and the incidence-based non-parametric estimator Chao2 (Chao and Jost, 2012). Considering that the number of sampling was not the same in all localities, we also estimate the sample completeness for each one, this measure allows us to infer the representativeness of the sampling effort at each locality. The interpolation of completeness was used to compare the local richness for a common completeness value of 0.9 (Chao et al., 2009; Chao and Jost, 2012). The analyses were done with the statistical software R (R Core Team, 2013) using the package iNEXT (Hsieh et al., 2016).

### Patterns of Hydrocarbons Pollution and Environmental Variation

Individual concentrations that were less than the limits of detection were assigned a value of zero for statistical estimations. Concentrations of PAHs were classified and summed according to the number of rings of each molecule (i.e., 2–3 rings, 4 rings, 5–6 rings), and then totalized ( $\Sigma$ PAHs). Similarly, aliphatic hydrocarbons were classified and summed according to the molecular structure (odd and even carbon number) and summed as total ( $\Sigma$ n-alkanes). To identify the potential source of aliphatic compounds, the Carbon Preference Index (CPI) was estimated as:

$$\frac{\sum \text{odd carbon number } n - \text{alkanes}}{\sum \text{even carbon number } n - \text{alkanes}}$$

where values greater than 1 indicate natural sources, while values lesser than 1 indicate anthropogenic sources (Marzi et al., 1993). Then, patterns of spatial heterogeneity in PAHs and n-alkanes were visualized using standard statistical representations of totals and the respective fraction of classified molecules. Besides, the null hypothesis of equal concentrations of these molecules between localities was tested using multivariate analyses. For this, data was transformed to a common scale (centered in mean zero with variance unit, aka normalization), then, a matrix of Euclidean distances was estimated, and total variation partitioned using a one-way permutational analysis of variances. For this, 9999 permutations of raw data were used to generate the null distribution of *pseudo-F* values.

### Sampling Effort for Future Assessments

The criterion for redefining sampling effort was the optimization of precision, that is, estimating the number of samples to improve the precision in the estimates of variability in assemblage structure and concentration of hydrocarbons at a reasonable cost, in terms of the number of samples at each locality. For this, we use data of this study as pilot data. For changes in the structure of the assemblages, multivariate standard error (*MultSE*) (Anderson and Santana-Garcon, 2015) were analyzed for several sampling efforts using simulations of data and the R package SSP (Guerra-Castro et al., 2020). For each stratum at each locality, 20 virtual

sites were simulated, each one with  $N = 100$  potential sample cores. Resampling were done for each combination of  $n = 2$  to  $n = 20$  and sites  $m = 2$  to  $m = 20$ . For each combination of  $n$  and  $m$ , *MultSE* was estimated; this estimation was repeated 10 times. All these processes were repeated for 10 simulated data sets. Then, a metanalysis about the behavior *MultSE* for each sampling effort was done projecting the *MultSe* – *sampling effort* relationship. The optimal sampling effort was defined as the range in which an additional sampling unit improves the worst precision by 10%, but not beyond 2.5%. Beyond this point, it was considered unnecessary sampling efforts. For pollutants, we used the equation  $n = [s / (p\bar{x})]^2$ , being  $n$  the sampling effort,  $s$  the standard deviation,  $\bar{x}$  de arithmetic mean of the sample, and  $p$  a standardized precision (i.e., 0.2) (Andrew and Mapstone, 1987). The variables used for these estimations were  $\Sigma$ PAHs and  $\Sigma$ n-alkanes, and the estimations were done for each locality. The codes for these analyses are available as **Supplementary Material**.

## RESULTS

### Patterns of Species Diversity

A total of 31 taxa/species were registered in 225 core samples, of which 15 were arthropods (13 crustaceans), 10 annelids (mainly polychaetes), 4 mollusks, and 2 bryozoans. The list of species (including main biological traits) is available in **Supplementary Table 2**, and the spatial distribution of each species can be visualized at OBIS (Guerra-Castro, 2019) and accessed at Zenodo (Guerra-Castro et al., 2019). Significant statistical differences in the structure of the assemblage were detected in all the spatial scales (**Table 2A**,  $p$ -values  $< 0.05$ ). The potential effect of the zone (i.e., littoral strata) varied among sites (**Table 2A**, interaction term Strata x Site (Locality) with  $p$ -value  $< 0.05$ ). The largest source of variation was the residuals: cores of the same littoral strata in the same site. This source of variation was about 34% in Bray Curtis dissimilarity and about 44% of the total variation. The second source of variation was the difference among localities (square root of components of variation 22% of Bray-Curtis dissimilarity), followed by variability among sites (18%) and difference among littoral strata (13%). El Cuyo and Dzilam were the most different localities (**Figure 2**), the rest of the localities were more similar between them but different from El Cuyo and Dzilam (**Figure 2**). Despite these differences, it can be noted that all sites present a community structure with the same four dominant species: the polychaete *Polyophthalmus pictus*, the oligochaete *Tubificoides diazi*, and the isopods *Excirrolana mayana* and *E. braziliensis* (**Figure 3**). In general, differences among localities were explained by a pool of 4–7 species confined to each locality (**Figure 3**). Regarding beta diversity, the total multi-site Jaccard dissimilarity was 0.91, indicating that only 9% of species were shared across all sites. In general, the turnover component was considerably higher (0.87) than the nestedness component (0.04). This spatial pattern of dissimilarities was weakly correlated with spatial distances ( $\rho = 0.26$ ,  $p < 0.001$ ).

The density of species, as well as the density of individuals, were statistically significant at the scale of locality (**Tables 2B,C**,



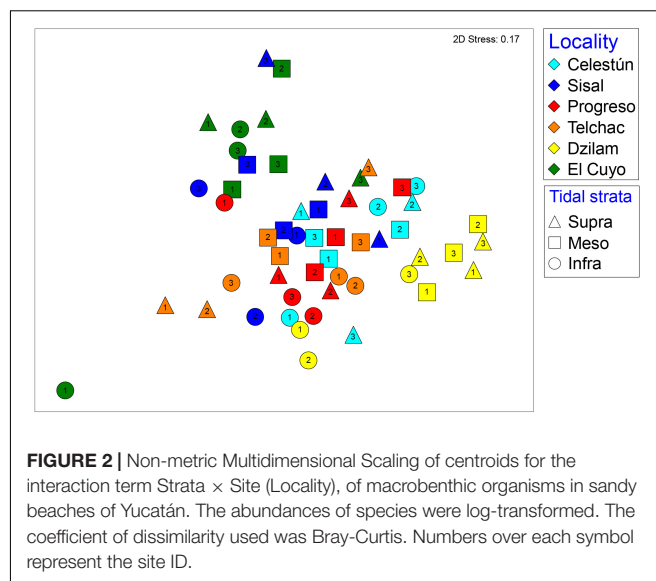
**TABLE 2 |** Permutational Analyses of Variances to evaluate spatial patterns of variability in the structure of intertidal macrofauna in sandy beaches of Yucatán, according to a multifactorial linear model that includes locality (L), site (S) and littoral strata (St).

<b>A</b>						
Source	df	MS	Pseudo-F	P (perm)	$\sqrt{CV}$	%CV
Strata	2	11807	4.86	0.0001	13	6
Locality	5	18273	4.37	0.0002	22	19
Site (L)	12	4221	3.75	0.0001	18	13
St × L	10	3042	1.24	0.1436	8	2
St × S (L)	24	2489	2.21	0.0001	20	15
Residuals	171	1126			34	44
Total	224					
<b>B</b>						
Source	df	MS	Pseudo-F	P (perm)	$\sqrt{CV}$	%CV
Strata	2	4.9	1.79	0.1780	0.2	2
Locality	5	12.4	5.58	0.0190	0.6	16
Site (L)	12	2.2	1.88	0.0450	0.3	5
St × L	10	3.9	1.40	0.2480	0.3	5
St × S (L)	24	2.8	2.38	0.0010	0.7	21
Residuals	171	1.2			1.1	52
Total	224					100
<b>C</b>						
Source	df	MS	Pseudo-F	P (perm)	$\sqrt{CV}$	%CV
Strata	2	8856	0.44	0.6440	0	0
Locality	5	124380	7.62	0.0070	61	20
Site (L)	12	16360	1.30	0.2480	20	2
St × L	10	11435	0.56	0.8260	0	0
St × S (L)	24	20646	1.65	0.1400	48	12
Residuals	171	12540			112	66
Total	224					100

(A) Structure of assemblages using Bray-Curtis dissimilarities over natural logarithms (+1) of abundances, (B) Density of species per core, (C) Density of individuals per core. The square root of the components of variation, as well as their relative importance, are presented.

factor Locality with  $p$ -values  $<0.05$ ). These metrics were higher in Dzilam (Figure 4), specifically, the average richness per core was around 4 species, while the density was very variable but always over 100 individuals, with a mean around 200 individuals. In the other localities, the density of species averaged between 2 and 3, and the number of individuals averaged between 25 and 50 individuals. The effect of strata was significant for the density of species, but such effect was variable among sites of the same locality (Table 2B, interaction term Strata × Site (Locality) with  $p$ -value  $<0.05$ ). No statistical variability in the density of individuals was detected among sites, neither difference between littoral strata.

The localities with higher richness registered were Dzilam and El Cuyo, with 15 species each. Paradoxically, Dzilam was the locality with the smallest number of samples (26 cores, due to the narrow littoral zone), while El Cuyo was the locality with a larger sampling effort (44 cores). On the other hand, the localities with the lower richness of species were Celestún and Progreso, both with 9 species (Figure 5A). Between these extremes of diversity, Telchac and Sisal account for 12 and 13 species,

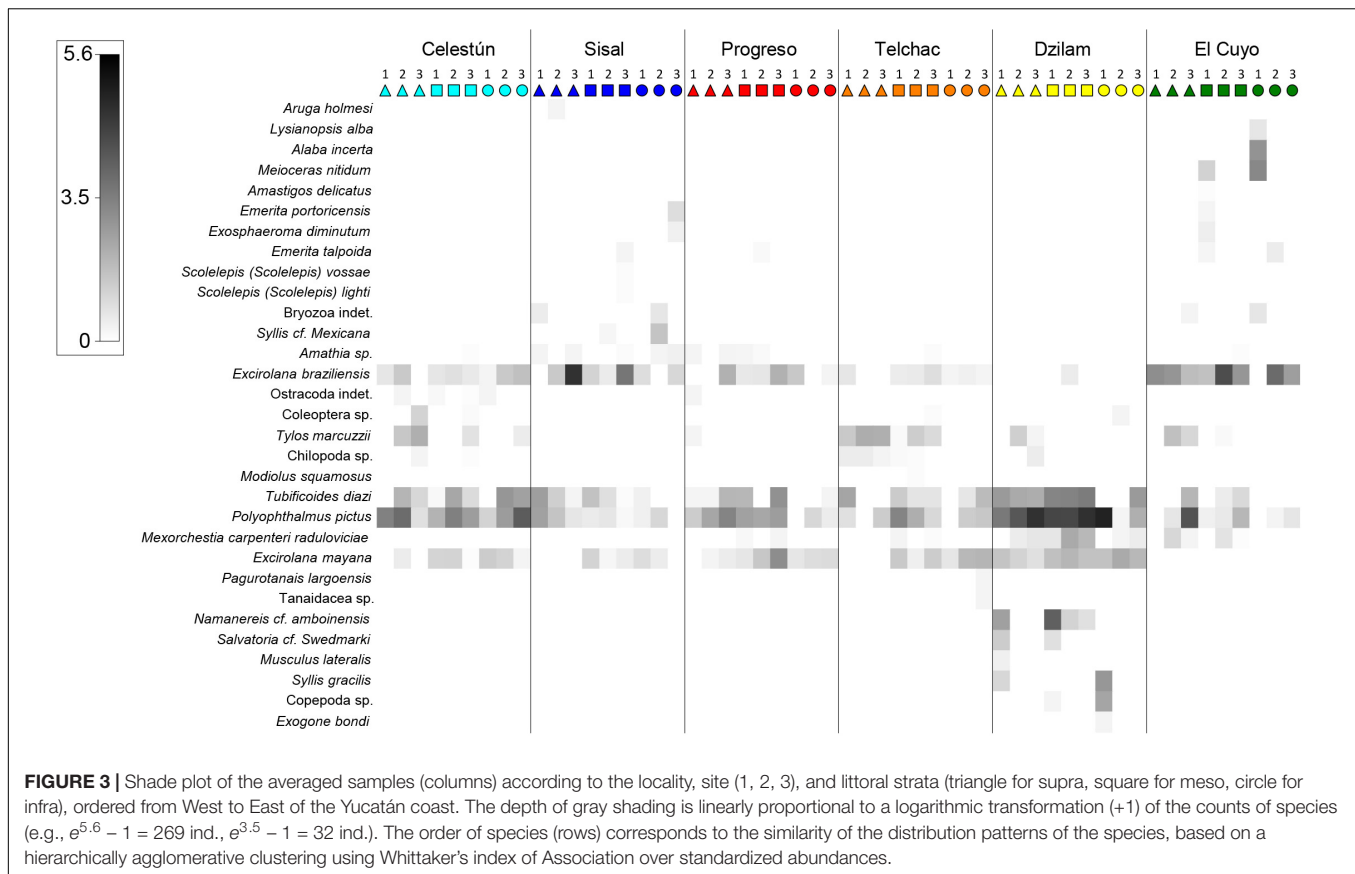


**FIGURE 2 |** Non-metric Multidimensional Scaling of centroids for the interaction term Strata × Site (Locality), of macrobenthic organisms in sandy beaches of Yucatán. The abundances of species were log-transformed. The coefficient of dissimilarity used was Bray-Curtis. Numbers over each symbol represent the site ID.

respectively (Figure 5A). In all cases, the sample completeness was greater than 0.9 (Figure 5B), which supposes a deficit in the detection of species lesser than 10% in all localities. After the evaluation of the interpolation of richness for completeness at 0.9, it was detected that Dzilam, El Cuyo, Sisal, and Telchac are the localities with higher richness, while Celestún and Progreso were the sites with lower species richness (Figure 5C). The gamma diversity, extrapolated using the Chao2 estimator, could be greater than 60 species. The actual sample completeness is 0.885, however, from Figure 5D it seems that the richness of species of the Yucatán beaches could be much higher than that reported in this study.

## Patterns of Hydrocarbons Pollution and Granulometry

Average and standard deviation of the individual concentration of 16 PAHs and 28 aliphatic hydrocarbons are listed in Supplementary Table 3. In general, the highest values of ΣPAHs were measured in Progreso, followed by Sisal and Telchac (Figure 6A). Molecules with 2–3 rings tend to predominate in all localities except in Progreso, where the concentrations of 4 rings and 5–6 rings molecules were as high as 2–3 ring PAH content. PAHs with 4 rings and 5–6 rings were 2–3 times higher in Progreso than in other localities (Figure 6A). Similarly, the highest values of Σn-alkanes were measured in Sisal, Progreso, and Telchac, doubling values concerning other localities (Figure 6B). In all cases, the CPI was around to unity (Figure 6B). Besides the apparent spatial trends in PAHs and aliphatic hydrocarbons along the coast of Yucatán, especially nearby Progreso (Figures 6A,B), there was no statistical evidence to reject the null hypothesis of equal concentration of pollutants across these localities (PERMANOVA,  $Pseudo-F = 1.38$ ,  $p$ -value  $>0.05$ ). Although it is not possible to perform an analysis of power on this test to assess the probability of type II error (failure to reject the null hypothesis), the low number of samples per



**FIGURE 3 |** Shade plot of the averaged samples (columns) according to the locality, site (1, 2, 3), and littoral strata (triangle for supra, square for meso, circle for infra), ordered from West to East of the Yucatán coast. The depth of gray shading is linearly proportional to a logarithmic transformation (+1) of the counts of species (e.g.,  $e^{5.6} - 1 = 269$  ind.,  $e^{3.5} - 1 = 32$  ind.). The order of species (rows) corresponds to the similarity of the distribution patterns of the species, based on a hierarchically agglomerative clustering using Whittaker's index of Association over standardized abundances.

location ( $n = 4$ ) and the high variability within locations may have influenced the significance of the test.

Regarding granulometry, a statistically significant difference was found between localities (PERMANOVA,  $Pseudo-F = 7.23$ ,  $p$ -value  $< 0.05$ ); specifically, El Cuyo compared to the other localities (Pair-wise  $t$ -test,  $p < 0.05$ ). Except for El Cuyo, the entire coast was characterized by sediments with a greater proportion of medium to coarse and very coarse sands ( $> 80\%$ , **Figure 6C**). El Cuyo was characterized by having more abundant fine and very fine sands fractions ( $> 70\%$ , **Figure 6C**) than in the rest of the localities ( $< 20\%$ , **Figure 6C**).

## Estimation of Sampling Effort for Future Assessments

The optimal sampling effort to characterize the macrofauna ranged between 7 and 10 samples per strata (**Figure 7**, dark gray area in upper panels). This sampling effort would allow obtaining a  $MultSE$  between 0.9 and 0.175, corresponding the 45 and 55% of the  $MultSE$  obtained with a sampling effort of two samples and two sites, respectively. The analysis highlights that the estimated range of effort varies according to stratum and localities. Consistently, Dzilam is the site that requires the lower sampling effort in all strata; on the other hand, El Cuyo requires the greatest sampling effort for the supra and infralittoral strata, and Telchac the locality that requires the greatest sampling effort in the mesolittoral strata (**Figure 7**, dark gray area in upper panels). In all cases, the sampling range should be between 7 and

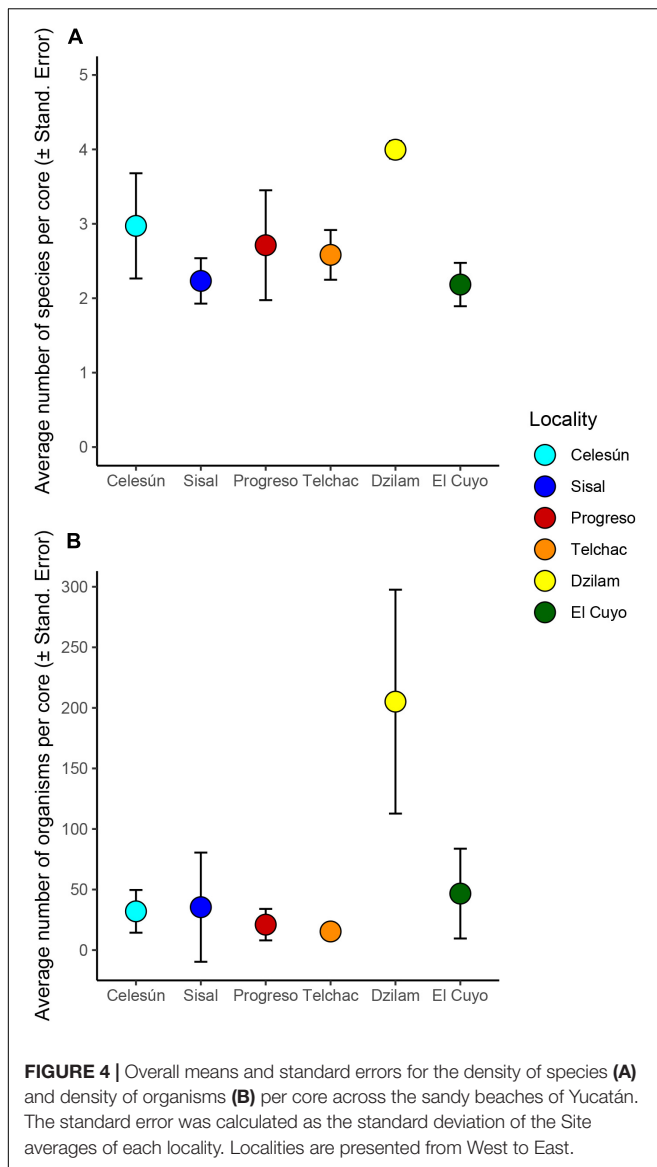
10 samples per strata at each site. Regarding the number of sites, the optimal improvement number was estimated between 4 and 11 sites per locality. This effort would reduce the  $MultSE$  from 0.03 to 0.009–0.02 (**Figure 7**, dark gray area in lower panels). Based on these estimates, we recommend increasing the number of samples for strata to 8, and the number of sites to 4. This recommendation will be analyzed in section “Discussion.”

To characterize the hydrocarbon concentration with a precision of 0.2, the range of samples varied by locality and according to the type of hydrocarbon. The greatest effort is required for PAHs (**Table 3**), the range of sampling effort ranges from 4 to 14 samples per location. The localities that require more effort are Dzilam, El Cuyo, and Sisal. On the other hand, aliphatic hydrocarbons require less effort, the range is from 2 to 8 samples (**Table 3**). The site that requires the greatest sampling effort is El Cuyo, followed by Progreso, Sisal, and Celestún. Based on these ranges (see bottom of **Table 3**), we recommend sampling between 8 and 10 samples for PAHs and 6–8 samples for aliphatic hydrocarbons. As for macrofauna, these recommendations will be analyzed in terms of cost in the discussion section.

## DISCUSSION

### Biological Patterns

The patterns of distribution and abundance of species in sandy beaches of Yucatán State showed the following features: (1) there was a base community structure along the entire

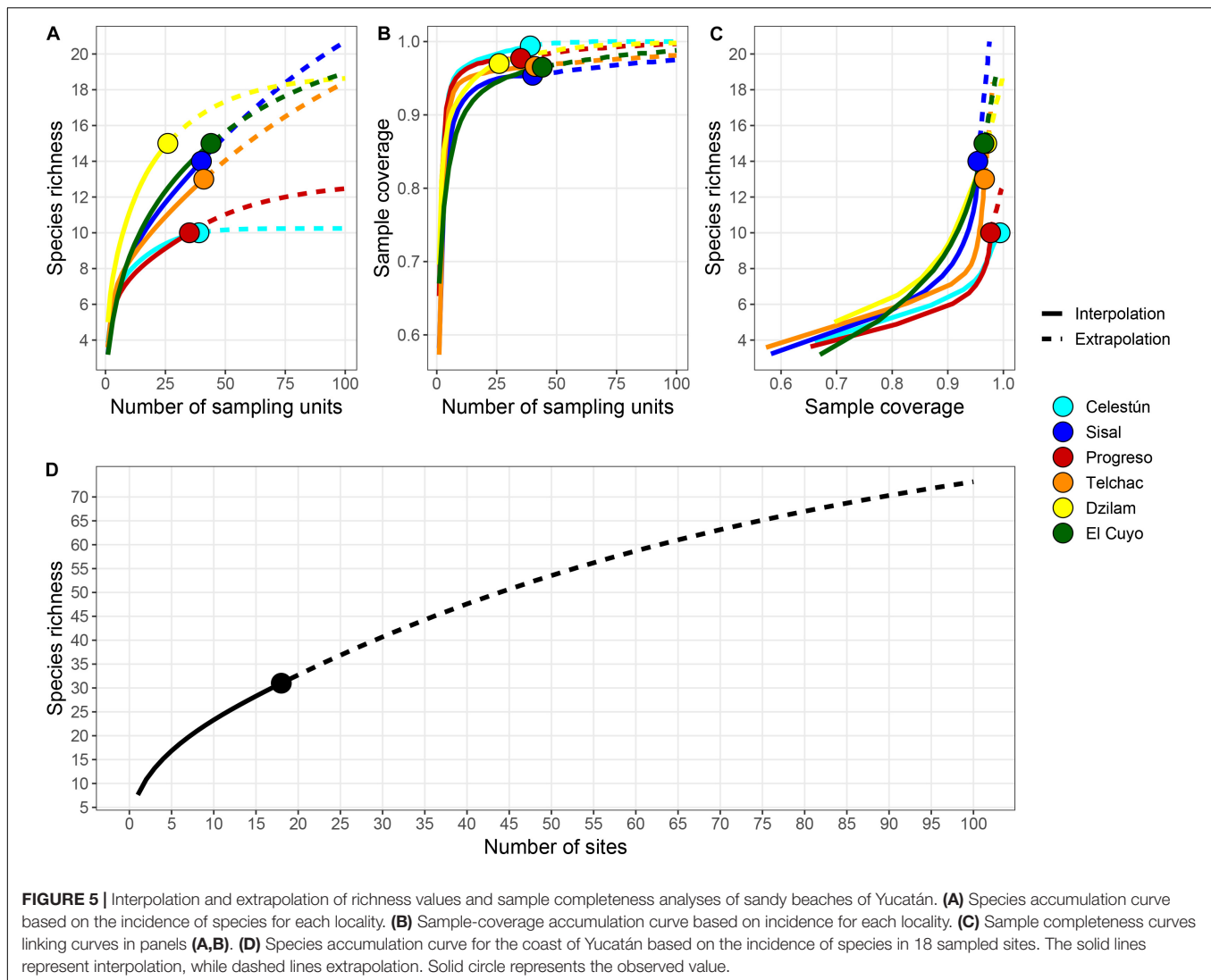


coast dominated by four species: the polychaete *Polyophthalmus pictus*, the oligochaete *Tubificoides diazi*, the isopods *Excirolana mayana* and *E. braziliensis*. Beyond these species, the community structure was highly variable in just few meters apart at the same tidal strata, but also, the effects of the tidal strata on the community structure varied within few kilometers (i.e., among sites of the same locality). (2) In general, the density of species of macrofauna was relatively low (averages between 2 and 4 species/0.01 m<sup>3</sup>) and the density of individuals was high (averages between 20 and 200 ind./0.01 m<sup>3</sup>); although both metrics were particularly higher in Dzilam. (3) The beta diversity was higher between localities with good environmental health (i.e., Dzilam and El Cuyo) but was lower between zones with regular and poor environmental health. (4) The estimated alpha diversities did not show a pattern regarding the health of the coast, they were high (> 18 species) in four of six beaches. Lastly, the overall number of species reported, as well as the extrapolated, suggest that gamma

diversity of the macrofauna in sandy beaches of Yucatán is within the highest known for sandy beaches.

In general, the available information about sandy beaches biodiversity around the world show a consistent pattern: richness decreases from tropical to temperate regions and from macrotidal dissipative beaches to microtidal reflective beaches (Barboza and Defeo, 2015; Fanini et al., 2020). However, besides being tropical, beaches in Yucatán are microtidal, sea breeze dominated, with a medium-grained sedimentary matrix of low content of organic matter. Therefore, considering the known patterns, the species richness reported for this region represents an atypical diversity value that motivates several ecological questions. For example, is the availability of organic matter the primary environmental filter in sandy beaches? How does the availability of organic matter interact with the morphodynamics of the beach in the stability of the macrofauna? Although these questions have been addressed previously (Defeo and McLachlan, 2005, 2013; Bozzeda et al., 2016), the pattern of diversity reported in Yucatán suggests that there is still room to address these questions in the context of beach ecology.

In Yucatán, the patterns of diversity of species do not show any geographical gradient, suggesting that local environmental/geomorphological properties might be driving the actual variation in the distribution of species. Within this context, some hypotheses that could explain these spatial patterns of species diversity are: (i) Massive seaweed accumulations as wrack during the influence of cold fronts and in dry season. The accumulation of wrack in the intertidal zone is spatially heterogeneous but widespread in this region (as evidenced in pictures of Figure 1); these accumulations in low quantities can be a source of energy and nutrients, promoting circumstantial high diversity of macrofauna (Rodil et al., 2008; Barreiro et al., 2013; Orr et al., 2014), but in large quantities could cause anoxia and large amounts of toxic leachates with negative effects on the macrofaunal community (Quillien et al., 2015). Although this process is not as evident as that of *Sargassum* in the Caribbean (Rodríguez-Martínez et al., 2019), it is a process that occurs annually in the coast of Yucatán State. (ii) Spatially differentiated groundwater discharges, with greater effect at the extremes of the cenote ring (Dzilam/el Cuyo and Sisal/Celesún) (Perry et al., 1995) could also generate environmental conditions for the macrofauna of the beaches. (iii) The morphodynamic conditions of each site (e.g., beach slope, swash length, erosion) might also influence in the microhabitat properties and act as an environmental filter (McLachlan and Dorvlo, 2005; Barboza et al., 2012; Barboza and Defeo, 2015). (iv) Actual anthropogenic disturbances could be reducing the beta diversity within and among some localities, especially in areas of poor and regular environmental health. To measure the plausibility of these hypotheses, it will be necessary to measure the patterns of variation in the diversity of species in times/localities with and without macrophytes wrack, with adequate spatial and temporal replication, as well as to measure environmental properties of the interstitial water (e.g., organic matter content, ammonium, redox potential, dissolved oxygen, etc.) and the morphodynamic characteristics of each site.

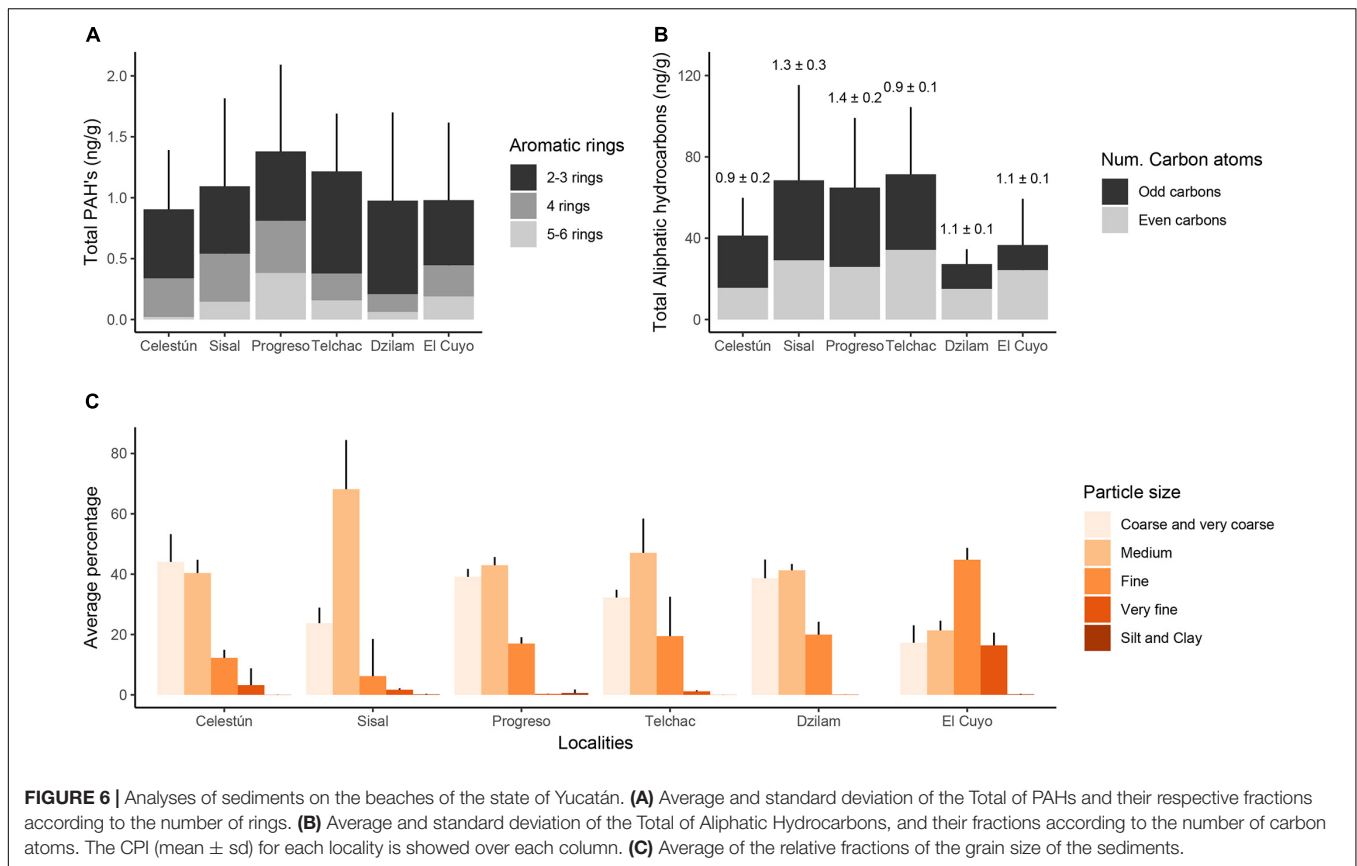


Regarding species distribution, at least three of the four species with wide presence along the coast of the State of Yucatán have been reported for inhabiting other sandy beaches around the world. The polychaete *Polyophthalmus pictus* is spread along the tropical coasts of America, but also in the Mediterranean Sea, the European Atlantic coast, South Africa, and some regions of the Pacific (Read and Fauchald, 2020). This species is recognized as a selective deposit feeder (Faulwetter et al., 2014) but also for being sensitive to organic enrichment and reported as present under unpolluted conditions (Borja et al., 2000). The oligochaete *Tubificoides diazi* has tanylobous prostomium and widely paired lumbricine arrangement of chaetae, this organism feeds on dissolved and particulate organic material and detritus in the surf zone. The isopod *Excirolana mayana*, one of the most abundant species in the present study, has been reported in the Atlantic from the Gulf of Mexico to South America, as well as in the Pacific coast of America, from Mexico to Chile (Dexter, 1976; Defeo et al., 1997; Dominici-Arosemena and Garcés, 2000). This species has been described as a very voracious predator (Brusca

et al., 1995), and is one of the largest isopods in the intertidal zone (Dominici-Arosemena and Garcés, 2000). Similarly, *Excirolana braziliensis* has been also documented as abundant species in sandy beaches of both coasts of America as well as an important predator (Glynn et al., 1975). In Yucatán, both *Excirolana* species seems to compete strongly for habitat, although not explored deeply, preliminary analyzes indicate co-occurrence of only 23% on their incidences, being *E. mayana* the most frequent and abundant in four of six localities. Isopods of the genus *Excirolana* are dominant inhabitants of the supralittoral and intertidal zones of sandy beaches around the world (Omar et al., 1992). It has already been indicated that competition may be a process that promotes the exclusion and low co-occurrence of species of the genus *Excirolana* on sandy beaches (Defeo et al., 1997).

The study of macrofauna of beaches in Mexico dates back to the 1970s (Dexter, 1976). This first study highlights Gulf of Mexico beaches for being considerably poorer in species richness than the Caribbean beaches of Costa Rica and Panama. This appreciation changed with Méndez et al.





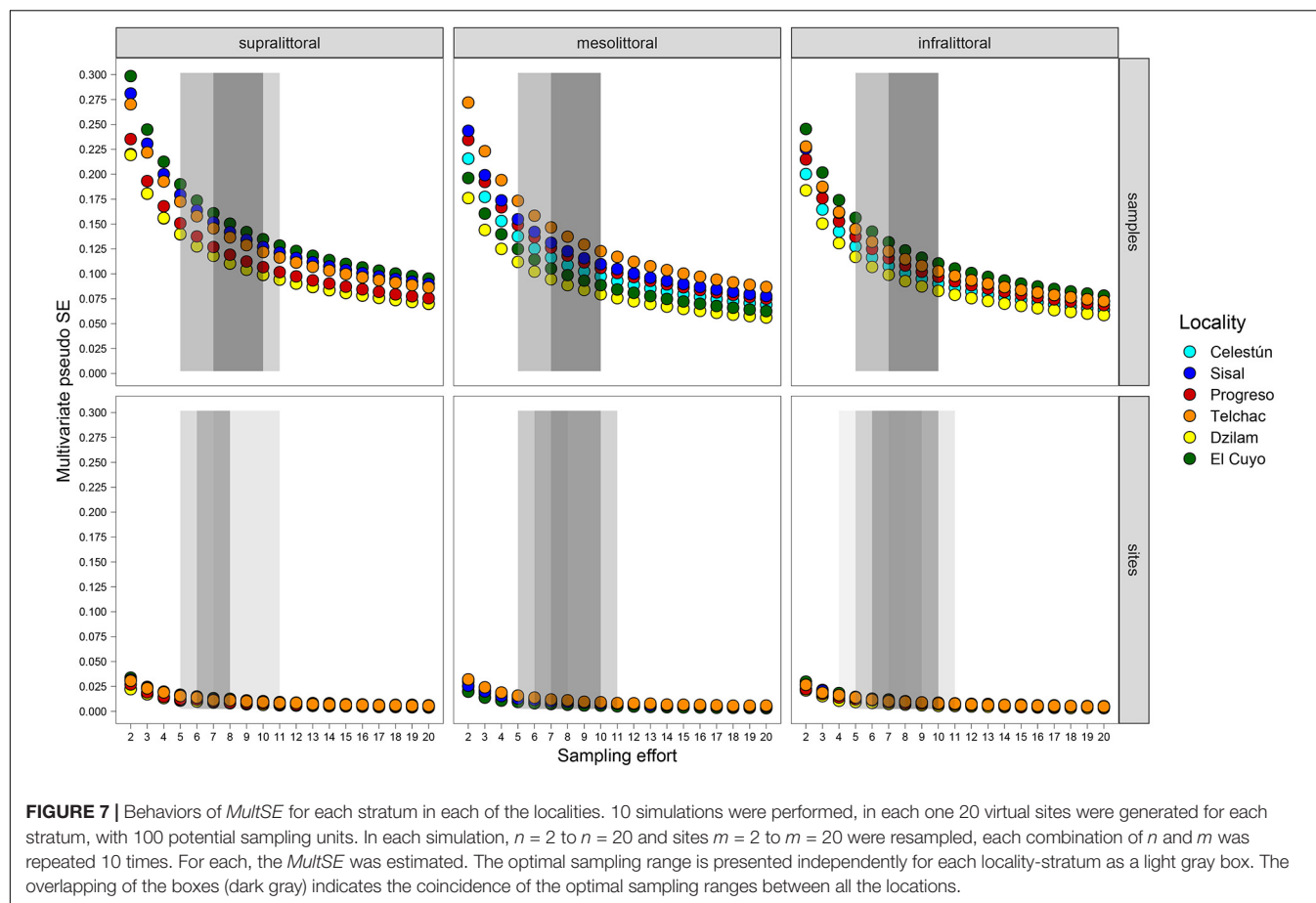
(1985), who reported 28 species in a very extensive study (29 localities) along the >650 km of coastline of Veracruz. In the same region, Hidalgo (2017) described seasonal variability of the macrofauna, reporting 37 species. It is noticeable that the dominant species of the macrofauna in beaches of Yucatán, as well as the main assemblages' patterns, differ from beaches of the Veracruz coast (Hidalgo, 2017). Local-scale geomorphologic and morphodynamical conditions seem to be important drivers of such differences, mainly the influence of salinity, sediment composition, wave energy, and organic input (Hidalgo et al., 2016).

Beyond these studies, and others more localized about crustaceans (Rocha-Ramírez et al., 2010; Paz-Ríos and Ardisson, 2013; Paz-Ríos et al., 2013; Rocha-Ramírez et al., 2016; Ortigosa et al., 2018), there is no information about the diversity of sandy beaches in the Gulf of Mexico. In the Caribbean, the most extensive studies are from Cuba (Ocaña et al., 2012, 2020), in which 30 species were reported; as well as some localities in Costa Rica and Panamá, with diversity varying between 3 and 15 species (Dexter, 1974). Besides these, data about the diversity of the beaches of the tropical western Atlantic is scarce. Indeed, the most important reviews about global patterns of diversity on this habitat have not included any beach of the Gulf of Mexico, neither the Caribbean (Defeo and McLachlan, 2005, 2013; Barboza and Defeo, 2015). In any case, making comparative analyzes of species richness between studies represents a challenge due to the differences in sampling effort and the extension of each study area

(Nel et al., 2014). Much progress has been made using ecoregions (defined by Spalding et al., 2007) as a geographical spatial unit of comparison. For example, the richness of species in South American ecoregions ranges from 1 to 37, the peaks are located at the tropical North Brazil Shelf Province and in Guayaquil and Panama Bight (Jaramillo, 1994; Defeo et al., 2017). Other highly diverse ecoregions are from the Arabian Sea, also with richness around 21–33 species (Defeo and McLachlan, 2013; Barboza and Defeo, 2015). Therefore, from a global perspective, the species richness reported here for the coast of the State of Yucatán stands out among the highest reported worldwide.

## Pollutants Patterns

Levels of hydrocarbons detected in this study are very low compared to the concentrations reported for other coastal areas of the Gulf of Mexico (GoM), both before and after Deepwater Horizon (DWH) oil spill in April 2010 (Botello et al., 2015; Bociu et al., 2019). Adhikari et al. (2016) report concentrations of  $\Sigma\text{PAH}_{43}$  ranging from 68 to 160 ng/g in surface sediments collected in coastal stations in 2011 and 2013 (1 and 3 years after DWH oil spill) in the northern zone (NgoM), an area influenced by river discharges, natural oil seeps, and industrial activities including petroleum exploration/transportation (Joye, 2016). Regarding the presence of hydrocarbons in the southern part of the GoM (SGoM), De Jesús-Navarrete (1993) found concentrations of 0.8–22.6 and 34.7–79.6  $\mu\text{g/g}$  of aliphatics and total PAHs, respectively,



**TABLE 3 |** Sampling effort for estimation of hydrocarbons in sediments from intertidal strata of sandy beaches in Yucatán State, with a precision of 0.2.

Localidad	Sample size for PAHs	Sample size for aliphatic hydrocarbons
Celestún	7	7
Sisal	11	7
Progreso	7	7
Telchac	4	6
Dzilam	14	2
El Cuyo	11	8
Range	4–14	2–8
Mean	9	6
Suggested	8–10	6–8

in sediments of the Campeche Sound, an area impacted by oil industry activities; Quintanilla-Mena et al. (2020) analyzed PAH content in sediment samples collected in the coasts of Mexican GoM from Tamaulipas to Yucatán, detecting the highest PAH levels in Tamaulipas ( $3.33 \pm 5.66 \mu\text{g/g}$ ) and lowest in Yucatán shores ( $0.04 \pm 0.06 \mu\text{g/g}$ ).

On the other hand, pollution studies on the coasts of the State of Yucatán are scarce. Valenzuela et al. (2005) refer maximum levels of  $6.8 \mu\text{g/g}$  of aliphatics and  $55.5 \mu\text{g/g}$  of total PAHs in

sediments from Chelem and Progreso; Kuk-Dzul et al. (2012) report  $0\text{--}3.55 \mu\text{g/g}$  of aliphatics and  $0.5\text{--}5.3 \mu\text{g/g}$  of PAHs in sediments collected in four Yucatán coastal lagoons (Celestún, Chelem, Dzilam, and Ria Lagartos) in 2005; while in sediment cores collected in the sheltered port of Sisal in 2009, mean aliphatic concentrations of  $1.4\text{--}9.7 \mu\text{g/g}$  and  $\Sigma\text{PAH}_{16}$  of  $9.9\text{--}42.8 \text{ ng/g}$  were detected (Noreña-Barroso et al., 2017). It can be seen that the concentrations previously reported are higher than those detected in this work, including areas with the highest presence of hydrocarbons such as Progreso, Telchac and Sisal; however, it is important to consider that the sediments analyzed in those studies were collected in the coastal lagoons, which have a dynamic that makes them more vulnerable to contamination. The low levels of hydrocarbons detected on Yucatán's sandy beaches are not surprising since the presence of these organic compounds is influenced by the potential sources of contamination, grain size (higher concentrations in fine particles) and the type of organic matter associated with the sediments (Wang et al., 2014). Sediments analyzed in this study were predominantly sandy (medium to coarse and very coarse sands) and samples were collected in areas with little industrial influence and without the presence of surface rivers. PAH concentrations in this study are several orders of magnitude lower than those considered as lower-threshold values (TEs,  $312 \text{ ng/g}$  for low MW PAHs,  $655 \text{ ng/g}$  for high MW PAHs and

1,684 ng/g for total PAHs) for marine sediment according to the quality guidelines established by NOAA's Screening Quick Reference Tables (SQUIRTs), suggesting that PAH content has a low probability of being toxic and exert a negative effect upon the benthos (Long et al., 1995; Buchman, 2008).

Beyond the oil industry's threats, the pressure on macrofauna diversity in Yucatán could also be associated with erosion and the local strategies implemented for sediment retention. The beach erosion is a critical process in several areas of the Yucatán shoreline (Appendini et al., 2012; Cuevas Jiménez et al., 2016). In general, the transport of sediment is westward all the year; this makes the beach very vulnerable to littoral barriers, frequently used in urbanized zones to increase the width of the beach (Medellín et al., 2015; Ruiz-Martínez et al., 2016). Some of these strategies include groins, geotextile tubes, breakwaters, and beach nourishment (Ruiz-Martínez et al., 2016); however, most of these engineering strategies currently used generate down-drift erosion problems (Medellín et al., 2015; Ruiz-Martínez et al., 2016). The effects of these sedimentary dynamics on the diversity and community structure of the macrofauna have not been evaluated in this region, but it has been demonstrated in other latitudes (Walker et al., 2008; Schlacher et al., 2012; Munari, 2013). In addition, there are other sources of pollution related to the karstic characteristics of the Yucatan Peninsula, that allow pollutants generated by activities carried out inland to permeate, flow and enter to the coast by submerged groundwater discharges; some evidence of that is the presence of human fecal material (coprostanol and epicoprostanol) in sediments surrounding the springs located in Dzilam de Bravo (Kantun-Manzano et al., 2018), as well as the results reported by Arcega-Cabrera et al. (2015) concerning heavy metal pollution in Chelem Lagoon connected to inland anthropogenic activities along with local factors.

## Sampling Effort

For macrofauna, we recommend that the sampling effort for future ecological assessments on sandy beaches of Yucatán should be of eight cores per stratum at each site, with four sites (separated by 2–3 km) for each one of the six localities, at least three times annually, considering the temporal variation of beach morphodynamics (i.e., erosion, accretion and accumulation of algae) (Medellín and Torres-Freyermuth, 2019). This full design would improve the precision with which the species composition is estimated along the coast of Yucatán, as well as the natural temporal variability. It also will allow to obtain a total sampling area for each site of about 3.6 m<sup>2</sup>; a bit above the minimum recommended by Schlacher et al. (2008) for sites in microtidal beaches with less than 50 m beach width (i.e., between 2 and 3 m<sup>2</sup>). Especially, this full design would allow *bbACI* analyses (beyond Before – After × Control – Impact sensu Underwood, 1992) in the context of oil spills or any other major disturbance that might occur on the beaches of Yucatán (Bejarano and Michel, 2016). However, supporting this sampling effort for the six beaches might be not affordable in terms of the time and personnel required to process so many samples. In such a situation, three strategies could be applied to reduce the sampling effort: (1) reclassifying littoral zones into dry zone and swash

zone, as recommended by MBON P2P (Pole, 2019) for microtidal beaches; (2) dispensing to sample in two or three localities with proved redundant information (e.g., Celestún, Progreso, Telchac); and (3) reducing to two annual samplings. Hence, keeping the most biodiverse localities (i.e., Dzilam and El Cuyo) and one of the remaining locations in the sampling design (e.g., Sisal) would ensure that the spatial patterns of biodiversity will be represented and measured twice a year, although potential reference localities would be sacrificed, as well as the temporal variability, which would imply a weakening of the *bbACI* analysis. Put in numbers, the full design would involve taking and processing 576 samples each time (1,728 samples per year), while the reduced sampling would involve 192 samples (384 samples per year). As a reference, this study involved processing and analysis of 225 sediment samples.

For pollutants, statistical estimations indicated sample sizes of 8–10 samples for PAHs and 6–8 samples for aliphatic hydrocarbons at each stratum. Based on these, we recommend taking eight sand samples at each stratum for both kinds of pollutants, for each of the four sites of each of six localities. As for macrofauna, this sampling effort generates several benefits. The first is the high statistical precision (and power) to detect changes in a highly variable system, using a *bbACI* analysis. The second is the feasibility of building regression models between the biological properties of the macrofauna concerning the variations of the pollutants in sediments. Although this is not informative in the actual circumstances (due to the extremely low concentrations of pollutants), it will be highly informative in case of an oil spill in the future. The great limitation of this sampling design is the economic feasibility; estimating PAH and aliphatic hydrocarbons is expensive, in orders of magnitude higher than the processing of biological samples. Hence, a reduction of the sampling effort as the one proposed for the macrofauna could also be applied for contaminants, with the disadvantage of losing information on potential reference locations.

## Conclusions

In this work, we demonstrate that the diversity of macrofauna is heterogeneous along the coast but especially high on the east side of the state. We also demonstrate that the current levels of PAHs and aliphatic hydrocarbons in beaches are low. Both situations indicate that it is an appropriate time to start long-term monitoring of the environmental health of Yucatán beaches, even more now when energy development (mainly oil & gas) in the Yucatán platform is imminent. It is necessary to advance in the understanding of the temporal patterns of diversity and abundance of species to complement the ecological baseline necessary to identify environmental impacts. The sampling designs we suggest are based on statistical precision and in recommendations previously formulated by experts in beach ecology. We also propose alternatives to reduce sampling effort concerning the ideal design considering possible resource limitations (e.g., funds, personnel, etc.), which, as in most cases, is usually the limiting factor for robust environmental impact assessments. The sampling protocol developed by the MBON

Pole to Pole will allow comparisons to be made with other beaches throughout the Americas.

Further research directions must include the role of morphodynamics (natural and human-induced) and temporal variability in the supply of energy and nutrients as main environmental drivers of macrofauna diversity. Besides, keeping the focus of biological and pollutant spatiotemporal patterns, and developing long-term data sets with international standards, are within the expectations for modern integrative beach ecology and assessment of environmental impacts.

## DATA AVAILABILITY STATEMENT

The datasets presented in this study can be found simultaneously in OBIS or Zenodo data repositories with the respective accession codes: OBIS – <https://obis.org/dataset/5700fdc3-956f-4e33-903b-e66ba38d980c> and ZENODO – doi: 10.5281/zenodo.3771828.

## AUTHOR CONTRIBUTIONS

NS, MM, EN-B, GH, and EG-C contributed to the conception and design of the study. EG-C, GH, and RC-C did fieldwork. GH, RC-C, and MM-R processed biological samples. JQ-D and EN-B did granulometric and chemical analyses. GH, JQ-D, and EG-C organized the database. EG-C performed statistical analyses. EG-C wrote the first draft of the manuscript, with the collaboration of NS, MM-R, and EN-B. All authors contributed to manuscript revision, read, and approved the submitted version.

## REFERENCES

- Adhikari, P. L., Maiti, K., Overton, E. B., Rosenheim, B. E., and Marx, B. D. (2016). Distributions and accumulation rates of polycyclic aromatic hydrocarbons in the northern Gulf of Mexico sediments. *Environ. Pollut.* 212, 413–423. doi: 10.1016/j.envpol.2016.01.064
- Anderson, M. J., Crist, T. O., Chase, J. M., Vellend, M., Inouye, B. D., Freestone, A. L., et al. (2010). Navigating the multiple meanings of (diversity): a roadmap for the practicing ecologist. *Ecol. Lett.* 14, 19–28. doi: 10.1111/j.1461-0248.2010.01552.x
- Anderson, M. J. (ed.). (2017). “Permutational multivariate analysis of variance (PERMANOVA),” in *Wiley StatsRef: Statistics Reference Online*, (Hoboken, NJ: John Wiley & Sons, Ltd). doi: 10.1002/9781118445112.stat07841
- Anderson, M. J., and Santana-Garcon, J. (2015). Measures of precision for dissimilarity-based multivariate analysis of ecological communities. *Ecol. Lett.* 18, 66–73. doi: 10.1111/ele.12385
- Anderson, M. J., and Ter Braak, C. J. F. (2003). Permutation test for multifactorial analysis of variance. *J. Stat. Comput. Simul.* 73, 85–113. doi: 10.1080/00949650215733
- Andrade, M. (2010). “Transformación de los sistemas naturales por actividades antropogénicas,” in *Biodiversidad y Desarrollo Humano en Yucatán*, eds R. Durán and M. Méndez (México: CICY, PPD-FMAM, CONABIO, SEDUMA), 316–319.
- Andrew, N. L., and Mapstone, B. D. (1987). “Sampling and the description of spatial pattern in marine ecology,” in *Oceanography and Marine Biology: an Annual Review*, eds H. Barnes and M. Barnes (Aberdeen: Aberdeen University Press), 39–90.

## FUNDING

This project was funded by the 2018 CONACyT 293354 grant “Laboratorio Nacional de Resiliencia Costera.” The continuity of this research is financed by the grant IA206320 (PAPIIT, Universidad Nacional Autónoma de México) under the supervision of EG-C. Funding was also provided by the Harte Research Institute for Gulf of Mexico Studies and the Harte Charitable Foundation through the “Biodiversity of the southern Gulf of Mexico” project under the supervision of NS and the support of the BDMY research group. NS holds the Furgason Fellowship International Chair for Coastal and Marine Studies in México.

## ACKNOWLEDGMENTS

Special thanks to the coordinators of the Pole to Pole of the Americas network, as well as to all its members for their positive comments and constructive criticism of this work in the workshop held in Puerto Morelos, Mexico, in 2018. We extend our gratitude to Dr. Frank Ocaña, who actively participated at an early stage of the design of this project. This work benefited greatly from important insights and comments given by reviewers.

## SUPPLEMENTARY MATERIAL

The Supplementary Material for this article can be found online at: <https://www.frontiersin.org/articles/10.3389/fmars.2020.589656/full#supplementary-material>

- Appendini, C. M., Salles, P., Mendoza, E. T., López, J., and Torres-Freyermuth, A. (2012). Longshore sediment transport on the northern coast of the Yucatan Peninsula. *J. Coast. Res.* 28, 1404–1417. doi: 10.2112/jcoastres-d-11-00162.1
- Arcega-Cabrera, F., Garza-Pérez, R., Noreña-Barroso, E., and Ocegueda-vargas, I. (2015). Impacts of geochemical and environmental factors on seasonal variation of heavy metals in a coastal lagoon Yucatan, Mexico. *Bull. Environ. Contam. Toxicol.* 94, 58–65. doi: 10.1007/s00128-014-1416-1
- Arturo Lopez, O., Lynch, J. F., and de Montes, B. M. K. (1989). New and noteworthy records of birds from the eastern Yucatán peninsula. *Wilson Bull.* 101, 390–409.
- Barboza, F. R., and Defeo, O. (2015). Global diversity patterns in sandy beach macrofauna: a biogeographic analysis. *Sci. Rep.* 5:14515. doi: 10.1038/srep14515
- Barboza, F. R., Gómez, J., Lercari, D., and Defeo, O. (2012). Disentangling diversity patterns in sandy beaches along environmental gradients. *PLoS One* 7:e40468. doi: 10.1371/journal.pone.0040468
- Barreiro, F., Gómez, M., López, J., Lastra, M., and de la Huz, R. (2013). Coupling between macroalgal inputs and nutrients outcrop in exposed sandy beaches. *Hydrobiologia* 700, 73–84. doi: 10.1007/s10750-012-1220-z
- Baselga, A. (2010). Partitioning the turnover and nestedness components of beta diversity. *Glob. Ecol. Biogeogr.* 19, 134–143. doi: 10.1111/j.1466-8238.2009.00490.x
- Baselga, A., and Orme, C. D. L. (2012). betapart: an R package for the study of beta diversity. *Methods Ecol. Evol.* 3, 808–812. doi: 10.1111/j.2041-210X.2012.00224.x
- Bejarano, A. C., and Michel, J. (2016). Oil spills and their impacts on sand beach invertebrate communities: a literature review. *Environ. Pollut.* 218, 709–722. doi: 10.1016/j.envpol.2016.07.065



- Bociu, I., Shin, B., Wells, W. B., Kostka, J. E., Konstantinidis, K. T., and Huettel, M. (2019). Decomposition of sediment-oil-agglomerates in a Gulf of Mexico sandy beach. *Sci. Rep.* 9:10071. doi: 10.1038/s41598-019-46301-w
- Borja, A., Franco, J., and Pérez, V. (2000). A marine biotic index to establish the ecological quality of soft-bottom benthos within European estuarine and coastal environments. *Mar. Pollut. Bull.* 40, 1100–1114. doi: 10.1016/s0025-326x(00)00061-8
- Botello, A. V., Soto, L. A., Ponce-Vélez, G., and Villanueva, F. S. (2015). Baseline for PAHs and metals in NW Gulf of Mexico related to the Deepwater Horizon oil spill. *Estuar. Coast. Shelf Sci.* 156, 124–133. doi: 10.1016/j.ecss.2014.11.010
- Bozzeda, F., Zangrilli, M. P., and Defeo, O. (2016). Assessing sandy beach macrofaunal patterns along large-scale environmental gradients: a Fuzzy Naïve Bayes approach. *Estuar. Coast. Shelf Sci.* 175, 70–78. doi: 10.1016/j.ecss.2016.03.025
- Brusca, R. C., Wetzer, R., and France, S. C. (1995). Cirolanidae (Crustacea: Isopoda: Flabellifera) of the tropical eastern Pacific. *Oceanogr. Lit. Rev.* 11:1001.
- Buchman, M. F. (ed.). (2008). “NOAA screening quick reference tables,” in *NOAA OR&R Report 08-1*, (Seattle, WA: National Oceanic and Atmospheric Administration).
- Bulleri, F., Underwood, A. J., and Benedetti-Cecchi, L. (2007). The assessment and interpretation of ecological impacts in human-dominated environments. *Environ. Conserv.* 34, 181–182. doi: 10.1017/s0376892907004201
- Canonic, G., Buttigieg, P. L., Montes, E., Muller-Karger, F. E., Stepien, C., Wright, D., et al. (2019). Global observational needs and resources for marine biodiversity. *Front. Mar. Sci.* 6:367. doi: 10.3389/fmars.2019.00367
- Chao, A., Colwell, R. K., Lin, C.-W., and Gotelli, N. J. (2009). Sufficient sampling for asymptotic minimum species richness estimators. *Ecology* 90, 1125–1133. doi: 10.1890/07-2147.1
- Chao, A., and Jost, L. (2012). Coverage-based rarefaction and extrapolation: standardizing samples by completeness rather than size. *Ecology* 93, 2533–2547. doi: 10.1890/11-1952.1
- Clarke, K. R., Gorley, R. N., Somerfield, P. J., and Warwick, R. M. (2014a). *Change in Marine Communities: an Approach to Statistical analysis and Interpretation*. Plymouth: PRIMER-E, Ltd.
- Clarke, K. R., Tweedley, J. R., and Valesini, F. J. (2014b). Simple shade plots aid better long-term choices of data pre-treatment in multivariate assemblage studies. *J. Mar. Biol. Assoc. U.K.* 94, 1–16. doi: 10.1017/S0025315413001227
- Cruz-Motta, J. J., Petkoff, I., Klein, E., and Alvarez, H. (2007). “Detection of impacts in a changing and highly variable world: the case of a floating storage and offloading (FSO) unit in the Gulf of Paria (Venezuela). SPE international,” in *Proceedings of the E&P Environmental and Safety Conference*, San Antonio, TX, 1–7. doi: 10.2118/106606-MS
- Cuevas, E., de los Ángeles Liceaga-Correa, M., and Mariño-Tapia, I. (2010). Influence of beach slope and width on hawksbill (*Eretmochelys imbricata*) and green turtle (*Chelonia mydas*) nesting activity in El Cuyo, Yucatán, México. *Chelonian Conserv. Biol.* 9, 262–267. doi: 10.2744/ccb-0819.1
- Cuevas Jiménez, A., Euán Ávila, J. I., Villatoro Lacouture, M. M., and Silva Casarín, R. (2016). Classification of beach erosion vulnerability on the Yucatan coast. *Coast. Manag.* 44, 333–349. doi: 10.1080/08920753.2016.1155038
- De Jesús-Navarrete, A. (1993). Concentración de hidrocarburos totales en los sedimentos de la Sonda de Campeche, México. *Caribb. J. Sci.* 29, 99–105.
- Defeo, O., Barboza, C. A. M., Barboza, F. R., Aeberhard, W. H., Cabrini, T. M. B., Cardoso, R. S., et al. (2017). Aggregate patterns of macrofaunal diversity: an interocean comparison. *Glob. Ecol. Biogeogr.* 26, 823–834. doi: 10.1111/geb.12588
- Defeo, O., Brazeiro, A., de Alava, A., and Riestra, G. (1997). Is sandy beach macrofauna only physically controlled? Role of substrate and competition in isopods. *Estuar. Coast. Shelf Sci.* 45, 453–462. doi: 10.1006/ecss.1996.0200
- Defeo, O., and McLachlan, A. (2005). Patterns, processes and regulatory mechanisms in sandy beach macrofauna: a multi-scale analysis. *Mar. Ecol. Prog. Ser.* 295, 1–20. doi: 10.3354/meps295001
- Defeo, O., and McLachlan, A. (2013). Global patterns in sandy beach macrofauna: species richness, abundance, biomass and body size. *Geomorphology* 199, 106–114. doi: 10.1016/j.geomorph.2013.04.013
- Defeo, O., McLachlan, A., Schoeman, D. S., Schlacher, T. A., Dugan, J., Jones, A., et al. (2009). Threats to sandy beach ecosystems: a review. *Estuar. Coast. Shelf Sci.* 81, 1–12.
- Dexter, D. M. (1974). Sandy-beach fauna of the Pacific and Atlantic coasts of Costa Rica and Colombia. *Rev. Biol. Trop.* 22, 51–66.
- Dexter, D. M. (1976). The sandy-beach fauna of Mexico. *Southwest. Nat.* 20, 479–485. doi: 10.2307/3669864
- Dominici-Arosemena, A., and Garcés, H. (2000). Occurrence of *Exciliorana mayana* (Isopoda: Cirolanidae) in a sandy mid-littoral beach of Punta Paitilla, Pacific coast of Panamá. *Bol. Cent. Investig. Biol. Univ. Zulia* 34, 410–415.
- Enriquez, C., Mariño-Tapia, I. J., and Herrera-Silveira, J. A. (2010). Dispersion in the Yucatan coastal zone: implications for red tide events. *Cont. Shelf Res.* 30, 127–137. doi: 10.1016/j.csr.2009.10.005
- Espejel, I. (1984). La vegetación de las dunas costeras de la península de Yucatán. I. Análisis florístico del estado de Yucatán. *Biótica* 9, 183–210.
- Fanini, L., Defeo, O., and Elliott, M. (2020). Advances in sandy beach research – Local and global perspectives. *Estuar. Coast. Shelf Sci.* 234:106646. doi: 10.1016/j.ecss.2020.106646
- Faulwetter, S., Markantonatou, V., Pavludi, C., Papageorgiou, N., Keklikoglou, K., Chatziniakolau, E., et al. (2014). *Polytraits*: a database on biological traits of marine polychaetes. *Biodivers. Data J.* 2:e1024. doi: 10.3897/BDJ.2.e1024
- Glynn, P. W., Dexter, D. M., and Bowman, T. E. (1975). *Exciliorana braziliensis*, a Pan-American sand beach isopod: taxonomic status, zonation and distribution. *J. Zool.* 175, 509–521. doi: 10.1111/j.1469-7998.1975.tb01414.x
- González-Muñoz, R. E., Simões, N., Tello-Musi, J. L., and Rodríguez, E. (2013). Sea anemones (Cnidaria, Anthozoa, Actiniaria) from coral reefs in the southern Gulf of Mexico. *Zookeys* 341, 77–106. doi: 10.3897/zookeys.341.5816
- Guerra-Castro, E. (ed.). (2019). “MBON pole to pole: sandy beach biodiversity of Yucatán coast,” in *Ocean Biogeographic Information System*, (Caribbean: Caribbean OBIS Node).
- Guerra-Castro, E., Hidalgo, G., Castillo, R., Muciño-Reyes, M., Noreña-Barroso, E., Quiroz Deadquino, J., et al. (2019). Macrofauna, granulometry, n-alkanes and PAHs in sediments of the sandy beaches of the state of Yucatán: November 2018. Zenodo, 1.0.0.0. doi: 10.5281/zenodo.3771829
- Guerra-Castro, E. J., Cajas, J. C., Dias Marques Simoes, F. N., Cruz-Motta, J. J., and Mascaró, M. (2020). SSP: an R package to estimate sampling effort in studies of ecological communities. *bioRxiv* [Preprint]. doi: 10.1101/2020.03.19.996991
- Herrera-Silveira, J. A., Javier Ramírez, R., and Arturo Zaldivar, J. (1998). Overview and characterization of the hydrology and primary producer communities of selected coastal lagoons of Yucatán, México. *Aquat. Ecosyst. Health Manag.* 1, 353–372. doi: 10.1080/14634989808656930
- Hidalgo, G. (2017). *Comunidades Intermareales de la Macrofauna en Playas Arenosas del Litoral Central de Veracruz, Golfo de México: un Enfoque de Integridad Ecológica*. Ph.D. thesis, Universidad Veracruzana, Veracruz, 158.
- Hidalgo, G., Castañeda-Chávez, M. R., Granados-Barba, A., and Sánchez, B. E. (2016). Environmental variability of tropical sandy beaches across an anthropic gradient: the case of central Veracruz (Southwestern Gulf of Mexico). *Int. J. Environ. Res.* 10, 481–490. doi: 10.22059/ijer.2016.59600
- Hsieh, T. C., Ma, K. H., and Chao, A. (2016). iNEXT: an R package for rarefaction and extrapolation of species diversity (Hill numbers). *Methods Ecol. Evol.* 7, 1451–1456. doi: 10.1111/2041-210x.12613
- Islebe, G. A., Sánchez-Sánchez, O., Valdéz-Hernández, M., and Weissenberger, H. (2015). “Distribution of vegetation types,” in *Biodiversity and Conservation of the Yucatán Peninsula*, eds G. A. Islebe, S. Calmé, J. L. León-Cortés, and B. Schmook (Cham: Springer International Publishing), 39–53.
- Jaramillo, E. (1994). Patterns of species richness in sandy beaches of South America. *S. Afr. J. Zool.* 29, 227–234. doi: 10.1080/02541858.1994.11448355
- Jernelov, A. (2010). How to defend against future oil spills. *Nature* 466, 182–183. doi: 10.1038/466182a
- Jernelov, A., and Linden, O. (1981). Ixtoc I: a case study of the world's largest oil spill. *Ambio* 10, 299–306.
- Joye, S. B. (2016). The Gulf of Mexico ecosystem – Before, during and after the Deepwater Horizon oil well blowout. *Deep Sea Res. II Top. Stud. Oceanogr.* 129:1. doi: 10.1016/j.dsr2.2016.04.022
- Kantun-Manzano, C., Árcaga-Cabrera, F., Derrien, M., Noreña-Barroso, E., and Herrera-Silveira, J. (2018). Submerged groundwater discharges as sources of fecal material in protected Karstic coastal areas. *Geofluids* 2018:9736260.
- Keith, L. H. (1996). *Compilation of EPA's Sampling and Analysis Methods*. Boca Raton, FL: CRC Press.
- Kingston, P. F. (2002). Long-term environmental impact of oil spills. *Spill Sci. Technol. Bull.* 7, 53–61. doi: 10.1016/s1353-2561(02)00051-8

- Kuk-Dzul, J. G., Gold-Bouchot, G., and Ardisson, P. L. (2012). Benthic infauna variability in relation to environmental factors and organic pollutants in tropical coastal lagoons from the northern Yucatán Peninsula. *Mar. Pollut. Bull.* 64, 2725–2733. doi: 10.1016/j.marpolbul.2012.09.022
- LANRESC (2017). *Tarjeta de Reporte de la Costa de Yucatán*. Mexico: CONACYT.
- Long, E. R., Macdonald, D. D., Smith, S. L., and Calder, F. D. (1995). Incidence of adverse biological effects within ranges of chemical concentrations in marine and estuarine sediments. *Environ. Manag.* 19, 81–97. doi: 10.1007/BF02472006
- Mareddy, A. R. (2017). “3 - Baseline data and environmental setting,” in *Environmental Impact Assessment*, ed. A. R. Mareddy (Oxford: Butterworth-Heinemann), 61–128. doi: 10.1016/b978-0-12-811139-0.00003-7
- Martínez, A., Eckert, E. M., Artois, T., Careddu, G., Casu, M., Curini-Galletti, M., et al. (2020). Human access impacts biodiversity of microscopic animals in sandy beaches. *Commun. Biol.* 3, 1–9.
- Marzi, R., Torkelson, B. E., and Olson, R. K. (1993). A revised carbon preference index. *Org. Geochem.* 20, 1303–1306. doi: 10.1016/0146-6380(93)90016-5
- McLachlan, A., and Dorvlo, A. (2005). Global patterns in sandy beach macrobenthic communities. *J. Coast. Res.* 21, 674–687. doi: 10.2112/03-0114.1
- Medellín, G., Mariño-Tapia, I., and Euán-Ávila, J. (2015). The influence of a seawall on postnourishment evolution in a sea-breeze-dominated microtidal beach. *J. Coast. Res.* 31, 1449–1458. doi: 10.2112/jcoastres-d-13-00194.1
- Medellín, G., and Torres-Freyermuth, A. (2019). Morphodynamics along a microtidal sea breeze dominated beach in the vicinity of coastal structures. *Mar. Geol.* 417:106013. doi: 10.1016/j.margeo.2019.106013
- Méndez, U. M. N., Solís-Weiss, V., and Carranza-Edwards, A. (1985). La importancia de la granulometría en la distribución de organismos bentónicos. Estudio de playas del estado de Veracruz, México. *Anal. Inst. Cienc. Limnol.* 13, 45–56.
- Mendoza-Becerril, M. A., Simões, N., and Genzano, G. (2018). Benthic hydroids (Cnidaria, Hydrozoa) from Alacranes reef, gulf of Mexico, Mexico. *Bull. Mar. Sci.* 94, 125–142. doi: 10.5343/bms.2017.1072
- Meyer-Arendt, K. J. (2001). Recreational development and shoreline modification along the north coast of Yucatán, Mexico. *Tour. Geogr.* 3, 87–104. doi: 10.1080/14616680010008720
- Munari, C. (2013). Benthic community and biological trait composition in respect to artificial coastal defence structures: a study case in the northern Adriatic Sea. *Mar. Environ. Res.* 90, 47–54. doi: 10.1016/j.marenvres.2013.05.011
- National Ocean Service NOAA (2011). *The Gulf of Mexico at a Glance: a Second Glance*. Washington, DC: Department of Commerce.
- Nel, R., Campbell, E. E., Harris, L., Hauser, L., Schoeman, D. S., McLachlan, A., et al. (2014). The status of sandy beach science: past trends, progress, and possible futures. *Estuar. Coast. Shelf Sci.* 150, 1–10. doi: 10.1016/j.ecss.2014.07.016
- Noreña-Barroso, E., Iturria-Dawn, R. A., and Árcega-Cabrera, F. (2017). “Contaminación histórica por hidrocarburos en el Puerto de Sisal, Yucatán,” in *Caracterización Multidisciplinaria de la Zona Costera de Sisal, Yucatán*, eds J. R. Garza-Pérez and I. A. R. Ize-Lema (Yucatán: LANRESC), 138–151.
- Ocaña, F. A., Apín, Y., Cala, Y., Vega, A., Fernández, A., and Córdova, E. (2012). Distribución espacial de los macroinvertebrados de playas arenosas de Cuba oriental. *Rev. Investig. Mar.* 32, 30–37.
- Ocaña, F. A., Mouso-Batista, M. M., and Hernández-Ávila, I. (2020). Macrofaunal assemblages from two low-energy sandy beaches within contrasting salinity environments in Northeastern Cuba. *Reg. Stud. Mar. Sci.* 2020:101484. doi: 10.1016/j.risma.2020.101484
- Oksanen, J., Blanchet, F. G., Kindt, R., Legendre, P., Minchin, P. R., O'Hara, R. B., et al. (2015). *Vegan: Community Ecology Package. R package version 2.3-0*.
- Omar, D., Jaramillo, E., and Anibal, L. (1992). Community structure and intertidal zonation of the macroinfauna on the Atlantic coast of Uruguay. *J. Coast. Res.* 8, 830–839.
- Orr, K. K., Wilding, T. A., Horstmeyer, L., Weigl, S., and Heymans, J. J. (2014). Detached macroalgae: its importance to inshore sandy beach fauna. *Estuar. Coast. Shelf Sci.* 150, 125–135. doi: 10.1016/j.ecss.2013.12.011
- Ortigosa, D., Lemus-Santana, E., and Simões, N. (2015). New records of ‘opisthobranchs’ (Gastropoda: Heterobranchia) from Arrecife Alacranes national park, Yucatán, Mexico. *Mar. Biodivers. Rec.* 8:e117. doi: 10.1017/S1755267215000925
- Ortigosa, D., Suárez-Mozo, N. Y., Barrera, N. C., and Simões, N. (2018). First survey of Intertidal molluscs from Cayo Nuevo, Campeche Bank, Gulf of Mexico. *Zookeys* 779, 1–17. doi: 10.3897/zookeys.779.24562
- Palomino-Alvarez, L. A., Rocha, R. M., and Simões, N. (2019). Checklist of ascidians (Chordata, Tunicata) from the southern Gulf of Mexico. *Zookeys* 832, 1–33. doi: 10.3897/zookeys.832.31712
- Paz-Ríos, C. E., and Ardisson, P.-L. (2013). Caribboecetes progreso, a new species of sand-dwelling amphipod (Amphipoda: Corophiidae: Ischyroceridae) from the Gulf of Mexico, with a key for the genus. *Zootaxa* 3652, 370–380. doi: 10.11646/zootaxa.3652.3.5
- Paz-Ríos, C. E., Pech, D., Mariño-Tapia, I., and Simões, N. (2020). Influence of bottom environment conditions and hydrographic variability on spatiotemporal trends of macrofaunal amphipods on the Yucatán continental shelf. *Cont. Shelf Res.* 198:104098. doi: 10.1016/j.csr.2020.104098
- Paz-Ríos, C. E., Simões, N., and Ardisson, P.-L. (2013). Intertidal and shallow water amphipods (Amphipoda: Gammaridea and Corophiidea) from Isla Pérez, Alacranes reef, southern Gulf of Mexico. *Nauplius* 21, 179–194. doi: 10.1590/s0104-64972013000200005
- Paz-Ríos, C. E., Simões, N., and Pech, D. (2019). Species richness and spatial distribution of benthic amphipods (Crustacea: Peracarida) in the Alacranes Reef National Park, Gulf of Mexico. *Mar. Biodivers.* 49, 673–682. doi: 10.1007/s12526-017-0843-8
- Pech Pool, D., Mascaró, M., Simoes, N., and Enríquez Ortiz, C. (2010). “Ambientes marinos,” in *Biodiversidad y Desarrollo Humano en Yucatán*, eds R. Durán and M. Méndez (México: CICY, PPD-FMAM, CONABIO, SEDUMA).
- Perry, E., Marin, L., McClain, J., and Velazquez, G. (1995). Ring of cenotes (sinkholes), northwest Yucatán, Mexico: its hydrogeologic characteristics and possible association with the Chicxulub impact crater. *Geology* 23, 17–20. doi: 10.1130/0091-7613(1995)023<0017:rocsny>2.3.co;2
- Peterson, C. H., Kennicutt, M. C. II, Green, R. H., Montagna, P., Harper, J. D. E., Powell, E. N., et al. (1996). Ecological consequences of environmental perturbations associated with offshore hydrocarbon production: a perspective on long-term exposures in the Gulf of Mexico. *Can. J. Fish. Aquat. Sci.* 53, 2637–2654. doi: 10.1139/f96-220
- Pole, M. P. T. (ed.). (2019). “Sampling protocol for assessment of marine diversity on sandy beaches,” in *Marine Biodiversity Observation Network Pole to Pole of the Americas*, (Oostende: OceanBestPractices Repository).
- Quillien, N., Nordström, M. C., Gauthier, O., Bonsdorff, E., Paulet, Y. M., and Grall, J. (2015). Effects of macroalgal accumulations on the variability in zoobenthos of high-energy macrotidal sandy beaches. *Mar. Ecol. Prog. Ser.* 522, 97–114. doi: 10.3354/meps11151
- Quintanilla-Mena, M., Gold-Bouchot, G., Zapata-Pérez, O., Rubio-Piña, J., Quiroz-Moreno, A., Vidal-Martínez, V. M., et al. (2020). Biological responses of shoal flounder (*Syacium gunteri*) to toxic environmental pollutants from the southern Gulf of Mexico. *Environ. Pollut.* 258:113669. doi: 10.1016/j.envpol.2019.113669
- R Core Team (2013). *R: A Language and Environment for Statistical Computing*, 1 Edn. Vienna: Austria: R Foundation for Statistical Computing.
- Ramos, E. L. (1975). “Geological summary of the Yucatán Peninsula,” in *The Gulf of Mexico and the Caribbean*, eds A. E. M. Nairn and F. G. Stehli (Boston, MA: Springer), 257–282. doi: 10.1007/978-1-4684-8535-6\_7
- Read, G., and Fauchald, K. (eds). (2020). *World Polychaeta Database. Polyophtalmus pictus (Dujardin, 1839)*. Accessed through: World Register of Marine Species. Available online at: <https://www.marinespecies.org/aphia.php?p=taxdetails&id=130510> (accessed June 3, 2020).
- Robertson, D. R., Domínguez-Domínguez, O., López Aroyo, Y. M., Moreno Mendoza, R., and Simões, N. (2019). Reef-associated fishes from the offshore reefs of western Campeche Bank, Mexico, with a discussion of mangroves and Seagrass beds as nursery habitats. *Zookeys* 843, 71–115. doi: 10.3897/zookeys.843.33873
- Rocha-Ramírez, A., Chávez-López, R., Antillón-Zaragoza, I., and Fuentes-Mendoza, F. A. (2016). Variación nictemeral de los ensamblajes de macrocrustáceos en una playa arenosa del centro-norte de Veracruz, México. *Rev. Mex. Biodivers.* 87, 92–100. doi: 10.1016/j.rmb.2016.01.025
- Rocha-Ramírez, A., Chávez-López, R., and Peláez-Rodríguez, E. (2010). *Ancinus jarocho* (Isopoda: Sphaeromatidea: Ancinidae), a new species from the central Gulf of Mexico, Mexico. *Zootaxa* 2397, 48–60. doi: 10.11646/zootaxa.2397.1.6
- Rodil, I. F., Compton, T. J., and Lastra, M. (2014). Geographic variation in sandy beach macrofauna community and functional traits. *Estuar. Coast. Shelf Sci.* 150, 102–110. doi: 10.1016/j.ecss.2013.06.019

- Rodil, I. F., Olabarria, C., Lastra, M., and López, J. (2008). Differential effects of native and invasive algal wrack on macrofaunal assemblages inhabiting exposed sandy beaches. *J. Exp. Mar. Biol. Ecol.* 358, 1–13. doi: 10.1016/j.jembe.2007.12.030
- Rodríguez-Martínez, R. E., Medina-Valmaseda, A. E., Blanchon, P., Monroy-Velázquez, L. V., Almazán-Becerril, A., Delgado-Pech, B., et al. (2019). Faunal mortality associated with massive beaching and decomposition of pelagic Sargassum. *Mar. Pollut. Bull.* 146, 201–205. doi: 10.1016/j.marpolbul.2019.06.015
- Rodríguez-Revelo, N., Espejel, I., García, C. A., Ojeda-Revah, L., and Vázquez, M. A. S. (2018). “Environmental services of beaches and coastal sand dunes as a tool for their conservation,” in *Beach Management Tools-Concepts, Methodologies and Case Studies*, Vol. 24, eds C. Botero, O. Cervantes, and C. Finkl (Cham: Springer), 75–100. doi: 10.1007/978-3-319-58304-4\_5
- Ruiz-Martínez, G., Mariño-Tapia, I., Baldwin, E. G. M., Casarín, R. S., and Ortiz, C. E. E. (2016). Identifying coastal defence schemes through morphodynamic numerical simulations along the northern coast of Yucatan, Mexico. *J. Coast. Res.* 32, 651–669. doi: 10.2112/jcoastres-d-15-00009.1
- Schlacher, T. A., Noriega, R., Jones, A., and Dye, T. (2012). The effects of beach nourishment on benthic invertebrates in eastern Australia: impacts and variable recovery. *Sci. Total Environ.* 435–436, 411–417. doi: 10.1016/j.scitotenv.2012.06.071
- Schlacher, T. A., Schoeman, D. S., Dugan, J., Lastra, M., Jones, A., Scapini, F., et al. (2008). Sandy beach ecosystems: key features, sampling issues, management challenges and climate change impacts. *Mar. Ecol.* 29, 70–90. doi: 10.1111/j.1439-0485.2007.00204.x
- SENER (2015). *Plan Quinquenal de Licitaciones Para la Exploración y Extracción de Hidrocarburos 2015 – 2019*. Mexico: Secretaría de Energía.
- Spalding, M. D., Fox, H. E., Allen, G. R., Davidson, N., Ferdaña, Z. A., Finlayson, M., et al. (2007). Marine ecoregions of the world: a bioregionalization of coastal and shelf areas. *Bioscience* 57, 573–583. doi: 10.1641/b570707
- Sun, S., Hu, C., and Tunnell, J. W. (2015). Surface oil footprint and trajectory of the Ixtoc-I oil spill determined from Landsat/MSS and CZCS observations. *Mar. Pollut. Bull.* 101, 632–641. doi: 10.1016/j.marpolbul.2015.10.036
- Tapia González, F. U., Herrera-Silveira, J. A., and Aguirre-Macedo, M. L. (2008). Water quality variability and eutrophic trends in karstic tropical coastal lagoons of the Yucatán Peninsula. *Estuar. Coast. Shelf Sci.* 76, 418–430. doi: 10.1016/j.ecss.2007.07.025
- Teal, J. M., and Howarth, R. W. (1984). Oil spill studies: a review of ecological effects. *Environ. Manag.* 8, 27–44. doi: 10.1007/bf01867871
- Thom, B. (2020). “29 - Future challenges in beach management as contested spaces,” in *Sandy Beach Morphodynamics*, eds D. W. T. Jackson and A. D. Short (Amsterdam: Elsevier), 711–731. doi: 10.1016/b978-0-08-102927-5.00029-1
- Ugalde, D., Gómez, P., and Simoes, N. (2015). Marine sponges (Porifera: Demospongiae) from the Gulf of México, new records and redescription of *Erylus trisphaerus* (de Laubenfels, 1953). *Zootaxa* 3911, 151–183. doi: 10.11646/zootaxa.3911.2.1
- Underwood, A. J. (1991). Beyond BACI: experimental designs for detecting human environmental impacts on temporal variations in natural populations. *Aust. J. Mar. Freshw. Res.* 42, 569–587. doi: 10.1071/mf9910569
- Underwood, A. J. (1992). Beyond BACI: the detection of environmental impacts on populations in the real, but variable, world. *J. Exp. Mar. Biol. Ecol.* 161, 145–178. doi: 10.1016/0022-0981(92)90094-q
- Underwood, A. J., and Chapman, M. G. (2003). Power, precaution, type II error and sampling design in assessment of environmental impacts. *J. Exp. Mar. Biol. Ecol.* 296, 49–70. doi: 10.1016/s0022-0981(03)00304-6
- US EPA (2007a). *Semivolatile Organic Compounds by Gas Chromatography/Mass Spectrometry (GC/MS). Method 8270D, Revision 4*. Washington, DC: United States Environmental Protection Agency.
- US EPA (2007b). *Solid-Phase Extraction. Method 3535A, Revision 1*. Washington, DC: United States Environmental Protection Agency.
- US EPA (2007c). *Ultrasonic Extraction. Method 3550C, Revision 3*. Washington, DC: United States Environmental Protection Agency.
- Valenzuela, S., Gold-Bouchot, G., and Ceja, M. (2005). “Hidrocarburos en agua y sedimentos de la laguna de Chelem y puerto Progreso, Yucatán, México,” in *Golfo de México Contaminación e Impacto Ambiental: Diagnóstico y Tendencias*, eds A. Botello, R. V. Osten, G. Gold-Bouchot, and C. Agraz-Hernández (Campeche, TX: Universidad Autónoma de Campeche), 311–328.
- Walker, S. J., Schlacher, T. A., and Thompson, L. M. C. (2008). Habitat modification in a dynamic environment: the influence of a small artificial groyne on macrofaunal assemblages of a sandy beach. *Estuar. Coast. Shelf Sci.* 79, 24–34. doi: 10.1016/j.ecss.2008.03.011
- Wang, Z., Liu, Z., Xu, K., Mayer, L. M., Zhang, Z., Kolker, A. S., et al. (2014). Concentrations and sources of polycyclic aromatic hydrocarbons in surface coastal sediments of the northern Gulf of Mexico. *Geochem. Trans.* 15:2.
- Yoskowitz, D., Leon, C., Gibeau, J., Lupher, B., Lopez, M., Santos, C., et al. (2013). *Gulf 360: State of the Gulf of Mexico*. Harte Research Institute for Gulf of Mexico Studies. Corpus Christi, TX: Texas A&M University-Corpus Christi.

**Conflict of Interest:** The authors declare that the research was conducted in the absence of any commercial or financial relationships that could be construed as a potential conflict of interest.

Copyright © 2020 Guerra-Castro, Hidalgo, Castillo-Cupul, Muciño-Reyes, Noreña-Barroso, Quiroz-Deaquino, Mascaro and Simoes. This is an open-access article distributed under the terms of the Creative Commons Attribution License (CC BY). The use, distribution or reproduction in other forums is permitted, provided the original author(s) and the copyright owner(s) are credited and that the original publication in this journal is cited, in accordance with accepted academic practice. No use, distribution or reproduction is permitted which does not comply with these terms.





# A Marine Biodiversity Observation Network for Genetic Monitoring of Hard-Bottom Communities (ARMS-MBON)

## OPEN ACCESS

### Edited by:

Frank Edgar Muller-Karger,  
University of South Florida,  
United States

### Reviewed by:

Lara Jane Atkinson,  
University of Cape Town, South Africa  
Christopher Sinigalliano,  
Atlantic Oceanographic and  
Meteorological Laboratory (NOAA),  
Miami, United States

### \*Correspondence:

Matthias Obst  
matthias.obst@marine.gu.se  
orcid.org/0000-0003-0264-9631

### Specialty section:

This article was submitted to  
Ocean Observation,  
a section of the journal  
Frontiers in Marine Science

**Received:** 15 June 2020

**Accepted:** 05 November 2020

**Published:** 30 November 2020

### Citation:

Obst M, Exter K, Allcock AL,  
Arvanitidis C, Axberg A,  
Bustamante M, Cancio I,  
Carreira-Flores D, Chatzinikolaou E,  
Chatzigeorgiou G, Christmas N,  
Clark MS, Comtet T, Dailianis T,  
Davies N, Deneudt K, de Cerio OD,  
Fortič A, Gerovasileiou V, Hablützel P,  
Keklikoglou K, Kotoulas G, Lasota R,  
Leite BR, Loisel S, Lévêque L, Levy L,  
Malachowicz M, Mavrič B, Meyer C,  
Mortelmans J, Norkko J, Pade N,  
Power AM, Ramšak A, Reiss H,  
Solbakken J, Staehr PA, Sundberg P,  
Thyrring J, Troncoso JS, Viard F,  
Wenne R, Yperifanou EI, Zbawicka M  
and Pavloudi C (2020) A Marine  
Biodiversity Observation Network for  
Genetic Monitoring of Hard-Bottom  
Communities (ARMS-MBON).  
*Front. Mar. Sci.* 7:572680.  
doi: 10.3389/fmars.2020.572680

Matthias Obst<sup>1\*</sup>, Katrina Exter<sup>2</sup>, A. Louise Allcock<sup>3</sup>, Christos Arvanitidis<sup>4,5</sup>, Alizz Axberg<sup>1</sup>, Maria Bustamante<sup>6</sup>, Ibon Cancio<sup>6</sup>, Diego Carreira-Flores<sup>7,8,9</sup>, Eva Chatzinikolaou<sup>4</sup>, Giorgos Chatzigeorgiou<sup>4</sup>, Nathan Christmas<sup>10</sup>, Melody S. Clark<sup>11</sup>, Thierry Comtet<sup>12</sup>, Thanos Dailianis<sup>4</sup>, Neil Davies<sup>13</sup>, Klaas Deneudt<sup>2</sup>, Oihane Diaz de Cerio<sup>5</sup>, Ana Fortič<sup>14</sup>, Vasilis Gerovasileiou<sup>4</sup>, Pascal I. Hablützel<sup>2</sup>, Kleoniki Keklikoglou<sup>4,15</sup>, Georgios Kotoulas<sup>4</sup>, Rafal Lasota<sup>16</sup>, Barbara R. Leite<sup>7,17,18</sup>, Stéphane Loisel<sup>12</sup>, Laurent Lévêque<sup>12</sup>, Liraz Levy<sup>19</sup>, Magdalena Malachowicz<sup>20</sup>, Borut Mavrič<sup>14</sup>, Christopher Meyer<sup>21</sup>, Jonas Mortelmans<sup>2</sup>, Joanna Norkko<sup>22</sup>, Nicolas Pade<sup>23</sup>, Anne Marie Power<sup>3</sup>, Andreja Ramšak<sup>14</sup>, Henning Reiss<sup>24</sup>, Jostein Solbakken<sup>22</sup>, Peter A. Staehr<sup>25</sup>, Per Sundberg<sup>1</sup>, Jakob Thyrring<sup>26,27</sup>, Jesus S. Troncoso<sup>17,28</sup>, Frédérique Viard<sup>12,29</sup>, Roman Wenne<sup>20</sup>, Eleni Ioanna Yperifanou<sup>4,30</sup>, Malgorzata Zbawicka<sup>20</sup> and Christina Pavloudi<sup>4</sup>

<sup>1</sup> Department of Marine Sciences, University of Gothenburg, Gothenburg, Sweden, <sup>2</sup> Flanders Marine Institute (VLIZ), Oostende, Belgium, <sup>3</sup> School of Natural Sciences, Ryan Institute, National University of Ireland Galway, Galway, Ireland, <sup>4</sup> Hellenic Centre for Marine Research, Institute of Marine Biology, Biotechnology and Aquaculture, Heraklion, Greece, <sup>5</sup> LifeWatch ERIC, Seville, Spain, <sup>6</sup> Plentzia Marine Station (PiE-UPV/EHU), University of the Basque Country, European Marine Biological Resource Centre, Plentzia, Spain, <sup>7</sup> Department of Biology, CBMA—Centre of Molecular and Environmental Biology, University of Minho, Braga, Portugal, <sup>8</sup> Marine Biology Station of A Graña, University of Santiago de Compostela, Ferrol, Spain, <sup>9</sup> Department of Biology and Environment, Centre for the Research and Technology of Agro-Environmental and Biological Sciences (CITAB), University of Trás-os Montes and Alto Douro, Vila Real, Portugal, <sup>10</sup> Marine Biological Association of the UK, Citadel Hill, Plymouth, United Kingdom, <sup>11</sup> British Antarctic Survey, Cambridge, United Kingdom, <sup>12</sup> Sorbonne Université, CNRS, Station Biologique de Roscoff, Place Georges Teissier, Roscoff, France, <sup>13</sup> Gump South Pacific Research Station, University of California Berkeley, Moorea, French Polynesia, <sup>14</sup> National Institute of Biology, Marine Biology Station Piran, Piran, Slovenia, <sup>15</sup> Biology Department, University of Crete, Heraklion, Greece, <sup>16</sup> Department of Marine Ecosystems Functioning, Institute of Oceanography, University of Gdansk, Gdynia, Poland, <sup>17</sup> IB-S—Institute of Science and Innovation for Bio-Sustainability, University of Minho, Braga, Portugal, <sup>18</sup> UVIGO Marine Research Centre (Centro de Investigación Mariña), Toralla Marine Science Station, Vigo, Spain, <sup>19</sup> The Interuniversity Institute of Marine Sciences in Eilat, Eilat, Israel, <sup>20</sup> Institute of Oceanology of the Polish Academy of Sciences (IOPAN), Sopot, Poland, <sup>21</sup> Department of Invertebrate Zoology, National Museum of Natural History, Smithsonian Institution, Washington, DC, United States, <sup>22</sup> Tvärminne Zoological Station, University of Helsinki, Hanko, Finland, <sup>23</sup> EMBRC-ERIC Headquarters, Sorbonne Université, Paris, France, <sup>24</sup> Faculty of Biosciences and Aquaculture, Nord University, Bodo, Norway, <sup>25</sup> Department of Bioscience, Aarhus University, Roskilde, Denmark, <sup>26</sup> Department of Zoology, University of British Columbia, Vancouver, BC, Canada, <sup>27</sup> Department of Bioscience, Marine Ecology, Aarhus University, Silkeborg, Denmark, <sup>28</sup> Department of Ecology and Animal Biology, Marine Sciences Faculty, University of Vigo, Vigo, Spain, <sup>29</sup> ISEM, Univ Montpellier, CNRS, EPHE, IRD, Montpellier, France, <sup>30</sup> School of Biology, Aristotle University of Thessaloniki, Thessaloniki, Greece

Marine hard-bottom communities are undergoing severe change under the influence of multiple drivers, notably climate change, extraction of natural resources, pollution and eutrophication, habitat degradation, and invasive species. Monitoring marine biodiversity in such habitats is, however, challenging as it typically involves expensive, non-standardized, and often destructive sampling methods that limit its scalability. Differences in monitoring approaches furthermore hinders inter-comparison among monitoring programs. Here, we announce a Marine Biodiversity Observation Network (MBON) consisting of Autonomous Reef Monitoring Structures (ARMS) with the aim



to assess the status and changes in benthic fauna with genomic-based methods, notably DNA metabarcoding, in combination with image-based identifications. This article presents the results of a 30-month pilot phase in which we established an operational and geographically expansive ARMS-MBON. The network currently consists of 20 observatories distributed across European coastal waters and the polar regions, in which 134 ARMS have been deployed to date. Sampling takes place annually, either as short-term deployments during the summer or as long-term deployments starting in spring. The pilot phase was used to establish a common set of standards for field sampling, genetic analysis, data management, and legal compliance, which are presented here. We also tested the potential of ARMS for combining genetic and image-based identification methods in comparative studies of benthic diversity, as well as for detecting non-indigenous species. Results show that ARMS are suitable for monitoring hard-bottom environments as they provide genetic data that can be continuously enriched, re-analyzed, and integrated with conventional data to document benthic community composition and detect non-indigenous species. Finally, we provide guidelines to expand the network and present a sustainability plan as part of the European Marine Biological Resource Centre ([www.embrc.eu](http://www.embrc.eu)).

**Keywords:** benthic invertebrates, Marine Strategy Framework Directive (MSFD), Essential Biodiversity Variables (EBVs), Essential Ocean Variables (EOVs), European Marine Biological Resource Centre (EMBRC), non-indigenous species (NIS), Genomic Observatories, marine biodiversity assessment

## INTRODUCTION

Healthy ecosystems and the biodiversity they harbor are a prerequisite for the sustainable future of our planet (Rockström et al., 2009). Scientists are now more than ever forced to provide evidence to understand, and where possible counteract, the factors causing severe change in the biological composition of these environments. Such knowledge is critical as human pressures increase and accumulate, especially in coastal zones, from a combination of factors including traffic, wastewater discharges, energy production, aquaculture and fisheries, recreation, and tourism (Lotze et al., 2006; Worm et al., 2006; OSPAR, 2009). A key limitation to improved understanding of the impact of human activities on marine ecosystems is the ability to generate comparative biological time-series data at a large spatial scale (Richardson and Poloczanska, 2008; Dailianis et al., 2018; Guidi et al., 2020). There is therefore strong pressure on biological monitoring programs to implement standardized and scalable methods to assess status and change in marine biological communities in order to support marine research and policy (Bourlat et al., 2013; Borja et al., 2016; Danovaro et al., 2016; Bean et al., 2017; Bevilacqua et al., 2020). These methods need to fulfill several important criteria, including the implementation of common standards and protocols and to generate material samples and data that are FAIR: findable, accessible, interoperable, and re-usable (Tanhua et al., 2019).

Monitoring subtidal hard-bottom habitats is a challenge as they are three-dimensionally complex and inherently difficult to access (Bianchi et al., 2004; Beisiegel et al., 2017). In contrast to soft-bottom environments, which are widely sampled in a standardized fashion across countries and regions (e.g., with

box corers or grab samplers), hard-bottom communities are usually studied by individual assessments in smaller areas using video recordings and scientific diving. A promising approach, however, is the use of artificial substrates—passive samplers that can record the community composition on the seafloor in a standardized way. Artificial Substrate Units (ASU), for example, have been used for many years in individual field experiments (Menge et al., 2002; Gobin and Warwick, 2006), while some European monitoring programs also use settlement plates for monitoring non-indigenous species (HELCOM, 2013). Another popular system is provided by Autonomous Reef Monitoring Structures (ARMS) ([www.oceanarms.org](http://www.oceanarms.org)). These are three-dimensional units consisting of stacked settlement plates attached to the sea floor (David et al., 2019). Because of their three-dimensional structure, mimicking the complexity of hard bottom marine substrates, ARMS attract both sessile and motile benthic organisms. These monitoring systems were originally developed during the *Census of Marine Life* and are currently in broad use for integrated studies combining morphological identification with metabarcoding (Leray and Knowlton, 2015; Pearman et al., 2016, 2018; Cahill et al., 2018).

DNA-metabarcoding has been advocated for some years as a potential method for rapid, effective, and scalable measurements of community composition in marine habitats (Bourlat et al., 2013; Borja et al., 2016; Bean et al., 2017). Recent studies have also tested the applicability of this method for hard-bottom monitoring and non-indigenous species (NIS) detection, comparing genetic with conventional methods (Pearman et al., 2016; Kelly et al., 2017; Cahill et al., 2018; Couton et al., 2019). Most of these studies concluded that metabarcoding adds substantial value for monitoring marine biological communities,

especially when combined with other methods in biological monitoring programs.

The use of metabarcoding for rapid identification of species in marine communities, however, is not without limitations (e.g., Cahill et al., 2018). One obvious drawback is the still incomplete taxonomic reference databases, which limit positive identifications and can also lead to misidentifications (Meiklejohn et al., 2019; Weigand et al., 2019; Hestetun et al., 2020). It should be noted that alternative morphological-based identification also has flaws as the declining number of taxonomic experts and large numbers of cryptic species mean that mis-identification is commonplace, with important consequences especially for non-indigenous species (NIS) detection (e.g., Viard et al., 2019). Another important consideration of metabarcoding is the sensitivity of the results to primer choice and sequencing methods. A recent study by van der Loos and Nijland (2020) showed that there is a high degree of inconsistency in metabarcoding studies, which are often explorative and designed for a specific purpose, and hence not directly comparable. There is a need to move beyond episodic metabarcoding studies and build up time-series of genetic data (Danovaro et al., 2016; David et al., 2019).

Here we describe a contribution to the Marine Biodiversity Observation Network (MBON) consisting of Autonomous Reef Monitoring Structures (ARMS). The goal of the ARMS-MBON is to establish long-term assessments of status and change in hard-bottom communities in the European continental seas using standardized methodology and generating FAIR data. The network is initiated and maintained by European marine infrastructure programs and intends to contribute a community of practice to the Group on Earth Observations Biodiversity Observation Network, GEO BON (Kissling et al., 2018).

## MATERIALS AND METHODS

### Field Sampling and Processing

ARMS observatories were established in the vicinity of marinas, ports, marine protected areas (MPAs), and long-term ecological research (LTER) sites between December 2017 and May 2020 (**Supplementary Table 1**). The duration of sample events varied between short (2–3 months) and long (12–24 months) periods, and was repeated annually, when possible. Some deployment periods had to be extended during the COVID-19 pandemic due to travel and diving restrictions. In several cases, ARMS are deployed as part of national monitoring programs (e.g., Limfjord, Laeso, Swedish West coast, Getxo).

### Molecular and Image Analysis

Each sampling event produces at least three fractions (40  $\mu$ m sessile, 100–500  $\mu$ m, and 500  $\mu$ m –2 mm motile) as well as a stack of plate and specimen images. Images are analyzed by individual partners, while material samples are stored at –20°C and shipped for processing by the Institute of Marine Biology, Biotechnology and Aquaculture (IMBBC) of the Hellenic Centre for Marine Research (HCMR) in Greece. Detailed protocols for DNA extraction, PCR amplification, and sequencing are available on the website (<http://www.arms-mbon.eu/>) under Molecular Standard Operating Procedures (MSOP). In summary,

DNA extractions are performed with the DNeasy PowerSoil Kit (Qiagen), while PCR amplification follow a two-step PCR protocol for: the mitochondrial cytochrome c oxidase subunit I (COI), the nuclear 18S small ribosomal subunit (18S rRNA) (except for the samples of 2018), and the nuclear Internal Transcribed Spacer (ITS1). Resulting amplicons are further sequenced using Illumina MiSeq Reagent Kit v3 (2 × 300 bp). Currently, samples are processed and sequenced as batches twice a year. In the future, samples may be processed more frequently and potentially involving additional partners, if these follow the established protocols.

All raw sequence files produced by the network are submitted to the European Nucleotide Archive, ENA (Amid et al., 2020), and processed with the Pipeline for Environmental DNA Metabarcoding Analysis, PEMA (Zafeiropoulos et al., 2020). Repeatable workflow procedures for integrated processing of image and sequence data are currently under development as part of the LifeWatch-ERIC Internal Joint Initiative on non-indigenous species. The final cleaned sequence files are stored in the PlutoF data management system (Abarenkov et al., 2010) where they are accessible to all members of the network.

### Case Study

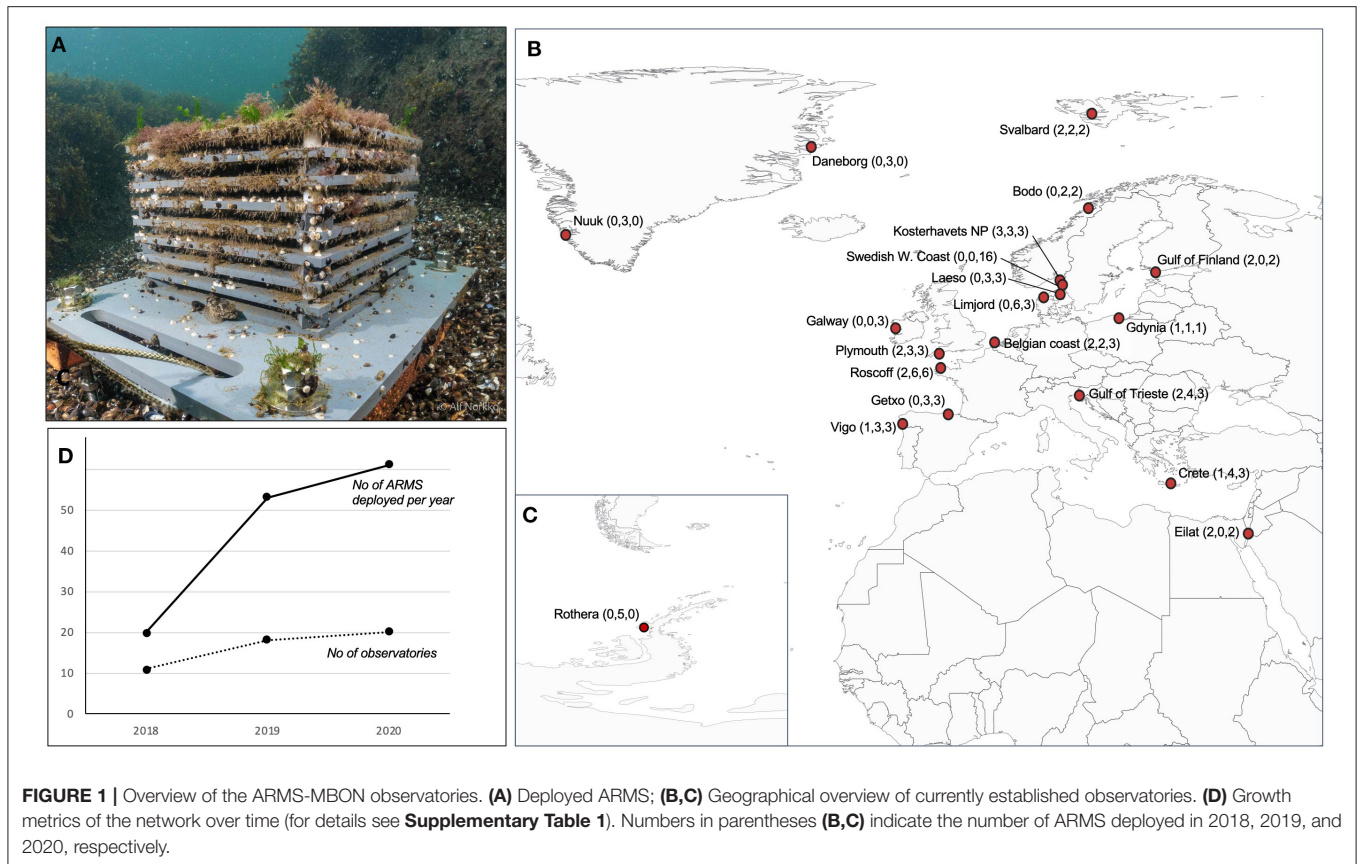
During the pilot phase, we used two ARMS for parallel sampling trials with alternative preservation methods, namely Dimethyl sulfoxide (DMSO) vs. ethanol (EtOH). One ARMS was located in a Marine Protected Area in Sweden, while the other one was located in a marina in Greece (**Supplementary Table 1**). The samples from these two sites were used to analyze the effects of the preservation method and compare the community composition between localities and fractions, as well as for identifying non-indigenous species.

## RESULTS

### The ARMS-MBON Network and Associated Standards

Currently, the network maintains 20 ARMS observatories in 14 European countries, as well as Greenland and Antarctica, ranging from tropical waters to polar environments (**Figure 1**, **Supplementary Table 1**). All major European continental seas are sampled, with exception of the Black Sea. To date, the network has deployed a total number of 134 ARMS units. The first sampling campaign (2018) deployed 20 ARMS across 11 sites, the second campaign (2019) deployed 53 ARMS across 18 sites, and the third campaign (2020) currently deploys 61 ARMS across 20 sites (**Figure 1**, **Supplementary Table 1**).

During the pilot phase, we customized the methodology of the global ARMS Program at the Smithsonian Institution ([www.oceanarms.org/](http://www.oceanarms.org/)) to match the purpose of ARMS-MBON. Detailed protocols for sampling and sample processing are documented in the Handbook and in the molecular standard operating procedures (MSOP) available at the ARMS-MBON website ([www.arms-mbon.eu](http://www.arms-mbon.eu)). In addition, we also developed a specific partner registration sheet to allow new partners to register new observatories and receive consultation as well as training.



**FIGURE 1 |** Overview of the ARMS-MBON observatories. **(A)** Deployed ARMS; **(B,C)** Geographical overview of currently established observatories. **(D)** Growth metrics of the network over time (for details see **Supplementary Table 1**). Numbers in parentheses **(B,C)** indicate the number of ARMS deployed in 2018, 2019, and 2020, respectively.

To date, 74% of all concluded sampling events have been sequenced (120 out of 162 material samples). The status of sequence processing and data publication is shown in **Supplementary Table 2** and will be updated regularly on the ARMS-MBON website ([www.arms-mbon.eu](http://www.arms-mbon.eu)).

## Data Management and Open Access Strategy for Sharing of Data

A model agreement for sample storage and Data Policy was developed in compliance with the Convention on Biological Diversity and the Nagoya Protocol on Access and Benefit Sharing (ABS) for the utilization of genetic resources in a fair and equitable way. Important documents associated with this model agreement include a Data Management Plan (DMP), Material Transfer Agreement (MTA), and Documents for Access and Benefit Sharing (ABS). All documents are available on the ARMS-MBON website (<http://www.arms-mbon.eu/>).

Data are published as packages—one for each ARMS (i.e., sampling event) and allow for continuous enrichment, as well as integration of sequence and image data during analysis (Exter et al., 2020). Detailed explanations of the ARMS-MBON data formats are given in the **Supplementary Material**. All data are published under the Open Access license CC BY 4.0, with a moratorium period of 1 year starting from the point when raw sequence data become available to the partner network. Two examples with data from the ARMS used in the case study are

available under the Data Availability Statement. Data from all remaining and future sampling events will become automatically available under the same license after the embargo period, starting in May 2021.

## Case Study

Comparison of sequence reads derived from DMSO and ethanol preserved samples showed a higher yield for DMSO in the sessile fraction and a lower yield for DMSO in the motile fraction from Greece (500  $\mu\text{m}$ ), while DMSO and EtOH yield were almost equal in the sessile fractions from Sweden (**Figure 2**). Despite this substantial variation of sequence reads in relation to the fixative, the representation of taxa, as well as the resulting species composition, remained very similar across both preservation methods (**Figures 2, 3**).

Combined analysis of genetic and image data resulted in 72 identified species from the Swedish ARMS, with 8% overlap between genetic and image-based species observations (**Figure 3**, **Supplementary Table 3**). In comparison, the analysis of the Greek ARMS resulted in 69 identified species with only 4% overlap between genetic and image-based communities, highlighting the high degree of complementarity of image and genetic data collected by the ARMS.

Comparison of the taxonomic composition between the three genetic fractions (40  $\mu\text{m}$  sessile, 100–500  $\mu\text{m}$ , and 500  $\mu\text{m}$  –2 mm motile) shows a shift in taxonomic dominance



between fractions and hence also indicates a high degree of complementarity (**Figure 2**). While the sessile fractions are dominated by sequences from chordates (tunicates), the motile fractions are co-dominated by arthropods, nematodes, mollusks, and single cellular eukaryotes. The complementarity between the fractions is also reflected by the distance between motile and sessile fractions in the NMDS plot (**Figure 3**).

We matched species observations obtained in the case study against the EASIN Catalog of Alien Species (<https://easin.jrc.ec.europa.eu/easin/Catalogue>) as well as the AquaNIS database (Olenin et al., 2014) and identified 16 non-indigenous species (NIS) that are either alien or cryptogenic in the region of detection (**Table 1**). Most of the NIS were tunicates, while all but one NIS were detected on the Greek ARMS. Such high numbers of NIS can be explained by the substantial biological invasion in the Eastern Mediterranean, as well as the placement of the Greek ARMS in a marina. In contrast, the low number of NIS on the Swedish ARMS can be explained by its placement in a Marine Protected Area. However, some NIS observations still need to be confirmed, either by taxonomic experts (e.g., in the case of *Botryllus* spp. in Greece) or by higher confidence estimates (e.g., in the case of *Ostraea angasi*). We also identified previously unknown NIS, as for example the first record of *Anteaeolidiella lurana* in the Eastern Mediterranean, a little-known nudibranch species which is suspected to have expanded its distribution range through shipping transport (Bariche et al., 2020).

## DISCUSSION

### Conclusions From the Case Study

Our results indicate that DMSO preservation does not impair the biological analysis, confirming earlier results by Ransome et al. (2017) who likewise found that DMSO is an appropriate preservative for estimating the sessile community in ARMS. Importantly, DMSO samples can be shipped across the network more easily. For this reason, all samples in ARMS-MBON are preserved in DMSO following the protocol of Seutin et al. (1991).

The low overlap between the communities identified by image and genetic analysis (**Figure 3**) demonstrates the strengths and weaknesses of both conventional and novel identification methods, while it also indicates how these methods complement each other. Genetic identifications are usually confined by incomplete reference libraries (Hestetun et al., 2020), while image-based identifications are confined by the available taxonomic expertise and image resolution. These limitations decline as genetic and image reference libraries continue to grow and computational image-based identification methods improve in the coming years. This will likely result in an increased number of identified species from ARMS.

Our case study shows that ARMS are well suited for hard-bottom monitoring as they provide standardized genetic data that can be continuously enriched and re-analyzed to document benthic community composition, obtain quantitative estimates from image analysis, and detect non-indigenous species. Although the species composition measured by ARMS might not always accurately reflect the biotic composition of surrounding natural substrates due to e.g., selective effects of the

substrate (Chase et al., 2016; Sanabria-Fernandez et al., 2018), the standardized method still allows for comparative studies of species assemblages across broad spatial and temporal scales.

### Application Potential of the Observatory Network

ARMS-MBON membership is open to new partners who may register through the program website ([www.arms-mbon.eu](http://www.arms-mbon.eu)), although support from central services provided by the European Marine Biological Resource Centre (EMBRC) may be subject to eligibility and availability of resources. Any new partner is expected to set up and maintain at least one observatory in coastal waters and follow the methods and protocols for sampling and sample processing. Partners will also be able to further develop and customize any of the current protocols and drive the scientific application of the data generated by the network. Examples include adaptation of the sampling design to collect data for descriptors in the Marine Strategy Framework Directive (MSFD). As an example, Descriptor 2 (D2) of the MSFD directs EU member states to develop monitoring schemes and management strategies to keep non-indigenous species (NIS) introduced by human activities at levels that do not adversely alter the ecosystems. Given that ports and marinas constitute major introduction hotspots and dispersion pathways for NIS (Ulman et al., 2017), the establishment of ARMS-MBON observatories in such environments is expected to enhance the timely detection of new NIS across the European regional seas. So far, at least nine observatories in the network are deploying ARMS for this purpose, while at least four observatories are part of national MSFD monitoring schemes in Sweden, Denmark, Greece, and Spain.

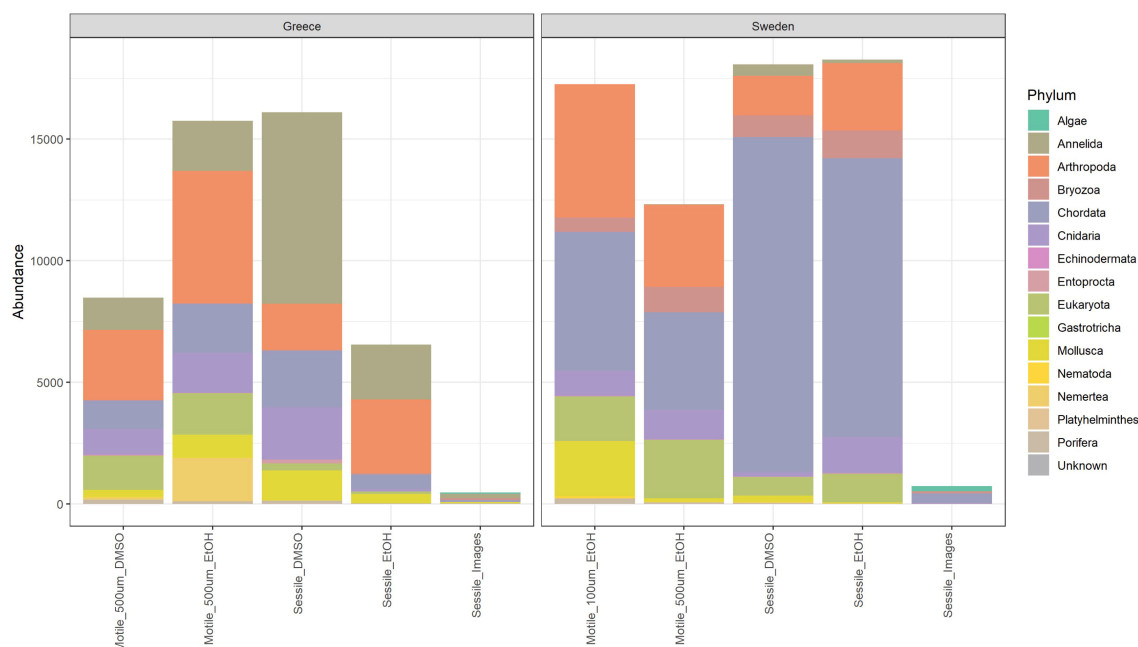
Another potential application area is the collection of data for calculating Essential Biodiversity Variables (EBV), as suggested by Kissling et al. (2018). EBVs emphasize standardized repeated measures of the same community in the same location at short to long time intervals required for reporting biodiversity change (Pereira et al., 2013). In the future, ARMS-MBON time-series data should be tested for such applications in EBVs.

Presence surveys provided by ARMS-MBON can provide occurrence data for prioritized taxa, including the AZTI Marine Biotic Index (Borja and Muxika, 2005) and Non-indigenous species (NIS). Finally, species traits can be derived from plate images recording the prevalence or relative composition of calcifying species or filter-feeding groups that might indicate important trends in ocean acidification or nutrient levels.

### Long-Term Sustainability and Integration

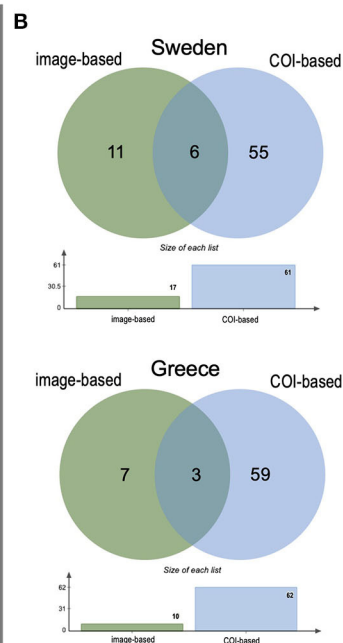
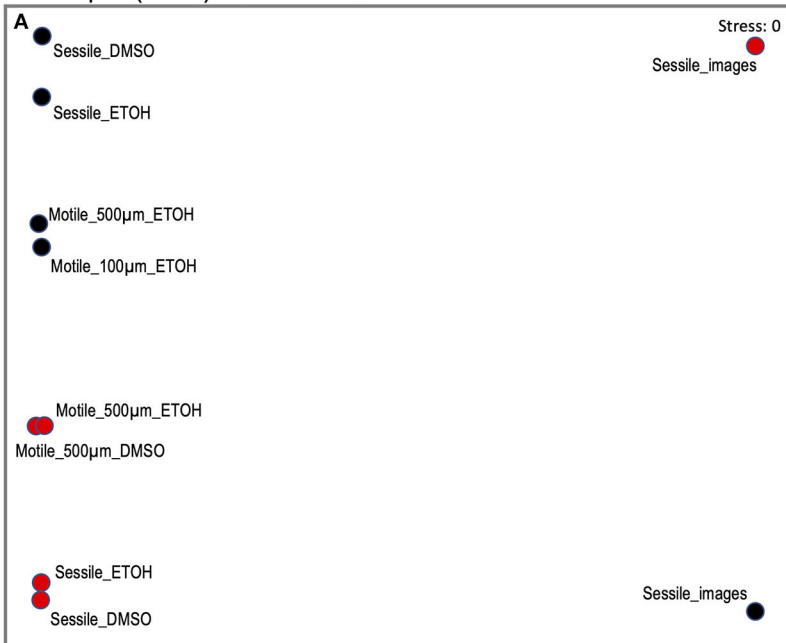
The ambition of ARMS-MBON is to maintain the current network and expand the coverage of the observatories with, spatially and temporally, more dense sampling events. The sustainability of the initiative as a long-term monitoring and observation asset needs to be ensured in as many sites as possible. This will be partly achieved by support from the European Marine Biological Resource Centre (EMBRC-ERIC), which provides access to marine biodiversity, ecosystems, experimental facilities, and expertise to facilitate research using marine organisms ([www.embrc.eu](http://www.embrc.eu)). As Europe's research infrastructure





**FIGURE 2 |** Bar chart showing the relative abundances of the main taxa based on the COI gene and image analysis, at the phylum level, across the different fractions of two ARMS (Greece ARMS: Crete\_1HERP\_180928-190128, Sweden ARMS: Koster\_VH2\_180418-180906).

### NMDS plot (Class) ● Sweden ● Greece



**FIGURE 3 |** Overview over variance and overlaps in composition of communities obtained from different fractions, preservations, as well as from plate images of two ARMS (Greece ARMS: Crete\_1HERP\_180928-190128, Sweden ARMS: Koster\_VH2\_180418-180906). **(A)** Non-metric Multi-dimensional Scaling (NMDS) plot at class level deduced from COI sequence and image analysis. **(B)** Venn diagram showing the overlap in the species identified from genetic data and images.

**TABLE 1 |** List of identified non-indigenous species (NIS) resulting from matching the complete species lists from two samples (Greece ARMS: Crete\_1HERP\_180928-190128, Sweden ARMS: Koster\_VH2\_180418-180906) against EASIN and AquaNIS databases.

Species	NIS status	Taxon	Source	Sequence reads	Confidence	ARMS
<i>Clytia linearis</i> (as <i>C. hemisphaerica</i> )	AL	Hydrozoa	ERR13:415770.613156	1	1.00	Greece
<i>Cephalothrix simula</i>	CR	Nemertea	ERR6:336120.637271	380	1.00	Greece
<i>Bugula neritina</i>	CR	Bryozoa	ERR3:1130880.648428	17	1.00	Greece
<i>Bugulina stolonifera</i> (as <i>Bugula stolonifera</i> )	CR	Bryozoa	ERR4:1011990.601062	30	1.00	Greece
<i>Amphibalanus amphitrite</i>	CR	Crustacea	ERR3:111700.649742	321	1.00	Greece
<i>Balanus trigonus</i>	AL	Crustacea	ERR9:501910.609480	32	1.00	Greece
<i>Monocorophium acherusicum</i>	CR	Crustacea	ERR5:433720.605205	96	1.00	Greece
<i>Ostrea angasi</i> (as <i>Ostrea angasi</i> )	AL	Mollusca	ERR15:100740.616292	110	0.59	Sweden
<i>Anteaeolidiella lurana</i>	CR	Mollusca	ERR3:1097540.663621	56	1.00	Greece
<i>Pinctada imbricata radiata</i> (as <i>Pinctada radiata</i> )	AL	Mollusca	Image	NA	NA	Greece
<i>Botryllus schlosseri</i>	CR	Tunicata	ERR3:1093300.604240	97	1.00	Greece
<i>Asciidiella aspersa</i>	AL	Tunicata	Image	NA	NA	Greece
			ERR16:281940.641233	6	1.00	
<i>Ciona robusta</i>	AL	Tunicata	Image	NA	NA	Greece
<i>Clavelina lepadiformis</i>	CR	Tunicata	Image	NA	NA	Greece
<i>Herdmania momus</i>	AL	Tunicata	ERR3:387270.604124	15	1.00	Greece
<i>Phallusia nigra</i>	AL	Tunicata	Image	NA	NA	Greece

AL, alien species; CR, cryptogenic species; NA, Non-applicable. Non-accepted names in the PEMA output were replaced with accepted synonyms.

(RI) for accessing and studying marine biodiversity, and with a functional lifespan of at least 20 years, EMBRC can offer a solid base for the long-term support of the ARMS-MBON for eligible partners in Europe.

EMBRC is currently developing an “Omics Observation network” to be deployed across its 9 member states, which is expected to cover pelagic and benthic sampling. Through the network of RIs in Europe, EMBRC will also work to develop new bioinformatics tools and analysis pipelines with its partners, such as ELIXIR and LifeWatch. The ambition is to ensure integration of ARMS-MBON (the European pilot described in this paper) into global efforts, such as the Global ARMS Program ([www.oceanarms.org](http://www.oceanarms.org)), Genomic Observatories Network (Davies et al., 2014), Global Omics Observatory Network GLOMICON (Buttigieg et al., 2019), as well as regional infrastructure networks in other regions, such as those under the umbrella of the World Association of Marine Stations (IOC) or the Partnership for Observation of the Global Ocean (POGO) to expand the ARMS-MBON further in the future.

The EMBRC “Omics Observatory” aims to ensure long-term, sustainable observation of marine biodiversity, integrated in a global setting. As such, the European research infrastructure can support the ARMS-MBON by providing increased visibility of the initiative to researchers and stakeholders in Europe and beyond. It will provide a platform for training and maintaining standards in the network, as well as expanding the coverage by integrating new sites from EMBRC. Furthermore, it is likely that the coordination and sequencing costs of the ARMS-MBON sites in EMBRC can be covered by its “Omics Observatory,” ensuring data collection from these sites for the foreseeable future. Such an initiative provides an important demonstration

and prototype for mainstreaming biodiversity observations at the molecular level into biodiversity monitoring programs and supports efforts led by a merger of the Genomic Observatories Network and GLOMICON (<https://glomicon.org/>) to establish an “Omics BON” (Buttigieg et al., 2019).

## DATA AVAILABILITY STATEMENT

The datasets presented in this study can be found in the Integrated Marine Information System (IMIS) datasets catalog under the following address: <http://www.assembleplus.eu/information-system?module=dataset&dasiid=6405>. The names of the repository/repositories and accession number(s) can also be found in the article/Supplementary Material.

## AUTHOR CONTRIBUTIONS

MO, CP, KE, and CA conceived the paper. MO coordinated the network. KE coordinated the data management. CP coordinated the sample processing and sequencing. All authors have contributed in an equal manner to the presented results in this paper and also revised the manuscript.

## FUNDING

This ARMS-MBON network is funded by the infrastructure programs ASSEMBLE Plus (grant no. 730984) and the European Marine Biological Resource Centre, EMBRC. Both programs establish and maintain the core network and provide services and consultation for deployment, sample processing, sequencing,

data management, and analysis. Funding for ARMS observatories in the North Sea Region was provided by the INTERREG project GEANS (North Sea Program of the European Regional Development Fund of the European Union) and the Swedish Agency for Marine and Water Management (grant no. 3181-2019), and the Flanders LifeWatch contribution (Research Foundation Flanders grant I000819N). The ARMS observatory in Roscoff also received support from the Aquanis 2.0 project (FONDATION Total). Data management and analysis was funded by Swedish LifeWatch grant from the Swedish Research council (grant no. 2017-00634) as well as the EOSC NORDIC project (grant no. 857652). Guiding documents to obtain ABS clearance for access to genetic resources were developed in the framework of projects INTERREG EBB (EAPA\_501/2016) and H2020 EOSC-Life (grant no. 824087).

## ACKNOWLEDGMENTS

We thank the LifeWatch ERIC and the Global ARMS Program for the helpful advice, especially Laetitia Plaisance at the Smithsonian Institution in Washington D.C. The ECIMAT Marine Station would like to thank Alberto Meizoso and Guillermo Díaz-Agras (Marine Biology Station of A Graña, University of Santiago de Compostela), Enrique Poza, Roberto Gómez and José González for their help on ARMS construction and deployment, and Prof. Pedro Gomes, Prof. Filipe Costa (CBMA, University of Minho) for help with sampling and lab processing and technical support. The MBA wish to thank John Bishop and Christine Wood for sample processing and technical support. HCMR thanks Argyro Zenetos for help confirming

of NIS observations. We are grateful to the participants of JRA5 (Scientific Diving) of the AssemblePlus program for their support in ARMS deployment in several of our observatories. The project is an activity of the Genomic Observatories network. We wish to remember Dawn Field, who founded both the Genomics Standards Consortium and the Genomic Observatories. JT was supported by a Marie Skłodowska-Curie Individual Fellowship (IF) under contract number 797387. This is publication ISEM 2020–283.

## SUPPLEMENTARY MATERIAL

The Supplementary Material for this article can be found online at: <https://www.frontiersin.org/articles/10.3389/fmars.2020.572680/full#supplementary-material>

**Supplementary Table 1** | Overview of observatories and sample events of the ARMS-MBON pilot phase.

**Supplementary Table 2** | Overview of genetic data generated during the ARMS-MBON pilot phase.

**Supplementary Table 3** | Output file consisting of seven spreadsheets showing the results of the sequence analysis of two samples (Greece ARMS: Crete\_1HERP\_180928-190128, Sweden ARMS: Koster\_VH2\_180418-180906) with ASV relative abundances across the various fractions and taxonomic assignments. Confidence estimates are provided for ASV and after each taxonomic level. Assignments with confidence estimates lower than 0.20 were not included in the statistical analysis and the lowest taxonomic level with higher confidence estimate was used instead. The eighth sheet (named “image-based observations”) shows the results of the manual species identification from image data, with measures of abundance and reference to the ARMS plate of origin.

**Supplementary Material** | Explanation of the ARMS-MBON data formats.

## REFERENCES

- Abarenkov, K., Tedersoo, L., Nilsson, R. H., Vellak, K., Saar, I., Veldre, V., et al. (2010). PlutoF—a web based workbench for ecological and taxonomic research, with an online implementation for fungal ITS sequences. *Evol. Bioinform.* 6, 189–196. doi: 10.4137/EBO.S6271
- Amid, C., Alako, B. T. F., Kadhivelu, V. B., Burdett, T., Burgin, J., Fan, J., et al. (2020). The European Nucleotide Archive in 2019. *Nucleic Acids Res.* 48, D70–D76. doi: 10.1093/nar/gkz1063
- Bariche, M., Al-Mabruk, S. A. A., Ates, M. A., Buyuk, A., Crocetta, F., Dritsas, M., et al. (2020). New alien Mediterranean biodiversity records (March 2020). *Mediterr. Mar. Sci.* 21, 129–145. doi: 10.12681/mms.21987
- Bean, T. P., Greenwood, N., Beckett, R., Biermann, L., Bignell, J. P., Brant, J. L., et al. (2017). A review of the tools used for marine monitoring in the UK: Combining historic and contemporary methods with modeling and socioeconomics to fulfill legislative needs and scientific ambitions. *Front. Mar. Sci.* 4, 263. doi: 10.3389/fmars.2017.00263
- Beisiegel, K., Darr, A., Gogina, M., and Zettler, M. L. (2017). Benefits and shortcomings of non-destructive benthic imagery for monitoring hard-bottom habitats. *Mar. Pollut. Bull.* 121, 5–15. doi: 10.1016/j.marpolbul.2017.04.009
- Bevilacqua, S., Katsanevakis, S., Micheli, F., Sala, E., Rilov, G., Sarà, G., et al. (2020). The status of coastal benthic ecosystems in the Mediterranean Sea: evidence from ecological indicators. *Front. Mar. Sci.* 7, 475. doi: 10.3389/fmars.2020.00475
- Bianchi, C. N., Pronzato, R., Cattaneo-Vietti, R., Benedetti-Cecchi, L., Morri, C., Pansini, M., et al. (2004). “Mediterranean marine benthos: a manual of methods for its sampling and study,” in *Biologia Marina Mediterranea*, Vol. 11, eds M. C. Gambi, M. Dappiano (Genoa: SIBM), 185–216.
- Borja, A., Elliott, M., Andersen, J. H., Berg, T., Carstensen, J., Halpern, B. S., et al. (2016). Overview of integrative assessment of marine systems: the ecosystem approach in practice. *Front. Mar. Sci.* 3, 20. doi: 10.3389/fmars.2016.00020
- Borja, A., and Muxika, H. (2005). Guidelines for the use of AMBI (AZTI's Marine Biotic Index) in the assessment of the benthic ecological quality. *Mar. Pollut. Bull.* 50, 787–789. doi: 10.1016/j.marpolbul.2005.04.040
- Bourlat, S. J., Borja, A., Gilbert, J., Taylor, M. I., Davies, N., Weisberg, S. B., et al. (2013). Genomics in marine monitoring: new opportunities for assessing marine health status. *Mar. Pollut. Bull.* 74, 19–31. doi: 10.1016/j.marpolbul.2013.05.042
- Buttigieg, P. L., Janssen, F., Macklin, J., and Pitz, K. (2019). The Global Omics Observatory Network: Shaping standards for long-term molecular observation. *Biodivers. Inf. Sci. Stand.* 3, e36712. doi: 10.3897/biss.3.36712
- Cahill, A. E., Pearman, J. K., Borja, A., Carugati, L., Carvalho, S., Danovaro, R., et al. (2018). A comparative analysis of metabarcoding and morphology-based identification of benthic communities across different regional seas. *Ecol. Evol.* 8, 8908–8920. doi: 10.1002/ece3.4283
- Chase, A. L., Dijkstra, J. A., and Harris, L. G. (2016). The influence of substrate material on ascidian larval settlement. *Mar. Pollut. Bull.* 106, 35–42. doi: 10.1016/j.marpolbul.2016.03.049
- Couton, M., Comtet, T., Le Cam, S., Corre, E., and Viard, F. (2019). Metabarcoding on planktonic larval stages: an efficient approach for detecting and investigating life cycle dynamics of benthic aliens. *Manag. Biol. Invasion* 10, 657–689. doi: 10.3391/mbi.2019.10.4.06
- Dailianis, T., Smith, C. J., Papadopoulou, N., Gerovasileiou, V., Sevastou, K., Bekkby, T., et al. (2018). Human activities and resultant pressures on key

- European marine habitats: an analysis of mapped resources. *Mar. Pol.* 98, 1–10. doi: 10.1016/j.marpol.2018.08.038
- Danovaro, R., Carugati, L., Berzano, M., Cahill, A. E., Carvalho, S., Chenuil, A., et al. (2016). Implementing and innovating marine monitoring approaches for assessing marine environmental status. *Front. Mar. Sci.* 3:213. doi: 10.3389/fmars.2016.00213
- David, R., Uyarra, M. C., Carvalho, S., Anlauf, H., Borja, A., Cahill, A. E., et al. (2019). Lessons from photo analyses of Autonomous Reef Monitoring Structures as tools to detect (bio-)geographical, spatial, and environmental effects. *Mar. Pollut. Bull.* 141, 420–429. doi: 10.1016/j.marpolbul.2019.02.066
- Davies, N., Field, D., Amaral-Zettler, L., Clark, M. S., Deck, J., Drummond, A., et al. (2014). The founding charter of the Genomic Observatories Network. *Gigascience* 3, 2. doi: 10.1186/2047-217X-3-2
- Exter, K., Decruw, C., Portier, M., Gerovasileiou, V., Pavloudi, C., and Obst, M. (2020). Genomics Observatory Use-Case: the challenge to standardise image and sequence data to Darwin Core format. *Biodivers. Inf. Sci. Stand.* 4, e58938. doi: 10.3897/biss.4.58938
- Gobin, J. F., and Warwick, R. M. (2006). Geographical variation in species diversity: a comparison of marine polychaetes and nematodes. *J. Exp. Mar. Biol. Ecol.* 330, 234–244. doi: 10.1016/j.jembe.2005.12.030
- Guidi, L., Guerra, A. F., Canchaya, C., Curry, E., Foglini, F., Irissou, J.-O., et al. (2020). “Big data in marine science,” in *Future Science Brief 6 of the European Marine Board*, eds B. Alexander, J. J. Heymans, A. Muñiz Piniella, P. Kellett, J. Coopman (Ostend: European Marine Board), 1–52. doi: 10.5281/zenodo.3755793
- HELCOM (2013). *HELCOM ALIENS 2- Non-Native Species Port Survey Protocols, Target Species Selection and Risk Assessment Tools for the Baltic Sea*, 34.
- Hestetun, J. T., Bye-Ingebrigtsen, E., Nilsson, R. H., Glover, A. G., Johansen, P. O., and Dahlgren, T. G. (2020). Significant taxon sampling gaps in DNA databases limit the operational use of marine macrofauna metabarcoding. *Mar. Biodivers.* 50, 70. doi: 10.1007/s12526-020-01093-5
- Kelly, R. P., Closek, C. J., O'Donnell, J. L., Kralj, J. E., Shelton, A. O., and Samhour, J. F. (2017). Genetic and manual survey methods yield different and complementary views of an ecosystem. *Front. Mar. Sci.* 3:283. doi: 10.3389/fmars.2016.00283
- Kissling, W. D., Ahumada, J. A., Bowser, A., Fernandez, M., Fernandez, N., Garcia, E. A., et al. (2018). Building essential biodiversity variables (EBVs) of species distribution and abundance at a global scale. *Biol. Rev.* 93, 600–625. doi: 10.1111/brev.12359
- Leray, M., and Knowlton, N. (2015). DNA barcoding and metabarcoding of standardized samples reveal patterns of marine benthic diversity. *Proc. Natl. Acad. Sci. U. S. A.* 112, 2076–2081. doi: 10.1073/pnas.1424997112
- Lotze, H. K., Lenihan, H. S., Bourque, B. J., Bradbury, R. H., Cooke, R. G., Kay, M. C., et al. (2006). Depletion, degradation, and recovery potential of estuaries and coastal seas. *Science* 312, 1806–1809. doi: 10.1126/science.1128035
- Meiklejohn, K. A., Damaso, N., and Robertson, J. M. (2019). Assessment of BOLD and GenBank - their accuracy and reliability for the identification of biological materials. *PLoS ONE* 14:e217084. doi: 10.1371/journal.pone.0217084
- Menge, B. A., Sanford, E., Daley, B. A., Freidenburg, T. L., Hudson, G., and Lubchenko, J. (2002). Inter-hemispheric comparison of bottom-up effects on community structure: insights revealed using the comparative-experimental approach. *Ecol. Res.* 17, 1–16. doi: 10.1046/j.1440-1703.2002.00458.x
- Olenin, S., Narščiū, A., Minchin, D., David, M., Galil, B., Gollasch, S., et al. (2014). Making non-indigenous species information systems practical for management and useful for research: an aquatic perspective. *Biol. Conserv.* 173, 98–107. doi: 10.1016/j.biocon.2013.07.040
- OSPAR (2009). *Trend Analysis of Maritime Human Activities and Their Collective Impact on the OSPAR Maritime Area*, 443. ISBN: 978-1-906840-83-9.
- Pearman, J. K., Anlauf, H., Irigoien, X., and Carvalho, S. (2016). Please mind the gap - visual census and cryptic biodiversity assessment at central Red Sea coral reefs. *Mar. Environ. Res.* 118, 20–30. doi: 10.1016/j.marenvres.2016.04.011
- Pearman, J. K., Leray, M., Villalobos, R., Machida, R. J., Berumen, M. L., Knowlton, N., et al. (2018). Cross-shelf investigation of coral reef cryptic benthic organisms reveals diversity patterns of the hidden majority. *Sci. Rep.* 8:8090. doi: 10.1038/s41598-018-26332-5
- Pereira, H. M., Ferrier, S., Walters, M., Geller, G. N., Jongman, R. H. G., Scholes, R. J., et al. (2013). Essential biodiversity variables. *Science* 339, 277–278. doi: 10.1126/science.1229931
- Ransome, E., Geller, J. B., Timmers, M., Leray, M., Mahardini, A., Sembiring, A., et al. (2017). The importance of standardization for biodiversity comparisons: a case study using autonomous reef monitoring structures (ARMS) and metabarcoding to measure cryptic diversity on Moorea coral reefs, French Polynesia. *PLoS One* 12:e0175066. doi: 10.1371/journal.pone.0175066
- Richardson, A. J., and Poloczanska, E. S. (2008). Ocean science - Under-resourced, under threat. *Science* 320, 1294–1295. doi: 10.1126/science.1156129
- Rockström, J., Steffen, W., Noone, K., Persson, A., Chapin, F. S., Lambin, E. F., et al. (2009). A safe operating space for humanity. *Nature* 461, 472–475. doi: 10.1038/461472a
- Sanabria-Fernandez, J. A., Lazzari, N., Riera, R., and Becerro, M. A. (2018). Building up marine biodiversity loss: artificial substrates hold lower number and abundance of low occupancy benthic and sessile species. *Mar. Environ. Res.* 140, 190–199. doi: 10.1016/j.marenvres.2018.06.010
- Seutin, G., White, B. N., and Boag, P. T. (1991). Preservation of avian blood and tissue samples for DNA analyses. *Can. J. Zool.-Rev. Can. Zool.* 69, 82–90. doi: 10.1139/z91-013
- Tanhua, T., Pouliquen, S., Hausman, J., O'Brien, K., Bricher, P., de Bruin, T., et al. (2019). Ocean FAIR data services. *Front. Mar. Sci.* 6, 440. doi: 10.3389/fmars.2019.00440
- Ulman, A., Ferrario, J., Occhipinti-Ambrogi, A., Arvanitidis, C., Bandi, A., Bertolino, M., et al. (2017). A massive update of non-indigenous species records in Mediterranean marinas. *PeerJ* 5, e3954. doi: 10.7717/peerj.3954
- van der Loos, L., and Nijland, R. (2020). Biases in bulk: DNA metabarcoding of marine communities and the methodology involved. *Mol. Ecol.* doi: 10.1111/mec.15592. [Epub ahead of print].
- Viard, F., Roby, C., Turon, X., Bouchemousse, S., and Bishop, J. (2019). Cryptic diversity and database errors challenge non-indigenous species surveys: an illustration with *Botrylloides* spp. in the English Channel and Mediterranean Sea. *Front. Mar. Sci.* 6:615. doi: 10.3389/fmars.2019.00615
- Weigand, H., Beermann, A. J., Ciampor, F., Costa, F. O., Csabai, Z., Duarte, S., et al. (2019). DNA barcode reference libraries for the monitoring of aquatic biota in Europe: gap-analysis and recommendations for future work. *Sci. Total Environ.* 678, 499–524. doi: 10.1016/j.scitotenv.2019.04.247
- Worm, B., Barbier, E. B., Beaumont, N., Duffy, J. E., Folke, C., Halpern, B. S., et al. (2006). Impacts of biodiversity loss on ocean ecosystem services. *Science* 314, 787–790. doi: 10.1126/science.1132294
- Zafeiropoulos, H., H. Q., Viet, K., Vasileiadou, A., Potirakis, C., Arvanitidis, P., et al. (2020). PEMA: from the raw.fastq files of 16S rRNA and COI marker genes to the (M)OTU-table, a thorough metabarcoding analysis. *GigaScience* 9, 1–12. doi: 10.1093/gigascience/giaa022

**Conflict of Interest:** The authors declare that the research was conducted in the absence of any commercial or financial relationships that could be construed as a potential conflict of interest.

Copyright © 2020 Obst, Exter, Allcock, Arvanitidis, Axberg, Bustamante, Cancio, Carreira-Flores, Chatzinikolaou, Chatzigeorgiou, Chrismas, Clark, Comtet, Dailianis, Davies, Deneudt, de Cerio, Fortič, Gerovasileiou, Hablützel, Keklikoglou, Kotoulas, Lasota, Leite, Loisel, Lévêque, Levy, Malachowicz, Mavrič, Meyer, Mortelmans, Norkko, Pade, Power, Ramšak, Reiss, Solbakken, Staehr, Sundberg, Thyrning, Troncoso, Viard, Wenne, Yperifanou, Zbawicka and Pavloudi. This is an open-access article distributed under the terms of the Creative Commons Attribution License (CC BY). The use, distribution or reproduction in other forums is permitted, provided the original author(s) and the copyright owner(s) are credited and that the original publication in this journal is cited, in accordance with accepted academic practice. No use, distribution or reproduction is permitted which does not comply with these terms.





# The Importance of Surface Orientation in Biodiversity Monitoring Protocols: The Case of Patagonian Rocky Reefs

Gonzalo Bravo<sup>1,2</sup>, Juan Pablo Livore<sup>1\*</sup> and Gregorio Bigatti<sup>1,2,3</sup>

<sup>1</sup> Laboratorio de Reproducción y Biología Integrativa de Invertebrados Marinos, Centro Científico Tecnológico CONICET-CENPAT, Instituto de Biología de Organismos Marinos, Puerto Madryn, Argentina, <sup>2</sup> Facultad de Ciencias Naturales, Universidad Nacional de la Patagonia San Juan Bosco, Puerto Madryn, Argentina, <sup>3</sup> Universidad Espíritu Santo, Guayaquil, Ecuador

## OPEN ACCESS

### Edited by:

Juan Carlos Azofeifa-Solano,  
University of Costa Rica, Costa Rica

### Reviewed by:

Jeffrey Sibaja-Cordero,  
University of Costa Rica, Costa Rica  
Andrés Beita-Jiménez,  
Memorial University of Newfoundland,  
Canada

### \*Correspondence:

Juan Pablo Livore  
livore@cenpat-conicet.gob.ar

### Specialty section:

This article was submitted to  
Ocean Observation,  
a section of the journal  
Frontiers in Marine Science

**Received:** 30 June 2020

**Accepted:** 03 December 2020

**Published:** 23 December 2020

### Citation:

Bravo G, Livore JP and Bigatti G  
(2020) The Importance of Surface  
Orientation in Biodiversity Monitoring  
Protocols: The Case of Patagonian  
Rocky Reefs.  
Front. Mar. Sci. 7:578595.  
doi: 10.3389/fmars.2020.578595

Temperate rocky reefs in Atlantic Patagonia are productive areas that support a high diversity of invertebrates, algae, and fishes. Complex surface structures on rocky reefs offer a range of microhabitats, which in turn, lead to a broad variety of co-existing species. Despite their ecological importance and the ecosystem services they provide, Patagonian rocky reef habitats have received limited attention. Until now studies have not discerned nor consequently described the assemblages found on each of the different surface orientations, namely horizontal, vertical, overhang and cavefloor. During this study we developed a protocol for sampling different surface orientations on subtidal rocky reefs using georeferenced high-resolution photoquadrats. We described and compared the epibenthic assemblage of surface orientations on 7 rocky reefs within 1–25 m depth in a northern Patagonia gulf. A total of 70 taxa were identified (12 macroalgae, 44 invertebrates, 10 tunicates, and 4 fishes), which doubles the number of species previously reported for the area. Each surface orientation presented a different assemblage structure while species richness was higher on vertical surfaces. The overhang surfaces had the most distinct assemblage conformed by cnidarians, tunicates, sponges and the absence of algae. The average overall species richness increased with depth due to the increase of sponge and tunicate species. Our results highlight the need of including several surface orientations in rocky reef biodiversity monitoring. This study offers a protocol for large-scale programs aimed at monitoring changes in biodiversity, which is broadly accessible and will provide accurate information. With robust yet simple, non-destructive and relatively low-cost practices this protocol can adequately assess changes in marine habitats, which provide important ecosystem services.

**Keywords:** epibenthic survey, large-scale monitoring, photoquadrats, MBON, benthos, subtidal, Southwestern Atlantic

## INTRODUCTION

Rocky subtidal reefs are recognized as highly biodiverse and productive areas, particularly in temperate waters of the world where other types of communities, such as coral reefs are scarce or absent. These areas generally support communities dominated by macroalgae that are habitat forming species that provide shelter, food and substrate for a broad range of organisms in turn

sustaining high biodiversity and ecosystem services (Steneck et al., 2002; Worm et al., 2006). Some rocky shore subtidal areas, such as part of the Mediterranean, the NE Pacific or the coasts of Australia have been extensively studied for decades and a wealth of knowledge including ecological theories have developed from them (Dayton et al., 1984; Edgar and Stuart-Smith, 2009). Large-scale patterns have been described and changes in species distributions and community structure due to the rapidly changing climate have been detected and are being studied (e.g., Ling, 2008; Marzinelli et al., 2015). However, other parts of the world, with less resources, have received much less attention and what little is known generally derives from fragmented information of local scale studies.

The lack of basic biological knowledge may lead to well-intended but uninformed decisions by policymakers and the ensuing creation of marine protected areas that may not entirely serve the intended purpose (Carpenter et al., 2009; Leenhardt et al., 2015). There is, therefore, an urgent need to acquire data of under-sampled marine areas in order to collect baseline information that may allow the detection of changes in species composition due to environmental or anthropogenic stressors and to identify sites that are biodiversity hotspots. As part of the effort to monitor and understand changes in marine biodiversity as a consequence of anthropogenic stressors a range of biological and ecological Essential Ocean Variables (EOVs) and emerging EOVs have been proposed (Miloslavich et al., 2018). Monitoring of EOVs are intended to provide the scientific, governance and policy baselines against which anthropogenic driven effects may be measured and reported. This knowledge is needed for conservation and management of ecosystem functions and services of subtidal rocky reefs that are often overlooked. Long term monitoring programs, such as MBON (Marine Biodiversity Observation Network) Pole to Pole<sup>1</sup> which monitor biodiversity on rocky shores from the American continent, could be a way of coordinating activities that may fill local knowledge gaps whilst simultaneously providing broader scale information on the effects of global change.

Rocky reefs are unique habitats because of the presence of outcrops, crevices, small caves and other microhabitats that provide refuge for organisms that are only found in these environments (Witman and Dayton, 2001; Stephens et al., 2006; Galván et al., 2009). As in most parts of the world, in Atlantic Patagonia there is more knowledge about intertidal than subtidal habitats. Patagonian rocky reefs include large areas that remain largely unexplored regarding subtidal benthic life. These gaps of knowledge impede the detection of changes in local and regional biodiversity if they were occurring (Fraschetti et al., 2008; Halpern et al., 2008; Claudet and Fraschetti, 2010; Duffy et al., 2013). For example, chronic impact of diving tourism has already been detected on these reefs (Bravo et al., 2015) while unregulated fisheries has led to local depletion of certain species (Venerus et al., 2014). Hence, targeting these habitats for subtidal monitoring programs is useful to detect changes that may occur in the future due to rising sea-water temperature, the increase and severity of extreme weather events as well as anthropogenic

stressors that are on the rise (Harley et al., 2006; Hawkins et al., 2008; Wernberg et al., 2011; Cheung et al., 2012).

On land, ecologists have used emerging technologies such as remote sensing to establish ecological patterns which have been the baseline for comparison to determine the changes produced by changing climate or other stressors (Pan et al., 2013). However, marine ecologist attempting to describe patterns have consistently encountered time restriction problems which determines the number of samples (Bianchi et al., 2004; Murray et al., 2006). Subtidal sampling that involves SCUBA diving enhances this restriction and generally limits the extent of the studies. Developing technologies such as remotely operated underwater vehicles and autonomous underwater vehicles have been successfully used to describe large-scale patterns in subtidal habitats (Marzinelli et al., 2015). However, these technologies tend to be inaccessible for regions of the world with financial restrictions that are coincidentally poorly studied. Thus, emerging large-scale monitoring programs need to address these issues.

The effect of surface orientation on benthic communities has been observed in various parts of the world (for references see Miller and Etter, 2011) and studied using manipulative field experiments (e.g., Irving and Connell, 2002). Light intensity (Glasby, 1999; Miller and Etter, 2008), sedimentation (Irving and Connell, 2002), water flow (Leichter and Witman, 1997), predation pressure (Jones and Andrew, 1990; Andrew and Underwood, 1993), larvae settlement process (Saunders and Connell, 2001) and spatial refuge (Witman, 1985) are the main factors structuring the benthic assemblages on adjacent surfaces inclinations. Environmental variables that are correlated with depth also have an effect on benthic communities (Garrahou et al., 2002; Heyns et al., 2016). However, sampling protocols for monitoring benthic assemblages in subaquatic programs tend to focus mainly on horizontal benthic surfaces and ignore other microhabitats such as vertical surfaces, overhangs and cavefloors (but see Jørgensen and Gulliksen, 2001; Virgilio et al., 2006; Cárdenas and Montiel, 2015).

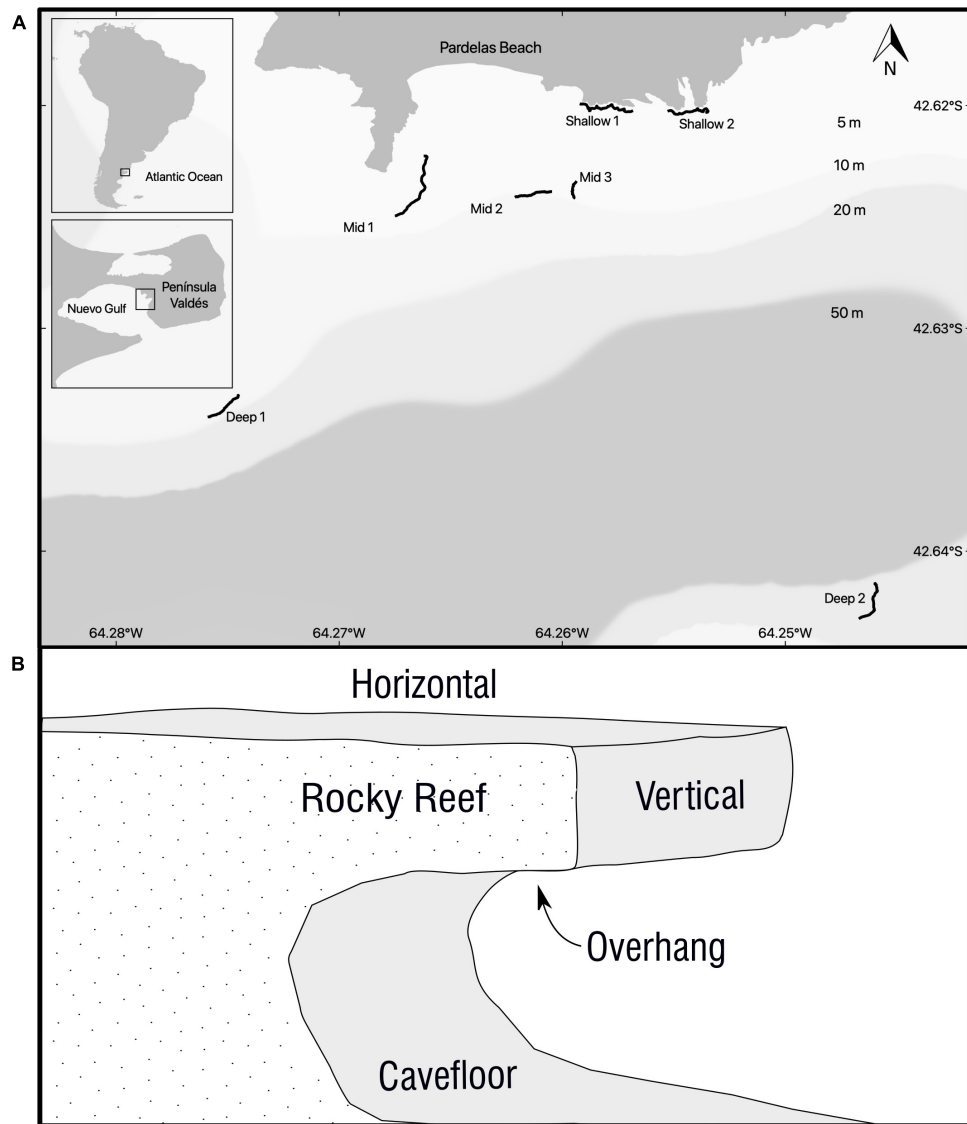
In this study, benthic rocky reef images from four contrasting surface orientations (horizontal, vertical, overhang, and cavefloor) at three different depth ranges were collected by SCUBA diving using georeferenced benthic digital images. Our goals were to: (a) determine and describe the species contribution to local assemblages of each surface orientation, (b) describe and compare species richness of each surface orientation among depths using the proposed method and (c) based on (a) and (b) propose a simple and comprehensive sampling protocol for large scale, long-term monitoring programs.

## MATERIALS AND METHODS

### Study Site

Seven rocky reefs grouped in an area of almost 11 km<sup>2</sup> were sampled off the coast of Punta Pardelas Bay (42° 37.737'S, 64° 15.739'W) inside Nuevo Gulf (**Figure 1A**) during March 2019. The region is considered as an ecotone of two marine biogeographic provinces (Argentinian and Magellanic), with

<sup>1</sup><https://marinebon.org/p2p/>



**FIGURE 1 | (A)** Study site, location and extension of all the rocky reefs sampled. Black lines are the GPS track of the rocky reefs ledges. **(B)** Diagram of a transversal view of a typical Patagonian rocky reefs where surface orientations (horizontal, vertical, overhang, and cavefloor) are represented.

both warm temperate and cold temperate species represented (Balech and Ehrlich, 2008). The tide regime is semidiurnal with a mean amplitude of 3.8 m and spring tides of up to 5.73 m. Hence, rocky reefs were sampled at three different depth ranges 1–7 m: “shallow rocky reefs” ( $n = 2$  reefs), 8–15 m: “mid depth rocky reefs” ( $n = 3$  reefs) and 16–25 m: “deep rocky reefs” ( $n = 2$  reefs) during the same week. Sedimentation traps (aspect ratio  $> 3$  as recommended by Hakanson et al., 1989), light loggers (Hobo MX2202), alabaster blocks (Jokiel and Morrissey, 1993) and temperature loggers (iButton type z) were deployed at each depth range during the time of the study to characterize the differences among depths (Table 1). Protocol is available on protocols.io<sup>2</sup>.

<sup>2</sup><https://www.protocols.io/view/simple-subtidal-rocky-reef-environmental-parameter-3vdgn26>

All rocky reefs were  $> 80$  m length and separated by at least 100 m (Figure 1A).

## Selection of Methods

Ledge borders were followed as underwater transects in all rocky reefs (Figure 1B). Photoquadrats (25 × 25 cm) spaced at 2–5 m intervals were taken by scuba diving. Preliminary test showed that a focal length of 50 cm, which in turn determined quadrat size, was the best to reduce the negative influence of water turbidity on the resolution of the image. The presence of cavities of 1.5–3 m high below the rocky ledges provided enough space to sample 4 different surface orientations, Figure 1B. On a preliminary study we determined that 80 photoquadrats (20 per surface orientation) represented 70% of the total richness. This

**TABLE 1** | Summary of physical variables measured at rocky reefs with different depth.

Rocky reef	Sedimentation (g m <sup>-2</sup> d <sup>-1</sup> ± SD)	Mean ± SD of daily max light intensity (LUX)	Alabaster blocks Diffusion factor ± SD	Mean ± SD of daily temperature range (°C)
Shallow	–	13,776.21 ± 5,272.72	6.03 ± 0.28	0.40 ± 0.20
Mid	16.81 ± 2.73	2,235.47 ± 2,779.37	4.38 ± 0.53	0.25 ± 0.16
Deep	4.63 ± 0.46	443.60 ± 570.10	4.03 ± 0.51	0.13 ± 0.09

Diffusion factor (DF) of alabaster blocks was calculated as Doty (1971).

replication could be obtained along transects of more than 100 m on 30' dives at the deepest rocky reef. Voucher samples were collected to confirm photo identifications when necessary. Divers were equipped with a Canon 100D camera and two Ikelite DS-161 strobes mounted on a stainless-steel structure with a 0.0625 m<sup>2</sup> quadrat (0.25 × 0.25 m). The camera had a 18–55 mm Canon lens and all the images were taken with the 18 mm setting, auto focus, ISO 400, Exposure 1/200 s at f/11 and flashes set on automatic TTL. A dive computer (Oceanic Geo2) was mounted on one side of the quadrat to register depth and temperature of each photoquadrat. Divers carried a monofilament line that towed a surface buoy with a GPS loading a waypoint every 3 seconds. Camera and GPS clocks were synchronized before each dive in order to georeference photographs by matching time.

## Image Analyses

Images were prepared for analysis using photo processing software (Adobe Lightroom Classic version: 9.1). All the images passed through the same workflow: (1) Georeferencing with the.gpx file; (2) registering depth, site and orientation data on photo's metadata; (3) white balance; (4) crop the area of interest (i.e., quadrat); and (5) lens distortion correction. Blurry or out of focus images were discarded.

All photos were uploaded to a public CoralNet source<sup>3</sup>, an open source and free software for benthic image analysis (Beijbom et al., 2015). Percentage cover of algae, sessile invertebrates and bare substrate was estimated by using a 100 point grid with 2.5 cm separation among points. When large mobile fauna covered points of the grid, those points were not considered for the cover estimation in each photo. On the same image the presence of mobile fauna larger than 2 cm was recorded for the creation of a presence-absence matrix. Species which were difficult to identify to low taxonomic levels by photo were grouped into a category or taxonomic group.

## Data Analyses

The dataset that resulted from photoquadrats analyses was divided into two matrices. A percentage cover matrix and presence-absence matrix. The latter uses species identities and was created by the combination of sessile and mobile taxa recorded in each photo.

Multivariate comparison of percentage cover of epibenthic community structure across reef surface orientations at each depth were visually inspected using non-metric Multi Dimensional Scaling (nMDS) ordinations and differences

were evaluated using Permutational Analysis of Variance (PERMANOVA,  $n = 999$ , Bray-Curtis dissimilarity,  $\log(x + 1)$  transformed data) followed by multiple comparisons using the function “pairwise.adonis” (Martinez Arbizu, 2017). Prior to PERMANOVA, multivariate dispersion homogeneity was tested using the “betadisper” function of the R package “vegan” (Oksanen et al., 2019). When PERMANOVA and “betadisper” are significant, differences may be due to factors (i.e., surface orientations), dispersion effects or both.

An Indicator Species Analysis (IndVal; Dufrêne and Legendre, 1997) was used to detect which taxa were indicative of each surface orientation. The “multipatt” function of the R package “Indispecies” using data from all depths (pooled). This function looks for indicator species based on the Indicator Value method as explained in De Cáceres et al. (2010), reflecting both the conditional probability of the taxa as an indicator of a particular surface orientation (A) and the probability of finding the taxa in samples from this surface orientation (B). High values in the component A indicate specificity or positive predictive value of the taxon as indicator of that surface orientation. High values of the component B indicate that the taxon occurs consistently in most photoquadrats within that surface orientation.

We analyzed the average number of species and cumulative richness of epibenthic assemblage from each surface orientation and depth using the R package “rich” (Rossi, 2011) with the presence-absence matrix as input. This package offers two functions “c2cv” and “c2m,” which allows the comparison of cumulative and average species richness, respectively, over two set of samples using randomization tests (Rossi, 2011). In contrast to standard parametric tests, randomization tests do not require distributional assumptions (Manly, 1991). Shared species between different surface orientations and depths were computed by the function “shared” of the same R package. Chao 2 estimation for the whole set of photoquadrats was calculated using the function “specpool” of the “Vegan” package (Oksanen et al., 2019). All plots and statistical analyses were carried out using R software V 3.6.2 (R Development Core Team, 2018).

## RESULTS

A total of 70 taxa were identified from 560 georeferenced photoquadrats covering more than 1,500 m of rocky reef ledge (Supplementary Table 1). The more diverse groups registered by photoquadrats were Mollusca, macroalgae, Ascidiacea, Porifera, Equinodermata, and Cnidaria. A lower diversity was found for Arthropoda, Annelida, Hydrozoa, Bryozoa, Brachiopoda, and Platyhelminthes. Some cryptic fishes were also recorded in the

<sup>3</sup><https://coralnet.ucsd.edu/source/1933/>



photoquadrats. The expected number of species estimated by Chao2 (71.99) for this study suggests that the majority of species were recorded (97%).

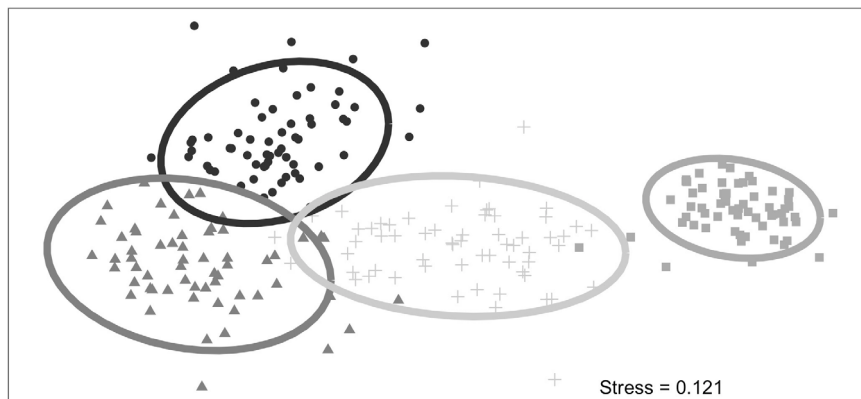
The nMDS ordination (**Figure 2**) showed that each surface orientation had a distinct assemblage. The separation

among epibenthic assemblages, in each surface orientation, increased with depth. Shallow assemblages show a small overlap of samples, particularly between vertical, horizontal and cavefloor surfaces (**Figure 2A**). This overlap is less pronounced and absent in mid depth and deep assemblages,

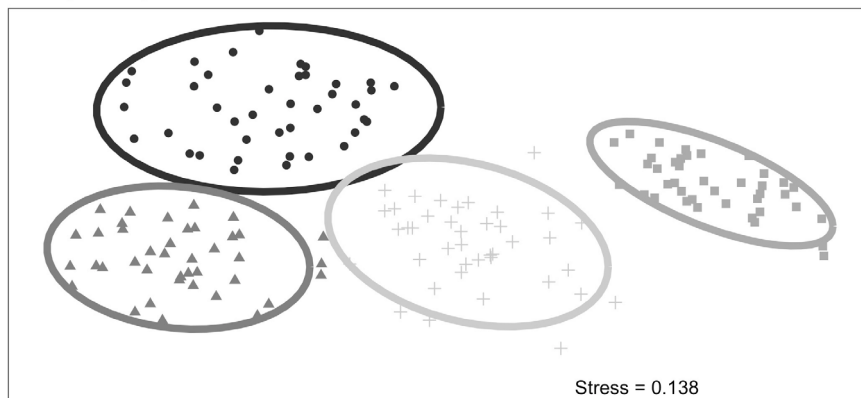
### A Shallow Rocky Reefs



### B Mid Rocky Reefs



### C Deep Rocky Reefs



Reef surface orientation    ● Cavefloor    ▲ Horizontal    ■ Overhang    + Vertical

**FIGURE 2 |** nMDS ordination plots of rocky reef surface orientation of epibenthic assemblage by depth (**A**) shallow, (**B**) mid, and (**C**) deep reefs. Ellipses represent 95% confidence interval. Based on Bray-Curtis distance metric and with log (x+1) transformed data.

respectively (Figures 2B,C). Pairwise comparisons (Table 2) indicated that all surface orientations had distinct epibenthic assemblages within each depth. However, only two surfaces combinations, horizontal/vertical and vertical/cavefloor, presented multivariate dispersion homogeneity throughout all depth ranges suggesting that differences were effectively due to factor and not dispersion.

Macroalgae covered on average 71% of horizontal surfaces, 40% of vertical surfaces, 20% of cavefloor surfaces and less than 1% of overhang surfaces. The most prevalent algal group on horizontal surfaces were filamentous algae (47%) composed primarily by *Anotrichium furcellatum* and *Ceramium* sp., which were identified by extractive vouchers. *Dyctyota dichotoma* was the second most prevalent alga (10%) followed by crustose coralline algae (4%). On the vertical surfaces average algal cover was ~40% followed by the anemone *Corynactis carnea* (32%), filter feeders such as the bivalve *Aulacomya atra* (4%) and sponges (4%). On the overhang surfaces suspension feeder cnidarians with 70% (*Corynactis carnea*, 62%, *Halcurias* sp. 7%, and *Anthothoe chilensis* 1%) and filter feeders with 24% (sponges 14%, *Aulacomya atra* 5%, rock boring bivalves 4%, and tunicates 1%) were the dominant groups. The highest percentage of bare substrate was found on cavefloor surfaces (65%) where a significant percentage of colonial tunicates was observed (5%). A decrease in macroalgal cover was recorded with higher depths for all orientations, while filter feeders became more abundant (Figure 3). On overhang surfaces percentage cover of filter

feeders (Porifera, tunicates, and bivalves) decreased with depth while suspension feeders increased.

A total of 31 sessile indicator taxa were identified, varying for overhang (10), cavefloor (8), horizontal (7), and vertical (6) surfaces (Table 3). The indicative taxa for overhang surfaces were 4 sponges, 2 anemones, 2 bivalves, 1 Brachiopoda (*Magellania venosa*), and 1 bryozoan. The indicative taxa in the cavefloor surfaces were mostly tunicates along with bare substrate, a sponge and tube worms. Macroalgae taxa were indicative from horizontal surfaces together with the tunicate *Diplosoma listerianum* and polychaeta Terebelidae. The vertical surfaces presented the lowest number of indicator taxa (2 algae, 2 sponges, 1 solitary tunicate, and 1 anemone) and all indicator indexes were below 0.56.

Average species richness of epibenthic communities increased with depth (Figure 4) and all depth ranges were significantly different from each other (Table 4). We found no differences in cumulative richness between deep (58) and mid (61) depth rocky reefs, but both were statistically different to shallow reefs (48) (Table 4). The sum of species observed between mid and deep reefs (67) represented 96% of the total number of species registered in this study and the mid depth shared the most species with the other two depths (Figure 5). Analysis of assemblages of a single surface orientation at different depths through a one-way PERMANOVA showed that each depth had a different assemblage for all surface orientations (Supplementary Table 2).

Vertical surfaces presented the highest species richness, ranging from 4 to 16 species by photoquadrat with a cumulative richness of 54, representing 77.14% of the total richness (Table 5). Average richness for this surface ( $9.06 \pm 0.19$  SE) was significantly higher than the other surfaces ( $p < 0.001$ ) (Figure 6). Horizontal surfaces with 1–14 species by sample (mean  $7.8 \pm 0.19$  SE) and 48 species in total had the second highest species richness. Among all the invertebrates species found using this protocol, four were recorded in a single photoquadrat. From these species, one was observed on the horizontal, one on the vertical, two on the overhang and three on the cavefloor surfaces exclusively, the other four were observed on at least two surfaces.

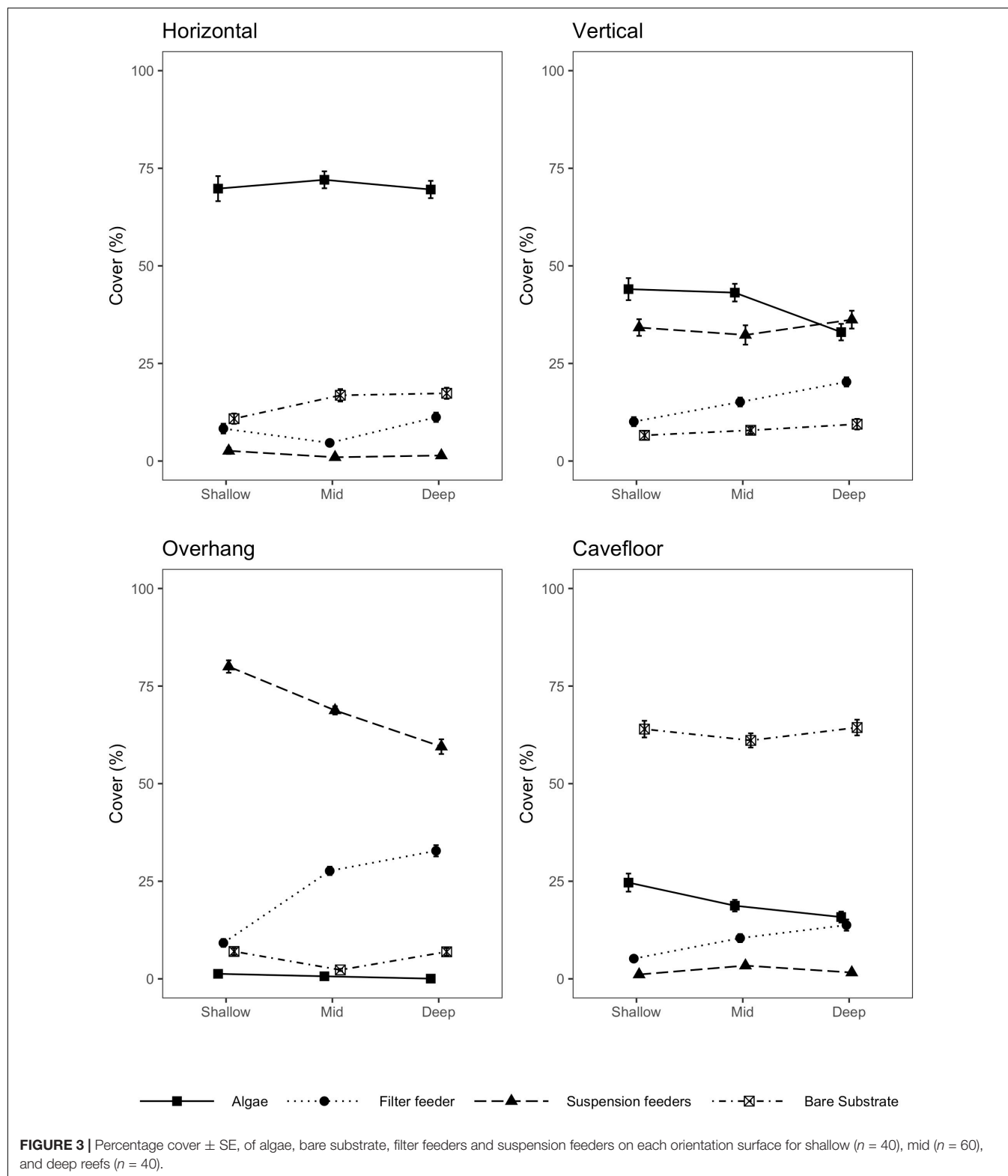
## DISCUSSION

This paper highlights the importance of sampling different surface orientations in subtidal monitoring programs as distinct epibenthic assemblages were associated to each orientation of the rocky reefs. In contrast with other similar approaches, the protocol proposed in this study simultaneously detected differences among rocky reef surface orientations and depths, whilst capturing 90% of the estimated species richness in a non-destructive manner. By sampling all available surfaces a more precise estimation of the local biodiversity can be achieved to detect temporal changes while monitoring rocky benthic assemblages. The georeferencing of photoquadrats used in our work provides the possibility of returning to specific places of the reef where an interesting feature was detected. Through this protocol that considers surface orientations, this study reports uncited species for the area such as *Halcurias* sp., *Darwinella* cf. *rosacea*, and calcareous sponges.

**TABLE 2 |** Multivariate tests used to detect differences between surface orientations among depths.

	PERMDISP		PERMANOVA		
	<i>P</i>	<i>SS</i>	<i>F</i>	<i>R</i> <sup>2</sup>	<i>p</i> -perm
<b>Shallow</b>					
Horizontal vs. Vertical	0.118	1.645	27.336	0.256	0.006**
Horizontal vs. Overhang	0.736	8.450	174.454	0.691	0.006**
Horizontal vs. Cavefloor	0.120	2.805	46.962	0.376	0.006**
Vertical vs. Overhang	0.007**	3.946	65.882	0.458	0.006**
Vertical vs. Cavefloor	0.999	3.946	58.545	0.429	0.006**
Overhang vs. Cavefloor	0.007**	8.761	157.386	0.669	0.006**
<b>Mid</b>					
Horizontal vs. Vertical	0.394	4.887	62.442	0.346	0.006**
Horizontal vs. Overhang	<0.001***	19.199	305.419	0.721	0.006**
Horizontal vs. Cavefloor	0.009**	4.484	61.388	0.342	0.006**
Vertical vs. Overhang	<0.001***	6.443	114.073	0.491	0.006**
Vertical vs. Cavefloor	0.379	5.829	87.441	0.426	0.006**
Overhang vs. Cavefloor	0.997	16.073	313.529	0.727	0.006**
<b>Deep</b>					
Horizontal vs. Vertical	0.521	5.294	73.784	0.486	0.006**
Horizontal vs. Overhang	<0.001***	14.408	242.490	0.757	0.006**
Horizontal vs. Cavefloor	0.691	8.556	165.107	0.679	0.006**
Vertical vs. Overhang	0.001***	3.275	46.933	0.376	0.006**
Vertical vs. Cavefloor	0.070	10.062	161.757	0.675	0.006**
Overhang vs. Cavefloor	<0.001***	13.535	271.392	0.777	0.006**

Bray-Curtis similarity with  $\log(x + 1)$  transformed data was used. The significance is indicated by asterisks \* $p < 0.05$ , \*\* $p < 0.01$ , \*\*\* $p < 0.001$ .



Our results indicate that all surfaces orientations must be contemplated in order to obtain high quality estimations of epibenthic biodiversity of coastal rocky reefs. Sampling all surface orientations increases the number of rare species that

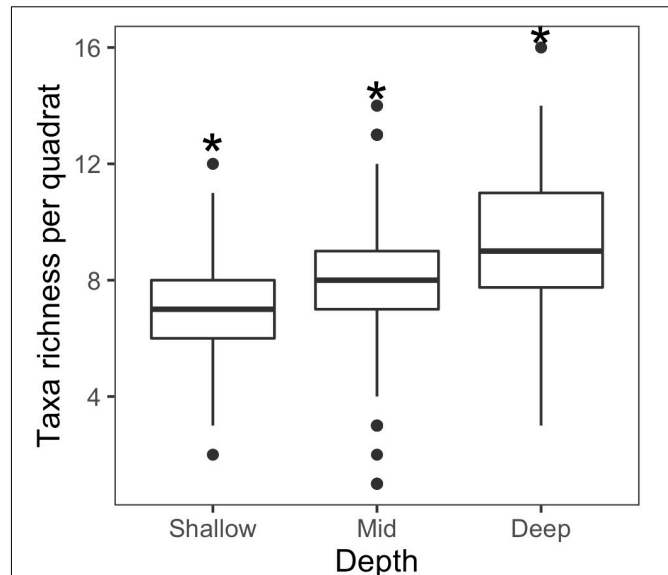
are normally difficult to detect. This also reduces the risk of not detecting species that may be limited to a specific microhabitat consequently giving more accuracy to richness estimations. When diving time restrictions impede sampling

**TABLE 3 |** Indicator value indices for each surface orientation within all depth.

Taxa	Indicator value index	A	B	p-value
<b>Horizontal</b>				
Macroalgae filamentous	0.73	0.533	1	0.001***
<i>Dictyota dichotoma</i>	0.714	0.729	0.7	0.001***
<i>Codium vermicularia/C. fragile</i>	0.601	0.904	0.4	0.001***
Brown encrusting algae	0.504	0.670	0.379	0.001***
<i>Ulva</i> sp.	0.469	0.669	0.329	0.001***
<i>Diplosoma listerianum</i>	0.447	0.754	0.264	0.001***
Terebellidae	0.319	0.491	0.207	0.001***
<b>Vertical</b>				
Crustose coralline algae	0.560	0.398	0.786	0.001***
Delesseriaceae	0.450	0.450	0.450	0.001***
Sponge tubular	0.410	0.462	0.364	0.001***
<i>Clathria</i> sp.	0.396	0.880	0.179	0.001***
<i>Ciona robusta</i>	0.228	0.912	0.057	0.001***
<i>Parabunodactis imperfecta</i>	0.216	0.819	0.057	0.004**
<b>Overhang</b>				
Sponge encrusting	0.862	0.754	0.986	0.001***
<i>Halcurias</i> sp.	0.854	0.992	0.736	0.001***
<i>Corynactis carnea</i>	0.798	0.637	1.000	0.001***
Sponge massive	0.662	0.653	0.671	0.001***
Rock boring bivalves	0.610	0.410	0.907	0.001***
<i>Aulacomys atra</i>	0.574	0.496	0.664	0.001***
Sponge repent	0.517	0.812	0.329	0.001***
Bryozoan	0.382	0.816	0.179	0.001***
<i>Darwinella cf. rosacea</i>	0.229	0.430	0.121	0.036*
<i>Magellania venosa</i>	0.180	0.565	0.057	0.016*
<b>Cavefloor</b>				
Bare substrate	0.831	0.690	1.000	0.001***
Colonial tunicate	0.714	0.700	0.729	0.001***
<i>Lissoclinum fragile</i>	0.402	0.515	0.314	0.001***
Sponge massive violet	0.342	0.632	0.186	0.001***
Tube worms	0.326	0.676	0.157	0.001***
<i>Ascidella aspersa</i>	0.323	0.488	0.214	0.001***
<i>Corella eumyota</i>	0.189	1.000	0.036	0.002**
<i>Paramolgula gregaria</i>	0.176	0.867	0.036	0.015*

A, the conditional probability of the taxa as an indicator of the surface orientation; B, the probability of finding the taxa in samples belonging to the surface orientation. Only significant taxa are included and significance is indicated by asterisks \* $p < 0.05$ , \*\* $p < 0.01$ , \*\*\* $p < 0.001$ .

all surfaces, horizontal and vertical orientations combined were the most efficient and comprehensive approach to capture species richness. This has also been suggested for algae and invertebrates of Mediterranean rocky shores where both vertical and horizontal surfaces better represented the spatial variability (Benedetti-Cecchi, 2001). Our study also identified strong associations between specific taxa and surface orientations which should be considered in studies aimed at describing those taxa. For example, overhang surfaces in our study showed a unique assemblage and the highest number of indicative sessile species. A great diversity of sponges was found in the overhang surface as has been previously observed in rocky reefs from other parts of the world (Preciado and Maldonado, 2005; Maldonado et al., 2016). Invertebrate

**FIGURE 4 |** Boxplot of species richness among shallow, mid, and deep reefs. The \* indicates  $p < 0.001$  obtained by randomization test.**TABLE 4 |** Results of comparison of cumulative species richness (c2cv) and mean species richness (c2m) by depth levels with randomization procedure.

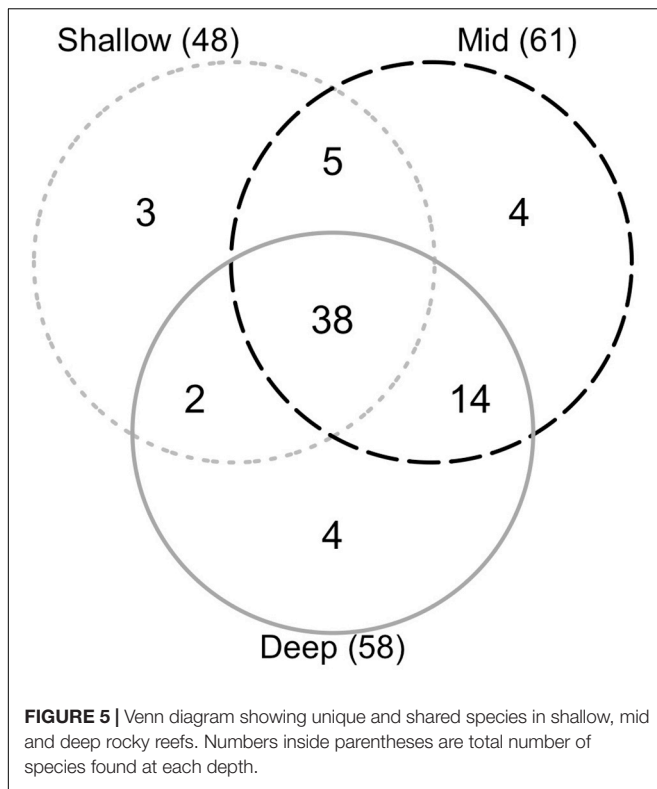
	cv1–cv2	c2cv (p-value)	mv1–mv2	c2m (p-value)
Shallow vs. Mid	–13	0.025**	–0.85	0.001***
Shallow vs. Deep	–10	0.011***	–2.15	0.001***
Mid vs. Deep	3	0.722	–1.30	0.001***

cv1–cv2 and mv1–mv2 represents the difference between observed cumulative and average richness, respectively, between community 1 and community 2. The significance is indicated by asterisks \* $p < 0.05$ , \*\* $p < 0.01$ , \*\*\* $p < 0.001$ .

assemblages were found to be richest on vertical surfaces which coincides with Witman et al. (2004) who on a global description of epibenthic species richness used rocky walls instead of horizontal surfaces. They found invertebrate richness ranged from 50 to 130 for rocky walls in Chile, South Africa and New Zealand that are similar to our results (Witman et al., 2004). Finally, three species of nudibranchs and one species of platyhelminth were exclusively found on cavefloor surfaces. This surface orientation presented an important cover of sponges and colonial tunicates which likely explain the presence of the nudibranchs and flat worm. Sea slugs for example, live in close association with their diets (Scoresby and Graham, 2013) and most of the species are carnivores that prey on sponges, tunicates, hydroids and bryozoans (Rudman and Bergquist, 2007).

Shade and low sedimentation surfaces support a larger number of sessile invertebrates (Irving and Connell, 2002) and benthic assemblage structure can vary along gradients of sedimentation (Naranjo et al., 1996). Therefore, the lower sedimentation rates and light intensity found on deeper reefs may explain the observed differences on the horizontal and cavefloor surfaces at varying depths. Sessile invertebrates were



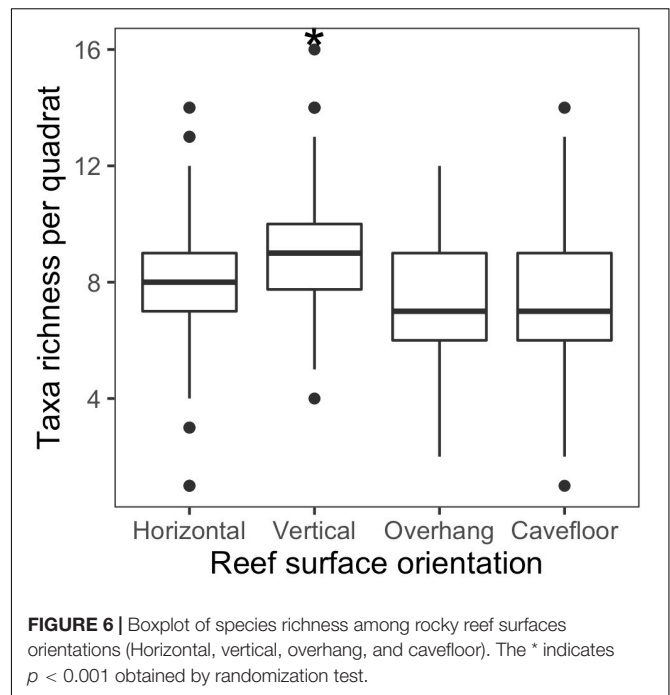


**TABLE 5 |** Species richness and shared species of benthic assemblage over rocky reefs surface orientations.

S = 70	Horizontal	Vertical	Overhang	Cavefloor
Horizontal	48 (68.57%)	41	27	37
Vertical	61	54 (77.14%)	36	38
Overhang	61	58	40 (57.14%)	28
Cavefloor	59	64	60	48 (68.57%)

On diagonal: observed species richness and in parentheses the corresponding ratio to the total number of species ( $S = 70$ ). Above diagonal: absolute number of species shared by orientation pairs. Below diagonal: the total number of species collected in orientation pairs.

more abundant in vertical and overhang surfaces as reported in other studies in Patagonian Magellan Strait (Cárdenas and Montiel, 2015). These results are consistent with studies from other latitudes that observed distinctions between horizontal and vertical rocky surface communities (Sebens, 1986; Baynes, 1999; Miller and Etter, 2011), between vertical and overhang surfaces (Virgilio et al., 2006; Cárdenas et al., 2012; Cárdenas and Montiel, 2015) and also between horizontal, vertical and overhang surfaces (Jørgensen and Gulliksen, 2001). The macroalgal richness in this study was well represented on horizontal surfaces orientations (10 of 11 recorded taxa) suggesting that this orientation should be sampled if the diving time is scarce and algae are of main interest. Our methodology is adequate for estimations of algal cover by functional groups, but if more detailed taxonomic resolution is required, voucher samples should be collected, since filamentous and crustose algal groups contain several species otherwise unidentifiable.



Our sampling found almost the same number of species on mid and deep rocky reefs, but the average number of species registered by individual photoquadrats was significantly higher on deep reefs. Similar results were found in several Antarctic rocky reefs, where species and phylum richness increased with depth in similar depth ranges (Barnes, 1995; Gambi et al., 2000; Nonato et al., 2000; Smale, 2007). This may be the consequence of a decrease in algal cover that in turn releases more settlement surfaces for sessile invertebrates which were more diverse per unit area than algae, a pattern that was also observed on Mediterranean rocky bottoms (Garrabou et al., 2002). As diving logistics and security protocols become stricter for diving at 30 m depth for  $>30'$ , we propose that rocky reef sampling for large-scale monitoring programs should be done at depths around 8–15 m where species richness is comparable to deeper reefs but diving limitations and risks are fewer. Hence, large-scale biodiversity monitoring programs should consider these findings and include this perspective when designing subtidal sampling protocols in rocky reefs.

The choice of the sampling unit should consider the size of the sampled organism and the aggregation among them (Underwood and Chapman, 2013). However, water visibility must also be considered when using photoquadrats. Using  $25 \times 25$  cm quadrats ensures good quality photos even with low visibility (e.g., up to 1 m). In the cases where macroalgae species are bigger than the size of the quadrat a solution could be taking 4 photos with  $25 \times 25$  cm quadrats together and then pool the photos for analysis (see Parravicini et al., 2009). The Reef Life Survey (RLS) created a sampling protocol and collected data using an international group of trained divers (Edgar and Stuart-Smith, 2014). Even though the RLS has similar

features to our protocol such as  $n = 20$  photoquadrats of  $\sim 30 \times 30$  cm or smaller, there is no special consideration on the use of quadrats in overhang or cavefloor surfaces, losing detail in the species composition of the rocky reef. Furthermore, there is no precise georeferencing in the RLS protocol. Using the protocol presented here where all the surface orientations are considered for the first time in the region, we could detect more than 90% of species estimated for the zone and more species than those recorded previously through extractive methods (Olivier et al., 1966; Bravo, 2013; Rechimont et al., 2013). The distinctive aspect of our study and likely the principal explanation of such disparity in species richness is that in addition to the horizontal surface, vertical, overhang and cavefloor surfaces were included in the sampling design.

The use of remotely operated vehicles or towed cameras has considerably increased spatial extent of benthic surveys. However, exploring overhang or cave surfaces with these technologies is at least challenging when not impossible. Overall, it is clear that a combination of techniques, when available, will get a broader and more precise picture of subtidal habitats (Van Rein et al., 2009). An important complement to our protocol, could be the use of towed cameras or a second diver counting fishes. Employing semi-automated annotation of images by deep machine learning (Beijbom et al., 2015) could also improve this protocol by decreasing the analysis time per photo.

All considered, we propose the use of this protocol to monitor rocky reefs in large-scale long-term benthic biodiversity programs since it amalgamates technical, academic and financial aspects that make it applicable across the globe. Low cost and simple, it is capable of sampling different surface orientations and detecting a broad range of species. The proposed protocol adequately estimates macroalgal cover, benthic invertebrate abundance and benthic invertebrate diversity which were identified as Essential Ocean Variables (EOVs) or emerging EOVs by the Global Ocean Observing System (GOOS) (Miloslavich et al., 2018) and as Essential Biodiversity Variables (EBVs) by the Group on Earth Observations (GEO BON) (Pereira et al., 2013). In this context, the proposed protocol can be useful for monitoring rapid changes in rocky reef biodiversity through periodic sampling, and can be implemented as part of large monitoring programs such as MBON Pole to Pole to detect less tangible changes in fragile marine habitats, which provide important ecosystem services to society.

## DATA AVAILABILITY STATEMENT

The datasets presented in this study can be found in online repository <https://doi.org/10.15468/xqgdsm>. The R codes

are available in [https://github.com/gonzalobravoargentina/SupplementaryMaterials\\_Bravo-et-al.2020](https://github.com/gonzalobravoargentina/SupplementaryMaterials_Bravo-et-al.2020).

## AUTHOR CONTRIBUTIONS

GBi and JPL supervised the study that forms part of the Ph.D. thesis of GBr. All authors designed the study and wrote the first manuscript. GBr collected the data and did the statistical analysis and plots. All authors contributed to manuscript revision, read and approved the submitted version.

## FUNDING

Funding for this work was provided by the Rapid Ocean Conservation grants (ROC) from Waitt foundation (<https://www.waittfoundation.org/>) granted to GBr. National Scientific and Technical Research Council—Argentina (CONICET) supports GBr Ph.D. grant and Livore and Bigatti's salary. Part of the financial support came from the PICT 2018-0969, ProyectoSub foundation and Instituto de Conservación de Ballenas (ICB) with the Australis award.

## ACKNOWLEDGMENTS

We are grateful to the team members: Ricardo Vera, Néstor Ortiz, Facundo Irigoyen, Fabián Quiroga, Julio Rua, Nicolás Battini, Martín Brogger, Juan Pablo Laclaud, Estefanía Alvarez, and Yann Herrera Fuchs (Rolex scholar 2018) for participated in the field work. Special thanks to Punta Ballena (<https://www.puntaballena.com.ar/>) and Claudio Nicolini for logistical assistance in Puerto Pirámides. GBi acknowledges Alejo Irigoyen for the help with the rocky reef locations and fish identification. Special mention to all the taxonomists that helped with identification, Paula Raffo (Algae), Marianela Gastaldi (Porifera), Cristian Lager (Tunicates), Daniel Lauretta (Cnidaria), and all the members of LARBIM laboratory. Ezequiel Marzinelli for statistical advice. We also wish to thank the two reviewers whose suggestions enhanced this manuscript. This is publication N\_140 of the Laboratorio de Reproducción y Biología Integrativa de Invertebrados Marinos (LARBIM).

## SUPPLEMENTARY MATERIAL

The Supplementary Material for this article can be found online at: <https://www.frontiersin.org/articles/10.3389/fmars.2020.578595/full#supplementary-material>

## REFERENCES

- Andrew, N., and Underwood, A. (1993). Density-dependent foraging in the sea urchin *Centrostephanus rodgersii* on shallow subtidal reefs in New South Wales. *Aust. Mar. Ecol. Prog. Ser.* 99, 89–98. doi: 10.3354/meps09089
- Balech, E., and Ehrlich, M. (2008). Esquema biogeográfico del Mar Argentino. *Rev. Invest. y Desarro. Pesq.* 19, 45–75.
- Barnes, D. K. A. (1995). Sublittoral epifaunal communities at Signy Island, Antarctica. II. Below the ice-foot zone. *Mar. Biol.* 121, 565–572. doi: 10.1007/BF00349467

- Baynes, T. W. (1999). Factors structuring a subtidal encrusting community in the southern Gulf of California. *Bull. Mar. Sci.* 64, 419–450.
- Beijbom, O., Edmunds, P. J., Roelfsema, C., Smith, J., Kline, D. I., Neal, B. P., et al. (2015). Towards automated annotation of benthic survey images: variability of human experts and operational modes of automation. *PLoS One* 10:e0130312. doi: 10.1371/journal.pone.0130312
- Benedetti-Cecchi, L. (2001). Variability in abundance of algae and invertebrates at different spatial scales on rocky sea shores. *Mar. Ecol. Prog. Ser.* 215, 79–92. doi: 10.3354/meps215079
- Bianchi, C. N., Pronzato, R., Cattaneo-Vietti, R., Benedetti-Cecchi, L., Morri, C., Pansini, M., et al. (2004). “Hard Bottoms,” in *Mediterranean Marine Benthos: A Manual of Methods for Its Sampling And Study*, eds M. C. Gambi and M. Dappiano (Genova: SIBM), 185–215.
- Bravo, G. (2013). *Efecto del Buceo Sobre Organismos Bentónicos En Los Parques Subacuáticos de Puerto Madryn, Chubut, Argentina*. Bachelor Thesis, Univ. Nac. la Patagon. San Juan Bosco, Puerto Madryn.
- Bravo, G., Márquez, F., Marzinelli, E. M., Mendez, M. M., and Bigatti, G. (2015). Effect of recreational diving on Patagonian rocky reefs. *Mar. Environ. Res.* 104, 31–36. doi: 10.1016/j.marenvres.2014.12.002
- Cárdenas, C., Davy, S., and Bell, J. (2012). Correlations between algal abundance, environmental variables and sponge distribution patterns on southern hemisphere temperate rocky reefs. *Aquat. Biol.* 16, 229–239. doi: 10.3354/ab00449
- Cárdenas, C. A., and Montiel, A. (2015). The influence of depth and substrate inclination on sessile assemblages in subantarctic rocky reefs (Magellan region). *Polar Biol.* 38, 1631–1644. doi: 10.1007/s00300-015-1729-5
- Carpenter, S. R., Mooney, H. A., Agard, J., Capistrano, D., DeFries, R. S., Diaz, S., et al. (2009). Science for managing ecosystem services: beyond the millennium ecosystem assessment. *Proc. Natl. Acad. Sci. U. S. A.* 106, 1305–1312. doi: 10.1073/pnas.0808772106
- Cheung, W. W. L., Meeuwig, J. J., Feng, M., Harvey, E., Lam, V. W. Y., Langlois, T., et al. (2012). Climate-change induced tropicalisation of marine communities in Western Australia. *Mar. Freshw. Res.* 63, 415–427. doi: 10.1071/MF11205
- Claudet, J., and Fraschetti, S. (2010). Human-driven impacts on marine habitats: a regional meta-analysis in the Mediterranean Sea. *Biol. Conserv.* 143, 2195–2206. doi: 10.1016/j.biocon.2010.06.004
- Dayton, P. K., Currie, V., Gerrodette, T., Keller, B. D., Rosenthal, R., and Tresca, D. V. (1984). Patch dynamics and stability of some California Kelp communities. *Ecol. Monogr.* 54, 253–289. doi: 10.2307/1942498
- De Cáceres, M., Legendre, P., and Moretti, M. (2010). Improving indicator species analysis by combining groups of sites. *Oikos* 119, 1674–1684. doi: 10.1111/j.1600-0706.2010.18334.x
- Doty, M. S. (1971). Measurement of water movement in reference to Benthic Algal Growth. *Bot. Mar.* 14, 32–35. doi: 10.1515/botm.1971.14.1.32
- Duffy, J. E., Amaral-Zettler, L. A., Fautin, D. G., Paulay, G., Ryeanson, T. A., Sosik, H. M., et al. (2013). Envisioning a marine biodiversity observation network. *Bioscience* 63, 350–361. doi: 10.1525/bio.2013.63.5.8
- Dufrène, M., and Legendre, P. (1997). Species assemblages and indicator species: the need for a flexible asymmetrical approach. *Ecol. Monogr.* 67, 345–366. doi: 10.2307/2963459
- Edgar, G., and Stuart-Smith, R. (2009). Ecological effects of marine protected areas on rocky reef communities—a continental-scale analysis. *Mar. Ecol. Prog. Ser.* 388, 51–62. doi: 10.3354/meps08149
- Edgar, G. J., and Stuart-Smith, R. D. (2014). Systematic global assessment of reef fish communities by the Reef Life Survey program. *Sci. Data* 1:140007. doi: 10.1038/sdata.2014.7
- Fraschetti, S., Terlizzi, A., and Boero, F. (2008). How many habitats are there in the sea (and where)? *J. Exp. Mar. Bio. Ecol.* 366, 109–115. doi: 10.1016/j.jembe.2008.07.015
- Galván, D. E., Venerus, L. A., and Irigoyen, A. J. (2009). The reef-fish Fauna of the Northern Patagonian Gulfs, Argentina, South-western Atlantic. *Open Fish Sci. J.* 2, 90–98. doi: 10.2174/1874401X00902010090
- Gambi, M. C., Buia, M. C., Mazzella, L., Lorenti, M., and Scipione, M. B. (2000). “Spatio-temporal variability in the structure of benthic populations in a physically controlled system off Terra Nova Bay: the shallow hard bottoms,” in *Ross Sea Ecology*, eds M. F. Francesco, G. Letterio, and A. Lanora (Berlin: Springer), 527–538. doi: 10.1007/978-3-642-59607-0\_38
- Garrahou, J., Ballesteros, E., and Zabala, M. (2002). Structure and dynamics of North-western Mediterranean Rocky Benthic communities along a Depth Gradient. *Estuar. Coast. Shelf Sci.* 55, 493–508. doi: 10.1006/ecss.2001.0920
- Glasby, T. M. (1999). Effects of shading on subtidal epibiotic assemblages. *J. Exp. Mar. Bio. Ecol.* 234, 275–290. doi: 10.1016/S0022-0981(98)00156-7
- Hakanson, L., Floderus, S., and Wallin, M. (1989). “Sediment trap assemblages a methodological description,” in *Sediment/Water Interaction*, eds P. G. Sly and B. T. Hart (Dordrecht: Springer), 481–490. doi: 10.1007/978-94-009-2376-8\_46
- Halpern, B. S., Walbridge, S., Selkoe, K. A., Kappel, C. V., Micheli, F., D’Agrosa, C., et al. (2008). A global map of human impact on marine ecosystems. *Science* 319, 948–952. doi: 10.1126/science.1149345
- Harley, C. D. G., Randall Hughes, A., Hultgren, K. M., Miner, B. G., Sorte, C. J. B., Thornber, C. S., et al. (2006). The impacts of climate change in coastal marine systems. *Ecol. Lett.* 9, 228–241. doi: 10.1111/j.1461-0248.2005.00871.x
- Hawkins, S., Moore, P., Burrows, M., Poloczanska, E., Mieszkowska, N., Herbert, R., et al. (2008). Complex interactions in a rapidly changing world: responses of rocky shore communities to recent climate change. *Clim. Res.* 37, 123–133. doi: 10.3354/cr00768
- Heys, E. R., Bernard, A. T. F., Richoux, N. B., and Götz, A. (2016). Depth-related distribution patterns of subtidal macrobenthos in a well-established marine protected area. *Mar. Biol.* 163:39. doi: 10.1007/s00227-016-2816-z
- Irving, A., and Connell, S. (2002). Sedimentation and light penetration interact to maintain heterogeneity of subtidal habitats: algal versus invertebrate dominated assemblages. *Mar. Ecol. Prog. Ser.* 245, 83–91. doi: 10.3354/meps245083
- Jokiel, P., and Morrissey, J. (1993). Water motion on coral reefs: evaluation of the “clod card” technique. *Mar. Ecol. Prog. Ser.* 93, 175–181. doi: 10.3354/meps093175
- Jones, G. P., and Andrew, N. L. (1990). Herbivory and patch dynamics on rocky reefs in temperate Australasia: the roles of fish and sea urchins. *Aust. Ecol.* 15, 505–520. doi: 10.1111/j.1442-9993.1990.tb01474.x
- Jørgensen, L. L., and Gulliksen, B. (2001). Rocky bottom fauna in arctic Kongsfjord (Svalbard) studied by means of suction sampling and photography. *Polar Biol.* 24, 113–121. doi: 10.1007/s003000000182
- Leenhardt, P., Low, N., Pascal, N., Micheli, F., and Claudet, J. (2015). “The role of marine protected areas in providing ecosystem services,” in *Aquatic Functional Biodiversity*, eds A. Belgrano, G. Woodward, and U. Jacob (San Diego: Elsevier), 211–239. doi: 10.1016/b978-0-12-417015-5.00009-8
- Leichter, J. J., and Witman, J. D. (1997). Water flow over subtidal rock walls: relation to distributions and growth rates of sessile suspension feeders in the Gulf of Maine Water flow and growth rates. *J. Exp. Mar. Bio. Ecol.* 209, 293–307. doi: 10.1016/S0022-0981(96)02702-5
- Ling, S. D. (2008). Range expansion of a habitat-modifying species leads to loss of taxonomic diversity: a new and impoverished reef state. *Oecologia* 156, 883–894. doi: 10.1007/s00442-008-1043-9
- Maldonado, M., Aguilar, R., Bannister, R. J., James, J. B., Conway, K. W., Dayton, P. K., et al. (2016). “Sponge grounds as key marine habitats: a synthetic review of types, structure, functional roles, and conservation concerns,” in *Marine Animal Forests*, eds S. Rossi, A. Gori, L. Bramanti, and C. Orejas (Cham: Springer International Publishing), 1–39. doi: 10.1007/978-3-319-17001-5\_24-1
- Manly, B. F. J. (1991). *Randomization and Monte Carlo Methods in Biology*. London, UK: Chapman and Hall.
- Martinez Arbizu, P. (2017). *pairwiseAdonis: Pairwise multilevel comparison using adonis*. Boston, MA: R Package.
- Marzinelli, E. M., Williams, S. B., Babcock, R. C., Barrett, N. S., Johnson, C. R., Jordan, A., et al. (2015). Large-Scale geographic variation in distribution and abundance of Australian deep-water kelp forests. *PLoS One* 10:e0118390. doi: 10.1371/journal.pone.0118390
- Miller, R., and Etter, R. (2011). Rock walls: small-scale diversity hotspots in the subtidal Gulf of Maine. *Mar. Ecol. Prog. Ser.* 425, 153–165. doi: 10.3354/meps09025
- Miller, R. J., and Etter, R. J. (2008). Shading facilitates sessile invertebrate dominance in the rocky subtidal gulf of maine. *Ecology* 89, 452–462. doi: 10.1890/06-1099.1
- Miloslavich, P., Bax, N. J., Simmons, S. E., Klein, E., Appeltans, W., Aburto-Oropeza, O., et al. (2018). Essential ocean variables for global sustained observations of biodiversity and ecosystem changes. *Glob. Chang. Biol.* 24, 2416–2433. doi: 10.1111/gcb.14108

- Murray, S. N., Ambrose, R., and Dethier, M. N. (2006). *Monitoring rocky shores*. London: University of California Press.
- Naranjo, S. A., Carballo, J., and García-Gómez, J. (1996). Effects of environmental stress on ascidian populations in Algeciras Bay (Southern Spain). Possible marine bioindicators? *Mar. Ecol. Prog. Ser.* 144, 119–131. doi: 10.3354/meps144119
- Nonato, E. F., Brito, T. A. S., De Paiva, P. C., Petti, M. A. V., and Corbisier, T. N. (2000). Benthic megafauna of the nearshore zone of Martel Inlet (King George Island, South Shetland Islands, Antarctica): depth zonation and underwater observations. *Polar Biol.* 23, 580–588. doi: 10.1007/s003000000129
- Oksanen, J., Blanchet, F. G., Friendly, M., Kindt, R., Legendre, P., McGinnis, D., et al. (2019). *Vegan: Community Ecology Package*. Boston, MA: R Package.
- Olivier, S. R., Paternoster, I. K., and Bastida, R. (1966). Estudios biocenóticos en las costas de Chubut (Argentina) I. Zonación biocenológica de Puerto Pardelas (Golfo Nuevo). *Inst. Biol. Mar.* 10, 1–71. doi: 10.11646/zootaxa.172.1.1
- Pan, Y., Birdsey, R. A., Phillips, O. L., and Jackson, R. B. (2013). The structure, distribution, and biomass of the world's forests. *Annu. Rev. Ecol. Evol. Syst.* 44, 593–622. doi: 10.1146/annurev-ecolsys-110512-135914
- Parravicini, V., Morri, C., Ciribilli, G., Montefalcone, M., Albertelli, G., and Bianchi, C. N. (2009). Size matters more than method: Visual quadrats vs photography in measuring human impact on Mediterranean rocky reef communities. *Estuar. Coast. Shelf Sci.* 81, 359–367. doi: 10.1016/j.ecss.2008.11.007
- Pereira, H. M., Ferrier, S., Walters, M., Geller, G. N., Jongman, R. H. G., Scholes, R. J., et al. (2013). Essential biodiversity variables. *Science* 339, 277–278. doi: 10.1126/science.1229931
- Preciado, I., and Maldonado, M. (2005). Reassessing the spatial relationship between sponges and macroalgae in sublittoral rocky bottoms: a descriptive approach. *Helgol. Mar. Res.* 59, 141–150. doi: 10.1007/s10152-004-0213-3
- R Development Core Team. (2018). *A Language and Environment for Statistical Computing*. New York, NY: R Development Core Team.
- Rechimont, M. E., Galván, D. E., Sueiro, M. C., Casas, G., Piriz, M. L., Diez, M. E., et al. (2013). Benthic diversity and assemblage structure of a north Patagonian rocky shore: a monitoring legacy of the NaGISA project. *J. Mar. Biol. Assoc. United Kingdom* 93, 2049–2058. doi: 10.1017/S0025315413001069
- Rossi, J.-P. (2011). rich: an R Package to analyse species richness. *Diversity* 3, 112–120. doi: 10.3390/d3010112
- Rudman, W. B., and Bergquist, P. R. (2007). A review of feeding specificity in the sponge-feeding Chromodorididae (Nudibranchia: Mollusca). *Molluscan Res.* 27, 60–88.
- Saunders, R. J., and Connell, S. D. (2001). Interactive effects of shade and surface orientation on the recruitment of spirorbid polychaetes. *Aust. Ecol.* 26, 109–115. doi: 10.1111/j.1442-9993.2001.01090.pp.x
- Scoresby, S., and Graham, E. (2013). in *Ecology of Australian Temperate Reefs: The Unique South*, eds S. Scoresby and E. Graham Collingwood (Australia: CSIRO publishing).
- Sebens, K. P. (1986). "Community ecology of vertical rock walls in the Gulf of Maine, USA: small-scale processes and alternative community states," in *The Ecology of Rocky Coasts*, eds P. G. Moore and R. Seed (New York, NY: Columbia Univ. Press), 346–371.
- Smale, D. A. (2007). Continuous benthic community change along a depth gradient in Antarctic shallows: evidence of patchiness but not zonation. *Polar Biol.* 31, 189–198. doi: 10.1007/s00300-007-0346-3
- Steneck, R. S., Graham, M. H., Bourque, B. J., Corbett, D., Erlandson, J. M., Estes, J. A., et al. (2002). Kelp forest ecosystems: biodiversity, stability, resilience and future. *Environ. Conserv.* 29, 436–459. doi: 10.1017/S0376892902000322
- Stephens, J. S., Larson, R. J., and Pondella, D. J. (2006). "Rocky Reefs and Kelp Beds," in *The Ecology of Marine Fishes: California and Adjacent Waters*, eds L. G. Allen, D. J. Pondella, and M. H. Horn (Berkeley: University of California Press), 227–252. doi: 10.1525/9780520932470-011
- Underwood, A. J., and Chapman, M. G. (2013). "Design and analysis in benthic surveys in environmental sampling," in *Methods for the Study of Marine Benthos*, ed. A. Eleftheriou (Oxford, UK: John Wiley & Sons, Ltd), 1–45. doi: 10.1002/9781118542392.ch1
- Van Rein, H., Brown, C., Quinn, R., and Breen, J. (2009). A review of sublittoral monitoring methods in temperate waters: a focus on scale. *Underw. Technol.* 28, 99–113. doi: 10.3723/ut.28.099
- Venerus, L. A., Irigoyen, A. J., Galván, D. E., and Parma, A. M. (2014). Spatial dynamics of the Argentine sandperch, *Pseudoperca semifasciata* (Pinguipedidae), in temperate rocky reefs from northern Patagonia, Argentina. *Mar. Freshw. Res.* 65, 39–49. doi: 10.1071/MF12163
- Virgilio, M., Airolidi, L., and Abbiati, M. (2006). Spatial and temporal variations of assemblages in a Mediterranean coralligenous reef and relationships with surface orientation. *Coral Reefs* 25, 265–272. doi: 10.1007/s00338-006-0100-2
- Wernberg, T., Russell, B. D., Moore, P. J., Ling, S. D., Smale, D. A., Campbell, A., et al. (2011). Impacts of climate change in a global hotspot for temperate marine biodiversity and ocean warming. *J. Exp. Mar. Bio. Ecol.* 400, 7–16. doi: 10.1016/j.jembe.2011.02.021
- Witman, J. D. (1985). Refuges, biological disturbance, and rocky subtidal community structure in New England. *Ecol. Monogr.* 55, 421–445. doi: 10.2307/2937130
- Witman, J. D., and Dayton, P. K. (2001). "Rocky subtidal communities," in *Marine community ecology*, eds M. D. Bertness, S. D. Gaines, and M. E. Hay (Sunderland, MA: Sinauer Associates), 339–366.
- Witman, J. D., Etter, R. J., and Smith, F. (2004). The relationship between regional and local species diversity in marine benthic communities: a global perspective. *Proc. Natl. Acad. Sci.* 101, 15664–15669. doi: 10.1073/pnas.0404300101
- Worm, B., Barbier, E. B., Beaumont, N., Duffy, J. E., Folke, C., Halpern, B. S., et al. (2006). Impacts of biodiversity loss on Ocean ecosystem services. *Science* 314, 787–790. doi: 10.1126/science.1132294

**Conflict of Interest:** The authors declare that the research was conducted in the absence of any commercial or financial relationships that could be construed as a potential conflict of interest.

Copyright © 2020 Bravo, Livore and Bigatti. This is an open-access article distributed under the terms of the Creative Commons Attribution License (CC BY). The use, distribution or reproduction in other forums is permitted, provided the original author(s) and the copyright owner(s) are credited and that the original publication in this journal is cited, in accordance with accepted academic practice. No use, distribution or reproduction is permitted which does not comply with these terms.





# The National Geographic Society Deep-Sea Camera System: A Low-Cost Remote Video Survey Instrument to Advance Biodiversity Observation in the Deep Ocean

Jonatha Giddens<sup>1\*</sup>, Alan Turchik<sup>1</sup>, Whitney Goodell<sup>1,2</sup>, Michelle Rodriguez<sup>1</sup> and Denley Delaney<sup>1</sup>

<sup>1</sup> Exploration Technology Lab, National Geographic Society, Washington, DC, United States, <sup>2</sup> Pristine Seas, National Geographic Society, Washington, DC, United States

## OPEN ACCESS

### Edited by:

Enrique Montes,  
University of South Florida,  
United States

### Reviewed by:

Emmanuel Boss,  
The University of Maine, United States  
Natalya D. Gallo,  
University of California, San Diego,  
United States

### \*Correspondence:

Jonatha Giddens  
jonatha@hawaii.edu

### Specialty section:

This article was submitted to  
Ocean Observation,  
a section of the journal  
Frontiers in Marine Science

**Received:** 31 August 2020

**Accepted:** 07 December 2020

**Published:** 11 January 2021

### Citation:

Giddens J, Turchik A, Goodell W,  
Rodriguez M and Delaney D (2021)  
The National Geographic Society  
Deep-Sea Camera System:  
A Low-Cost Remote Video Survey  
Instrument to Advance Biodiversity  
Observation in the Deep Ocean.  
*Front. Mar. Sci.* 7:601411.  
doi: 10.3389/fmars.2020.601411

There is a growing need for marine biodiversity baseline and monitoring data to assess ocean ecosystem health, especially in the deep sea, where data are notoriously sparse. Baited cameras are a biological observing method especially useful in the deep ocean to estimate relative abundances of scavenging fishes and invertebrates. The National Geographic Society Exploration Technology Lab developed an autonomous benthic lander platform with a baited camera system to conduct stationary video surveys of deep-sea megafauna. The first-generation landers were capable of sampling to full ocean depth, however, the form factor, power requirements, and cost of the system limited deployment opportunities. Therefore, a miniaturized version (76 cm × 76 cm × 36 cm, 18 kg in air) was developed to provide a cost-effective method to observe ocean life to 6000 m depth. Here, we detail this next-generation deep-sea camera system, including the structural design, scientific payload, and the procedures for deployment. We provide an overview of NGS deep-sea camera system deployments over the past decade with a focus on the performance improvements of the next-generation system, which began field operations in 2017 and have performed 264 deployments. We present example imagery and discuss the strengths and limitations of the instrument in the context of existing complementary survey methods, and for use in down-stream data products. The key operational advantages of this new instrument are spatial flexibility and cost-efficiency. The instrument can be hand-deployed by a single operator from a small craft concurrent with other shipboard operations. The main limitation of the system is battery power, which allows for 6 h of continuous recording, and takes up to 8 h to recharge between deployments. Like many baited-camera methods, this instrument is specialized to measure the relative abundance of mobile megafauna that are attracted to bait, which results in a stochastic snapshot of the

species at the deployment location and time. The small size and ease of deployment of this next-generation camera system allows for increased sample replication on expeditions, and presents a path forward to advance cost-effective biological observing and sustained monitoring in the deep ocean.

**Keywords:** BRUVS, Bathyal, autonomous vehicle, remote imaging, Essential Biodiversity Variables, Essential Ocean Variables, benthic lander, scavenging megafauna

## INTRODUCTION

There is a growing need for marine biodiversity baseline and monitoring data to assess ocean ecosystem health, especially in the deep sea, where data is notoriously sparse (Costello et al., 2010; Levin et al., 2019; Rogers et al., 2020). Emerging deep-sea methods and technologies, such as remote autonomous benthic landers with high-definition imaging capability, can aid international biodiversity monitoring networks (e.g., the Marine Biodiversity Observation Network), extend observing capacity into the deep ocean (Muller-Karger et al., 2018; Moltmann et al., 2019; Rogers et al., 2020), and aid scientific networks (e.g., Biology and Ecosystems Panel of the Global Ocean Observing System; Deep Ocean Observing Strategy) to incorporate cost-effective biological observing capabilities into integrated deep ocean assessments (Levin et al., 2019). Harnessing emerging technologies for deep-sea biological observation is critical to creating a global knowledge base of this ecosystem about which very little is known (Levin et al., 2019).

New biological data obtained from high definition imaging can be used to build the marine Essential Biodiversity Variables (EBVs) (Pereira et al., 2013; Muller-Karger et al., 2018) and biological Essential Ocean Variables (EOVs) (Milosavljevic et al., 2018; Bax et al., 2019). These variables are necessary for ecosystem indicator development and reporting over the Ocean Decade (Moltmann et al., 2019; Ryabinin et al., 2019; Tanhua et al., 2019), which help to build a better understanding of the health of ocean ecosystems. However, it is critical that the strengths and limitations inherent to emerging observing methods are transparent. This enables observers and users to converge on agreed data standards and practices that complement existing approaches (Pearlman et al., 2019). Such transparency and data standards are necessary to ensure that data obtained from emerging methods contribute to the development of ecosystem indicators that address policy and management requirements (e.g., suitable for building EBV/EOV data products) (Hardisty et al., 2019; Jetz et al., 2019).

Autonomous free-fall lander vehicles (untethered instrumented seafloor platforms) for deep-sea research were developed in the 1930s (Ewing and Vine, 1938), and have since been used successfully to sample full ocean depth (Jamieson et al., 2009; Hardy et al., 2013), and for a variety of deep-sea research purposes (Phleger and Soutar, 1971; Smith et al., 1976). Landers offer many advantages over human-operated submersible vehicles, and ship-tethered equipment such as Remote Operated Vehicles (ROVs), towed camera sleds, and trawls (Isaacs and Schick, 1960; Worcester et al., 1997; Priede and Bagley, 2000). The main advantage is that autonomous

landers enable simultaneous deployments to obtain spatial replication of surveys, and can be conducted while the ship performs concurrent operations, significantly optimizing expensive ship time (Brandt et al., 2016). To unlock the potential to sample the deep ocean at scale, autonomous lander vehicles offer a promising direction for the future of deep-sea research with improved sampling efficiency compared to ship-tethered equipment (Brandt et al., 2016).

Landers equipped with baited cameras have proven to be an especially useful tool for biological observation in the deep ocean where food is limited (Willis and Babcock, 2000; Trenkel et al., 2004; Bailey et al., 2007; Drazen and Sutton, 2017). The bait attracts mobile fishes and invertebrates to the camera, and data extracted from the footage can be used to estimate relative abundances of these scavenging taxa (Farnsworth et al., 2007; Harvey et al., 2007; Yeh and Drazen, 2011; Linley et al., 2016; Leitner et al., 2017). Therefore, baited cameras are commonly used to study top predator communities in the deep sea (Priede and Bagley, 2000; Bailey et al., 2007; Yeh and Drazen, 2009; Drazen and Sutton, 2017), and share many common sampling features with shallow-water Baited Remote Underwater Video Station (BRUVS) techniques (Langlois et al., 2018), so that standards can be shared and data could be comparable among methodologies (Whitmarsh et al., 2017).

However, due to their size and weight, many lander vehicles still require large ships with winch capabilities to operate them (e.g., Hardy et al., 2013; but see Phillips et al., 2019; Gallo et al., 2020). In 2009, the National Geographic Society (NGS) Exploration Technology Lab developed a hand-deployable deep-sea lander and camera system that has since been deployed opportunistically across the world's ocean, largely on NGS Pristine Seas expeditions (e.g., Friedlander et al., 2019; Giddens et al., 2019; **Table 1**). The instrument is a remote autonomous benthic lander with a baited camera system, and is used for stationary video surveys of deep-sea demersal scavenging megafauna. The first-generation landers were capable of sampling to full ocean depth (Turchik et al., 2015) however the form factor (size and weight), power requirements, and cost of the system limited deployment opportunities. Therefore a next-generation miniaturized version was developed to optimize the physical design and scientific payload, providing improved efficiency and a cost-effective method to observe life in the deep sea to 6000 m depth.

In this paper we detail the novel next-generation NGS deep-sea camera system, including the structural design and scientific payload, and describe the methodological procedures, including set up, deployment, recovery, and data management.

**TABLE 1** | Expeditions on which NGS deep-sea camera systems have been deployed.

Expedition	Year	Average Latitude	Average Longitude	Depth min (m)	Depth max (m)	# deployments	Range of deployment length (hrs)	Total footage (hh:mm)	Average footage per deployment (hh:mm)	Environment	EMUs represented
Puerto Rico	2010			7526	7618	2				Trench	
Porcupine Abyssal Plain	2010				~4000	2				Abyssal plain	
Sala y Gomez	2011	−26.690	−106.830	552	1849	21	5–5	45:25	2:09	Oceanic island, Seamount	11, 13, 33, 36, 37
Marianas	2011			3682	10641	3				Trench	
Pitcairn	2012	−24.505	−128.921	142	1585	22	5–5			Oceanic island	8, 11, 13, 24, 33, 37
Tonga Trench	2012			7300	9200	2				Trench	
Desventuradas	2013	−26.111	−80.288	75	2363	28	1–3	52:25	1:52	Oceanic island, Seamount	3, 8, 10, 13, 14, 26, 33, 37
Franz Josef Land	2013	80.717	55.426	32	392	24	1–3	45:00	1:52	Arctic, Shelf	14, 29, 31, 35, 36
Mozambique	2014	−22.298	35.577	46	222	10	2–8			Shelf, Coastal	11, 26
Palmyra	2014	5.868	−162.132	189	1555	11	17–24	56:51	5:10	Oceanic island	3, 10, 33
Puerto Rico	2014	17.950	−65.535	2329	2329	1				Trench	36
Palau	2014	7.367	134.431	38	2400	28	3–3	36:03	1:17	Oceanic island	3, 8, 10, 13, 24, 26, 33, 37
Rapa	2014	−27.646	−144.190	30	1057	15	1–3	13:25	0:53	Oceanic island	8, 11, 37
Chagos	2015	−6.388	72.193	34	3359	21				Oceanic island	10, 13, 14, 24, 33, 36
Solomons	2015	−8.938	158.054	28	1761	7	1–8	16:40	2:22	Oceanic island	13, 24, 33, 36, 37
Seychelles	2015	−9.713	47.182	173	2095	7	5–10	17:50	2:32	Oceanic island	13, 26, 33, 37
Selvagens	2015	30.092	−15.954	112	2294	12	3–5	46:45	3:53	Oceanic island	10, 11, 26, 36
Galapagos	2015	0.706	−91.691	531	1825	26	1–3	37:05	1:25	Oceanic island	3, 13, 33, 36, 37
Clipperton	2016	10.304	−109.234	230	1497	14	5–10	40:00	2:51	Oceanic island	3, 8, 33, 36, 37
Revillagigedo	2016	18.889	−111.039	49	2285	15	5–10	45:00	3:00	Oceanic island	3, 10, 13, 26, 33, 36, 37
Niue	2016	−19.475	−168.951	274	2447	11	5–9			Oceanic island	3, 11, 13, 14, 26, 33, 36, 37

(Continued)

**TABLE 1** | Continued

Expedition	Year	Average Latitude	Average Longitude	Depth min (m)	Depth max (m)	# deployments	Range of deployment length (hrs)	Total footage (hh:mm)	Average footage per deployment (hh:mm)	Environment	EMUs represented
Tristan	2017	−38.012	−11.732	164	1414	23	1–2	28:40	1:14	Oceanic island	8, 14, 19, 36, 37
Tierra del Fuego	2017	−56.062	−67.795	53	105	12	3–9	46:19	3:51	Shelf, Oceanic island	19, 31
Juan Fernandez	2017	−33.678	−79.786	71	1575	24	4–6	63:00	2:37	Oceanic island	8, 10, 13, 33, 36, 37
Ascension	2017	−9.674	−12.798	100	2184	15	4–15	68:15	4:33	Oceanic island	10, 26, 36, 37
Yaganes	2018	−54.818	−64.648	31	505	21	1–5	51:35	2:27	Shelf, Strait	19, 30, 31
Malpelo	2018	4.029	−81.622	107	2195	29	1–6			Oceanic island	3, 8, 10, 13, 26, 33, 36, 37
Azores	2018	39.100	−30.314	240	1340	42	2–12	94:05	2:14	Oceanic island, Seamount	8, 10, 11, 26, 29, 36
Islas Marias	2018	21.547	−106.629	501	1666	10				Oceanic island	3, 13, 33, 36, 37
Clarion-Clipperton Fracture Zone	2018	15.471	−154.147	1010	5296	4	3–6	7:25	1:51	Abyssal plain	3, 13, 14
Birdwood Bank	2018	−54.622	−63.349	75	800	6				Bank, Seamount	19, 31, 36, 37
Antarctica	2019	63.551	60.839	90	797	25	3–3	75:15	3:00	Antarctic, Shelf	14, 15, 25, 29, 35
Seychelles	2019	7.729	49.957	310	338	5	12–12	14:57	2:59	Oceanic island	10, 26
Costa Rica	2019	8.585	40.625	48	1850	28	1–3	43:45	1:33	Shelf, Coastal	3, 10, 11, 13, 26, 33, 36, 37
Bermuda	2019	32.325	−64.584			4				Oceanic island	
Pacific Seamounts	2019	30.859	−136.671	3675	3675	1	15			Seamount	14
Southeast Alaska	2019	57.442	−106.181	60	250	19	3–7			Fjords	19, 23, 30, 31, 37
Galapagos	2019	−0.530	−90.476	150	1500	32	3–7	77:15	2:24	Oceanic island	3, 10, 33, 36
Chile	2020	−51.919	−74.003	65	600	12	1–5	16:20	1:21	Fjords	19, 36

Ecological Marine Units (EMUs) refer to numbered clusters of ecologically unique water masses (Sayre et al., 2017). Expeditions prior to 2018 (solid horizontal line) were conducted with the first-generation version of the camera system, with the last three expeditions of 2017 (between dashed and solid horizontal lines) involving both the first-generation and next-generation systems.



We describe instrument uses over a decade of operation (2010–2020) and discuss the performance of the next-generation system, which was used from 2017 onward for improved efficiency in deep-ocean benthic observing. Example imagery is presented, and discussed in terms of the strengths and limitations of the observing method in relationship to existing complementary BRUVS survey methods. The resulting data dimensions and attributes from the observing instrument and sampling approach are discussed in terms of suitability for use in downstream EBV/EOV data products. This work represents a significant step forward in improved efficiency and cost-reduction to conduct stationary video surveys in the deep ocean, increase opportunities for sampling, and obtain marine biodiversity baseline and monitoring data to assess ocean ecosystem health.

## MATERIALS AND EQUIPMENT

### The NGS Deep-Sea Camera System

While the first iteration of the deep-sea camera system was developed to reach full ocean depth (Turchik et al., 2015), subsequent improvements in design and economy present increased opportunities for deployment and use for the marine biodiversity observing community. Below we describe the next generation of the “mini” NGS deep-sea camera system (rated to 6000 m depth), which is small (76 cm × 76 cm × 36 cm), lightweight (18 kg in air), and low-cost (~ \$10,000 USD to manufacture) compared to many existing technologies. Details of build (mechanical illustration, electrical block diagrams, firmware state machine diagram) are available at <https://github.com/NGS-Exploration-Technology/Deep-Sea-Camera-System>.

#### Structural Design

The physical layout of the deep-sea camera system consists of a glass housing with external lights, a shaft that holds a bait canister, and the release mechanism that attaches to the anchor (**Figure 1**). The glass pressure housing is a 33 cm diameter, 1.2 cm thick borosilicate glass sphere (Vitrovex, Nautilus Marine, GmbH). The upper and lower hemispheres are sealed at the center with butyl rubber tape followed by vinyl tape, to maintain 0.6 atm inside the sphere during operation. The bottom hemisphere houses a high definition (HD) camera, the camera controller, and batteries (details below) (**Figure 2A**). The upper hemisphere contains the Argos satellite beacon and VHF beacon used for recovery (details below), and the electrical bulkhead for data download and battery charging (**Figure 2B**). A set of magnet switches activates the camera controller and the recovery beacon (**Figure 2B**).

The stainless steel detachable bottom shaft (4.5 cm diameter, 41 cm long) holds the bait canister, which is a removable PVC pipe perforated with 1.3 cm holes (3.2 cm horizontal distance between holes, 2.5 cm vertical distance between holes) to allow the odor of the bait to disperse without loss of bait. At the bottom of the shaft is an attachment point for the release system (details below) and temporary anchor (**Figure 1**). The anchor is comprised of a piece of biodegradable line tied to a 100% cotton biodegradable pillowcase filled with local sand (measured to weigh 10 kg). With a 10 kg anchor, the instrument descends

at ~ 1.1 m/s. The anchor line extends 2 m from the seafloor to optimize the field of view to both capture large mobile scavenging megafauna and allow for identification of organisms on or above the benthos.

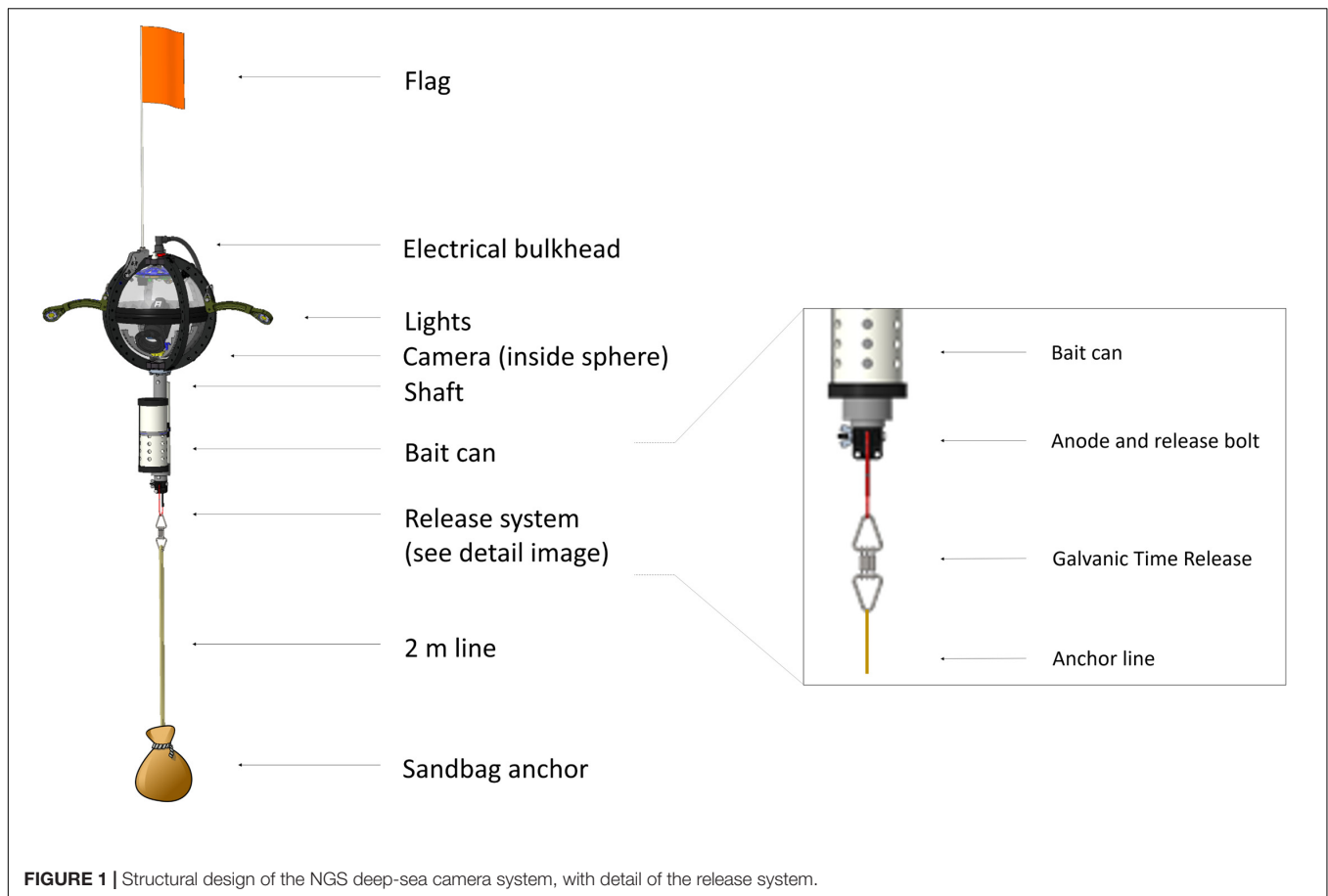
The release system consists of a single-use burn-wire and a back-up Galvanic Time Release (GTR) (Neptune Marine Supply) (**Figure 1**). The primary burn-wire system consists of a stainless steel nylon-coated wire with a 6 mm section of coating removed. The exposed wire is connected to a bolt. At the user-designated pre-programmed time, these components are energized via the camera controller and pressure-housing bulkhead, which causes the exposed wire to disintegrate through electrolytic erosion. This releases the anchor, and the camera system ascends to the surface under its own buoyancy (9.28 N) at ~ 1 m/s. Should the primary release mechanism fail, the GTR serves a back-up function. The GTR (secured between the shaft/burn-wire and the anchor system) begins corroding upon immersion in salt water, and takes between 24 and 36 h to completely disintegrate, depending on seawater temperature and salinity.

The recovery beacon is activated with a magnet switch, and consists of a 401 MHz Argos satellite transmitter (Telonics), for global tracking, and a 150 MHz VHF transmitter (Telonics) (for short-range tracking). The beacon is powered by four parallel 3.6 V, 3.4 Ah lithium ion primary batteries, with 1-year battery life in continuous operation. The camera controller consists of a custom-designed PCB based on the Microchip Technology PIC24 series microcontroller. A single waterproof bulkhead (BH10FTI, SubConn), externally located on the upper hemisphere, provides an electrical connection for charging and data retrieval and can be accessed through this bulkhead. The camera system is powered by a bank of 14.4 V, 2.6 Ah lithium ion batteries providing 337 Wh., with the capacity for 6 h of video recording with illumination (see **Supplementary Table 1** for battery-duration field-testing results).

The deep-sea camera system uses a high efficiency LED lighting system (Cree XLamp CMT1930 LED), which consists of two lights each placed approximately 318 mm from the center of the sphere, with a viewing angle of 115°. The lights are angled downward at a constant 45° from the horizontal plane, with an illumination of 1530 lm and a color temperature of 4000 K.

#### Scientific Payload

The camera is a Sony Handycam, FDR-AX33 4K Ultra-High Definition (3840 × 2160) video camera with a 20.6 megapixel still image capability. The camera is fixed at a 45° declination from the horizontal plane and has a 35 mm equivalent focal length of 29.8 mm, which results in a horizontal 62.27° and a vertical 37.53° angular field-of-view. The camera has a wide-angle adapter, which provides a 0.70 nominal magnification factor. Video is stored as an mp4 file. Typically the camera is programmed to record 2 out of 10 min, and turns on 10 s before the lights, though mission parameters are fully customizable depending on user needs, programmed through the externally located electrical bulkhead. Additionally, onboard sensors measure temperature (Texas Instruments, LM34CAZ) and pressure (Keller, 7LY HP) for each deployment.



**FIGURE 1** | Structural design of the NGS deep-sea camera system, with detail of the release system.

## METHODS

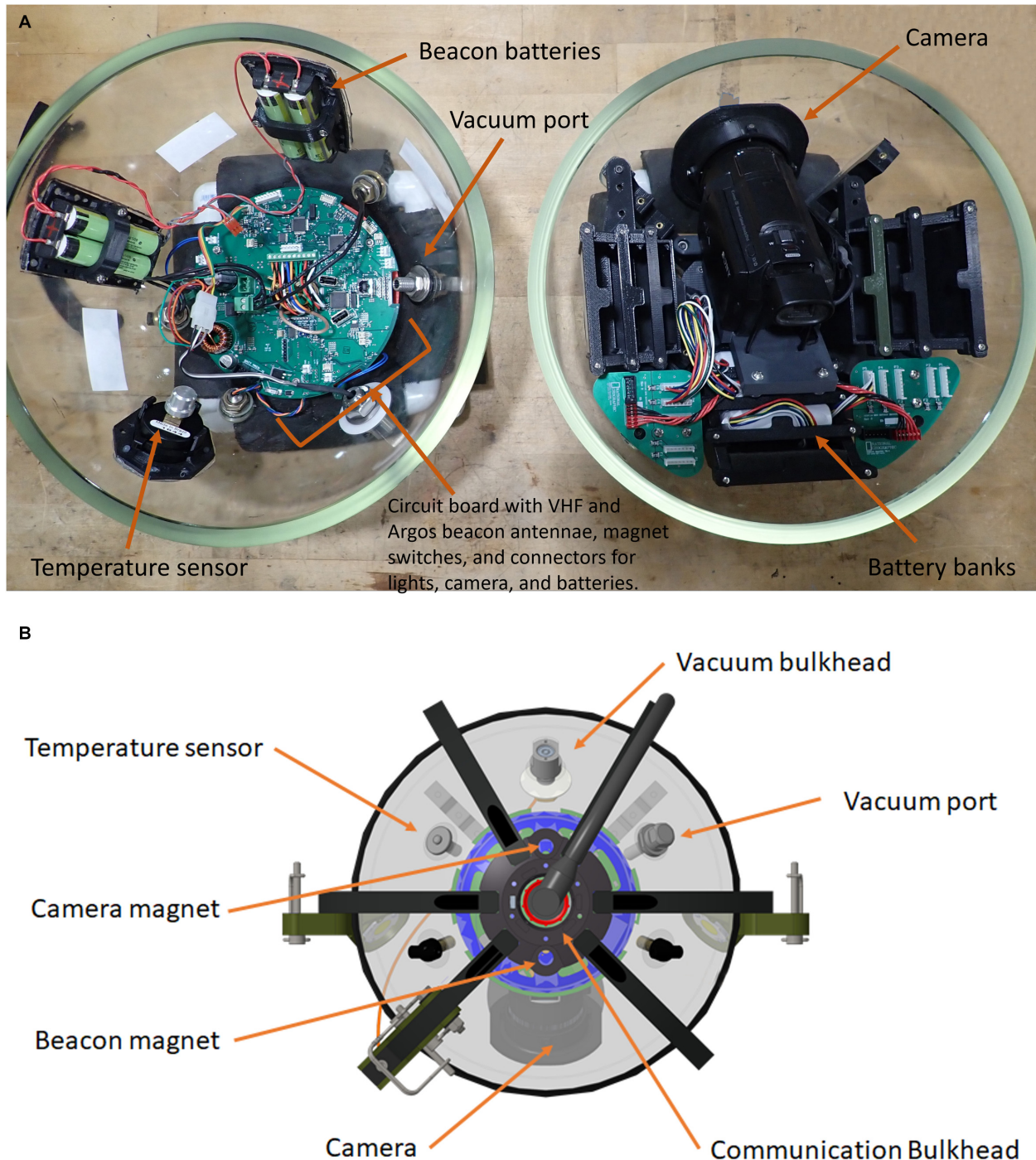
The objective of this method is to conduct stationary video surveys of bathyal demersal mobile scavenging megafauna, and to contribute fish and invertebrate abundance and distribution observations to the global ocean and biodiversity observing community. The deep-sea camera system deployment process has four stages: setup (~ 30 min.), deployment (~ 15 min.), recovery (depends on sea state), and data management (30 min download time for 1 h of video footage). Battery-charging time can take up to 8 h. The set up process includes testing and loading the mission, setting up the release mechanism, attaching the anchor, and loading the bait. Further details for each step are found in the Users Manual at <https://github.com/NGS-Exploration-Technology/Deep-Sea-Camera-System>.

### Deployment Process

Deploying the camera system takes one or two people, and can be done from a range of craft sizes, from small rigid inflatables to a large research vessel. If the water line is not directly accessible from a vessel, a slip line can be used to lower the instrument slowly into the water, however, it is preferable to remove any unnecessary lines as they present opportunity for entanglement.

The video survey time is programmed prior to deployment. It is likely that deep-sea camera deployments should last a minimum of 6 h, even at the shallow depth-range (e.g., 200 m), based on the bait plume detection (Priede and Merrett, 1998; Jamieson, 2016). Just prior to deployment, the beacon and camera system are activated by removing magnets that otherwise keep those systems off. A GPS location and time (UTC) is marked upon deployment. Based on the pre-programmed deployment time, and the calculation of ascent rate, the operator can estimate the expected time of surfacing, and arrive to the deployment area for device recovery, ready to retrieve the camera upon surfacing.

For instrument recovery, if the operator is within several hundred meters of the device, it can be detected visually by the high-visibility orange flag (during daylight hours) or reflective bands on the flag (during nighttime hours). Additionally, external lights flash every 10 s once the mission timer has elapsed, aiding visual detection at night. If the operator on the open ocean is within 10 km of the device at the surface, the bearing for navigation can be determined using a directional Yagi antenna with a radio receiver tuned to the specific frequency of the instrument's VHF beacon. The radio signal is, however, inhibited by landmasses and should be considered when deploying in settings such as fjord lands or around small islands. Beyond 10 km distance, the operator can track the device using location



**FIGURE 2 | (A)** Two hemispheres of the NGS deep-sea camera system; lower hemisphere (right) contains the high definition (HD) camera; upper hemisphere (left) contains the Argos satellite beacon and VHF beacon, and the electrical bulkhead for data download and battery charging; **(B)** outside view diagram of upper hemisphere; communication bulkhead in the center, along with magnets, sensors, and vacuum port.

fixes from the Argos satellite network forwarded to an operator's satellite phone. Fair seas and frequent Argos satellite passing can provide a location fix with an accuracy of within 250 m. However, the accuracy of the location coordinates can vary greatly (e.g.,

sea state, broadcast signal strength, etc.) therefore this system should be used only in case of unforeseen circumstances (e.g., early release, deteriorated sea state prohibiting retrieval when the device first reaches the surface).



Following retrieval, video footage and sensor data are downloaded from the device to an external hard drive and the system batteries are recharged. All of this is executed through the single waterproof bulkhead, thus the hemispheres do not need to be separated between deployments, and barring unforeseen complications, should be able to remain intact throughout the duration of an expedition. The same bulkhead and cabling used for data download is also used to set the next mission's parameters.

## Data Management

To efficiently process and manage the data, the video files are stored in "Tator," which is a cloud-based collaborative video annotation platform developed by CVisionAI<sup>1</sup>. Annotations are made in Tator and proceed from a standard annotation methodology currently in development for the NGS deep-sea camera system's remote video surveys (Marsh et al., in prep). This annotation protocol is Darwin Core compliant with standardized taxonomic nomenclature according to the World Register of Marine Species (WoRMS), and adheres to the Ocean Biodiversity Information System (OBIS) data standard formats for image-based marine biology (Costello et al., 2013; De Pooter et al., 2017; Provoost et al., 2017). Uncertainty classification is provided with controlled vocabulary according to the "Open Nomenclature" standard identification qualifiers (e.g., comments on video quality and taxonomic identification resolution) (Sigovini et al., 2016).

## Metrics and Biodiversity Analyses

In the video analysis stage, annotations are made from the video footage to identify species to the highest taxonomic resolution, and obtain a relative abundance metric (maximum number per frame, or MaxN). The maximum number of individuals of each species in a video frame, rather than a total tally per deployment, is recorded to ensure that individuals are not double counted (Langlois et al., 2018). Other variables that may be quantified from this approach include time of first arrival of a taxon, and time at which the maximum number of a taxon is observed, time being relative to the landing of the device on the seafloor (e.g., Leitner et al., 2017; Linley et al., 2018).

To assess biodiversity across sites, Hill numbers (the effective number of species) can be used as a unified way to compare measures of biodiversity with varying sample coverage (Chao et al., 2014). Coverage-based rarefaction (interpolation) and extrapolation (prediction) curves with a bootstrap routine can be produced in R (iNEXT package; Hsieh et al., 2016), and used to estimate asymptotic diversity. For example, Giddens et al. (2019) used data from the deep-sea camera system to produced fish family accumulation curves for four sites in the Tropical Eastern Pacific, and found that sample completeness ranged from 84.3% at Clipperton (13 deployments) to 100% at Malpelo (19 deployments). Further, multivariate statistics and generalized hierarchical models can be used to compare community structure between depths and habitat types and, coupled with publicly available oceanographic data, across

regions to evaluate environmental drivers of biodiversity (e.g., Giddens et al., 2019).

## RESULTS

### NGS Deep-Sea Camera System Uses

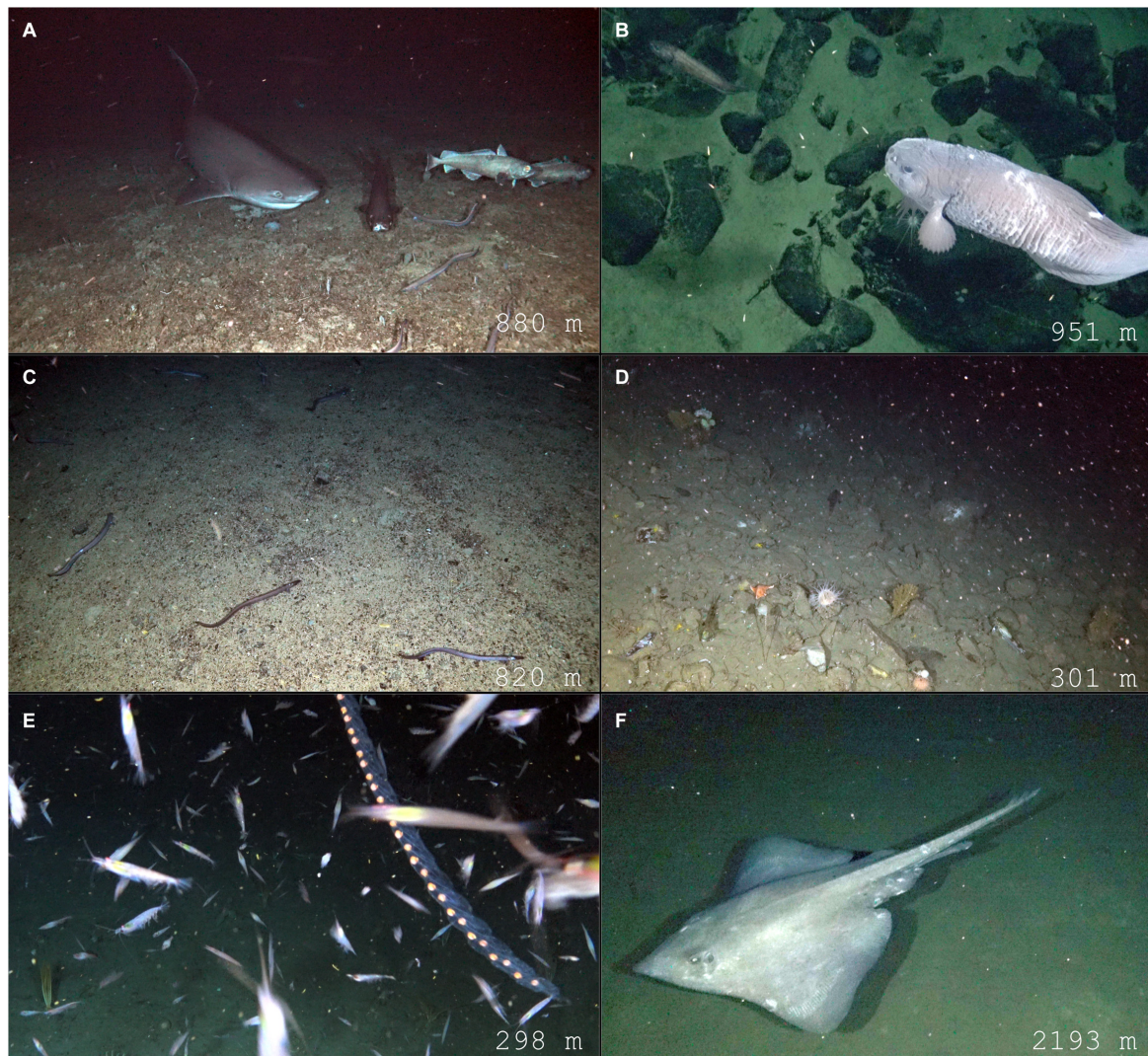
With the NGS deep-sea camera system, 595 deployments have been conducted on 39 expeditions from 2010 to 2020 (Table 1). For the next-generation version, which was used from 2017 onward, 264 deployments were conducted on 17 expeditions. Deployments for the next-generation system ranged in depth from 31 to 5296 m, and in duration from 7 to 94 h per expedition. Deployment length ranged from 1 to 12 h, and the average video length obtained per deployment ranged from 1 h 21 min to 4 h 33 min per deployment (Table 1). Example imagery is shown in Figure 3, illustrating a diversity of taxa, habitats, depths, and geographies imaged during expeditions. Complete annotations for all previous expeditions are still in process, thus the number of organisms observed in this dataset are not reported here. However, previous studies have assessed local biodiversity and community composition from shallow to deep ecosystems (e.g., Friedlander et al., 2019) performed regional comparisons in bathyal demersal scavenging megafauna (e.g., Tropical Eastern Pacific; Giddens et al., 2020), published new species records (e.g., Galapagos; Buglass et al., 2020), and described novel behavioral observations (e.g., Eastern Pacific Black Ghost Shark [*Hydrolagus melanophasma*]; Giddens et al., 2020).

The NGS deep-sea camera system has been used across a variety of different geomorphological zones and habitats (Table 1). It has been used extensively on seamounts (e.g., Easton et al., 2017; Buglass et al., 2020), in oceanic island/archipelagos (e.g., Giddens et al., 2020), polar shelf areas (e.g., Friedlander et al., 2020) and fjordlands (Chile, Southeast Alaska; Table 1). While the first-generation landers made exploratory deployments to hadal zones in ocean trenches (e.g., Puerto Rico, Tonga and Marianas Trenches) up to 10,641 m depth, the majority of deployments made with the next-generation deep-sea camera system have been conducted in <3000 m (Table 1). The current deployment dataset represents 19 of the 37 different Ecological Marine Units (EMUs; Sayre et al., 2017), with deployments in water masses of varying temperatures, oxygen levels, and chemical properties (nitrate, phosphate, silicate) (Sayre et al., 2017). Most expeditions represented 4–6 different EMUs, with some expeditions in the Pacific Ocean sampling up to 8 different EMUs (e.g., Desventuradas, Palau, Niue, Malpelo, Costa Rica) (Table 1).

The deep-sea camera system is usually deployed and recovered once per day from the main ship or a support vessel (e.g., zodiac), while other operations are carried out simultaneously. The device can be hand-deployed and requires just one operator. Typically, 2–4 instruments are brought on expeditions to allow for simultaneous deployments. This spatial flexibility and cost-efficiency in deployment operations, including reduced ship and personnel time required, are the key operational advantages of this method over larger lander systems and ship-tethered equipment.

<sup>1</sup><http://cvisionai.com/>





**FIGURE 3 |** Example imagery from NGS deep-sea camera system: **(A)** *Hexanchus griseus*, *Dalatias licha*, Synaphobranchidae, and *Mora moro*, at 880 m on a seamount in the Azores; **(B)** Liparid at 951 m at Malpelo Island; **(C)** Elongate taxa, *Synaphobranchus* sp., at 820 m in the Azores; **(D)** Benthic taxa in background of a frame can be difficult or impossible to confidently identify; 301 m on the Antarctic shelf; **(E)** Siphonophora and light-attracted krill (Euphausiidae); 298 m on the Antarctic shelf; **(F)** *Bathyraja spinosissima*, at 2193 m at Malpelo Island.

The main limitations of the method are battery power, which limits recording time to 6 h in total per deployment, and the battery charging time between deployments, which can take up to 8 h. However, because of the single bulkhead for data retrieval, battery charging, and mission programming, the pressure housing remains sealed over the course of the expedition, which makes the deployment turnaround process simple and relatively time efficient. Thus, the system can be in near continuous operation over the course of an expedition, factoring in time for data retrieval and battery charging.

### NGS Deep-Sea Lander Performance

The next-generation NGS deep-sea camera system performed successfully over the 264 deployments conducted since 2017 (Table 1). The instrument has been recovered on 100% of

its deployments, though it has relied on the back-up release mechanism (GTR) and back-up Argos satellite tracking system on occasion. Release issues were most commonly due to flawed electrical connection to the burn-wire (user error in set up), or sharks biting the burn-wire release cable causing an early release. In the Seychelles, surface currents were strong enough that after a shark-induced early release, the system was carried away from the deployment site. In this case, the Argos satellite tracking provided device location after surfacing. On one occasion in the Galapagos (Tropical Eastern Pacific), the device became entangled with the substrate after release, but eventually freed itself and was recovered using the Argos satellite tracking system on the surface. The first-generation system suffered two losses in ocean trenches and abyssal plains >6000 m, surmised to be from defects in the glass that caused a catastrophic implosion

(Turchik et al., 2015). However, for the next-generation system described here, no structural errors persist and the instrument has performed successfully on its 264 deployments above 6000 m.

## NGS Deep-Sea Imaging System Performance

The NGS deep-sea camera system has produced high-quality imagery of the deep-benthos (Figure 3). The system is designed to optimize the survey field of view and the ability to identify distinguishing characteristics of mobile taxa (e.g., pectoral and anal fins, head characteristics) (Figures 3A,B,F). This optimization is achieved with the oblique camera angle, which permits larger areas of seafloor to be visible compared with downward-facing (vertical) photography (Jamieson, 2016). This combination of camera and angle (Ultra-High Definition at 45°), LED lighting (1530 lm), and altitude (2 m above the seafloor) provides sufficient field of view (horizontal = 62.27°, vertical = 37.53°) and lighting to identify large mobile taxa. However, small sessile fauna (e.g., meiofauna, infauna) in the background of a frame can be difficult or impossible to confidently identify (e.g., Figure 3D), therefore this method focuses on assessments of mobile megafauna.

The NGS deep-sea camera system is free to spin in full 360-degree rotation around the anchor line axis, typically due to current, or an animal coming into physical contact with the camera. One disadvantage of this design compared to downward facing cameras, is that if the angled camera is facing away from where the animal is approaching, the video could miss the exact time of arrival (Jamieson, 2016). To capture the variability of survey area observed, rotation degree is recorded in the annotation process, quantified as a portion of a full 360-degree view (e.g., 90, 180, 270, and 360) represented during the deployment.

One challenge in animal identification with the current system is that the bait canister is situated below the camera and outside the field of view (Figure 1). Initially designed to keep the video frame unobstructed, this placement can, however, make taxonomic identification more challenging, as some animals approach the bait and obscure the camera lens. Future design improvements are planned to modify this feature so that the bait is within the field of view to aid in species identification to the highest possible taxonomic resolution.

## DISCUSSION

The next-generation NGS deep-sea camera system and deployment process has proven to be a robust and efficient deep-sea stationary video survey method. To ensure that data obtained is suitable for downstream use in EBV/EOV data product development, and interoperable with existing survey methods, we discuss the strengths and limitations of the method for consideration in future use.

### Advantages and Limitations of Method

A major advantage of the NGS deep-sea camera system method, as with other BRUVS, is that it is a non-extractive technique,

and can be used in delicate habitats (e.g., deep-sea coral gardens) (Jamieson, 2016; Whitmarsh et al., 2017; Levin et al., 2019). Further, for fish communities, an advantage of video rather than physical sampling, is that slender bodied species (e.g., *Synphobranchius* sp.) (Figure 3C) can escape through mesh used in physical sampling, creating a sampling artifact based on body-size and form (Clark et al., 2016). However, as a BRUVS survey method, the NGS deep-sea camera system is specialized to assess a target group (mobile predators with scavenging tendencies that are attracted to the bait), and is not intended to gather data on the full biological community (Farnsworth et al., 2007; Yeh and Drazen, 2011) as this method cannot consistently image small sessile fauna (e.g., meiofauna, infauna) (Bailey et al., 2007; e.g., Figure 3D). Further, chance encounters with non-attracted species (e.g., Siphonophora, Figure 3E) are not uncommon, but should be analyzed separately from bait-attracted taxa. Similarly, some animals are attracted not by the bait, but by some other disturbance introduced by the camera system, such as light (e.g., Euphausiidae, Figure 3E). These non-bait-attracted animal observations are noted during video review and annotation, and filtered accordingly in statistical analyses and inference of the mobile scavenging megafaunal assemblage. This limitation should be transparent in any presentation or discussion of the interpreted data.

Measures of density per unit volume are not obtained directly from survey footage because the current speed and direction affect the bait plume area of detection (Priede and Merrett, 1998). Therefore, any measure of density from baited cameras is considered theoretical based on models of the bait plume over distance and time (Priede and Merrett, 1998; Jamieson, 2016). The odor detection threshold is unknown for most species, however theoretical models predict a plume area of 0.6 km<sup>2</sup> after 6 h, and 2.4 km<sup>2</sup> after 12 h (assuming an average current speed of 0.05 ms<sup>-1</sup>) (Jamieson, 2016). Relative (rather than absolute) measures of abundance (MaxN) from the resultant footage is emphasized in data products and metadata to acknowledge the systemic bias of the method, not only for bait-attracted fauna in general, but also for varying behavior effects within the scavenging and predator assemblage (e.g., behavior to different bait-types, and species-specific reactions to artificial illumination). Species-specific reactions are expected to be consistent across sampling, so relative estimates are achievable with a consistent survey method. With these caveats noted, this method is specialized to measure the relative abundance and distribution for target taxa.

### Avoidance Behavior

Many deep-sea species are highly sensitive to artificial illumination, and so are repelled rather than attracted to the survey area (Fitzpatrick et al., 2013). While there is no evidence for absence of species due to artificial illumination, visual impairment can result in behavior change and thus uncertainty in baited camera results (Jamieson, 2016). A variety of animal responses to light are noted in the literature and range from blindness for some species to no effect for others (Jamieson,



2016). For example, deep-water eels (*Synaphobranchus kaupii*) decreased in numbers with illumination (Bailey et al., 2005) and sablefish (*Anoplopoma fimbria*) showed a flight response with white, but not far red light (Raymond and Widder, 2007). The Eastern Pacific Black Ghost shark (*Hydrolagus melanophasma*) was deterred from un-baited ROV surveys (James et al., 2009), however we saw no flight response in this species when using the NGS deep-sea camera system at Clipperton Atoll in the Tropical eastern Pacific (Giddens et al., 2020). As baited cameras typically use lower intensity and less-sustained illumination, compared to ROV and submersible surveys, the BRUVS method is less likely to disturb deep-sea fauna (Jamieson, 2016). Because of the systemic bias of artificial light introduced to a dark environment during deep-sea deployments, it is important that lighting intensity remains consistent among video surveys, in order to produce comparative relative estimates of biodiversity and community composition among locations (Hammerschlag et al., 2017).

For bait-selection, fishes that are native to the experimental site are more representative of the natural setting (Jamieson, 2016). Therefore, the specific bait type will vary among sampling campaigns specific to the region (Langlois et al., 2018). However, the use of deep-sea fish as bait may cause avoidance in conspecifics (Barry and Drazen, 2007), so surface-dwelling or pelagic fishes of the region should be used.

## Sampling Approach

The current NGS deep-sea camera system dataset (from years 2010 to 2020) consists of baseline observations and opportunistic sampling with point video surveys, producing species inventories for bait-attracted fauna. However, given the opportunistic model, past sampling campaigns rarely sampled evenly among depth strata and habitat types. Given variation in detectability among species and habitats, species-absences may be less-reliably measured by opportunistic point video surveys (Jetz et al., 2019). Especially for mobile groups such as predators and scavenging megafauna, larger or longer-lasting survey campaigns offer more reliable evidence of taxon absence. Repeated surveys that use a standardized protocol for sampling presence-absence at multiple time points are currently in development. Metadata reporting for each campaign, past and planned, will provide information about the extent, resolution, measurement units, and uncertainties of spatial, temporal, and taxonomic data dimensions (Jetz et al., 2019).

## Deployment Time per Depth

Generally, as depth increases, faunal density decreases over the vast expanse of the seafloor (Schiaparelli et al., 2016). Therefore, it is expected that with greater depth, a longer sampling time is needed to assess biodiversity and scavenger community composition with baited camera surveys (Whitmarsh et al., 2017). Sampling methods for shallow-water BRUVS (e.g., 0–100 m) are well established, and consistently use 1-hour deployment times (Langlois et al., 2018). However, the optimum sampling time in bathyal and abyssal depths are still unknown (Whitmarsh et al., 2017). To optimize deep BRUVS deployment protocols, a measure of the minimum time for video deployments per depth

strata is needed to ensure adequate sampling for MaxN without diminishing returns on recording time invested (Giddens et al., in prep). Further, as the density of organisms is expected to vary with levels of particulate organic carbon (POC) reaching the deep-sea from the surface waters (Levin et al., 2001) measures of time-to-MaxN should be determined for an array of seascape regimes (Giddens et al., in prep).

## CONCLUSION

The deep ocean presents a unique challenge for biological observing. While the density of any kind of data in the deep ocean is low, this is especially true for biological observations (Levin et al., 2019). Routine observations over time will be essential for environmental monitoring of the deep ocean, especially for Ecosystem Impact Assessments associated with resource extraction, area-based management, and climate change studies (Levin et al., 2019). To attain this data requirement efficiently, there is a need to incorporate emerging technology, such as low-cost imaging, into observing strategy plans (Canonico et al., 2019; Levin et al., 2019).

The next-generation NGS deep-sea camera system described here is a low-cost, lightweight device that can be deployed from nearly any vessel and added to an existing monitoring program to extend biological observing capacity into the deep sea. By detailing the deep-sea camera system elements and deployment protocols, along with the strengths and limitations of the method, our intention is to connect this information with ocean observers using similar methods and sampling approaches, and work toward common data standards to enable interoperability. Harmonized data streams can be used in conjunction to measure and report on the status of benthic fish assemblages at a global scale, and advance decadal goals for an integrated ocean observing system (Pearlman et al., 2019; Ryabinin et al., 2019).

## DATA AVAILABILITY STATEMENT

The original contributions presented in the study are included in the article/**Supplementary Material**, further inquiries can be directed to the corresponding author.

## AUTHOR CONTRIBUTIONS

JG and AT conceived the manuscript. JG coordinated the author contributions, wrote the text, edited, and contributed to the figures. WG and MR contributed to the manuscript figures and text. DD and AT contributed to the manuscript ideas and text. All authors approved the submission.

## FUNDING

This work was funded by the National Geographic Society.

## ACKNOWLEDGMENTS

We thank Enric Sala, Alan Friedlander, and the Pristine Seas team for their support of the NGS Deep-Sea Research Project. We also thank Alex Moen and the Explorer Engagement Program at NGS, and Deep-Sea Research team members Benjamin Woodward, Leigh Marsh, Jeffrey Drazen, Virginia Moriwake, and Katherine Croff Bell. We would like to thank Kasie Cocco, Kyler Abernathy, and the Exploration Technology Lab members past and present, including Eric Berkenpas, Mike Shepard, Brad

Henning, Jessica Elfadl, and Fabien Laurier. Finally we thank the editor and the two reviewers, whose comments have greatly improved this manuscript.

## SUPPLEMENTARY MATERIAL

The Supplementary Material for this article can be found online at: <https://www.frontiersin.org/articles/10.3389/fmars.2020.601411/full#supplementary-material>

## REFERENCES

- Bailey, D. M., Genard, B., Collins, M. A., Rees, J. F., Unsworth, S. K., Battle, E. J., et al. (2005). High swimming and metabolic activity in the deep-sea eel *Synaphobranchus kaupii* revealed by integrated in situ and in vitro measurements. *Physiol. Biochem. Zool.* 78, 335–346. doi: 10.1086/430042
- Bailey, D. M., King, N. J., and Priede, I. G. (2007). Cameras and carcasses: historical and current methods for using artificial food falls to study deep-water animals. *Mar. Ecol. Prog. Ser.* 350, 179–191. doi: 10.3354/meps07187
- Barry, J. P., and Drazen, J. C. (2007). Response of deep-sea scavengers to ocean acidification and the odor from a dead grenadier. *Mar. Ecol. Prog. Ser.* 350, 193–207. doi: 10.3354/meps07188
- Bax, N. J., Milosavljevic, P., Muller-Karger, F. E., Allain, V., Appeltans, W., Batten, S. D., et al. (2019). A response to scientific and societal needs for marine biological observations. *Front. Mar. Sci.* 6:395. doi: 10.3389/fmars.2019.00395
- Brandt, A., Gutt, J., Hildebrandt, M., Pawlowski, J., Schwendner, J., Soltwedel, T., et al. (2016). Cutting the umbilical: new technological perspectives in benthic deep-sea research. *J. Mar. Sci. Eng.* 4:36. doi: 10.3390/jmse4020036
- Buglass, S., Nagy, S., Ebert, D., Sepa, P., Turchik, A., Bell, K. L., et al. (2020). First records of the seven-gilled *Notorynchus cepedianus* and six-gilled *Hexanchus griseus* sharks (Chondrichthyes: Hexanchiformes: Hexanchidae) found in the Galápagos marine reserve. *J. Fish Biol.* 97, 926–929. doi: 10.1111/jfb.14447
- Canonica, G., Buttigieg, P. L., Montes, E., Stepien, C. A., Wright, D., Benson, A., et al. (2019). Global observational needs and resources for marine biodiversity. *Front. Mar. Sci.* 6:367. doi: 10.3389/fmars.2019.00367
- Chao, A., Gotelli, N. J., Hsieh, T. C., Sander, E. L., Ma, K. H., Colwell, R. K., et al. (2014). Rarefaction and extrapolation with Hill numbers: a framework for sampling and estimation in species diversity studies. *Ecol. Monogr.* 84, 45–67. doi: 10.1890/13-0133.1
- Clark, M. R., Bagley, N. W., and Harley, B. (2016). “Trawls,” in *Biological Sampling in the Deep Sea*, eds M. R. Clark, M. Consalvey, and A. A. Rowden (Oxford: Wiley Blackwell), 16–35.
- Costello, M. J., Bouchet, P., Boxshall, G., Fauchald, K., Gordon, D., Hoeksema, B. W., et al. (2013). Global coordination and standardisation in marine biodiversity through the World Register of Marine Species (WoRMS) and related databases. *PLoS One* 8:e51629. doi: 10.1371/journal.pone.0051629
- Costello, M. J., Coll, M., Danovaro, R., Halpin, P., Ojaveer, H., and Milosavljevic, P. (2010). A census of marine biodiversity knowledge, resources, and future challenges. *PLoS One* 5:e12110. doi: 10.1371/journal.pone.0012110
- De Pooter, D., Appeltans, W., Bailly, N., Bristol, S., Deneudt, K., Eliezer, M., et al. (2017). Toward a new data standard for combined marine biological and environmental datasets-expanding OBIS beyond species occurrences. *Biodivers. Data J.* 5:e10989. doi: 10.3389/bdj.5.e10989
- Drazen, J. C., and Sutton, T. T. (2017). Dining in the deep: the feeding ecology of deep-sea fishes. *Ann. Rev. Mar. Sci.* 9, 337–366. doi: 10.1146/annurev-marine-010816-060543
- Easton, E. E., Sellanes, J., Gaymer, C. F., Morales, N., Gorny, M., and Berkenpas, E. (2017). Diversity of deep-sea fishes of the Easter Island Ecoregion. *Deep Sea Res. 2 Top. Stud. Oceanogr.* 137, 78–88. doi: 10.1016/j.dsr2.2016.12.006
- Ewing, M., and Vine, A. (1938). Deep-sea measurements without wires or cables. *Eos Trans. Am. Geophys. Union* 19, 248–251. doi: 10.1029/tr019i001p00248
- Farnsworth, K. D., Thygesen, U. H., Ditlevsen, S., and King, N. J. (2007). How to estimate scavenger fish abundance using baited camera data. *Mar. Ecol. Prog. Ser.* 350, 223–234. doi: 10.3354/meps07190
- Fitzpatrick, C., McLean, D., and Harvey, E. S. (2013). Using artificial illumination to survey nocturnal reef fish. *Fish. Res.* 146, 41–50. doi: 10.1016/j.fishres.2013.03.016
- Friedlander, A. M., Giddens, J., Ballesteros, E., Blum, S., Brown, E. K., Caselle, J. E., et al. (2019). Marine biodiversity from zero to a thousand meters at Clipperton Atoll (Île de La Passion), Tropical Eastern Pacific. *PeerJ* 7:e7279. doi: 10.7717/peerj.7279
- Friedlander, A. M., Goodell, W., Salinas-de-León, P., Ballesteros, E., Berkenpas, E., Capurro, A. P., et al. (2020). Spatial patterns of continental shelf faunal community structure along the Western Antarctic Peninsula. *PLoS One* 15:e0239895. doi: 10.1371/journal.pone.0239895
- Gallo, N. D., Hardy, K., Wegner, N. C., Nicoll, A., Yang, H., and Levin, L. A. (2020). Characterizing deepwater oxygen variability and seafloor community responses using a novel autonomous lander. *Biogeosciences* 17, 3943–3960. doi: 10.5194/bg-17-3943-2020
- Giddens, J., Goodell, W., Friedlander, A., Salinas-de-León, P., Shepard, C., Henning, B., et al. (2019). Patterns in bathyal demersal biodiversity and community composition around archipelagos in the Tropical Eastern Pacific. *Front. Mar. Sci.* 6:388. doi: 10.3389/fmars.2019.00388
- Giddens, J., Salinas-de-León, P., Friedlander, A., Ebert, D. A., Henning, B., and Turchik, A. (2020). First observation of a *Hydrolagus melanophasma* (Chondrichthyes, Chimaeriformes, Holocephali) aggregation with egg cases extruding from a female. *Mar. Biodivers.* 50:91. doi: 10.1007/s12526-020-01122-3
- Hammerslag, N., Meyer, C. G., Grace, M. S., Kessel, S. T., Sutton, T. T., Harvey, E. S., et al. (2017). Shining a light on fish at night: an overview of fish and fisheries in the dark of night, and in deep and polar seas. *Bull. Mar. Sci.* 93, 253–284. doi: 10.5343/bms.2016.1082
- Hardisty, A. R., Michener, W. K., Agosti, D., García, E. A., Bastin, L., Belbin, L., et al. (2019). The Bari Manifesto: an interoperability framework for essential biodiversity variables. *Ecol. Inform.* 49, 22–31. doi: 10.1016/j.ecoinf.2018.11.003
- Hardy, K., Cameron, J., Herbst, L., Bulman, T., and Pausch, S. (2013). “Hadal landers: the DEEPSEA CHALLENGE ocean trench free vehicles,” in *Proceedings of the Oceans 2013 MTS/IEEE - San Diego*, (New York, NY: IEEE), 1–10.
- Harvey, E. S., Cappel, M., Butler, J. J., Hall, N., and Kendrick, G. A. (2007). Bait attraction affects the performance of remote underwater video stations in assessment of demersal fish community structure. *Mar. Ecol. Prog. Ser.* 350, 245–254. doi: 10.3354/meps07192
- Hsieh, T. C., Ma, K. H., and Chao, A. (2016). iNEXT: an R package for rarefaction and extrapolation of species diversity (Hill numbers). *Methods Ecol. Evol.* 7, 1451–1456. doi: 10.1111/2041-210X.12613
- Isaacs, J. D., and Schick, G. B. (1960). Deep-sea free instrument vehicle. *Deep Sea Res.* (1953) 7, 61–67. doi: 10.1016/0146-6313(60)90009-5
- James, K. C., Ebert, D. A., Long, D. J., and Didier, D. A. (2009). A new species of chimaera, *Hydrolagus melanophasma* sp. nov. (Chondrichthyes: Chimaeriformes: Chimaeridae), from the eastern North Pacific. *Zootaxa* 2218, 59–68. doi: 10.11646/zootaxa.2218.1.3
- Jamieson, A. J. (2016). “Landers baited cameras and traps,” in *Biological Sampling in the Deep Sea*, eds M. R. Clark, M. Consalvey, and A. A. Rowden (Hoboken, NJ: John Wiley & Sons), 228–259. doi: 10.1002/9781118332535.ch11
- Jamieson, A. J., Solan, M., and Fujii, T. (2009). Imaging deep-sea life beyond the abyssal zone. *Sea Technol.* 50, 41–46.



- Jetz, W., McGeoch, M. A., Guralnick, R., Ferrier, S., Beck, J., Costello, M. J., et al. (2019). Essential biodiversity variables for mapping and monitoring species populations. *Nat. Ecol. Evol.* 3, 539–551. doi: 10.1038/s41559-019-0826-1
- Langlois, T., Williams, J., Monk, J., Bouchet, P., Currey, L., Goetze, J., et al. (2018). “Marine sampling field manual for benthic stereo BRUVS (Baited Remote Underwater Videos),” in *Field Manuals for Marine Sampling to Monitor Australian Waters*, eds R. Przeslawski, and S. Foster (Canberra, ACT: National Environment Science Programme Marine Biodiversity Hub), 82–104.
- Leitner, A. B., Neuheimer, A. B., Donlon, E., Smith, C. R., and Drazen, J. C. (2017). Environmental and bathymetric influences on abyssal bait-attending communities of the Clarion Clipperton Zone. *Deep Sea Res. 1 Oceanogr. Res. Pap.* 125, 65–80. doi: 10.1016/j.dsr.2017.04.017
- Levin, L. A., Bett, B. J., Gates, A. R., Heimbach, P., Howe, B. M., Janssen, F., et al. (2019). Global observing needs in the deep ocean. *Front. Mar. Sci.* 6:241. doi: 10.3389/fmars.2019.00241
- Levin, L. A., Etter, R. J., Rex, M. A., Gooday, A. J., Smith, C. R., Pineda, J., et al. (2001). Environmental influences on regional deep-sea species diversity. *Annu. Rev. Ecol. Syst.* 32, 51–93. doi: 10.1146/annurev.ecolsys.32.081501.114002
- Linley, T. D., Craig, J., Jamieson, A. J., and Priede, I. G. (2018). Bathyal and abyssal demersal bait-attending fauna of the Eastern Mediterranean Sea. *Mar. Biol.* 165:159.
- Linley, T. D., Gerringer, M. E., Yancey, P. H., Drazen, J. C., Weinstock, C. L., and Jamieson, A. J. (2016). Fishes of the hadal zone including new species, in situ observations and depth records of Liparidae. *Deep Sea Res. 1 Oceanogr. Res. Pap.* 114, 99–110. doi: 10.1016/j.dsr.2016.05.003
- Miloslavich, P., Bax, N. J., Simmons, S. E., Klein, E., Appeltans, W., Aburto—Oropeza, O., et al. (2018). Essential ocean variables for global sustained observations of biodiversity and ecosystem changes. *Glob. Change Biol.* 24, 2416–2433. doi: 10.1111/gcb.14108
- Moltmann, T., Zhang, H. M., Turton, J. D., Nolan, G., Gouldman, C. C., Griesbauer, L., et al. (2019). A Global Ocean Observing System (GOOS), delivered through enhanced collaboration across regions, communities, and new technologies. *Front. Mar. Sci.* 6:291. doi: 10.3389/fmars.2019.00291
- Muller-Karger, F. E., Miloslavich, P., Bax, N. J., Simmons, S., Costello, M. J., Sousa Pinto, I., et al. (2018). Advancing marine biological observations and data requirements of the complementary essential ocean variables (EOVs) and essential biodiversity variables (EBVs) frameworks. *Front. Mar. Sci.* 5:211. doi: 10.3389/fmars.2018.00211
- Pearlman, J., Bushnell, M., Coppola, L., Karstensen, J., Buttigieg, P. L., Pearlman, F., et al. (2019). Evolving and sustaining ocean best practices and standards for the next decade. *Front. Mar. Sci.* 6:277. doi: 10.3389/fmars.2019.00277
- Pereira, H. M., Ferrier, S., Walters, M., Geller, G. N., Jongman, R. H. G., Scholes, R. J., et al. (2013). Essential biodiversity variables. *Science* 339, 277–278.
- Phillips, B. T., Licht, S., Haiat, K. S., Bonney, J., Allder, J., Chaloux, N., et al. (2019). DEEPI: a miniaturized, robust, and economical camera and computer system for deep-sea exploration. *Deep Sea Res. 1 Oceanogr. Res. Pap.* 153:103136. doi: 10.1016/j.dsr.2019.103136
- Phleger, C. F., and Soutar, A. (1971). Free vehicles and deep-sea biology. *Am. Zool.* 11, 409–418. doi: 10.1093/icb/11.3.409
- Priede, I. G., and Bagley, P. M. (2000). In situ studies on deep-sea demersal fishes using autonomous unmanned lander platforms. *Oceanogr. Mar. Biol.* 38, 357–392.
- Priede, I. G., and Merrett, N. R. (1998). The relationship between numbers of fish attracted to baited cameras and population density: studies on demersal grenadiers *Coryphaenoides (Nematonurus) armatus* in the abyssal NE Atlantic Ocean. *Fish. Res.* 36, 133–137. doi: 10.1016/s0165-7836(98)00105-2
- Provoost, P., De Pooter, D., Appeltans, W., Bailly, N., Bristol, S., Deneudt, K., et al. (2017). Expanding the Ocean Biogeographic Information System (OBIS) beyond species occurrences. *Biodivers. Inform. Sci. Stand.* 1:e20515. doi: 10.3897/dtwgproceedings.1.20515
- Raymond, E. H., and Widder, E. A. (2007). Behavioral responses of two deep-sea fish species to red, far-red, and white light. *Mar. Ecol. Prog. Ser.* 350, 291–298. doi: 10.3354/meps07196
- Rogers, A., Aburto-Oropeza, O., Appeltans, W., Assis, J., Ballance, L. T., Cury, P., et al. (2020). *Critical Habitats and Biodiversity: Inventory, Thresholds and Governance*. Washington, DC: World Resources Institute.
- Ryabinin, V., Barbière, J., Haugan, P., Kullenberg, G., Smith, N., McLean, C., et al. (2019). The UN decade of ocean science for sustainable development. *Front. Mar. Sci.* 6:470. doi: 10.3389/fmars.2019.00470
- Sayre, R. G., Wright, D. J., Breyer, S. P., Butler, K. A., Van Graafeiland, K., Costello, M. J., et al. (2017). A three-dimensional mapping of the ocean based on environmental data. *Oceanography* 30, 90–103. doi: 10.5670/oceanog.2017.116
- Schiaparelli, S., Rowden, A. A., and Clark, M. R. (2016). “Deep-sea fauna,” in *Biological Sampling in the Deep Sea*, eds M. R. Clark, M. Consalvey, and A. A. Rowden (Oxford: Wiley Blackwell), 16–35.
- Sigovini, M., Keppel, E., and Tagliapietra, D. (2016). Open nomenclature in the biodiversity era. *Methods Ecol. Evol.* 7, 1217–1225. doi: 10.1111/2041-210x.12594
- Smith, K. L. Jr., Clifford, C. H., Eliason, A. H., Walden, B., Rowe, G. T., and Teal, J. M. (1976). A free vehicle for measuring benthic community metabolism 1. *Limnol. Oceanogr.* 21, 164–170. doi: 10.4319/lo.1976.21.1.0164
- Tanhua, T., McCurdy, A., Fischer, A., Appeltans, W., Bax, N., Currie, K., et al. (2019). What we have learned from the framework for ocean observing: evolution of the global ocean observing system. *Front. Mar. Sci.* 6:471. doi: 10.3389/fmars.2019.00471
- Trenkel, V. M., Lorange, P., and Mahévas, S. (2004). Do visual transects provide true population density estimates for deepwater fish? *ICES J. Mar. Sci.* 61, 1050–1056. doi: 10.1016/j.icesjms.2004.06.002
- Turchik, A. J., Berkenpas, E. J., Henning, B. S., and Shepard, C. M. (2015). “The deep ocean dropcam: a highly deployable benthic survey tool,” in *Proceedings of the OCEANS 2015-MTS/IEEE Washington*, (New York, NY: IEEE), 1–8. doi: 10.1016/j.dsr.2014.07.011
- Whitmarsh, S. K., Fairweather, P. G., and Huveneers, C. (2017). What is big BRUVver up to? Methods and uses of baited underwater video. *Rev. Fish Biol. Fish.* 27, 53–73. doi: 10.1007/s11160-016-9450-1
- Willis, T. J., and Babcock, R. C. (2000). A baited underwater video system for the determination of relative density of carnivorous reef fish. *Mar. Freshw. Res.* 51, 755–763. doi: 10.1071/mf00010
- Worcester, P. F., Hardy, K. R., Horwitt, D. D., and Peckham, D. A. (1997). A deep ocean data recovery module. *Oceanogr. Lit. Rev.* 8:901.
- Yeh, J., and Drazen, J. C. (2009). Depth zonation and bathymetric trends of deepsea megafaunal scavengers of the Hawaiian Islands. *Deep Sea Res. 1 Oceanogr. Res. Pap.* 56, 251–266. doi: 10.1016/j.dsr.2008.08.005
- Yeh, J., and Drazen, J. C. (2011). Baited-camera observations of deep-sea megafaunal scavenger ecology on the California slope. *Mar. Ecol. Prog. Ser.* 424, 145–156. doi: 10.3354/meps08972

**Conflict of Interest:** The authors declare that the research was conducted in the absence of any commercial or financial relationships that could be construed as a potential conflict of interest.

Copyright © 2021 Giddens, Turchik, Goodell, Rodriguez and Delaney. This is an open-access article distributed under the terms of the Creative Commons Attribution License (CC BY). The use, distribution or reproduction in other forums is permitted, provided the original author(s) and the copyright owner(s) are credited and that the original publication in this journal is cited, in accordance with accepted academic practice. No use, distribution or reproduction is permitted which does not comply with these terms.



# Mass Mortality of Foundation Species on Rocky Shores: Testing a Methodology for a Continental Monitoring Program

**María M. Mendez<sup>1,2\*</sup>, Juan P. Livore<sup>1</sup>, Federico Márquez<sup>1,2</sup> and Gregorio Bigatti<sup>1,2,3</sup>**

<sup>1</sup> Laboratorio de Reproducción y Biología Integrativa de Invertebrados Marinos, Instituto de Biología de Organismos Marinos-Consejo Nacional de Investigaciones Científicas y Técnicas, Puerto Madryn, Argentina, <sup>2</sup> Universidad Nacional de la Patagonia San Juan Bosco, Puerto Madryn, Argentina, <sup>3</sup> Universidad Espíritu Santo, Samborombón, Ecuador

## OPEN ACCESS

### Edited by:

Juan Carlos Azofeifa-Solano,  
University of Costa Rica, Costa Rica

### Reviewed by:

Michelle Jillian Devlin,  
Centre for Environment, Fisheries and  
Aquaculture Science (CEFAS),  
United Kingdom  
María Gabriela Palomo,  
Independent Researcher, Buenos  
Aires, Argentina

### \*Correspondence:

María M. Mendez  
mendez@cenpat-conicet.gob.ar

### Specialty section:

This article was submitted to  
Ocean Observation,  
a section of the journal  
Frontiers in Marine Science

**Received:** 23 October 2020

**Accepted:** 15 January 2021

**Published:** 09 February 2021

### Citation:

Mendez MM, Livore JP, Márquez F  
and Bigatti G (2021) Mass Mortality of  
Foundation Species on Rocky Shores:  
Testing a Methodology for a  
Continental Monitoring Program.  
Front. Mar. Sci. 8:620866.  
doi: 10.3389/fmars.2021.620866

Global concern around substantial losses of biodiversity has led to the development of a number of monitoring programs. Networks were established to obtain appropriate data on the spatial and temporal variation of marine species on rocky shores. Recently, the Marine Biodiversity Observation Network Pole to Pole of the Americas (MBON P2P) program was established and is coordinating biodiversity surveys along coastal areas throughout the continent. The goal of this paper was to test the usefulness and adequacy of a methodology proposed for the MBON P2P program. Changes in benthic assemblage cover were studied on monitored sites in northern Patagonia before and after the 2019 austral summer. Long-term dynamics of mussel bed is described based on existing data. Results showed that assemblages before the 2019 austral summer were different from assemblages after it. Thus, a mussel mass mortality event could be detected with this methodology. It took less than a year for mussel cover to drop from 90 to almost 0%; even where substantial changes in mussel bed cover were not registered in the previous ~20 years at the study area. This simple methodology is an adequate tool for monitoring rocky intertidal habitats. Yearly monitoring is needed, as a minimum, to perceive this kind of process timely. Real-time detection offers the opportunity of properly understanding the causes that lead to the loss of key community components, such as these foundation species. Furthermore, it would provide early warning to decision-makers enhancing the chances of conservation of natural environments and their ecosystem services.

**Keywords:** benthos, disturbance, conservation, mussels, ecosystem services, intertidal

## INTRODUCTION

Rocky shores are one of the most widely distributed coastal habitats throughout the world (Thompson et al., 2002). Different human stressors, including introduction of species, physical modification of the coast, contamination, recreation, and the changes in climate are continuously threatening these habitats (Halpern et al., 2015; Duffy et al., 2019). Several efforts have been made to build coordinated international monitoring networks across the world aimed at obtaining temporal data on biodiversity, community structure, and dynamics of rocky shores (Canónico et al., 2019; Duffy et al., 2019). Starting with

the Marine Biodiversity and Climate Change Project (MarClim) in 1950 on the coast of United Kingdom and France, different programs have been developed with this premise around the world.

The history of monitoring networks in South America is relatively short; with three main efforts recorded in the last 20 years. The Natural Geography in Shore Areas (NaGISA) project of the Census of Marine Life (CoML) program (2000–2010) and its sequel the South American Research Group on Coastal Ecosystems (SARCE) (since 2011), together monitored rocky shores over more than 60° of latitude across 150 sites. Such monitoring described and analyzed biodiversity patterns across latitudinal gradients and linked them with ecosystem functioning and human stressors (Miloslavich et al., 2016; Cruz Motta et al., 2020). Lastly in 2016, the Pole to Pole project of the Marine Biodiversity Observation Network (MBON P2P) was established with a goal of using common methods for the collection of biological information in coastal habitats throughout the American continent (Canonico et al., 2019; Duffy et al., 2019).

Argentinean Patagonia (41–55°S; 63–70°W) rocky intertidal shores were included as sampling sites since 2007 in the NaGISA and SARCE projects (Miloslavich et al., 2016; Cruz Motta et al., 2020) and are currently being included in MBON P2P. One of the most important features on these shores is the extreme desiccation that intertidal organisms are exposed to through a combination of strong dry winds, low humidity and scarce rainfall (Bertness et al., 2006). Scorched mussel beds of the mid intertidal are a distinctive component of the shores and a dense matrix of the two species, *Brachidontes rodriguezii* and *Perumytilus purpuratus*, dominate the physiognomy of the rocky shore communities (Bertness et al., 2006; Silliman et al., 2011; Miloslavich et al., 2016). These communities are unique because almost all mid intertidal organisms are unable to survive outside of the mussel bed; hence community structure and its diversity along with ecosystem function in these shores are obligately dependent on these foundation species (Bertness et al., 2006). Historically, mussel beds from this region show simple structure, uniform appearance and disturbance-generated bare space throughout the bed is strikingly rare (Bertness et al., 2006; Adami et al., 2018). However, losses in cover of scorched mussels were visually observed at different monitored sites after the 2019 austral summer. The goal of this paper was to test the usefulness and adequacy of a simple, low-cost, low-tech methodology proposed for the recently established MBON P2P program (Livore et al., 2021). To do this, we compare the mid intertidal benthic assemblage before and after the 2019 austral summer using this methodology. A description of the long-term cover dynamics of the mid intertidal foundation species is given in order to provide a context of the temporal scale of natural fluctuations in the study area.

## MATERIALS AND METHODS

### Study Sites and Sampling Design

The study was performed at three rocky shores (Punta Cuevas: PC, Punta Este: PE and Punta Loma: PL; **Figure 1**)

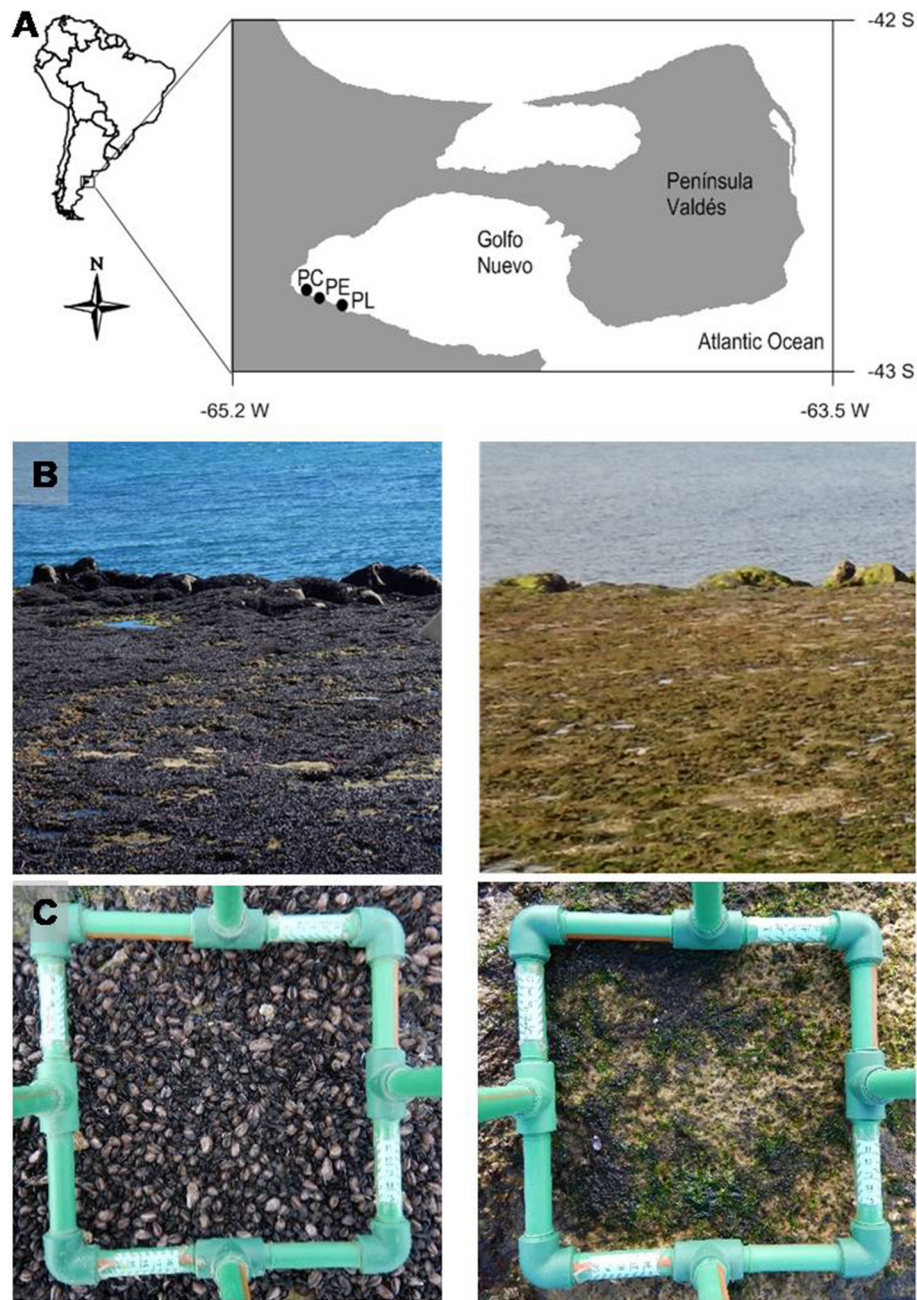
on the southwest coast of Golfo Nuevo, Chubut, Patagonia Argentina. Sites have similar slope, and semidiurnal tides with mean amplitude of ~4 m, which exposes a sedimentary rock platform (consolidated mudstone). The characteristic three-level biological zonation of Patagonian rocky shores (Bertness et al., 2006; Rechimont et al., 2013; Miloslavich et al., 2016) was present at the three studied sites. The high intertidal zone has a large proportion of bare soil, being the invasive barnacle *Balanus glandula* and the limpet *Siphonaria lessonii* abundant. The mid-intertidal is typically dominated by matrix of scorched mussels, *Brachidontes rodriguezii* and *Perumytilus purpuratus*. The low intertidal level is characterized by several ephemeral algal species and a large proportion of the calcareous alga *Corallina officinalis*. PC and PE were monitoring sites of the SARCE project and the three sites are currently part of the MBON P2P program.

As mentioned in the Introduction, losses in scorched mussel cover were visually observed in the mid intertidal at several sites along the coast of Golfo Nuevo after the 2019 austral summer (**Figure 1**). Thus, we compare the mid intertidal benthic assemblage in two different times: before and after this event using data collected through a simple, low-cost, low-tech methodology proposed for the MBON P2P program. For the before samplings, data was obtained from previous surveys performed in October 2014 (at PL site) and in October 2018 (at PC and PE sites). After samplings were conducted in June 2019 at the three sites. A specifically designed protocol to study changes in rocky shore communities was used in all sampling events (adapted from Ocean Best Practices: <http://dx.doi.org/10.25607/OBP-5>). Briefly, percentage cover of benthic organisms was estimated inside 25 × 25 cm photoquadrats haphazardly placed on the substrate ( $n = 5\text{--}10$  per sampling;  $N = 50$ ). Recently, this methodology was compared to a previously used *in situ* visual methodology and both similarly detected spatial and temporal variability of rocky shores assemblages (Livore et al., 2021). In the lab, 100 equidistant points were placed over the digital image using the free software Coral Point Count (CPCe V 4.1, Kohler and Gill, 2006) and organisms observed under each point were determined to the lowest possible taxonomic level.

Non-metric multi-dimensional scaling (nMDS) was used to visualize multivariate patterns in benthic assemblages. Percentage covers of benthic taxa were analyzed using permutational analysis of variance (PERMANOVA). Similarity matrices based on Bray-Curtis measure were generated for the analyses, which used 9,999 permutations of residuals under a reduced model. PERMANOVA model had two factors: sites (Si, fixed, three levels: PC, PE, and PL) and Time (Ti, fixed, two levels: before and after). Pairwise comparisons were performed among all pair of sites for the two times levels. A similarity percentage analysis (SIMPER) was performed to determine the taxa responsible for the similarities among sites and the dissimilarities between times. All the multivariate analysis were performed using PRIMER v6.1.7 software.

To describe the long-term natural dynamics of mid intertidal foundation species we collected historical data from Punta Cuevas. This intertidal is located at the southern end of the



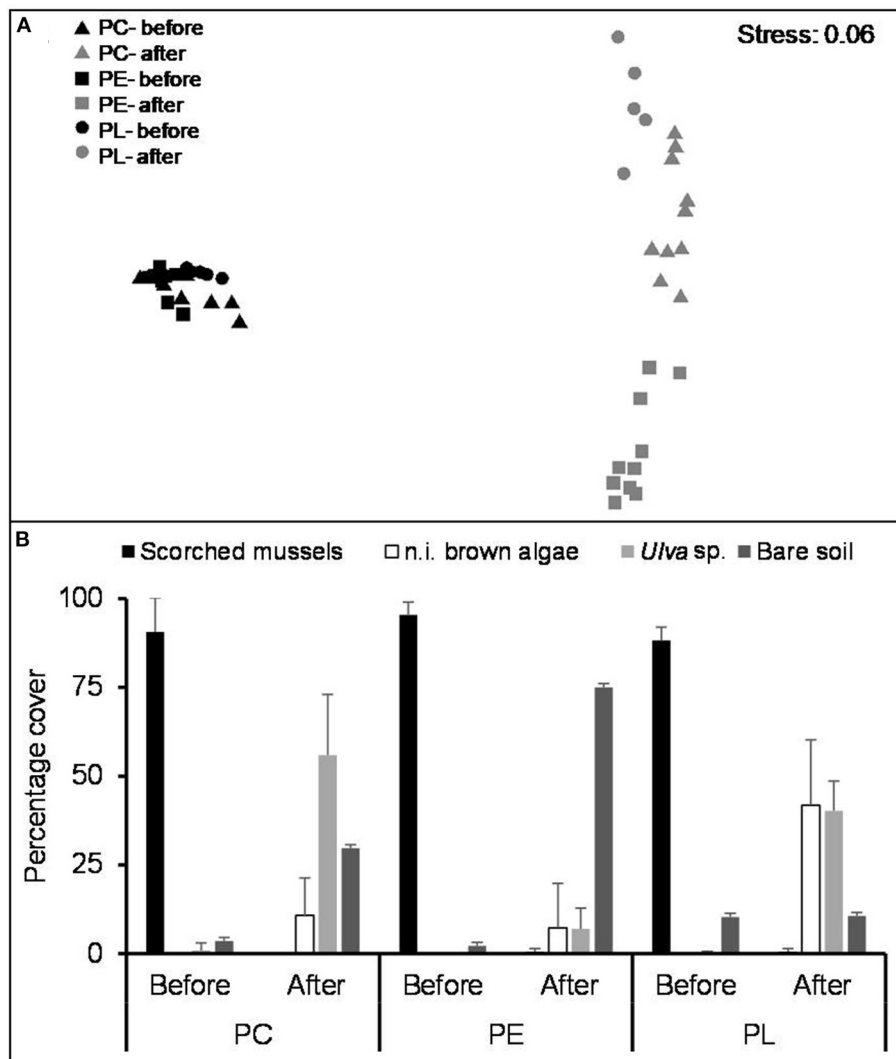


**FIGURE 1 | (A)** Map of South America showing the location of the study sites. PC, Punta Cuevas; PE, Punta Este; and PL, Punta Loma. **(B)** Punta Loma mid intertidal rocky shore showing the typical cover of the mussel bed in February 2018 (left) and in May 2019 (right). **(C)** Plots in the mid intertidal of Punta Cuevas in October 2018 (left) and after the mass mortality event, when mussels were absent on all horizontal surfaces in June 2019 (right).

city of Puerto Madryn, 500 meters from the CCT CONICET-CENPAT and the Universidad Nacional de la Patagonia (the authors' workplaces). Both scientist and biology professors, from these institutions, regularly use the site for academic and scholar field trips. Thus, quantitative (for example, percentage cover) and qualitative (for example, panoramic photographs) data was obtained almost annually for the last ~20 years to examine the stability and resilience of the mid intertidal. Due

to the heterogeneity in the nature of the data a qualitative description of mussel cover at Punta Cuevas over the past ~20 years was obtained. Landscape photographs, occurrence data and percentage cover data of organisms at the site were considered (for details see **Table 2**). From these sources, scorched mussel cover was estimated into three categories: <50, 50–80, and >80%. Large bare soil patches (>10 m<sup>2</sup>) in photographs, if present, were recorded.





**FIGURE 2 | (A)** Two-dimensional MDS ordination comparing benthic assemblages associated with the three sites before and after the 2019 austral summer. **(B)** Mean (SD) scorched mussel, not identified (n.i.) brown algae, *Ulva* sp., and bare soil cover for the three samplings sites before and after the 2019 austral summer. These taxa explain >90% of the observed differences in the assemblages between sampling times (SIMPER analysis, **Table 1**).

## RESULTS

Benthic assemblages before the 2019 austral summer were dissimilar to assemblages after it (**Figure 2A**). No clear separation between sites was distinguished in the before samplings, but samples were grouped by sites in the after samplings (**Figure 2A**). The assemblages before the 2019 austral summer were significantly different from the assemblages after it and among sampling sites [PERMANOVA, SixTi: pseudo- $F = 29.14$ ,  $df = 2$ ,  $p(\text{perm}) < 0.05$ ]. Pairwise comparisons showed that for the before samplings,  $PC = PE$ ,  $PC = PL$  [ $p(\text{perm}) > 0.05$ ] and  $PE \neq PL$  [ $p(\text{perm}) < 0.05$ ]. For the after samplings, instead, all sites were different from each other [ $p(\text{perm}) < 0.05$ ]. SIMPER analysis showed that scorched mussels were responsible for most of the similarity between

sites in the before samplings (**Table 1**). Cover of bare soil, *Ulva* sp., and a not identified brown algae, mostly contribute to the similarities between sites after the 2019 summer (**Table 1**). When before and after samplings were compared, scorched mussels, bare soil, *Ulva* sp., and a not identified brown algae cover explain the high dissimilarity found between times (**Table 1** and **Figure 2B**).

The examination of the available occurrence and cover data and photographs suggests that the natural dynamics of the mid intertidal at the studied site is very stable and uniform through time. Throughout the last ~20 years, mussel cover was >80%, and no substantial changes in cover were registered at the site (**Table 2**). Furthermore, bare soil patches >10 m<sup>2</sup> were not observed in the mussel bed during this period.

**TABLE 1 |** SIMPER routine results showing taxa with the greatest contributions to similarity among sites and the dissimilarities between times.

	Contrib%	Cum.%
<b>Time: before (average similarity: 92.11%)</b>		
Scorched mussels	96.56	96.56
<b>Time: after (average similarity: 75.30%)</b>		
Bare soil	54.32	54.32
<i>Ulva</i> sp.	34.24	88.55
n.i. brown algae	8.01	96.56
<b>Before vs. after (average dissimilarity = 94.60%)</b>		
Scorched mussels	48.72	48.72
Bare soil	23.5	72.21
<i>Ulva</i> sp.	16.91	89.13
n.i. brown algae	6.71	95.83

n.i., not identified.

**TABLE 2 |** Natural dynamics of Punta Cuevas mussel bed between 1998 and 2020.

Period	Sampling	Mussel bed cover estimation
1998–2001	Occurrence frequency <sup>1</sup> and landscape photographs	>80%
2002–2005	Occurrence frequency <sup>1</sup> and landscape photographs	>80%
2006–2009	Occurrence frequency <sup>2</sup> and landscape photographs	>80%
2010–2013	Cover data, <sup>3,4</sup> occurrence frequency, <sup>2</sup> and landscape photographs	>80%
2014–2017	Cover data, <sup>3,4</sup> occurrence frequency, <sup>2</sup> and landscape photographs	>80%
2018–2020	Cover data, <sup>5</sup> occurrence frequency, <sup>2</sup> and landscape photographs	No mussels after 2019 summer

Data collected from: <sup>1</sup>Torres and Caille (2009), <sup>2</sup>“Community ecology” samplings (Prof. A. Bisigato, UNPSJB), <sup>3</sup>“Malacology” sampling (Prof. G. Bigatti, UNPSJB), <sup>4</sup>SARCE samplings, <sup>5</sup>MBON samplings and a vast photographic record of the site.

## DISCUSSION

This study shows how a simple low-cost and non-extractive methodology was able to detect changes in mid intertidal rocky shore assemblages, as a scorched mussel mass mortality event on Patagonian coasts. Anthropogenic pressure on coastal areas is increasing worldwide, and detecting temporal and spatial changes in rocky shore biodiversity is critical for its conservation (Duffy et al., 2019). Those sites suffering significant changes in biodiversity are considered degraded or unhealthy ecosystems. This equates to risks to different ecosystem services for billions of people, some as essential as human nutrition and health, recreation attractions or public safety (Canonico et al., 2019). One way to detect biodiversity changes is the implementation of monitoring programs. Although the history of these programs is quite young in South America, the present study provides empirical evidence on the efficacy of their methodologies in

detecting rapid biodiversity changes. In the study area, dense beds of scorched mussels are a distinct component and the foundation species in the mid intertidal (Bertness et al., 2006; Miloslavich et al., 2016; Adami et al., 2018). In the present work, we found that mussel bed cover at different sites of Golfo Nuevo was close to 90% before the 2019 austral summer. However, almost no scorched mussels were registered at the sites after the 2019 summer, being replaced with bare soil and different algae (Figure 1).

In northern Patagonian rocky shores, desiccation plays a fundamental role in community structure (Bertness et al., 2006). Only a few habitat-forming species are capable of tolerating the extreme physical conditions. Several studies have described in detail the role of scorched mussels as ecosystem engineer species and in the provision of habitats and refuge for other organisms (Bertness et al., 2006; Silliman et al., 2011; Rechimont et al., 2013; Arribas et al., 2014, 2019). These studies report that more than 40 invertebrate species live associated with mussel beds avoiding environmental stress. In order to prevent the removal of living organisms and degradation of natural sites, global monitoring programs try to incorporate non-destructive sampling methodologies, like the one used here. Undoubtedly, there are some limitations related to this type of sampling, such as not detecting organisms associated with mussel beds. In this sense, the present work aimed at studying changes in cover on the dominant sessile intertidal species. However, the observed loss of the mussel cover and its replacement by ephemeral algae and bare soil would likely have important indirect effects on the associated assemblage through the absence of tens of species.

Our examination of the natural dynamics of Punta Cuevas mid intertidal showed that scorched mussel beds are highly stable and resistant to disturbance, as was suggested by Bertness et al. (2006) for central Patagonian rocky shores. This contrasts with mussel beds on the Atlantic and Pacific coasts of North America, for example, where disturbance-generated patches are common (Paine and Levin, 1981). The registered stability could be related to the small size of scorched mussels (usually about 0.20 cm long) and its strong byssal attachment strength (Bertness et al., 2006; Mendez et al., 2019). The pattern described in this study suggests that the drastic decline of scorched mussel cover observed at the study sites was not a consequence of the natural dynamics of the mussel bed and that this event was not part of the baseline fluctuations of the mid rocky shore assemblage.

From a conservation perspective, it is essential to consider the recovery time needed by a given community to reestablish after drastic changes in foundation species cover as the one detected here. Although *B. rodriguezii* has been observed to recruit continuously during the year in northern Atlantic Patagonia (Arribas et al., 2015), it would take up to a decade to reach the full recovery of the mussel bed (Bertness et al., 2006; Mendez et al., 2017). In this sense, the possibility of natural recovery from this event will depend on different processes related to larval recruitment, including larvae arrival from unaffected areas, and the reproduction of individuals in the affected areas (Kersting et al., 2020). We found that after the mass mortality event of scorched mussels, different opportunistic algae and bare soil dominated the mid intertidal. The switch

in species dominance at the sites (i.e., algae and bare soil replacing mussels) could last several years and would influence local biological interactions with important consequences for community structure. Furthermore, the assemblages of the studied sites responded differently to mussel losses. After the 2019 austral summer, heterogeneity of the assemblages increased among sites and samples. This suggests that the effects of the mussel mortality are site-specific and could be hard to predict. Thus, in systems exposed to high physical stress where foundation species are dominant, management and conservation efforts should be focused on the foundation species instead of charismatic organisms that live associated to them (Bertness et al., 2006).

When massive mortalities occur, there is a need to study the causes of the event. Fungi, parasites, bacteria, viruses or toxic blooms have been reported as responsible agents for this kind of events in bivalves (Peperzak and Poelman, 2008; Vázquez et al., 2016; Kersting et al., 2020). More recently, several studies documented how extreme weather events (e.g., heatwaves) can be responsible for mass mortalities in dominant organisms (Zamir et al., 2018), including mytilids (Seuront et al., 2019; Lupo et al., 2021). The fact that the changes in mussel cover were detected after a summer suggests that mortality could be related to weather conditions. Even though no extraordinary storm events were registered in the 2019 summer, the loss of scorched mussels cover coincided with high atmospheric temperature ( $>35^{\circ}\text{C}$ ) and strong winds ( $>30$  knots) occurring simultaneously during low tides that exposed these organisms to prolonged thermal and desiccation stress over several continuous days (Mendez et al., 2020). These atmospheric conditions also coincided with sea surface temperature anomalies exceeding  $1^{\circ}\text{C}$  occurring in Golfo Nuevo, indicating the presence of heatwaves during the 2019 austral summer (Mendez et al., 2020). Also, different parasites and viruses were reported in the area, several of them directly affecting local bivalve species (Vázquez et al., 2020). Thus, different drivers or a combination of them can be causing the registered mortality of scorched mussels (Lupo et al., 2021). At the time of publication, potential causes for this sudden mass mortality are being studied, and none of them could be completely ruled out.

In this work a scorched mussel mass mortality event was detected, taking  $<6$  months (summer 2019) for the mussel beds to decline from 90% to losing all of its cover (**Figure 1**). Significant effort is spent on debating sampling frequency in

monitoring programs; our results contribute empiric evidence that highlights the need to have at least yearly monitoring. It is important to note that without periodic monitoring, this mortality case would not have been detected in its beginnings and the causes that led to it could not have been appropriately studied. The immediacy of the detection gives us the opportunity to study the changes in the community from the start and to follow the entire recovery process, whilst considering the concomitant effects on ecosystem function. Studies of this nature, derived from monitoring programs, can give an early alarm to decision-makers and provide a timely response action that mitigates the impacts on coastal zones and preserves rocky shore environments and their ecosystem services.

## DATA AVAILABILITY STATEMENT

The raw data supporting the conclusions of this article will be made available by the authors, without undue reservation.

## AUTHOR CONTRIBUTIONS

MMM analyse the data and wrote the manuscript with contribution from all authors. All authors conceived the project and participated in data collection in the field.

## FUNDING

Field work was partially financially supported by ANPCyT-FONCyT (PICT 2018-0969). Field work was also supported by Total Foundation (SARCE program) and NASA under the A.50 AmeriGEO Work Program of the Group on Earth Observations with grant number 80NSSC18K0318 (Laying the foundations of the Pole-to-Pole Marine Biodiversity Observation Network of the Americas [MBON Pole to Pole]).

## ACKNOWLEDGMENTS

We were grateful to all the colleges and friends that kindly share information and photographs of Punta Cuevas. We thank Pepe Ojeda for technical support. The manuscript was greatly improved by the comments of two reviewers. This was publication #142 of the Laboratorio de Reproducción y Biología Integrativa de Invertebrados Marinos (LARBIM).

## REFERENCES

- Adami, M., Schwindt, E., Tablado, A., Calcagno, J., Labraga, J. C., and Orensanz, J. M. (2018). Intertidal mussel beds from the South-western Atlantic show simple structure and uniform appearance: does environmental harshness explain the community? *Mar. Biol. Res.* 14, 403–419. doi: 10.1080/17451000.2017.1417603
- Arribas, L. P., Bagur, M., Gutiérrez, J. L., and Palomo, M. G. (2015). Matching spatial scales of variation in mussel recruitment and adult densities across southwestern Atlantic rocky shores. *J. Sea Res.* 95, 16–21. doi: 10.1016/j.seares.2014.10.015
- Arribas, L. P., Donnarumma, L., Palomo, M. G., and Scrosati, R. A. (2014). Intertidal mussels as ecosystem engineers: their associated invertebrate biodiversity under contrasting wave exposures. *Mar. Biodiv.* 44, 203–211. doi: 10.1007/s12526-014-0201-z
- Arribas, L. P., Gutiérrez, J. L., Bagur, M., Soria, S. A., Penchaszadeh, P. E., and Palomo, M. G. (2019). Variation in aggregate descriptors of rocky shore communities: a test of synchrony across spatial scales. *Mar. Biol.* 166:44. doi: 10.1007/s00227-019-3492-6
- Bertness, M. D., Crain, C. M., Silliman, B. R., Bazterrica, M. C., Reyna, M. V., Hidalgo, F., et al. (2006). The community structure of Western Atlantic Patagonian rocky shores. *Ecol. Monogr.* 76, 439–460. doi: 10.1890/0012-9615(2006)076[0439:TCSOWA]2.0.CO;2
- Canonico, G., Buttigieg, P. L., Montes, E., Muller-Karger, F. E., Stepien, C. A., Wright, D., et al. (2019). Global observational needs and resources

- for marine biodiversity. *Front. Mar. Sci.* 6:367. doi: 10.3389/fmars.2019.00367
- Cruz Motta, J. J., Miloslavich, P., Guerra-Castro, E., Hernández-Agreda, A., Herrera, C., Barros, et al. (2020). Latitudinal patterns of species diversity on South American rocky shores: local processes lead to contrasting trends in regional and local species diversity. *J. Biogeogr.* 47, 1966–1979. doi: 10.1111/jbi.13869
- Duffy, J. E., Benedetti-Cecchi, L., Trinanès, J., Muller-Karger, F. E., Ambo-Rappe, R., Boström, C., et al. (2019). Toward a coordinated global observing system for seagrasses and marine macroalgae. *Front. Mar. Sci.* 6:317. doi: 10.3389/fmars.2019.00317
- Halpern, B. S., Frazier, M., Potapenko, J., Casey, K. S., Koenig, K., Longo, K., et al. (2015). Spatial and temporal changes in cumulative human impacts on the world's ocean. *Nat. Commun.* 6:7615. doi: 10.1038/ncomms8615
- Kersting, D. K., Vázquez-Luis, M., Mourre, B., Belkhamssa, F. Z., Álvarez, E., Bakran-Petricoli, T., et al. (2020). Recruitment disruption and the role of unaffected populations for potential recovery after the *Pinna nobilis* mass mortality event. *Front. Mar. Sci.* 7:594378. doi: 10.3389/fmars.2020.594378
- Kohler, K. E., and Gill, S. M. (2006). Coral Point Count with Excel extensions (CPCe): a visual basic program for the determination of coral and substrate coverage using random point count methodology. *Comput. Geosci.* 32, 1259–1269. doi: 10.1016/j.cageo.2005.11.009
- Livore, J. P., Mendez, M. M., Miloslavich, P., Rilov, G., and Bigatti, G. (2021). Biodiversity monitoring in rocky shores: challenges of devising a globally applicable and cost-effective protocol. *Ocean Coast. Manage.* (in press).
- Lupo, C., Bougeard, S., Le Bihan, V., Blin, J. L., Allain, G., Azéma, P., et al. (2021). Mortality of marine mussels *Mytilus edulis* and *M. galloprovincialis*: systematic literature review of risk factors and recommendations for future research. *Rev. Aquacult.* 13, 504–536. doi: 10.1111/raq.12484
- Mendez, M. M., Livore, J. P., and Bigatti, G. (2019). Interaction of natural and anthropogenic stressors on rocky shores: community resistance to trampling. *Mar. Ecol. Prog. Ser.* 631, 117–126. doi: 10.3354/meps13144
- Mendez, M. M., Livore, J. P., Bigatti, G., and Montes, E. (2020). “Integrating *in situ* and satellite-based observations to unravel a mass mortality event of mussel beds in Patagonia, Argentina,” in *AGU Fall Meeting, Virtual Meeting, 1–17 December*. San Francisco, CA.
- Mendez, M. M., Livore, J. P., Calcagno, J. A., and Bigatti, G. (2017). Effects of recreational activities on Patagonian rocky shores. *Mar. Environ. Res.* 130, 213–220. doi: 10.1016/j.marenvres.2017.07.023
- Miloslavich, P., Cruz-Motta, J. J., Hernandez, A., Herrera, C. A., Klein, E., Barros, F., et al. (2016). “Benthic assemblages in South American intertidal rocky shores: biodiversity, services, and threats,” in *Marine Benthos: Biology, Ecosystem Functions and Environmental Impact*, ed R. R. Rodríguez (New York, NY: Nova Science Publishers).
- Paine, R. T., and Levin, S. A. (1981). Intertidal landscapes: disturbance and the dynamics of pattern. *Ecol. Monogr.* 51, 145–178. doi: 10.2307/2937261
- Peperzak, L., and Poelman, M. (2008). Mass mussel mortality in The Netherlands after a bloom of *Phaeocystis globosa* (Prymnesiophyceae). *J. Sea Res.* 60, 220–222. doi: 10.1016/j.seares.2008.06.001
- Rechimont, M. E., Galvan, D. E., Sueiro, M. C., Casas, G., Piriz, M. L., Diez, M. E., et al. (2013). Benthic diversity and assemblage structure of a north Patagonian rocky shore: a monitoring legacy of the NaGISA project. *J. Mar. Biol. Assoc. U.K.* 93, 2049–2058. doi: 10.1017/S0025315413001069
- Seuront, L., Nicastro, K. R., Zardi, G. I., and Goberville, E. (2019). Decreased thermal tolerance under recurrent heat stress conditions explains summer mass mortality of the blue mussel *Mytilus edulis*. *Sci. Rep.* 9:17498. doi: 10.1038/s41598-019-53580-w
- Silliman, B. R., Bertness, M. D., Altieri, A. H., Griffin, J. N., Bazterrica, M. C., Hidalgo, F. J., et al. (2011). Whole-community facilitation regulates biodiversity on Patagonian rocky shores. *PLoS ONE* 6:e24502. doi: 10.1371/journal.pone.0024502
- Thompson, R. C., Crowe, T. P., and Hawkins, S. J. (2002). Rocky intertidal communities: past environmental changes, present status and predictions for the next 25 years. *Environ. Conserv.* 29, 168–191. doi: 10.1017/S0376892902000115
- Torres, A., and Caille, G. (2009). Las comunidades del intermareal rocoso antes y después de la eliminación de un disturbio antropogénico: un caso de estudio en las costas de Puerto Madryn (Patagonia, Argentina). *Rev. Biol. Mar. Oceanogr.* 44, 517–521. doi: 10.4067/S0718-19572009000200024
- Vázquez, N., Fiori, S., Arzul, I., Carcedo, C., and Cremonte, F. (2016). Mass mortalities affecting populations of the yellow clam *Amarilladessa mactroides* along its geographic range. *J. Shellfish Res.* 35, 739–745. doi: 10.2983/035.035.0403
- Vázquez, N., Frizzera, A., and Cremonte, F. (2020). Diseases and parasites of wild and cultivated mussels along the Patagonian coast of Argentina, southwest Atlantic Ocean. *Dis. Aquat. Organ.* 139, 139–152. doi: 10.3354/dao 03467
- Zamir, R., Alpert, P., and Rilov, G. (2018). Increase in weather patterns generating extreme desiccation events: implications for Mediterranean rocky shore ecosystems. *Estuar. Coasts* 41, 1868–1884. doi: 10.1007/s12237-018-0408-5

**Conflict of Interest:** The authors declare that the research was conducted in the absence of any commercial or financial relationships that could be construed as a potential conflict of interest.

Copyright © 2021 Mendez, Livore, Márquez and Bigatti. This is an open-access article distributed under the terms of the Creative Commons Attribution License (CC BY). The use, distribution or reproduction in other forums is permitted, provided the original author(s) and the copyright owner(s) are credited and that the original publication in this journal is cited, in accordance with accepted academic practice. No use, distribution or reproduction is permitted which does not comply with these terms.





# Time-Varying Epipelagic Community Seascapes: Assessing and Predicting Species Composition in the Northeastern Pacific Ocean

Caren Barceló<sup>1\*</sup>, Richard D. Brodeur<sup>2</sup>, Lorenzo Ciannelli<sup>1</sup>, Elizabeth A. Daly<sup>3</sup>, Craig M. Risien<sup>1</sup>, Gonzalo S. Saldías<sup>4</sup> and Jameal F. Samhouri<sup>5</sup>

## OPEN ACCESS

### Edited by:

Frank Edgar Muller-Karger,  
University of South Florida,  
United States

### Reviewed by:

Tom William Bell,  
University of California,  
Santa Barbara, United States  
Stefano Allani,  
National Research Council (CNR), Italy

### \*Correspondence:

Caren Barceló  
caren.barcelo@gmail.com;  
caren.barcelo@noaa.gov

### † Present address:

Caren Barceló,  
ECS Federal, LLC on behalf of the  
Office of Science and Technology,  
NOAA Fisheries, Silver Spring, MD,  
United States

### Specialty section:

This article was submitted to  
Marine Ecosystem Ecology,  
a section of the journal  
Frontiers in Marine Science

**Received:** 23 July 2020

**Accepted:** 11 January 2021

**Published:** 12 February 2021

### Citation:

Barceló C, Brodeur RD,  
Ciannelli L, Daly EA, Risien CM,  
Saldías GS and Samhouri JF (2021)  
Time-Varying Epipelagic Community  
Seascapes: Assessing and Predicting  
Species Composition  
in the Northeastern Pacific Ocean.  
*Front. Mar. Sci.* 8:586677.  
doi: 10.3389/fmars.2021.586677

<sup>1</sup> College of Earth, Ocean, and Atmospheric Sciences, Oregon State University, Corvallis, OR, United States, <sup>2</sup> Fish Ecology Division, Northwest Fisheries Science Center, National Oceanic and Atmospheric Administration, Newport, OR, United States, <sup>3</sup> Cooperative Institute of Marine Resource Studies, Oregon State University, Newport, OR, United States, <sup>4</sup> Departamento de Física, Facultad de Ciencias, Universidad del Bío-Bío, Concepción, Chile, <sup>5</sup> Conservation Biology Division, Northwest Fisheries Science Center, National Marine Fisheries Service, National Oceanic and Atmospheric Administration, Seattle, WA, United States

The vast spatial extent of the ocean presents a major challenge for monitoring changes in marine biodiversity and connecting those changes to management practices. Remote-sensing offers promise for overcoming this problem in a cost-effective, tractable way, but requires interdisciplinary expertise to identify robust approaches. In this study, we use generalized additive mixed models to evaluate the relationship between an epipelagic fish community in the Northeastern Pacific Ocean and oceanographic predictor variables, quantified in situ as well as via remote-sensing. We demonstrate the utility of using MODIS Rrs555 fields at monthly and interannual timescales to better understand how freshwater input into the Northern California Current region affects higher trophic level biology. These relationships also allow us to identify a gradient in community composition characteristic of warmer, offshore areas and cooler, nearshore areas over the period 2003–2012, and predict community characteristics outside of sampled species data from 2013 to 2015. These spatial maps therefore represent a new, temporally and spatially explicit index of community differences, potentially useful for filling gaps in regional ecosystem status reports and is germane to the broader ecosystem-based fisheries management context.

**Keywords:** pelagic ecosystem, community composition and assembly, generalized additive models, remote sensing, ecosystem indicators, Northern California Current, Northeastern Pacific Ocean

## INTRODUCTION

Major initiatives worldwide have recognized the importance of measuring diversity and community structure as indicators of ecosystem condition (Skidmore and Pettorelli, 2015). Satellite-based remote sensing (RS) is a tool that provides habitat information across large extents at high spatial and temporal resolutions, having the potential to describe the distribution of multiple facets of biodiversity, including species distributions, alpha diversity, predator-prey overlap, and community composition (Skidmore and Pettorelli, 2015; Pittman, 2017; Wallis et al., 2017;

Walters and Scholes, 2017; Muller-Karger et al., 2018). As a greater variety of RS-based oceanographic information becomes increasingly available and accessible, scientists have coupled these data with biological datasets collected in situ to develop knowledge in key areas of seascape ecology research, which are in turn useful for fisheries management and dynamic ocean management (Zwolinski et al., 2011; Hazen et al., 2013; Scales et al., 2017). Three key topic areas of seascape ecology research [i.e., research linking oceanography with landscape ecology (Pittman et al., 2011)] include: (1) a better understanding of how terrestrial landscapes affect adjacent seascape patterns and processes, (2) determining which structural attributes of seascapes (defined in Pittman et al., 2011, as: ‘wholly or partially submerged marine landscapes’) drive biotic assemblages and distribution of biodiversity, and (3) quantifying the impacts of climate change on seascape patterns (Pittman et al., 2011). In this study, we address the first two areas and demonstrate potential applicability of our approach to the third.

Pelagic fish and invertebrate communities are among the most ecologically, culturally, and economically important components of marine ecosystems worldwide (Pikitch et al., 2014). The species we focus on here (salmon, sardines, anchovies, squid and mackerel) are at once the object of dedicated and emerging fisheries and critical links connecting lower and higher trophic levels in the coastal ocean (Pikitch et al., 2014; Szoboszlai et al., 2015). As such, understanding the dynamics of pelagic communities is fundamental to ecosystem-based fisheries management efforts. As in other regions, the pelagic community composition of the California Current Large Marine Ecosystem (CCLME) has varied substantially in response to changes in environmental conditions (Brodeur et al., 2006; Ralston et al., 2015; Peterson et al., 2017; Morgan et al., 2019). One of the major environmental drivers influencing the coastal ocean off Washington, Oregon, and northern California is the input of freshwater from the Columbia River (e.g., Hickey et al., 2005; Henderikx Freitas et al., 2018) and the small coastal rivers along the coast (Mazzini et al., 2014; Saldías et al., 2020). These freshwater outflows are a significant source of nutrients, sediments, organic matter and other constituents for the coastal ocean (Sigleo and Frick, 2007; Goñi et al., 2013). The Columbia River plume has been identified as a crucial environment providing nutrients and enhancing the coastal productivity to sustain the ecosystem during periods of delayed upwelling (Hickey and Banas, 2008; Kudela et al., 2010). Thus, the plume can modulate plankton distribution and the aggregation of zooplankton around plume fronts (e.g., Morgan et al., 2005; Hickey et al., 2010). However, the use of RS data products related to coastal freshwater input in the study of epipelagic community dynamics is very limited.

Moving toward ecosystem-based fisheries management of the CCLME requires consideration of the effects of environmental variability and climate on the biota (Field et al., 2006), including the development and evaluation of ecological indicators that directly and indirectly measure environmental impacts on marine communities (Levin et al., 2009; Samhoury et al., 2014; Thompson et al., 2019). Under current marine management policies, predictions of species and ecosystem distributions are

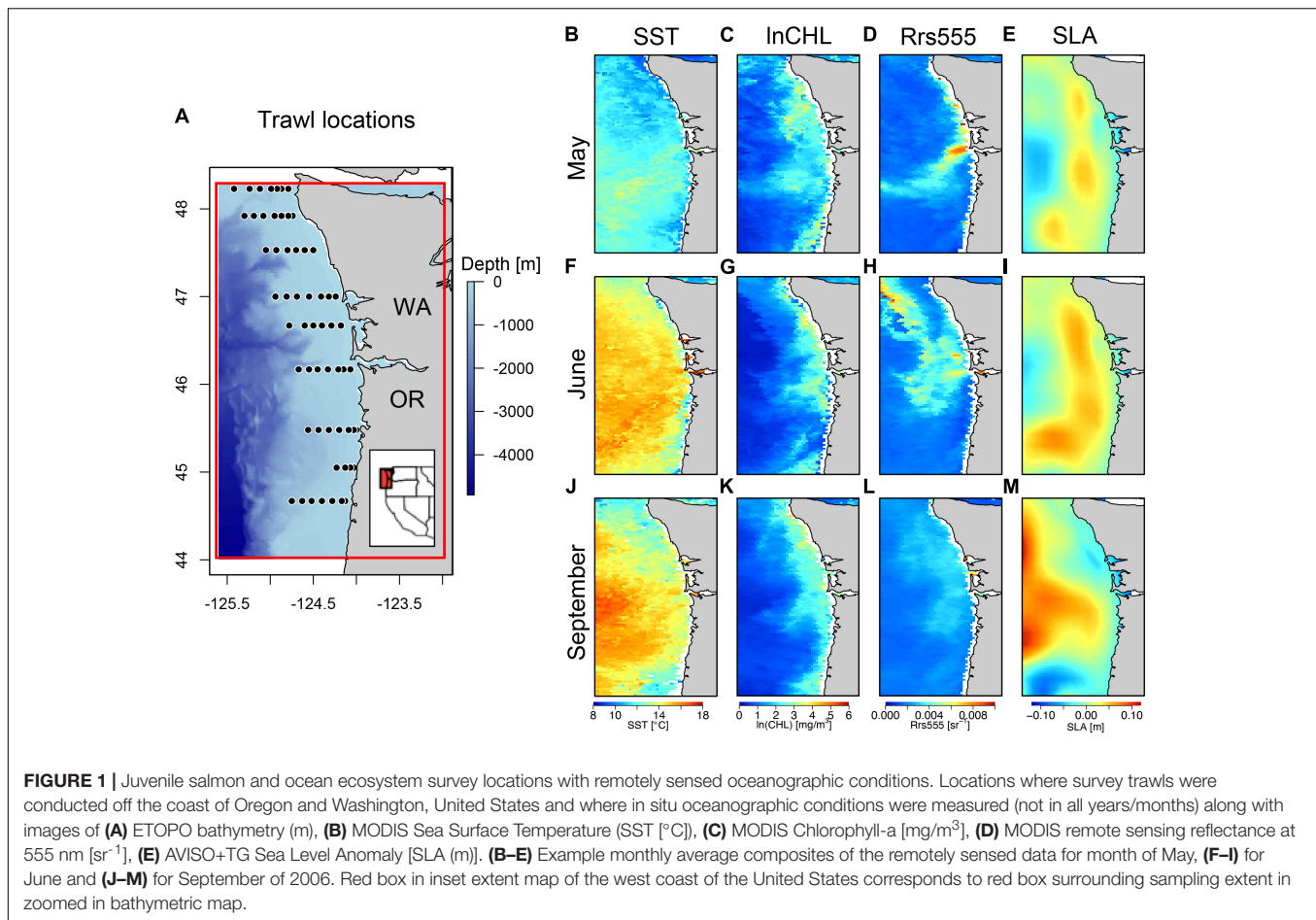
necessary for ongoing integrated ecosystem assessments and indicator development (Hidalgo et al., 2016). Leveraging RS data, predictive statistical models can allow for near real-time and hind-casted distributions of individual species as well as community metrics onto multi-layered RS fields. Innovative methods are being used to couple high-resolution RS data with field survey data via statistical modeling techniques to generate fine-resolution predictive maps (Manderson et al., 2011; Hobday and Hartog, 2014; Thorson et al., 2020). However, research that integrates satellite RS data with species diversity, has largely focused on alpha-diversity metrics (e.g., Pittman et al., 2007; Hazen et al., 2013) and less on other community metrics, such as ordination scores representative of assemblage similarities/dissimilarities. Ultimately, forecasts of individual species distributions and community composition metrics can provide an important foundational layer to be used in marine spatial planning, such as dynamic ocean management (Lewison et al., 2015; Maxwell et al., 2015 and references therein).

In this study, we use a pelagic seascape approach and model the epipelagic fish and macro-invertebrate community structure off the coasts of Oregon and Washington using RS and in situ oceanographic biophysical data. First, we assess the relationships among species across different months and community groups. To understand the relationship between community structure and the environment, we use generalized additive mixed effects models (GAMMs) and couple ordination scores with both local in situ collected environmental data and remotely sensed oceanographic data fields. Using the results of these community seascape models, we construct predictive spatial maps of community composition onto the RS layers as hind-casts and predictions at yearly and seasonal scales. From these community structure prediction maps, we extract time series of predicted community gradients. We propose that by coupling readily available RS data with community metrics, we can predict community species composition in the pelagic marine realm, gaining information that can potentially be of use for dynamic regional ocean management.

## MATERIALS AND METHODS

### Survey Specifics

From 1998 to 2012 NOAA's Northwest Fisheries Science Center's Fish Ecology Division regularly conducted pelagic surface trawl surveys within the Northern California Current (NCC) epipelagic ecosystem with the primary goal of quantifying the marine survival and habitat associations of juvenile salmonids [*Juvenile Salmon and Ocean Ecosystem Survey (JSOES)*; Brodeur et al., 2005]. These surveys were conducted regularly each year in spring-early summer, and late summer, off the coasts of Oregon and Washington between 44.25 and 48.23°N and -125.61 and -123.97°W (**Figure 1A**). Here, we analyze survey data collected between 2003 to 2012 in order to synchronize with MODIS data availability. The sampling methodology of these surveys was altered after 2012 with respect to the geographical and temporal extent of sampling, and modifications to the gear, impacting catchability and abundance estimates of certain



species (Wainwright et al., 2019). However, while comparable ecosystem data (with similar gear configuration) from 2013 to 2015 were collected, they were not made available to us for this analysis/validation purposes. Approximately, 10 transects consisting of between 6 and 8 stations extend from the nearshore to off the continental shelf (approximately 50 km from shore). Thirty-minute surface tows were conducted at each station with a Nordic 264 rope trawl (Nor'Eastern Trawl Systems, Inc., Bainbridge Island, WA, United States) at a speed over ground of approximately 6 km/h. The length of the trawl is 108 m long with a mouth opening of 30 m  $\times$  20 m, and the head rope at approximately 1 m from the surface. The mesh size varies along the length of the rope trawl, ranging between 162.6 cm at the mouth to 8.9 cm at the cod end, which had a 0.8 cm liner inside.

## Species Data

For this study, we restricted the hauls to only those conducted exclusively during daylight hours of the months of May, June, and September. The cruises occurred during the last half of the cruise month, however, on few occasions, some trawls were conducted into the first few days of the next month (into July for example for the June cruise, similarly for May and September). Due to the mesh size used in the trawl, we restricted our community analysis to those species quantitatively retained by the trawl,

including both invertebrate and fish species. All species captured in the trawl were identified, counted and measured, with the exception of large catches, where a random sub-sample of fish from each species was measured, counted and weighed and then total abundance re-calculated based on total weight. Catches were standardized by calculating catch-per-unit-effort (CPUE, number per  $\text{km}^2$ ) using the distance fished (geographic distance between beginning and end of trawl) (Figure 1A; Daly et al., 2012). Of the total quantitatively sampled species captured between 2003 and 2012 in May, June, and September, we restricted the epipelagic community analysis presented here to species that were found in 3% or more of the sampled stations.

## In situ and Remotely Sensed Oceanographic Data

In situ (IS) ocean temperature, salinity, and pressure were recorded at each meter of the water column down to 5 m from the bottom, or to 100 m depth, either prior to or immediately after conducting each surface trawl at a station using a Sea-Bird SBE 19 SeaCAT conductivity/temperature/depth profiler (CTD). At each trawl station (Figure 1A), water samples were collected with a Niskin bottle at a depth of 3 m, and filtered at sea. Pigments were later extracted and analyzed using acetone (90% HPLC grade). Sample fluorescence was measured with a Turner Designs

fluorometer (Arar and Collins, 1997). Following Lentz (1992), we calculated mixed layer depth as the depth where the temperature difference relative to the sea surface exceeded  $0.02^{\circ}\text{C}$ .

Moderate Resolution Imaging Spectroradiometer (MODIS) Aqua ocean temperature and multi-spectral color fields for the region off Oregon and Washington were acquired from <http://ocean.color.gsfc.nasa.gov/>. Specifically, sea surface temperature (SST), chlorophyll-a (CHL), and Remote sensing reflectance at 555 nm (Rrs555) fields were used. SST and satellite derived metrics of primary productivity have been commonly used to define marine habitat for pelagic species as they describe both the thermal conditions as well as potential prey availability (Suryan et al., 2012). Rrs555 fields have been previously used to map the surface expansion of the Columbia River plume throughout the annual cycle (Thomas and Weatherbee, 2006; Mazzini et al., 2015; Saldías et al., 2016) and is likely a good descriptor of community differences due to biological responses to plume-influenced waters (Saldías et al., 2016). All MODIS fields were smoothed using a two-dimensional  $3 \times 3$  grid cell median filter to reduce noise associated with cloud edges and to enhance frontal features in satellite images (Wall et al., 2008; Saldías et al., 2016).

Sea level anomaly (SLA) data were obtained by combining gridded, daily AVISO altimeter fields (Pujol et al., 2016) with low-pass filtered coastal tide gauge data (Risien and Strub, 2016). This  $0.25^{\circ} \times 0.25^{\circ}$ , blended dataset improves SLA estimates along the coast by removing altimeter data approximately 55–70 km from the coastline and replacing it with a linear interpolation between the tide gauge and remaining offshore altimeter data (Risien and Strub, 2016). In order to have a consistent grid resolution for all RS data fields, we interpolated the blended SLA data to the 4 km MODIS grid using a Barnes objective analysis scheme (Barnes, 1964; Emery and Thomson, 2004). As we were interested in quantifying the distinct water properties associated with distributions of species in the local community, we used both SST and SLA in this study (as done in other species distribution studies, see Becker et al., 2016). SLA and SST are correlated at large scales (Emery et al., 2011) and in the data used here. While MODIS SST is limited to the skin of the sea surface (top 10 microns), SLA is integrative, providing information about the density structure of the water column. As SLA is related to pycnocline depth it may impact habitat quality and availability for distinct species (e.g., a higher SLA is indicative of a deeper pycnocline and therefore potentially more diluted prey availability for pelagic fish and invertebrates, whereas a lower SLA is indicative of a shallower pycnocline which may in turn concentrate prey for pelagic species).

We collocated sampling dates (using actual trawl dates, rather than assigned cruise month) and locations (midpoint of the start and end locations) of surface trawls (Figure 1) with coincident 8-day MODIS and SLA data to the nearest 4 km grid cell for all fields. As we were interested in understanding the fluctuations of the community associated with the regional features (upwelling front, Columbia River plume, eddies) at monthly and interannual time scales, we used 8-day MODIS composites, which McKibben et al. (2012) show to be adequate for comparing IS with RS data off central Oregon. While the sampled species and in situ

time series begin in 1998, the time series analyzed here begins in 2003 to allow for the use of consistent RS fields and temporally congruent IS data. Prior to 2003, AVHRR SST and SeaWiFS ocean color data were collected by two distinct satellites with different orbits and timings. The MODIS-Aqua instrument collects SST and ocean color information simultaneously, thus avoiding the issue of mismatched data in time and space. Additionally, SeaWiFS data are only available through mid-December 2010, which does not cover the in situ sampling time series (up to 2012) or the prediction period (up to 2015). To better understand the correlations of IS and collocated RS fields across all stations, all months, and all years, we ran Pearson correlations and report the correlation values (Supplementary Figure 1). In order to create maps of predicted community gradients and to maximize the number of cloud-free grid cells, we created monthly composites of all MODIS and blended SLA fields for the period 2003 to 2012 and predicted community scores onto 3 years (2013–2015) outside of the in situ monthly data collections (2003–2012) (Figures 1B–E). The RS-based oceanographic monthly composited images for the months of May, June, and September between 2003 and 2015 are presented in the *Supplemental Information* (Supplementary Figures 2–5, respectively).

## Community Analysis of the Epipelagic

Non-metric multidimensional scaling (NMDS) ordination (Clarke and Warwick, 2001; McCune and Grace, 2002) using Bray–Curtis dissimilarities was used to quantify the variability in community composition by year and season of the epipelagic juvenile and adult nekton and associated macro-invertebrate community. We specifically chose to use NMDS ordination to quantify the community composition as we do not assume that species are linearly related to each other [a central assumption of principal component analysis (PCAs)/empirical orthogonal functions (EOFs)] (McCune and Grace, 2002).

To explore the spatial changes of the epipelagic nekton and associated macro-invertebrate community by year and season, we performed a NMDS ordination of hauls in species space with a random starting configuration, calculating a dissimilarity matrix using the Bray–Curtis distance measure. The community dataset was composed of 23 relative species abundances (CPUE) by 1215 individual hauls as sample units. The 23 species consisted of salmon, forage fish, and some top predator species, as well as several gelatinous macro-zooplankton and squid representing the macroinvertebrate community. The relative species abundances (CPUE) were  $\log_{10}(x + 1)$  transformed to reduce the variation between different species abundances. In order to visualize the relationships of in situ and RS data in relation to axes of the NMDS ordination – we used *vegan's envfit* (Wood and Scheipl, 2014) function to first obtain a vector overlay on the ordination representing a linear regression of the environmental variables with each NMDS axes. Next, to visualize potential non-linear relationships between each environmental variable and the ordination, we used the *ordisurf* function that fits a generalized additive model with each variable individually, and produces response surfaces of oceanographic conditions overlaid on the ordination using 2-D thin-plate regression splines. The



degree of smoothing is automatically selected by cross validation (Wood and Scheipl, 2014).

We performed a hierarchical cluster analysis to define two community clusters (refer to dendrogram of hauls in **Supplementary Figure 6**), henceforth referred to as cold and warm communities as they were distributed along the temperature gradient associated with NMDS axis 1. Multiple Response Permutation Procedure (MRPP) was used to determine if the two clusters were significantly different from one another (refer to McCune and Grace, 2002 for a methodological description of MRPP) (A-statistic = 0.056,  $p < 0.01$ ). MRPP was also conducted by year and month to determine whether these two clusters were significantly different from one another across all years and months (A-statistic range: 0.046 to 0.057,  $p < 0.01$ ). To assess the exclusivity and fidelity of the species to particular clusters, as well as the statistical significance of the relationship between species abundance and groups of sites in each month, we performed an indicator species analysis (ISA) (McCune and Grace, 2002) on the two groups identified *a priori* by the hierarchical cluster analysis for each season of data. All non-parametric multivariate statistical analyses were done in R v. 3.4.0 (R Core Team, 2019) using the *vegan* and *indicspecies* libraries (Oksanen et al., 2019; R Core Team, 2019; De Cáceres and Jansen, 2020).

## Relating Community Composition to in situ or Remotely Sensed Oceanographic Data

We used the dimensionless NMDS axis 1 scores from the ordination of hauls in species space as response variables in GAMMs (Zuur et al., 2009) to explore the non-linear effects of oceanographic conditions on the community structure. The GAMM analyses focus on the cold to warm community gradients and how the Columbia River plume affected species communities. We constructed two model set ups, using NMDS axis 1 as the response variables and either in situ and remotely sensed variables as co-variables (i.e., NMDS1~IS covariates and NMDS1~RS covariates) (**Table 3**). We selected the best fit models for each based on minimization of the AIC. All final models and model selection details for NMDS1 are reported in **Table 3**. Only the community seascape model (NMDS1~RS) results are discussed here, the other model (NMDS1~IS) and their resulting functional relationships with environmental co-variables are presented in the *Supplemental Information*.

Using the linear and non-linear functional relationships of RS environmental data with NMDS axis 1 derived from the GAMM, we predicted the spatial distribution of the response variable (NMDS axis 1) for the different years (2003–2012) and month (May, June, and September) combinations, using monthly composited satellite images. We also used the relationships of NMDS axis 1 to RS covariates, to predict outside the range of the data (2013–2015 in May, June, and September) used here. Spatial predictions were restricted to within the minimum convex hull surrounding the sampled locations.

Generalized additive mixed effects models are a non-linear regression technique where the covariates (environmental

variables) are modeled with non-parametric smoothing functions (Hastie and Tibshirani, 1990; Wood, 2015) in the *gam4* library of R (Wood and Scheipl, 2014). GAMMs do not require an *a priori* assumption of the type of relationship between the covariates and response variables in a model. The environmental co-variables were used as the fixed effects in the models and individual stations as the random effect to account for within station correlation. Variable selection was achieved by minimizing the Akaike information criterion (AIC) as well as the genuine cross validation (gCV) score for each set of models. To calculate gCV, we fit each model to a randomly selected training dataset (with 90% of the total observations), generated predictions for a validation dataset (with the remaining 10% of the observations) and then calculated the prediction error. This procedure was repeated a total of 500 times and a model gCV criterion score was computed by taking the mean squared prediction error (Ciannelli et al., 2007, 2012). The candidate model with the lowest combined AIC (weighted more heavily) and gCV criterion scores was determined to be the best model for determining local IS and RS data relationships with NMDS1.

## RESULTS

### Oceanographic Correlates With Individual NCC Epipelagic Species

For each species (at stations with positive catch only), we provide the median and range values of remotely sensed oceanographic data (SLA, SST, CHL, Rrs555) in **Table 1**. The median and range of in situ sampled oceanographic variables (temperature, salinity, density at 10 m depth, and chlorophyll-a (CHL) concentration sampled at 3 m depth), for all 23 species included in this analysis are included in **Supplementary Table 1**.

Starry flounder (*Platichthys stellatus*) followed by surf smelt (*Hypomesus pretiosus*) were caught most often at the lowest temperatures (median in situ temperature: 10.2, 10.95°C, for each species, respectively), whereas ocean sunfish (*Mola mola*), followed by sablefish (*Anoplopoma fimbria*) and then Pacific saury (*Cololabis saira*), were caught most often at the highest temperatures (median in situ temperature at 10 m depth of 14.2, 13.78, 13.25°C, for each species, respectively). Sablefish (median: 0.657 mg/m<sup>3</sup>) followed by Pacific saury (median: 0.669 mg/m<sup>3</sup>) and steelhead (*Oncorhynchus mykiss*; median: 0.933 mg/m<sup>3</sup>) were more often caught at stations that had low chlorophyll concentrations, in contrast to starry flounder (median: 1.74 mg/m<sup>3</sup>) and surf smelt (1.69 mg/m<sup>3</sup>). Starry flounder was also present in the most saline waters (median salinity: 32.49) followed by pink salmon (*O. gorbuscha*; median salinity: 32.12), in contrast to steelhead (median salinity: 31.45) and sockeye salmon (*O. nerka*; median salinity: 31.70). Rrs555 fields were effective at identifying plume vs. non-plume species during sampled months. Specifically, species shown previously to have an affinity for plume waters (Brodeur et al., 2005) including market squid (*Doryteuthis opalescens*), wolf eel (*Anarrhichthys*

**TABLE 1 |** Summarized remotely sensed collocated data with positive presence for each species present in more than 3% of the total hauls conducted between 2003 and 2012 during the spring-summer season.

Common name	Scientific name	SST (median)	SST (mean)	SST (range)	InCHL (median)	InCHL (mean)	InCHL (range)	SLA (median)	SLA (mean)	SLA (range)	Rrs555 (median)	Rrs555 (mean)	Rrs555 (range)
Starry flounder	<i>Platichthys stellatus</i>	12.33	12.88	10.75–15.78	2.06	2.26	1.54–3.43	−0.071	−0.07	−0.12–0	0.00342	0.00418	0.0021–0.0072
Spiny dogfish	<i>Squalus acanthias</i>	12.74	13.27	10.75–17.38	2.09	2.039	0.72–3.58	−0.054	−0.052	−0.12–0.01	0.00326	0.00402	0.0016–0.0099
Steelhead	<i>Oncorhynchus mykiss</i>	12.92	12.91	9.47–16.81	1.61	1.688	0.44–3.26	−0.038	−0.032	−0.1–0.04	0.00269	0.00333	0.0014–0.0099
Sockeye salmon	<i>Oncorhynchus nerka</i>	12.93	12.85	9.47–15.18	1.49	1.666	0.44–3.58	−0.048	−0.045	−0.12–0.03	0.00332	0.00383	0.0015–0.0128
Chum salmon	<i>Oncorhynchus keta</i>	13.02	13.31	9.47–17.57	1.47	1.571	0.36–3.58	−0.041	−0.041	−0.12–0.03	0.00303	0.00361	0.0015–0.0128
Chinook salmon	<i>Oncorhynchus tshawytscha</i>	13.08	13.39	9.47–17.42	1.82	1.813	0.36–3.58	−0.047	−0.048	−0.14–0.03	0.00312	0.00362	0.0011–0.0128
Surf smelt	<i>Hypomesus pretiosus</i>	13.17	13.48	10.39–16.47	2.19	2.3	1.29–3.43	−0.06	−0.06	−0.14–0.04	0.003375	0.00405	0.0018–0.0095
Coho salmon	<i>Oncorhynchus kisutch</i>	13.31	13.50	9.47–17.74	1.70	1.765	0.36–3.62	−0.044	−0.045	−0.12–0.03	0.0031	0.00352	0.0011–0.0128
Pink salmon	<i>Oncorhynchus gorbuscha</i>	13.42	13.14	10.55–16.98	1.87	1.908	0.94–3.05	−0.049	−0.048	−0.12–0.02	0.002275	0.00262	0.0015–0.0083
Wolf eel	<i>Anarrhichthys ocellatus</i>	13.45	13.51	10.54–16.45	1.57	1.672	0.31–3.58	−0.039	−0.042	−0.12–0.03	0.00329	0.00398	0.0012–0.0128
Pacific herring	<i>Clupea pallasii</i>	13.77	13.67	10.39–17.42	2.04	2.051	0.46–3.62	−0.052	−0.054	−0.12–0.03	0.00311	0.00362	0.0017–0.0117
Tope shark	<i>Galeorhinus zyopterus</i>	13.89	13.97	11.41–17.38	1.72	1.726	0.62–2.81	−0.029	−0.038	−0.11–0.02	0.00326	0.00393	0.0012–0.0128
Market squid	<i>Doryteuthis opalescens</i>	14.00	14.16	10.39–17.57	1.74	1.809	0.51–3.4	−0.039	−0.041	−0.12–0.03	0.00333	0.00374	0.0013–0.0099
Pacific sardine	<i>Sardinops sagax</i>	14.44	14.38	10.51–18.48	1.74	1.754	0.23–3.62	−0.026	−0.026	−0.12–0.04	0.00288	0.00316	0.0012–0.0111
Sea nettle jelly	<i>Chrysaora fuscescens</i>	14.65	14.25	10.39–17.2	1.90	1.907	0.6–3.52	−0.043	−0.045	−0.14–0.04	0.002965	0.00323	0.0011–0.0099
Jack mackerel	<i>Trachurus symmetricus</i>	14.73	14.73	11.73–16.87	1.43	1.474	0.66–3.09	−0.022	−0.018	−0.09–0.04	0.00278	0.00312	0.0012–0.0117
Water jelly	<i>Aequorea victoria</i>	14.74	14.40	10.54–18.49	1.42	1.532	0.23–3.62	−0.03	−0.031	−0.12–0.04	0.00252	0.00289	0.0011–0.01
Pacific saury	<i>Cololabis saira</i>	14.75	14.63	11.26–18.49	1.49	1.565	0.31–3.62	−0.003	−0.006	−0.06–0.04	0.00232	0.00249	0.0012–0.0083
Moon jelly	<i>Aurelia labiata</i>	14.79	14.44	9.9–17.78	1.86	1.783	0.46–3.62	−0.032	−0.036	−0.12–0.04	0.00258	0.00276	0.0012–0.0068
Egg yolk jelly	<i>Phacellophora camtschatica</i>	14.97	14.55	11–18.48	1.19	1.293	0.22–2.95	−0.02	−0.025	−0.11–0.04	0.00256	0.00296	0.0013–0.01
Northern anchovy	<i>Engraulis mordax</i>	15.10	14.94	10.39–18.49	1.69	1.682	0.23–3.43	−0.024	−0.026	−0.12–0.04	0.00294	0.00334	0.0011–0.0128
Sablefish	<i>Anoplopoma fimbria</i>	15.14	15.27	12.73–18.48	1.08	1.132	0.23–3.05	0.002	−0.006	−0.08–0.04	0.003005	0.00333	0.0013–0.0083
Ocean sunfish	<i>Mola mola</i>	15.51	15.27	12.01–16.78	1.25	1.349	0.46–3.35	0.001	−0.002	−0.05–0.04	0.00186	0.00224	0.0012–0.0128

Coloration is relative to each environmental covariate (SST, CHL, SLA, or Rrs555) with respect to the mean or median. The species in the table are ordered with respect to increasing median SST.

*ocellatus*), and tope shark (*Galeorhinus zyopterus*), were captured at relatively high Rrs555 values ( $>0.003 \text{ sr}^{-1}$ ). Other species, such as Pacific saury, ocean sunfish, pink salmon, and jellies [including, egg-yolk jelly (*Phacellophora camtschatica*), moon jelly (*Aurelia labiata*), and water jelly (*Aequorea victoria*)], species characteristically associated with the warm community (Brodeur et al., 2005), were captured at relatively low Rrs555 values.

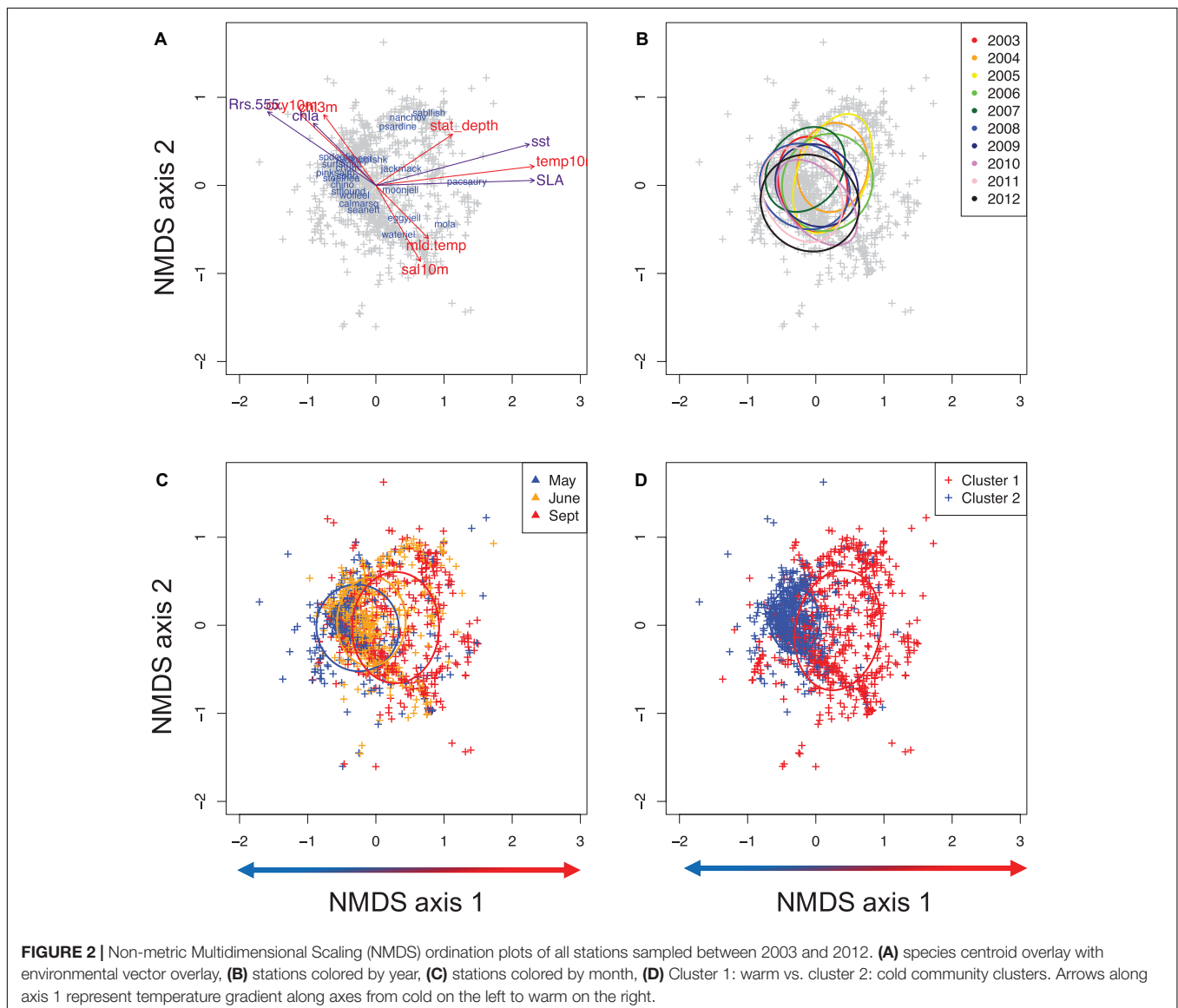
## Interannual and Monthly Community Variability

The NMDS 2-D ordination of the survey hauls (1215 total hauls and 23 species) had a final stress of 0.42 (Figures 2A–D). There were significant differences in the communities of fish and macroinvertebrates sampled off Oregon and Washington amongst years (data from months and stations for a given year) (Table 2). However,

the degree of differentiation between years was low given the large variability associated with spatial variables and ocean conditions (e.g., Oregon vs. Washington and cold vs. warm conditions) (Figure 2B). The overall yearly MRPP A-statistic was 0.013 ( $p < 0.05$ ) for year-to-year comparisons when using sample units from the full sampling grid in each month.

## Indicator Species of Monthly Community Clusters

Indicator species of monthly communities are presented in Table 2. Pacific saury was the only consistent warm community indicator across all three cruise months. The other warm indicator species differed by month (Table 2). The months of May and June included egg-yolk jelly and sablefish as indicators of the warm community, while in June, Jack mackerel (*Trachurus symmetricus*) was also an indicator of this warm



**TABLE 2 |** Indicator species for both warm and cold community clusters by cruise month.

Month	Species	A	B	Stat	p-value
<b>WARM COMMUNITY INDICATOR SPECIES</b>					
MAY	Egg-yolk jelly	0.96641	0.23077	0.472	0.005
	Pacific saury	0.76976	0.11538	0.298	0.005
	Sablefish	0.94233	0.03846	0.19	0.01
JUNE	Sablefish	0.97492	0.29843	0.539	0.005
	Egg-yolk jelly	0.76287	0.1466	0.334	0.005
	Jack mackerel	0.74862	0.09948	0.273	0.005
SEPTEMBER	Pacific saury	0.82358	0.08377	0.263	0.005
	Ocean sunfish	0.81366	0.22297	0.426	0.005
	Jack mackerel	0.83395	0.15541	0.36	0.01
<b>COLD COMMUNITY INDICATOR SPECIES</b>					
MAY	Steelhead	0.86628	0.43379	0.613	0.005
	Chum salmon	0.91165	0.33333	0.551	0.005
	Sockeye salmon	0.81154	0.34247	0.527	0.005
	Wolf eel	0.91449	0.10502	0.31	0.015
	Surf smelt	0.81638	0.11416	0.305	0.05
	Spiny dogfish	0.93023	0.07306	0.261	0.01
JUNE	Chinook salmon	0.76566	0.89691	0.829	0.005
	Pacific herring	0.82997	0.2921	0.492	0.005
	Wolf eel	0.90958	0.23711	0.464	0.005
	Spiny dogfish	0.9393	0.21306	0.447	0.005
	Sockeye salmon	0.7646	0.23024	0.42	0.005
	Surf smelt	1	0.13402	0.366	0.005
	Tope shark	0.92824	0.12715	0.344	0.005
	Starry flounder	0.92957	0.09278	0.294	0.005
	Pink salmon	0.88939	0.04811	0.207	0.01
	Chinook salmon	0.79736	0.7193	0.757	0.005
SEPTEMBER	Sea nettle jelly	0.71834	0.64912	0.683	0.005
	Pacific herring	0.85574	0.46491	0.631	0.005
	Coho salmon	0.76041	0.5	0.617	0.005
	Chum salmon	0.90692	0.24561	0.472	0.005
	Pink salmon	0.98274	0.19298	0.435	0.005
	Surf smelt	0.9712	0.18421	0.423	0.005
	Spiny dogfish	0.86376	0.14912	0.359	0.005
	Tope shark	1	0.11404	0.338	0.005
	Wolf eel	0.96993	0.09649	0.306	0.005
	Market squid	0.7073	0.13158	0.305	0.01
	Starry flounder	1	0.07895	0.281	0.005

Component 'A' is the probability that the surveyed sample unit belongs to the target site group given the fact that the species has been found (or specificity) and 'B' is the probability of finding the species in sites belonging to a particular cluster (or fidelity) and 'stat' is the indicator value (composed of both components).

community cluster. The warm community in September included Pacific saury and Jack mackerel as well as ocean sunfish. The indicator species of the cold community cluster were more variable than those of the warm cluster. The cold cluster indicator species across all months, included salmonids [Chum (*O. keta*), Chinook (*O. tshawytscha*), Coho (*O. kisutch*), Sockeye, Pink salmon], Pacific herring (*Clupea pallasii*), surf smelt, as well as wolf eel, and Spiny dogfish (*Squalus acanthias*) (see **Table 2**). Market squid was a significant cold indicator species

in September but not in other months. Steelhead was also found to be an indicator species for the cold community only for the month of May. Species differed by month in their specificity, probability and fidelity to a particular community cluster (**Table 2**).

## In situ Environment Relationships With Community Composition

With respect to the in situ sampled environment, the ordination had a notable cold-warm gradient along NMDS axis 1 and a salinity gradient along NMDS axis 2 (henceforth referred to as NMDS1 and NMDS2). Simple linear regressions indicated that NMDS1 was positively correlated with in situ temperature at 10 m depth and the seafloor depth of the sampling location, which was also partially negatively correlated with NMDS2 (**Figure 2A**). In situ salinity was positively correlated along NMDS2 while mixed layer depth was positively correlated along both NMDS1 and NMDS2. In situ chlorophyll (at 3 m depth) was negatively correlated with NMDS1 and NMDS2 (**Figures 2A, 3A–H**). The surfaces of each in situ physical and biological variable overlaid on the NMDS ordination presents the non-linear component of each variable in relation to the community composition (with both NMDS axes) of each haul the ordination (**Figures 3A–H**). Temperature at 10 m depth had higher temperatures at positive NMDS1 scores and lower temperatures at negative NMDS1, while having both high and low values of temperature at both extremes of NMDS2 (**Figures 3A–H**). Salinity was more linearly related to NMDS2, indicating a gradient of fresh to warm waters with a positive correlation along NMDS2 (**Figures 2A, 3A–H**). Chlorophyll had a negative relationship with both NMDS axes (**Figure 2A**). While oxygen was only sampled from 2006 to 2012, we overlay the non-linear relationship with the community (**Figure 3D**), but do not use it in the analyses. Communities sampled at shallower stations were concentrated in the upper left quadrant of the ordination (low values of NMDS axis 1 and high NMDS2) whereas communities sampled the deeper water column stations were on the right side of the NMDS ordination (all NMDS2, and NMDS1 values > 0) (**Figure 3E**). Mixed layer depth largely showed a positive linear relationship with both NMDS axes (**Figure 3F**). Relationships with latitude, longitude are also presented (**Figures 3G,H**).

## Remotely Sensed Environment Relationships With Community Composition

The relationships of the RS data fields showed slightly different patterns than the IS data as expected, given the different data sources and depth at which the variables were measured relative to satellite data measurements (see **Figures 3, 4**). MODIS-Aqua SST had a different pattern compared to the in situ data at 10 m depth. Relatively warm SST (>14°C) ranged between −0.5 to 1.5 values along NMDS1 and along almost the entire NMDS2 (**Figure 4A**). SST of less than 13°C was restricted to the far-right side of the ordination (NMDS1 values less than −0.5) (**Figure 4A**). Rrs555 showed a similar pattern to in situ salinity



**TABLE 3 |** Generalized additive mixed model structures and results for models of NMDS axis 1 and NMDS axis 2 with in situ or remotely sensed co-variables and model performance metrics.

Models	Model structure	AIC	gCV	Adj. $R^2$	Hauls
NMDS1~RS	Community seascape model				
	NMDS1~ai+(Lat,Lon)+(SST,SLA)+Rrs555+ln(CHL)+depth	501.3	0.178	0.457	380
	NMDS1~ai+(Lat,Lon)+(SST,SLA)+Rrs555+ln(CHL)	499	0.132	0.459	380
	<b>NMDS1~ai+(Lat,Lon)+(SST,SLA)+Rrs555</b>	<b>491.3</b>	<b>0.124</b>	<b>0.458</b>	<b>380</b>
NMDS1~IS	NMDS1~ai+(Lat,Lon)+temp10m+sal10m+mld+ln(chl3m)+depth	869.43	0.167	0.488	769
	<b>NMDS1~ai+(Lat,Lon)+temp10m+sal10m+ln(chl3m)+depth</b>	<b>862.76</b>	<b>0.145</b>	<b>0.487</b>	<b>773</b>

Best models for NMDS axis 1 (NMDS1) are highlighted in bold and are based minimization of AIC. RS, remotely sensed environmental co-variables; IS, in situ environmental co-variables. Abbreviations used in table as follows: NMDS1, non-metric multidimensional scaling ordination axis 1; Lat, latitude; Lon, longitude; temp10m, CTD temperature at 10 m depth; sal10m, CTD salinity at 10 m depth; mld, mixed layer depth; chl3m, chlorophyll-a concentration at 3 m depth; depth, station bathymetric depth; SST, MODIS SST; SLA, AVISO sea level anomaly; Rrs555, MODIS Remote sensing reflectance 555; CHL, MODIS chlorophyll-a; ai, random intercept term; AIC, Akaike information criterion; gCV, genuine cross validation; Adj.  $R^2$ , adjusted  $R^2$ ; hauls, trawls included as sample units.

in relation to the ordination, with high values in the lower right quadrant of the NMDS (**Figure 4B**). MODIS Chl-a demonstrated an almost identical pattern to that observed with in situ Chl-a collected at 3 m depth (**Figure 4C**).

## Community Seascape Model Results

The final RS NMDS axis 1 model explained 45.8% of the variability in NMDS axis 1 and included as covariates: (1) an interaction of latitude and longitude, (2) an interaction of SLA, SST, and (3) Rrs555 (**Table 3**). The average spatial pattern of NMDS axis 1, with low NMDS axis 1 values distributed along most of Washington and higher NMDS axis 1 values distributed off Oregon (**Figure 5A**). The GAMM interaction biplot of SST and SLA showed a positive relationship of NMDS axis 1 with both SST and SLA (**Figure 5B**). There was a non-linear relationship of NMDS1 to the Rrs555 data field, with high NMDS1 at low values of Rrs555 ( $<0.004 \text{ sr}^{-1}$ ). At Rrs555 values  $>0.004 \text{ sr}^{-1}$  there was a quasi-linear relationship with negative NMDS axis 1 scores (**Figure 5C**).

## Remote Sensing-Based Prediction of Ordination Scores

The best fit NMDS1~RS model (community seascape model) had significant correlations with the interaction term of latitude and longitude, interaction of MODIS SST with AVISO+TG SLA, and with Rrs555 (**Figure 5**). Positive values of NMDS1 were generally found offshore, and at higher SST and SLA values and vice-versa for negative NMDS1 values. While a formal threshold analysis was not done here, the Rrs555 value where there is no change in NMDS1 occurs at approximately  $0.004 \text{ sr}^{-1}$ .

Based on the community seascape model (NMDS1~RS; **Figure 5**), spatial predictions of NMDS axis 1 values (indicating the gradient from cold to warm communities) indicated differences across years and months (**Figure 6**). Based on boxplots of extracted predicted NMDS axis 1 values for the Oregon and Washington regions as well as the whole sampled region, Oregon had a higher presence of warm community during all months-years (**Figure 7**), while Washington had a greater presence of the cold community across all months-years (**Figure 5**). During some months and years (May 2005, May 2008,

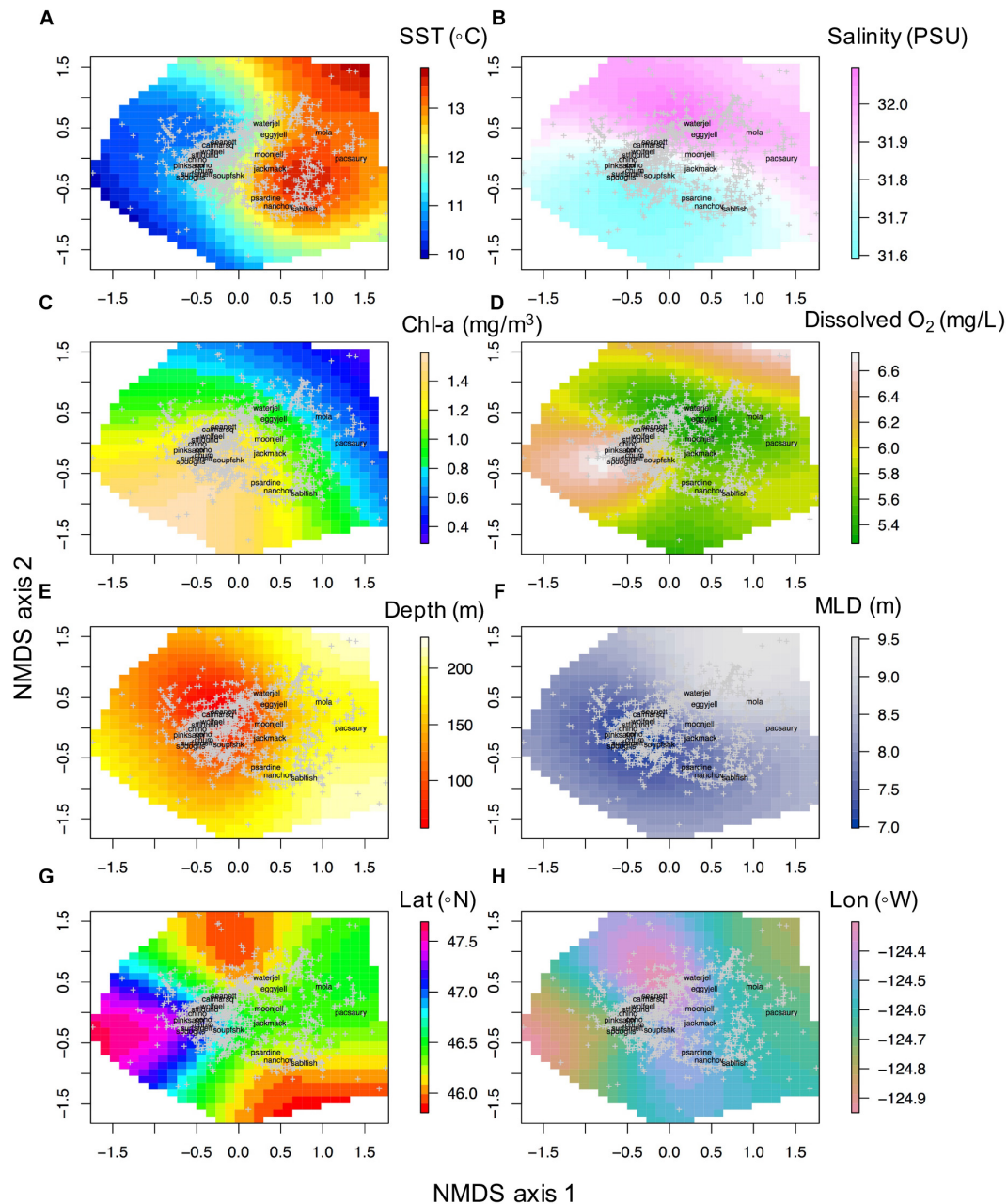
June 2008, June 2012, June 2006, September 2006, September 2012, June 2014), the difference between Oregon and Washington was pronounced (**Figure 7**).

In May, the period between 2003 and 2005 had a higher presence of the warm community across the entire sampled extent, with a greater presence of the warm community in Oregon than for Washington or the full region (**Figure 7**). For this month, from 2006 to 2012, there was a lower presence of cold community across the whole region (**Figure 7**). For May 2013–2015, a significant increase in the presence of the warm community was predicted for all regions, with 2015 having the highest presence of the warm-offshore community within our hind-casted and fore-casted time series. In June, between 2003 and 2005 there was a greater incursion of the warm community than other years (**Figure 7**). Years with little to no presence of the warm community included 2007 and 2008 (**Figures 5, 6**). For both Oregon and Washington, September of 2004 and 2009 had the highest predicted warm community presence.

Between 2013 and 2015, for May and September there was a pronounced predicted increase in the presence of the warm-offshore community, especially off Oregon (high positive values of NMDS1). June and September of 2014 both had notably higher predicted presence of the warm community relative to the full area and to the Washington area. For all regions, June 2015 was similar to the long-term mean predicted NMDS1 scores. However, in both May and September, the predicted NMDS1 scores were higher than any previous year and had values greater than the most positive of the observed NMDS1 scores (up to 2012).

## DISCUSSION

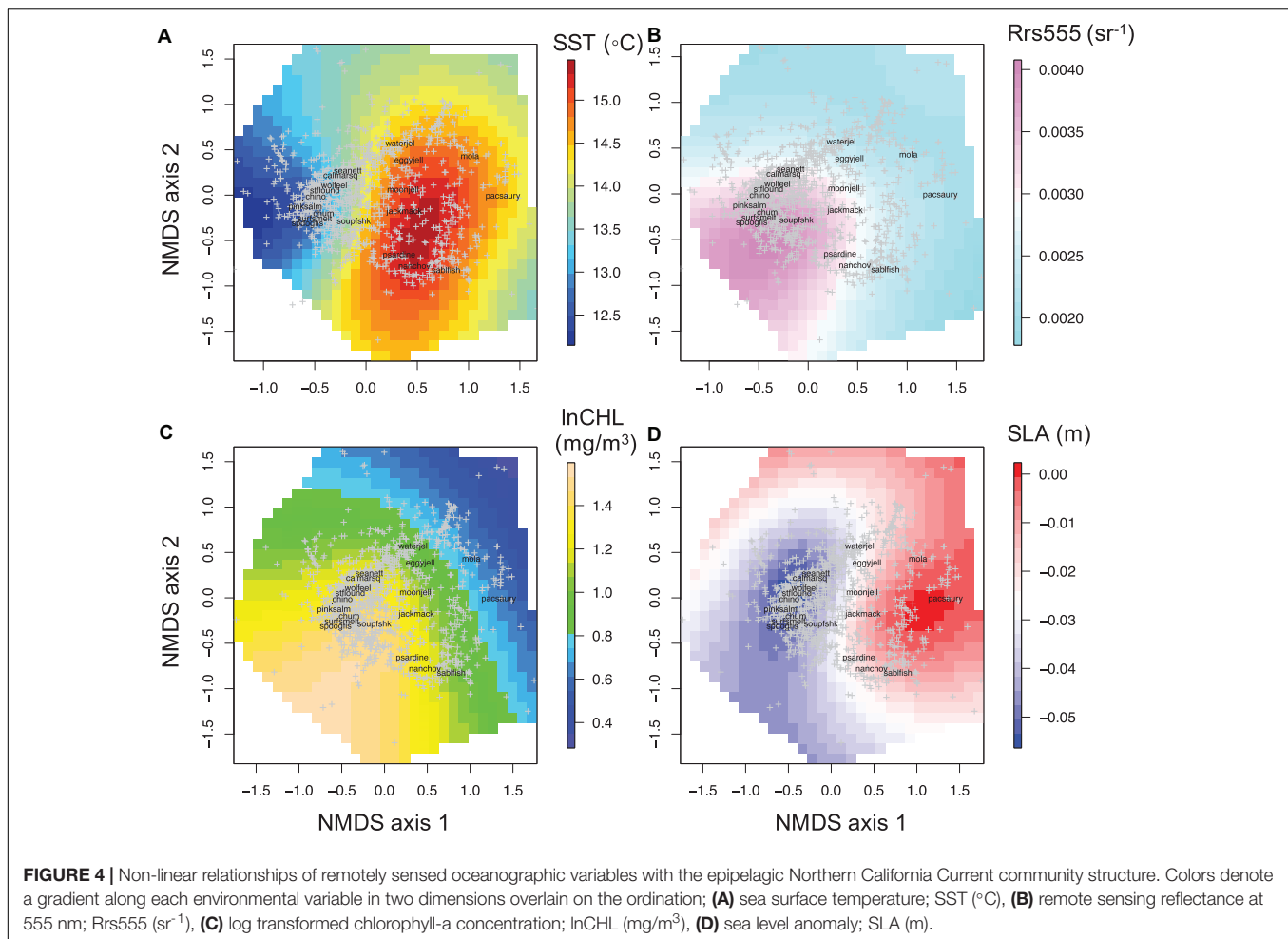
The field of pelagic seascape ecology so far has dealt mainly with the prediction of species distributions onto RS data fields (e.g., Alvarez-Berastegui et al., 2014, 2016), as well as the long-standing tradition of categorizing ocean waters based on RS data (Jerlov, 1968; Kavanaugh et al., 2014). More recently, predicting individual species distributions onto clustered RS data fields has also been attempted. For example, Breece et al. (2016) classified MODIS ocean color and SST fields, and then predicted Atlantic



**FIGURE 3 |** Non-linear relationships of in situ CTD derived oceanographic variables with community structure NMDS axis 1 and axis 2. **(A)** Temperature at 10 m depth (SST, °C), **(B)** salinity at 10 m depth (psu), **(C)** log (chlorophyll at 3 m depth) ( $\text{mg}/\text{m}^3$ ), **(D)** dissolved oxygen concentration at 10 m depth ( $\text{mg}/\text{L}$ ), **(E)** station bathymetric depth (m), **(F)** mixed layer depth (m), **(G)** latitude (Lat, °N), **(H)** longitude (Lon, °W).

sturgeon habitat (using acoustic receiver tracked movements of individuals) onto categorized images based on a cluster analysis of multiple RS data fields. Here, we chose a different seascape approach: prediction of community gradients onto RS data by linking ordination axes describing community composition onto statistically amalgamated RS-data fields given the relationships defined by non-linear regressions (GAMMs). The relationships between marine species distributions and the environment are often non-linear (McCune, 2006; Lintz et al., 2011), as

are the relationships of gradations in community composition to the environment. Our use of a continuous community gradient response variable (ordination axes) avoids drawbacks associated with classified community clusters, which includes unrealistic crisp borders and potential misclassification of species to distinct clusters (Lintz et al., 2011). It also allows for the description of non-linearities between individual RS data fields and community gradients (e.g., **Figures 4A–D**). Our approach of using a community metric has been instrumental in uncovering

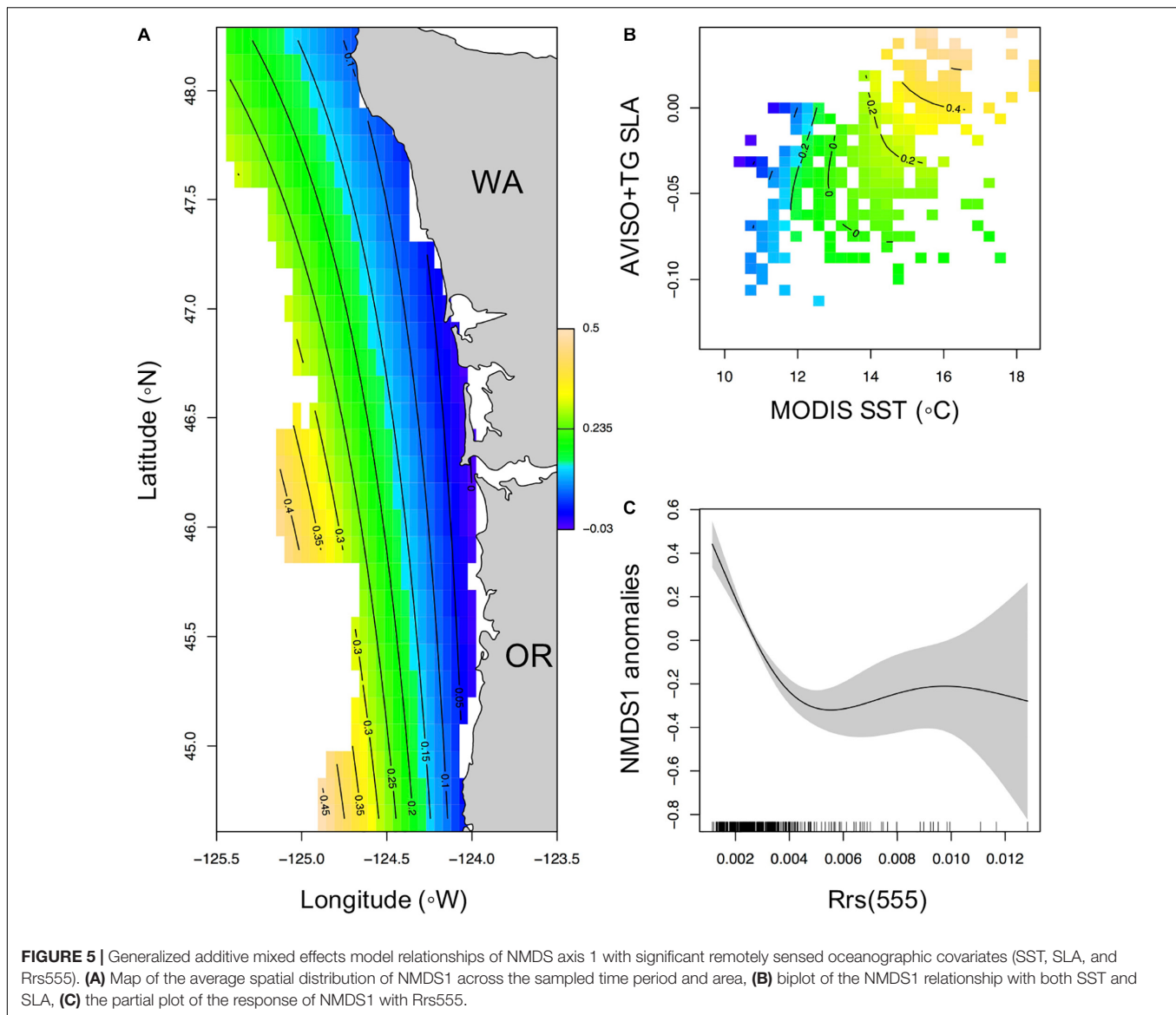


useful ecological information that other approaches could not have revealed. Notably, we found that at the community level, spatial and temporal dynamics are well represented by and correlated with remotely sensed and in situ oceanographic variables, indicating a high degree of spatio-temporal variability of each identified assemblage (e.g., warm–cold) in the NCC.

This is the first study in this region that assesses Rrs555 in relation to the nekton and macro-invertebrate community. MODIS Rrs555 data are known to be related to pelagic biology in this region (Thomas and Weatherbee, 2006; Saldías et al., 2016), but this is the first study in this region to demonstrate the utility of using MODIS Rrs555 fields for biological studies. Furthermore, the species associated with the highest Rrs555 median values are generally understood to be related to the plume or relatively fresh waters, while those with the lowest Rrs555 median values given their distributions during this sampling period are indicators for the ‘warm community’ (Brodeur et al., 2005). In addition, we demonstrate the utility of using the interaction of both SST and SLA, as together they capture the local physical expression of ocean indices such as PDO and the North Pacific Gyre Oscillation in species distribution models, rather than individually or together as additive co-variables (as is often done in species distribution modeling of organisms).

SST in this region is at times strongly influenced by the warmer Columbia River plume waters (Saldías et al., 2016) and relatively cool upwelled waters during the spring–summer season. From our correlations of collocated MODIS SST and SLA at sampling locations, SST is positively correlated with SLA, indicating that these variables capture complementary yet distinct aspects of the marine environment (SST is only representative of the surface skin conditions of the ocean and SLA provides a more depth integrative understanding of the surface ocean capturing both density and regional circulation features).

The GAMM models predicted community differences based on RS oceanographic variables, capturing predicted NMDS1 scores outside the range observed during the sampled 10 years during all months. This is likely indicative of a distinct offshore community configuration occurring in the Oregon and Washington shelf and slope waters during the 2014–2015 (variable by season) period, due to anomalously warm water temperatures during 2014–2015 heatwave years (Gentemann et al., 2017; Peterson et al., 2017; Brodeur et al., 2019; Morgan et al., 2019). There are limitations with respect to the inferences we can make about the spatio-temporal community predictions past the extent of our empirical sampled data. That said, our results do suggest an anomalous offshore

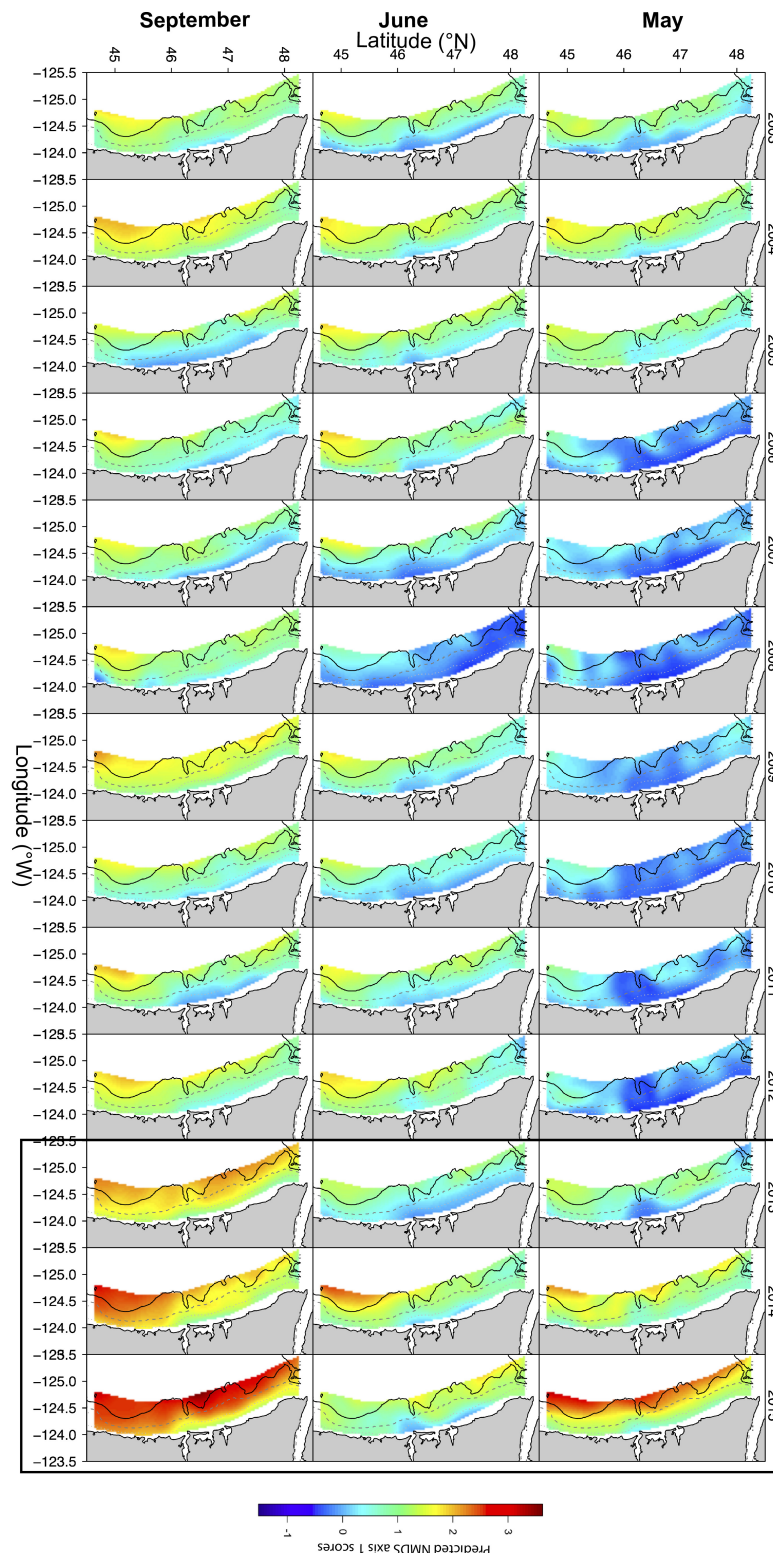


community in 2014–2015 which agrees with results from other studies in the region and adjacent that analyzed empirical data from that time period (e.g., Brodeur et al., 2019; Morgan et al., 2019). For example, Auth et al. (2018) recently identified novel ichthyoplankton assemblages in this region after 2014, due to the Northeastern Pacific (NEP) marine heatwave of 2014–2016 influencing the early and more coastal spawning of northern anchovy and Pacific sardine, and the more northerly and coastal spawning of Pacific hake (*Merluccius productus*). In the central California Current System, Santora et al. (2017) identified anomalously high diversity during this 2014–2016 NEP marine heatwave. Our prediction of community composition onto RS-data fields allowed for the spatial distribution of the compositional gradient, and thus has broader ecological implications. Almost all years and months had a significantly lower presence of the warm community along the Washington shelf than off Oregon (Figures 5, 6). This region is similar to

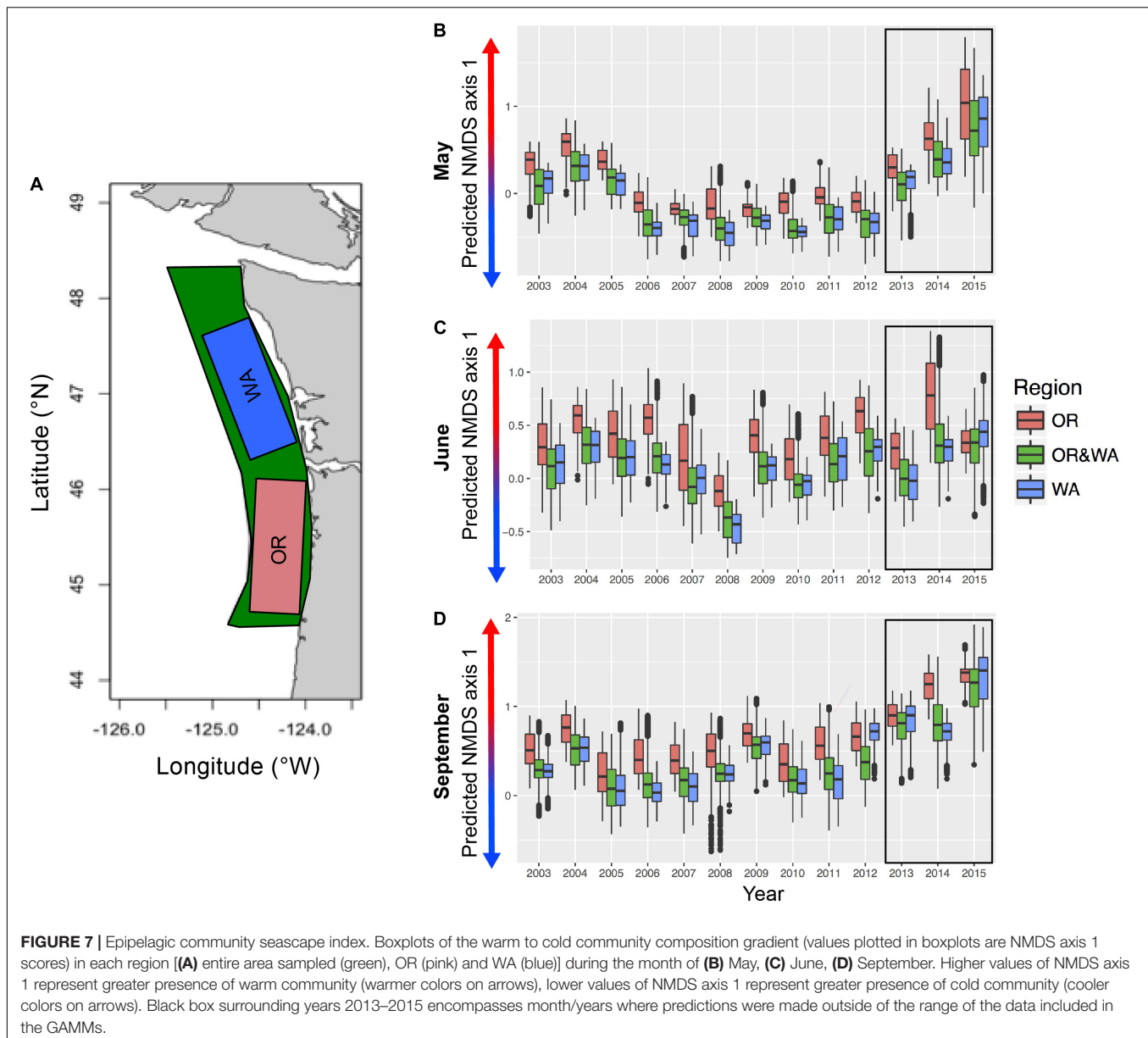
that identified by Barceló et al. (2018) as a cold water refugia and provides evidence that the coastal region off southern Washington has a consistent onshore affinity community that is consistent across multiple months during the spring-summer upwelling season.

The two community clusters identified in this study, represent what we describe as the ‘cold community’ or the ‘warm community.’ These communities are represented by pelagic species that have either warm (offshore and/or southern) or cold-water (northern and/or nearshore) affinities (Brodeur et al., 2003). The ‘warm community’ might be further subdivided into a Columbia River plume vs. the warm, but non-plume community (Supplementary Figure 6). However, this separation was not distinguished in this study, and possibly not clearly defined for all months due to the variable spatial extent of the plume as well as the use of the plume by a wide range of both warm and cold affinity, nearshore and offshore species.





**FIGURE 6 |** Spatial predictions of NMDS axis 1 (representing the warm to cold-onshore community composition gradient) onto statistically (GAMM) combined remotely sensed MODIS data products in May (top row), June (middle row) and September (bottom row) between 2003 and 2012. May, June and September months of years 2013–2015 are predicted using prior data. Black box surrounding years 2013–2015 encompasses month/years where predictions were made outside of the range of the data included in the GAMMs.



Northern anchovy and Pacific sardine clustered together with sablefish in the ordination (**Figure 2A**) in a different region of the ordination than either Pacific saury or ocean sunfish, and are species known to be associated with the Columbia River Plume during the spring-summer upwelling season (Emmett et al., 2004; Litz et al., 2008).

The indicator species in each month for the monthly warm clusters (**Table 1**) consistently had Pacific saury as an indicator. This species is often captured at offshore stations; however, its schooling behavior leads to a highly variable catch predictability in these stations (Brodeur and Pearcy, 1986; Brodeur et al., 2004, 2005). Sablefish (age-0) was also an indicator of the ‘warm community’ in May and June, but given median values of CTD salinity and Rrs555 it may also be a Columbia River plume associated species (Brodeur and Pearcy, 1986).

The ISA indicated that September also included Jack mackerel and ocean sunfish, likely due to an increased presence of warm offshore water along the shelf. With respect to the shared indicator species among the 3 months, May and June shared two of the species, and June and September shared two different species, while all 3 months shared Pacific saury. This is indicative of an expected, compositional continuum (vs. completely different warm communities between May to September) throughout the spring-summer season of makeup of the offshore community composition.

The fluctuation of the warm vs. cold community gradient has implications from a food-web and fisheries perspective. The closer to shore the preferred habitat for species of warm water affinity is, the higher the degree of competition and/or potential habitat compression for colder affinity

species (such as juvenile and sub-adult salmonids). This concept is analogous to vertical habitat compression of the mesopelagic community due to the vertical expansion of oxygen minimum zones (Stewart et al., 2014; Checkley et al., 2017), but instead, from a horizontal perspective. A concentrated presence of the cold community into the near-shore implies potentially higher competition among similar trophic level species, leading to reduced success, as well as higher predation by coastal predators (colonial seabirds and pinnipeds), potentially further reducing already low populations of forage fish and salmon species. On the other hand, the near-shore intrusion and increased presence of the offshore community may introduce higher trophic level species (e.g., Santora et al., 2020), such as albacore, making these species more easily available to the fishery (less travel time to fishing grounds for fishers).

Further, community seascape derived indices can add to integrated ecosystem assessments, by filling in gaps in survey coverage (e.g., resulting from global pandemics) and providing information about the state of the ecosystem that can then be used to relate to other trophic levels and human activities. Similar to the cold-water lipid-rich copepod community versus warm-water, lipid-poor copepods in the northeastern Pacific Ocean (Peterson et al., 2017), the warm-cold community gradient metrics described here (**Figures 5, 6**) have both spatial and temporal qualities. As such, they measure both the ‘flavor’ of the regional community, as well as the spatial presence of different community groups. This metric of warm-cold epipelagic fish fluctuations could be added to the suite of regional biological condition indicators of the upper ocean that have been related to higher trophic levels, such as salmon returns (Burke et al., 2013), or as a predictor for the yearly distribution of albacore habitat for fishermen. This metric also could contribute to the suite of diversity indicators used in the California Current Integrated Ecosystem Assessments as a new, community composition-based indicator of upper ocean ecosystem state. Furthermore, these data and community predictions could be integrated into seasonal forecasting products, such as J-SCOPE<sup>1</sup> (Siedlecki et al., 2016; Malick et al., 2020) and extended to use Regional Ocean Model System (ROMS) data to provide useful information on coastal pelagic species’ essential fish habitat.

In this study, we combined analytical techniques for understanding community structure with in situ and RS oceanographic observations to develop a better understanding of the community seascape. This analysis determined the habitat associations and community gradients in this upwelling and river-plume influenced pelagic marine ecosystem. These results demonstrated a statistically significant relationship between in situ and remotely sensed environmental variables and community composition that can have major benefits in monitoring and managing multi-species communities regionally, ranging from zooplankton to mammal and seabird communities. Daily satellite passes, and calculated satellite data composites (weekly, monthly) allow for continually updating community

seascape maps that can be easily visualized by managers and stakeholders. The information gained by this approach allows for the identification of distinct communities and associated habitat characteristics for the whole community as well as distinct species and is directly applicable to ecosystem-based management as this metric could be linked to salmon returns data (Burke et al., 2013) and landings data of other species. This index, however, does not replace the important need for maintaining long time series of biological fishery independent surveys in the ocean so as to be able to “seatruth” (Barth et al., 2019) these remotely sensed derived indices.

## DATA AVAILABILITY STATEMENT

Publicly available datasets were analyzed in this study. These data are available through a data request to NOAA-NWFSC’s Estuarine and Ocean Ecology Program [contact: David Huff (david.huff@noaa.gov) or Brian Burke (brian.burke@noaa.gov)].

## ETHICS STATEMENT

All animal work was conducted according to relevant national guidelines. Fish were collected under the Endangered Species Act (ESA) Section 10 permit #1410-7A, which is the federal procedure for research directed by NOAA that includes ESA-listed species. Neither NOAA nor OSU collections of fishes required a separate review by an Institutional Animal Care and Use Committee.

## AUTHOR CONTRIBUTIONS

CB with input from all authors, developed concept. RB and ED contributed biological and oceanographic data. LC provided base generalized additive model and gCV code. GS and CR contributed satellite data. CB conducted analysis and developed all figures and tables. All authors discussed the results and edited the manuscript.

## FUNDING

This study was result of research supported by NOAA’s Fisheries and the Environment Program (NOAA FATE Project ID: 12-01), NSF’s Graduate Research Fellowship Program (Grant No: 1214109 to CB). Contributing support for this work was provided by NOAA’s Integrated Ecosystem Assessment (NOAA IEA) Program via the OSU/NOAA’s Cooperative Institute of Marine Resources Studies (CIMRS). Publication funds for this article were provided by CIMRS-OSU and NRT-DESE: Risk and uncertainty quantification in marine science’ (Grant No: 1545188 to LC).

<sup>1</sup> www.nanoos.org/products/j-scope/home.php

# ACKNOWLEDGMENTS

We are indebted to the dedication of the many scientists who participated on the cruises, and to the captain and crew of the fishing vessels that assisted in sampling throughout the years. We thank federal agencies: Bonneville Power Administration (Department of Energy) and NOAA Fisheries - Northwest Fisheries Science Center (Department of Commerce) for providing funding for the Juvenile Salmon and Ocean Ecosystem Survey and personnel throughout the years. We are particularly thankful for helpful comments on earlier

versions of the manuscript received by reviewers and the editor, FM-K, and two reviewers, as well as internal NOAA-NMFS-NWFSC reviews received by Dr. Brian Burke and Dr. Rich Zabel.

# SUPPLEMENTARY MATERIAL

The Supplementary Material for this article can be found online at: <https://www.frontiersin.org/articles/10.3389/fmars.2021.586677/full#supplementary-material>

# REFERENCES

- Alvarez-Berastegui, D., Ciannelli, L., Aparicio-Gonzalez, A., Reglero, P., Hidalgo, M., Lopez-Jurado, J. L., et al. (2014). Spatial scale, means and gradients of hydrographic variables define pelagic seascapes of bluefin and bullet tuna spawning distribution. *PLoS One* 9:e109338. doi: 10.1371/journal.pone.0109338
- Alvarez-Berastegui, D., Hidalgo, M., Tugores, M. P., Reglero, P., Aparicio-González, A., Ciannelli, L., et al. (2016). Pelagic seascape ecology for operational fisheries oceanography: modelling and predicting spawning distribution of Atlantic bluefin tuna in western Mediterranean. *ICES J. Mar. Sci.* 73, 1851–1862. doi: 10.1093/icesjms/fsw041
- Arar, E. J., and Collins, G. B. (1997). In Vitro Determination of Chlorophyll a and Pheophytin a in Marine and Freshwater Algae by Fluorescence US EPA Method 445.0. Available online at: <https://permanent.fdlp.gov/lps68140/m445-0.pdf> (accessed July 9, 2017).
- Auth, T. D., Daly, E. A., Brodeur, B. D., and Fisher, J. L. (2018). Phenological and distributional shifts in ichthyoplankton associated with recent warming in the northeast Pacific Ocean. *Glob. Chang. Biol.* 24, 259–272. doi: 10.1111/gcb.13872
- Barceló, C., Ciannelli, L., and Brodeur, R. D. (2018). Pelagic marine refugia and climatically sensitive areas in an eastern boundary current upwelling system. *Glob. Chang. Biol.* 24, 668–680. doi: 10.1111/gcb.13857
- Barnes, S. L. (1964). A technique for maximizing details in numerical weather map analysis. *J. Appl. Meteorol. Climatol.* 3, 396–409. doi: 10.1175/1520-0450(1964)003<0396:atfmdi>2.0.co;2
- Barth, J. A., Allen, S. E., Dever, E. P., Evans, W., Feely, R. A., Fisher, J. L., et al. (2019). Better regional ocean observing through cross-national cooperation: a case study from the northeast pacific. *Front. Mar. Sci.* 6:93. doi: 10.3389/fmars.2019.00093
- Becker, E., Forney, K., Fiedler, P. C., Barlow, J., Chivers, S. J., Edwards, C. A., et al. (2016). Moving towards dynamic ocean management: How well do modeled ocean products predict species distributions? *Remote Sens.* 8:149. doi: 10.3390/rs8020149
- Breece, M. W., Fox, D. A., Dunton, K. J., Frisk, M. G., Jordaan, A., and Oliver, M. J. (2016). Dynamic seascapes predict the marine occurrence of an endangered species: Atlantic sturgeon *Acipenser oxyrinchus oxyrinchus*. *Methods Ecol. Evol.* 7, 725–733. doi: 10.1111/2041-210x.12532
- Brodeur, R. D., Auth, T. D., and Phillips, A. J. (2019). Major shifts in pelagic micronekton and macrozooplankton community structure in an upwelling ecosystem related to an unprecedented marine heatwave. *Front. Mar. Sci.* 6:212. doi: 10.3389/fmars.2019.00212
- Brodeur, R. D., Fisher, J. P., Emmett, R. L., Morgan, C. A., and Casillas, E. (2005). Species composition and community structure of pelagic nekton off Oregon and Washington under variable oceanographic conditions. *Mar. Ecol. Prog. Ser.* 298, 41–57. doi: 10.3354/meps298041
- Brodeur, R. D., Fisher, J. P., Teel, D. J., Emmett, R. L., Casillas, E., and Miller, T. W. (2004). Juvenile salmonid distribution, growth, condition, origin, and environmental and species associations in the northern California Current. *Fish. Bull.* 102, 24–46.
- Brodeur, R. D., and Pearcy, W. G. (1986). Distribution and relative abundance of pelagic non-salmonid nekton off Oregon and Washington, 1979–1984. *NOAA Tech. Rep.* 46, 515–535.
- Brodeur, R. D., Pearcy, W. G., and Ralston, S. (2003). Abundance and distribution patterns of nekton and micronekton in the northern California Current transition zone. *J. Oceanogr.* 59, 515–535.
- Brodeur, R. D., Ralston, S., Emmett, R. L., Trudel, M., Auth, T. D., and Phillips, A. J. (2006). Anomalous pelagic nekton abundance, distribution, and apparent recruitment in the northern California current in 2004 and 2005. *Geophys. Res. Lett.* 33:L22S08.
- Burke, B. J., Peterson, W. T., Beckman, B. R., Morgan, C., Daly, E. A., and Litz, M. (2013). Multivariate models of adult Pacific Salmon returns. *PLoS One* 8:e54134. doi: 10.1371/journal.pone.0054134
- Checkley, D. M., Asch, R. G., and Rykaczewski, R. R. (2017). Climate, Anchovy, and Sardine. *Annu. Rev. Mar. Sci.* 9, 469–493. doi: 10.1146/annurev-marine-122414-033819
- Ciannelli, L., Bailey, K. M., Chan, K.-S., and Stenseth, N. C. (2007). Phenological and geographical patterns of walleye pollock (*Theragra chalcogramma*) spawning in the western Gulf of Alaska. *Can. J. Fish. Aquat. Sci.* 64, 713–722. doi: 10.1139/f07-049
- Ciannelli, L., Bartolino, V., and Chan, K.-S. (2012). Non-additive and non-stationary properties in the spatial distribution of a large marine fish population. *Proc. Biol. Sci.* 279, 3635–3642. doi: 10.1098/rspb.2012.0849
- Clarke, K. R., and Warwick, R. M. (2001). *Changes in Marine Communities: An Approach to Statistical Analysis and Interpretation*, 2nd Edn. Plymouth: PRIMER-E, Ltd.
- Daly, E. A., Brodeur, R. D., Fisher, J. P., Weitkamp, L. A., Teel, D. J., and Beckman, B. R. (2012). Spatial and trophic overlap of marked and unmarked Columbia River basin spring Chinook salmon during early marine residence with implications for competition between hatchery and naturally produced fish. *Environ. Biol. Fish.* 94, 117–134. doi: 10.1007/s10641-011-9857-4
- De Caceres, M., and Jansen, F. (2020). Package ‘Indicspecies’. Function to Assess the Strength and Significance of Relationships of Species Site Group Associations. Version 1.5.1 edn.
- Emery, W. J., Strub, T., Leben, R., Foreman, M., McWilliams, J. C., Han, G., et al. (2011). “Satellite altimetry applications off the coasts of North America,” in *Coastal Altimetry*, eds S. Vignudelli, A. Kostianoy, P. Cipollini, and J. Benveniste (Berlin: Springer), 417–451. doi: 10.1007/978-3-642-12796-0\_16
- Emery, W. J., and Thomson, R. E. (2004). *Data Analysis Methods in Physical Oceanography*, 2nd Edn. Amsterdam: Elsevier.
- Emmett, R. L., Brodeur, R. D., and Orton, P. M. (2004). The vertical distribution of juvenile salmon (*Oncorhynchus* spp.) and associated fishes in the Columbia River plume. *Fish. Oceanogr.* 13, 392–402. doi: 10.1111/j.1365-2419.2004.00294.x
- Field, J., Francis, R., and Aydin, K. (2006). Top-down modeling and bottom-up dynamics: linking a fisheries-based ecosystem model with climate hypotheses in the Northern California Current. *Prog. Oceanogr.* 68, 238–270. doi: 10.1016/j.pocean.2006.02.010
- Gentemann, C., Fewings, M., and Garcia-Reyes, M. (2017). Satellite sea surface temperatures along the West Coast of the United States during the 2014–2016 northeast pacific marine heat wave. *Geophys. Res. Lett.* 44, 312–319. doi: 10.1002/2016gl071039



- Goni, M. A., Hatten, J. A., Wheatcroft, R. A., and Borgeld, J. A. (2013). Particulate organic matter export by two contrasting small mountainous rivers from the Pacific Northwest, USA. *J. Geophys. Res. Biogeosci.* 118, 112–134. doi: 10.1002/jgrg.20024
- Hastie, T., and Tibshirani, R. (1990). *Generalized Additive Models*. London: Chapman and Hall.
- Hazen, E. L., Jorgensen, S., Rykaczewski, R. R., Bograd, S. J., Foley, D. G., Jonsen, I. D., et al. (2013). Predicted habitat shifts of Pacific top predators in a changing climate. *Nat. Clim. Change* 3, 234–238. doi: 10.1038/nclimate1686
- Henderikx Freitas, F., Saldias, G. S., Goni, M., Shearman, R. K., and White, A. E. (2018). Temporal and spatial dynamics of physical and biological properties along the Endurance Array of the California Current ecosystem. *Oceanography* 31, 80–89. doi: 10.5670/oceanog.2018.113
- Hickey, B., and Banas, N. (2008). Why is the northern end of the California Current System so productive? *Oceanography* 21, 90–107. doi: 10.5670/oceanog.2008.07
- Hickey, B., Geier, S., Kachel, N., and MacFadyen, A. (2005). A bi-directional river plume: the Columbia in summer. *Cont. Shelf Res.* 24, 1631–1656. doi: 10.1016/j.csr.2005.04.010
- Hickey, B., Kudela, R. M., Nash, J., Bruland, K. W., Peterson, W. T., MacCready, P., et al. (2010). River influences on shelf ecosystems: introduction and synthesis. *J. Geophys. Res. Oceans* 115:C00B17.
- Hidalgo, M., Secor, D. H., and Broman, H. I. (2016). Observing and managing seascapes: linking synoptic oceanography, ecological processes, and geospatial modelling. *ICES J. Mar. Sci.* 73, 1825–1830. doi: 10.1093/icesjms/fsw079
- Hobday, A. J., and Hartog, J. R. (2014). Derived ocean features for dynamic ocean management. *Oceanography* 27, 134–145. doi: 10.5670/oceanog.2014.92
- Jerlov, N. (1968). *Optical Oceanography*. New York, NY: Elsevier.
- Kavanaugh, M. T., Hales, B., Saraceno, M., Spitz, Y. H., White, A. E., and Letelier, R. M. (2014). Hierarchical and dynamic seascapes: a quantitative framework for scaling pelagic biogeochemistry and ecology. *Prog. Oceanogr.* 120, 291–304. doi: 10.1016/j.pocean.2013.10.013
- Kudela, R. M., Horner-Devine, A. R., Banas, N. S., Hickey, B. M., Peterson, T. D., McCabe, R. M., et al. (2010). Multiple trophic levels fueled by recirculation in the Columbia river plume. *Geophys. Res. Lett.* 37:L18607. doi: 10.1029/2010GL044342
- Lentz, S. J. (1992). The surface boundary layer in coastal upwelling regions. *J. Phys. Oceanogr.* 22, 1517–1539. doi: 10.1175/1520-0485(1992)022<1517:tsblic>2.0.co;2
- Levin, P. S., Fogarty, M. J., Murawski, S. A., and Fluharty, D. (2009). Integrated ecosystem assessments: developing the scientific basis for ecosystem-based management of the ocean. *PLoS Biol.* 7:e1000014. doi: 10.1371/journal.pbio.1000014
- Lewison, R., Hobday, A. J., Maxwell, S., Hazen, E., Hartog, J. R., Dunn, D. C., et al. (2015). Dynamic ocean management: identifying the critical ingredients of dynamic approaches to ocean resource management. *Bioscience* 65, 486–498. doi: 10.1093/biosci/biv018
- Lintz, H. E., McCune, B., Gray, A. N., and McCulloh, K. A. (2011). Quantifying ecological thresholds from response surfaces. *Ecol. Model.* 222, 427–436. doi: 10.1016/j.ecolmodel.2010.10.017
- Litz, M. N. C., Heppell, S. R., Emmett, R. L., and Brodeur, R. (2008). Ecology and distribution of the northern subpopulation of northern anchovy (*Engraulis mordax*) off the US west coast. *Calif. Coop. Ocean. Fish. Invest. Rep.* 49, 167–182.
- Malick, M. J., Siedlecki, S. A., Norton, E. L., Kaplan, I. C., Haltuch, M. A., Hunsicker, M. E., et al. (2020). Environmentally driven seasonal forecasts of Pacific hake distribution. *Front. Mar. Sci.* 7:578490. doi: 10.3389/fmars.2020.578490
- Manderson, J., Palamara, L., Kohut, J., and Oliver, M. J. (2011). Ocean observatory data are useful for regional habitat modeling of species with different vertical habitat preferences. *Mar. Ecol. Prog. Ser.* 438, 1–17. doi: 10.3354/meps09308
- Maxwell, S. M., Hazen, E. L., Lewison, R. L., Dunn, D. C., Bailey, H., Bograd, S. J., et al. (2015). Dynamic ocean management: defining and conceptualizing real-time management of the ocean. *Mar. Policy* 58, 42–50. doi: 10.1016/j.marpol.2015.03.014
- Mazzini, P. L., Barth, J. A., Shearman, R. K., and Erofeev, A. (2014). Buoyancy-driven coastal currents off Oregon during fall and winter. *J. Phys. Oceanogr.* 44, 2854–2876. doi: 10.1175/jpo-d-14-0012.1
- Mazzini, P. L., Risien, C. M., Barth, J. A., Pierce, S. D., Erofeev, A., Dever, E. P., et al. (2015). Anomalous near-surface low-salinity pulses off the Central Oregon coast. *Sci. Rep.* 5:17145.
- McCune, B. (2006). Non-parametric habitat models with automatic interactions. *J. Veg. Sci.* 17, 819–830. doi: 10.1111/j.1654-1103.2006.tb02505.x
- McCune, B., and Grace, J. B. (2002). *Analysis of Ecological Communities*. (Gleneden Beach, OR: MjM Software), 304.
- McKibben, S. M., Strutton, P. G., Foley, D. G., Peterson, T. D., and White, A. E. (2012). Satellite-based detection and monitoring of phytoplankton blooms along the Oregon coast. *J. Geophys. Res. Oceans* 117:C12002.
- Morgan, C., Beckman, B., Weitkamp, L. A., and Fresh, K. L. (2019). Recent Ecosystem Disturbance in the Northern California Current. *Fisheries* 44, 465–474. doi: 10.1002/fsh.10273
- Morgan, C. A., De Robertis, A., and Zabel, R. W. (2005). Columbia River plume fronts. I. Hydrography, zooplankton distribution, and community composition. *Mar. Ecol. Prog. Ser.* 299, 19–31. doi: 10.3354/meps299019
- Muller-Karger, F. E., Hestir, E., Ade, C., Turpie, K., Roberts, D. A., Siegel, D., et al. (2018). Satellite sensor requirements for monitoring Essential Biodiversity Variables of coastal ecosystems. *Ecol. Appl.* 28, 749–760.
- Oksanen, J., Blanchet, F. G., Friendly, M., Kindt, R., Legendre, P., McGlinn, D., et al. (2019). *vegan: Community Ecology Package. R package version 2.5-6*. Available online at: <https://CRAN.R-project.org/package=vegan> (accessed July 9, 2017).
- Peterson, W. T., Fisher, J. L., Strub, P. T., Du, X., Risien, C., Peterson, J., et al. (2017). The pelagic ecosystem in the Northern California Current off Oregon during the 2014–2016 warm anomalies within the context of the past 20 years. *J. Geophys. Res. Oceans* 122, 7267–7290. doi: 10.1002/2017JC012952
- Pikitch, E. K., Rountos, K. J., Essington, T. E., Santora, C., Pauly, D., Watson, R., et al. (2014). The global contribution of forage fish to marine fisheries and ecosystems. *Fish. Fish.* 15, 43–64. doi: 10.1111/faf.12004
- Pittman, S., Christensen, J., Caldow, C., Menza, C., and Monaco, M. (2007). Predictive mapping of fish species richness across shallow-water seascapes in the Caribbean. *Ecol. Model.* 204, 9–21. doi: 10.1016/j.ecolmodel.2006.12.017
- Pittman, S., Kneib, R., Simenstad, C., and Nagelkerken, I. (2011). Seascape ecology: application of landscape ecology to the marine environment. *Mar. Ecol. Prog. Ser.* 427, 187–190. doi: 10.3354/meps09139
- Pittman S. (ed.). (2017). *Seascape ecology: Taking landscape ecology to the sea*. Wiley-Blackwell.
- Pujol, M.-I., Faugère, Y., Taburet, T., Dupuy, S., Pelloquin, C., Ablain, M., et al. (2016). DUACS DT2014: the new multi-mission altimeter data set reprocessed over 20 years. *Ocean Sci.* 12, 1067–1090. doi: 10.5194/os-12-1067-2016
- R Core Team (2019). *R: A Language and Environment for Statistical Computing*. Vienna: R Foundation for Statistical Computing.
- Ralston, S., Field, J. C., and Sakuma, K. M. (2015). Long-term variation in a central California pelagic forage assemblage. *J. Mar. Syst.* 146, 26–37. doi: 10.1016/j.jmarsys.2014.06.013
- Risien, C. M., and Strub, P. T. (2016). Blended sea level anomaly fields with enhanced coastal coverage along the US west coast. *Sci. Data* 3:160013.
- Saldias, G. S., Shearman, R. K., Barth, J. A., and Tuffiaro, N. (2016). Optics of the offshore Columbia River plume from glider observations and satellite imagery. *J. Geophys. Res. Oceans* 121, 2367–2384. doi: 10.1002/2015jc011431
- Saldias, G. S., Strub, P. T., and Shearman, R. K. (2020). Spatio-temporal variability and ENSO modulation of turbid freshwater plumes along the Oregon coast. *Estuar. Coast. Self Sci.* 243:106880. doi: 10.1016/j.ecss.2020.106880
- Samhouri, J. F., Haupt, A. J., Levin, P. S., Link, J. S., and Shufford, R. (2014). Lessons learned from developing integrated ecosystem assessments to inform ecosystem based management. *ICES J. Mar. Sci.* 71, 1205–1215. doi: 10.1093/icesjms/fst141
- Santora, J. A., Hazen, E. L., Schroeder, I. D., Bograd, S. J., Sakuma, K. M., and Field, J. C. (2017). Impacts of ocean climate variability on biodiversity of pelagic forage species in an upwelling ecosystem. *Mar. Ecol. Prog. Ser.* 580, 205–220. doi: 10.3354/meps12278
- Santora J. A., Mantua, N. J., Schroeder I. D., Field J. C., Hazen E. L., and Bograd S. J. (2020). Habitat compression and ecosystem shifts as potential links between marine heatwaves and record whale entanglements. *Nat. Commun.* 11:536. doi: 10.1038/s41467-019-14215-w
- Scales, K. L., Schorr, G. S., Hazen, E. L., Bograd, S. J., Miller, P. I., Andrews, R. D., et al. (2017). Should I stay or should I go? Modelling year-round habitat

- suitability and drivers of residency for fin whales in the California Current. *Divers. Distrib.* 23, 1204–1215. doi: 10.1111/ddi.12611
- Siedlecki, S. A., Kaplan, I. C., Hermann, A. J., Nguyen, T. T., Bond, N. A., Newton, J. A., et al. (2016). Experiments with seasonal forecasts of ocean conditions for the northern region of the California Current upwelling system. *Sci. Rep.* 6:27203.
- Sigleo, A., and Frick, W. (2007). Seasonal variations in river flow and nutrient concentrations in a Northwestern USA watershed. *Estuar. Coast. Shelf Sci.* 73, 368–378.
- Skidmore, A. K., and Pettorelli, A. (2015). Agree on biodiversity metrics to track from space: ecologists and space agencies must forge a global monitoring strategy. *Nature* 523, 403–406. doi: 10.1038/523403a
- Stewart, J. S., Hazen, E. L., Bograd, S., Byrnes, J. E. K., Foley, D. G., Gilly, W. F., et al. (2014). Combined climate- and prey-mediated range expansion of Humboldt squid (*Dosidicus gigas*), a large marine predator in the California Current System. *Glob. Change Biol.* 20, 1832–1843. doi: 10.1111/gcb.12502
- Suryan, R. M., Santora, J. A., and Sydeman, W. J. (2012). New approach for using remotely sensed chlorophyll a to identify seabird hotspots. *Mar. Ecol. Prog. Ser.* 451, 213–225. doi: 10.3354/meps09597
- Szoboszlai, A. I., Thayer, J. A., Wood, S. A., Sydeman, W. J., and Koehn, L. E. (2015). Forage species in predator diets: synthesis of data from the California Current. *Ecol. Inform.* 29, 45–56. doi: 10.1016/j.ecoinf.2015.07.003
- Thomas, A. C., and Weatherbee, R. A. (2006). Satellite-measured temporal variability of the Columbia River plume. *Remote Sens. Environ.* 100, 167–178. doi: 10.1016/j.rse.2005.10.018
- Thompson, A., Harvey, C. J., Sydeman, W. J., Barceló, C., Bograd, S. J., Brodeur, R. D., et al. (2019). Indicators of pelagic forage community shifts in the California Current Large Marine Ecosystem, 1998–2016. *Ecol. Indic.* 105, 215–228. doi: 10.1016/j.ecolind.2019.05.057
- Thorson, J., Cheng, W., Hermann, A. J., Iannelli, J. N., Litzow, M. A., O’Leary, C. A., et al. (2020). Empirical orthogonal function regression: linking population biology to spatial varying environmental conditions using climate projections. *Glob. Change Biol.* 26, 4638–4649. doi: 10.1111/gcb.15149
- Wainwright T. C., Emmett R. L., Weitkamp L. A., Hayes S. A., Bentley P. J., and Harding J. A. (2019). Effect of marine mammal excluder device on trawl catches of salmon and other pelagic animals. *Mar. Coast. Fish.* 11, 17–31. doi: 10.1002/mcf2.10057
- Wall, C. C., Muller-Karger, F. E., Roffer, M. A., Hu, C., Yao, W., and Luther, M. E. (2008). Satellite remote sensing of surface oceanic fronts in coastal waters off west-central Florida. *Remote Sens. Environ.* 112, 2963–2976. doi: 10.1016/j.rse.2008.02.007
- Wallis, C. I., Brehm, G., Donoso, D. A., Fiedler, K., Homeier, J., Paulsch, D., et al. (2017). Remote sensing improves prediction of tropical montane species diversity but performance differs among taxa. *Ecol. Indic.* 83, 538–549. doi: 10.1016/j.ecolind.2017.01.022
- Walters, M., and Scholes, R. (eds) (2017). *The GEO Handbook on Biodiversity Observation Networks*. (Berlin: Springer), 39–78.
- Wood, S. (2015). *Mixed GAM Computation Vehicle with GCV/AIC/REML Smoothness Estimation R package version 1.8-6*. Available online at: <https://mran.microsoft.com/snapshot/2015-10-27/web/packages/mgcv/mgcv.pdf> (accessed July 9, 2017).
- Wood, S., and Scheipl, F. (2014). *gamm4: Generalized Additive Mixed Models Using mgcv and lme4. R package version 0.2-3*. Available online at: <http://CRAN.R-project.org/package=gamm4> (accessed July 9, 2017).
- Zuur, A., Ieno, E. N., and Walker, N. (2009). *Mixed Effects Models and Extensions in Ecology*. New York, NY: Springer.
- Zwolinski, J. P., Emmett, R. L., and Demer, D. A. (2011). Predicting habitat to optimize sampling of Pacific sardine (*Sardinops sagax*). *ICES J. Mar. Sci.* 68, 867–879. doi: 10.1093/icesjms/fsr038

**Conflict of Interest:** The authors declare that the research was conducted in the absence of any commercial or financial relationships that could be construed as a potential conflict of interest.

Copyright © 2021 Barceló, Brodeur, Ciannelli, Daly, Risien, Saldías and Samhoury. This is an open-access article distributed under the terms of the Creative Commons Attribution License (CC BY). The use, distribution or reproduction in other forums is permitted, provided the original author(s) and the copyright owner(s) are credited and that the original publication in this journal is cited, in accordance with accepted academic practice. No use, distribution or reproduction is permitted which does not comply with these terms.



# Low Densities of the Ghost Crab *Ocypode quadrata* Related to Large Scale Human Modification of Sandy Shores

Carlos A. M. Barboza<sup>1,2\*</sup>, Gustavo Mattos<sup>3</sup>, Abílio Soares-Gomes<sup>4</sup>,  
Ilana Rosental Zalmon<sup>5</sup> and Leonardo Lopes Costa<sup>5</sup>

<sup>1</sup> Laboratório de Biologia de Invertebrados, Instituto de Biodiversidade e Sustentabilidade NUPEM, Universidade Federal do Rio de Janeiro, Macaé, Brazil, <sup>2</sup> Laboratório Integrado de Biologia Marinha, Instituto de Biodiversidade e Sustentabilidade NUPEM, Universidade Federal do Rio de Janeiro, Macaé, Brazil, <sup>3</sup> Laboratório de Polychaeta, Instituto de Biologia, Departamento de Zoologia, Universidade Federal do Rio de Janeiro, Rio de Janeiro, Brazil, <sup>4</sup> Laboratório de Ecologia de Sedimentos, Departamento de Biologia Marinha, Universidade Federal Fluminense, Niterói, Brazil, <sup>5</sup> Laboratório de Ciências Ambientais, Centro de Biociências e Biotecnologia, Universidade Estadual do Norte Fluminense Darcy Ribeiro, Campos dos Goytacazes, Brazil

## OPEN ACCESS

### Edited by:

Enrique Montes,  
University of South Florida,  
United States

### Reviewed by:

Maíra Pombo,  
Universidade Federal do Amapá,  
Brazil  
Edlin José Guerra-Castro,  
National Autonomous University of  
Mexico, Mexico

### \*Correspondence:

Carlos A. M. Barboza  
carlosambarboza@ufrj.br;  
carlosambarboza@gmail.com

### Specialty section:

This article was submitted to  
Marine Ecosystem Ecology,  
a section of the journal  
Frontiers in Marine Science

**Received:** 30 July 2020

**Accepted:** 26 January 2021

**Published:** 11 March 2021

### Citation:

Barboza CAM, Mattos G,  
Soares-Gomes A, Zalmon IR and  
Costa LL (2021) Low Densities of  
the Ghost Crab *Ocypode quadrata*  
Related to Large Scale Human  
Modification of Sandy Shores.  
Front. Mar. Sci. 8:589542.  
doi: 10.3389/fmars.2021.589542

Sandy beaches are the most common ecosystems of coastal regions and provide direct and indirect essential services for millions of people, such as coastal protection, fishing, tourism, and recreational activities. However, the natural habitats of sandy shores are being modified at rates never experienced before, making beaches key monitoring sites of marine ecosystems worldwide. The ghost crab species *Ocypode quadrata* is the most conspicuous crustacean of sandy beaches along the Western Atlantic coast and has been successfully used as an indicator of anthropogenic disturbance and environmental variability. To investigate the potential role of a “triple whammy” [(1) urbanization; (2) use of resources; (3) decreasing resilience] on the most common bioindicator of sandy shores, we compiled a dataset including 214 records of burrows density from 94 microtidal sandy beach sectors covering a range of over 65° of latitude. The response of burrows density to synergetic effects of human modification of natural systems and environmental changes was investigated using linear models. We used the cumulative Human Modification (HMc) index, a standardized geographic projection of changes of natural systems, as a predictor of urbanization, industrialization and use of resources. The predictor wave energy, tidal range and temperature (sea surface and air) were included as potential effects of climate changes. Literature review showed records mainly concentrated at sub-tropical and temperate regions. HMc values were clearly negatively related to burrows density, thereby supporting an effect of modification of natural habitat at large spatial scale. Sea surface temperature and air temperature were positive related with density and the lack of a general pattern of the relationship between burrows density, interactions between wave energy and tide range, supported unclear patterns reported at regional scales. Finally, we argue that ghost crabs are valuable targets for protection actions on sandy beaches that can benefit coexisting species and provide natural habitat conservation.

**Keywords:** sandy shores, habitat loss, marine essential biodiversity variables, human impact, crustaceans, biological indicator

## INTRODUCTION

Concentrating almost half of the world's population,<sup>1</sup> coastal regions (<100 km from line coast) play a major role in providing ecological services and promote human well-being (Costanza et al., 2014). Although the United Nations 2030 Sustainable Development Goals calls for the protection, restoration, and sustainable use of ecosystems (Cowie et al., 2018), coastal regions are being transformed at rates never experienced before, even in face of evidences that natural systems generate social and economic benefits which exceed those obtained from habitat conversion (Balmford et al., 2002; Xavier et al., 2020).

Recognizing the importance of these services, numerous international collaborations (Benson et al., 2018; Canonico et al., 2019) have centered their efforts to enhance monitoring, setting essential physical, chemical, and marine biological variables to be measured through standardized methods and best practices of data acquisition to subsidize conservation, management, and stakeholders decisions (Pereira et al., 2013; Miloslavich et al., 2018; Fanini et al., 2020; Guerra-Castro et al., 2020). In this sense, sandy beaches are key monitoring sites. Sandy shores are the most common ecosystems of coastal regions and provide direct and indirect essential services for millions of people, such as coastal protection, fishing, and recreational activities (Micallef and Williams, 2009; McLachlan and Defeo, 2018). Negative synergetic effects on biodiversity and ecosystems functions due to multiple human activities co-occurring in a region, are commonly higher when compared to single effects (Raiter et al., 2014; Costa et al., 2020a). This is what Defeo and Elliot (2020) characterized as “triple whammy” on worldwide sandy shores subject to three major threats: (1) increasing urbanization and industrialization; (2) increasing use of resources; (3) increasing susceptibility and decreasing resilience and resistance to the effects of climate change. Thus, a pragmatic implementation of ecosystems management and monitoring efforts on sandy beaches is a major challenge (Schlacher et al., 2014). A complex scenario is presented because sandy beaches should be considered as social-ecological systems, with interactions between human activities and environmental processes involved (Micallef and Williams, 2009; Xavier et al., 2020). Values and conservation goals should be carefully addressed for a broad and successful inclusion of multiple segments of society (Harris et al., 2014; Schlacher et al., 2016).

Monitoring single species, particularly “charismatic” ones due to a public appeal, is perhaps the most common and effective way to monitor environment variability and include social interactions on conservation activities (Micallef and Williams, 2009; Siddig et al., 2016; Xavier et al., 2020). Ghost crabs (Crustacea: Ocypodidae) are the largest crustaceans from sandy beaches with a distribution from the tropics to temperate latitudes (Sakai and Türkay, 2013). *Ocypode quadrata* (Fabricius, 1787) is the unique ghost crab species from Western Atlantic. Commonly abundant in sandy shores, they are relatively large semi-terrestrial species that inhabit the intertidal-dune interface. Ghost crabs not only respond to anthropogenic drivers, but

also to physical environment features such as morphodynamic characteristics (Pombo et al., 2017; Gül and Griffen, 2019) or biological changes like food supply (Tewfik et al., 2016). There are a number of evidences to a common local or regional pattern of burrow density reduction on urban beaches affected by trampling, vehicle traffic, beach cleaning, litter pollution, recreational harvesting, prey depletion and/or armoring (de Souza et al., 2017; Gül and Griffen, 2018; Pombo and Turra, 2019; Costa et al., 2020c). Different preferences of ghost crabs species for across shore zones according to local beach characteristics (Gül and Griffen, 2018; Ocaña et al., 2018) could reveal distinct response to natural habitat modification. Because they are typical upper-shore semi-terrestrial crustaceans, that are theoretically less affected by swash climate and wave action than other macrofauna, they are commonly neglected as a component of beach communities in classical ecological hypotheses (Defeo and McLachlan, 2005; Defeo et al., 2017).

Although some biases of quantification have been raised (Pombo and Turra, 2013), the indirect estimates of ghost-crab population sizes are a non-destructive, friendly, and low cost sampling and, has been used as a valuable and efficient strategy tool by researchers for impact assessments on sandy beaches and today these data represent an important historical of records. At the same time the increasing possibilities to apply remote-sensing technologies enable the application of spatially explicit information on conservation and management effort (Monsarrat et al., 2019; El Mahradi et al., 2020). A big effort is being dedicated to make friendly available global scale data set of environmental variables (Fick and Hijmans, 2017; Assis et al., 2018) and intensity of human modification of natural systems, for example the Global Human Footprint (Venter et al., 2016) or the cumulative Human Modification (HMc) (Kennedy et al., 2019, 2020). Associating remote sensing data to the available records of the single ghost crab from Western Atlantic, enabled investigate large scale correlations between environmental drivers and standardized metrics of the magnitude of human modifications of sandy shores. For this purpose, we compiled a dataset including records of burrow density, as a proxy of population density, from pristine to urbanized beach sectors. For the first time, large scale patterns of population densities were related to key marine variables of species distributions and to a standardized geographic projection of changes on natural systems. We brought new insights on *O. quadrata* distribution and verified the potential role of a “triple whammy” from (1) synergetic effects of resource exploitation and (2) coastal urbanization (HMc), as also from (3) climate changes (wave energy, tidal range, and environment temperature) on the most common bioindicator of sandy shores.

## MATERIALS AND METHODS

### Ghost Crab Data

Studies about the ghost crab *O. quadrata* were first obtained by searching the databases of Web of Science, Scopus, and Google Scholar using “*Ocypode quadrata*” as key-word. Additional studies were then sourced by cited references on this pool of

<sup>1</sup><https://www.un.org/en/about-un/>



documents. For quality control purposes, only studies with peer-review or an equivalent process completed were kept. There is a great variability in methodological approaches used in the literature (for example regarding the area of the beach that is sampled or the metric that counts are reported) that represent a big challenge to investigate spatial and temporal patterns. From this primary source we selected only reports that estimated population size using density of burrows (ind/m<sup>2</sup>) or all information necessary to estimate this metric. Only studies where densities were estimated from the entire across-shore area (waterline to upper supralittoral) were used to avoid bias in the estimate of densities. Data that were only available in figures were extracted using the WebPlotDigitizer Program (Rohatgi, 2013). The dataset from four sandy beaches of the coast of Rio de Janeiro (Cavaleiros: −22.4059°/−41.7985°, Pecado: −22.4150°/−41.8150°, Barreto: −22.3364°/−41.7236°, and Jurubatiba −22.2969/41.6845) monitored by adapting the standardized sampling protocol from Mbon Pole to Pole (2019) is available as **Supplementary Material**. The protocol allows obtaining comparable information across beaches with different morphodynamic states and was recognized as an Ocean Best Practice initiative of UNESCO/IODE. Barreto Beach and Jurubatiba Beach are located inside marine protected areas and License for activities at protected areas was conceived by ICMBio 65087-1. Jurubatiba Beach is monitored by the Brazilian Long-Term Ecological Research (RLaC; CNPq 441610/2016-1). Studies used contiguous sample units for each transect perpendicular to the waterline that varied from 1 to 38 m wide ( $8.4 \pm 12.6$ ), random quadrats or units in plots established at each beach zone (supra, meso, and infralittoral). The final list of studies included in the analyses is available on **Supplementary Material**. Our final data matrix included 214 records from 94 sandy beach sectors (**Figure 1**).

## Environmental Variables: The Potential Role of Climate Changes

Temperature plays a key role in ghost crab biology because it influences critical physiological and metabolic processes (Weinstein and Full, 1994, 1998), survival, distributional limits (Schoeman et al., 2015), reproduction habits (Negreiros-Fransozo et al., 2002) and behavior (Lucrezi and Schlacher, 2014). Mean sea surface temperature (SST, °C) was extracted from the Bio-ORACLEv2.0 database, which offers averages data for the period of 2000–2014. Data source is from Global Observed Ocean Physics Reprocessing (resolution: 0.258/33 vertical levels), and the pre-processed global ocean re-analyses combining satellite and *in situ* observations generated global data with a resolution of 5 arc-minutes (Tyberghein et al., 2012; Assis et al., 2018).<sup>2</sup> Average values (°C) of air temperature were obtained from the WorldClim database, which provides long-term bioclimatic data from land areas with a resolution of 5 arc-minutes (Hijmans et al., 2005).<sup>3</sup>

The physical environment of sandy beaches is driven by the interaction between wind, sand, waves and tides where

resident sandy beach fauna species are thought to be influenced by these physical drivers (Defeo et al., 2017; McLachlan and Defeo, 2018). Data of wave energy (kW/m) were retrieved from the Marine Socio-Environmental Covariates – MSEC database (Yeager et al., 2017).<sup>4</sup> The wave energy values are a product of a wave forecasting model based on wind input for a span of 31 years (1979–2009), including sheltered-coastline corrections (Yeager et al., 2017). The annual average tidal amplitude (cm) was extracted from the AVISO+ data service, which contains global tidal variables with a resolution of 3.75 arc-minutes (Vestbo et al., 2018).<sup>5</sup> The geographical coordinates from each beach sector were used to extract the variables' values. Layers from Bio-ORACLEv2.0, WorldClim and MARSPEC were accessed through the sdmpredictors package (Bosch, 2018) of the R Program (R Core Team, 2020), and layers from AVISO+ were downloaded from the above-cited websites, and manipulated using the raster package (Hijmans et al., 2016).

## Human Modification: The Potential Role of Synergetic Effects of Coastal Urbanization and Resource Exploitation

To quantify human modification of natural habitat we used the HMc values (Kennedy et al., 2019, 2020). The index is a degree of human modification across global terrestrial lands and was calculated as the per pixel (1 km<sup>2</sup>) product (HMs) of the spatial extent and the expected intensity of impact across five major groups of human stressors: (1) human settlement (population density, built up areas), (2) agriculture (cropland, livestock), (3) transportation (major roads, minor roads, two tracks, railroads), (4) mining and energy production (mining, oil wells, wind turbines), and (5) electrical infrastructure (powerlines, nighttime lights). Thus the HMc capture two of the three whammys defined by Defeo and Elliot (2020). For each stressor the median and mean values are from 2016 and 2014, respectively. The final human modification model is defined as:

$$\text{HMc} = 1.00 - \prod_{s=1}^n (1 - (\text{HMs}))$$

This fuzzy sum is a function that assumes the contribution of a given factor decreases as values from other stressors co-occur. In this way, the HMc is a continuous parsimonious gradient of modification effect that calibrates landscape impacts and ultimately converges to 1.00 (Kennedy et al., 2019).

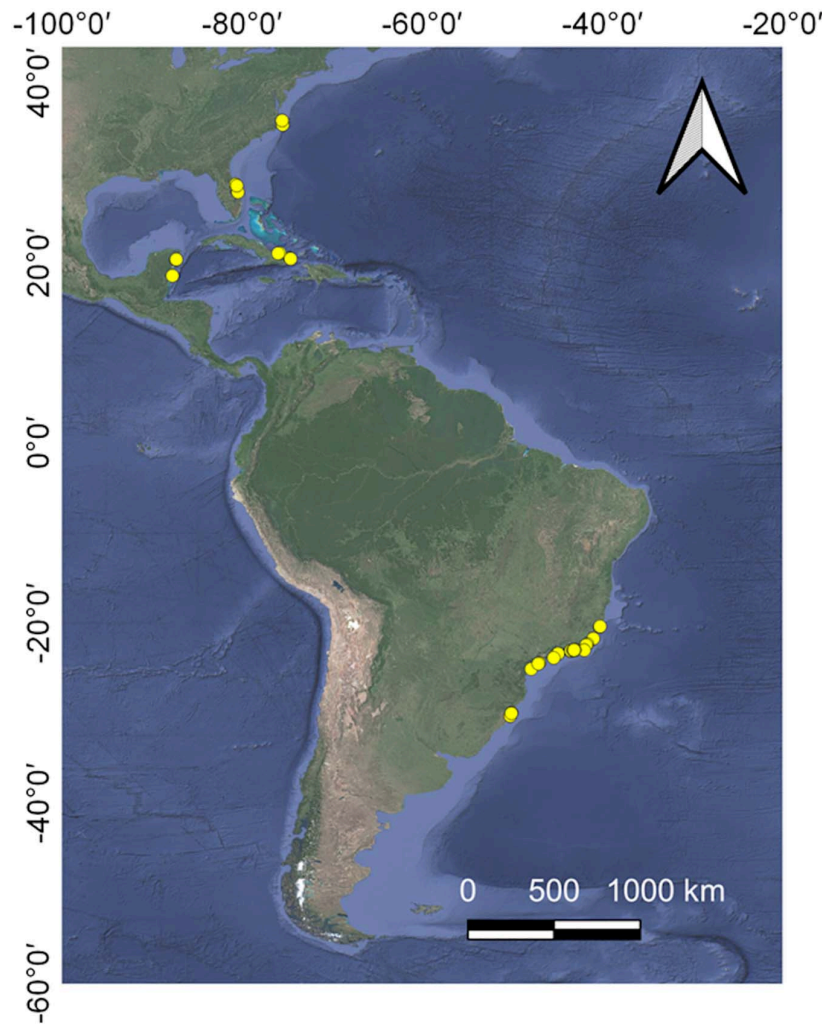
We also independently accessed the magnitude of human modification of natural habitat at a local spatial scale by applying a categorical classification of impact on the beach record. The classification was primarily assigned following the original descriptions provided by the authors of each study, and calibrated across sites. In some cases, the intensity of environmental modification was not directly declared by the authors; thereby we used Google Earth images and additional public information (i.e., government reports) from each location to assign a common classification. This classification Google

<sup>2</sup><https://www.bio-oracle.org/>

<sup>3</sup><https://www.worldclim.org/>

<sup>4</sup><https://shiny.sesync.org/apps/msec/>

<sup>5</sup><https://snd.gu.se/en/catalogue/study/ecds0243>



**FIGURE 1** | Locations of the records of burrow density from 94 beach sectors in Western Atlantic Coast.

Earth images was done based on the image from the year of survey or as close as possible. Our classification included four levels: High Impact – records on beach sectors with completely modified and suppressed supralittoral zone, with easy access (e.g., presence of runway), buildings and markets, and absence of dune/vegetation; Moderate Impact – urbanized beach sectors, but with some degree of conservation of the supralittoral zone and dune vegetation; Low Impact – beaches with difficult or restricted access, relatively preserved supralittoral zone and exclusively impacted by low number of beachgoers; None Impact – totally preserved beaches commonly located at protected areas. Finally, we assessed the relationship between the HMc values and our categorical classification of local human modification. By this way we can estimate some mismatch between the spatial and temporal variability of both indicators.

## Data Analysis

For investigate the potential effects of a “triple whammy” on populations of the ghost crab *O. quadarta* we used linear models.

The density of burrows was included as a response variable. HMc represented the effect of natural modification and the predictor sea surface temperature, air temperature, wave energy and tidal range proxies of the role of climate changes. In a first step a global linear model was run using the response variable burrows density and the linear predictors HMc, SST, air temperature, wave energy, and the interactions wave SST  $\times$  air temperature and wave energy  $\times$  tidal range. A fourth-root transformation was applied on burrow densities and the predictors SST, air temperature, wave energy and tide range were standardized. The presence of multicollinearity on predictors was assessed by the variation inflation factor (VIF) and we used a threshold of  $VIF \geq 3$  to variable exclusion. We applied the Moran's I test (Cliff and Ord, 1981) for spatial autocorrelation in residuals and rejected the null hypothesis of independence. Thus we used the Moran eigenvector approach (Dray et al., 2006) for construct a matrix of spatial patterns that represents the spatial dependence present in the residuals and can be allocated into the linear model. For construct the spatial model we used the package

“spdep” (Bivand and Wong, 2018) from the R Program (R Core Team, 2020) and defined a spatial matrix on the indices of points belonging to the set of  $k = 5, 10, 15$ , and 20 nearest neighbors. The neighbors of region points were identified by great circle distance and weights matrices were generated. The package *spatialreg* (Bivand and Piras, 2015) was used to select the optimal subset of eigenvectors and remove spatial dependence on errors. This spatial eigenvectors matrix was included in the linear model and a second stage of model test was applied. Because the model captures the spatial pattern it represents also local environmental variables that were not explicitly inserted in our model. For the validation of the best linear model we plotted residuals against fitted values and each explanatory variable to identify patterns, and violation of homogeneity dependence; histogram of residuals was used to verify normality assumptions (Supplementary Material; Zuur et al., 2009).

## RESULTS

### Dataset Coverage and Properties

Data included records from Brazil (77%), United States (15%), Mexico (4%), and Cuba (4 distributed from 35.83° N to 30.28° S (Figure 1). Sampling year ranged from 1991 to 2019 with a median value at the year 2012 (only one study occurred before the year 2000). From the total number of beach sectors included in the dataset, 81% have temporal replication (at least two records from the same beach sector) ranging from 2 to 5 replicates.

The coastal region analyzed were represent by microtidal sandy beaches of sub-tropical and temperate shores and the summary statistics of the environmental variables are presented on Table 1. HMc values included pristine to very urbanized sandy beaches and varied between 0.036 and 0.92 with a median value equal to 0.53 (Figure 2). We found a general congruence between HMc values and the local impact classification applied. Some degree of mismatch between both indicators revealed that human modification can be captured at distinct spatial scales and possibly temporal and that local characteristics are potential small scale patterns that influence density.

### Relationship Between Burrow Density, Human Modification, Environmental and Spatial Predictors

Burrows density ranged from 0 to 1.53 ind/m<sup>2</sup> with a mean of 0.17 ind/m<sup>2</sup>. We identified values of  $VIF \geq 3$  for SST and air temperature and run two independent models selection including each predictor at each run. Independent spatial matrices were constructed for each model. The best model (using SST) retained the predictors HMc, tidal range, wave energy, SST the interaction tidal range  $\times$  wave energy and nine spatial eigenvectors (Table 2), thus supporting the effect of a triple whammy on ghost crabs populations. The best spatial matrix was defined using  $k = 5$  nearest neighbors and we got a significant increase in the model fitting when including the spatial eigenvectors (LR test  $F = 29.026$ ,  $p < 0.001$ ). For a model including air temperature this variable

was positively related with burrow density (estimate = 0.022) with a marginal significance ( $p = 0.057$ ) (Supplementary Material).

Figure 3 shows the mean partial effects of each predictor on burrows density of *O. quadrata*. Density clearly decreased with increasing HMc values. We found a positive relationship between burrows density and SST. The interaction between tidal range and wave energy revealed distinct effects along these gradients. We found a positive mean partial effect of wave energy across average and minor values of tide, and a negative effect on beaches with higher values of tidal range.

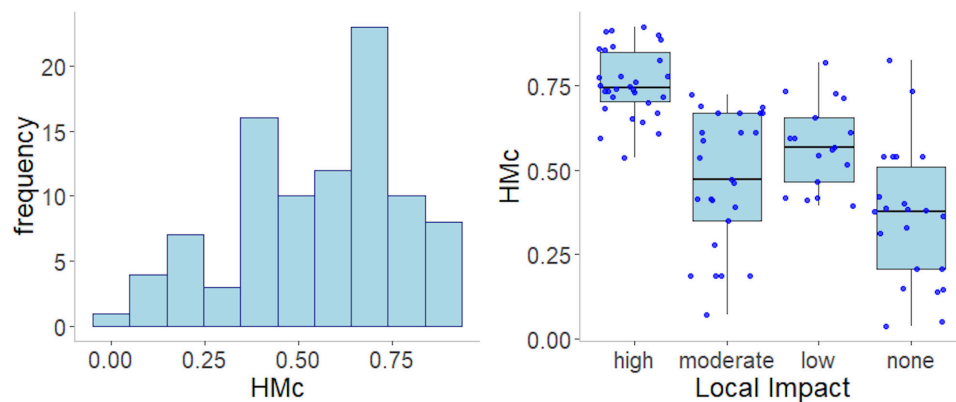
## DISCUSSION

Our results broadly support existent data at local and regional scales indicating a general negative anthropogenic impact on populations of *O. quadrata*. Using records from sandy beach sectors with multiple morphodynamic states across a range of over 65° of latitude along the Western Atlantic coast, we showed evidences of a potential role of a “triple whammy” on densities of the ghost crab *O. quadrata*. Herein density was clearly negatively related to HMc values that capture the extent of human settlement measured by metrics such as population density, built-up areas and the presence of major roads. For the first time a global standardized metric of human modification of natural system was related to densities of a sandy beach species, thereby supporting the effect of large scale urbanization (*sensu* Defeo and Elliot, 2020) on the biodiversity of sandy shores. Environmental variables were also important predictors of burrow densities and, the interaction between tidal range and wave energy effects evidenced the lack of a general relationship between ghost crab distributions and environmental drivers. Local spatial variability could only be captured by the spatial model due to our spatial resolution of the environmental predictors. This potentially include unknown precitors explaining density at those scales. Because the same or neighbour sectors were sampled at different times this spatial model could be, in some way, biased by a temporal effect.

The main human intervention on sandy shores consists of physical modifications which have critical effects on coastal ecosystem dynamics by reducing natural habitat suitability (Jones et al., 2017). Particularly higher human population sizes are related to easy access, efficient public transportation and recreational facilities as restaurants, bars and hotels over beach sectors that enhance their social value. In fact, this is the case of hundreds of beaches from the coast of Brazil (Amaral et al., 2016). Recreation-associated disturbances, such as trampling and vehicle traffic, clearly impair invertebrate macrofauna (Gheskiere et al., 2005; Schlacher and Thompson, 2012), including ghost crabs (Schlacher et al., 2007; Lucrezi et al., 2009; Costa et al., 2019, 2020c). The suppression of the dry upper beach zone extirpates semi-terrestrial invertebrates due to habitat loss (Dugan et al., 2008; Hubbard et al., 2014; Cardoso et al., 2016). Although ghost crabs can cover the entire extent of the beach face, they depend directly on supralittoral to mid-intertidal zones to feed and to construct their semi-permanent burrows (Lucrezi and Schlacher, 2014).

**TABLE 1** | Summary statistics from the environmental variables of 94 beach sandy beach sectors of Western Atlantic.

Variable	Unit	Median value	Dataset range	Source
Sea surface temperature	°C	23.39	18.90–28.03	Bio-ORACLEv2.0 <a href="http://www.bio-oracle.org">www.bio-oracle.org</a>
Air temperature	°C	22.27	16.50–26.30	WorldClim <a href="http://www.worldclim.org">www.worldclim.org</a>
Wave energy	kW/m	5.48	0.002–16.36	MSEC <a href="http://shiny.sesync.org/apps/msec">shiny.sesync.org/apps/msec</a>
Tide range	cm	77.48	15.65–117.38	AVISO+ <a href="http://snd.gu.se/en/catalogue/study/ecds0243">snd.gu.se/en/catalogue/study/ecds0243</a>

**FIGURE 2** | Histogram of values of the cumulative Human Modification (HMc) and relationship with the local human modification levels of 94 sandy beach sectors from Western Atlantic coast.**TABLE 2** | Summary statistics of the final best model relating the 214 records of burrows density of the ghost crab *Ocypode quadrata* from 94 sandy beach sectors from Western Atlantic coast, environmental variables, HMc values and spatial eigenvectors.

	Estimate	SE	t	p
<b>Environmental Changes</b>				
HMc	−0.667	0.049	−13.585	< 0.001
Tide range	−0.046	0.010	−4.453	0.001
Wave energy	0.055	0.012	4.679	< 0.001
SST	0.070	0.012	5.762	< 0.001
Tide range × wave energy	−0.104	0.014	−7.643	< 0.001
<b>Spatial Structure</b>				
MEM6	−1.028	0.148	6.940	< 0.001
MEM4	−0.682	0.148	−4.603	< 0.001
MEM5	0.763	0.148	−5.123	< 0.001
MEM7	−0.060	0.148	−7.156	< 0.001
MEM1	0.390	0.148	2.634	0.009
MEM3	0.276	0.148	1.870	0.063
MEM12	−0.521	0.148	−3.515	< 0.001
MEM9	−0.358	0.148	−2.414	0.017
MEM10	0.324	0.148	2.188	0.030

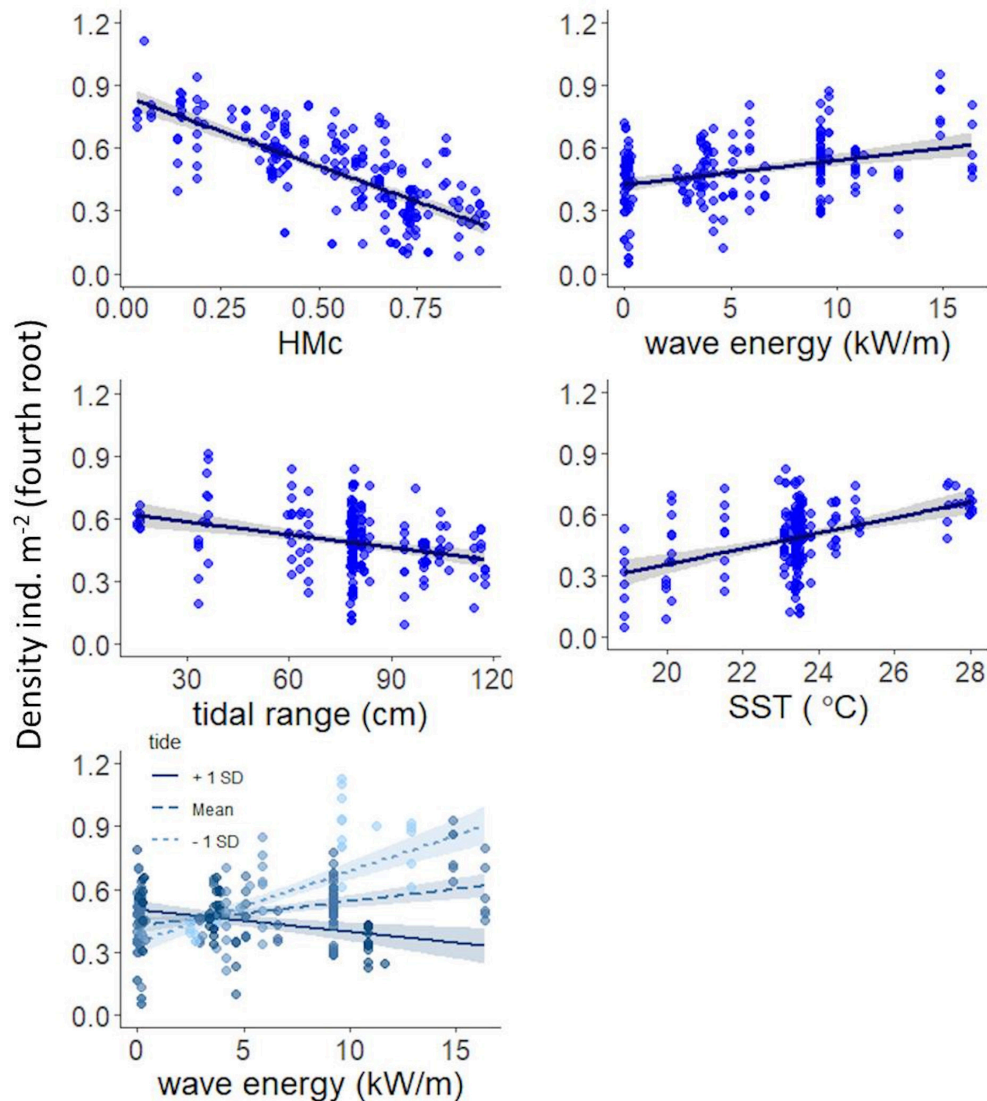
Adjusted  $R^2 = 0.67$ .

The levels in the categorization used here to measure local impact relied mainly on physical modification of natural features characterizing the urbanization effects of the “triple whammy.” Some mismatch between this classification and HMc values revealed important distinctness between the spatial scales of the metric to be used. For example, we can have a preserved supralittoral zone of a beach sector located at a metropolitan area. Backshore vegetation is successfully used

as a metric of natural habitat modification of sandy beaches (Schlacher et al., 2008; Orlando et al., 2020) and is an important habitat for *O. quadrata*, providing shelter, burrow stabilization, foraging area, and protection from storms (Lucrezi et al., 2010; Schlacher et al., 2011; Gül and Griffen, 2019). This is also true for other species of macrofauna. Cardoso et al. (2016) reported that despite having some infrastructure facilities, beaches with well-preserved backshore vegetation in Rio de Janeiro state, Brazil, supported higher densities of the sandhopper *Atlantorchestoidea brasiliensis*, a mobile crustacean typically found from the supralittoral to the upper midlittoral zone (Cardoso and Veloso, 2001; Gómez et al., 2013). Similarly, Orlando et al. (2020) reported that macrofauna community richness is usually higher in areas with preserved vegetation on sandy shores. Therefore, it is expected that ghost crab conservation confers a “protection wave” to numerous coexisting species (beneficiary species “under the umbrella”) (Simberloff, 1998; Fleishman et al., 2001), and can co-occur with the control of erosive processes through the maintenance of coastal vegetation.

Although neglected in sandy beach impact assessments (González et al., 2014; Duarte et al., 2016) nightlight, also weighted on HMc values and related to urbanization, can affect ghost crab sensorial responses (Silva et al., 2017). Costa et al. (2020b) tested whether artificial light attracts ghost crabs inland toward roads nearby sandy beaches, but evidences that light pollution predicts ghost crabs road-kills (car-crab collisions) were not found. In an extensive meta-analysis, Schlacher et al. (2016) pointed out that mechanistic processes and suitable sampling design concerning impacts of artificial nightlight on macrofauna species remain underreported, even though foraging behavior





**FIGURE 3 |** Best model relating burrows density of the ghost crab *Ocypode quadrata*, environmental variables and cumulative Human Modification (HMc) values. Mean partial effects of HMc, wave energy, tidal range, and SST are shown by solid lines. Mean partial effects for different values of wave energy are shown by solid and dashed lines across distinct values of tidal range. A shaded envelope represents the 95% of confidence intervals.

and activity rhythms may be sensitive to artificial light and could possibly have fitness implications for ghost crabs species.

The resilience to synergetic effects of these rate of coastal modification and environmental change includes the combination of the capacity to resist to increasingly frequent and severe disturbances and to adapt to new environmental conditions, that is enhanced by high population sizes and dispersal rates (Bernhardt and Leslie, 2011). Thus, we expect that population decrease on urbanized sandy shores will increase susceptibility and decrease resilience and resistance to the effects of environmental changes. Understand how these changes will disturb ghost crab populations includes establish ecological theories about patterns of macrofauna communities of sandy beaches to morphodynamic features.

The Swash Exclusion Hypothesis and the Habitat Harshness Hypothesis propose that macrofauna along a morphodynamic gradient is limited by the swash climate; and then, species richness, abundance and biomass increase from reflective to dissipative beaches (McLachlan et al., 1993; Defeo and McLachlan, 2005). For our data the interaction between tidal range and wave energy indicated the importance of these environment predictors to population densities. A positive effect of wave energy was estimated to sandy beaches with lower values of tide range, particularly characteristic from temperate regions of South America with dissipative beaches with high wave energy and high primary productivity (Odebrecht et al., 2014). A weak but negative effect of wave energy occurred for higher values of tide range, that are characteristic of sandy beaches

from southeast coast of Brazil (Amaral et al., 2016), the region that included the majority of records in our data. In ghost crabs literature we have quite different results. For example, Quijón et al. (2001) reported no clear response of *Ocypode gaudichaudii* to morphodynamic variables on sandy beaches in the North of Chile. Counting indistinguishable burrows of three ghost crab species, Lucrezi (2015) observed an increase in burrow densities toward dissipative conditions on four warm-temperate microtidal sandy beaches in South Africa. Oppositely, Defeo and McLachlan (2011) found increase, but not very clear, in burrow densities of *O. quadrata* from dissipative to reflective beaches and coarser grain sizes, compiling information from microtidal sandy beaches from the warm temperate Southwestern Atlantic province. Finally, analyzing densities along nine pristine areas with distinct morphodynamic states and wave exposure levels, Pombo et al. (2017) reported no clear response to slope, but an increased burrow density in finer-grained beaches. These evidences supported that beach morphodynamic state alone could be insufficient to predict population and community parameters, that impose some challenges in proposing forecasting scenarios, especially for supralittoral species which are not directly exposed to swash conditions (Contreras et al., 2003; Defeo and Gómez, 2005).

Because *O. quadrata* has an indirect development with a long-lived larval stage and populations sharing haplotypes over ~7,000 km (Mattos et al., 2019) is expected that not only coastal modification and beach characteristic will influence population densities, but also oceanic variables. Although sandy beaches occupy about one-third of ice-free coastline (Luijendijk et al., 2018), large scale (i.e., regional and continental) oceanic environmental drivers of macrofauna distribution have only been investigated quite recently (Defeo et al., 2017). The positive effect of SST, as well as of for air temperature when SST is excluded, should be evaluated with care because it seems that these predictors can act distinctly on ghost crabs distribution according to ontogenetic stage. *O. quadrata* has a planktonic larvae phase, thus sea temperature is more likely to be related to larvae metabolism, development rates, metamorphosis and time spent in the plankton (O'Connor et al., 2009; Gerber et al., 2014). Recently, Meerhoff et al. (2020) showed the influence of seasonal winds and associated ocean circulation patterns to larval connectivity of the mole crab *Emerita brasiliensis*. Local hydrodynamic regimes may have great potential to influence larval settlement. On the other hand, air temperature is likely to be related with population establishment, distribution range and burrowing activity. Schoeman et al. (2015) showed that distribution range of *Ocypode cordimanus* is not primarily determined by recruitment limitation along the Central to Northern East coast of Australia. In that region, both air and ocean temperatures decrease from north to south, but with a stronger spatial gradient in seawater than in air temperatures. Abundance of species is usually lower near its range edge (Bates et al., 2014) and this is in part coherent with our findings, which show decreasing burrow densities toward lower sea surface and air temperatures.

In conclusion, we showed evidences that coastal modification plays a potential major role on the population density of the ghost crab *O. quadrata* along the Western Atlantic coast and, these

effects should vary across environment characteristics. Effects at continental scales seems not only disturb densities of but also individuals size (Schlacher et al., 2016). The species is a model of key element in sandy beach trophic webs and thus indicates that natural habitat loss at a continental scale will certainly bring changes on patterns of the land-sea interface processes. Urbanization of sandy beaches has an intrinsic relation with widely used indicators of natural habitat urbanization, such as human population density and nighttime light intensity, here identified as potential and promising proxies of biological disturbance at large spatial scales. Ghost crabs conservation will benefit coexisting species, because it requires protection to sandy shores' natural habitat. In addition, maintenance of coastal vegetation was found to be essential for ghost crabs conservation, and it indirectly allows the control of erosive processes. Therefore, targeting ghost crabs as umbrella and indicator species is a valuable strategy for the conservation and monitoring of coastal regions. Our dataset is may be influenced by intrinsic processes of the Brazilian coast, the area with the greatest research effort for this species. Also, data is restricted to microtidal sandy beaches with a lack of existent reports from tropical coasts and macrotidal regimes. However, we argue that the number of records included here, with a wide range of morphodynamic states across a continental scale covering the entire gradient of urbanization levels, supports our findings in this domain and, brings new insights for the ecology of ghost crabs. We strongly recommend increasing monitoring data on the tropical coasts of the Western Atlantic, mainly sandy beaches along the Caribbean Sea and the Gulf of Mexico. Finally, manipulative experiments using standardized protocols that include key environmental variables at large scales are pivotal, particularly to disentangle causality relationships between reduction of ghost crab populations and human stressors.

## DATA AVAILABILITY STATEMENT

The raw data supporting the conclusions of this article will be made available by the authors, without undue reservation.

## AUTHOR CONTRIBUTIONS

CB led the analyses and writing of the manuscript in close collaboration with GM and LC. AS-G and IZ contributed critically to the drafts and gave final approval for publication. All authors contributed to the article and approved the submitted version.

## FUNDING

The work was supported by NASA under the A.50 AmeriGEO Work Programme of the Group on Earth Observations with grant number 80NSSC18K0318 ['Laying the foundations of the Pole-to-Pole Marine Biodiversity Observation Network of the Americas (MBON Pole to Pole)']. IZ was supported by Conselho Nacional de Desenvolvimento Científico e Tecnológico

(CNPq Proc. 301203/2019-9). AS-G was supported by Conselho Nacional de Desenvolvimento Científico e Tecnológico (CNPq Proc. 301475/2017-2). LC was supported by Coordenação de Aperfeiçoamento de Pessoal de Nível Superior (CAPES Proc. 88882.463168/2019-01).

## ACKNOWLEDGMENTS

We thank Marine Biodiversity Observation Network Pole to Pole of the Americas for their support. We thank María Chaumet and

Paula Debiassi for English and figures edition, respectively. We also thank the two reviewers for a careful revision and Maikon Di Domenico for valuable comments.

## SUPPLEMENTARY MATERIAL

The Supplementary Material for this article can be found online at: <https://www.frontiersin.org/articles/10.3389/fmars.2021.589542/full#supplementary-material>

## REFERENCES

- Amaral, A. C. Z., Corte, G. N., Filho, J. S. R., Denadai, M. R., Colling, L. A., Borzone, C., et al. (2016). Brazilian sandy beaches: characteristics, ecosystem services, impacts, knowledge and priorities. *Brazilian J. Oceanogr.* 64, 5–16. doi: 10.1590/s1679-875920160933064sp2
- Assis, J., Tyberghein, L., Bosch, S., Verbruggen, H., Serrão, E. A., and De Clerck, O. (2018). Bio-ORACLE v2.0: extending marine data layers for bioclimatic modelling. *Glob. Ecol. Biogeogr.* 27, 277–284. doi: 10.1111/geb.12693
- Balmford, A., Bruner, A., Cooper, P., Costanza, R., Farber, S., Green, R. E., et al. (2002). Ecology: economic reasons for conserving wild nature. *Science* 297, 950–953. doi: 10.1126/science.1073947
- Bates, A. E., Pecl, G. T., Frusher, S., Hobday, A. J., Wernberg, T., Smale, D. A., et al. (2014). Defining and observing stages of climate-mediated range shifts in marine systems. *Glob. Environ. Chang.* 26, 27–38. doi: 10.1016/j.gloenvcha.2014.03.009
- Benson, A., Brooks, C. M., Canonico, G., Duffy, E., Muller-Karger, F., Sosik, H. M., et al. (2018). Integrated observations and informatics improve understanding of changing marine ecosystems. *Front. Mar. Sci.* 5:428.
- Bernhardt, J. R., and Leslie, H. M. (2011). Resilience to climate change in coastal marine ecosystems. *Annu. Rev. Marine. Sci.* 5, 371–392. doi: 10.1146/annurev-marine-121211-172411
- Bivand, R. S., and Piras, G. (2015). Comparing implementations of estimation methods for spatial econometrics. *J. Stat. Softw.* 63, 1–36.
- Bivand, R. S., and Wong, D. W. S. (2018). Comparing implementations of global and local indicators of spatial association. *Test* 27, 716–748. doi: 10.1007/s11749-018-0599-x
- Bosch, S. (2018). *Package “sdmpredictors” - Species Distribution Modelling Predictor Datasets*. Available online at: <http://cran.r-project.org/web/packages/sdmpredictors>.
- Canonico, G., Buttigieg, P. L., Montes, E., Muller-Karger, F. E., Stepien, C., Wright, D., et al. (2019). Global observational needs and resources for marine biodiversity. *Front. Mar. Sci.* 6:367.
- Cardoso, R. S., and Veloso, V. G. (2001). Embryonic development and reproductive strategy of *Pseudorchestoidea brasiliensis* (Amphipoda: Talitridae) at Prainha beach. *Brazil. J. Nat. Hist.* 35, 201–211. doi: 10.1080/00222930150215332
- Cardoso, R. S., Barboza, C. A. M., Skinner, V. B., and Cabrini, T. M. B. (2016). Crustaceans as ecological indicators of metropolitan sandy beaches health. *Ecol. Indic.* 62, 154–162. doi: 10.1016/j.ecolind.2015.11.039
- Cliff, A. D., and Ord, J. K. (1981). Spatial processes. models and applications. *Cartography* 13, 59–60.
- Contreras, H., Jaramillo, E., Duarte, C., and McLachlan, A. (2003). Population abundances, growth and natural mortality of the crustacean macroinfauna at two sand beach morphodynamic types in southern Chile. *Rev. Chil. Hist. Nat.* 76, 543–561.
- Costa, L. L., Fanini, L., Zalmon, I. R., and Defeo, O. (2020a). Macroinvertebrates as indicators of human disturbances: a global review. *Ecol. Indic.* 118:106764. doi: 10.1016/j.ecolind.2020.106764
- Costa, L. L., Madureira, J. F., and Zalmon, I. R. (2019). Changes in the behaviour of *Ocypode quadrata* (Fabricius, 1787) after experimental trampling. *J. Mar. Biol. Assoc. U K* 99, 1135–1140. doi: 10.1017/s0025315418001030
- Costa, L. L., Mothé, N. A., and Zalmon, I. R. (2020b). Light pollution and ghost crab road-kill on coastal habitats. *Reg. Stud. Mar. Sci.* 39:101457. doi: 10.1016/j.rsma.2020.101457
- Costa, L. L., Secco, H., Arueira, V. F., and Zalmon, I. R. (2020c). Mortality of the Atlantic ghost crab *Ocypode quadrata* (Fabricius, 1787) due to vehicle traffic on sandy beaches: a road ecology approach. *J. Environ. Manag.* 260:110168. doi: 10.1016/j.jenvman.2020.110168
- Costanza, R., Groot, R., Sutton, P., Ploeg, S., Anderson, S. J., Kubiszewski, I., et al. (2014). Changes in the global value of ecosystem services. *Glob. Environ. Change* 26, 152–158.
- Cowie, A. L., Orr, B. J., Castillo Sanchez, V. M., Chase, P., Crossman, N. D., Erlewein, A., et al. (2018). Land in balance: the scientific conceptual framework for land degradation neutrality. *Environ. Sci. Policy* 79, 25–35. doi: 10.1016/j.envsci.2017.10.011
- de Souza, G. N., Oliveira, C. A. G., Tardem, A. S., and Soares-Gomes, A. (2017). Counting and measuring ghost crab burrows as a way to assess the environmental quality of beaches. *Ocean Coast. Manag.* 140, 1–10. doi: 10.1016/j.ocecoaman.2017.02.007
- Defeo, O., and Elliot, M. (2020). The ‘triple whammy’ of coasts under threat – why we should be worried! *Mar. Poll. Bull.* doi: 10.1016/j.marpolbul.2020.111832 Online ahead of print.
- Defeo, O., and Gómez, J. (2005). Morphodynamics and habitat safety in sandy beaches: life-history adaptations in a supralittoral amphipod. *Mar. Ecol. Prog. Ser.* 293, 143–153. doi: 10.3354/meps293143
- Defeo, O., and McLachlan, A. (2005). Patterns, processes and regulatory mechanisms in sandy beach macrofauna: a multi-scale analysis. *Mar. Ecol. Prog. Ser.* 295, 1–20. doi: 10.3354/meps295001
- Defeo, O., and McLachlan, A. (2011). Coupling between macrofauna community structure and beach type: a deconstructive meta-analysis. *Mar. Ecol. Prog. Ser.* 433, 29–41. doi: 10.3354/meps09206
- Defeo, O., Barboza, C. A. M., Barboza, F. R., Aeberhard, W. H., Cabrini, T. M. B., Cardoso, R. S., et al. (2017). Aggregate patterns of macrofaunal diversity: an interocean comparison. *Glob. Ecol. Biogeogr.* 26, 823–834. doi: 10.1111/geb.12588
- Dray, E., Legendre, P., and Peres-Neto, P. R. (2006). Spatial modelling: a comprehensive framework for principal coordinate analysis of neighbour matrices (PCNM). *Eco. Modell.* 196, 483–493. doi: 10.1016/j.ecolmodel.2006.02.015
- Dugan, J. E., Hubbard, D. M., Rodil, I. F., Revell, D. L., and Schroeter, S. (2008). Ecological effects of coastal armoring on sandy beaches. *Mar. Ecol.* 29, 160–170. doi: 10.1111/j.1439-0485.2008.00231.x
- El Mahrad, B., Newton, A., Icely, J. D., Kacimi, I., Abalansa, S., and Snoussi, M. (2020). Contribution of remote sensing technologies to a holistic coastal and marine environmental management framework: a review. *Remote Sens.* 12:2313. doi: 10.3390/rs12142313
- Fabricius, J. C. (1787). *Mantissa Insectorum Sistens Eorum Species Nuper Detectas Adjectis Characteribus Genericis Differentiis Specificis, Emendationibus, Observationibus. Tome I.* (Hafniae: Christ. Gottl. Proft.), 348.
- Fanini, L., Defeo, O., and Elliott, M. (2020). Advances in sandy beach research local and global perspectives. *Estuar. Coast. Shelf Sci.* 234:106646. doi: 10.1016/j.ecss.2020.106646

- Fick, S., and Hijmans, R. (2017). WorldClim 2: new 1-km spatial resolution climate surfaces for global land areas. *Int. J. Climatol.* 37, 4302–4315. doi: 10.1002/joc.5086
- Fleishman, E., Blair, R. B., and Murphy, D. D. (2001). Empirical validation of a method for umbrella species selection. *Ecol. Appl.* 11, 1489–1501. doi: 10.1890/1051-0761(2001)011[1489:evoamf]2.0.co;2
- Gerber, L. R., Del Mar, Mancha-Cisneros, M., O'Connor, M. I., and Selig, E. R. (2014). Climate change impacts on connectivity in the ocean: implications for conservation. *Ecosphere* 5, 1–18. doi: 10.1093/acprof:oso/9780199368747.003.0001
- Gheskiere, T., Vincx, M., Weslawski, J. M., Scapini, F., and Degraer, S. (2005). Meiofauna as descriptor of tourism-induced changes at sandy beaches. *Mar. Environ. Res.* 60, 245–265. doi: 10.1016/j.marenvres.2004.10.006
- Gómez, J., Barboza, F. R., and Defeo, O. (2013). Environmental drivers defining linkages among life-history traits: mechanistic insights from a semiterrestrial amphipod subjected to macroscale gradients. *Ecol. Evol.* 3, 3918–3924. doi: 10.1002/ece3.759
- González, S. A., Yáñez-Navea, K., and Muñoz, M. (2014). Effect of coastal urbanization on sandy beach coleoptera Phaleria maculata (Kulzer, 1959) in northern Chile. *Mar. Pollut. Bull.* 83, 265–274. doi: 10.1016/j.marpolbul.2014.03.042
- Guerra-Castro, E., Hidalgo, G., Castillo-Cupul, R. E., Muciño-Reyes, M., Noreña-Barroso, E., Quiroz-Deaquino, J., et al. (2020). Sandy beach macrofauna of Yucatán state (Mexico) and oil industry development in the gulf of Mexico: first approach for detecting environmental impacts. *Front. Mar. Sci.* 7:589656.
- Gül, M. R., and Griffen, B. D. (2018). Impacts of human disturbance on ghost crab burrow morphology and distribution on sandy shores. *PLoS One* 13:e0209977. doi: 10.1371/journal.pone.0209977
- Gül, M. R., and Griffen, B. D. (2019). Combined impacts of natural and anthropogenic disturbances on the bioindicator *Ocypode quadrata* (Fabricius, 1787). *J. Exp. Mar. Bio. Ecol.* 519:151185. doi: 10.1016/j.jembe.2019.151185
- Harris, L., Nel, R., Holness, S., Sink, K., and Schoeman, D. (2014). Setting conservation targets for sandy beach ecosystems. *Estuar. Coast. Shelf Sci.* 150, 45–57. doi: 10.1016/j.ecss.2013.05.016
- Hijmans, R. J., Cameron, S. E., Parra, J. L., Jones, G., and Jarvis, A. (2005). Very high resolution interpolated climate surfaces for global land areas. *Int. J. Climatol.* 1978, 1965–1978. doi: 10.1002/joc.1276
- Hijmans, R., van Etten, J., Sumner, M., Cheng, J., Baston, D., Bevan, A., et al. (2016). *Raster: Geographic Analysis and Modeling*. Available online at: <http://cran.r-project.org/web/packages/raster>.
- Hubbard, D. M., Dugan, J. E., Schooler, N. K., and Viola, S. M. (2014). Local extirpations and regional declines of endemic upper beach invertebrates in southern California. *Estuar. Coast. Shelf Sci.* 150, 67–75. doi: 10.1016/j.ecss.2013.06.017
- Jones, A. R., Schlacher, T. A., Schoeman, D. S., Weston, M. A., and Withycombe, G. M. (2017). Ecological research questions to inform policy and the management of sandy beaches. *Ocean Coast. Manag.* 148, 158–163. doi: 10.1016/j.ocecoaman.2017.07.020
- Kennedy, C. M., Oakleaf, J. R., Theobald, D. M., Baruch-Mordo, S., and Kiesecker, J. (2019). Managing the middle: a shift in conservation priorities based on the global human modification gradient. *Glob. Chang. Biol.* 25, 811–826. doi: 10.1111/gcb.14549
- Kennedy, C. M., Oakleaf, J. R., Theobald, D. M., Baruch-Mordo, S., and Kiesecker, J. (2020). *Global Human Modification of Terrestrial Systems*. Palisades, NY: NASA Socioeconomic Data and Applications Center (SEDAC).
- Luarte, T., Bonta, C. C., Silva-Rodríguez, E. A., Quijón, P. A., Miranda, C., Farias, A. A., et al. (2016). Light pollution reduces activity, food consumption and growth rates in a sandy beach invertebrate. *Environ. Pollut.* 218, 1147–1153. doi: 10.1016/j.envpol.2016.08.068
- Lucrezi, S. (2015). Ghost crab populations respond to changing morphodynamic and habitat properties on sandy beaches. *Acta Oecologica* 62, 18–31. doi: 10.1016/j.actao.2014.11.004
- Lucrezi, S., and Schlacher, T. A. (2014). The ecology of ghost crabs. *Oceanogr. Mar. Biol. An Annu. Rev.* 52, 201–256. doi: 10.1201/b17143-5
- Lucrezi, S., Schlacher, T. A., and Robinson, W. (2009). Human disturbance as a cause of bias in ecological indicators for sandy beaches: experimental evidence for the effects of human trampling on ghost crabs (*Ocypode* spp.). *Ecol. Indic.* 9, 913–921. doi: 10.1016/j.ecolind.2008.10.013
- Lucrezi, S., Schlacher, T. A., and Robinson, W. (2010). Can storms and shore armouring exert additive effects on sandy-beach habitats and biota? *Mar. Freshw. Res.* 61, 951–962. doi: 10.1071/mf09259
- Luijendijk, A., Hagenaars, G., Ranasinghe, R., Baart, F., Donchyts, G., and Aarninkhof, S. (2018). The state of the world's beaches. *Sci. Rep.* 8:6641.
- Mattos, G., Seixas, V. C., and Paiva, P. C. (2019). Comparative phylogeography and genetic connectivity of two crustacean species with contrasting life histories on South Atlantic sandy beaches. *Hydrobiologia* 826, 319–330. doi: 10.1007/s10750-018-3744-3
- Mbon Pole to Pole (2019). *Sampling Protocol for Assessment of Marine Diversity on Sandy Beaches*. Available online at: [https://marinebon.org/p2p/methods\\_field\\_protocols.html](https://marinebon.org/p2p/methods_field_protocols.html).
- McLachlan, A., and Defeo, O. (2018). *The Ecology of Sandy Shores*. Cambridge, MA: Academic Press.
- McLachlan, A., Jaramillo, E., Donn, T. E., and Wessels, F. (1993). Sandy beach macrofauna communities and their control by the physical environment: a geographical comparison. *J. Coast. Res.* 15, 27–38.
- Meerhoff, E., Defeo, O., Combes, V., Franco, B. C., Matano, R. P., Piola, A. R., et al. (2020). Assessment of larval connectivity in a sandy beach mole crab through a coupled bio-oceanographic model. *Estuar. Coast. Shelf Sci.* 246:107035. doi: 10.1016/j.ecss.2020.107035
- Micallef, A., and Williams, A. (2009). *Beach Management*. Milton Park: Routledge.
- Milosavljech, P., Bax, N. J., Simmons, S. E., Klein, E., Appeltans, W., Aburto-Oropeza, O., et al. (2018). Essential ocean variables for global sustained observations of biodiversity and ecosystem changes. *Glob. Chang. Biol.* 24, 2416–2433. doi: 10.1111/gcb.14108
- Monsarrat, S., Jarvie, S., and Svenning, J. C. (2019). Anthropocene refugia: integrating history and predictive modelling to assess the space available for biodiversity in a human-dominated world. *bioRxiv. [preprint]* doi: 10.1101/722132
- Negreiros-Fransozo, M., Fransozo, A., and Bertini, G. (2002). Reproductive cycle and recruitment period of *Ocypode quadrata* (Decapoda, Ocypodidae) at a sandy beach in southeastern Brazil. *J. Crustac.* 22, 157–161.
- O'Connor, M. I., Piehler, M. F., Leech, D. M., Anton, A., and Bruno, J. F. (2009). Warming and resource availability shift food web structure and metabolism. *PLoS Biol.* 7:e1000178. doi: 10.1371/annotation/73c277f8-421a-4843-9171-403be1a014c7
- Ocaña, F. A., De Jesús-Navarrete, A., and Hernández-Arana, H. A. (2018). Across-shore distribution of *Ocypode quadrata* burrows in relation to beach features and human disturbance. *J. Nat. Hist.* 52, 2185–2196. doi: 10.1080/00222933.2018.1524030
- Odebrecht, C., Du Preez, D. R., Abreu, P. C., and Campbell, E. E. (2014). Surf zone diatoms: a review of the drivers, patterns and role in sandy beaches food chains. *Estuar. Coast. Shelf Sci.* 150, 24–35. doi: 10.1016/j.ecss.2013.07.011
- Orlando, L., Ortega, L., and Defeo, O. (2020). Urbanization effects on sandy beach macrofauna along an estuarine gradient. *Ecol. Indic.* 111:106036. doi: 10.1016/j.ecolind.2019.106036
- Pereira, H. M., Ferrier, S., Walters, M., Geller, G. N., Jongman, R. H. G., Scholes, R. J., et al. (2013). Essential biodiversity variables. *Science* 339, 277–278. doi: 10.1126/science.1229931
- Pombo, M., and Turra, A. (2013). Issues to be considered in counting burrows as a measure of atlantic ghost crab populations, an important bioindicator of sandy beaches. *PLoS One* 8:e83792. doi: 10.1371/journal.pone.0083792
- Pombo, M., and Turra, A. (2019). The burrow resetting method, an easy and effective approach to improve indirect ghost-crab population assessments. *Ecol. Indic.* 104, 422–428. doi: 10.1016/j.ecolind.2019.05.010
- Pombo, M., Oliveira, A., Xavier, L., Siegle, E., and Turra, A. (2017). Natural drivers of distribution of ghost crabs *Ocypode quadrata* and the implications of estimates from burrows. *Mar. Ecol. Prog. Ser.* 565, 131–147. doi: 10.3354/meps11991
- Quijón, P., Jaramillo, E., and Contreras, H. (2001). Distribution and habitat structure of *Ocypode gaudichaudii* H. Milne Edwards & Lucas, 1843, in sandy beaches of northern Chile. *Crustaceana* 74, 91–103. doi: 10.1163/156854001505460
- R Core Team (2020). *R: A Language and Environment for Statistical Computing*. Available online at: <https://www.R-project.org/>



- Raiter, K. G., Possingham, H. P., Prober, S. M., and Hobbs, R. J. (2014). Under the radar: mitigating enigmatic ecological impacts. *Trends Ecol. Evol.* 29, 635–644. doi: 10.1016/j.tree.2014.09.003
- Rohatgi, A. (2013). *WebPlotDigitizer*. Available online at: <https://automeris.io/WebPlotDigitizer/>.
- Sakai, K., and Türkay, M. (2013). Revision of the genus *Ocypode* with the description of a new genus, *Hoplocypode* (Crustacea: Decapoda: Brachyura). *Mem. Queensl. Museum* 56, 665–793.
- Schlacher, T. A., and Thompson, L. (2012). Beach recreation impacts benthic invertebrates on ocean-exposed sandy shores. *Biol. Conserv.* 147, 123–132. doi: 10.1016/j.biocon.2011.12.022
- Schlacher, T. A., De Jager, R., and Nielsen, T. (2011). Vegetation and ghost crabs in coastal dunes as indicators of putative stressors from tourism. *Ecol. Indic.* 11, 284–294. doi: 10.1016/j.ecolind.2010.05.006
- Schlacher, T. A., Lucenzi, S., Connolly, R. M., Peterson, C. H., Gilby, B. L., Maslo, B., et al. (2016). Human threats to sandy beaches: a meta-analysis of ghost crabs illustrates global anthropogenic impacts. *Estuar. Coast. Shelf Sci.* 169, 56–73. doi: 10.1016/j.ecss.2015.11.025
- Schlacher, T. A., Schoeman, D. S., Dugan, J., Lastra, M., Jones, A., Scapini, F., et al. (2008). Sandy beach ecosystems: key features, sampling issues, management challenges and climate change impacts. *Mar. Ecol.* 29, 70–90. doi: 10.1111/j.1439-0485.2007.00204.x
- Schlacher, T. A., Schoeman, D. S., Jones, A. R., Dugan, J. E., Hubbard, D. M., Defeo, O., et al. (2014). Metrics to assess ecological condition, change, and impacts in sandy beach ecosystems. *J. Environ. Manag.* 144, 322–335. doi: 10.1016/j.jenvman.2014.05.036
- Schlacher, T. A., Thompson, L., and Price, S. (2007). Vehicles versus conservation of invertebrates on sandy beaches: mortalities inflicted by off-road vehicles on ghost crabs. *Mar. Ecol.* 28, 354–367. doi: 10.1111/j.1439-0485.2007.00156.x
- Schoeman, D. S., Schlacher, T. A., Jones, A. R., Murray, A., Huijbers, C. M., Olds, A. D., et al. (2015). Edging along a warming coast: a range extension for a common sandy beach crab. *PLoS One* 10:e0141976. doi: 10.1371/journal.pone.0141976
- Siddig, A. A. H., Ellison, A. M., Ochs, A., Villar-Leeman, C., and Lau, M. K. (2016). How do ecologists select and use indicator species to monitor ecological change? insights from 14 years of publication in ecological indicators. *Ecol. Indic.* 60, 223–230. doi: 10.1016/j.ecolind.2015.06.036
- Silva, E., Marco, A., da Graça, J., Pérez, H., Abella, E., Patino-Martinez, J., et al. (2017). Light pollution affects nesting behavior of loggerhead turtles and predation risk of nests and hatchlings. *J. Photochem. Photobiol. B Biol.* 173, 240–2496. doi: 10.1016/j.jphotobiol.2017.06.006
- Simberloff, D. (1998). Flagships, umbrellas, and keystones: is single-species management passé in the landscape era? *Biol. Conserv.* 83, 247–257. doi: 10.1016/S0006-3207(97)00081-5
- Tewfik, A., Bell, S. S., McCann, K. S., and Morrow, K. (2016). Predator diet and trophic position modified with altered habitat morphology. *PLoS One* 11:e0147759. doi: 10.1371/journal.pone.0147759
- Tyberghein, L., Verbruggen, H., Pauly, K., Troupin, C., Mineur, F., and De Clerck, O. (2012). Bio-ORACLE: a global environmental dataset for marine species distribution modelling. *Glob. Ecol. Biogeogr.* 21, 272–281. doi: 10.1111/j.1466-8238.2011.00656.x
- Venter, O., Sanderson, E., Magrath, A., et al. (2016). Global terrestrial human footprint maps for (1993) and 2009. *Sci Data* 3:160067. doi: 10.1038/sdata.2016.67
- Vestbo, S., Obst, M., Fernandez, F. J. Q., Intanai, I., and Funch, P. (2018). Present and potential future distributions of asian horseshoe crabs determine areas for conservation. *Front. Mar. Sci.* 5:164. doi: 10.3389/fmars.2018.00164
- Weinstein, R. B., and Full, R. J. (1994). Thermal dependence of locomotor energetics and endurance capacity in the ghost crab, *Ocypode quadrata*. *Physiol. Zool.* 67, 855–872. doi: 10.1086/physzool.67.4.30163868
- Weinstein, R. B., and Full, R. J. (1998). Performance limits of low-temperature, continuous locomotion are exceeded when locomotion is intermittent in the ghost crab. *Physiol. Zool.* 71, 274–284. doi: 10.1086/515927
- Xavier, L. Y., Gonçalves, L. R., Checon, H. H., Corte, G., and Turra, A. (2020). Are we missing the bigger picture? an analysis of how science can contribute to an ecosystem-based approach for beach management on the São Paulo macrometropolis. *Ambient. Soc.* 23:e01411. doi: 10.1590/1809-4422asoc20190141r1vu2020l2de
- Yeager, L. A., Philippe, M., Gill, D., Baum, J. K., and McPherson, J. M. (2017). MSEC: queryable global layers of environmental and anthropogenic variables for marine ecosystem studies. *Ecology* 98:1976. doi: 10.1002/ecy.1884
- Zuur, A. F., Ieno, Walker, N., Saveliev, A. A., and Smith, G. M. (2009). *Mixed Effects Models and Extensions in Ecology with R*. Berlin: Springer. doi: 10.1007/978-0-387-87458-6

**Conflict of Interest:** The authors declare that the research was conducted in the absence of any commercial or financial relationships that could be construed as a potential conflict of interest.

Copyright © 2021 Barboza, Mattos, Soares-Gomes, Zalmon and Costa. This is an open-access article distributed under the terms of the Creative Commons Attribution License (CC BY). The use, distribution or reproduction in other forums is permitted, provided the original author(s) and the copyright owner(s) are credited and that the original publication in this journal is cited, in accordance with accepted academic practice. No use, distribution or reproduction is permitted which does not comply with these terms.



# Metabarcoding Analysis of Ichthyoplankton in the East/Japan Sea Using the Novel Fish-Specific Universal Primer Set

Ah Ran Kim<sup>1</sup>, Tae-Ho Yoon<sup>1,2</sup>, Chung Il Lee<sup>3</sup>, Chang-Keun Kang<sup>4</sup> and Hyun-Woo Kim<sup>1,5\*</sup>

<sup>1</sup> Interdisciplinary Program of Biomedical, Mechanical and Electrical Engineering, Pukyong National University, Busan, South Korea, <sup>2</sup> Aquatic Living Resources Division, FIRA (Korea Fisheries Resources Agency), Busan, South Korea, <sup>3</sup> Department of Marine Bioscience, Gangneung-Wonju National University, Gangneung, South Korea, <sup>4</sup> School of Earth Sciences and Environmental Engineering, Gwangju Institute of Science and Technology, Gwangju, South Korea, <sup>5</sup> Department of Marine Biology, Pukyong National University, Busan, South Korea

## OPEN ACCESS

### Edited by:

Dominique Pelletier,  
Institut Français de Recherche pour  
l'Exploitation de la Mer (IFREMER),  
France

### Reviewed by:

Simo Njabulo Maduna,  
Norwegian Institute of Bioeconomy  
Research (NIBIO), Norway  
Ka Yan Ma,  
Sun Yat-sen University, China

### \*Correspondence:

Hyun-Woo Kim  
kimhw@pknu.ac.kr

### Specialty section:

This article was submitted to  
Marine Molecular Biology  
and Ecology,  
a section of the journal  
Frontiers in Marine Science

**Received:** 06 October 2020

**Accepted:** 03 February 2021

**Published:** 17 March 2021

### Citation:

Kim AR, Yoon T-H, Lee CI,  
Kang C-K and Kim H-W (2021)  
Metabarcoding Analysis  
of Ichthyoplankton in the East/Japan  
Sea Using the Novel Fish-Specific  
Universal Primer Set.  
Front. Mar. Sci. 8:614394.  
doi: 10.3389/fmars.2021.614394

The spatiotemporal distribution of fish larvae and eggs is fundamental for their reproduction and recruitment in aquatic ecosystems. Here, a metabarcoding strategy was employed as an alternative to a conventional ichthyoplankton survey, which requires a considerable amount of time, labor, and cost. First, a piscine-specific universal primer set (FishU) was designed to amplify the region, flanking the highly conserved mitochondrial 12S and 16S ribosomal genes, and it was optimized for the MiSeq platform. Based on both *in silico* and *in vitro* analyses, the newly designed FishU primers outperformed the two previously reported fish-specific universal primer sets (ecoPrimer and MiFish) in taxon coverage, specificity, and accuracy in species identification. The metabarcoding results by FishU primers successfully presented the diversity of ichthyoplankton directly from the zooplankton net samples in the East/Japan Sea, presenting more accurate and plentiful species numbers than those by MiFish primers. Thus, the metabarcoding analysis of ichthyoplankton using the newly designed FishU primers is a promising tool for obtaining useful data to understand the reproduction of fish, such as spawning sites, reproductive periods, population structures, feeding ecology, and diet.

**Keywords:** metabarcoding, ichthyoplankton, Korea, next-generation sequencing, environmental DNA

## INTRODUCTION

DNA metabarcoding is a recently established technique that makes it possible to conduct taxonomic identification of entire assemblages in environmental samples via high-throughput sequencing (Yu et al., 2012). Because of its reliable results with relatively low cost and labor, this technique has become one of the most widely used methods in ecological studies, including biodiversity assessment (Valentini et al., 2016; Bylemans et al., 2018), the detection of invasive species (Borrell et al., 2017; Klymus et al., 2017), and feeding ecology (Iwanowicz et al., 2016; Yoon et al., 2017; Hawlitschek et al., 2018). The environmental DNA (eDNA) derived from organisms in water samples can also be directly analyzed by eDNA metabarcoding, another promising method that has little impact on the ecosystem during sample collection (Thomsen et al., 2012;

Sigsgaard et al., 2017; Yamamoto et al., 2017; Bylemans et al., 2019; McDevitt et al., 2019). As a result, metabarcoding is now being considered by many researchers as a reliable alternative to replace time-consuming and laborious traditional survey methods (Berry et al., 2015; Aylagas et al., 2016; Shaw et al., 2016; Watts et al., 2019).

Most metabarcoding analyses are currently based on the assemblage of PCR products amplified by a universal primer for specific taxa. Several fish-specific universal primers have been developed targeting 12S rRNA regions, such as EcoPrimers (Riaz et al., 2011) and MiFish (Miya et al., 2015), 16S rRNA region primers (Evans et al., 2016; Shaw et al., 2016), cytochrome b (Minamoto et al., 2012; Thomsen et al., 2012) and cytochrome c oxidase I (Balasingham et al., 2018; Collins et al., 2019). Among them, the primers targeting the 12S rRNA and 16S rRNA regions generally showed higher performance in the broader taxonomic range and species-level assignment than the primers targeting the cytochrome b region (Zhang et al., 2020). The MiFish primer set demonstrated reliability for fish biodiversity analysis of eDNA samples for both seawater (Ushio et al., 2017; Yamamoto et al., 2017) and freshwater (Sato et al., 2018). The bioinformatics tool, web-based MiFish pipeline<sup>1</sup> also provides a standardized and convenient bioinformatic platform, which has helped researchers obtain reliable metabarcoding data without considering the complicated bioinformatics processes from the raw reads generated by the sequencer (Sato et al., 2018). Therefore, the MiFish platform is now being widely used for the study of fish biodiversity using eDNA metabarcoding analysis (Andruszkiewicz et al., 2017; Yamamoto et al., 2017; Bylemans et al., 2019). In particular, owing to its small amplicon size (~170 bp), the MiFish platform is currently considered one of most reliable tools for the eDNA metabarcoding analysis of fish taxa. However, the small amplicon size of MiFish is a double-faceted property. Although it may increase the chance of detection rate, its small amplicon size may not have enough sequence to discriminate a species from the closely related ones (Bylemans et al., 2018; Zhang et al., 2020). In fact, MiFish sequences could not discriminate species in several genera, including *Sebastes* and *Takifugu* (Yamamoto et al., 2017). In addition, the short MiFish sequence may require sufficient reference sequences in the database for the local fish assemblage, which would be another barrier to adopting the MiFish platform directly for local analysis. Even a single nucleotide difference in the region may result in the assignment of a wrong species in the MiFish platform (Yamamoto et al., 2017). Therefore, it was necessary to design a primer set covering larger barcode sequences for higher discrimination power.

Ichthyoplankton refers to the eggs and larvae of fish, which is usually found at depths of less than 200 m, in what is known as the epipelagic zone. Their surveys have been conducted for a long time in the East/Japan Sea to obtain information about fish resources, ranging from the spawning areas and seasons to the estimated numbers of spawning stocks and changes in the distribution of certain species (Keller et al., 1999; Shoji et al., 2011). Due to the simple coastlines, fisheries in the East/Japan

Sea have been strongly affected by the collision of two main currents along with the Korean peninsula: the North Korea cold current (NKCC) from the North and East Korea warm current (EKWC), a branch of the Tsushima current (Kim et al., 2007b). In addition, the transport processes of eggs and larvae are largely dependent on the variability in these two currents, affecting the recruitment and productivity of each fish stock (Yatsu et al., 2005). Therefore, ichthyoplankton surveys have been one of the main methods to understand fisheries in the East/Japan Sea. However, traditional ichthyoplankton surveys depend mainly on microscopic morphological observations, which require a considerable amount of time and effort to sort and count the eggs and larval fish from the zooplankton net samples. In addition, morphological identification of several fish larvae and eggs remains a challenge even for experienced specialists. These drawbacks have been a major bottleneck in conducting large-scale ichthyoplankton surveys.

Therefore, there is a need for the use of metabarcoding analysis for ichthyoplankton surveys. However, the use of short barcodes, such as MiFish, often results in the misidentification of exotic species due to ichthyoplankton being transported from distant locations by currents. To avoid potential issues with identification, an accurate species analysis using longer barcodes was needed. In this study, we designed novel fish-specific universal primers (FishU) to analyze ichthyoplankton from the zooplankton net samples. FishU yields longer amplicons that have a higher taxon specificity than MiFish. Their reliability was compared with previously designed fish-specific universal primers, including ecoPrimer and MiFish. We also compared the metabarcoding data generated by two primers, MiFish and FishU, using zooplankton samples obtained from the East/Japan Sea. These data show the FishU primer set provides a higher accuracy in species assignment and recovers more species than the MiFish primer set. Thus, the newly developed FishU primers represent a useful tool for ichthyoplankton surveys in countries with relatively limited reference sequence information, facilitating a molecular strategy in fishery surveys.

## MATERIALS AND METHODS

### Design of Universal Primer Set for Fish Taxa

A pair of universal fish primer sets (FishU) was designed to meet three goals: (i) wide taxon coverage to present most of the fish species, (ii) a high degree of taxon specificity to amplify fish DNA from mixed zooplankton samples, and (iii) an optimized amplicon size for the Illumina MiSeq platform (300–500 bp). FishU primers were designed to amplify the region between the end of 12S and 16S based on the multiple alignment of 1,808 fish mitogenome sequences obtained from the MITOFISH database (Iwasaki et al., 2013) (**Supplementary data 1**). The expected amplicon size by FishU was approximately 373 bp (**Figure 1**).

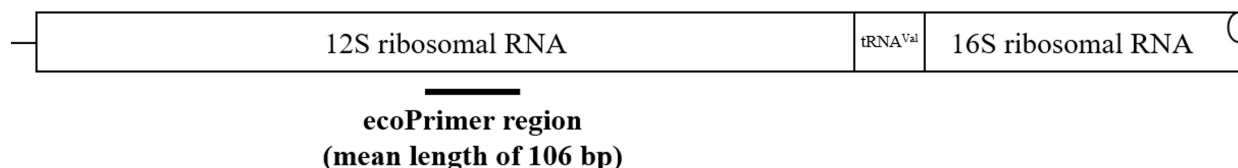
The FishU primers were validated by *in silico* analysis using 1,808 fish mitogenome sequences in the database. The OBITools software (Boyer et al., 2016) was used to calculate the amplified

<sup>1</sup><http://mitofish.aori.u-tokyo.ac.jp/MiFish/>

A

**MiFish region**  
(mean length of 172 bp)

**FishU region**  
(mean length of 373 bp)



B

Sequence of FishU-F	5'-	A	C	A	Y	A	C	C	G	C	C	C	G	T	C	A	C	Y	C	T	C	-3'
A		1,807	0	1,808	3	1,808	0	0	0	0	0	0	0	0	0	1,796	4	0	1	0	0	
		99.9	0	100	0.2	100	0	0	0	0	0	0	0	0	0	99.3	0.2	0	0.1	0	0	
C		1	1,808	0	1,702	0	1,779	1,806	0	1,805	1,808	1,802	0	0	1,808	1	1,789	167	1,800	15	1,806	
		0.1	100	0	94.1	0	98.4	99.9	0	99.8	100	99.7	0	0	100	0.1	98.9	9.2	99.6	0.8	99.9	
G		0	0	0	2	0	0	0	1,807	2	0	3	1,808	0	0	11	0	0	0	0	0	
		0	0	0	0.1	0	0	0	99.9	0.1	0	0.2	100	0	0	0.6	0	0	0	0	0	
T		0	0	0	101	0	27	0	1	1	0	1	0	1,808	0	0	15	1,641	7	1,793	2	
		0	0	0	5.6	0	1.5	0	0.1	0.1	0	0.1	0	100	0	0	0.8	90.8	0.4	99.2	0.1	
-		0	0	0	0	0	2	2	0	0	0	2	0	0	0	0	0	0	0	0	0	
		0	0	0	0	0	0.1	0.1	0	0	0	0.1	0	0	0	0	0	0	0	0	0	

C

Consensus sequences	5'-	C	Y	Y	G	T	A	C	C	T	T	T	T	G	C	A	T	C	A	T	G	-3'
Sequence of FishU-R	3'-	G	R	R	C	A	T	G	G	A	A	A	A	C	G	T	A	G	T	A	C	-5'
A		0	0	0	1	0	1,802	2	0	0	0	0	0	0	0	1,807	1	4	1,807	1	1	
		0	0	0	0.1	0	99.7	0.1	0	0	0	0	0	0	0	99.9	0.1	0.2	99.9	0.1	0.1	
C		1,805	56	1,343	0	0	0	1,806	1,808	2	6	0	41	0	1,806	1	1	1,798	1	1	0	
		99.8	3.1	74.3	0	0	0	99.9	100	0.1	0.3	0	2.3	0	99.9	0.1	0.1	99.4	0.1	0.1	0	
G		0	0	0	1,806	1	1	0	0	0	0	0	1	1,807	1	0	0	0	0	3	1,805	
		0	0	0	99.9	0.1	0.1	0	0	0	0	0	0.1	99.9	0.1	0	0	0	0	0.2	99.8	
T		3	1,752	465	0	1,807	3	0	0	1,805	1,801	1,808	1,765	1	1	0	1,806	6	0	1,803	2	
		0.2	96.9	25.7	0	99.9	0.2	0	0	99.8	99.6	100	97.6	0.1	0.1	0	99.9	0.3	0	99.7	0.1	
-		0	0	0	1	0	2	0	0	1	1	0	1	0	0	0	0	0	0	0	0	
		0	0	0	0.1	0	0.1	0	0	0.1	0.1	0	0.1	0	0	0	0	0	0	0	0	

**FIGURE 1 |** Primer region schematic representation. **(A)** The position of the primer used in this study is represented in the structure of general mtDNA, including 12S and 16S rRNA genes. MiFish has a mean length of 172 bp; FishU has a mean length of 373 bp. **(B)** Consensus nucleotide sequences of the forward primer. **(C)** Consensus nucleotide sequences of the reverse primer.

species numbers according to the mismatched nucleotide numbers of the three universal primers (ecoPrimer, MiFish, and FishU). Taxonomic resolutions amplified by three primers were calculated by *in silico* PCR using the *ecotaxspecifity* script of OBITools (Boyer et al., 2016).

## Examination of the Reliability of the FishU Primer Set

The taxon specificity of the FishU primer set was examined by PCR analysis (Figure 2). The amplification by FishU was tested with 51 individual fish samples collected from Korean waters, which covered 50 genera, 37 families, and 14 orders.

Specificity for fish species was tested by PCR with the most abundant invertebrate taxa in the zooplankton net samples, including *Metridia pacifica* (copepod), *Euphausia pacifica* (krill), *Sagitta elegans* (arrow worm), and *Penaeus monodon* (shrimp). Genomic DNA was extracted using the AccuPrep® Genomic DNA Extraction Kit (Bioneer, Republic of Korea) following the manufacturer's instructions. PCR amplification was performed with extracted DNA as templates and three different primer sets (ecoPrimer, MiFish, and FishU). PCR amplification with the FishU primer set was conducted using the following cycling conditions: initial denaturation at 94°C for 3 min, followed by 35 cycles of 94°C for 30 s, 48°C for 30 s, and 72°C for 30 s with a final extension at 72°C for 3 min.



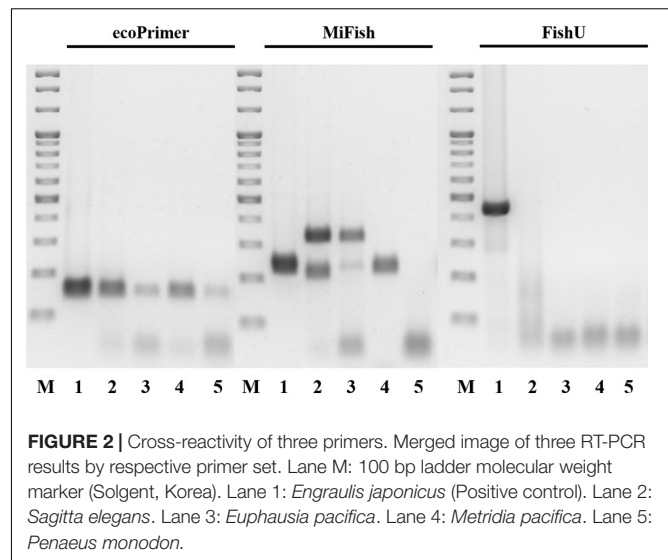
PCR conditions with MiFish and ecoPrimer sets were the same as above except for the annealing step at 50°C for 10 s. The PCR reaction mixture (20 µL) contained 100 ng template, 1 µL of each primer (10 pmol), 2 µL of dNTPs (10 mM), 0.2 µL exTaq HS (Takara, Japan), and 2 µL of 10 × buffer and distilled water to a final volume of 20 µL. The amplification products were separated by 1.5% agarose gel electrophoresis and stained with loading star dye (Dynebio, Republic of Korea).

The taxon coverage and specificity of the three primers was also compared through metabarcoding analysis. The library for MiSeq sequencing was constructed using the Nextera XT index kit (Illumina, United States). Genomic DNA (200 ng) in two random zooplankton samples was amplified using three primer sets with the adapter. The first PCR conditions of FishU involved initial denaturation at 94°C for 3 min, followed by 30 cycles of 94°C for 30 s, 48°C for 30 s, and 72°C for 30 s with a final extension at 72°C for 3 min. The first PCR amplification was performed with a 20 µL reaction volume containing 200 ng of template, 1 µL of each FishU with adapter primer (20 pmol), 0.5 µL of dNTPs (10 mM), 0.2 µL of ex hot start Taq (TaKaRa, Japan), and 2 µL of 10 × exTaq buffer. The PCR reaction mixture and conditions with the MiFish and ecoPrimer set were identical to the FishU mixture except for the primer with adapter (each 5 pmol). The first amplicons were visualized by 1.5% agarose gel electrophoresis, and the fragment of expected size was collected. The collected fragments of each primer set were purified using the AccuPrep® Gel Purification Kit (Bioneer, Republic of Korea) and eluted with 20 µL of elution buffer. The purified products were used to construct a library using the Nextera XT index kit (Illumina, United States) according to the manufacturer's instructions. Nextera libraries were purified using the AccuPrep® Gel Purification Kit (Bioneer, Republic of Korea). After the quality and quantity of the library were measured using the 2100 Bioanalyzer (Agilent Technologies, United States) and qubit dsDNA HS Assay Kit (Invitrogen, United States), sequencing was performed using the Illumina MiSeq (2 × 300 bp pair ends).

## Metabarcoding Analysis of Ichthyoplankton From Zooplankton Net Sample

Zooplankton net samples were collected from 12 sample stations from the coastal waters along the Korean Peninsula as part of a project funded by the Ministry of Oceans and Fisheries, Korea (Figure 3, Supplementary Table 1). Plankton samples were collected by oblique tows using a bongo net (60 cm in diameter, 330 µm in mesh size) monthly from January to June 2016. The collected zooplankton samples were immediately stored in five volumes of 99.5% ethanol (Daejung Chemicals & Metals Co., Ltd., Republic of Korea), transferred to the laboratory, and stored at −20°C until further analysis.

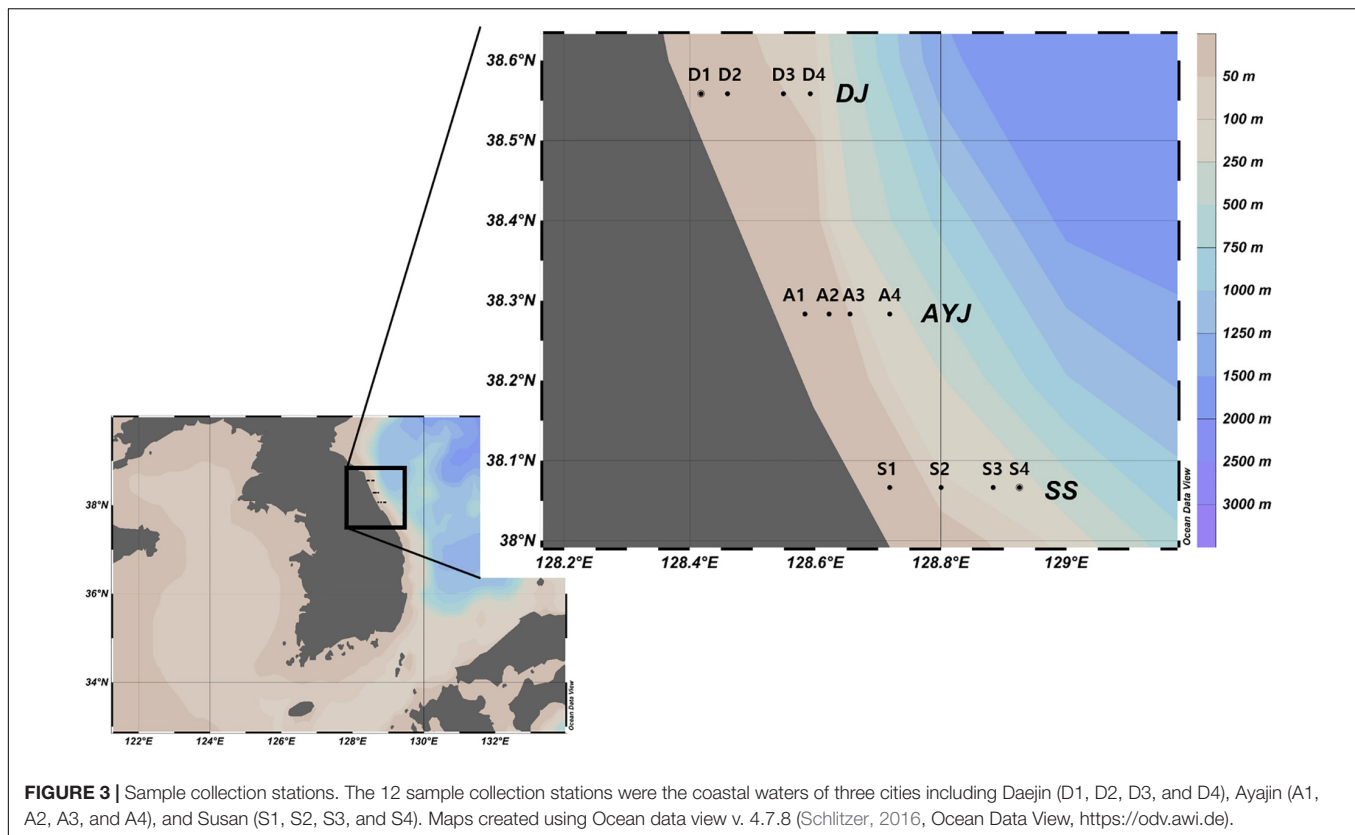
After rinsing with distilled water using a sieve (pore size, 200 µm), each zooplankton net sample was divided into two halves. The wet weight of half of the sample was measured, and six volumes of lysis buffer (Biosesang, Republic of Korea) were



added for genomic DNA extraction. Genomic DNA was extracted with 700 µL of homogenized sample using an AccuPrep® genomic DNA extraction kit (Bioneer, Republic of Korea) following the manufacturer's instructions. The isolated DNA was quantified using a NanoDrop™ 1,000 Spectrophotometer (Thermo Fisher Scientific, United States) and qualified by agarose gel electrophoresis. The other half of the sample was used for the measurement of dry weight, according to a previous study (Jacobs and Grant, 1978). The comparisons of biodiversity between FishU and MiFish for ichthyoplankton were determined by NGS analysis. The library was constructed as mentioned above, but the first PCR products were pooled monthly and purified. Nextera libraries were sequenced from Illumina using 2 × 300 bp sequencing on MiSeq.

## NGS Data Analysis

Using the CLC Genomic Workbench v.8.0 (CLC Bio, United States), the short reads (<100 bp) and low-quality sequences (QV <20) were trimmed from the raw data. Paired-end reads of FishU sequences were assembled using Mothur software (Schloss et al., 2009). From the assembled reads, the reads that overlapped by >6 bp, no mismatches, and sizes between 350 and 500 bp were filtered. The reads that could not be matched with options were discarded. The sequences of the forward and reverse primer regions were trimmed with one nucleotide mismatch option. Using the UCHIME software package (Edgar et al., 2011), operational taxonomic units (OTUs) were assigned at 99.7% identity from the obtained paired-end contigs, and chimeric sequences were removed based on *de novo* chimera detection. After OTUs with fewer than 10 contigs were removed, the species name was assigned using the BLASTn algorithm of BLAST + 2.2.38 (Camacho et al., 2009) against the NCBI non-redundant nucleotide database (accession date: 09/04/2019). The top-scored species name was assigned for each OTU with >97% sequence identity to the database. OTUs between 95 and 97% identity to the database were described as “genus name with highest score” followed by “sp.” OTUs



with an identity of less than 95% were classified as “unknown.” MiFish raw reads were processed using the MiFish pipeline with default settings (Sato et al., 2018). The OTUs obtained from MiFish were assigned to the highest blast score species at the species level with at least 97% sequence identity, and those between 95 and less than 97% sequences were assigned to the same genus. The representative haplotypes of two primers were designated in OTUs with abundances of more than 10% in each species, and these OTUs were subjected to phylogenetic analysis by maximum-likelihood algorithm using MEGA-X (Kumar et al., 2018). To compare the species resolution between the two primers, we calculated the genetic distance using MEGA-X based on the pairwise distances ( $p$ -distance).

## RESULTS

### Design of Fish-Specific Universal Primer, FishU

After comparing the mitochondrial rRNA sequences from 1808 fish species in the database, a universal primer set, FishU, was designed to amplify the variable region between the highly conserved mitochondrial 12S and 16S ribosomal sequences (Figure 1). The predicted size of PCR products amplified by the FishU primer ranged from 300 to 400 bp with an average of 373 bp, which was optimized to the MiSeq platform. Unusually large amplicons were identified in only 14 species, including

*Hoplostilatus cuniculus* (818 bp), *Centropyge multicolor* (558 bp), and *Centropyge jocularis* (558 bp).

The amplification efficiency of the newly developed FishU primers was compared with two previously designed fish-specific universal primers, ecoPrimer and MiFish. The recovered species numbers by the different mismatched bases within the primer sequences were compared (Table 1 and Supplementary Tables 2–4). When PCR was conducted without any mismatch, the highest number of species was amplified by the FishU primer set, in which 1,529 species out of a total of 1,683 examined bony fish species (Actinopteri) were able to be recovered (90.85%). Although the ecoPrimer set also amplified 82.06% of them, only 7.13% of the examined species were amplified using MiFish, and only 7.13% of the examined species were amplified using MiFish primers (Table 1). When one mismatch was allowed, the percentage recovered by the MiFish primer increased up to 81.28% while 94 and 98.10% of the examined species could be amplified by ecoPrimer and FishU primer, respectively. As the mismatch numbers increased to three, the amplification success rates became similar among all three compared primers (94.18% by ecoPrimer, 97.39% by MiFish, and 98.46% by FishU). In contrast to the other two universal primers, the FishU primer also showed a high recovery percentage in the Chondrichthyes, up to 98.99% (Table 1). However, only 0–13.13% of the Chondrichthyes species could be amplified by ecoPrimer and MiFish primer sets with up to one mismatch.

**TABLE 1** | The numbers and percentage (in parentheses) of the amplified species by *in silico* PCR with three fish-specific universal primers.

Primer	Sequences (5'–3')	Average amplicon size	Class	Species number	Number of mismatches			
					0	1	2	3
ecoPrimer (Riaz et al., 2011)	F–ACTGGGATTAGATACCCC	106 bp	Actinopteri	1683	1,381 (82.06)	1,582 (94)	1,584 (94.12)	1,585 (94.18)
	R–TAGAACAGGCTCCTCTAG		Chondrichthyes	99	13 (13.13)	13 (13.13)	13 (13.13)	13 (13.13)
MiFish (Miya et al., 2015)	F–GTCGGTAAACTCGTGCCAGC	172 bp	Actinopteri	1683	120 (7.13)	1,368 (81.28)	1,584 (94.12)	1,639 (97.39)
	R–CATAGTGGGGTATCTAATCCCAGT TTG		Chondrichthyes	99	0 (0)	0 (0)	26 (26.26)	95 (95.96)
FishU (present study)	F–ACAYACCGCCCGTCACYCTC	373 bp	Actinopteri	1683	1,529 (90.85)	1,651 (98.10)	1,656 (98.40)	1,657 (98.46)
	R–CATGATGCAAAGGTACRRG		Chondrichthyes	99	91 (91.92)	98 (98.99)	98 (98.99)	98 (98.99)

**TABLE 2** | Percentage of accurately assigned taxa in three fish barcodes by the different mismatches.

Primer (mean length)	Taxonomic level	Number of nucleotide differences				
		1 bp	2 bp	3 bp	4 bp	5 bp
ecoPrimer (106 bp)	Order	97.18%	92.96%	88.73%	81.69%	77.46%
	Family	94.27%	90.76%	83.12%	71.97%	64.97%
	Genus	72.74%	64.10%	56.92%	48.18%	42.66%
	Species	57.63%	47.52%	38.54%	32.02%	27.12%
MiFish (171 bp)	Order	100%	95.06%	93.83%	93.83%	93.83%
	Family	99.42%	97.12%	96.54%	96.54%	95.97%
	Genus	90.92%	88.53%	86.42%	84.13%	79.73%
	Species	81.15%	75.53%	70.91%	65.70%	60.50%
FishU (373 bp)	Order	96.34%	93.90%	93.90%	93.90%	93.90%
	Family	98.32%	97.76%	97.76%	97.20%	97.20%
	Genus	95.67%	94.07%	93.03%	90.96%	89.17%
	Species	89.85%	86.66%	84.38%	81.07%	78.56%

The taxonomic resolutions of the region amplified by the three universal primers were compared (Table 2). The sequence variations and the length of the barcode region by each universal primer set are key to the high degree of taxonomic resolution. The percentage of correctly assigned species numbers by different universal primers was calculated. Barcodes using ecoPrimer showed the highest misidentification percentage by one nucleotide mismatch with 42.37% misassigned rates (Table 2). By contrast, only 10.15% were misidentified by one nucleotide mismatch in the FishU primer. Even in five nucleotide mismatches, 78.56% of the barcodes by FishU were correctly assigned, and only 27.12% of those by ecoPrimer were adequately assigned. Compared with those by ecoPrimer, barcodes by MiFish showed a much higher accuracy in the taxon assignment ranging from 81.15 to 60.50% according to the number of mismatches. However, its rates were lower than those by FishU (Table 2).

The taxon specificity of the three fish universal primers, namely ecoPrimer, MiFish, and FishU, were compared

with four individual zooplankton, which were among the most abundant taxa in the zooplankton net samples (Figure 2). FishU amplified only *Engraulis japonicus* (415 bp), and ecoPrimer and MiFish showed a high degree of cross-reactivity in the examined invertebrate species, including *Sagitta elegans*, *Euphausia pacifica*, *Metridia pacifica*, and *Penaeus monodon* (Figure 2). The metabarcoding analysis of the zooplankton net samples was performed with three fish-specific universal primer sets to analyze the ichthyoplankton assemblage (Table 3). Only ecoPrimer showed cross-reactivity with low proportions of Arthropoda (1.2 and 5.2%), Mammalian (0.002% in S2), and Enteropneusta (0.1 and 0.03%). In contrast, both MiFish and FishU presented only fish taxa. These results indicate that FishU primers are useful for examining the assemblage of ichthyoplankton directly from zooplankton net samples with a long barcode size, a low cross-reactivity, and a high specificity for fish taxa.

**TABLE 3 |** Relative abundances of the different phyla detected from three primers.

		% Read counts (S: Sample)					
Phylum	Class	ecoPrimer (S1)	ecoPrimer (S2)	MiFish (S1)	MiFish (S2)	FishU (S1)	FishU (S2)
Arthropoda	Insecta	0.005	0.011	0	0	0	0
	Malacostraca	1.225	5.151	0	0	0	0
Chordata	Actinopterygii	98.061	94.683	72.031	99.885	86.021	84.825
	Mammalia	0	0.008	0	0	0	0
Hemichordata	Enteropneusta	0.128	0.034	0	0	0	0
Unknown		0.581	0.113	27.969	0.115	13.979	15.175
		100	100	100	100	100	100

**TABLE 4 |** Summary of read numbers generated from three primers during the bioinformatics process.

	Raw reads		Processed reads (%)		Fish reads (%) *		Fish OTUs *	
	MiFish	FishU	MiFish	FishU	MiFish	FishU	MiFish	FishU
Jan	252,843	649,175	174,876 (72)	115,403 (21)	174,876 (69)	114,895 (18)	432	20
Feb	364,476	1,122,967	243,537 (72)	231,404 (23)	243,537 (67)	63,019 (06)	1,149	25
Mar	296,678	627,978	199,069 (72)	143,120 (25)	199,069 (67)	116,834 (19)	1,038	41
Apr	342,439	792,879	232,165 (72)	225,633 (30)	232,165 (68)	105,074 (13)	1,290	20
May	317,982	510,666	214,275 (70)	252,194 (55)	214,275 (67)	246,288 (48)	922	69
Jun	242,167	680,254	157,384 (69)	357,704 (58)	157,384 (65)	356,277 (52)	955	34
Average	302,764	730,653	203,551 (67)	220,909 (35)	203,551 (67)	167,064 (26)	964	35

\*Fish reads and OTUs referred to the number of reads identified as fish taxa as a result of a BLAST search.

## Comparative Analysis of Ichthyoplankton Survey in East/Japan Sea by Two Universal Primers: MiFish and FishU

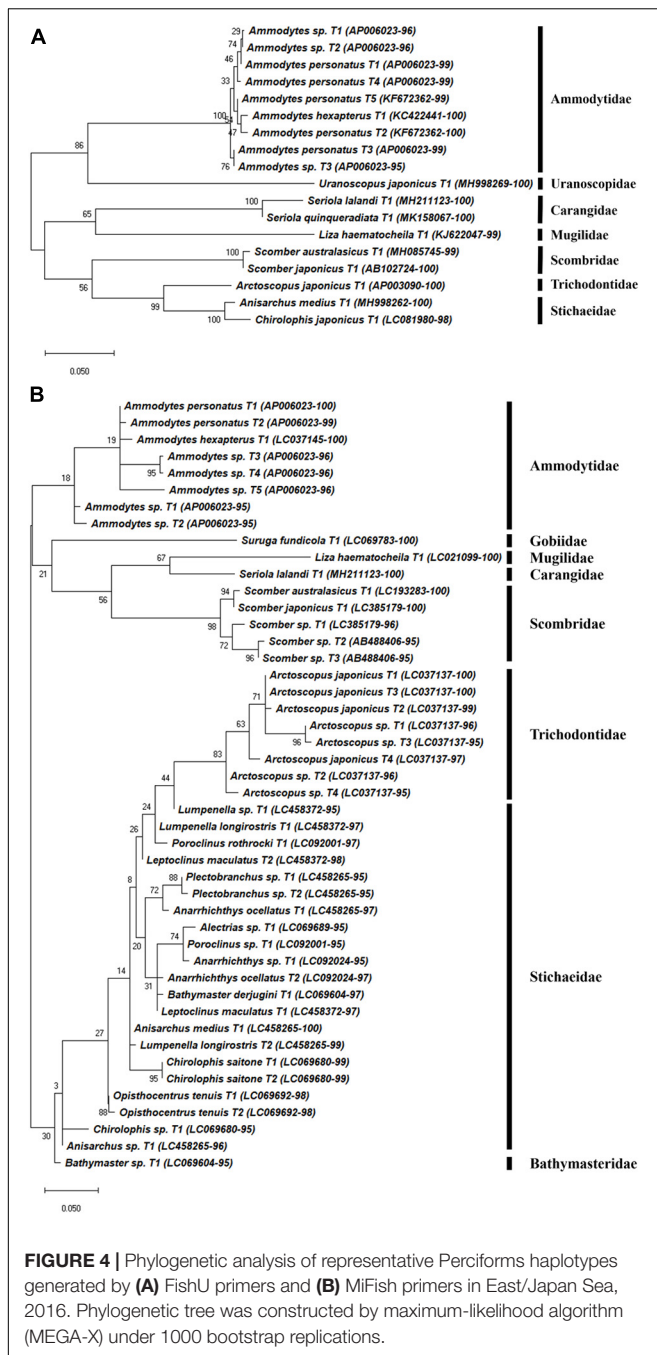
Metabarcoding analyses of ichthyoplankton from the zooplankton net samples were conducted using two fish-specific universal primer sets (MiFish and FishU). A total of 1,816,585 and 4,383,919 raw reads from 6 month samples were generated using the MiFish and FishU primer set, respectively (Table 4). On average, 203,551 merged reads were obtained using the MiFish primer after eliminating the low-quality reads, accounting for approximately 67% of the raw reads. All processed merged reads were identified as fish taxa (Table 4). Compared with those by MiFish, only 35% (220,909) of raw reads by the FishU primer were successfully merged, representing a 2.01-fold decrease compared with those by MiFish. An average of 75% of merged reads were identified as fish barcodes in those by FishU primer (Table 4).

A total of 180 representative haplotypes were obtained from the MiFish primer set, including 42 species in 22 families in 6 orders. Forty-seven haplotypes from 33 species in 21 families in 9 orders were obtained by the FishU primer set, which was fewer than those from the MiFish primer set (Figures 4–6). Among them, only 16 species were commonly identified by the two primers, which were 38.1 and 48.5% of those by MiFish and FishU, respectively. In the order Perciformes, 46 (8 families) and 18 haplotypes (7 families) were obtained using the MiFish and FishU primers, respectively (Figure 4). Three (*Seriola quinqueradiata*, *Chirolophis japonicus*, and *Uranoscopus japonicus*) and two (*Suruga fundicola* and *Chirolophis saitone*)

species were detected only by the FishU and MiFish primers, respectively (Table 5). MiFish generated a higher number of haplotypes in each species compared with those by FishU primers. In particular, haplotypes with a low identity to the reference database, such as those in the Stichaeidae and Trichodontidae, were more difficult to assign to their correct species (Figure 4B). In contrast, multiple haplotypes were identified in only a limited number of species in those by FishU primers. Some haplotypes were assigned different species names, presumably based on different reference data. For example, only a single nucleotide was different between *Chirolophis saitone* by MiFish and *Chirolophis japonicus* by FishU (Figure 4). The reference sequence of *C. saitone* for the FishU barcode has not yet been deposited in the database, and it should be supplemented.

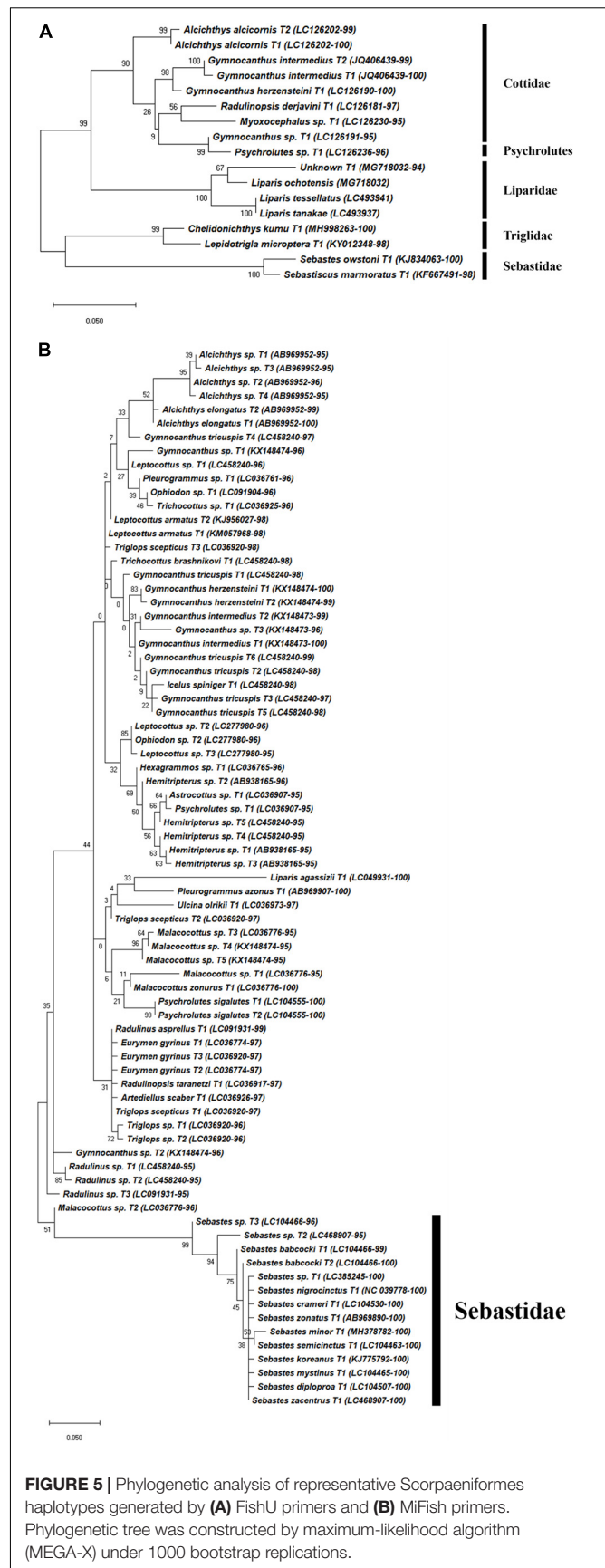
Haplotypes in the Scorpaeniformes, especially those in the families Cottidae and Psychrolutidae, showed a low identity to the reference database in both primers, indicating that the reference data in the family should be supplemented in the East Sea (Figure 5). In addition, haplotypes in the family Sebastidae by MiFish showed a 100% identity to multiple species, indicating the low resolution of the MiFish region to distinguish those taxa (Figure 5B), which was also identified in a previous study (Yamamoto et al., 2017). In contrast, two sebastids, *Sebastes owstoni* and *Sebastes marmoratus*, were clearly assigned by FishU with 99% identity to the database (Figure 5A), which was supported by a previous conventional survey (Sohn et al., 2014). In addition, the assignment of species in Pleuronectidae were highly different between MiFish and FishU. Two species, *P. yokohamae* and *G. zachirus*, were assigned by the MiFish

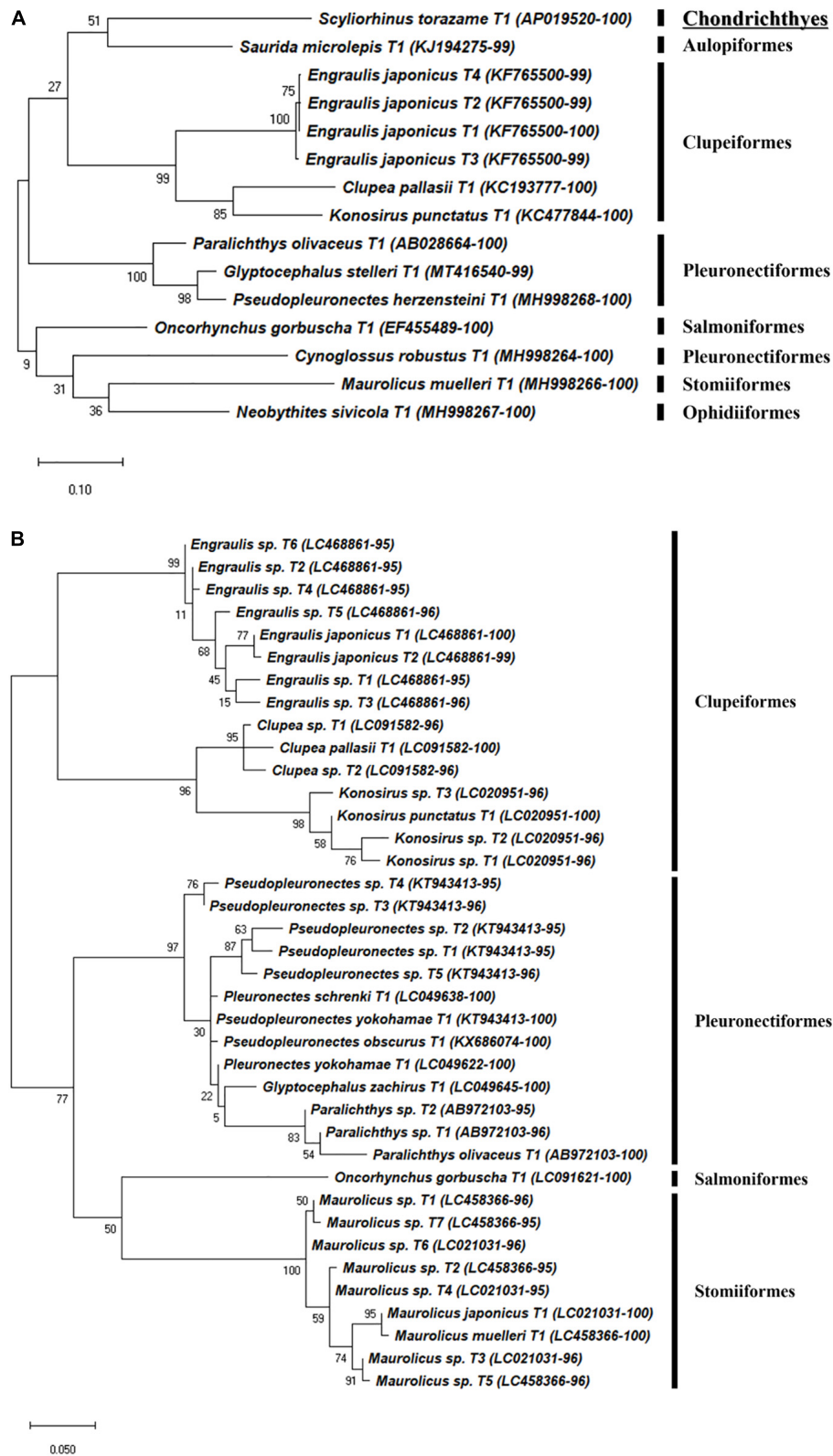




pipeline, and *P. herzensteini* and *G. stelleri* were assigned by FishU (Figure 6). The habitats of these two pleuronectid species by MiFish did not match the information of FishBase<sup>2</sup>. For example, *G. zachirus* is distributed from the Kuril Island to the Bering Sea coasts of Russia, not the coastal water of the East/Japan Sea, suggesting an incorrect species assignment by the MiFish pipeline. In addition to those in the family Sebastidae, species in the Pleuronectidae assigned by the MiFish pipeline should be manually checked before their use in regional/local surveys.

<sup>2</sup>www.fishbase.org





**FIGURE 6 |** Phylogenetic analysis of representative haplotypes belongs to eight orders generated by (A) FishU primers and (B) MiFish primers. Phylogenetic tree was constructed by maximum-likelihood algorithm (MEGA-X) under 1000 bootstrap replications.

Based on the metabarcoding analysis of zooplankton net samples using the two primers, the spawning period of each species was estimated in the East/Japan Sea (Table 5). The average species richness by MiFish was 8.3, ranging from 5 to 13, and 9.8 by FishU, ranging from 4 to 14. Four species, including *Konosirus punctatus*, *Engraulis japonicus*, *Ammodytes personatus*, and *Scomber japonicus*, were detected with a similar pattern by both primers. Although the spawning periods for two related species, *S. lalandi* and *S. quinqueradiata*, were similar to each other from April to May along the Korean waters (Shiraishi et al., 2010; Miura et al., 2020), ichthyoplankton for *S. quinqueradiata* were detected only by the FishU primer in June (Table 5). *Chirolophis japonicus* and *Liza haematocheila* were also detected in January and June as reported in previous studies (Kim et al., 2015; Park et al., 2015). In the species belonging to Pleuronectiformes, two species were identified in the genus *Glyptocephalus*: *Glyptocephalus stelleri* by FishU and *Glyptocephalus zachirus* by MiFish (Figure 6). According to the previous study, the main spawning season for *G. stelleri* is from April to May (Cha et al., 2008). Two species belonging to the genus *Pseudopleuronectes* were also detected from March to June: *Pseudopleuronectes herzensteini* by FishU and *Pseudopleuronectes yokohamae* by MiFish. The previously reported reproduction periods of *P. herzensteini* eggs also support the correct species assignment by the metabarcoding of the FishU primer (Lee and Kim, 2016). Collectively, the FishU primers outperformed MiFish in ichthyoplankton metabarcoding analysis because of the longer barcode, allowing for a clearer species assignment and a broader taxon coverage, representing more taxa, including Synodontidae, Ophidiidae, Uranoscopidae, Cynoglossidae, and Triglididae.

The ichthyoplankton metabarcoding results and previous records for the spawning season were compared (Table 5). Because most of the studies on the spawning seasons have been conducted in commercially important species, including *Scomber japonicus*, *Ammodytes personatus*, and *Engraulis japonicus*, our comparisons were limited to these species (Table 5; shown in blue). The detection of ichthyoplankton generally reflects the spawning season. For instance, *Sebastes marmoratus* and *Maurolicus muelleri* showed spawning periods similar to those reported in previous studies (Yuuki, 1982; Takano et al., 1991). Metabarcoding analysis successfully discriminated the spawning season of two relative species, *Ammodytes personatus* and *Ammodytes hexapterus* (Table 5). However, the onset time of larval detection in other species was often identified some months after the previous records. For instance, the spawning period of *Konosirus punctatus* was known to be from March (Kim et al., 2007a), and its larvae were first identified in June (Table 5). Similarly, two species belonging to the genera *Scomber*, *S. japonicus*, and *S. australasicus*, were detected in June, 3 months after their recorded reproduction periods. The spawning period of *G. herzensteini* was known from December to February (Park et al., 2007), but was detected from February to April.

Our ichthyoplankton metabarcoding analyses also revealed unreported spawning seasons of some species. For instance, we were able to detect the larvae of *Cynoglossus robustus* in the East/Japan Sea from January to April, and it was previously found on the southeastern coast of Korean peninsula from June to

July (Park et al., 2013). In addition, the spawning seasons of several species, including *Suruga fundicola*, *Anisarchus medius*, *Uranoscopus japonicus*, *Lepidotrigla microptera*, and *Neobythites sivicola*, were first estimated in this study. Collectively, the metabarcoding analysis of ichthyoplankton shows great potential for understanding the reproduction of fish species around the Korean peninsula. However, further study is needed to produce data comparable to the conventional ichthyoplankton surveys.

## DISCUSSION

In the present study, we designed a novel fish-specific universal primer set, FishU, for the metabarcoding analysis of ichthyoplankton and compared its reliability with two currently used universal primers, ecoPrimer and MiFish. Because most of the current metabarcoding analyses are conducted based on PCR analysis amplified by universal primers, the choice of the universal primer is crucial. FishU outperformed the other two fish-specific universal primers for the ichthyoplankton survey in several aspects. First, the FishU primer showed a high degree of taxon specificity, amplifying almost exclusively fish taxa directly from the zooplankton net samples. In addition to the sequence specificity within the primer region, the barcode region amplified by FishU contained tRNA<sup>val</sup> flanked by the 12S and 16S regions, a characteristic structure of the fish mitogenome (Figure 2). Therefore, each primer can land on different genes, 12S and 16S, respectively, lowering the chance of amplifying different taxa. By contrast, ecoPrimer and MiFish primers have been designed within the 12S gene, increasing the chance of amplifying a similar sequence of other taxa (Figures 1, 2). Copepods, euphausiid, and Chaetognatha species are among the major zooplankton taxa (Iguchi, 2004), and even a low degree of cross-reactivity to those species would be problematic for the metabarcoding of ichthyoplankton directly from the net sample.

In addition to taxon specificity, the longer barcodes of the FishU primer contributed to a higher accuracy in species identification by both *in silico* and zooplankton net sample analyses. The average length of the barcodes generated by FishU was 373 bp, which represents a 3.5- and 2.2-fold increase compared with those generated by ecoPrimer (106 bp) and MiFish (172 bp), respectively. Although 200 bp or smaller sizes have been reported as the ideal length for metabarcoding to maximize the recovered species numbers (Coissac et al., 2012; Clarke et al., 2017), these small-sized barcodes may trade off the accuracy of species identification. For example, a single base substitution in the barcodes by ecoPrimers resulted in almost half of the barcode not being able to correctly assign species (Table 2). In addition, the short length of the MiFish barcode may not be variable enough to discriminate between closely related species, especially in Pleuronectiformes or Scorpaeniformes, as reported in previous studies (Yamamoto et al., 2017). By contrast, *Pseudopleuronectes herzensteini* and *Sebastes owstoni* in those orders were accurately assigned only by FishU, which was supported by previous studies (Sohn et al., 2014; Lee and Kim, 2016). In addition to these two orders, two related species in each genus, *Alcichthys alcicornis* and *Alcichthys elongatus* and *Maurolicus japonicus* and *Maurolicus muelleri*, should be reexamined.

**TABLE 5 |** Detection of ichthyoplankton in each month by metabarcoding analysis with two universal primers, MiFish (M) and FishU (U).

Order	Family	Species	Jan		Feb		Mar		Apr		May		Jun	
			M	U	M	U	M	U	M	U	M	U	M	U
Actinopteri														
Aulopiformes	Synodontidae	<i>Saurida microlepis</i>						○						
Clupeiformes	Clupeidae	<i>Clupea pallasii</i>	■	■	○	○	■	■	■	■	■	■	⊙	●
		<i>Konosirus punctatus</i>			■	■	■	■	■	■	■	■	⊙	
		<i>Konosirus</i> sp.											⊙	
	Engraulidae	<i>Engraulis japonicus</i>		○			■	○	⊙	⊙	⊙	●	⊙	●
		<i>Engraulis</i> sp.							○		⊙		⊙	
Ophidiiformes	Ophidiidae	<i>Neobythites sivicola</i>			○		○		○					
Perciformes	Ammodytidae	<i>Ammodytes hexapterus</i>	○	⊙										
		<i>Ammodytes personatus</i>	●	●	●	●	●	●	○	○	○		○	
		<i>Ammodytes</i> sp.	⊙	○	⊙	○	⊙	○						
	Carangidae	<i>Seriola lalandi</i>							■	■	■	■	○	○
		<i>Seriola quinqueradiata</i>							■	■	■	■		○
	Gobiidae	<i>Suruga fundicola</i>							○					
	Mugilidae	<i>Liza haematocheila</i>									■	■	○	○
	Scombridae	<i>Scomber australasicus</i>			■	■	■	■	■	■			○	⊙
		<i>Scomber japonicus</i>					■	■	■	■	○	■	⊙	○
		<i>Scomber</i> sp.											○	
	Stichaeidae	<i>Anisarchus medius</i>			⊙	⊙								
		<i>Anisarchus</i> sp.			○									
		<i>Chirolophis japonicus</i>	■	○										
		<i>Chirolophis saitone</i>	○											
		<i>Opisthocentrus</i> sp.			○									
		<i>Poroclinus</i> sp.			○									
	Trichodontidae	<i>Arctoscopus japonicus</i>	○	■	⊙	⊙	○	○						
		<i>Arctoscopus</i> sp.			⊙		○							
	Uranoscopidae	<i>Uranoscopus japonicus</i>								○				
Pleuronectiformes	Cynoglossidae	<i>Cynoglossus robustus</i>		○		○	○			○			■	■
	Paralichthyidae	<i>Paralichthys olivaceus</i>			■	■	■	■	■	■	■	■	⊙	○
		<i>Paralichthys</i> sp.											○	
	Pleuronectidae	<i>Glyptocephalus stelleri</i>							■	○	■	■		
		<i>Glyptocephalus zachirus</i>							○					
		<i>Pseudopleuronectes yokohamae</i>	■	■	■	■			⊙		⊙		⊙	
		<i>Pseudopleuronectes herzensteini</i>			■	■	■	○	■	●	■	⊙	■	○
		<i>Pseudopleuronectes schrenki</i>							○					
		<i>Pseudopleuronectes</i> sp.							⊙		○		○	
Salmoniformes	Salmonidae	<i>Oncorhynchus gorboscha</i>					○	○						
Scorpaeniformes	Agonidae	<i>Ulcina</i> sp.					○							
	Cottidae	<i>Alcichthys alcornis</i>							■	⊙	■	■	■	■
		<i>Alcichthys elongatus</i>					○		⊙	■	■	■		
		<i>Alcichthys</i> sp.							⊙					
		<i>Cottus</i> sp.			○									
		<i>Gymnocanthus herzensteini</i>	■	■	⊙	○	⊙	⊙	○	○				
		<i>Gymnocanthus intermedius</i>					⊙	○	⊙	⊙				
		<i>Gymnocanthus</i> sp.			○		⊙	○	○					
		<i>Leptocottus</i> sp.			⊙		○							
		<i>Myoxocephalus</i> sp.				○		○						
		<i>Phasmatocottus</i> sp.			○									
		<i>Radulinopsis derjavini</i>										○		
		<i>Radulinus asprellus</i>										○		
		<i>Radulinus</i> sp.										○		

(Continued)



TABLE 5 | Continued

Order	Family	Species	Jan		Feb		Mar		Apr		May		Jun	
			M	U	M	U	M	U	M	U	M	U	M	U
Stomiiformes	Hemirhamphidae	<i>Stelgistrum</i> sp.									○			
		<i>Trichocottus</i> sp.			○									
		<i>Triglops</i> sp.									⊙			
		<i>Hemirhamphus</i> sp.			○									
		<i>Hexagrammos</i> sp.			○									
		<i>Pleurogrammus azonus</i>							○					
		<i>Liparis agassizii</i>					○		○					
		<i>Liparis</i> sp.			○		○	○		○				
		<i>Malacocottus</i> sp.			○		⊙							
		<i>Psychrolutes sigalutes</i>	○											
		<i>Psychrolutes</i> sp.					⊙							
		<i>Sebastes babcocki</i>									○			
		<i>Sebastes hubbsi</i>									⊙		○	
		<i>Sebastes minor</i>									○			
		<i>Sebastes owstoni</i>									⊙			○
		<i>Sebastes</i> sp.									○			
		<i>Sebastes marmoratus</i>	■	○	■	⊙	■	○	■	⊙				
		<i>Chelidonichthys kumu</i>												○
		<i>Lepidotrigla microptera</i>		○		○		○		○				
Stomiiformes	Sternoptychidae	<i>Maurollicus japonicus</i>							⊙				⊙	
		<i>Maurollicus muelleri</i>					■	○	⊙	⊙	■	■	⊙	⊙
		<i>Maurollicus</i> sp.							⊙				○	
Chondrichthyes														
Carcharhiniformes	Scyliorhinidae	<i>Scyliorhinus torazame</i>								○				
		Unknown	○		○		○		○		○		○	

● relative proportion of each month was 50–100%, ⊙ relative proportion of each month was 1–50%, ○ relative proportion of each month was 0–1% (except 0%). The spawning periods from the previous studies are blue-shaded.

The application of the MiFish pipeline requires careful attention from those who would like to use the data directly from its bioinformatic analysis for the analysis of local fish assemblages. Although much higher haplotypes (180) and species numbers (42) were obtained by the MiFish pipeline in this study compared with those by the FishU platform (51 haplotypes and 31 species), most of the species assigned only by MiFish showed a low similarity to the database (Table 5). Those assigned as genus names, such as *Konosirus* sp., *Engraulis* sp., or *Ammodytes* sp., may have come from the short barcode length. When merging each pair read generated by the MiSeq platform, it was especially challenging to eliminate chimeric sequences for multiple haplotypes, species with a high degree of genetic similarity, or lack of a reference database. For instance, three species in the genus *Ammodytes* could not be adequately assigned by the MiFish pipeline, generating a high number of haplotypes with low similarities, mainly due to the genetic similarity among those species and the lack of the local reference sequences in the database (Figure 4). The chimeric sequences generated by MiFish would be problematic, exaggerating the species numbers for countries without a sufficiently large reference database. In contrast, the barcodes by FishU showed no chimeric haplotypes with long read lengths. In fact, all the species exclusively identified by FishU primers showed a high sequence identity, with an

identity of more than 99% to the database, which included *Clupea pallasii*, *Neobythites sivicola*, *Seriola quinqueradiata*, *Uranoscopus japonicus*, and *Radulinopsis derjavini* (Table 5). This result indicates that FishU provides species information with a high degree of accuracy in ichthyoplankton metabarcoding analysis. The longer barcode size by FishU was not a problem, at least for ichthyoplankton metabarcoding. Instead, FishU outperformed the other two fish-specific universal primers in the ichthyoplankton survey with higher accuracy and reliability.

Compared with the other two fish-specific universal primers, the use of FishU for the ichthyoplankton metabarcoding has several advantages, including higher taxon coverage and specificity and accurate species identification. However, there are still several shortcomings in adopting the primer. The barcode region by FishU includes the tRNA-valine flanked by the partial 12S rRNA and 16S rRNA, whose reference sequences are fewer than those of the typically used barcodes, such as COI or MiFish region. Notably, there is much less information regarding those that have little commercial value. Because taxonomic identification in metabarcoding is entirely dependent on the reference database, the reference sequences for the FishU region, especially those for the local or indigenous species, should be supplemented. The recent fast growth of complete mitochondrial DNA information of various fish taxa

is also helpful to compensate for these shortcomings (Iwasaki et al., 2013). Another factor to consider in choosing FishU is the low yield of merged reads from the raw data (Table 5). The proportions of the average merged fish barcode numbers generated by the FishU primer were 35%, which was twofold lower than that by MiFish. These results are mainly due to the low merged rates for the longer barcodes by the FishU primer (Elbrecht and Leese, 2017). These low merged-read rates can be compensated by the increased raw reads. To obtain processed merged reads similar to those of MiFish in this study, approximately twofold higher raw read numbers were required in the FishU platform (Table 4). Because longer barcodes have many advantages in ichthyoplankton metabarcoding, metabarcoding analysis by FishU would trade off the shortcoming in the cost. Storage after sample collection may also affect the recovery of longer barcodes by FishU, and we cannot rule out that the low merged-read numbers from January to April may have arisen due to the degradation of DNA after a long period of storage (Table 4) because it is widely known that DNA can be degraded over long storage times (Vamos et al., 2017). Therefore, higher merged reads could be achieved by metabarcoding immediately after the extraction of total genomic DNA.

Here, we attempted to determine the spawning season based on the metabarcoding analysis of ichthyoplankton from zooplankton net samples. The metabarcoding analysis of ichthyoplankton provides many useful data to understand the reproduction of fish, including details of their spawning sites, reproductive periods, and population structures, at relatively low cost and labor. The large amount of data obtained by metabarcoding analysis can be used for various purposes not previously possible using conventional ichthyoplankton surveys, including the effects of climate change during the spawning season in each species, an understanding of the reproduction of rare species, or the genetic populations of ichthyoplankton. In addition, the transport routes of fish eggs and larvae in the East/Japan Sea can also be understood by its larval metabarcoding analysis. Waters in the East/Japan Sea are the place where two main currents along the Korean peninsula, the NKCC from the north and EKCW, collide. Therefore, transportation and settlement of ichthyoplankton are largely dependent on the dynamics of these currents. In fact, we were able to identify a small number of tropical and cold-water fish larvae, which are further used as indicators of the spatiotemporal dynamics of these currents. For instance, *Saurida microlepis* and *Chelidonichthys kumu* have been conveyed from the South Pacific Ocean by the Kuroshio warm current and Tsushima current entering the East/Japan Sea through the Korean Strait. Because the Kuroshio current begins with the water around the Philippines and Taiwan, which is known to be the spawning site of many fish species, the abundance of these tropical fish would explain the effects of the warm current on fisheries in the East/Japan Sea. In contrast, some species detected during the winter season may have been conveyed from the NKCC. For example, *Anisarchus medius* is a demersal species, preferring water at temperatures below 0°C, and its larvae were only found in February although *A. hexapterus* was originally distributed in cold waters from Arctic Alaska to the northern Pacific. Therefore, changes in the abundance of tropical

or cold ichthyoplankton help explain the effects of the dynamics of the two main currents on fisheries in the East/Japan Sea.

Although it is a useful tool for the ichthyoplankton survey, metabarcoding analysis is not likely to replace currently used methods in the near future. In addition to diversity, several data, such as morphological or developmental parameters, can be obtained only using the conventional ichthyoplankton survey. For example, egg or larval fish abundances cannot be obtained by metabarcoding analysis using the current methodology. It is also unclear whether metabarcoding analysis can explain the behavioral characteristics, such as diurnal vertical migrations, of fish larvae or spawning ecology. Quantitative analysis is another issue to establish the correlation between metabarcoding analysis and conventional survey. Although it is generally accepted that there is a quantitative relationship between the sequence reads and biomass (Deagle et al., 2019; Lamb et al., 2019), a clear consensus has yet to be reached with regards to the quantification methodology and continues to vary between research groups. Furthermore, there are many chances for bias throughout the metabarcoding pipeline from the sample collection to the bioinformatic processes, making it more difficult to achieve an accurate quantification (Juen and Traugott, 2006; Plummer et al., 2015; Smith et al., 2017). We also identified the delayed detection of ichthyoplankton in many species compared with the previously known spawning season (Table 5). The reproductive period of a species is usually estimated by the combination of gonad maturation and ichthyoplankton survey (Murua et al., 2003; Lowerre-Barbieri et al., 2011). The delayed detection can be explained by the lower chance of detection in eggs, which have lower copies of DNA, compared with those of larvae. As cell numbers increase from eggs to fish larvae during the developmental stages, the chance of detection is much higher for the larval stage than for eggs (Takeuchi et al., 2019). Therefore, further studies should be conducted to identify the spawning seasons more precisely via the metabarcoding analysis of ichthyoplankton.

Despite its current limitations, the metabarcoding analysis of ichthyoplankton remains a promising strategy to supplement conventional surveys. As the data accumulates by comparative analysis with conventional microscopic observation, this technique provides more reliable data. Once a universal and automated metabarcoding platform is established, cost-effective and long-term ichthyoplankton surveys with a higher degree of statistical reliability will be possible, which would provide useful information for the scientific management of local fish resources.

## DATA AVAILABILITY STATEMENT

The sequencing data from this study has been deposited in BioProject (accession: PRJNA682864).

## AUTHOR CONTRIBUTIONS

AK designed the experiments, performed the experiments, analyzed the data, prepared figures and tables, and wrote the manuscript. T-HY designed the experiments, analyzed the data, and prepared figures and tables. CL and C-KK conceived and

designed the experiments, contributed reagents, materials, and analysis tools. H-WK conceived and designed the experiments, performed the experiments, analyzed the data, contributed reagents, materials, analysis tools, prepared figures and tables, authored and reviewed drafts of the manuscript, and approved the final draft. All authors contributed to the article and approved the submitted version.

## FUNDING

This research was a part of the project titled “Walleye Pollock stock management based on Marine Information

and Communication Technology,” funded by the Ministry of Oceans and Fisheries, Korea and partly supported by Basic Science Research Program through the National Research Foundation of Korea (NRF) funded by the Ministry of Education (2020R1I1A3072978).

## SUPPLEMENTARY MATERIAL

The Supplementary Material for this article can be found online at: <https://www.frontiersin.org/articles/10.3389/fmars.2021.614394/full#supplementary-material>

## REFERENCES

- Andruszkiewicz, E. A., Starks, H. A., Chavez, F. P., Sassoubre, L. M., Block, B. A., and Boehm, A. B. (2017). Biomonitoring of marine vertebrates in Monterey Bay using eDNA metabarcoding. *PLoS One* 12:e0176343. doi: 10.1371/journal.pone.0176343
- Aylagas, E., Borja, A., Irigoien, X., and Rodríguez-Ezpeleta, N. (2016). Benchmarking DNA metabarcoding for biodiversity-based monitoring and assessment. *Front. Mar. Sci.* 3:96. doi: 10.3389/fmars.2016.00096
- Balasingham, K. D., Walter, R. P., Mandrak, N. E., and Heath, D. D. (2018). Environmental DNA detection of rare and invasive fish species in two Great Lakes tributaries. *Mol. Ecol.* 27, 112–127. doi: 10.1111/mec.14395
- Berry, O., Bulman, C., Bunce, M., Coghlan, M., Murray, D. C., and Ward, R. D. (2015). Comparison of morphological and DNA metabarcoding analyses of diets in exploited marine fishes. *Mar. Ecol. Prog. Ser.* 540, 167–181. doi: 10.3354/meps11524
- Borrell, Y. J., Miralles, L., Do Huu, H., Mohammed-Geba, K., and Garcia-Vazquez, E. (2017). DNA in a bottle—Rapid metabarcoding survey for early alerts of invasive species in ports. *PLoS One* 12:e0183347. doi: 10.1371/journal.pone.0183347
- Boyer, F., Mercier, C., Bonin, A., Le Bras, Y., Taberlet, P., and Coissac, E. (2016). obitools: a unix-inspired software package for DNA metabarcoding. *Mol. Ecol. Resour.* 16, 176–182. doi: 10.1111/1755-0998.12428
- Bylemans, J., Gleeson, D. M., Duncan, R. P., Hardy, C. M., and Furlan, E. M. (2019). A performance evaluation of targeted eDNA and eDNA metabarcoding analyses for freshwater fishes. *Environ. DNA* 1, 402–414. doi: 10.1002/edn3.41
- Bylemans, J., Gleeson, D. M., Hardy, C. M., and Furlan, E. (2018). Toward an ecoregion scale evaluation of eDNA metabarcoding primers: a case study for the freshwater fish biodiversity of the murray-darling basin (Australia). *Ecol. Evol.* 8, 8697–8712. doi: 10.1002/ece3.4387
- Camacho, C., Coulouris, G., Avagyan, V., Ma, N., Papadopoulos, J., Bealer, K., et al. (2009). BLAST+: architecture and applications. *BMC Bioinformatics* 10:421. doi: 10.1186/1471-2105-10-421
- Cha, H. K., Kwon, H. C., Lee, S. I., Yang, J. H., Chang, D. S., and Chun, Y. Y. (2008). Maturity and spawning of Korean flounder *Glyptocephalus stelleri* (Schmidt) in the East Sea of Korea. *Korean J. Ichthyol.* 20, 263–271.
- Clarke, L. J., Beard, J. M., Swadling, K. M., and Deagle, B. E. (2017). Effect of marker choice and thermal cycling protocol on zooplankton DNA metabarcoding studies. *Ecol. Evol.* 7, 873–883. doi: 10.1002/ece3.2667
- Coissac, E., Riaz, T., and Puillandre, N. (2012). Bioinformatic challenges for DNA metabarcoding of plants and animals. *Mol. Ecol.* 21, 1834–1847. doi: 10.1111/j.1365-294X.2012.05550.x
- Collins, R. A., Bakker, J., Wangenstein, O. S., Soto, A. Z., Corrigan, L., Sims, D. W., et al. (2019). Non-specific amplification compromises environmental DNA metabarcoding with COI. *Methods Ecol. Evol.* 10, 1985–2001. doi: 10.1111/2041-210X.13276
- Deagle, B. E., Thomas, A. C., McInnes, J. C., Clarke, L. J., Vesterinen, E. J., Clare, E. L., et al. (2019). Counting with DNA in metabarcoding studies: how should we convert sequence reads to dietary data? *Mol. Ecol.* 28, 391–406. doi: 10.1111/mec.14734
- Edgar, R. C., Haas, B. J., Clemente, J. C., Quince, C., and Knight, R. (2011). UCHIME improves sensitivity and speed of chimera detection. *Bioinformatics* 27, 2194–2200. doi: 10.1093/bioinformatics/btr381
- Elbrecht, V., and Leese, F. (2017). Validation and development of COI metabarcoding primers for freshwater macroinvertebrate bioassessment. *Front. Environ. Sci.* 5:11. doi: 10.1371/journal.pone.0177643
- Evans, N. T., Olds, B. P., Renshaw, M. A., Turner, C. R., Li, Y., Jerde, C. L., et al. (2016). Quantification of mesocosm fish and amphibian species diversity via environmental DNA metabarcoding. *Mol. Ecol. Resour.* 16, 29–41. doi: 10.1111/1755-0998.12433
- Hawltischek, O., Fernandez-Gonzalez, A., Balmori-De La Puente, A., and Castresana, J. (2018). A pipeline for metabarcoding and diet analysis from fecal samples developed for a small semi-aquatic mammal. *PLoS One* 13:e0201763. doi: 10.1371/journal.pone.0201763
- Iguchi, N. (2004). Spatial/temporal variations in zooplankton biomass and ecological characteristics of major species in the southern part of the Japan Sea: a review. *Prog. Oceanogr.* 61, 213–225. doi: 10.1016/j.pocean.2004.06.007
- Iwanowicz, D. D., Vandergast, A. G., Cornman, R. S., Adams, C. R., Kohn, J. R., Fisher, R. N., et al. (2016). Metabarcoding of fecal samples to determine herbivore diets: a case study of the endangered pacific pocket mouse. *PLoS One* 11:e0165366. doi: 10.1371/journal.pone.0165366
- Iwasaki, W., Fukunaga, T., Isagozawa, R., Yamada, K., Maeda, Y., Satoh, T. P., et al. (2013). MitoFish and MitoAnnotator: a mitochondrial genome database of fish with an accurate and automatic annotation pipeline. *Mol. Biol. Evol.* 30, 2531–2540. doi: 10.1093/molbev/mst141
- Jacobs, F., and Grant, G. C. (1978). *Guidelines for Zooplankton Sampling in Quantitative Baseline and Monitoring Programs*. Jacksonville, FL: National Information Service.
- Juen, A., and Traugott, M. (2006). Amplification facilitators and multiplex PCR: tools to overcome PCR-inhibition in DNA-gut-content analysis of soil-living invertebrates. *Soil Biology Biochem.* 38, 1872–1879. doi: 10.1016/j.soilbio.2005.11.034
- Keller, A. A., Klein-Macphree, G., and Burns, J. S. O. (1999). Abundance and distribution of ichthyoplankton in Narragansett Bay, Rhode Island, 1989–1990. *Estuaries* 22, 149–163. doi: 10.2307/1352935
- Kim, S., Han, K.-H., Lee, J.-H., Lee, S.-H., Kim, C.-C., Ko, H.-J., et al. (2007a). Egg development and morphology of larva and juvenile of the konoshiro gizzard shad, *Konosirus punctatus*. *Dev. Reprod.* 11, 127–135.
- Kim, S., Zhang, C.-I., Kim, J.-Y., Oh, J.-H., Kang, S., and Lee, J. B. (2007b). Climate variability and its effects on major fisheries in Korea. *Ocean Sci. J.* 42, 179–192. doi: 10.1007/BF03020922
- Kim, M.-K., Choi, K.-S., Shin, M.-K., Kim, B.-P., and Han, K.-N. (2015). Age and Growth of Redlip Mullet (*Chelon haematocheilus*) in the Han River Estuary, Korea. *Korean J. Ichthyol.* 27, 133–141.
- Klym, K. E., Marshall, N. T., and Stepien, C. A. (2017). Environmental DNA (eDNA) metabarcoding assays to detect invasive invertebrate species in the Great Lakes. *PLoS One* 12:e0177643. doi: 10.1371/journal.pone.0177643
- Kumar, S., Stecher, G., Li, M., Knyaz, C., and Tamura, K. (2018). MEGA X: molecular evolutionary genetics analysis across computing platforms. *Mol. Biol. Evol.* 35, 1547–1549. doi: 10.1093/molbev/msy096

- Lamb, P. D., Hunter, E., Pinnegar, J. K., Creer, S., Davies, R. G., and Taylor, M. I. (2019). How quantitative is metabarcoding: a meta-analytical approach. *Mol. Ecol.* 28, 420–430. doi: 10.1111/mec.14920
- Lee, S. J., and Kim, J.-K. (2016). Morphological characteristics and distribution of Pleuronectidae (Pisces) eggs in the western margin of the East Sea. *Ocean Sci. J.* 51, 13–20. doi: 10.1007/s12601-016-0002-3
- Lowerre-Barbieri, S. K., Ganas, K., Saborido-Rey, F., Murua, H., and Hunter, J. R. (2011). Reproductive timing in marine fishes: variability, temporal scales, and methods. *Mar. Coast. Fish.* 3, 71–91. doi: 10.1080/19425120.2011.556932
- McDevitt, A. D., Sales, N. G., Browett, S. S., Sparnenn, A. O., Mariani, S., Wangenstein, O. S., et al. (2019). Environmental DNA metabarcoding as an effective and rapid tool for fish monitoring in canals. *J. Fish Biol.* 95, 679–682. doi: 10.1111/jfb.14053
- Minamoto, T., Yamanaka, H., Takahara, T., Honjo, M. N., and Kawabata, Z. I. (2012). Surveillance of fish species composition using environmental DNA. *Limnology* 13, 193–197. doi: 10.1007/s10201-011-0362-4
- Miura, C., Hayashi, D., and Miura, T. (2020). Relationship between gonadal maturation and kyphosis in cultured yellowtail (*Seriola quinqueradiata*). *Aquaculture* 520:734667. doi: 10.1016/j.aquaculture.2019.734667
- Miya, M., Sato, Y., Fukunaga, T., Sado, T., Poulsen, J. Y., Sato, K., et al. (2015). MiFish, a set of universal PCR primers for metabarcoding environmental DNA from fishes: detection of more than 230 subtropical marine species. *R. Soc. Open Sci.* 2:150088. doi: 10.1098/rsos.150088
- Murua, H., Kraus, G., Saborido-Rey, F., Witthames, P., Thorsen, A., and Junquera, S. (2003). Procedures to estimate fecundity of marine fish species from field samples in relation to reproductive strategy. *J. Northw. Atlantic Fish. Sci.* 33, 33–54. doi: 10.2960/J.v33.a3
- Park, J. M., Hashimoto, H., Jeong, J. M., Kim, H. J., and Baek, G. W. (2013). Age and growth of the robust tonguefish *Cynoglossus robustus* in the Seto Inland Sea. *Jpn. Anim. Cells Syst.* 17, 290–297. doi: 10.1080/19768354.2013.826281
- Park, J. M., Lee, S. H., Choi, J. Y., and Han, K. H. (2015). Spawning behavior and morphological development of the eggs and larvae of the fringed blenny, *Chirolophis japonicus* from Korea (Pisces: Stichaeidae). *Korean J. Ichthyol.* 27, 63–70.
- Park, K. Y., Park, K. H., Lee, S. I., Park, H. W., Hong, S. E., Yang, J. H., et al. (2007). Maturity and spawning of black edged sculpin, *Gymnocanthus herzensteini* in the East Sea. *Korean J. Ichthyol.* 19, 101–106.
- Plummer, E., Twin, J., Bulach, D. M., Garland, S. M., and Tabrizi, S. N. (2015). A comparison of three bioinformatics pipelines for the analysis of preterm gut microbiota using 16S rRNA gene sequencing data. *J. Proteom. Bioinform.* 8, 283–291. doi: 10.4172/jpb.1000381
- Riaz, T., Shehzad, W., Viari, A., Pompanon, F., Taberlet, P., and Coissac, E. (2011). ecoPrimers: inference of new DNA barcode markers from whole genome sequence analysis. *Nucleic Acids Res.* 39:e145. doi: 10.1093/nar/gkr732
- Sato, Y., Miya, M., Fukunaga, T., Sado, T., and Iwasaki, W. (2018). MitoFish and MiFish pipeline: a mitochondrial genome database of fish with an analysis pipeline for environmental DNA metabarcoding. *Mol. Biol. Evol.* 35, 1553–1555. doi: 10.1093/molbev/msy074
- Schlitzer, R. (2016). *Ocean Data View, version 4.7.8*.
- Schloss, P. D., Westcott, S. L., Ryabin, T., Hall, J. R., Hartmann, M., Hollister, E. B., et al. (2009). Introducing mothur: open-source, platform-independent, community-supported software for describing and comparing microbial communities. *Appl. Environ. Microbiol.* 75, 7537–7541. doi: 10.1128/AEM.01541-09
- Shaw, J. L. A., Clarke, L. J., Wedderburn, S. D., Barnes, T. C., Weyrich, L. S., and Cooper, A. (2016). Comparison of environmental DNA metabarcoding and conventional fish survey methods in a river system. *Biol. Conserv.* 197, 131–138. doi: 10.1016/j.biocon.2016.03.010
- Shiraishi, T., Ohshimo, S., and Yukami, R. (2010). Age, growth and reproductive characteristics of gold striped amberjack 1 *Seriola lalandi* in the waters off western Kyushu, Japan. *N. Zeal. J. Mar. Freshw. Res.* 44, 117–127. doi: 10.1080/00288330.2010.488787
- Shoji, J., Toshito, S.-I., Mizuno, K.-I., Kamimura, Y., Hori, M., and Hirakawa, K. (2011). Possible effects of global warming on fish recruitment: shifts in spawning season and latitudinal distribution can alter growth of fish early life stages through changes in daylength. *ICES J. Mar. Sci.* 68, 1165–1169. doi: 10.1093/icesjms/fsr059
- Sigsgaard, E. E., Nielsen, I. B., Carl, H., Krag, M. A., Knudsen, S. W., Xing, Y., et al. (2017). Seawater environmental DNA reflects seasonality of a coastal fish community. *Mar. Biol.* 164:128. doi: 10.1007/s00227-017-3147-4
- Smith, K. F., Kohli, G. S., Murray, S. A., and Rhodes, L. L. (2017). Assessment of the metabarcoding approach for community analysis of benthic-epiphytic dinoflagellates using mock communities. *N. Zeal. J. Mar. Freshw. Res.* 51, 555–576. doi: 10.1080/00288330.2017.1298632
- Sohn, M. H., Yoon, B. S., Park, J.-H., Choi, Y. M., and Yang, J. H. (2014). Species composition and distribution of trammel net catches in the coastal waters of Gangwon province, Korea. *Korean J. Fish. Aquat. Sci.* 47, 945–959. doi: 10.5657/KFAS.2014.0945
- Takano, K., Takemura, A., Furihata, M., Nakanishi, T., and Hara, A. (1991). “Annual reproductive and spawning cycles of female *Sebastiscus marmoratus*,” in *Rockfishes of the Genus Sebastes: Their Reproduction and Early Life History*, eds J. Yamada and G. W. Boehlert (Berlin: Springer), 39–48. doi: 10.1007/978-94-011-3792-8\_5
- Takeuchi, A., Iijima, T., Kakuzen, W., Watanabe, S., Yamada, Y., Okamura, A., et al. (2019). Release of eDNA by different life history stages and during spawning activities of laboratory-reared Japanese eels for interpretation of oceanic survey data. *Sci. Rep.* 9, 1–9. doi: 10.1038/s41598-019-42641-9
- Thomsen, P. F., Kielgast, J., Iversen, L. L., Møller, P. R., Rasmussen, M., and Willerslev, E. (2012). Detection of a diverse marine fish fauna using environmental DNA from seawater samples. *PLoS One* 7:e41732. doi: 10.1371/journal.pone.0041732
- Ushio, M., Murakami, H., Masuda, R., Sado, T., Miya, M., Sakurai, S., et al. (2017). Quantitative monitoring of multispecies fish environmental DNA using high-throughput sequencing. *bioRxiv* [Preprint]. doi: 10.3897/mbmg.2.23297
- Valentini, A., Taberlet, P., Miaud, C., Civate, R., Herder, J., Thomsen, P. F., et al. (2016). Next-generation monitoring of aquatic biodiversity using environmental DNA metabarcoding. *Mol. Ecol.* 25, 929–942. doi: 10.1111/mec.13428
- Vamos, E. E., Elbrecht, V., and Leese, F. (2017). Short COI markers for freshwater macroinvertebrate metabarcoding. *PeerJ* 1:e14625. doi: 10.3897/mbmg.1.14625
- Watts, C., Dopheide, A., Holdaway, R., Davis, C., Wood, J., Thornburrow, D., et al. (2019). DNA metabarcoding as a tool for invertebrate community monitoring: a case study comparison with conventional techniques. *Austral. Entomol.* 58, 675–686. doi: 10.1111/aen.12384
- Yamamoto, S., Masuda, R., Sato, Y., Sado, T., Araki, H., Kondoh, M., et al. (2017). Environmental DNA metabarcoding reveals local fish communities in a species-rich coastal sea. *Sci. Rep.* 7:40368. doi: 10.1038/srep40368
- Yatsu, A., Watanabe, T., Ishida, M., Sugisaki, H., and Jacobson, L. D. (2005). Environmental effects on recruitment and productivity of Japanese sardine *Sardinops melanostictus* and chub mackerel *Scomber japonicus* with recommendations for management. *Fish. Oceanogr.* 14, 263–278. doi: 10.1111/j.1365-2419.2005.00335.x
- Yoon, T. H., Kang, H. E., Lee, S. R., Lee, J. B., Baek, G. W., Park, H., et al. (2017). Metabarcoding analysis of the stomach contents of the Antarctic Toothfish (*Dissostichus mawsoni*) collected in the Antarctic Ocean. *PeerJ* 5:e3977. doi: 10.7717/peerj.3977
- Yu, D. W., Ji, Y., Emerson, B. C., Wang, X., Ye, C., Yang, C., et al. (2012). Biodiversity soup: metabarcoding of arthropods for rapid biodiversity assessment and biomonitoring. *Methods Ecol. Evol.* 3, 613–623. doi: 10.1111/j.2041-210X.2012.00198.x
- Yuuki, Y. (1982). Spawning and maturity of a sternopterychid fish *Maurollicus muelleri* in the south western waters of the Sea of Japan. *Bull. Jpn. Soc. Sci. Fish.* 48, 749–753. doi: 10.2331/suisan.48.749
- Zhang, S., Zhao, J., and Yao, M. (2020). A comprehensive and comparative evaluation of primers for metabarcoding eDNA from fish. *Methods Ecol. Evol.* 11, 1609–1625. doi: 10.1111/2041-210X.13485

**Conflict of Interest:** The authors declare that the research was conducted in the absence of any commercial or financial relationships that could be construed as a potential conflict of interest.

Copyright © 2021 Kim, Yoon, Lee, Kang and Kim. This is an open-access article distributed under the terms of the Creative Commons Attribution License (CC BY). The use, distribution or reproduction in other forums is permitted, provided the original author(s) and the copyright owner(s) are credited and that the original publication in this journal is cited, in accordance with accepted academic practice. No use, distribution or reproduction is permitted which does not comply with these terms.





# Application of a Simple, Low-Cost, Low-Tech Method to Monitor Intertidal Rocky Shore Assemblages on a Broad Geographic Scale

Juan Pablo Livore<sup>1</sup>, María M. Mendez<sup>2,3\*</sup>, Eduardo Klein<sup>4</sup>, Lorena Arribas<sup>1,3</sup> and Gregorio Bigatti<sup>1,3,5</sup>

<sup>1</sup> Laboratorio de Reproducción y Biología Integrativa de Invertebrados Marinos, Instituto de Biología de Organismos Marinos (IBIOMAR-CONICET), Puerto Madryn, Argentina, <sup>2</sup> Instituto de Biología de Organismos Marinos (IBIOMAR-CONICET), Puerto Madryn, Argentina, <sup>3</sup> Universidad Nacional de la Patagonia San Juan Bosco, Puerto Madryn, Argentina, <sup>4</sup> Departamento de Estudios Ambientales, Universidad Simón Bolívar, Caracas, Venezuela, <sup>5</sup> Universidad Espíritu Santo, Samborombón, Ecuador

## OPEN ACCESS

### Edited by:

Juan Carlos Azofeifa-Solano,  
University of Costa Rica, Costa Rica

### Reviewed by:

Iacopo Bertocci,  
University of Pisa, Italy  
Isabel Sousa Pinto,  
University of Porto, Portugal

### \*Correspondence:

María M. Mendez  
mendez@cenpat-conicet.gob.ar

### Specialty section:

This article was submitted to  
Ocean Observation,  
a section of the journal  
Frontiers in Marine Science

**Received:** 30 July 2020

**Accepted:** 08 March 2021

**Published:** 26 March 2021

### Citation:

Livore JP, Mendez MM, Klein E,  
Arribas L and Bigatti G (2021)  
Application of a Simple, Low-Cost,  
Low-Tech Method to Monitor  
Intertidal Rocky Shore Assemblages  
on a Broad Geographic Scale.  
*Front. Mar. Sci.* 8:589489.  
doi: 10.3389/fmars.2021.589489

Identifying susceptible regions where biodiversity changes occur at fast rates is essential in order to protect and ameliorate affected areas. Large-scale coastal monitoring programs that focus on long-term variability are scarce, yet the Marine Biodiversity Observation Network Pole to Pole is currently developing a regional collaboration throughout the American continent collecting biodiversity data in coastal habitats with a standardized systematic protocol. The use of photographic methods to collect assemblage data on intertidal rocky shores can be appropriate. The goal of this study was to analyze the performance of a simple, low-cost, non-destructive and low-tech photographic method on a broad geographical scale (~ 2,000 km) of Atlantic Patagonian coastline. Concurrently, we aimed to identify indicators whose cover, presence or condition can be followed in time and used as beacons of change in biodiversity on these rocky intertidal shores. We also explored the potential relationships between assemblage structure and environmental variables, such as seascape classes. We identified and propose cover of mytilids, *Corallina* spp. and bare substrate as indicators of change due to their ecological relevance in intertidal assemblages and their visible and rapid response to human stressors or changes in environmental conditions. Finally, we illustrate the practicality and usefulness of remotely accessible environmental data, for instance the seascape classes approach as an integrative tool for large-scale rocky shore studies.

**Keywords:** biodiversity, rocky shores, monitoring, intertidal, Patagonia

## INTRODUCTION

Coastal ecosystems generally present high biodiversity and provide valuable cultural, provisioning and regulating services (Galparsoro et al., 2014). Although they represent only 8% of global surface, these areas provide approximately 43% of the estimated value of ecosystem services worldwide. Concurrently, global average population density is estimated to be three times higher in coastal areas (Small and Nicholls, 2003) and these are also the most likely to be affected by natural hazards such as storm surges, hurricanes

and other extreme weather events including those related to climate change (Kron, 2013). Within this context, rocky shores form more than 80% of coastal shorelines worldwide (Emery and Kuhn, 1982; Granja, 2004). Hence, monitoring for rapid changes to ecosystems on coastal rocky shores is imperative for adequate management and conservation of the services they provide.

Large-scale ecosystem monitoring programs on rocky shores are few despite the logistic advantages of these ecosystems (Miloslavich et al., 2019). Long-term, sustained, time-series of biodiversity, community structure and dynamics in this generally accessible ecosystem are few, such as MarClim in western Europe, PISCO on the west coast of the United States and SARCE in South America. Furthermore, data of the existing programs may be incomparable due to variability in the collection methods, heterogeneity in spatial and temporal sampling, and in data formats (Duffy et al., 2019; Miloslavich et al., 2019). Monitoring efforts at large spatial scales that try to integrate long-term inter-annual and seasonal community variability are scarce, mostly because they are costly, logistically complex and require much coordination by different groups of scientists. In this sense, contrasting access to resources of dedicated scientists involved in large-scale monitoring often challenges the implementation of programs at the desired scale (Bax et al., 2019). The implementation of large-scale and long-term monitoring programs is a tool for detecting changes in rocky shore communities that may provide early alarms to decision makers allowing the opportunity of a timely response action.

A recently established large-scale and long-term program is the Marine Biodiversity Observation Network Pole to Pole of the Americas (MBON P2P). It was conceived as an international network of collaborating research institutions, marine laboratories, parks, and reserves seeking to address common problems related to sustaining ecosystem services through conservation ecology. This project was built on the efforts of two previous international projects, namely the Natural Geography in Shore Areas (NaGISA) of the Census of Marine Life (CoML) program and its sequel for South America the South American Research Group on Coastal Ecosystems (SARCE) (Miloslavich et al., 2016). MBON P2P is collecting biological data in coastal habitats (rocky shores and sandy beaches) and acting as a global community of practice for sustained, operationalized measurements of marine biodiversity (Canonico et al., 2019). All data collected by the MBON P2P project are open available and contribute to other programs as the Global Ocean Observing System (GOOS- UNESCO), under the framework of Essential Ocean Variables (EOVs). Within this framework, some of the identified EOVs that are achieved by the MBON P2P program is “macroalgal canopy cover and composition,” as well as the emerging EOV “benthic invertebrate abundance and distribution,” both relevant to rocky shores (Miloslavich et al., 2018).

Along both Pacific and Atlantic South American coasts, the development of large-scale programs provided evidence of strong changes in community diversity (Cruz-Motta et al., 2020). Sea surface temperature (SST) was the main variable that explained the changes, yet local factors were also important (Cruz-Motta et al., 2020). Previously, similar programs also

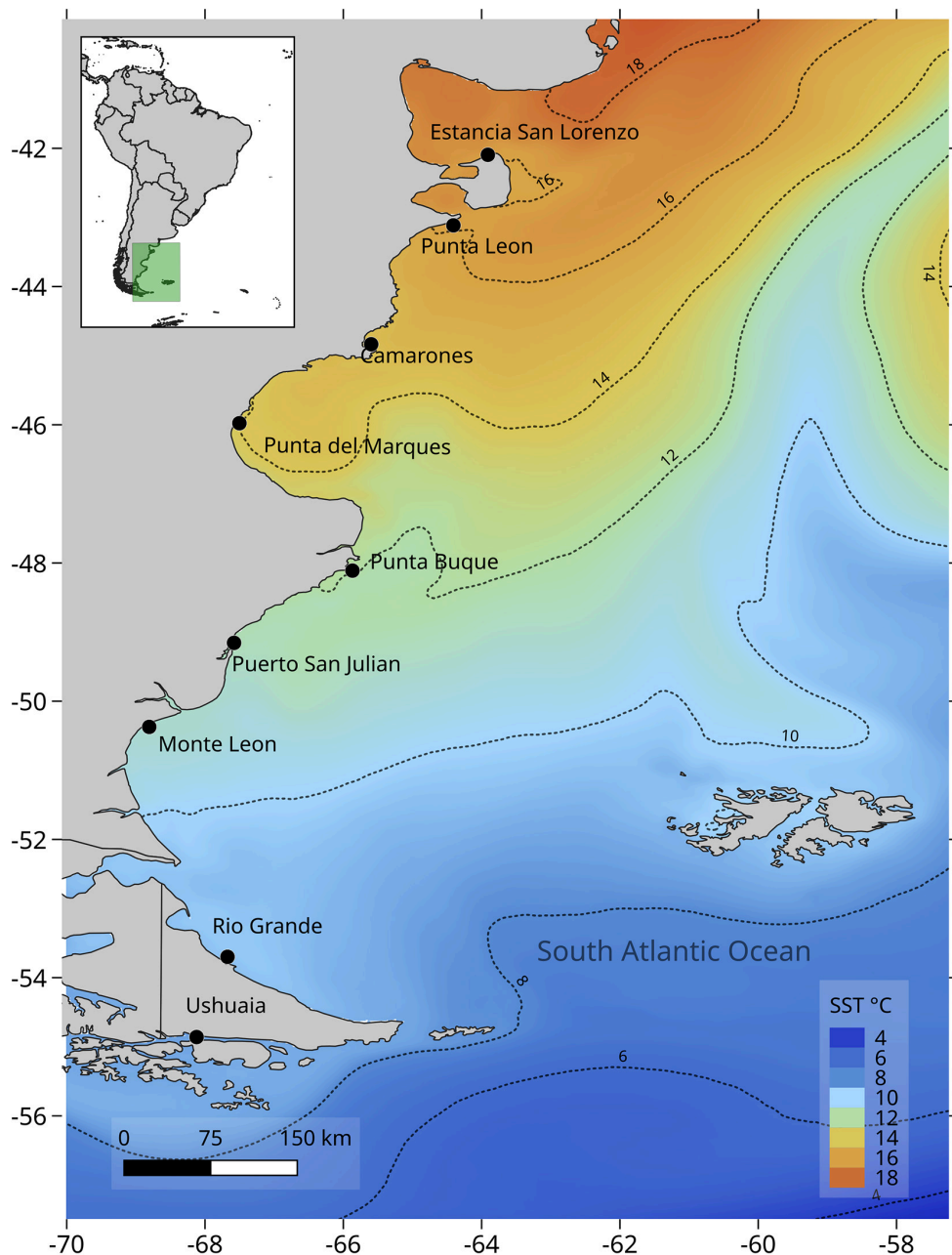
detected patterns in the distribution of the species assemblages on these coasts that were correlated with the SST and rainfall (Cruz-Motta et al., 2010). Atlantic Patagonia (41–55° S; 63–70° W) rocky intertidal shores were included as monitoring sites in the NaGISA-CoML and SARCE projects (Cruz-Motta et al., 2010, 2020; Rechimont et al., 2013; Miloslavich et al., 2016, among others) and are currently being included in MBON P2P. Communities within these habitats are exposed to particularly harsh environmental conditions that lead to adaptations of the local species (Bertness et al., 2006). In addition, a range of anthropogenic threats may add stress to communities and lead to changes in cover of dominant space occupiers (Mendez et al., 2017, 2021; Sorte et al., 2017).

Establishing a method that maximizes results and minimizes efforts is always a challenge for large-scale monitoring programs (Bax et al., 2019). Recently, a globally applicable and cost-effective method was tested for intertidal shore levels at two sites in northern Atlantic Patagonia by Livore et al. (2021). This method, non-destructive photographs of small parcels, showed similar results to others previously used for monitoring but required less time, knowledge and training in the field. The goal of the current study was to analyze that method's performance on a broader geographical scale. To do so, this study sampled intertidal assemblages along ~ 2,000 km of SW Atlantic Patagonian coastline using the afore mentioned method. The hypothesis was that the method would be capable of detecting differences among assemblages within two intertidal levels along the studied latitudinal scope as described by previous studies (Bertness et al., 2006; Rechimont et al., 2013; Raffo et al., 2014; Cruz-Motta et al., 2020). Furthermore, with the obtained data we identified biological indicators whose cover, presence or abundance can be followed in time through long-term monitoring programs on rocky intertidal shores. Finally, we explored potential relationships between the assemblages and relevant remotely sensed environmental variables (e.g., sea surface temperature, chlorophyll-*a* and seascape classes) as an illustration of their usefulness in long-term monitoring.

## MATERIALS AND METHODS

### Study Area

Sampling was carried out on the rocky intertidal shores of Atlantic Patagonia from Estancia San Lorenzo, Chubut (42.094° S; 63.910° W) to Ushuaia, Tierra del Fuego (54.849° S; 68.494° W). Nine locations were sampled along >2,000 km of coast (**Figure 1**). Rocky intertidal platforms sampled were exposed to semidiurnal tides with tidal amplitudes that ranged from 4 to 9 m. All locations presented an intertidal biological zonation: high (HT), mid (MT) and low (LT) intertidal. At some locations the HT were covered by pebbles and were impossible to sample, hence only MT and LT were included in this study. The MT was generally dominated by a matrix of mytilids that may include the scorched mussels *Brachidontes rodriguezii* and *Perumytilus purpuratus* as well as *Mytilus edulis*. The LT was generally characterized by several algal species including a large proportion of calcareous algae *Corallina* spp. as well as gastropods *Tegula*



**FIGURE 1** | Sampled locations in Atlantic Patagonia: Estancia San Lorenzo (ESL), Punta León (PLE), Camarones (CAM), Punta del Marqués (PMA), Punta Buque (PBU), Puerto San Julián (SJU), Monte León (MLE), Río Grande (RGR) and Ushuaia (USH). MUR SST mean climatological temperature for January–May. Source: <https://coastwatch.pfeg.noaa.gov/erddap/griddap/jplMURSST41clim.html>.

*patagonica* and *Trophon geversianus*, mytilids *Mytilus edulis* and *Aulacomya atra*, limpets from the genus *Nacella* and pulmonate limpets from the genus *Siphonaria* (Bertness et al., 2006; Raffo et al., 2014; Miloslavich et al., 2016).

## Sampling

Samples were collected between February and May 2017 during diurnal low tides. Percentage cover of sessile organisms was estimated from high definition photographs of 25 × 25 cm

quadrats haphazardly placed on the substrate ( $n = 15$  per level and location;  $n = 255$ , the LT of location San Julián could not be sampled). The compact camera (Nikon Coolpix AW 130) was fixed on a purposely built pvc-tube stand to standardize distance from the substrate. No zoom was used and the same setting was used throughout sampling. Photographs were analyzed using the free software Coral Point Count (CPCe V 4.1, Kohler and Gill, 2006). One hundred equidistant points were placed over the digital image and sessile organisms observed under each point

were registered to estimate cover. All organisms were identified to the lowest possible taxonomic level. Concurrently, all mobile organisms larger than  $\sim 1$  cm observed within the quadrat were also determined to the lowest possible taxonomic level and counted. For analysis, *Perumytilus purpuratus*, *Brachidontes rodriguezii*, *Aulacomya atra*, and *Mytilus edulis* were grouped within the category Mytilids, as identification to species level through photographs is unreliable. The same occurred for the red algae *Ceramium* sp. and *Polysiphonia* sp. and the pulmonate limpets *Siphonaria lessonii* and *S. lateralis*.

## Environmental Variables

Following the results of the SARCE project (Cruz-Motta et al., 2020), sea surface temperature (SST), chlorophyll-*a* concentration, photosynthetic active radiation (PAR), daily rainfall and air temperature, were extracted from different remote sensing sources (see **Supplementary Table S1** in the **Supplementary Material**). Data from 1 January 2016 to 31 May 2017 was used for all variables. Virtual stations were located up to 5 km offshore of the sampling station to avoid land interference and the land mask imposed by some of the products. The spatial resolution varied according to the data source, from 1 degree (air temperature) to 1 km [Multi-sensor Ultra-high Resolution (MUR)]. We included the novel seascape classification of the marine environment, as a multiscale, and synoptic characterization of the SST, salinity, chlorophyll-*a* and chromophoric dissolved organic matter (CDOM) represented as a catalog of classes (Kavanaugh et al., 2016).

## Data Analysis

Non-metric multi-dimensional scaling (nMDS) was used to visualize multivariate patterns in benthic assemblages cover at various scales. Benthic assemblage cover data were analyzed separately for each location and shore level using permutational analysis of variance (PERMANOVA) with the PERMANOVA extension in Primer v6.1.7 software (Anderson et al., 2008). Similarity matrices based on Bray-Curtis measure were generated on square-root transformed data for the analyses, which used 9,999 permutations of residuals under a reduced model (Anderson et al., 2008). PERMANOVA model had two factors: Location (Lo, random, 9 levels) and Intertidal Level (IL, fixed, 2 levels: MT and LT). Pairwise comparisons were performed among all pair of locations within each level to identify differences. SIMPER analyses were used to determine which taxa contributed more to similarity within samples. DistLM analyses were performed MT and LT assemblage data to identify and visualize taxa that contributed most ( $>0.60$  correlation) to the observed differences for each level.

A Kruskal-Wallis test was used to analyze differences in cover of the dominant categories for each intertidal level (i.e., Mytilids and bare substrate for MT and Coralline algae and bare substrate for LT), as they may be used as Environmental Ocean Variables in monitoring programs.

Abundances of mobile organisms that were recorded at five or more locations and exceeded a mean of 10 individuals  $m^{-2}$  across all locations, were compared through Kruskal-Wallis to analyze differences among locations. Taxa that were recorded at fewer

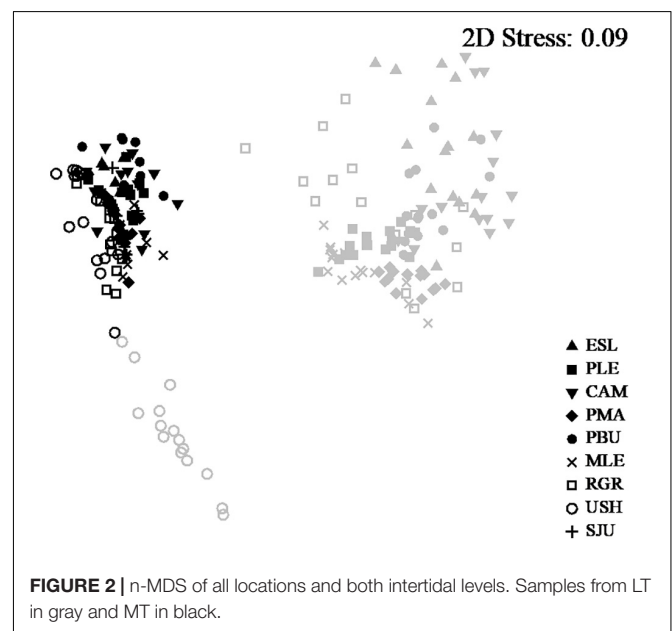
than five locations or had mean abundances  $<10$  individuals  $m^{-2}$  were not considered.

A correlation analysis between the Bray Curtis similarity matrix and the environmental variable matrix (using Gower similarity index) was performed with the BioEnv algorithm to establish potential relationships between both ordination arrangements (Clarke and Ainsworth, 1993).

## RESULTS

The photoquadrat protocol used in this study detected a total of 26 taxa for which cover was estimated from the MT and LT levels across more than 2,000 km of Atlantic Patagonian intertidal rocky shores. Four of these taxa were sessile invertebrates that include four species of mytilids (*Brachidontes rodriguezii*, *Perumytilus purpuratus*, *Mytilus edulis*, and *Aulacomya atra*) which were grouped for analysis and three species of barnacles (*Notobalanus flosculus*, *Notochthamalus scabrosus*, and *Balanus glandula*), whilst the remaining taxa were macroalgae.

The assemblages from the MT level were significantly different from the assemblages from the LT and among sampling Locations [PERMANOVA. LoxIL: *pseudo-F* = 27.82, *df* = 7, *p*(perm) < 0.001]. Pairwise comparisons showed that intertidal levels within each location differed significantly [all comparison (*p*(perm) > 0.001)]. In the same way, nm-MDS analysis showed separation of samples by intertidal level, with the LT of Ushuaia as the only assemblage that was clearly separate from all others (**Figure 2**). A high similarity within the studied range of both MT and LT was detected, with 84.92 and 76.71%, respectively. Within each level very few categories explained  $>80\%$  of the dissimilarity (**Table 1**). Those categories were Mytilids and to a lesser degree bare substrate in the MT. In the LT *Corallina* spp. was consistently the most explanatory category with several





**TABLE 1** | Results of SIMPER analysis for each location in the two tidal levels.

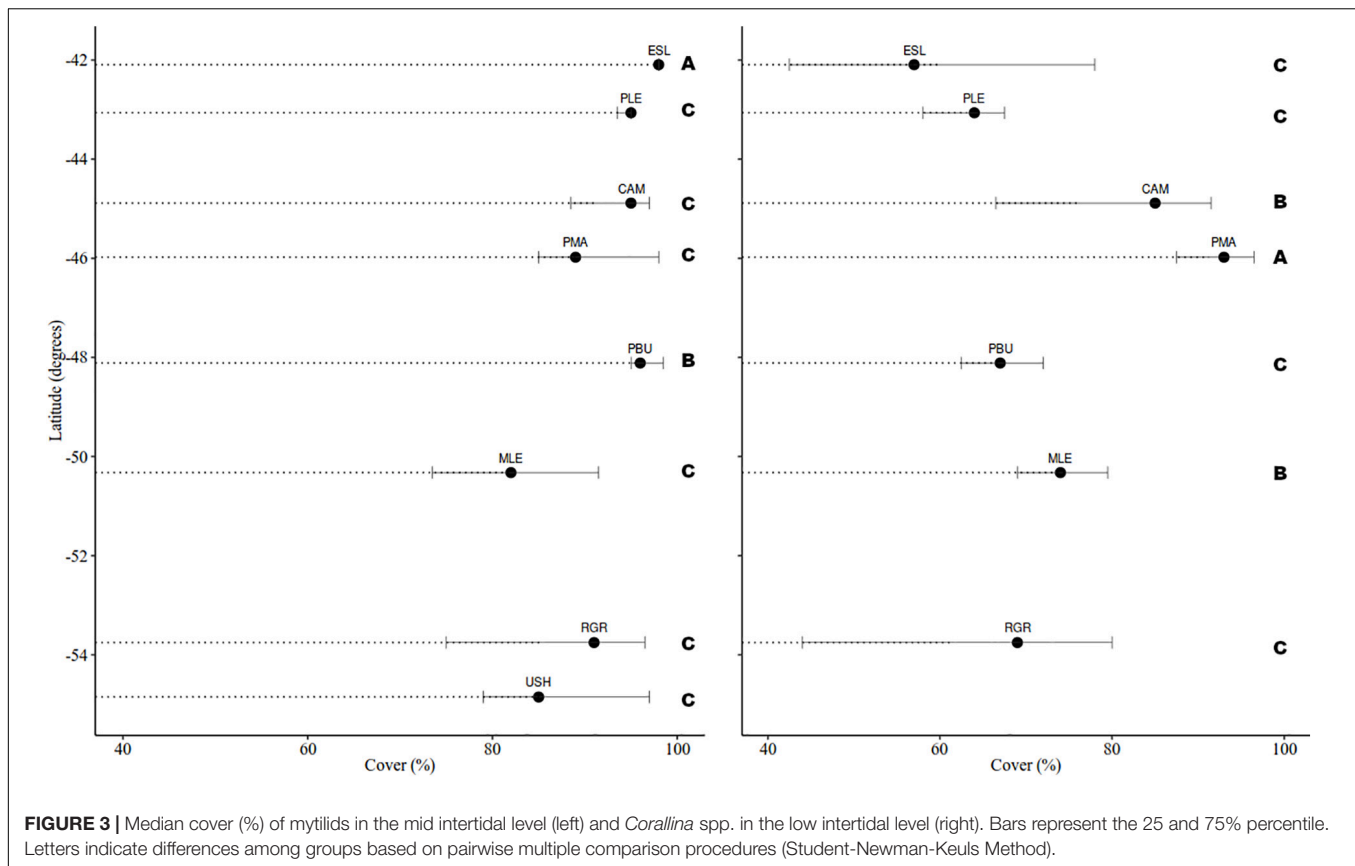
MT						LT				
	Species	Av.Abund	Av.Sim	Contrib%	Cum.%	Species	Av.Abund	Av.Sim	Contrib%	Cum.%
<b>ESL</b>			<b>Av. similarity: 95.79</b>					<b>Av. similarity: 73.19</b>		
	Mytilidae	9.89	82.31	85.93	85.93	<i>Corallina</i> spp.	7.61	43.81	59.85	59.85
						<i>Ulva</i> spp.	5.37	26.17	35.75	95.61
<b>PLE</b>			<b>Av. similarity: 92.27</b>					<b>Av. similarity: 83.75</b>		
	Mytilidae	9.68	70.89	76.83	76.83	<i>Corallina</i> spp.	7.94	40.7	48.6	48.6
	Bare substrate	1.89	10.66	11.56	88.38	Bare substrate	4.32	21.26	25.39	73.98
						<i>Ulva</i> spp.	2.45	10.04	11.99	85.98
<b>CAM</b>			<b>Av. similarity: 79.08</b>					<b>Av. similarity: 71.50</b>		
	Mytilidae	9.55	65.59	82.94	82.94	<i>Corallina</i> spp.	8.65	49.67	69.47	69.47
						<i>Ceramium</i> sp.	2.47	8.05	11.25	80.72
<b>PMA</b>			<b>Av. similarity: 85.53</b>					<b>Av. similarity: 89.23</b>		
	Mytilidae	9.41	71.93	84.1	84.1	<i>Corallina</i> spp.	9.55	71.65	80.3	80.3
<b>PBU</b>			<b>Av. similarity: 81.93</b>					<b>Av. similarity: 76.26</b>		
	Mytilidae	9.79	75	91.54	91.54	<i>Corallina</i> spp.	8.15	40.81	53.51	53.51
						<i>Ulva</i> spp.	2.96	11.71	15.36	68.87
						<i>Ceramium</i> sp.	2.73	9.75	12.78	81.65
<b>SJU</b>			<b>Av. similarity: 87.71</b>					<b>was not sampled</b>		
	Mytilidae	9.41	71.84	81.9	81.9					
<b>MLE</b>			<b>Av. similarity: 86.79</b>					<b>Av. similarity: 82.16</b>		
	Mytilidae	9.05	65.34	75.29	75.29	<i>Corallina</i> spp.	8.62	50.44	61.39	61.39
	Bare substrate	3.78	21.12	24.34	99.63	Mytilidae	3.38	15.37	18.71	80.1
								<b>Av. similarity: 65.55</b>		
<b>RGR</b>			<b>Av. similarity: 79.88</b>							
	Mytilidae	9.2	63.68	79.72	79.72	<i>Corallina</i> spp.	7.7	36.69	55.97	55.97
	Bare substrate	2.8	11.8	14.77	94.49	Mytilidae	3.6	10.23	15.6	71.57
						<i>Ulva</i> spp.	2.23	6.43	9.82	81.39
<b>USH</b>			<b>Av. similarity: 75.27</b>					<b>Av. similarity: 72.04</b>		
	Mytilidae	9.2	59.16	78.59	78.59	Bare substrate	5.04	19.6	27.21	27.21
	Undetermined algae	1.15	5.34	7.09	85.68	Encrusting coralline algae	4.9	19.23	26.69	53.9
						Mytilidae	4.26	15.29	21.22	75.12
						<i>Notochthamalus scabrosus</i>	4.2	14.81	20.56	95.69

other categories with much lower values alternating among locations (Table 1).

Cover in MT was consistently dominated by mytilids with average cover ranging from 82 to 98%, yet differences were detected among groups ( $H = 32.917$ ,  $df = 8$ ,  $p < 0.001$ ) (Figure 3). Bare substrate cover differed within the studied geographical range ( $H = 52.978$ ,  $df = 8$ ,  $p < 0.001$ ) and ranged from 0.27 to 16.53% (MLE > PMA = SJU = RGR > USH > PLE > CAM > PBU > ESL). In the MT bare substrate (50%), the alga *Pyropia* sp. (14%) and the two barnacles *Balanus glandula* (11%) and

*Notochthamalus scabrosus* (10%) explained 85% of the observed variation (Figure 4A).

Cover in the LT was generally dominated by the alga *Corallina* spp. except in USH where mytilids had larger cover (mean: 21.33%). *Corallina* spp. cover, when present, ranged from 60 to 91% and differences among groups were detected ( $H = 69.530$ ,  $df = 7$ ,  $p < 0.001$ ) (Figure 3). Bare substrate cover also differed within the studied area ( $H = 85.123$ ,  $df = 7$ ,  $p < 0.001$ ) and ranged from 27.80 to 0.40% (USH = PLE > MLE > PMA = PBU > RGR > CAM = ESL). In the LT *Corallina* spp. (47%), *Ulva* spp. (18%), *Ceramium* sp. and



*Polysiphonia* sp. (10%), mytilids (8%), and bare substrate (7%) accounted for 90% of the observed variation (Figure 4B).

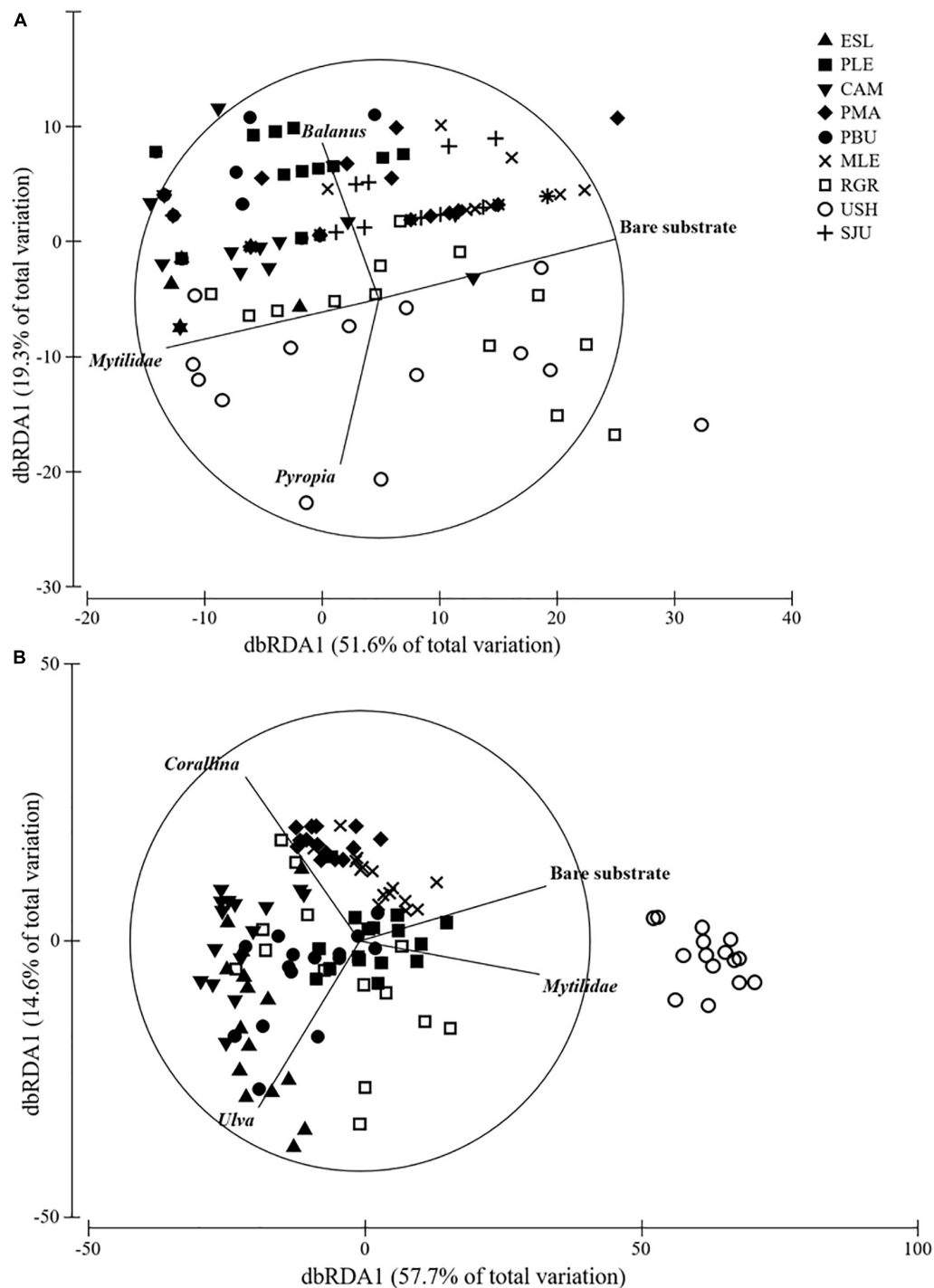
A total of 13 taxa of mobile macroinvertebrates were found within all the study locations: the sea anemones *Parabunodactis imperfecta* and *Bunodactis octoradiata*, the gastropods *Siphonaria lessonii*, *S. lateralis*, *Nacella magellanica*, *Pareuthria fuscata*, *Tegula patagonica*, *Fissurella radiosa*, and *Trophon geversianus*, undetermined chitons that were grouped, the isopod *Exosphaeroma* sp. and the sea urchin *Arbacia dufresnii*. Abundances of only *Siphonaria* spp. (*S. lessonii* and *S. lateralis*) in MT and *N. magellanica* in LT were of relevance (mean abundance  $>10$  individuals  $m^{-2}$ ) for statistical analysis. Abundance of *Siphonaria* spp. ranged from 0 to 512 individuals  $m^{-2}$  and differed among locations ( $H = 113.282$ ,  $df = 8$ ,  $p < 0.001$ ,  $SJU > MLE = USH > PLE > CAM = PMA = PBU > ESL = RGR$ ). *N. magellanica* ranged from 0 to 204 individuals  $m^{-2}$  being highest in USH and different than all other locations ( $H = 77.253$ ,  $df = 7$ ,  $p < 0.001$ ).

Three seascape classes were observed in the region during the studied period (Table 2). Among all the studied environmental variables, the number of seascapes classes alone, number of seascapes classes and PAR, and SST, number of seascapes classes and number of switches between seascapes classes were the models that best explained assemblage variability present at each sampling location during the 2017 summer (BioEnv  $r = 0.60, 0.59$ , and  $0.56$ , respectively).

## DISCUSSION

The results of this study demonstrate that the simple, low-cost, low-tech method used here is capable of detecting differences in assemblage structure along an extension of  $\sim 2,000$  kilometers of Atlantic Patagonian coast. Differences among assemblages from two levels of air exposure within this broad geographic scale were clearly identified. Despite the low variability in each exposure level, the method was able to detect differences among assemblages and in the dominant taxa percentage cover. The method allows for the adequate collection of useful cover data of sessile species and abundance of some slow moving taxa which can be linked to remotely accessible environmental data.

Visual methods performed *in situ*, such as the NaGISA protocols (Rigby et al., 2007) used in previous large-scale programs, can take up to 2 days at a single site to obtain the desired data whilst the method employed here required a single day. This non-destructive method can be repeated at the same locations throughout an extended period of time and can be applied by scientist globally due its simplicity and low cost. Concurrently, it is suitable to determine changes in cover or abundance in several indicators as reported here. Identification of organisms to a low taxonomic level and the impossibility of viewing primary cover when dense algal stands are present are the most important limitations the used method has (Livore et al., 2021). Hence, for detailed description of intertidal communities, such as species



**FIGURE 4 |** DistLM analysis of **(A)** MT and **(B)** LT assemblages. Vectors show variables that had >0.6 correlation (Spearman).

richness and diversity, this may not be suitable. However, for large-scale long-term studies focusing on major changes in primary space occupying species this method should be broadly applicable.

This study identified taxa whose changes in cover largely explained the changes in assemblage structure at the two

described intertidal levels. For the mid intertidal mytilids, bare substrate and *Balanus glandula* were the variables that better explained the observed patterns, whilst for the low intertidal *Corallina* spp., bare substrate and mytilids, explained most of the variability. We propose mytilids and *Corallina* spp., in particular, as biological indicators for broad scale monitoring

**TABLE 2 |** Seascapes classes present in the study region during the period January 2016–May 2017.

Seascape class ID number	Nominal descriptor	Latitude	Dominant hemisphere	Dominant season
14	Temperate blooms upwelling	Temperate/subpolar	Both	Spring summer
19	Arctic/subpolar shelves	Temperate/subpolar	Both	Year round
21	Warm, blooms, high nuts	Tropical/subtropical	Both	Winter/year-round

From Kavanaugh et al., 2016.

programs because they are cosmopolitan taxa with a conspicuous presence, they have a low probability of misidentification, they are ecologically relevant (i.e., habitat forming species that sustain many other dependent species) and they respond to human stressors or changes in environmental conditions (Kelaher, 2003; Liuzzi and López Gappa, 2008; Buschbaum et al., 2009; Olabarria et al., 2016; Vinagre et al., 2016). Concurrently, bare substrate is proposed as another indicator because changes in this variable reflect either settlement or disappearance of primary space holders, which are often also habitat forming species. Hence, changes in the relative cover of bare substrate directly indicate changes in assemblage structure (Pickett and White, 2013; Mendez et al., 2019). Two algae, *Pyropia* sp. and *Ulva* spp. also contributed to the observed patterns in the mid and low intertidal, respectively. However, the high natural fluctuation along with the limited distribution of these taxa suggest they may be less appropriate indicators for long-term, large-scale studies (Raffo et al., 2014). There may be other suitable indicators that may be considered upon application of the method along the American coastline.

The use of this simple method also allows the possibility of relating assemblages with remotely obtained environmental variables. This study was able to detect a correlation between seascape classes and biotic assemblages of individual locations. Linking environmental variables collected from remote sensing platforms offshore the sampling sites may represent a potential source of error (Turner et al., 2003). However, this feature provides easily accessible environmental data for remote locations where almost no local continuous environmental data exists. The global seascape classes appear as a very promising environmental predictor as they summarize the interaction and variability in time of multiple variables in a typology of pelagic realms (Kavanaugh et al., 2016). The correlation between the classes and the community structure of pelagic communities has recently been demonstrated (Montes et al., 2020). However, this is the first time that pelagic seascapes are related to rocky shores assemblages. The alternation between the predominant classes might result in a robust predictor for the changes in cover/abundance of the main groups that form the intertidal coastal communities. In this sense, long-term monitoring programs will provide replication in time of assemblage data and seascape information which combined, as in this study, can be used as a synoptic and integrating assessment tool.

The macroecology approach brought together ecology and biogeography in the early 1990s in the sense that ecologists recognized that external influences may strongly affect community structure, whilst biogeographers acknowledged that

community events may have broad significance on distribution patterns (Briggs, 2007). Within this framework, regional scale studies with consistent and extensive local sampling that describe assemblages are needed to appropriately address ecological process and geographic distribution. Without this knowledge there is a risk of a continuous description of heterogeneity without the capability of integration to address broader scale problems (Connell and Irving, 2008). The current study is a step in that direction, describing dissimilarities in assemblages along ~ 2,000 kilometers of largely unexplored coasts of Atlantic Patagonia. In our study changes in the assemblages were moderately associated to four environmental variables. The lack of a more distinct pattern in the studied assemblages could be suggesting that biodiversity of these rocky intertidal habitats is likely driven by a combination of factors that operate at different spatiotemporal scales as has been suggested for other marine communities (Witman et al., 2004; Connell and Irving, 2008; Cruz-Motta et al., 2020).

Whilst recent efforts are encouraging and supporting long-term and large-scale monitoring programs that integrate scientist at the continental level, they are still scarce (Canonico et al., 2019 and references therein). This could be due, at least in part, to the difficulties of finding methodologies that are both scientifically robust, practically achievable and logistically inexpensive in order for it to be accessible and feasible to a wider range of potential participants (Stephenson et al., 2017). The method employed here complies with all the above mentioned attributes and is therefore suggested for use in long-term and broad-scale monitoring programs such as MBON P2P. Its application within the MBON P2P will provide information on the associations among assemblages along the American coastline and test the proposed ecological indicators. When coupled with environmental variables that are remotely and easily accessible they could provide the tools for an integrative approach to an informed coastal management.

## DATA AVAILABILITY STATEMENT

The raw data supporting the conclusions of this article will be made available by the authors, without undue reservation.

## AUTHOR CONTRIBUTIONS

JL conceived the project, participated in data collection in the field and lab, data processing, and wrote the manuscript with contribution from all authors. MM conceived the project,



participated in data collection in the field and lab, and reviewed the manuscript. LA participated in data collection in the field and lab, and reviewed the manuscript. EK collected and processed environmental and seascape data and reviewed the manuscript. GB conceived the project and reviewed the manuscript.

## FUNDING

This work was financially supported by the Conservation, Food and Health Foundation, ANPCyT-FONCyT (PICT 2015-0841 and PICT 2018-0969).

## ACKNOWLEDGMENTS

We would like to thank Carmen Gilardoni for organization and support for field trips. We also thank Florencia Cremonte, Muriel Demetrio, Joaquin Vietto, Tabare Barreto, Lucía Epherra, and

Jose Fernandez Alfaya for field collaborations. The manuscript was improved by the comments of two reviewers. Special thanks to the provincial authorities of Chubut, Santa Cruz, and Tierra del Fuego, and Administración de Parques Nacionales for allowing us to work inside natural protected areas (permit number 143-SsCyAP/16). We also thank Estancia San Lorenzo for access to that sampling location. This is publication #153 of the Laboratorio de Reproducción y Biología Integrativa de Invertebrados Marinos (LAR BIM).

## SUPPLEMENTARY MATERIAL

The Supplementary Material for this article can be found online at: <https://www.frontiersin.org/articles/10.3389/fmars.2021.589489/full#supplementary-material>

**Supplementary Table 1** | List of environmental variables used in analyses.

## REFERENCES

- Anderson, M., Gorley, R., Clarke, K., Anderson, M., Gorley, R., Clarke, K., et al. (2008). *PERMANOVA+ for PRIMER. Guide to Software and Statistical Methods*. Plymouth: PRIMER-E.
- Bax, N. J., Miloslavich, P., Muller-Karger, F. E., Allain, V., Appeltans, W., Batten, S. D., et al. (2019). A response to scientific and societal needs for marine biological observations. *Front. Mar. Sci.* 6:395. doi: 10.3389/fmars.2019.00395
- Bertness, M. D., Crain, C. M., Silliman, B. R., Bazterrica, M. C., Reyna, M. V., Hildago, F., et al. (2006). The community structure of Western Atlantic Patagonian rocky shores. *Ecol. Monogr.* 76, 439–460.
- Briggs, J. C. (2007). Marine biogeography and ecology: invasions and introductions. *J. Biogeogr.* 34, 193–198. doi: 10.1111/j.1365-2699.2006.01632.x
- Buschbaum, C., Dittmann, S., Hong, J.-S., Hwang, I.-S., Strasser, M., Thiel, M., et al. (2009). Mytilid mussels: global habitat engineers in coastal sediments. *Helgol. Mar. Res.* 63, 47–58.
- Canonica, G., Buttigieg, P. L., Montes, E., Muller-Karger, F. E., Stepien, C., Wright, D., et al. (2019). Global observational needs and resources for marine biodiversity. *Front. Mar. Sci.* 6:367. doi: 10.3389/fmars.2019.00367
- Clarke, K. R., and Ainsworth, M. (1993). A method of linking multivariate community structure to environmental variables. *Mar. Ecol. Progr. Ser.* 92, 205–219.
- Connell, S. D., and Irving, A. D. (2008). Integrating ecology with biogeography using landscape characteristics: a case study of subtidal habitat across continental Australia. *J. Biogeogr.* 35, 1608–1621.
- Cruz-Motta, J. J., Miloslavich, P., Guerra-Castro, E., Hernández-Agreda, A., Herrera, C., Barros, F., et al. (2020). Latitudinal patterns of species diversity on South American rocky shores: local processes lead to contrasting trends in regional and local species diversity. *J. Biogeogr.* 47, 1966–1979. doi: 10.1111/jbi.13869
- Cruz-Motta, J. J., Miloslavich, P., Palomo, G., Iken, K., Konar, B., Pohle, G., et al. (2010). Patterns of spatial variation of assemblages associated with intertidal rocky shores: a global perspective. *PLoS One* 5:e14354. doi: 10.1371/journal.pone.0014354
- Duffy, J. E., Benedetti-Cecchi, L., Trínanes, J., Muller-Karger, F. E., Ambo-Rappe, R., Boström, C., et al. (2019). Toward a coordinated global observing system for seagrasses and marine macroalgae. *Front. Mar. Sci.* 6:317. doi: 10.3389/fmars.2019.00317
- Emery, K. O., and Kuhn, G. G. (1982). Sea cliffs: their processes, profiles, and classification. *GSA Bulletin* 93, 644–654.
- Galparsoro, I., Borja, A., and Uyarra, M. C. (2014). Mapping ecosystem services provided by benthic habitats in the European North Atlantic Ocean. *Front. Mar. Sci.* 1:23. doi: 10.3389/fmars.2014.00023
- Granja, H. M. (2004). “Rocky coasts,” in *Coastal Zone And Estuaries*, eds F. I. Isla and O. Iribarne (Oxford: EOLSS Publishers), 135–163.
- Kavanaugh, M. T., Oliver, M. J., Chavez, F. P., Letelier, R. M., Muller-Karger, F. E., and Doney, S. C. (2016). Seascapes as a new vernacular for pelagic ocean monitoring, management and conservation. *ICES J. Mar. Sci.* 73, 1839–1850.
- Kelaker, B. P. (2003). Changes in habitat complexity negatively affect diverse gastropod assemblages in coralline algal turf. *Oecologia* 135, 431–441.
- Kohler, K. E., and Gill, S. M. (2006). Coral point count with excel extensions (CPCe): a visual basic program for the determination of coral and substrate coverage using random point count methodology. *Comput. Geosci.* 32, 1259–1269. doi: 10.1016/j.cageo.2005.11.009
- Kron, W. (2013). Coasts: the high-risk areas of the world. *Nat. Hazards* 66, 1363–1382. doi: 10.1007/s11069-012-0215-4
- Liuzzi, M. G., and López Gappa, J. (2008). Macrofaunal assemblages associated with coralline turf: species turnover and changes in structure at different spatial scales. *Mar. Ecol. Progr. Ser.* 363, 147–156.
- Livore, J. P., Mendez, M. M., Miloslavich, P., Rilov, G., and Bigatti, G. (2021). Biodiversity monitoring in rocky shores: challenges of devising a globally applicable and cost-effective protocol. *Ocean Coast. Manag.* 205:105548.
- Mendez, M. M., Livore, J. P., and Bigatti, G. (2019). Interaction of natural and anthropogenic stressors on rocky shores: community resistance to trampling. *Mar. Ecol. Progr. Ser.* 631, 117–126.
- Mendez, M. M., Livore, J. P., Calcagno, J. A., and Bigatti, G. (2017). Effects of recreational activities on Patagonian rocky shores. *Mar. Environ. Res.* 130, 213–220.
- Mendez, M. M., Livore, J. P., Márquez, F., and Bigatti, G. (2021). Mass mortality of foundation species on rocky shores: testing a methodology for a continental monitoring program. *Front. Mar. Sci.* 8:620866. doi: 10.3389/fmars.2021.620866
- Miloslavich, P., Bax, N. J., Simmons, S. E., Klein, E., Appeltans, W., Aburto-Oropeza, O., et al. (2018). Essential ocean variables for global sustained observations of biodiversity and ecosystem changes. *Glob. Chang. Biol.* 24, 2416–2433. doi: 10.1111/gcb.14108
- Miloslavich, P., Cruz-Motta, J. J., Hernández, A., Herrera, C., Klein, E., Barros, F., et al. (2016). Benthic assemblages in South American intertidal rocky shores: biodiversity, services, and threats. *Mar. Benthos* 83–137.
- Miloslavich, P., Seeyave, S., Muller-Karger, F., Bax, N., Ali, E., Delgado, C., et al. (2019). Challenges for global ocean observation: the need for increased human capacity. *J. Operat. Oceanogr.* 12(sup2), S137–S156. doi: 10.1080/1755876X.2018.1526463
- Montes, E., Djurhuus, A., Muller-Karger, F. E., Otis, D., Kelble, C. R., and Kavanaugh, M. T. (2020). Dynamic satellite seascapes as a biogeographic framework for understanding phytoplankton assemblages in the Florida Keys

- National Marine Sanctuary, United States. *Front. Mar. Sci.* 7:575. doi: 10.3389/fmars.2020.00575
- Olabarria, C., Gestoso, I., Lima, F. P., Vázquez, E., Comeau, L. A., Gomes, F., et al. (2016). Response of Two Mytilids to a Heatwave: The Complex Interplay of Physiology, Behaviour and Ecological Interactions. *PLoS One* 11:e0164330. doi: 10.1371/journal.pone.0164330
- Pickett, S. T., and White, P. S (Eds.) (2013). *The Ecology of Natural Disturbance And Patch Dynamics*. New York, NY: Elsevier.
- Raffo, M. P., Lo Russo, V., and Schwindt, E. (2014). Introduced and native species on rocky shore macroalgal assemblages: zonation patterns, composition and diversity. *Aquat. Bot.* 112, 57–65. doi: 10.1016/j.aquabot.2013.07.011
- Rechimont, M. E., Galván, D. E., Sueiro, M. C., Casas, G., Piriz, M. L., Diez, M. E., et al. (2013). Benthic diversity and assemblage structure of a north Patagonian rocky shore: a monitoring legacy of the NaGISA project. *J. Mar. Biol. Assoc. U. K.* 93, 2049–2058. doi: 10.1017/S0025315413001069
- Rigby, P. R., Iken, K., and Shirayama, Y. (2007). *Sampling Biodiversity in Coastal Communities: NaGISA Protocols for Seagrass and Macroalgal Habitats*. Singapore: NUS Press.
- Small, C., and Nicholls, R. J. (2003). A global analysis of human settlement in coastal zones. *J. Coast. Res.* 19, 584–599.
- Sorte, C. J., Davidson, V. E., Franklin, M. C., Benes, K. M., Doellman, M. M., Etter, R. J., et al. (2017). Long-term declines in an intertidal foundation species parallel shifts in community composition. *Glob. Chang. Biol.* 23, 341–352.
- Stephenson, P. J., Bowles-Newark, N., Regan, E., Stanwell-Smith, D., Diagana, M., Höft, R., et al. (2017). Unblocking the flow of biodiversity data for decision-making in Africa. *Biol. Conserv.* 213, 335–340. doi: 10.1016/j.biocon.2016.09.003
- Turner, W., Spector, S., Gardiner, N., Fladeland, M., Sterling, E., and Steininger, M. (2003). Remote sensing for biodiversity science and conservation. *Trends Ecol. Evol.* 18, 306–314.
- Vinagre, P. A., Pais-Costa, A. J., Gaspar, R., Borja, Á, Marques, J. C., and Neto, J. M. (2016). Response of macroalgae and macroinvertebrates to anthropogenic disturbance gradients in rocky shores. *Ecol. Indic.* 61, 850–864. doi: 10.1016/j.ecolind.2015.10.038
- Witman, J. D., Etter, R. J., and Smith, F. (2004). The relationship between regional and local species diversity in marine benthic communities: a global perspective. *Proc. Nat. Acad. Sci. U.S.A.* 101:15664. doi: 10.1073/pnas.0404300101

**Conflict of Interest:** The authors declare that the research was conducted in the absence of any commercial or financial relationships that could be construed as a potential conflict of interest.

Copyright © 2021 Livore, Mendez, Klein, Arribas and Bigatti. This is an open-access article distributed under the terms of the Creative Commons Attribution License (CC BY). The use, distribution or reproduction in other forums is permitted, provided the original author(s) and the copyright owner(s) are credited and that the original publication in this journal is cited, in accordance with accepted academic practice. No use, distribution or reproduction is permitted which does not comply with these terms.



# Beyond Post-release Mortality: Inferences on Recovery Periods and Natural Mortality From Electronic Tagging Data for Discarded Lamnid Sharks

Heather D. Bowlby<sup>1\*</sup>, Hugues P. Benoît<sup>2</sup>, Warren Joyce<sup>1</sup>, James Sulikowski<sup>3</sup>, Rui Coelho<sup>4,5</sup>, Andrés Domingo<sup>6</sup>, Enric Cortés<sup>7</sup>, Fabio Hazin<sup>8</sup>, David Macias<sup>9</sup>, Gérard Biais<sup>10</sup>, Catarina Santos<sup>4,5</sup> and Brooke Anderson<sup>3</sup>

<sup>1</sup> Bedford Institute of Oceanography, Fisheries and Oceans Canada, Dartmouth, NS, Canada, <sup>2</sup> Institut Maurice-Lamontagne, Fisheries and Oceans Canada, Mont-Joli, QC, Canada, <sup>3</sup> School of Mathematical and Natural Sciences, Arizona State University, Glendale, AZ, United States, <sup>4</sup> Portuguese Institute for the Ocean and Atmosphere (IPMA, I.P.), Olhão, Portugal, <sup>5</sup> Centre of Marine Sciences of the Algarve (CCMAR), University of Algarve, Faro, Portugal, <sup>6</sup> Laboratorio de Recursos Pelágicos, Dirección Nacional de Recursos Acuáticos, Montevideo, Uruguay, <sup>7</sup> Panama City Laboratory, NOAA Fisheries, Southeast Fisheries Science Center, Panama, FL, United States, <sup>8</sup> Department of Fishing and Aquaculture, Universidade Federal Rural de Pernambuco, Recife, Brazil, <sup>9</sup> Oceanographic Center of Malaga, Spanish Institute of Oceanography, Málaga, Spain, <sup>10</sup> Ifremer, Laboratoire LIENSs, Université de La Rochelle, Nantes, France

## OPEN ACCESS

### Edited by:

Juan Carlos Azofeifa-Solano,  
University of Costa Rica, Costa Rica

### Reviewed by:

Luis Cardona,  
University of Barcelona, Spain  
Tatiana Araya,  
University of Costa Rica, Costa Rica

### \*Correspondence:

Heather D. Bowlby  
heather.bowlby@dfo-mpo.gc.ca

### Specialty section:

This article was submitted to  
Marine Megafauna,  
a section of the journal  
Frontiers in Marine Science

**Received:** 19 October 2020

**Accepted:** 15 March 2021

**Published:** 07 April 2021

### Citation:

Bowlby HD, Benoît HP, Joyce W, Sulikowski J, Coelho R, Domingo A, Cortés E, Hazin F, Macias D, Biais G, Santos C and Anderson B (2021) Beyond Post-release Mortality: Inferences on Recovery Periods and Natural Mortality From Electronic Tagging Data for Discarded Lamnid Sharks. *Front. Mar. Sci.* 8:619190. doi: 10.3389/fmars.2021.619190

Accurately characterizing the biology of a pelagic shark species is critical when assessing its status and resilience to fishing pressure. Natural mortality ( $M$ ) is well known to be a key parameter determining productivity and resilience, but also one for which estimates are most uncertain. While  $M$  can be inferred from life history, validated direct estimates are extremely rare for sharks. Porbeagle (*Lamna nasus*) and shortfin mako (*Isurus oxyrinchus*) are presently overfished in the North Atlantic, but there are no directed fisheries and successful live release of bycatch is believed to have increased. Understanding  $M$ , post-release mortality (PRM), and variables that affect mortality are necessary for management and effective bycatch mitigation. From 177 deployments of archival satellite tags, we inferred mortality events, characterized physiological recovery periods following release, and applied survival mixture models to assess  $M$  and PRM. We also evaluated covariate effects on the duration of any recovery period and PRM to inform mitigation. Although large sample sizes involving extended monitoring periods (>90 days) would be optimal to directly estimate  $M$  from survival data, it was possible to constrain estimates and infer probable values for both species. Furthermore, the consistency of  $M$  estimates with values derived from longevity information suggests that age determination is relatively accurate for these species. Regarding bycatch mitigation, our analyses suggest that juvenile porbeagle are more susceptible to harm during capture and handling, that keeping lamnid sharks in the water during release is optimal, and that circle hooks are associated with longer recovery periods for shortfin mako.

**Keywords:** Natural mortality, recovery period, lamnid sharks, Atlantic, survival, mitigation, bycatch

## INTRODUCTION

Quantifying fishing-related ( $F$ ) and natural ( $M$ ) mortality continues to be one of the main challenges in understanding and managing marine fauna. Representative starting values and priors for  $M$  are needed for demographic analyses (e.g., Cortés, 2016), evaluating resilience to population decline (e.g., Gedamke et al., 2007; Au et al., 2015), estimating extinction risk (e.g., García et al., 2008), and stock assessment (e.g., Cortés, 1998, 2002). For elasmobranchs in particular,  $M$  is typically approximated from life history information, using previously derived functional relationships with longevity, growth or size (Kenchington, 2014; Cortés, 2016; Pardo et al., 2016). To varying extents, common methods rely on age determination, and are calculated from theoretical longevity, length-at-age and weight-at-age relationships, and/or von Bertalanffy growth function parameters (reviewed in Kenchington, 2014). This means all methods are sensitive to the level of uncertainty in age determination for elasmobranchs, where longevity specifically may be systematically underestimated (Campana et al., 2002; Harry, 2018; Natanson et al., 2018). Underestimation of maximum age results in an overestimation of  $M$  from life-history based methods. There is a pressing need to move away from life-history based estimates of  $M$  to more direct estimates derived from species-specific data. Electronic tagging is an important source of information on movement, habitat associations and survival of large pelagic fishes (Hammerschlag and Sulikowski, 2011; Hazen et al., 2012), and provides an opportunity to directly estimate natural mortality from survival data (e.g., Benoît et al., 2015, 2020a). Nonetheless the substantial cost associated with archival tags still constrains sample sizes (Hazen et al., 2012) and poses a particular challenge for reliable estimation of  $M$  for long-lived species.

Pelagic sharks tend to have high interaction rates with high-seas fisheries targeting swordfish and tunas, and the majority of global shark catches represent bycatch (Lewison et al., 2004; Oliver et al., 2015). The magnitude of shark bycatch and the need for mitigation to reduce population declines (Dulvy et al., 2014) have driven recent research on shark survivorship following release (Ellis et al., 2017; Miller et al., 2020). In the North Atlantic, shortfin mako (*Isurus oxyrinchus*) and porbeagle (*Lamna nasus*) are two species for which landings have decreased in recent years and discard rates are increasing as a result of national and international management measures. A large proportion of discards have the potential to be released alive, given that estimated at-vessel mortality rates range from 35–56% for shortfin mako and 21–44% for porbeagle (reviewed in Ellis et al., 2017). Although quantifying rates of post-release mortality (PRM) remains a priority for future stock assessments to improve estimates of total removals, additional consideration of variables that affect survivorship is critical to develop effective bycatch mitigation measures (Davis, 2002; Ellis et al., 2017).

Capture and handling are two separate processes that can influence survivorship of bycatch (Benoît et al., 2012). For the majority of species, different handling protocols in addition to tagging effects are very rarely evaluated because they are assumed to be negligible in relation to capture effects (Musyl et al., 2009; Molina and Cooke, 2012; Jepsen et al., 2015). For sharks, research

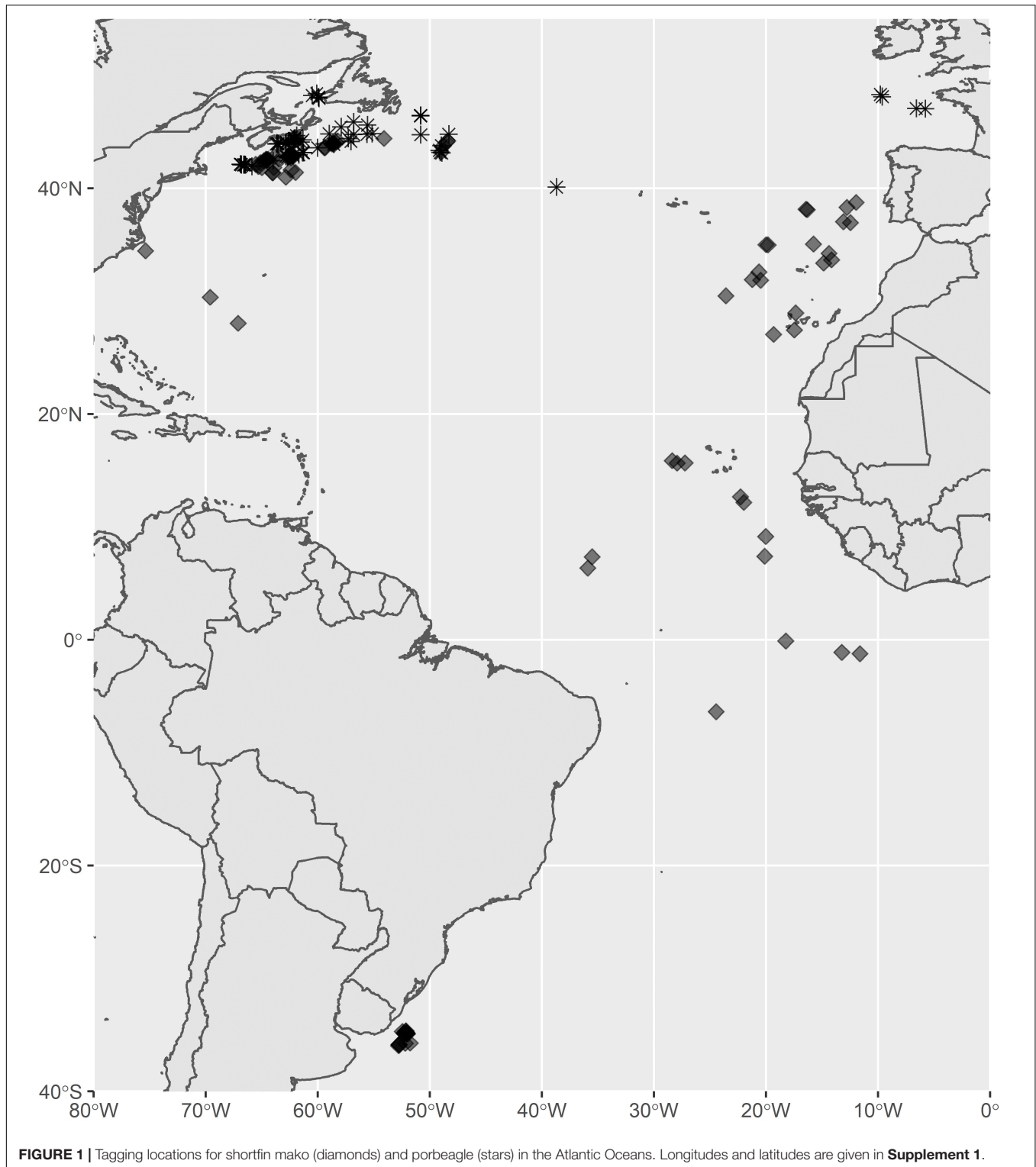
on survivorship tends to consider only covariates with at-vessel and/or post-release mortality. In general, lamnid sharks appear to be quite resilient to various types of capture and handling (Musyl and Gilman, 2019). However, sublethal effects on behavior and/or physiology are likely even though individuals survive (Skomal, 2007). Several studies report changes in swimming and dive behavior upon release, indicative of a recovery period (e.g., Skomal and Chase, 2002; Sippel et al., 2011; Wilson et al., 2014; Whitney et al., 2016). Any behavioral changes associated with recovery from physiological stress may ultimately contribute to mortality by making animals more susceptible to disease or predation, less able to forage, and/or more susceptible to recapture (Davis, 2002; Jepsen et al., 2015). Thus, mitigation measures designed to reduce the duration of any recovery period following release or to minimize capture and handling effects could be relevant when developing best practices to reduce shark bycatch mortality.

For this study, we compiled data from satellite tagging on porbeagle and shortfin mako sharks in the North Atlantic. Deployments were conducted by Canada, the United States, Portugal, and by the International Commission for the Conservation of Atlantic Tunas (ICCAT) through the Shark Research and Data Collection Program. Of the shark species whose status is regularly assessed at ICCAT, shortfin mako and porbeagle are currently considered overfished with a very high probability (ANON, 2019, 2020). Recovery planning for both species would benefit from improved mortality estimates for stock assessment, as well as from the development of best-practices for mitigation of bycatch mortality. For these purposes, our objectives were to infer  $M$  from survivorship data in light of relatively small sample size, to characterize any recovery period following tagging from changes in dive depths and periodicity, and to evaluate covariate effects on PRM and/or the duration of any recovery period.

## MATERIALS AND METHODS

This study combined data from 177 archival satellite tag deployments during 2001–2019 in the North Atlantic (**Figure 1**), 73 on porbeagle and 104 on shortfin mako (**Supplement 1**). Both species were captured during regular commercial fishing activities by pelagic longline fleets ( $N = 134$ ), scientific cruises using pelagic longline ( $N = 38$ ) or commercial trawl trips ( $N = 5$ ) and tagged by fisheries observers, science personnel, or fishermen trained by science personnel. Tags were attached to the sharks by tethering a dart anchor into the dorsal musculature, immediately beside the posterior end of the first dorsal fin (Campana et al., 2016; Musyl et al., 2011). Anchors consisted of either nylon umbrella darts (Domeier Anchor) or titanium darts, excluding the single deployment with an experimental fin clamp. Stainless steel wire or 400 lb test monofilament line (~15 cm) was used to tether the tags to the anchor and the wire/line was sheathed in high temperature heat-shrink tubing to prevent chaffing at the point of attachment and to protect the leader. The PSAT tags were programmed to release from the sharks with the anchor and wire assembly remaining attached to them.





Individuals were chosen opportunistically for tagging. Six different types of archival satellite tag were deployed: PSATLIFE survival tags ( $N = 39$ ; Lotek Wireless), survivalPAT ( $N = 13$ ; Wildlife Computers), miniPAT ( $N = 56$ ; Wildlife Computers), PAT4 ( $N = 1$ ; Wildlife Computers), PAT MK10 ( $N = 57$ ; Wildlife

Computers), and X-tags ( $N = 11$ ; Microwave Telemetry). All tags recorded depth, either directly or through pressure, which was used to evaluate behavior and survival following tagging (PSATLIFE tags 0.05% resolution for pressure; survivalPAT, miniPAT, PAT 4, and PAT Mk 10:  $\pm 0.5$  m depth; and

X-Tags: 0.34 m depth resolution). Each tag type reported the archived depth data at a different temporal resolution, ranging from a single daily maximum and minimum from survivalPAT tags to values at 5-min intervals from the PSATLIFE tags. Deployments were a maximum of 28 days for PSATLIFE tags and 30 days for survivalPAT tags. The PAT tag was deployed for 19 days with the experimental fin clamp. Longer-term deployments were possible from the other tag types and maximum deployment durations were 255 days for miniPATs, 204 days for X-tags, and 356 days for PAT MK10s (**Supplement 1**).

## Post-release Behavior and Inferring Mortalities

Behavioral changes following tagging were assessed from recorded depth (pressure) profiles. SurvivalPAT tags provided no information on daily dive variability and were not included in the behavioral analyses. Daily dive variance ( $\sigma^2$ ) was calculated from dive amplitudes and initially used to characterize behavior following tagging. For example, dive depth was calculated as the maximum minus the minimum depth recorded for each summary interval (4, 6, 8, or 12 h summaries) for miniPAT and PAT Mk 10 tags, and then variance was calculated from these depths for each day. No attempt was made to impute missing values for days without transmitted data. Porbeagle have been shown to exhibit limited vertical movement (i.e., low variability in dive depths) and residency at the surface following the physiological stresses associated with capture and release, indicative of a recovery period (Hoolihan et al., 2011). In our data, low variability in dive depths upon release was always associated with residency in the top 60 m of the water column. Thus, we identified the animals that exhibited a recovery period following capture and handling as those with low variability in dive depth coupled with residency in the top of the water column at the start of the deployment (**Supplement 2: Supplementary Figures 1C, 2B**). To quantify the duration of the recovery period, we identified the day on which dive variability markedly increased. Variance increased substantially once an animal started to dive more regularly and more deeply (i.e., maximum dive depths and periodicity increased). We identified the end of the recovery period as the day with the maximum difference between dive variance at the start of the deployment vs the remainder of the deployment. This involved sequentially calculating the difference in variance among time periods throughout the track, i.e., comparing day 1 vs day 2 onward, days 1–2 vs 3 onward, days 1–3 vs 4 onward, and so on (**Supplement 2: Supplementary Figure 2C**). Compared to analyses that use eigenfunctions and orthogonal axes to determine irregular post-release behavior (e.g., Hoolihan et al., 2011), using variance was computationally simpler and had a direct ecological interpretation in terms of how behavior was changing over time. Inconsistent sampling frequencies among the tag types and programmed settings prevented analyzing dive behavior using more sophisticated statistical methods such as Wavelet analyses (e.g., Thorburn et al., 2019) or the fast Fourier transform (e.g., Shepard

et al., 2006). It is important to note that some animals exhibited similarly restricted diving behavior at other times during monitoring, which may have been related to geographical position. However, if restricted diving behavior upon release was solely a function of geographical position, it would not be expected to be functionally related to tagging covariates. Although we report the estimated duration of recovery periods for each individual (**Supplement 1**), our analyses of recovery time is focused on comparisons of mean recovery time between two groups.

Mortality events were inferred from continual records at a constant depth for multiple days (indicative of a dead animal on the bottom) or pop-ups following progressively increasing depth records up to the tag crush depth (indicative of an animal that is sinking; e.g., Musyl et al., 2011). Thus, the tag data tracked survival in continuous time (days until death) with right-censored observations from individuals that lived until the end of the observation period. The observations were censored because the ultimate time of death of the individual is unknown, yet the animal was known to be alive until the end of the observation period (Cox and Oakes, 1984). To separate post-release mortality events (i.e., mortality associated with capture and handling) from natural mortality events (i.e., independent from the capture process), we evaluated patterns in dive behavior for animals that ultimately died. Similar to the evaluation of dive tracks from individuals that lived, we identified animals that were negatively affected by capture and handling as those with near-zero variability in dive depth coupled with residency in the top of the water column upon release. A mortality event that followed such a period of restricted diving behavior, with minimal evidence of re-establishment of cyclical movement, was considered post-release mortality and directly related to capture and handling. There was a single instance where an individual abruptly died yet had not exhibited any prior behavior that could be attributed to capture and handling. This mortality event was sudden and preceded by dive depths and periodicity consistent with those observed from animals that lived until the end of the observation period (comparison in **Supplement 2: Supplementary Figure 1**). This mortality was suspected to represent a natural mortality event.

## Factors Influencing Recovery and Survival

There were several characteristics of the capture and handling process that could be evaluated from these tag deployments. The covariates that were considered included fork length, stage (juvenile, adult), sex (male, female), gear type (longline, trawl), hook type (circle, J), hooking location (mouth, gut), and handling location (in water, on-board) (**Supplement 1**). Note that the gut category for hooking location included gut-hooked (5 shortfin mako, 10 porbeagle) and foul-hooked individuals (0 shortfin mako, 6 porbeagle; **Supplement 1**). When categorizing life stage, we used sex-specific length at 50% maturity to separate juveniles from adults, with values of 182 cm and 280 cm fork length (FL) for male and female shortfin mako (Natanson et al., 2020) and 174 cm and 218 cm FL for male and female porbeagle (Natanson

et al., 2002). There were only 58 deployments on shortfin mako and 57 on porbeagle that had information for the entire suite of covariates (**Supplement 1**).

The properties of the data on recovery times (e.g., sparse, zero-inflated) made typical parametric regression analyses unsuitable, so we used a randomization test to evaluate relationships with covariates. The main assumption underlying this approach is that the observed sample is representative of the larger population. We ran 10,000 samples to characterize the distribution for the mean difference in recovery times between factor levels of each covariate, implemented in the “simpleboot” package in R (Peng, 2019). The distribution of differences would be centered on zero if there was no effect of the covariate on recovery time and the proportion of samples with means that fell below zero represented the  $p$ -value for the comparison. To evaluate any association between recovery time and the continuous covariate FL, we used a Spearman Rank Correlation test. Relationships with hooking location and gear type could not be examined because there were insufficient data in one of the categories.

The influence of covariates on survivorship for each species was assessed using Cox proportional hazards models (CPHM; Cox, 1972; Therneau and Grambsch, 2000). CPHM are a well-established semi-parametric approach that estimates the multiplicative effect of covariates on a common hazard function, which describes the time-specific instantaneous probability of dying at a given time  $t$ , conditional on having survived to  $t$ . For each CPHM, the proportional hazards assumption was tested based on trends in the Schoenfeld residuals and was assessed visually by plotting the log of the negative log survivor function vs the log of event time. To provide the best inferences possible in light of missing covariate data, we undertook two series of analyses of the influence of covariates using CPHM. In the first, each covariate was modeled individually using all available observations, with no attempt to impute missing values. In the second series, we limited the data to observations for which values were available for all covariates ( $N = 58$  for shortfin mako and  $N = 57$  for porbeagle). This second series of analyses was intended to identify the suite of covariates associated with survivorship. A forward-selection scheme based on Akaike's Information Criterion (AIC) was employed. For shortfin mako, a model with hook-related injury resulted in a decrease in AIC of 10.5 compared to an intercept only model, but no other single or multiple covariate models were found to be comparable or superior based on AIC. For porbeagle, there were no models including a single covariate that resulted in a reduction in AIC of at least two units compared to an intercept-only model. Therefore, models incorporating multiple covariates were not pursued further and we report the results for individual covariates only, using all available observations. As in the behavioral analyses, statistical significance was accepted at  $p < 0.05$ .

## Estimating Post-release and Natural Mortality

A CPHM does not distinguish between components of mortality, so we used the parametric mixture model of Benoît et al. (2015)

to estimate separate rates of catch-related post-release mortality (PRM) and natural mortality ( $M$ ). Specifically, the survivorship to time  $t$ ,  $S(t)$ , was modeled as:

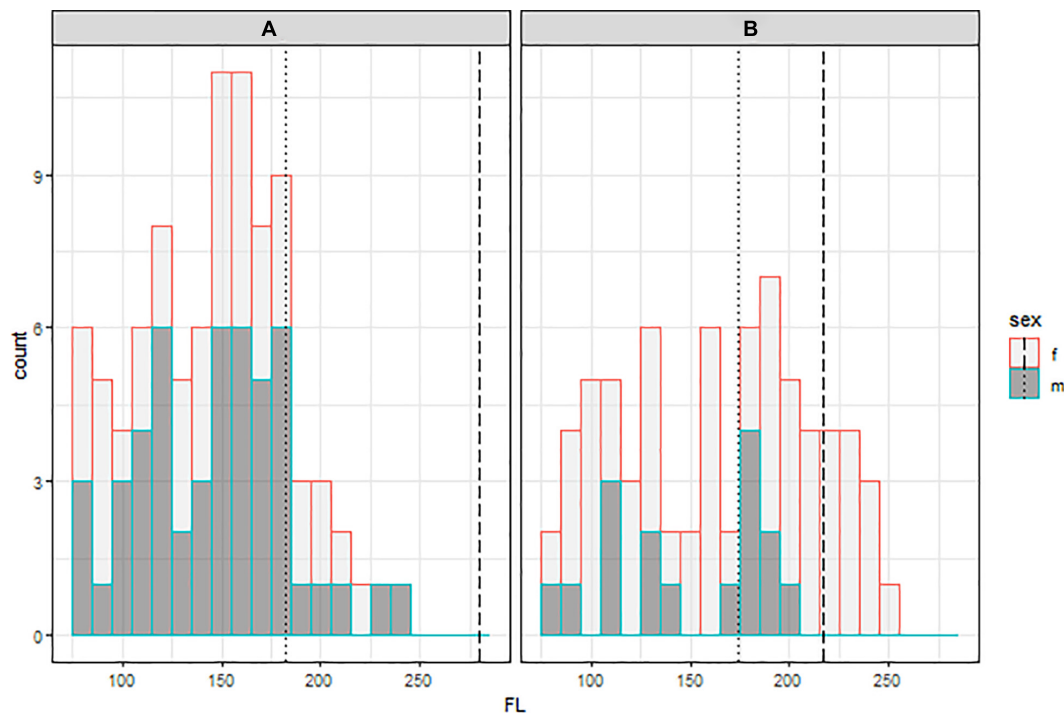
$$S(t) = (\pi \exp[-(\alpha t)^\gamma] + (1 - \pi)) \cdot \exp(-Mt) \quad (1)$$

where  $\alpha$  and  $\gamma$  are parameters of a Weibull survival function that describes the attrition of fish that will die after release due to the capture and release event,  $\pi$  is the post-release mortality rate, and  $M$  is the instantaneous annual rate of natural mortality (for a derivation see Benoît et al., 2015). Model parameters were estimated using maximum likelihood (details in Benoît et al., 2015, 2020b). The non-parametric Kaplan-Meier (KM) estimator (Cox and Oakes, 1984) was used to visualize the survivorship of the two species, providing a basis for visually assessing model fit.

The model in Equation 1 effectively parses out mortality into capture-related (PRM) and natural ( $M$ ) components based on their assumed time course. Post-release mortality is considered to asymptote over a finite timespan, typically within hours or days (reviewed in Musyl and Gilman, 2019). Meanwhile, released individuals are continuously at risk of dying from natural causes such as disease or predation, and an exponential function is commonly assumed in population modeling. The model can freely and reliably estimate the two mortality components provided that sufficient observations are available for both early rapid mortality and the later time periods (Benoît et al., 2015). Alternatively, the estimation can be aided by specifying the cause of mortality for some or all observations (Benoît et al., 2020a). In this study, patterns in dive depths and periodicity suggested that 33 of the mortalities of shortfin mako were catch-related, and only one had the potential to be natural. All mortalities of porbeagle appeared to be catch-related. Therefore, we fit the parametric model above with three variations: (1) fixing  $M = 0$ , which attributes all observed mortality events to PRM, (2) estimating  $M$  using the full model above, and (3) using the full model with cause-specific classifications of mortality (shortfin mako only). The cause-specific estimation for shortfin mako was accomplished by specifying different likelihood equations for the different classes of event observations (Benoît et al., 2020a; Kneebone et al., 2020). Specifically, observations for which the cause of death was inferred to be catch-related employed a likelihood in which  $M$  was fixed at 0, those for which the cause was assumed to be natural employed a likelihood in which  $\pi$  was fixed at zero, and those of uncertain cause employed the full likelihood for Equation 1. Similarly all censored observations employed the full likelihood as these individuals were at risk of dying from both catch-related and natural causes.

## Simulation Modeling to Further Infer Natural Mortality Rates

Life history-based estimates of  $M$  for pelagic sharks are very low relative to other fish species (Cortés, 2002), suggesting natural mortality events are rare. The probability of observing natural deaths during the course of a tagging experiment should be correspondingly low, particularly when the median deployment duration from all tag types was 28 days for both porbeagle and shortfin mako. This likely explained why a natural mortality event



**FIGURE 2 |** Size distribution of tagged male (dark gray) and female (light gray) shortfin mako **(A)** and porbeagle **(B)**. Sizes at 50% maturity for males (dotted) and females (dashed) of both species are shown by the vertical lines.

was only observed once in these data. We used a simulation model to allow for inferences on the probable magnitude of  $M$  for each species given the observations made in this study. Our approach determined the probability of observing no natural deaths during the experiments for porbeagle and the probability of one or fewer for shortfin mako, as a function of the natural mortality rate.

Following the method by Bender et al. (2005), each iteration of the simulation proceeded as follows. Vectors of mortality probabilities,  $Z(t)$ , with lengths corresponding to the total number of mortality event observations for each species were generated by randomly selecting values from a uniform distribution over the interval  $[0,1]$ . Assuming exponential natural mortality, mortality event times from each individual,  $t_{M,i}$  in days, associated with each value of  $Z(t)_i$  for a given simulated annual natural mortality rate  $M_s$  were calculated as:

$$t_{M,i} = -365 \log(Z(t)_i) / M_s \quad (2)$$

A censoring time,  $t_{C,i}$ , was simulated for each individual by sampling with replacement from among the mortality event times for each species in the tagging experiments. Instances in which  $t_{M,i} \leq t_{C,i}$  reflect a simulated instance in which an individual died from natural causes while or before dying from catch-related causes or having its tag detach. The proportion of iterations for which no individuals (porbeagle) or one or no individuals (shortfin mako) died from natural causes for a given value of  $M_s$  is the estimated probability that the observed number of natural deaths occurred at that rate of natural mortality. It becomes less

likely to observe no natural mortality events over the duration of the study as the magnitude of  $M$  increases. We also simulated the probability of observing no natural deaths for shortfin mako to illustrate the extent to which a single observation can change the probabilities associated with different natural mortality rates. Ten thousand iterations were undertaken for each  $M_s$  value, which ranged from 0.02 to 0.70, with increments of 0.02.

## RESULTS

The opportunistic tagging resulted in a range of sizes of both species and sexes, with slight oversampling of shortfin mako  $< 100$  cm FL and fewer than expected porbeagle between 150 and 170 cm FL (**Figure 2**) relative to typical length-frequency distributions from landings data (Coelho et al., 2018; Santos et al., 2020). The vast majority of tagging occurred on juvenile animals, consistent with the selectivity patterns in longline fisheries (ANON, 2019, 2020). Animals ranged in size from 78 to 249 cm FL (mean = 163 cm FL) for porbeagle and 66–240 cm FL (mean = 144 cm FL) for shortfin mako. The sex ratio of tagged animals was skewed in both species, with more females for porbeagle and more males for shortfin mako. Sample sizes varied substantially across the different tagging covariates (**Table 1**), as was expected from opportunistic tag deployments.

Given the tag types used, we could determine the recovery period following tagging for 59 shortfin mako and 53 porbeagle. We distinguished pre- and post-recovery periods using a sharp change in variance (**Supplement 2: Supplementary Figure 2C**),



**TABLE 1** | Summary of the covariate analyses showing the number of animals that lived (L), died (D) and total (T) for each comparison, plus the coefficients (coef), standard error (se), and *p*-values (pval) for differences in recovery time or mortality.

Covariate	Shortfin mako										Porbeagle									
	Tag summary					Recovery time					Mortality					Tag summary				
	Levels	L	D	T		Coef	SE	Pval			Coef	SE	Pval			L	D	T		
Fork length	NA	70	34	104		<b>-0.29<sup>^</sup></b>	-	<b>0.014</b>	0.083	0.005	-0.01	0.005	0.083	0.005	-0.11 <sup>^</sup>	61	12	73		
Sex	Male	32	18	50		-0.04	0.784	0.492	0.724	0.880	0.13	0.880	0.724	0.880	0.35	13	3	16		
	Female	27	13	40												47	8	55		
Stage	Juvenile	63	32	95		-0.80	0.936	0.979	0.968	0.971	0.03	0.971	0.968	0.971	<b>4.35</b>	43	10	53		
	Adult	7	2	9												17	2	19		
Gear type	Longline	70	34	104		-	-	-	-	-	-	-	-	-	-	57	11	68		
	Trawl	0	0	0												4	1	5		
Hook type	Circle	39	17	56		<b>1.97</b>	<b>0.851</b>	<b>0.003</b>	0.266	0.683	-0.38	0.683	0.266	0.683	-	53	10	63		
	J	25	17	42												4	1	5		
Hook injury*	Foul	0	0	0		-	-	-	-	-	<b>1.24</b>	<b>0.616</b>	<b>0.043</b>	<b>0.043</b>	-	4	2	6		
	Gut	2	3	5		-	-	-	-	-					1.38	4	6	10		
	Mouth	49	25	74												34	3	37		
Handling	In water	16	4	20		<b>-3.31</b>	<b>1.120</b>	<b>&lt;0.001</b>	<b>0.549</b>	<b>0.549</b>	<b>-1.08</b>	<b>0.549</b>	<b>0.048</b>	<b>0.048</b>	<b>-3.63</b>	11	3	14		
	Onboard	24	20	44												50	9	59		

<sup>^</sup>Coefficient based on Spearman's Rank Correlation (rho).

\*Mortality results for porbeagle are listed for fouthmouth and gut:mouth comparisons.

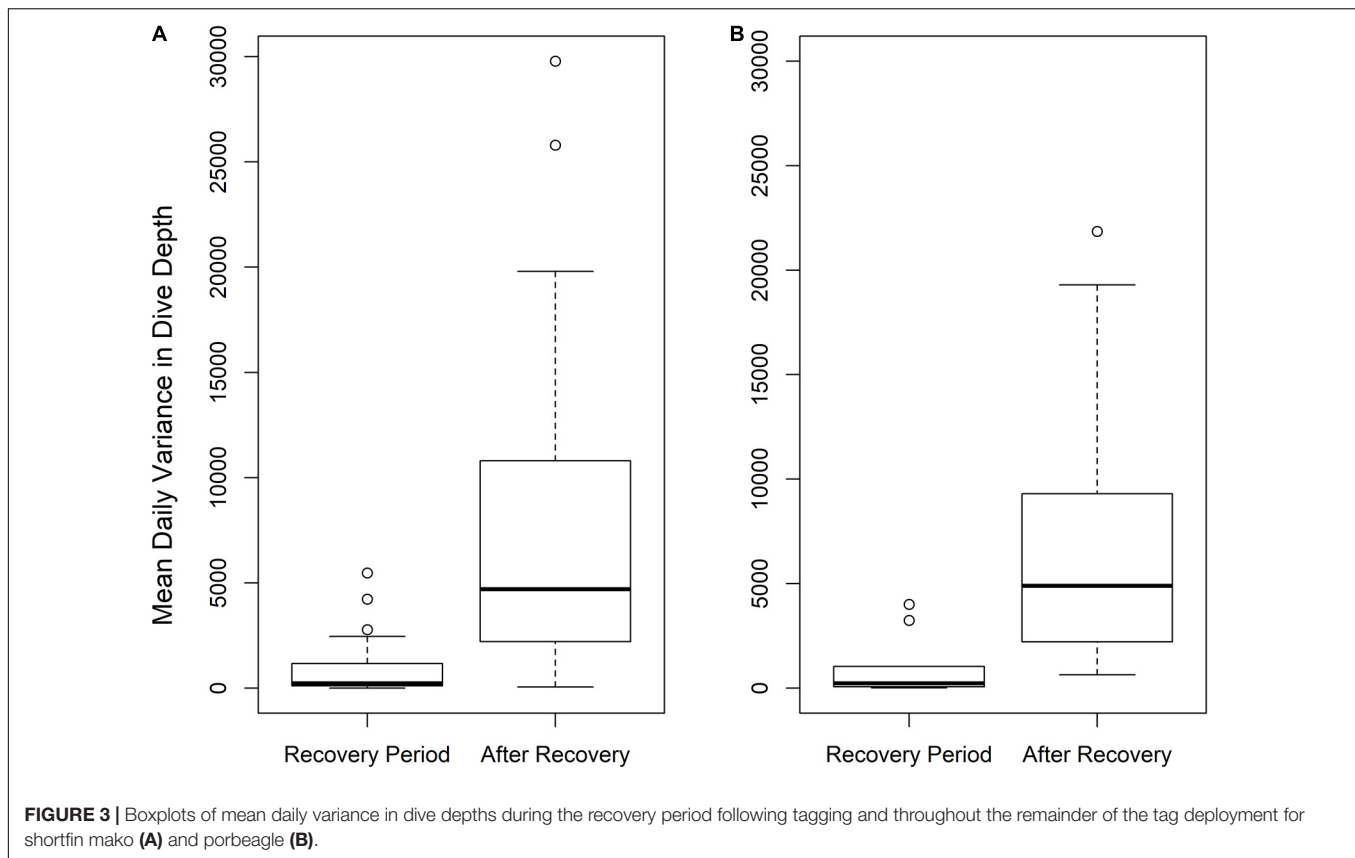
Significant relationships (pval < 0.05) are identified in bold.

and a comparison of mean daily dive variance during and following the recovery period showcases the substantial increase in dive depths and periodicity following recovery. During the inferred recovery period, the median variance was near-zero for both species, while it increased to ~5,000 following the recovery period (**Figure 3**). For individuals that remained in the top of the water column following tagging, there were no instances where dive variance was greater immediately following tagging than in the remainder of the deployment. The majority of sharks that died after tagging did so relatively quickly, many within hours. All mortalities of porbeagle occurred within 45 days of release and there were many long-term survivors, some with monitoring for up to a year (**Figure 4A** and **Supplement 1**). Similarly, all mortalities of shortfin mako shark occurred within 50 days of release, and there were many long-term survivors, including some with monitoring times in excess of 200 days (**Figure 4B** and **Supplement 1**).

## Factors Influencing Recovery and Survival

The estimated durations of recovery for porbeagle (mean = 9.1 days) were similar to previous evaluations of recovery periods based on dive behavior for multiple species of pelagic teleosts (mean = 7.1 days) and pelagic sharks (mean = 10.8 days) (Hoolihan et al., 2011; Musyl et al., 2015). The estimated durations of recovery for shortfin mako (mean = 3.8 days) tended to be lower. For the animals that survived, there were no differences in mean recovery time between the sexes of either species, between different hooking injury types for both species, or between juvenile and adult shortfin mako (**Table 1**). There was a negative relationship between recovery time and fork length for both species, which was significant only for shortfin mako (**Table 1**). For porbeagle, mean recovery times were 4.35 days longer (95% CI: 1.22–7.60) for juveniles and 3.63 days longer (95% CI: 0.87–6.77) when tagged onboard a vessel (**Table 1** and **Supplement 2: Supplementary Figures 3, 4**). For shortfin mako, recovery duration was 1.97 days longer (95% CI: 0.66–3.39) when captured on circle hooks as compared to J hooks, and 3.31 days longer (95% CI: 1.61–5.22) when tagged onboard a vessel as compared to in the water (**Table 1** and **Supplement 2: Supplementary Figures 4, 5**). The effect of hook type (circle, J) on porbeagle, or hook injury (foul, gut, and mouth) on shortfin mako or porbeagle could not be assessed due to extremely low or zero sample sizes in one of the categories (**Table 1**).

Survivorship of shortfin mako was significantly lower (at the 5% level) for individuals hooked in the gut rather than the mouth (**Table 1**), with a hazard ratio of 3.47 (95% CI: 1.04–11.61) (**Supplement 2: Supplementary Figure 6A**). Survivorship was also significantly lower for individuals tagged onboard rather than in-water, with a hazard ratio of 2.96 (95% CI: 1.01–8.67) (**Supplement 2: Supplementary Figure 6B**). Survivorship of porbeagle was significantly affected only by the manner in which fish were hooked on the fishing gear (**Table 1**). Compared to individuals hooked in the mouth, survivorship was reduced for individuals hooked in the gut or more generally



foul-hooked. Combining the latter two categories to increase sample size, the hazard ratio for fish hooked elsewhere than in the mouth was 8.49 (95% CI: 2.21–32.46), constituting an important reduction in survival (**Supplement 2: Supplementary Figure 7**). For both species, risk of mortality was negatively associated with increased fork length, though the effect was not statistically significant.

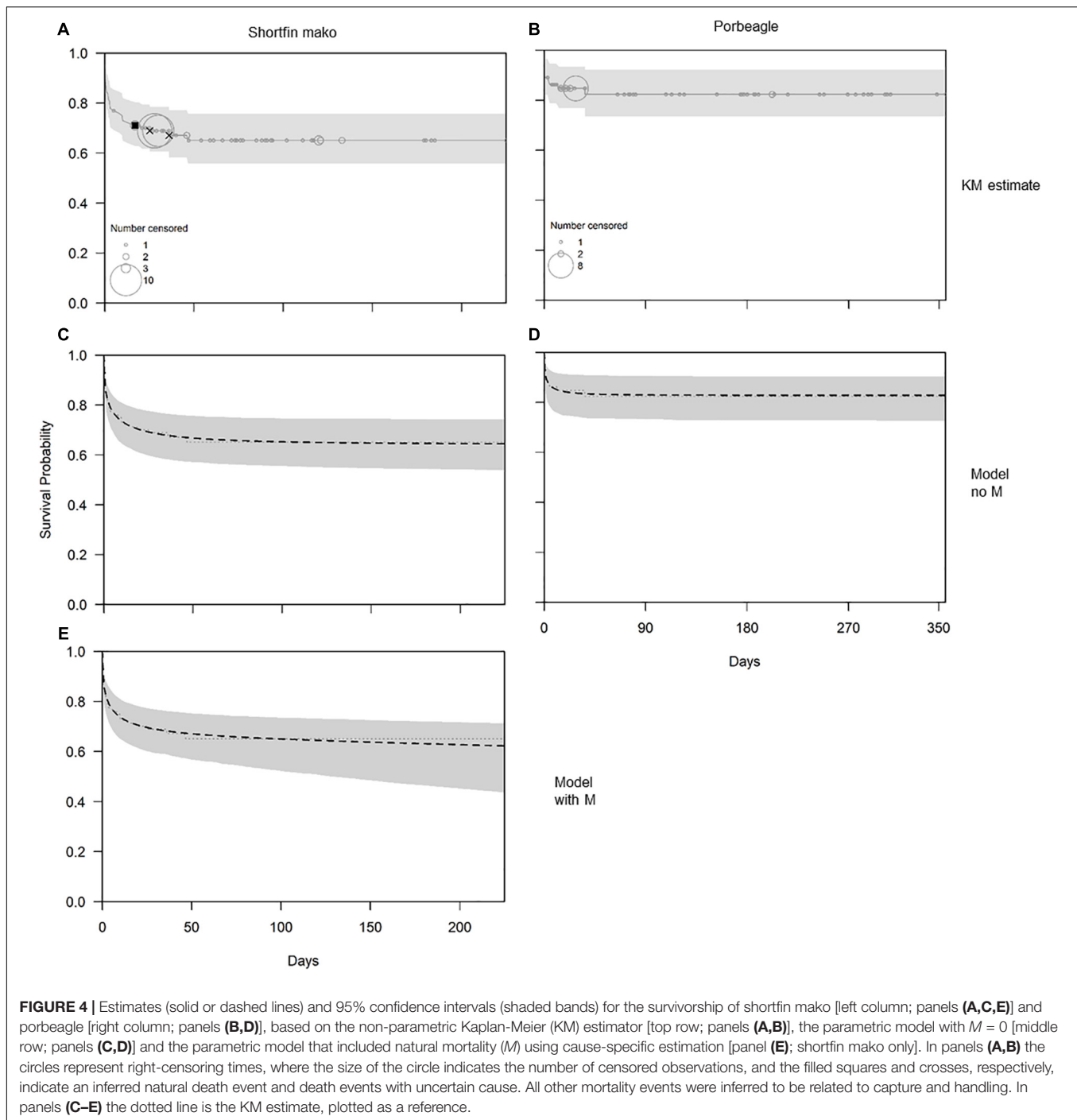
## Estimating Post-release and Natural Mortality

Visual evaluation suggested fits from the parametric survival model were comparable to those from the non-parametric Kaplan-Meier (KM) estimator (*c.f.* **Figures 4A–D**). For porbeagle shark, the parametric model with only post-release mortality (i.e.,  $M = 0$ ) fit the trends in survivorship very well, producing an estimate of PRM of 0.171 (95% confidence interval: 0.099–0.277) (**Table 2** and **Figure 4D**). An identical estimate of PRM was obtained when  $M$  was estimated in the model because the estimate of the  $M$  parameter was essentially zero, with an exceedingly wide confidence interval (results not shown). It is therefore not possible to directly estimate natural mortality for porbeagle using data from these tagging experiments. For shortfin mako, the parametric model with only post-release mortality fit the trends in survivorship very well, producing an estimate of PRM of 0.358 (95% confidence interval: 0.259–0.479) (**Table 2** and **Figure 4C**). As with porbeagle, the model that attempted to freely estimate natural mortality produced an

identical PRM estimate and an estimate of the  $M$  parameter that was essentially zero, with an exceedingly wide confidence interval (results not shown). In contrast, the cause-specific estimation (i.e., when one natural death event was identified in the data, see **Figure 4E**) produced an estimate of post-release mortality of 0.339 (0.246–0.453) and an estimate of natural mortality of 0.101 (0.016–0.659) (**Table 2**). This model also provided a good fit to the survivorship trend, although the uncertainty around survivorship at later times was greater and increasing in time compared to the model excluding natural mortality. This pattern reflected the uncertainty associated with the additional and ongoing natural mortality component (**Figure 4E**).

## Simulation Modeling

The absence of observations of natural deaths for porbeagle during the tagging experiments is consistent with the species' having low natural mortality. The simulation model suggests probabilities of  $\leq 0.10$  associated with each natural mortality rate above 0.15 (**Figure 5**). In contrast, the observation of a single natural death for shortfin mako resulted in substantially higher probabilities for the same natural mortality rates. The probability of observing one or no natural deaths only dropped below 0.10 when  $M$  was greater than 0.3. We also ran the simulations for a scenario assuming no natural deaths had been observed for shortfin mako, to evaluate how assigning cause to mortality events affects predicted PRM rates as well as how overall monitoring duration affects the simulations. In that scenario, the



simulated probability for shortfin mako was essentially double that of porbeagle at 0.2 when  $M = 0.15$  (Figure 5). There were 27 porbeagle that were monitored for > 90 days (~3 months) as compared to only 15 shortfin mako (Supplement 1). Extended monitoring periods using archival tags increases the chances of observing mortality from natural causes. If such mortality events are not observed despite longer monitoring, there is greater certainty that the rate of natural mortality is low, as was the case for porbeagle.

## DISCUSSION

Large sample sizes involving extended monitoring periods would be optimal to directly estimate  $M$  from satellite tagging data for lamnid sharks. Yet it remains possible to infer probable values or to constrain estimates, even in the absence of direct observations. For porbeagle, there was less than a 10% probability associated with values of  $M$  higher than 0.15 based on the simulation modeling. From the survival mixture model and a

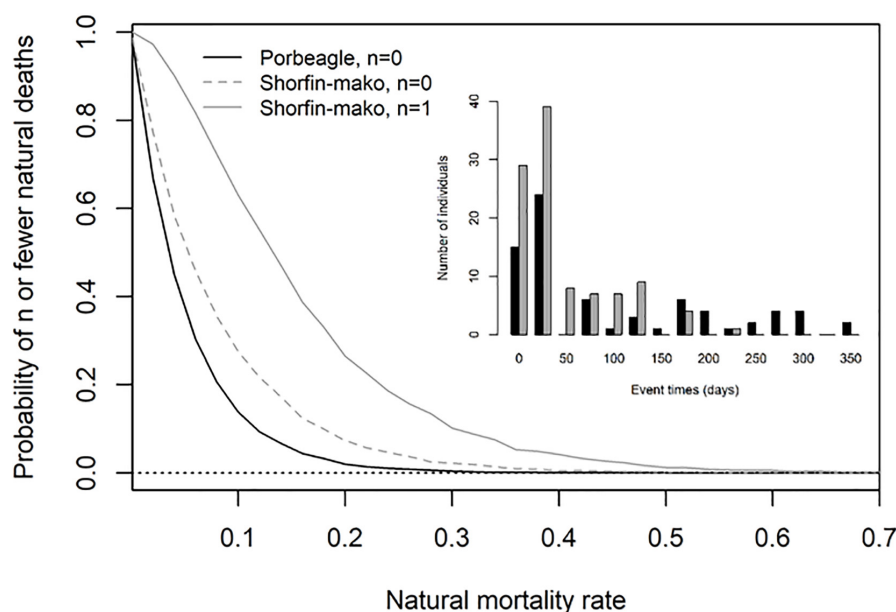
**TABLE 2** | Estimates of post-release mortality (PRM) and natural mortality ( $M$ ) for porbeagle and shortfin mako sharks based on a model that excluded natural mortality ( $M = 0$ ) and a model in which  $M$  was estimated using cause-specific parameter estimation (shortfin mako only).

Model	Shortfin mako		Porbeagle	
	PRM	$M$	PRM	$M$
1. No $M$	0.358 (0.259, 0.479)	0	0.171 (0.099, 0.277)	0
2. With $M$	0.339 (0.246, 0.453)	0.101 (0.016, 0.659)	–	–

single suspected natural mortality event, the maximum likelihood estimate of  $M$  was 0.101 for shortfin mako. To put these rates in perspective, approximately 1.5% of a population is expected to live to maximum age (Hewitt and Hoenig, 2005). Under a simple exponential model for mortality, 1.5% of the population would live to be ~28 years ( $M = 0.150$ ) for porbeagle and ~41 years ( $M = 0.101$ ) for shortfin mako. This would be on the lower end of longevity estimates for porbeagle in the Northwest Atlantic (24–43 years; Natanson et al., 2002), as might be expected from an upper limit of  $M$ . Our estimate of longevity for shortfin mako in the North Atlantic also falls within the expected range of longevity of 20–52 years (Natanson et al., 2006; Rosa et al., 2017). In all, there was fair correspondence with rates derived from life history for both species, even though our data came primarily from juvenile animals. Estimates of  $M$  based on age and growth parameters, maturity, and longevity most often yield a single value, and variability is generated by applying different types of estimators (e.g., Cortés, 2002, 2016) or by allowing for variability in longevity when using a single estimator (e.g., Bowlby and Gibson, 2020). Using the Then et al. (2015) suite

of estimators based on longevity and growth data,  $M$  ranged from 0.081 to 0.267 for porbeagle and from 0.068 to 0.318 for shortfin mako for males and females combined. Our estimates of  $M$  from survival data fell within these ranges, which lends credence to the natural mortality values currently being used in stock assessment (ANON, 2019, 2020) and gives independent support that our current understanding of these species' biology is largely representative.

Our results highlighted the types of information on survivorship that can be gained from long-term vs short-term tag deployments. Estimating post-release mortality and evaluating the influence of covariates with survivorship was the original goal for the majority of the tagging contributing to this study. This explains the predominance of satellite tag types optimized for  $\leq 30$  days; chosen to reduce cost and increase sample size, given that shorter monitoring periods are generally sufficient for estimating post-release mortality in large pelagic fish (e.g., Musyl and Gilman, 2019; Benoit et al., 2020b). Although our PRM rates were similar to those of previous studies on these species, there were still limited and unbalanced data relative to covariates, which reduced statistical power and thus detectability of relationships (Sippel et al., 2015). Mortality related to capture and handling apparently extended beyond a 30-day monitoring period, which suggests PRM rates for porbeagle and shortfin mako could have been slightly underestimated if derived exclusively from short-term deployments (e.g., Marçalo et al., 2018). Finally, short-term deployments reduced the potential for natural mortality events to be observed over the duration of the experiment, making them suboptimal for species characterized by low  $M$ . Our results support several of the discussion points from a recent



**FIGURE 5** | Simulated probability of observing  $n$  or fewer mortality events resulting from natural causes during the tagging experiments, as a function of the annual natural mortality rate for porbeagle ( $n = 0$ , black solid line) and shortfin mako ( $n = 0$ , dashed gray line;  $n = 1$ , solid gray line). The inset histogram summarizes the observed mortality event times for the tagged porbeagle (black) and shortfin mako (gray).



meta-analysis of post-release mortality in pelagic sharks (Musyl and Gilman, 2019), demonstrating that a substantial number of tag deployments is required to tease apart fishing-related mortality from  $M$ , that long-term deployments are necessary to increase precision of  $M$  estimates, and that a minimum 3-month pop-up period ( $>90$  days) would be useful when trying to separate post-release from natural mortality as opposed to relying on short-term archival tags.

There is some debate on whether delayed mortality for pelagic sharks can be linked to capture and handling or whether PRM would be expected to asymptote relatively quickly. Several survivorship studies in addition to ours have reported delayed mortality, up to 50 days following release (summarized in Musyl and Gilman, 2019). Although mortalities that occur within hours of the tagging event are readily ascribed as PRM (Sulikowski et al., 2020), it is less clear if longer-term mortalities should be attributed to capture and handling (Hutchinson et al., 2015). Sublethal effects, such as reduced activity levels upon release (e.g., Raoult et al., 2019), reflex impairment and physiological damage (e.g., Jerome et al., 2018), or measureable changes in distribution (e.g., Bullock et al., 2015) could ultimately result in delayed mortality due to increased susceptibility to disease and predation, or cessation of feeding (Davis, 2002; Campana et al., 2016). Also,  $M$  is continuous and can occur at any time, irrespective of the length of time since the capture event. Instead of categorizing mortality as PRM and  $M$  based on a subjective timeframe, we used dive behavior to indicate whether mortality was likely related to capture and handling. We felt this was appropriate given the definitive contrast in dive variability that characterized recovery, and the correspondence between our estimates of the duration of recovery and previous evaluations of dive behavior from archival satellite tagging data (e.g., Campana et al., 2009; Hoolihan et al., 2011). Interestingly, the only likely natural death was recorded from a mouth-hooked male shortfin mako (157 cm FL) within 17 days of tagging. This individual's dive track exhibited variability equivalent to recovered individuals until the mortality event. Given that this was one observation, it would be beneficial to explore the utility and robustness of behavior-based classifications of mortality in future research.

Evaluating capture and handling covariates relative to recovery time as well as survivorship allowed for a more fulsome use of the tagging data and strengthened the inferences that could be made. As in other PRM studies, the majority of tagged animals survived, giving relatively few observations of mortality events from which to infer the effect of covariates (Sippel et al., 2015). Incorporating behavioral analyses of dive patterns from surviving individuals was an inexpensive and straightforward way to increase the amount of information gained, with some of the differences in recovery period being significant even when differences in survivorship were not. For example, the estimated coefficients from the CPHM suggested a non-significant increase in survivorship of porbeagle with fork length. There was a corresponding significant increase in mean recovery time following release for juveniles as compared to adults (i.e., juveniles took longer to recover from capture and handling) as well as a significant decrease in recovery time with fork length for shortfin mako. Taken together, we conclude

that capture and handling was more detrimental to smaller juveniles of both species, although it is important to recognize that decreased swimming performance caused by carrying the tag would also be affecting these smaller animals (Todd Jones et al., 2013). Although enhanced international cooperation and additional tagging would be optimal to bolster sample sizes (Ellis et al., 2017; Harcourt et al., 2019), we suggest that quantifying recovery periods from surviving individuals is an additional avenue to explore the effect of covariates with capture and handling. Ideally, better standardization among tag types and programmed settings would support more complex statistical analyses of behavior (e.g., Shepard et al., 2006; Thorburn et al., 2019), and would be useful to give more precise estimates of the duration of recovery periods. In the absence of this, our comparisons provide meaningful information on sublethal effects that arise from specific characteristics of the capture and handling process for porbeagle and shortfin mako.

Revealing covariates with injury and mortality is important for developing mitigation options for non-retained bycatch (Molina and Cooke, 2012; Ellis et al., 2017). One of the most consistent relationships in our study was related to handling, specifically onboard vs in-water tagging. The  $>3$  day difference in recovery time for both species in addition to the significant reduction in shortfin mako survivorship suggests that physiological stresses associated with removal from the water significantly outweigh any benefit of gear removal following capture. Although trailing gear is commonly thought to contribute to PRM (Gilman et al., 2016), all animals that were tagged in the water for this study were released by cutting the gangion, thus retaining the hook plus an unquantified amount of monofilament leader (no weights or steel leaders). When tagged onboard, the shark remained under duress for a longer period and may have been subject to physiological damage when lifted out of the water and/or from the animal's inability to support its own weight while onboard (Musyl et al., 2009). Studies that directly evaluate handling effects (in isolation from capture effects) are rare, but longer handling times and increased exposure to air have also shown a significant negative effect on activity levels upon release for Squaliform and Carcharhiniform species (Raoult et al., 2019). Scientific work benefits from deep and precise insertion of the tag anchor to reduce the probability of pre-mature tag loss, which is easier to accomplish when the animal is onboard (Biais et al., 2017). In our study, in-water tagging of porbeagle used PSATLIFE tags only (28 day maximum deployment) and it was difficult to determine if pre-mature pop-ups were related to anchor placement. This batch of tags had a 40% non-transmission rate (Bowlby et al., 2019) indicating other tag construction and/or software issues. Shortfin mako that were tagged in the water had a longer median monitoring duration as compared to those tagged onboard (c.f. 60 days vs 57.5 days). Although it was not possible to determine the specific characteristics of boarding that increased recovery time for both species and decreased shortfin mako survival (e.g., the method of lifting the animal out of the water, the duration the animal was onboard, the method of gear removal), in-water release from commercial captures and in-water tagging for scientific work appears optimal for lamnid sharks.

In terms of best-practices for the release of bycatch from commercial interactions, our results support the recommendation to release sharks immediately upon capture, leaving embedded hooks and as little trailing line as possible (Musyl and Gilman, 2019). Contrary to earlier suggestions that handling practices have little influence on the condition of sharks upon release (Campana et al., 2009; Musyl and Gilman, 2019), handling in and of itself was associated with substantial sublethal effects. Our results also support the general recommendation to increase protection of the juvenile life stages of bycaught species (Ellis et al., 2017), optimally by minimizing the potential for interaction through spatial management. However, they are less clear relative to optimal hook type. On one hand, increased gut hooking is expected from capture on J hooks (Epperly et al., 2012; Gilman et al., 2016), where gut and foul hooking were associated with significantly higher post-release mortality for both species. However, shortfin mako exhibited longer recovery times following release when caught on circle as opposed to J hooks, possibly because circle hooks are harder to remove (Cooke and Suski, 2004) or may not be expelled from the jaw as quickly (Poisson et al., 2019). Such apparently contradictory results underscore the multi-faceted nature of bycatch mitigation, where it is often unclear if benefits relative to one component of the capture process are outweighed by detriments to another (Reinhardt et al., 2017). Ultimately, taking a holistic approach to bycatch mitigation is necessary, particularly to make any trade-offs explicit in the overall management approach (Gilman et al., 2019).

## DATA AVAILABILITY STATEMENT

The original contributions presented in the study are included in the article/Supplementary Material, further inquiries can be directed to the corresponding author/s.

## ETHICS STATEMENT

The animal study was reviewed and approved by Fisheries and Oceans regional Animal Care Committee.

## REFERENCES

- ANON (2019). Report of the 2019 shortfin mako shark stock assessment update meeting (Madrid, Spain, 20–24 May 2019). *ICCAT Col. Vol. Sci. Pap.* 76, 1–77.
- ANON (2020). Report of the 2020 Porbeagle shark stock assessment meeting (online, June 15–22). *ICCAT Col. Vol. Sci. Pap.* [Epub ahead of print]. (accessed March 24, 2021).
- Au, D. W., Smith, S. E., and Show, C. (2015). New abbreviated calculation for measuring intrinsic rebound potential in exploited fish populations – example for sharks. *Can. J. Fish. Aquat. Sci.* 72, 767–773. doi: 10.1139/cjfas-20140360
- Bender, R., Augustin, T., and Blettner, M. (2005). Generating survival times to simulate cox proportional hazard models. *Stat. Med.* 24, 1713–1723. doi: 10.1002/sim.2059
- Benoît, H. P., Capizzano, C. W., Knotek, R. J., Rudders, R. B., Sulikowski, J. A., Dean, M. J., et al. (2015). A generalized model for longitudinal short- and long-term mortality data for commercial fishery discards and recreational fishery catch-and-releases. *ICES J. Mar. Sci.* 72, 1834–1847. doi: 10.1093/icesjms/fsv039

## AUTHOR CONTRIBUTIONS

HDB conceived research, undertook data collection and fieldwork, developed analyses, wrote manuscript, and contributed in funding. HPB developed models, undertook analyses, and reviewed manuscript. WJ, CS, and BA undertook data collection and fieldwork and reviewed manuscript. JS, RC, AD, EC, FH, DM, and GB undertook data collection and fieldwork, reviewed manuscript, and contributed in funding. All authors contributed to the article and approved the submitted version.

## FUNDING

Tagging in Canadian waters was done in collaboration with the Nova Scotia Swordfish Association, Atlantic Shark Association, Javitech Atlantic Ltd., and Karlens Shipping Company Ltd., with funding provided under the International Governance Strategy of Fisheries and Oceans, Canada. Tagging on Portuguese vessels was carried out by onboard observers under the PNAB/EU-DCF (National Program for Biological Sampling, integrated in the EU Data Collection Framework), with additional tags coming from Project SAFEWATERS (Ref: EU/MARE/2012/21) and Project MAKOWIDE (Ref: FAPESP/19740/2014), funded by FCT, the Portuguese Science and Technology Foundation. Tagging by Ifremer (France) was done during a scientific survey in collaboration with the regional professional fishing organization of Pays de Loire and funded by the European Union. Deployments by ICCAT were funded by the European Union (EU Grant Agreements—*Strengthening the scientific basis for decision-making in ICCAT*) and by the Commission as part of the ICCAT regular budget. C. C. Santos is supported by a FCT Doctoral grant (Ref: SFRH/BD/139187/2018).

## SUPPLEMENTARY MATERIAL

The Supplementary Material for this article can be found online at: <https://www.frontiersin.org/articles/10.3389/fmars.2021.619190/full#supplementary-material>

- Benoît, H. P., Hurlbut, T., Chassé, J., and Jonsen, I. D. (2012). Estimating fishery-scale rates of discard mortality using conditional reasoning. *Fish. Res.* 125, 318–330. doi: 10.1016/j.fishres.2011.12.004
- Benoît, H. P., Kneebone, J., Tracey, S., Golet, W., and Bernal, D. (2020a). Distinguishing discard mortality from natural mortality in field experiments based on electronic tagging. *Fish. Res.* 230:105642. doi: 10.1016/j.fishres.2020.105642
- Benoît, H. P., Morfin, M., and Capizzano, C. W. (2020b). Improved estimation of discard mortality rates with in situ experiments involving electronic and traditional tagging. *Fish. Res.* 221:105398. doi: 10.1016/j.fishres.2019.105398
- Biais, G., Coupeau, Y., Séret, B., Calmettes, B., Lopez, R., Hetherington, S., et al. (2017). Return migration patterns of porbeagle shark (*Lamna nasus*) in the Northeast Atlantic: implications for stock range and structure. *ICES J. Mar. Sci.* 74, 1268–1276. doi: 10.1093/icesjms/fsw233
- Bowlby, H. D., and Gibson, A. J. F. (2020). Implications of life history uncertainty when evaluating status in the Northwest Atlantic population of white shark (*Carcharodon carcharias*). *Ecol. Evol.* 10, 4990–5000. doi: 10.1002/ece3.6252

- Bowlby, H. D., Joyce, W., Benoît, H. P., and Sulikowski, J. (2019). Evaluation of post-release mortality for porbeagle and shortfin mako sharks from the Canadian pelagic longline fishery. *ICCAT Col. Vol. Sci. Pap.* 76, 365–373.
- Bullock, R., Guttridge, T., Cowx, I., Elliott, M., and Gruber, S. (2015). The behaviour and recovery of juvenile lemon sharks *Negaprion brevirostris* in response to external accelerometer tag attachment. *J. Fish Biol.* 87, 1342–1354. doi: 10.1111/jfb.12808
- Campana, S. E., Joyce, W., Fowler, M., and Showell, M. (2016). Discards, hooking, and post-release mortality of porbeagle (*Lamna nasus*), shortfin mako (*Isurus oxyrinchus*), and blue shark (*Prionace glauca*) in the Canadian pelagic longline fishery. *ICES J. Mar. Sci.* 73, 520–528. doi: 10.1093/icesjms/fsv234
- Campana, S. E., Joyce, W., and Manning, M. J. (2009). Bycatch and discard mortality in commercially caught blue sharks *Prionace glauca* assessed using archival satellite pop-up tags. *Mar. Ecol. Prog. Ser.* 387, 241–253. doi: 10.3354/meps08109
- Campana, S. E., Natanson, L. J., and Myklevoll, S. (2002). Bomb dating and age determination of large pelagic sharks. *Can. J. Fish. Aquat. Sci.* 59, 450–455. doi: 10.1139/F02-027
- Coelho, R., Domingo, A., Courtney, D., Cortés, E., Arocha, F., Liu, K.-M., et al. (2018). An updated revision of shortfin mako size distributions in the Atlantic. *Collect. Vol. Sci. Pap. ICCAT* 75, 476–492.
- Cooke, S. J., and Suski, C. D. (2004). Are circle hooks an effective tool for conserving marine and freshwater recreational catch-and-release fisheries? *Aquat. Conserv. Mar. Freshw. Ecosyst.* 14, 299–326. doi: 10.1002/aqc.614
- Cortés, E. (1998). Demographic analysis as an aid in shark stock assessment and management. *Fish. Res.* 39, 199–208. doi: 10.1016/s0165-7836(98)00183-0
- Cortés, E. (2002). Incorporating uncertainty into demographic modeling: application to shark population and their conservation. *Conserv. Biol.* 16, 1048–1062. doi: 10.1046/j.1523-1739.2002.00423.x
- Cortés, E. (2016). Perspectives on the intrinsic rate of population growth. *Methods Ecol. Evol.* 7, 1136–1145. doi: 10.1111/2041-210X.12592
- Cox, D. R. (1972). Regression models and life tables. *J. R. Stat. Soc.* 34, 187–200.
- Cox, D. R., and Oakes, D. (1984). *Analysis of Survival Data*. London: Chapman and Hall Ltd.
- Davis, M. W. (2002). Key principles for understanding fish bycatch discard mortality. *Can. J. Fish. Aquat. Sci.* 59, 1834–1843. doi: 10.1139/F02-139
- Dulvy, N. K., Fowler, S. L., Musick, J. A., Cavanagh, R. D., Kyne, P. M., Harrison, L. R., et al. (2014). Extinction risk and conservation of the world's sharks and rays. *eLife* 3, 1–34. doi: 10.7554/eLife.00590
- Ellis, J. R., McCully, S. R., and Poisson, F. (2017). A review of capture and post-release mortality of elasmobranchs. *J. Fish Biol.* 90, 653–722. doi: 10.1111/jfb.13197
- Epperly, S. P., Watson, J. W., Foster, D. G., and Shah, A. K. (2012). Anatomical hooking location and condition of animals captured with pelagic longlines: the grand banks experiments 2002–2003. *Bull. Mar. Sci.* 88, 513–527. doi: 10.5343/bms.2011.1083
- García, V. B., Lucifora, L. O., and Myers, R. A. (2008). The importance of habitat and life history to extinction risk in sharks, skates, rays and chimaeras. *Proc. R. Soc. B.* 275, 83–89. doi: 10.1098/rspb.2007.1295
- Gedamke, T., Hoenig, J. M., Musick, J. A., DuPaul, W. D., and Gruber, S. H. (2007). Using demographic models to determine intrinsic rate of increase and sustainable fishing for elasmobranchs: pitfalls, advances and applications. *N. Am. J. Fish. Manage.* 27, 605–618. doi: 10.1577/M05-157.1
- Gilman, E., Chaloupka, M., Dagorn, L., Hall, M., Hobday, A., Musyl, M., et al. (2019). Robbing Peter to pay Paul: replacing unintended cross-taxa conflicts with intentional tradeoffs by moving from piecemeal to integrated fisheries bycatch management. *Rev. Fish. Biol. Fish.* 29, 93–123. doi: 10.1007/s11160-019-09547-1
- Gilman, E., Chaloupka, M., Swimmer, Y., and Piovano, S. (2016). A cross-taxa assessment of pelagic longline by-catch mitigation measures: conflicts and mutual benefits to elasmobranchs. *Fish Fish.* 17, 748–784. doi: 10.1111/faf.12143
- Hammerschlag, N., and Sulikowski, J. (2011). Killing for conservation: the need for alternatives to lethal sampling of apex predatory sharks. *Endanger. Species Res.* 14, 135–140. doi: 10.3354/esr00354
- Harcourt, R., Sequeira, A. M. M., Zhang, X., Roquet, F., Komatsu, K., Heupel, M., et al. (2019). Animal-borne telemetry: an integral component of the ocean observing toolkit. *Front. Mar. Sci.* 6:326. doi: 10.3389/fmars.2019.00326
- Harry, A. V. (2018). Evidence for systemic age underestimation in shark and ray ageing studies. *Fish Fish.* 19, 185–200. doi: 10.1111/FAF.12243
- Hazen, E. L., Maxwell, S. M., Bailey, H., Bograd, S. J., Hamann, M., and Gaspar, P. (2012). Ontogeny in marine tagging and tracking science: technologies and data gaps. *Mar. Ecol. Prog. Ser.* 457, 221–240. doi: 10.3354/meps09857
- Hewitt, D. A., and Hoenig, J. M. (2005). *Comparison Of Two Approaches For Estimating Natural Mortality Based On Longevity*. VIMS Articles. 566. Available online at: <https://scholarworks.wm.edu/vimsarticles/566> (accessed March 24, 2021).
- Hoolihan, J. P., Luo, J., Abascal, F. J., Campana, S. E., De Metrio, G., Deway, H., et al. (2011). Evaluating post-release behavior modification in large pelagic fish deployed with pop-up satellite archival tags. *ICES J. Mar. Sci.* 68, 880–889. doi: 10.1093/icesjms/fsr024
- Hutchinson, M. R., Itano, D. G., Muir, J. A., and Holland, K. N. (2015). Post-release survival of juvenile silky sharks captured in a tropical tuna purse seine fishery. *Mar. Ecol. Prog. Ser.* 521, 143–154. doi: 10.3354/meps11073
- Jepsen, N., Thorstad, E. B., Havn, T., and Lucas, M. C. (2015). The use of external electronic tags on fish: an evaluation of tag retention and tagging effects. *Anim. Biotelem.* 3:49. doi: 10.1186/s40317-015-0086-z
- Jerome, J., Gallagher, A., Cooke, S., and Hammerschlag, N. (2018). Integrating reflexes with physiological measures to evaluate coastal shark stress response to capture. *ICES J. Mar. Sci.* 75, 796–804. doi: 10.1093/icesjms/fsx191
- Kenchington, T. J. (2014). Natural mortality estimators for information-limited fisheries. *Fish Fish.* 15, 533–562. doi: 10.1111/faf.12027
- Kneebone, J., Benoît, H. P., Bernal, D., and Golet, W. (2020). Application of a parametric survival model to understand capture-related mortality and predation of yellowfin tuna (*Thunnus albacares*) released in a recreational fishery. *Can. J. Fish. Aquat. Sci.* (in press). doi: 10.1139/cjfas-2020-0266
- Lewison, R. L., Crowder, L. B., Read, A. J., and Freeman, S. A. (2004). Understanding impacts of fisheries bycatch on marine megafauna. *Trends Ecol. Evol.* 19, 598–604. doi: 10.1016/j.tree.2004.09.004
- Marçalo, A., Guerreiro, P. M., Bentes, L., Rangel, M., Monteiro, P., Oliveira, F., et al. (2018). Effects of different slipping methods on the mortality of sardine, *Sardina pilchardus*, after purse-seine capture off the Portuguese Southern coast (Algarve). *PLoS One* 13:e0195433. doi: 10.1371/journal.pone.0195433
- Miller, P., Santos, C. C., Carlson, J., Natanson, N., Cortés, E., Mas, F., et al. (2020). Updates on post-release mortality of shortfin mako in the Atlantic using satellite telemetry. *SCRS/2019/096. Collect. Vol. Sci. Pap. ICCAT* 76, 298–315.
- Molina, J. M., and Cooke, S. J. (2012). Trends in shark bycatch research: current status and research needs. *Rev. Fish Biol. Fish.* 22, 719–737. doi: 10.1007/s11160-012-9269-3
- Musyl, M. K., Domeier, M. L., Nasby-Lucas, N., Brill, R. W., McNaughton, L. M., Swimmer, J. Y., et al. (2011). Performance of pop-up satellite archival tags. *Mar. Ecol. Prog. Ser.* 433, 1–28. doi: 10.3354/meps09202
- Musyl, M. K., and Gilman, E. L. (2019). Meta-analysis of post-release fishing mortality in apex predatory pelagic sharks and white marlin. *Fish Fish.* 20, 466–500. doi: 10.1111/faf.12358
- Musyl, M. K., Moyes, C. D., Brill, R. W., and Fragoso, N. (2009). Factors influencing mortality estimates in post-release survival studies. *Mar. Ecol. Prog. Ser.* 396, 157–159. doi: 10.3354/meps08432
- Musyl, M. K., Moyes, C. D., Brill, R. W., Mourato, B. L., West, A., McNaughton, L. M., et al. (2015). Postrelease mortality in istiophorid billfish. *Can. J. Fish. Aquat. Sci.* 72, 1–19. doi: 10.1002/9780470935095.ch2
- Natanson, L. J., Kohler, N. E., Ardizzone, D., Cailliet, G. M., Wintner, S. P., and Mollet, H. F. (2006). Validated age and growth estimates for the shortfin mako, *Isurus oxyrinchus*, in the North Atlantic Ocean. *Environ. Biol. Fish.* 77, 367–383. doi: 10.1007/978-1-4020-5570-6\_16
- Natanson, L. J., Mello, J. J., and Campana, S. E. (2002). Validated age and growth of the porbeagle shark (*Lamna nasus*) in the western North Atlantic Ocean. *Fish Bull.* 100, 266–278.
- Natanson, L. J., Skomal, G. B., Hoffmann, S. L., Porter, M. E., Goldman, K. J., and Serra, D. (2018). Age and growth of sharks: do vertebral band pairs record age? *Mar. Freshwater Res.* 69, 1440–1452. doi: 10.1071/MF17279
- Natanson, L. J., Winton, M., Bowlby, H. D., Joyce, W., Deacy, B., Coelho, R., et al. (2020). Updated reproductive parameters for the shortfin mako (*Isurus oxyrinchus*) in the North Atlantic Ocean with inferences of distribution by sex and reproductive stage. *Fish Bull.* 118, 21–36. doi: 10.7755/FB.118.1.3

- Oliver, S., Braccini, M., Newman, S. J., and Harvey, E. S. (2015). Global patterns in the bycatch of sharks and rays. *Mar. Policy* 54, 86–97. doi: 10.1016/j.marpol.2014.12.017
- Pardo, S. A., Kindsvater, H. K., Reynolds, J. D., and Dulvy, N. K. (2016). Maximum intrinsic rate of population increase in sharks, rays, and chimaeras: the importance of survival to maturity. *Can. J. Fish. Aquat. Sci.* 73, 1159–1163. doi: 10.1139/cjfas-2016-0069
- Peng, R. D. (2019). *simpleboot: Simple Bootstrap Routines*. R package version 1.1-7. Available online at: <https://CRAN.R-project.org/package=simpleboot> (accessed March 24, 2021).
- Poisson, F., Catteau, S., Chiera, C., and Groul, J.-M. (2019). The effect of hook type and trailing gear on hook shedding and fate of pelagic stingray (*Pteroplatytrygon violacea*): New insights to develop effective mitigation approaches. *Mar. Policy* 107:103594. doi: 10.1016/j.marpol.2019.103594
- Raoult, V., Williamson, J. E., Smith, T. M., and Gaston, T. F. (2019). Effects of on-deck holding conditions and air exposure on post-release behaviours of sharks revealed by a remote operated vehicle. *J. Exper. Marine Biol. Ecol.* 511, 10–18. doi: 10.1016/j.jembe.2018.11.003
- Reinhardt, J. F., Weaver, J., Latham, P. J., Dell'Apa, A., Serafy, J. E., Browder, J. A., et al. (2017). Catch rate and at-vessel mortality of circle hooks versus J-hooks in pelagic longline fisheries: a global meta-analysis. *Fish. Fish.* 19, 413–430. doi: 10.1111/faf.12260
- Rosa, D., Mas, F., Mathers, A., Natanson, L. J., Domingo, A., Carlson, J., et al. (2017). *Age and Growth of Shortfin Mako in the North Atlantic, with Revised Parameters for Consideration to use in the Stock Assessment*. ICCAT-SCRS Document, SCRS/2017/111. Madrid: International Commission for the Conservation of Atlantic Tunas.
- Santos, C. C., Forselledo, R., Mas, F., Cortés, E., Carlson, J., Bowlby, H., et al. (2020). *Size Distribution of Porbeagle Shark in the North and South Atlantic using Data from Observer Programs*. ICCAT-SCRS Document, SCRS/2020/097. Madrid: International Commission for the Conservation of Atlantic Tunas.
- Shepard, E. L. C., Ahmed, M. Z., Southall, E. J., Witt, M. J., Metcalfe, J. D., and Sims, D. W. (2006). Diel and tidal rhythms in diving behavior of pelagic sharks identified by signal processing of archival tagging data. *Mar. Ecol. Prog. Ser.* 328, 205–213. doi: 10.3354/meps328205
- Sippel, T., Eveson, J. P., Galuardi, B., Lam, C., Hoyle, S., Maunder, M., et al. (2015). Using movement data from electronic tags in fisheries stock assessment: a review of models, technology and experimental design. *Fish. Res.* 163, 152–160. doi: 10.1016/j.fishres.2014.04.006
- Sippel, T., Holdsworth, J., Dennis, T., and Montgomery, J. (2011). Investigating behavior and population dynamics of striped marlin (*Kajikia audax*) from the Southwest Pacific Ocean with satellite tags. *PLoS One* 6:e21087. doi: 10.1371/journal.pone.0021087
- Skomal, G. B. (2007). Evaluating the physiological and physical consequences of capture on post-release survivorship in large pelagic fishes. *Fish. Manag. Ecol.* 14, 81–89. doi: 10.1111/j.1365-2400.2007.00528.x
- Skomal, G. B., and Chase, B. C. (2002). The physiological effects of angling on post-release survivorship in tunas, sharks and marlin. *Am. Fish. Soc. Symp.* 30, 135–138.
- Sulikowski, J., Golet, W., Hoffmayer, E., Driggers, W., Natanson, L., Carlson, A., et al. (2020). Observing post-release mortality for dusky sharks, *Carcharhinus obscurus*, captured in the U.S. pelagic longline fishery. *Fish. Res.* 221:105341. doi: 10.1016/j.fishres.2019.105341
- Then, A. Y., Hoenig, J. M., Hall, N. G., and Hewitt, D. A. (2015). Evaluating the predictive performance of empirical estimators of natural mortality rate using information on over 200 fish species. *ICES J. Mar. Sci.* 72, 82–92. doi: 10.1093/icesjms/fsu136
- Therneau, T. M., and Grambsch, T. M. (2000). *Modeling Survival Data: Extending the Cox Model*. New York, NY: Springer.
- Thorburn, J., Neat, F., Burrett, I., Henry, L.-A., Bailey, D. M., Jones, C. S., et al. (2019). Ontogenetic variation in movements and depth use, and evidence of partial migration in a benthopelagic elasmobranch. *Front. Ecol. Evol.* 7:353. doi: 10.3389/fevo.2019.00353
- Todd Jones, T., Van Houtan, S., Bostrom, B. L., Ostafichuk, P., Mikkelsen, J., Tezcan, E., et al. (2013). Calculating the ecological impacts of animal-borne instruments on aquatic organisms. *Methods Ecol. Evol.* 4, 1178–1186. doi: 10.1111/2041-210x.12109
- Whitney, N. M., White, C. F., Gleiss, A. C., Schwieterman, G. D., Anderson, P., Hueter, R. E., et al. (2016). A novel method for determining post-release mortality, behavior, and recovery period using acceleration data loggers. *Fish. Res.* 183, 210–221. doi: 10.1016/j.fishres.2016.06.003
- Wilson, S. M., Raby, G. D., Burnett, N. J., Hinch, S. G., and Cooke, S. J. (2014). Looking beyond the mortality of bycatch: sublethal effects of incidental capture on marine animals. *Biol. Conserv.* 171, 61–72. doi: 10.1016/j.biocon.2014.01.020

**Conflict of Interest:** The authors declare that the research was conducted in the absence of any commercial or financial relationships that could be construed as a potential conflict of interest.

Copyright © 2021 Bowlby, Benoît, Joyce, Sulikowski, Coelho, Domingo, Cortés, Hazin, Macias, Biaís, Santos and Anderson. This is an open-access article distributed under the terms of the Creative Commons Attribution License (CC BY). The use, distribution or reproduction in other forums is permitted, provided the original author(s) and the copyright owner(s) are credited and that the original publication in this journal is cited, in accordance with accepted academic practice. No use, distribution or reproduction is permitted which does not comply with these terms.





# Fieldable Environmental DNA Sequencing to Assess Jellyfish Biodiversity in Nearshore Waters of the Florida Keys, United States

Cheryl Lewis Ames<sup>1,2,3\*</sup>, Aki H. Ohdera<sup>3,4</sup>, Sophie M. Colston<sup>1</sup>, Allen G. Collins<sup>3,5</sup>, William K. Fitt<sup>6</sup>, André C. Morandini<sup>7,8</sup>, Jeffrey S. Erickson<sup>9</sup> and Gary J. Vora<sup>9\*</sup>

<sup>1</sup> National Research Council, National Academy of Sciences, U.S. Naval Research Laboratory, Washington, DC, United States, <sup>2</sup> Graduate School of Agricultural Science, Faculty of Agriculture, Tohoku University, Sendai, Japan, <sup>3</sup> Department of Invertebrate Zoology, National Museum of Natural History, Smithsonian Institution, Washington, DC, United States, <sup>4</sup> Division of Biology and Biological Engineering, California Institute of Technology, Pasadena, CA, United States, <sup>5</sup> National Systematics Laboratory of the National Oceanic Atmospheric Administration Fisheries Service, National Museum of Natural History, Smithsonian Institution, Washington, DC, United States, <sup>6</sup> Odum School of Ecology, University of Georgia, Athens, GA, United States, <sup>7</sup> Departamento de Zoologia, Instituto de Biociências, University of São Paulo, São Paulo, Brazil, <sup>8</sup> Centro de Biologia Marinha, University of São Paulo, São Sebastião, Brazil, <sup>9</sup> Center for Bio/Molecular Science and Engineering, U.S. Naval Research Laboratory, Washington, DC, United States

## OPEN ACCESS

### Edited by:

Frank Edgar Muller-Karger,  
University of South Florida,  
United States

### Reviewed by:

Chih-Ching Chung,  
National Taiwan Ocean University,  
Taiwan  
Yu Zhang,  
Shanghai Jiao Tong University, China

### \*Correspondence:

Cheryl Lewis Ames  
ames.cheryl.lynn.a1@tohoku.ac.jp  
Gary J. Vora  
gary.vora@nrl.navy.mil

### Specialty section:

This article was submitted to  
Marine Molecular Biology  
and Ecology,  
a section of the journal  
Frontiers in Marine Science

**Received:** 11 December 2020

**Accepted:** 22 March 2021

**Published:** 13 April 2021

### Citation:

Ames CL, Ohdera AH, Colston SM, Collins AG, Fitt WK, Morandini AC, Erickson JS and Vora GJ (2021) Fieldable Environmental DNA Sequencing to Assess Jellyfish Biodiversity in Nearshore Waters of the Florida Keys, United States.  
*Front. Mar. Sci.* 8:640527.  
doi: 10.3389/fmars.2021.640527

Recent advances in molecular sequencing technology and the increased availability of fieldable laboratory equipment have provided researchers with the opportunity to conduct real-time or near real-time gene-based biodiversity assessments of aquatic ecosystems. In this study, we developed a workflow and portable kit for fieldable environmental DNA sequencing (FeDS) and tested its efficacy by characterizing the breadth of jellyfish (Medusozoa) taxa in the coastal waters of the Upper and Lower Florida Keys. Environmental DNA was isolated from seawater collection events at eight sites and samples were subjected to medusozoan 16S rRNA gene and metazoan mitochondrial cytochrome oxidase 1 gene profiling via metabarcoding onsite. In total, FeDS yielded 175,326 processed sequence reads providing evidence for 53 medusozoan taxa. Our most salient findings revealed eDNA from: (1) two venomous box jellyfish (Cubozoa) species, including taxa whose stings cause the notorious Irukandji envenomation syndrome; (2) two species of potentially introduced stalked jellyfish (Staurozoa); and (3) a likely cryptic species of upside-down jellyfish (Scyphozoa). Taken together, the results of this study highlight the merits of FeDS in conducting biodiversity surveys of endemic and introduced species, and as a potential tool for assessing envenomation and/or conservation-related threats.

**Keywords:** eDNA, envenomation, upside-down jellyfish, conservation, biodiversity, portable lab kit

## INTRODUCTION

Over the past decade, the study of environmental DNA (eDNA) coupled with next-generation sequencing (NGS) has emerged as a promising means to assess and monitor the biodiversity of a habitat which may in turn influence conservation action and intervention. These techniques, which have been commonly used in microbial ecology studies for some time, are now being

similarly adopted for the study of macroorganismal ecology. Timely and accurate assessments of organisms in their native habitats are critical to understanding the dynamics of population trends with respect to normal conditions and potentially disruptive environmental events. Conservation interests have increasingly shifted from surveys with a narrow scope, such as single species, taxon-targeted approaches, to those that evaluate ecosystems more broadly (i.e., community-targeted approaches), within both healthy and compromised ecosystems (Thomsen et al., 2012; Thomsen and Willerslev, 2015; Goldberg et al., 2016; Port et al., 2016).

As the name indicates, eDNA is genetic material that has been deposited into the environment via numerous sources, such as skin, feces, urine, larvae, and gametes. DNA extracted directly from environmental samples (e.g., filtered seawater, soil, and sand) can be sequenced to identify source organisms occupying the proximate area of the collected sample (Laramie et al., 2015; Minamoto et al., 2016; Hinlo et al., 2017; Dibattista et al., 2020). Accordingly, eDNA-based investigations have proven to be as valuable as traditional survey methods that require capture and subsampling of target organisms. Importantly, eDNA methods are a less-intrusive approach to studying invasive or declining species (Zhou et al., 2013; Bucklin et al., 2016; Holman et al., 2019; Nelson-Chorney et al., 2019), documenting the distribution of difficult to sample taxa (Parsons et al., 2018), and estimating relative seasonal biomass of target species (Takasu et al., 2019; Stoeckle et al., 2020). Marine-derived eDNA has also been likened to a “barometer of disturbance” with respect to its potential to assess anthropogenic effects on ecosystems (Dibattista et al., 2020).

While the depth and resolution of eDNA sequencing make it an attractive approach for community characterization, often there is a significant delay between sample collection in the field and sequence generation and analysis in the laboratory. Marine ecosystems, which are dynamic and subject to fluctuations in tides, reproductive cycles, seasonal disasters and stochastic events, require the generation of actionable data in a timelier manner. For such applications, we developed the fieldable eDNA sequencing (FeDS) kit which utilizes the field-deployable MinION sequencing platform Oxford Nanopore Technologies (ONT) [reviewed in Jain et al. (2016); Pomerantz et al. (2018), Krehenwinkel et al. (2019); Watsa et al. (2020)].

In this study, FeDS was used to assess the biodiversity of jellyfishes (phylum Cnidaria; subphylum Medusozoa) in order to create a more comprehensive survey of medusozoan taxa surrounding the Florida Keys. A critical FeDS capability would be the detection of two resident species for which draft genomes were recently published (Ohdera et al., 2019) – the upside-down jellyfish *Cassiopea xamachana* (class Scyphozoa) and the venomous box jellyfish *Alatina alata* (class Cubozoa). *C. xamachana* is considered a valuable bioindicator species, with potential applications to ecotoxicological assessments (Ohdera et al., 2018). *A. alata* is known as a notorious stinger during monthly inshore spawning aggregations in tropical and subtropical waters (Lewis et al., 2013; Lewis Ames et al., 2016).

We deployed the FeDS kit at sampling locations in the Upper Keys (Key Largo and Marathon Key) where ongoing

studies on viable *C. xamachana* populations have continued for decades (Fitt and Trench, 1983; Hofmann et al., 1996; Fitt and Costley, 1998). As the life cycle of *Cassiopea* (like many other jellyfishes) involves an alternation of generations between a sexually reproducing jellyfish (medusa), microscopic swimming larva (planula), and a sessile asexual stage (polyp) (**Supplementary Figure 1**), we anticipated that there would be sufficient eDNA in the water column for FeDS-based detection of these medusozoans. Sampling sites were also selected in the Lower Keys (Fleming Key) to gauge the potential for FeDS to serve as a tool for assessing envenomation risks due to difficult-to-detect venomous jellyfish. These sites corresponded to locations where unresolved jellyfish stings had been reported (Grady and Burnett, 2003).

## MATERIALS AND METHODS

### Collection Sites and Samples

Triplicate seawater samples (1 L) were collected from the following locations: (a) three nearshore sites in Upper Keys (Key Largo, FL, United States) with one artificial site, as a positive control (May 14–16, 2018), and (b) four nearshore sites in Lower Keys (Fleming Key, FL, United States), with one of these sites serving as a process negative control (May 16–18, 2018) (**Table 1** and **Supplementary Figure 2**).

Collection sites in the Upper Keys, which included Key Largo and Marathon Key (BC01 – BC03) (**Table 1** and **Supplementary Figures 2A–E**), were chosen based on historic reports of large smacks of the upside-down jellyfish *C. xamachana* (**Figures 1a–c**), often together with *Cassiopea frondosa* (**Figures 1d–f**; Hofmann et al., 1996; Fitt and Costley, 1998; Ohdera et al., 2018). The presence of *Cassiopea* medusae has been documented at all four locations by participants of the Annual International *Cassiopea* Workshop, held at the Key Largo Marine Research Laboratory since May 2017. As an ostensible positive control (BC04), an outdoor aquarium was established at the Key Largo Marine Research Station, consisting of a 10 L plastic container filled with locally sourced seawater and live *C. frondosa* medusae ( $n = 6$ ) (**Figures 1g,h**) collected at BC02 (**Table 1**, **Supplementary Figure 2E**, and **Figures 1g,h**).

Collection sites in the Lower Keys – Fleming Key (BC05 – BC08) (**Table 1** and **Supplementary Figures 2F–H**) were primarily chosen based on proximity to the United States Special Forces Underwater Operations School (SFUWOS), where United States military divers previously reported experiencing systemic envenomation syndrome similar to “Irukandji syndrome” (Barnes, 1964), and at least one reported jellyfish-related fatality has been documented (Burnett and Gable, 1989; Grady and Burnett, 2003). Seawater samples were taken from BC08 – an artificial enclosure away from the dive drop sites, to serve as a process negative control (**Table 1**). Although no jellyfish species were positively identified in the reported sting incidences, the venomous box jellyfish *A. alata* is a suspected culprit, given its “Irukandji-like” sting and well-documented presence in Caribbean and Florida waters (Lawley et al., 2016; Lewis Ames et al., 2016; Bouyer-Monot et al., 2017).

**TABLE 1** | Florida Keys eDNA collection sites. “Sheltered” and “Pelagic” are qualitative descriptions of the general connectedness observed between the sites and open ocean.

Station	Location	Sampled	Coast
BC01	Quarry, Upper Keys <b>Figure 6B, Supplementary Figure 2A</b>	2018/5/15	Sheltered
BC02	Rock Harbor, Upper Keys <b>Figure 6C, Supplementary Figure 2B</b>	2018/5/15	Sheltered
BC03	Buttonwood Sound, Upper Keys <b>Figure 6A, Supplementary Figures 2C,D</b>	2018/5/15	Pelagic
BC04	Aquarium, Upper Keys <b>Figure 6D, Supplementary Figure 2E</b>	2018/5/15	N/A
BC05	SFUWOS Finger Pier, Lower Keys <b>Figure 6E, Supplementary Figure 2F</b>	2018/5/17	Pelagic
BC06	SFUWOS FAA Tower, Lower Keys <b>Figure 6F, Supplementary Figure 2G</b>	2018/5/17	Pelagic
BC07	SFUWO Drop, Lower Keys <b>Figure 6G, Supplementary Figure 2H</b>	2018/5/17	Pelagic
BC08	Enclosure, Lower Keys Not shown	2018/5/17	Pelagic

Corresponding to map in **Figure 6**.

## Filtration of Seawater Samples

Triplicate seawater samples from each site were collected by rinsing the contents of a plankton net (towed by kayaking or snorkeling in shallow coastal waters) into a 1 L bottle (Nalgene), and subjected to coarse filtration with 250  $\mu$ m sieve (20 cm mouth, Fisherbrand), homogenization by hand-held USB-powered Juicer Cup Blender (380 ml volume, Huatop) for 25–35 s to remove debris and large particles, and then fine filtration through a 47 mm diameter water-testing membrane filter (0.45  $\mu$ m Gridded Sterile Cellulose Nitrate Membrane, Sartorius) using a magnetic filter funnel (500 ml, PALL) attached to a polypropylene vacuum flask (1 L, #8 stopper, Nalgene) connected to a battery-powered portable vacuum filtration system (Argos Technologies PV000 P-VAC System) (**Figure 2A**). Filter membranes (containing eDNA filtrate) were transferred to custom-made 2-chamber tubes [0.5 ml PCR tubes with a hole drilled in the bottom, suspended within a 2 ml DNA LoBind tube (Eppendorf)] containing 400  $\mu$ l of tissue lysis buffer and 40  $\mu$ l of protease K (ATL Buffer, DNeasy Blood and Tissue Isolation Kit, Qiagen). Tubes containing membranes in buffer were kept at ambient temperature until DNA extraction was conducted (**Figure 2B**). All equipment was wiped between stations with HYPE-WIPE 3% Bleach Towlettes (7.6 cm, Current Technologies) and rinsed with distilled water and 70% ethanol, before processing subsequent samples.

## Isolation of eDNA From Filtrate

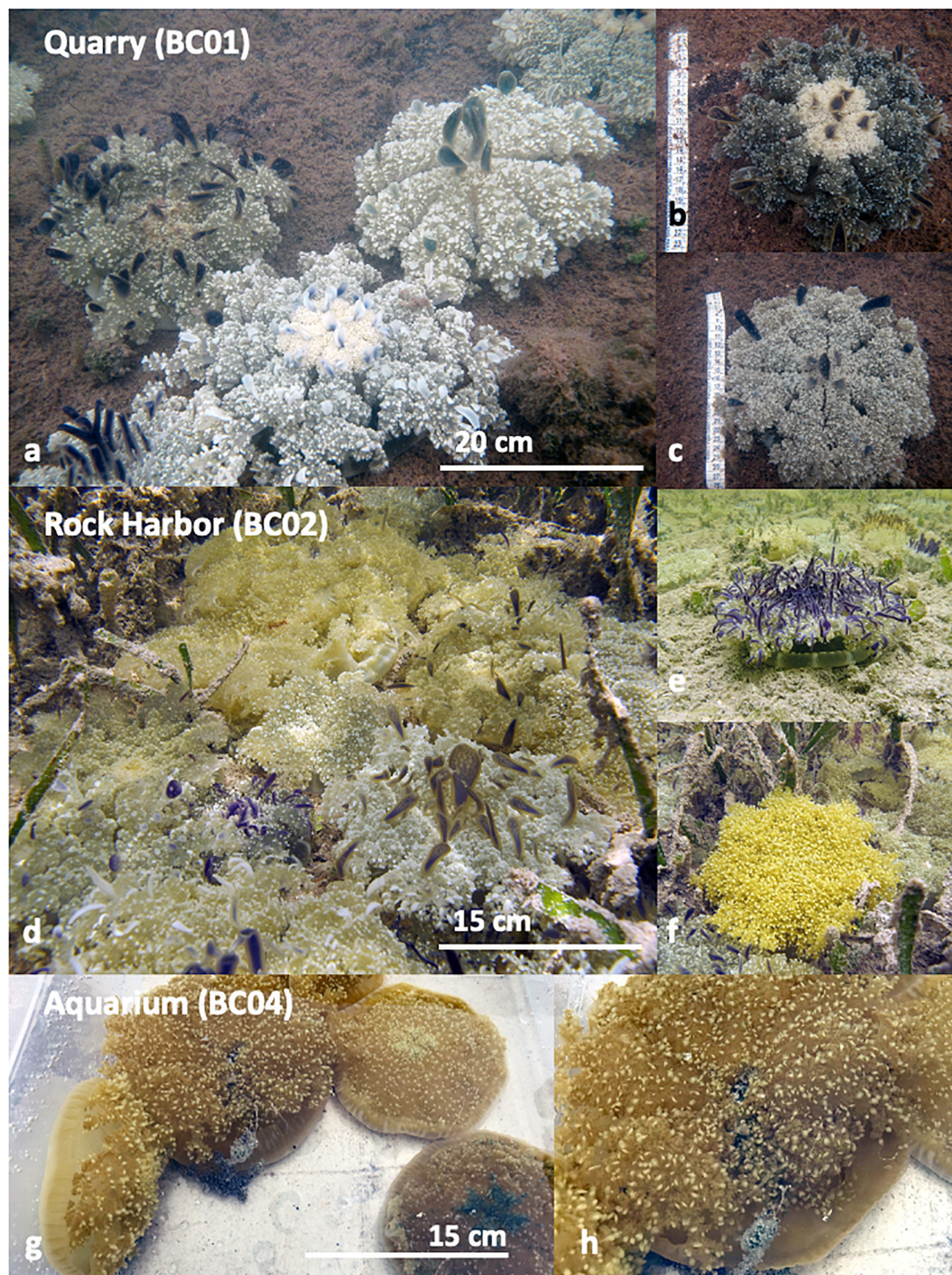
DNA extraction and molecular protocols were carried out using the following battery-operated (12V Lithium battery pack (RAVPower) portable equipment: mini centrifuge (6,000RPM/2,960G RPM, TOMY) (**Figure 2B**), mini dry bath (MyBlock, Benchmark Scientific) and USB-operated 8-well thermocycler (miniPCR) (**Figure 2C**), Mini Vortex mixer (NISSIN) (AA alkaline batteries), and USB-operated fluorometer (Quantus Promega) with the QuantiFluor ONE dsDNA System. Environmental DNA was extracted using modifications to the protocol for the DNeasy Blood and Tissue Isolation Kit (Qiagen), as previously published (Yamamoto et al., 2016). Specifically, tubes containing membranes in buffer were incubated for 90 min at 56°C, 200  $\mu$ l TE 1X buffer was added to membranes to maximize yield. After centrifugation, 600  $\mu$ l was added to the collected liquid (filter membrane discarded), and in the final

step eDNA was eluted in a volume of 70  $\mu$ l. Extracted eDNA was purified with AMPure XP beads (Agencourt AMPURE XP, Beckman Coulter) on a magnetic bead separation rack (Bel-Art™ SP Scienceware), at ambient temperature using a 1–1.6X ratio (to remove fragments smaller than 100 bp), and quantified using the fluorometer. Of the triplicate samples for each of the eight collection sites, the sample with the highest DNA concentration for each site was selected for downstream analysis, starting with first round PCR in the USB-operated 8-well thermocycler (miniPCR) (**Figures 2, 3**).

## Target eDNA Amplification, Sample Barcoding, and Pooling

Two mitochondrial gene fragments, one from the 16S rRNA gene (large subunit of the ribosome; 565 bp) and the other from cytochrome oxidase subunit 1 (COI) gene (720 bp), were targeted using primers with an additional 5' sequence which allows for unique ONT barcodes to be added during library preparation (**Figure 3**). The COI primers were designed to amplify a broad diversity of metazoans (Geller et al., 2013), while the 16S rRNA gene primers specifically target most medusozoans (Lawley et al., 2016). For each 20  $\mu$ l reaction, 3  $\mu$ l of template DNA was combined with 1.4  $\mu$ l dNTPs, 2  $\mu$ l Advantage 2 DNA buffer, Advantage 2 Polymerase (Advantage 2 Enzyme System Kit, Takara Bio), 1  $\mu$ l each of forward and reverse primers (10  $\mu$ M), and 11.2  $\mu$ l nuclease-free water. Subsequently, amplicons were prepared for sequencing using the 1D ligation kit (LSK-SQK108, ONT) in accordance with the manufacturer's instructions. All PCR steps were conducted on the miniPCR. First-round PCR (**Figure 3**, Step 1, Advantage 2 Enzyme System Kit, Takara Bio) conditions were as follows: initial denaturation at 95°C (5 min); three cycles of denaturation at 95°C (30 s), annealing at 54°C (30 s), and extension at 72°C (45 s), followed by a final extension executed at 72°C (5 min). Following first round PCR, amplicons for each gene were pooled by collection site by taking equimolar concentrations of each sample to generate a single 20  $\mu$ l purified amplicon sample. In the second round PCR (**Figure 3**, Step 2, Barcoding by PCR), unique ONT barcodes (EXP-PBC001, ONT) were added to each pooled amplicon sample using LongAmpTaq 2X master mix (New England BioLabs) with the following reaction conditions: initial denaturation at 95°C (3 min); 15 cycles of denaturation at 95°C (15 s), annealing at 62°C (15 s) and





**FIGURE 1 |** *Cassiopea* medusae at Upper Keys collection sites: **(a–c)** Quarry (BC01). **(a)** Large *C. xamachana* medusae in patches of high abundance ( $n = 5$  in view), on the substrate, but not overlapping, approximately 17–30 cm diameter. **(b)** Large individual *C. xamachana* medusa. **(c)** Large individual *C. xamachana* medusa. **(d–f)** Rock Harbor (BC02). **(d)** Medium to large *C. xamachana* and *C. frondosa* medusae on the substrate in high abundance ( $n = 16$  in view), overlapping one another, approximately 15–20 cm diameter. **(e)** Medium individual *C. xamachana* medusa. **(f)** Medium individual *C. frondosa* medusa. **(g,h)** Aquarium (BC04). **(g)** Medium *C. frondosa* medusae in aquarium with water from the local source. **(h)** Close up on medium *C. frondosa* medusae from **(g)**, showing mucus being released. No *Cassiopea* medusae were photographed from BC03, as only a few small medusae were witnessed. Sampling locations mapped in **Figure 6**.

extension at 65°C (45 s), followed by a final extension at 65°C (5 min). For final multiplex library preparation (**Figure 3**, Step 3), ~1 µg of input DNA (equimolar pooled barcoded amplicons)

was end-repaired and dA-tailed using NEBNext End Repair/dA-tailing (NEB), then incubated at 20°C (using Medi-Pak Instant Cold Packs) and then at 65°C for 5 min each. Adapters were





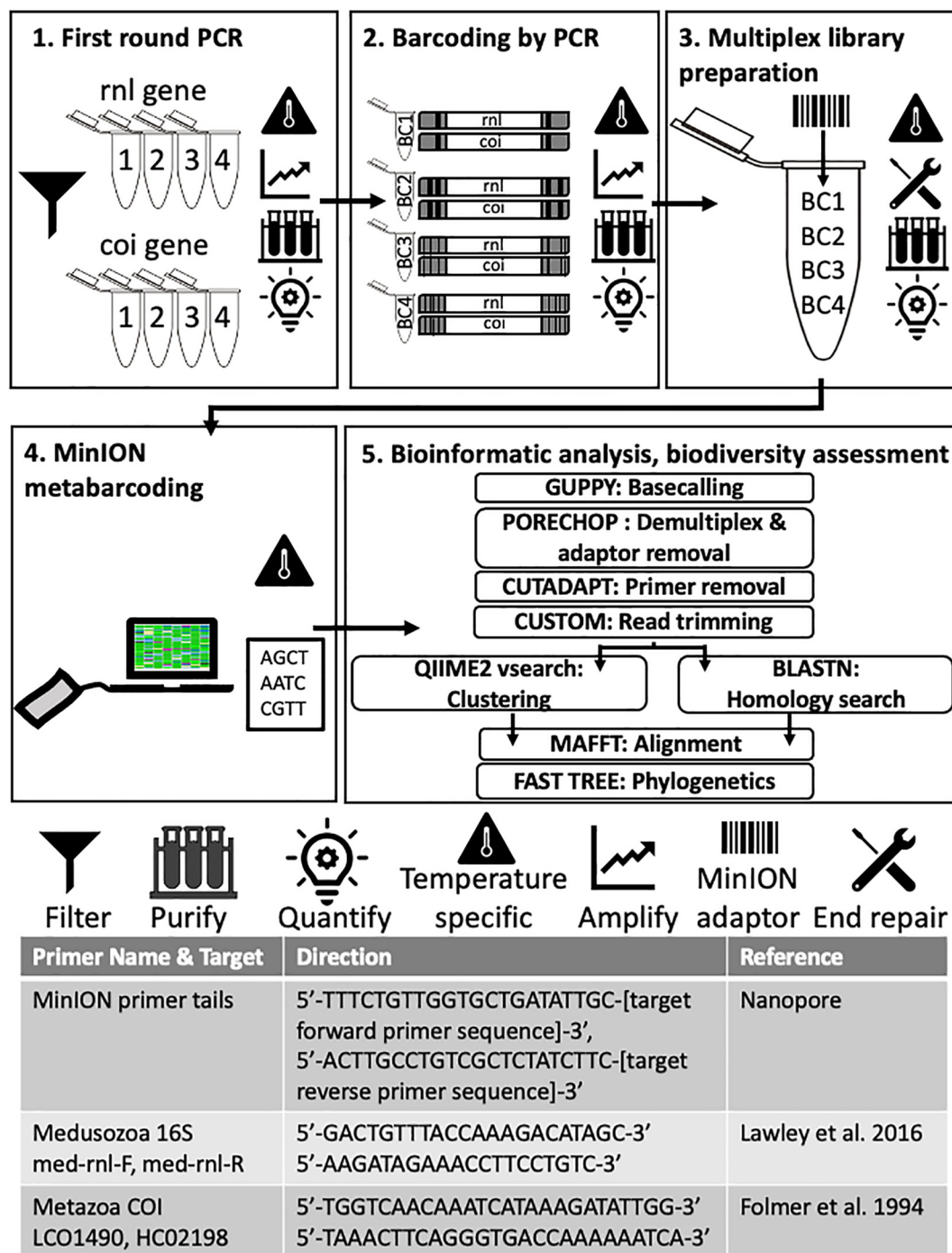
**FIGURE 2 |** Overview of FeDS workflow used in this study for collection sites in both Upper Keys (BC01 – BC04) and Lower Keys (BC05 – BC08). **(A)** Triplicate seawater samples were collected from each sampling location and processed in the field within 1–2 h post-collection. Coarse filtration was conducted, followed by homogenization and fine filtration on a water-testing membrane filter. **(B)** Filter membranes (containing eDNA filtrate) were kept in buffer at ambient temperature until eDNA was extracted; in the final step, isolated eDNA was concentrated in 70  $\mu$ l of elution buffer. All equipment was sanitized between stations. **(C)** Molecular protocols including PCR were carried out using an USB-operated 8-well thermocycler (miniPCR). **(D)** Nanopore sequencing metabarcoding with MinION commenced in Upper Keys (BC01 – BC04) outside on a bluff overlooking Buttonwood Sound, and in Key West (BC05 – BC08) in a rental car.

added in a ligation reaction using the 1D adapter mix (AMX) and Blunt/TA Ligase Master Mix (NEB) and incubated at ambient temperature for 10 min.

### MinION Metabarcoding

Separately for the Upper Keys and Lower Keys samples, the prepared library (~300 ng of NEB end-prepped template) was loaded onto an R9.4 flow cell (FLO-MIN106, ONT) and sequenced using the MinION Mk-1B and MinKNOW v 1.2.8 (offline version), on a MacBook Pro (Sierra Version 10.12.6, 16GB, 17 quad core) connected by an USB to USB-C adapter (Figure 3, Step 4). The resulting average sequence length of

16S rRNA gene and COI reads for the two MinION runs was 700 and 825 bp, respectively. MinION sequencing for BC01-BC04 was initiated at 21:55 (May 15, 2018) outside on a bluff (elevation ~ 4 m) overlooking Buttonwood Sound (ambient temperature 26.5°C, 81% humidity) (Figure 2D), completed inside the Key Largo Marine Science Station, and lasted 7 hrs and 50 min, generating 578K reads. MinION sequencing for BC05-BC08 was initiated at 12:00 (May 18, 2018) inside a rent-a-car (ambient temperature 27°C, 87% humidity) (Figure 2D), completed inside the Naval Research Laboratory, Key West, and lasted 4 hr and 30 min, generating 521K reads.



**FIGURE 3 |** Molecular and bioinformatic components of the FeDS workflow. **(1)** First round PCR. Two genetic targets were amplified from eDNA samples (16S rRNA gene and COI, 4 miniPCR wells each). Primers and MinION primer tails provided in the table at the bottom. Amplicons pooled by collection site. **(2)** Barcoding by PCR. In the second round PCR, unique nanopore barcodes were added to each pooled amplicon sample. **(3)** Multiplexed library preparation. Input DNA was end-repaired and dA-tailed, and adapters were added. **(4)** MinION metabarcoding. The prepared sequencing library was loaded onto an R9.4 flow cell (FLO-MIN106, ONT) and sequenced using the MinION Mk-1B and MinKNOW v 1.2.8. (offline version), on a laptop. Icons = Filter: Seawater filtered through 0.45  $\mu$ m Gridded Sterile Cellulose Nitrate Membrane, and eDNA isolated using extraction kit. Purification: Impurities removed with AMPure XP beads; purified DNA eluted in 31  $\mu$ l nuclease-free water followed by quantification with the QuantiFluor portable fluorometer using QuantiFluor ONE dsDNA HS assay, after every step. Temperature specific: PCR step (amplification), or cold incubation 20°C, or controlling MinION temperature (to = < 35°C) with battery-powered mini-fan. MinION adaptor: unique nanopore barcodes (EXP-PBC001, ONT) added to each amplicon sample. End repair: End-repaired and dA-tailed using NEBNext End Repair/dA-tailing (NEB). **(5)** Bioinformatic analyses and biodiversity assessments. Software programs in upper case letters, followed by respective application. Refer to code: [https://github.com/aohdera/Ames\\_et\\_al\\_2020](https://github.com/aohdera/Ames_et_al_2020).

## Metabarcoding Data Analysis and Interpretation

Bioinformatic analyses (Figure 3, Step 5) were conducted after returning from the field, on the Smithsonian Institution High Performance Cluster (SI/HPC) (Code available at: [https://github.com/aohdera/Ames\\_et\\_al\\_2020](https://github.com/aohdera/Ames_et_al_2020)). Basecalling of raw reads was done using Guppy (ONT) (Balachandran et al., 2017; Wick, 2017; De Coster et al., 2018) with a quality score cutoff of 9. Demultiplexing and barcode filtering were performed using Porechop v0.2.3 (Wick, 2017) with a strict 85% sequence identity for the forward and reverse barcodes. Alignments were conducted to effectively remove end adaptors and sequences with internal adaptors prior to downstream analyses. As an added conservative measure to ensure removal of residual MinION adaptors and barcodes, Nanofilt (De Coster et al., 2018) was used to trim 50 bp from either end of the sequences. Strictly filtered reads were further trimmed using Cutadapt (Martin, 2001) to specifically remove any untrimmed primers and MinION adaptors, and reads shorter than 550 bp were removed using a custom script<sup>1</sup>.

Reads were classified as either 16S rRNA gene or COI gene sequences using BLASTN against a curated NCBI nucleotide database installed locally from the MIDORI server<sup>2</sup> (Machida et al., 2017). Due to our rigorous quality control protocol and limited reference database, the number of reads with homology matches to metazoan taxa diminished the datasets for all eight metabarcoding samples. As expected, the number of reads represented by the process negative control (BC08) amounted to zero and, as such, BC08 was not included in downstream analyses. The seven remaining trimmed datasets (BC01-BC07) were subsequently concatenated into a single file (containing 64K sequences) for downstream biodiversity assessments (trimmed 16S rRNA gene and COI reads available at: [https://github.com/aohdera/Ames\\_et\\_al\\_2020](https://github.com/aohdera/Ames_et_al_2020)).

## Medusozoan Biodiversity Assessment

Classification of the eDNA samples was conducted using a modified pipeline for the Qiime2 software (Bolyen et al., 2019; Figure 3, Step 5). In order to capture a suitable number of OTUs that might reflect the true biodiversity at sample collection sites, we conducted closed vsearch trial runs in 5% increments for percent identity values from 70–95% (as *de novo* “open” vsearch analysis proved unsuitable for our dataset – see **Supplementary Figures 3,4**). Furthermore, homology search was also conducted with BLASTN on all reads meeting the quality threshold, with BLASTN hits filtered for coverage (80%) and two identity cutoffs of 80 and 90% for comparison (Figure 4). To validate our method, we compared species-richness calculated from the Qiime2 and BLASTN classification methods for both 80% and 90% identity cutoffs (**Supplementary Figure 5**), and settled on a vsearch threshold of 80% clustering. While separate Qiime2 and BLASTN analyses were conducted on both 16S rRNA gene and COI datasets using the above parameters, we focus mainly on the 16S rRNA gene results since those primers preferentially

target medusozoan taxa. The COI primers used in this study broadly target metazoans and were chosen to supplement the 16S rRNA gene libraries to ensure that the starting concentration of total DNA in the multiplex samples was sufficient for optimal sequencing on the MinION, in addition to the potential for recovering COI sequences of medusozoan taxa. To validate the Qiime2 taxonomic assignments, 16S rRNA gene reads showing greater than 80 and 90% similarity to sequences associated with species of the four medusozoan classes – Cubozoa, Hydrozoa, Scyphozoa, and Staurozoa – were aligned using MAFFT (E-INSI algorithm) (Katoh and Standley, 2013). Majority rule consensus sequences were generated in cases where three or more sequences corresponded to a given species (Table 2).

## Phylogenetic Reconstruction

Phylogenetic analyses were conducted using FastTree (Price et al., 2010) (assuming a GTR model of nucleotide evolution, with optimization of the Gamma20 likelihood) as a plugin in Geneious prime version 2019.1.1<sup>3</sup>. In order to assess the overall coherence of our metabarcoding data to the current understanding of medusozoan phylogeny (Zapata et al., 2015), we reconstructed a topology of all sequences (under both identity thresholds, >80% and >90%) including individual or pairs of reads when fewer than three sequences showed similarity to a given medusozoan target (Figure 5A). Separate trees were also constructed for the classes Cubozoa, Scyphozoa and Staurozoa that included sequences for our recovered medusozoan taxa, as well as corresponding 16S rRNA gene sequences from GenBank (Figure 5). Additionally, distance plots for selected taxa of these three classes were reconstructed to validate species-level matches to ascertain whether OTUs represented distinct species or genetic variants of a single species (calculations and distance plots available at [https://github.com/aohdera/Ames\\_et\\_al\\_2020](https://github.com/aohdera/Ames_et_al_2020)). Note that because of the much higher species richness for Hydrozoa (and associated large number of 16S rRNA gene sequences in GenBank), a summary tree was not constructed separately for this class.

## RESULTS

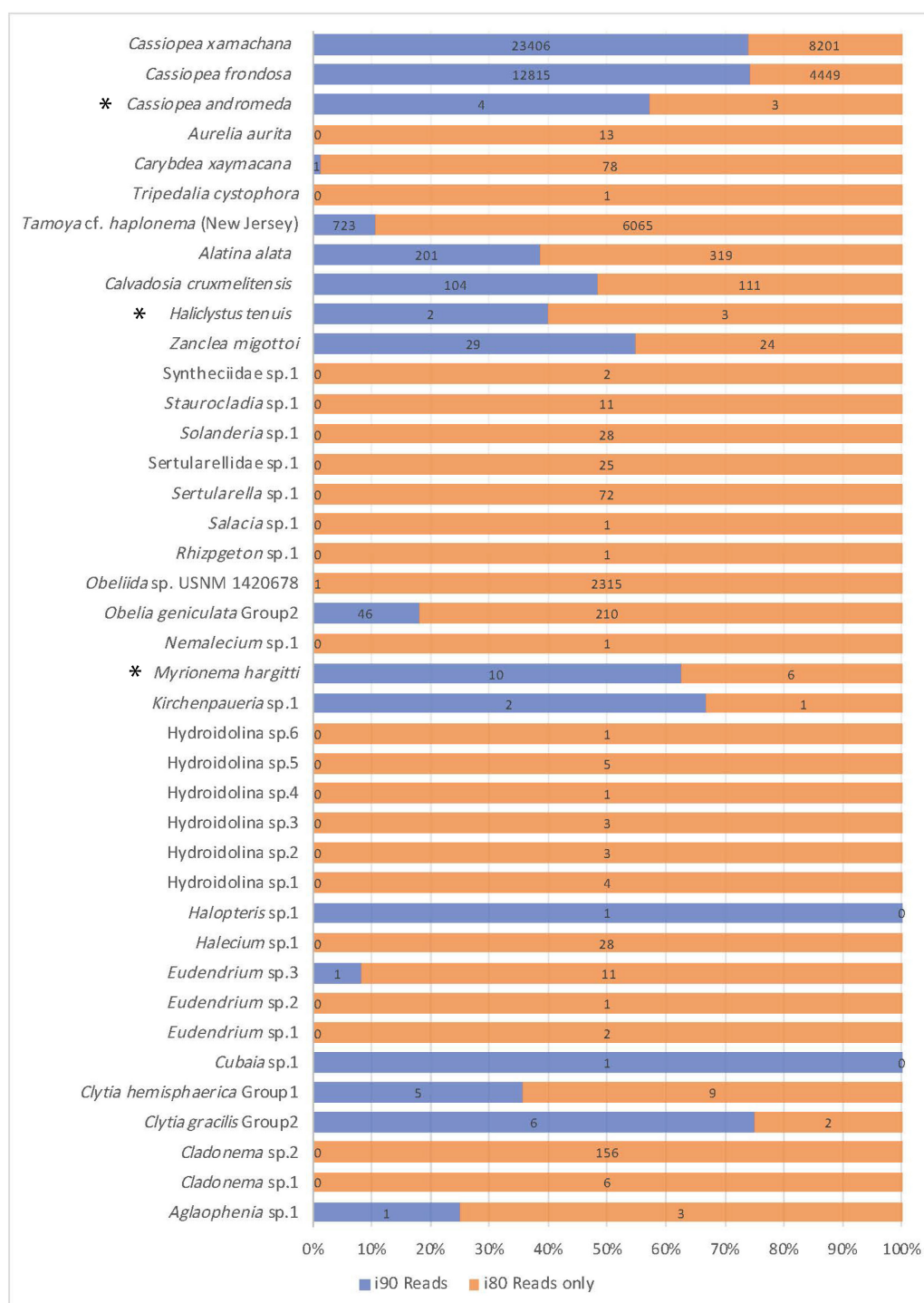
We retained 175,326 total reads after stringent quality filtering and trimming, ranging from 3,965 to 50,063 reads across the seven sampling sites. Of those, 59,705 were identified through BLAST as 16S rRNA gene sequences. BC07 retained the lowest number of reads with 506, while 27,629 reads remained for BC02. Qiime2 analysis using closed vsearch with an identity cutoff of 80% identified a total of 53 medusozoan OTUs (**Supplementary Figure 4**). Despite the low read count for several samples, alpha-diversity rarefaction analysis suggested our method were sufficient to assess progress in recovering representative medusozoan eDNA by sample location, given our sequencing depth (**Supplementary Figures 5,6**). A BLASTN search of our recovered 16S rRNA gene filtered dataset yielded 59 unique medusozoan taxa, suggesting minor discrepancies can occur

<sup>1</sup>[https://github.com/aohdera/Ames\\_et\\_al\\_2020](https://github.com/aohdera/Ames_et_al_2020)

<sup>2</sup><http://reference-midori.info/download.php#>

<sup>3</sup><https://www.geneious.com>





**FIGURE 4 |** Comparison of read number for jellyfish taxa recovered. Jellyfish taxa comprising 40 OTUs (putative species) identified at 80 and 90% identity cutoffs with BLASTN, recovered from medusozoan 16S rRNA gene eDNA metabarcoding data (shown are matches comprising three or more sequences). Taxonomic identity was determined against the GenBank sequence database (NCBI). Values reflect proportions prior to rarefaction analysis (subsample normalization), which resulted in loss of three minimally represented taxa (\*) across all sites.

with variations in database and algorithm (clustering versus homology) used for read classification. Furthermore, although sequences corresponding to eDNA for the COI gene were largely

a secondary target in this study, we were successful in detecting three medusozoan OTUs comprising two hydrozoans and *C. frondosa* (details provided in **Supplementary Figures 5A, B**);



**TABLE 2 |** GenBank accession numbers corresponding to consensus sequences (16S rRNA gene) for medusozoan taxa detected as eDNA using FeDS.

Class	Identification	Name	Accession
Cubozoa	<i>Alatina alata</i>	<i>Alatina alata</i> isolate CLAetal02	MT709254
Cubozoa	<i>Carybdea</i> sp.	<i>Carybdea</i> sp. CLAetal05	MT709257
Cubozoa	<i>Tamoya</i> sp.	<i>Tamoya</i> sp. CLAetal23	MT709275
Hydrozoa	<i>Aglaophenia</i> sp.	<i>Aglaophenia</i> sp. CLAetal01	MT709253
Hydrozoa	<i>Cladonema</i> sp.	<i>Cladonema</i> sp. CLAetal09	MT709261
Hydrozoa	<i>Clytia</i> sp.	<i>Clytia</i> sp. CLAetal10	MT709262
Hydrozoa	<i>Clytia</i> sp.	<i>Clytia</i> sp. CLAetal11	MT709263
Hydrozoa	<i>Eudendrium</i> sp.	<i>Eudendrium</i> sp. CLAetal12	MT709264
Hydrozoa	<i>Halecium</i> sp.	<i>Halecium</i> sp. CLAetal13	MT709265
Hydrozoa	<i>Kirchenpaueria</i> sp.	<i>Kirchenpaueria</i> sp. CLAetal15	MT709267
Hydrozoa	<i>Myrionema hargitti</i>	<i>Myrionema hargitti</i> isolate CLAetal16	MT709268
Hydrozoa	<i>Obelia</i> sp.	<i>Obelia</i> sp. CLAetal17	MT709269
Hydrozoa	<i>Obeliida</i> sp.	<i>Obeliida</i> sp. CLAetal18	MT709270
Hydrozoa	<i>Sertularella</i> sp.	<i>Sertularella</i> sp. CLAetal19	MT709271
Hydrozoa	<i>Sertulariellidae</i> sp.	<i>Sertulariellidae</i> sp. CLAetal20	MT709272
Hydrozoa	<i>Solanderia</i> sp.	<i>Solanderia</i> sp. CLAetal21	MT709273
Hydrozoa	<i>Staurocladia</i> sp.	<i>Staurocladia</i> sp. CLAetal22	MT709274
Hydrozoa	<i>Zanclea migottoi</i>	<i>Zanclea migottoi</i> isolate CLAetal24	MT709276
Scyphozoa	<i>Aurelia</i> sp.	<i>Aurelia</i> sp. CLAetal03	MT709255
Scyphozoa	<i>Cassiopea andromeda</i>	<i>Cassiopea andromeda</i> isolate CLAetal06	MT709258
Scyphozoa	<i>Cassiopea frondosa</i>	<i>Cassiopea frondosa</i> isolate CLAetal07	MT709259
Scyphozoa	<i>Cassiopea xamachana</i>	<i>Cassiopea xamachana</i> isolate CLAetal08	MT709260
Staurozoa	<i>Calvadosia cruxmelitensis</i>	<i>Calvadosia cruxmelitensis</i> isolate CLAetal04	MT709256
Staurozoa	<i>Halicystus</i> sp.	<i>Halicystus</i> sp. CLAetal14	MT709266

The table lists consensus sequences generated from multiple individual sequences identified at >80% and/or >90% identity threshold for each of the corresponding medusozoan taxa (for clusters comprising at least three sequences).

these data were not incorporated into our medusozoan biodiversity analyses.

## Medusozoan Fauna in the Florida Keys

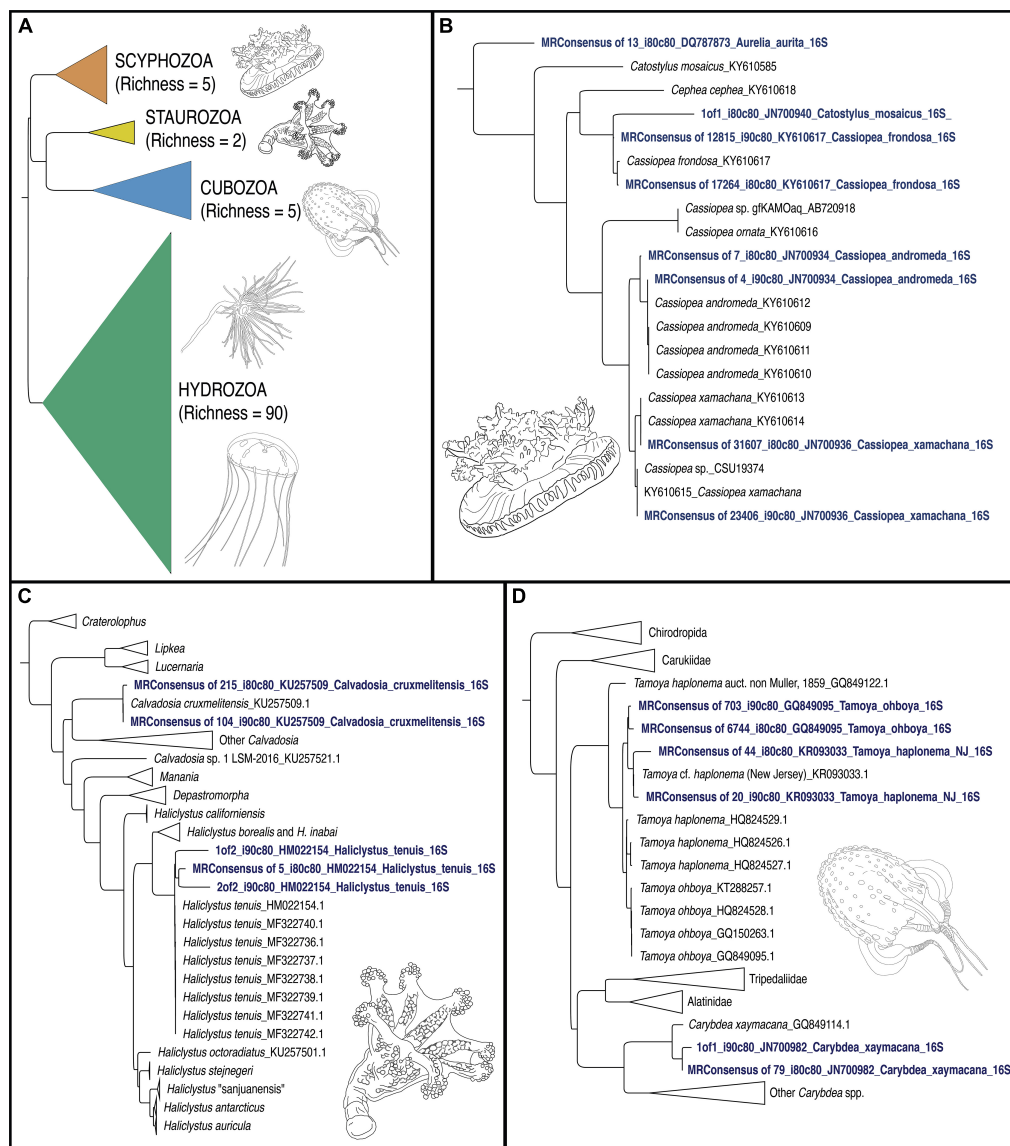
Overall, medusozoan OTU richness was lowest at Rock Harbor-BC02 (24 OTUs), followed by the Aquarium control-BC04 (15 OTUs) (**Figures 6C,D**). Buttonwood Sound (BC03) and Finger Pier (BC05), both pelagic habitats, had the greatest number of OTUs (42) (**Figures 6B,E**). On average, we detected 30 OTUs from sheltered sites (BC01 and BC02) and 36 OTUs from pelagic sites (BC03, BC05, BC06, and BC07) (**Figure 6**). Although Hydrozoa represented the class with the highest number of OTUs detected, on average, 65.2% of reads were assigned to Scyphozoa, 26.7% to Hydrozoa, followed by 18.6% to Cubozoa, with Staurozoa represented by the fewest reads (0.9%). With the exception of Buttonwood Sound, *Cassiopea* was consistently the most represented taxon (based on total corresponding reads) at each site.

*Cassiopea* reads were recovered from all sampling sites, but most of the reads were from sheltered sites, with *C. xamachana* reads encompassing 96.3% of *Cassiopea* reads generated for Rock Harbor (**Figure 6** and **Supplementary Figure 6**). Although *Cassiopea* medusae were not visually confirmed at Fleming Key, the detection of eDNA for this taxon was expected given that the upside-down jellyfish is the most common jellyfish in the Florida Keys and has been documented in mangroves of neighboring

Key West, several kilometers away (NOAA, 2020). Phylogenetic analysis of consensus reads, as determined by BLASTN revealed that three putative *Cassiopea* species are likely present in the Florida Keys. *C. xamachana* dominates throughout the Florida Keys with respect to detected eDNA (**Figure 7**) and visual confirmation (Ohdera et al., 2018), whereas *C. frondosa* occurs less frequently (**Table 1**).

In addition to *Cassiopea*, we detected a second scyphozoan genus *Aurelia*, for which the consensus of reads at the 80% identity threshold (BLASTN) shared ~86% similarity to *Aurelia aurita* (GenBank DQ787873) – a broadly distributed species complex of jellyfish known as moon jellyfish (Dawson, 2003), with at least one species known in Florida waters (**Figure 7**). Using Qiime2, this match was only recovered using percent identity cutoffs below 75%. Interestingly, the consensus of reads at the 80% identity threshold in our BLASTN search showed >98% identity to unpublished sequences of *Aurelia* sp. samples from southern Brazil (J. Lawley, pers. comm.). Therefore, it is likely that the DNA sequences of the species we detected is yet lacking from GenBank, highlighting the importance of building robust reference databases of genetic barcodes.

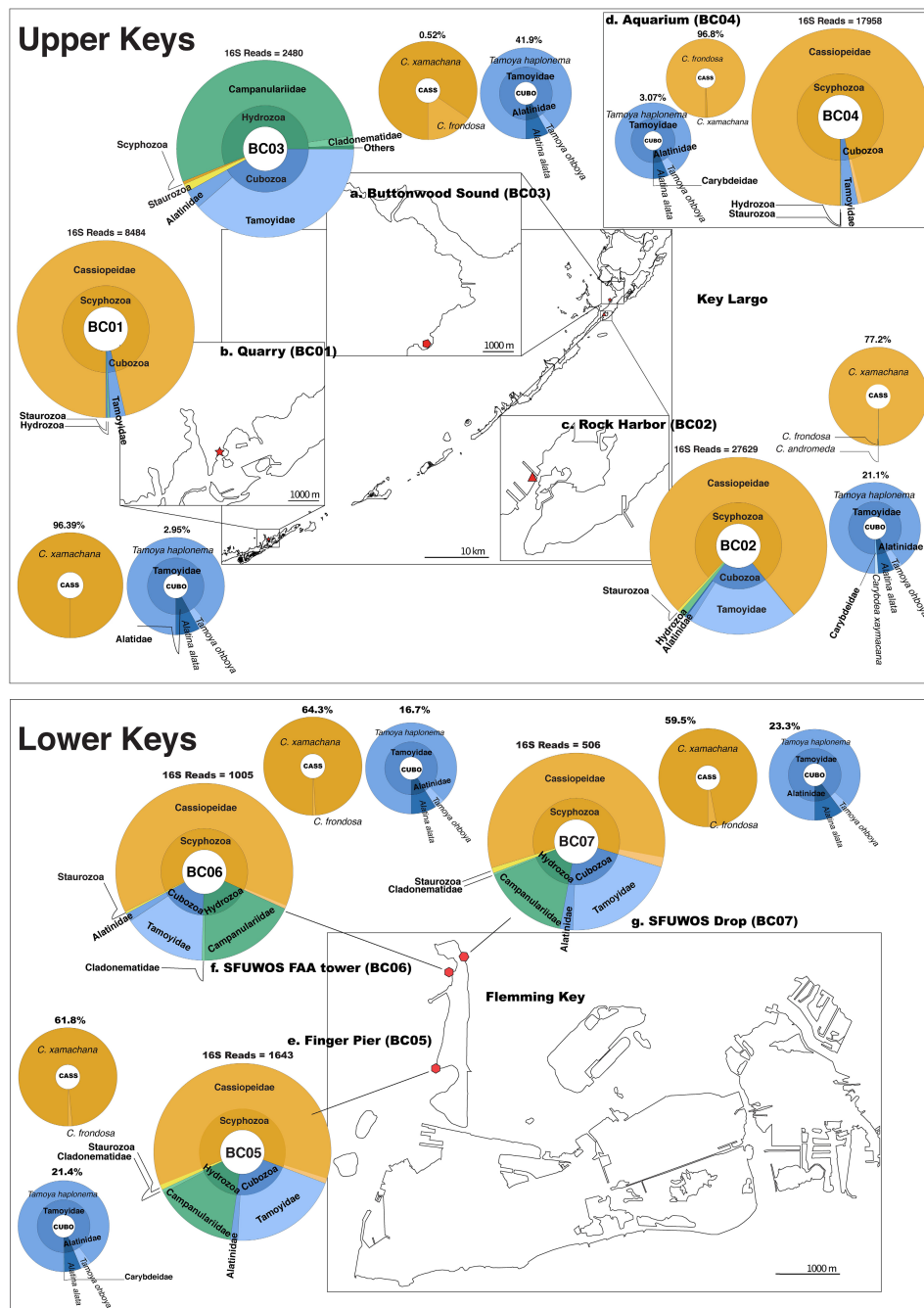
Venomous species of box jellyfish (Cubozoa) detected by eDNA metabarcoding include taxa of the cubozoan families Alatinidae and Tamoyidae (**Figures 4–7**). Though previously reported from the Caribbean and Florida Keys region (**Figure 7**), no medusa of either family was visually confirmed during this



**FIGURE 5 |** Phylogenetic trees of jellyfish (Medusozoa) based on mitochondrial 16S rRNA gene eDNA profiling from the Florida Keys. **(A)** Phylogenetic reconstruction of representatives of all four medusozoan classes detected in eDNA samples. Terminal taxa consist of majority-rule consensus sequences of aligned sequence reads that showed BLAST similarity to target sequences at two thresholds (1) Percent identity > 90% and percent coverage > 80%, and (2) Percent identity > 80% and percent coverage > 80% in cases where there were three or more such reads (see **Figure 4**). In cases where there were less than three such reads, these reads were included as terminals (GenBank accession numbers in **Table 2**). Richness refers to the number of OTUs for each class. Colors correspond to classes represented in mapped pie charts in **Figure 6**. Phylogenetic reconstruction of 16S rRNA gene sequences in GenBank (NCBI) in tandem with relevant taxa detected as metabarcodes (denoted in blue letters). **(B)** Scyphozoa. Note that one read identified as > 80% identical to *Catostylus mosaicus* (an Indo-Pacific species) appears more likely to represent an aberrant read of *C. fronsosa*. **(C)** Staurozoa. Representing the first record of Staurozoa in the Florida Keys. **(D)** Cubozoa. Note that two sets of reads showing high identity to *Tamoya cf. haplonema* from New Jersey (KR093033) and *T. ohboya* (GQ849095), respectively, both group with *Tamoya cf. haplonema* from New Jersey (KR093033) suggesting that the two sets of sequences may be associated with a single species rather than two. Hydrozoa phylogenetic tree not provided. Sequence alignments conducted with MAFFT (E-INSI algorithm), and tree reconstructed with FASTTREE on Geneious Prime version 2019.1.1.

study. As these box jellyfish medusae are rather large and conspicuous (**Figure 7**), it is conceivable that our sequences corresponded to eDNA from microscopic life stages (planulae or polyps) present at collection sites, in line with recent findings of eDNA signal detected for benthic cnidarians (Sawaya et al., 2019; Bolte et al., 2021). *A. alata* is the best documented species of the

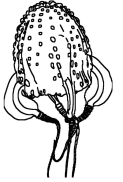

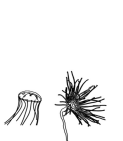

family Alatinidae, but at least one other has been reported in the Gulf of Mexico (Graham, 1998; Lewis et al., 2013; Lasley et al., 2016; Lawley et al., 2016). Our initial results indicated that two species of Tamoyidae had been detected in this study: *Tamoya cf. haplonema* (matching a New Jersey sample; GenBank KR093033) and a very similar sequence of *Tamoya ohboya* (matching a



**FIGURE 6 |** Map depicting distribution of jellyfish species at Florida Keys sampling sites based on 16S rRNA gene. Upper Keys (Key Largo and Marathon Key), water samples (May 14–16, 2018). **(a)** Buttonwood Sound (BC03). 25.10143, –80.43861. **(b)** Quarry (BC01). 24.74975, –80.97812. **(c)** Rock Harbor (BC02). 25.07924, –80.45245. **(d)** Aquarium (BC04). 25.10135, –80.43861. Lower Keys (Fleming Key), water samples (May 17, 2018). **(e)** Finger Pier (BC05). 24.57581, –81.79922. **(f)** SFUWOS FAA Tower (BC06). 24.59015, –81.79704. **(g)** SFUWOS Drop (BC07). 24.59181, –81.79487; Negative control (BC08) not depicted. Red symbols correspond to sampling locations on the map. Large, multicolored pie charts show medusozoan diversity detected at each site and total number of 16S rRNA gene reads detected per location based on Qiime2 analysis. Percentages above smaller monochromatic pie charts highlight the percent of total reads corresponding to *Cassiopea* and cubozoan species, respectively. Results from the Qiime2 barplot function were modified and visualized here using Krona (Ondov et al., 2011). Percentages reflect proportions prior to rarefaction analysis (subsample normalization), which resulted in loss of three minimally represented taxa.

Caribbean sample; GenBank GQ150263). *Tamoya* species have been previously reported in this geographical region (Collins et al., 2011; **Figure 7**), although further studies are needed to

properly delineate species within this genus. While two different exemplar sequences were identified by maximal BLASTN scores, consensus sequences of these reads both had nearly 100%

	Class	Taxon Detected in This Study	Resident in Florida/ Nearest Locality	Pelagic Stage	Specimen(s) FLMNH/ NMNH	Size Range at Maturity (cm)	Sting Risk	Polyp Stage	References
	Cubozoa	<i>Alatina alata</i>	Resident	Yes	Yes / No	8-10 (BH)	Serious	Solitary	Kramp 1961
		<i>Carybdea xaymacana</i>	Bahamas	Yes	No / No	4 (BH)	Mild	Solitary	Connant 1898 (Jamaica); Larson 1976 (Puerto Rico); Mayer 1910 (Bahamas)
	Scyphozoa	<i>Tamoya</i> sp.	Resident ( <i>T. cf. haplonema</i> )	Yes	No / Yes	9 (BH)	Serious	Solitary	Calder, 2009
		<i>Tripedalia cystophora</i>	Resident	Yes	No / No	1 (BH)	ND	Solitary	Orellan and Collins 2011
	Scyphozoa	<i>Aurelia</i> sp.	Resident ( <i>A. aurita</i> )	Yes	Yes / Yes	2-5 (BH)	Mild	Solitary	Kramp, 1961
		<i>Cassiopea andromeda</i>	Resident	Yes	No / No	10-25 (BW)	Medium	Solitary	Holland et al. 2004; Stamper et al. 2020
	Hydrozoa	<i>Cassiopea frondosa</i>	Resident	Yes	No / Yes	10-28 (BW)	Mild	Solitary	Kramp, 1961
		<i>Cassiopea xamachana</i>	Resident	Yes	Yes / Yes	10-28 (BW)	Mild	Solitary	Kramp, 1961
	Hydrozoa	<i>Aglaophenia</i> sp.	Resident (multiple spp.)	No	Yes / Yes	2-10 (L)	Mild	Colonial	Calder 2013; Vervoort 1968
		<i>Clytia</i> spp.	Resident (multiple spp.)	Yes	Yes / Yes	0.2-0.8 (BH)	ND	Colonial	Calder 2013; Vervoort 1968
	Hydrozoa	<i>Cubaia</i> sp.	Resident ( <i>C. aphrodite</i> )	Yes	No / No	0.2-0.4 (BH)	ND	Solitary	Mayer, 1910
		<i>Eudendrium</i> sp.	Resident (multiple spp.)	No	Yes / No	1-2 (L)	ND	Colonial	Calder 2013; Vervoort 1968
	Hydrozoa	<i>Halopteris</i> sp.	Resident (multiple spp.)	No	No / Yes	1-13 (L)	ND	Colonial	Calder 2013; Vervoort 1968
		<i>Kirchenpaueria</i> sp.	Resident ( <i>K. halecioides</i> )	Yes	No / No	<0.1 (BH)	ND	Colonial	Calder 2013; Vervoort 1968
	Hydrozoa	<i>Myrionema hargitti</i>	Resident	No	Yes / No	2-10 (L)	ND	Colonial	Vervoort 1968
		<i>Obelia</i> sp.	Resident (multiple spp.)	Yes	Yes / Yes	0.1-0.2 (BH)	ND	Colonial	Calder 2013; Vervoort 1968
	Hydrozoa	<i>Obeliida</i> sp.	Belize	Unknown	No / No	0.1-0.4 (L)	ND	Colonial	Cunha et al. 2017
		<i>Zanclea migottii</i>	Southern Gulf of Mexico	Presumed	No / No	Not known	ND	Colonial	Mendoza-Becerril et al. 2018
	Staurozoa	<i>Haliclystus</i> sp.	Northern Japan ( <i>H. tenuis</i> )	No	No / No	1-3 (L)	ND	Solitary	Miranda et al. 2018
		<i>Calvadosia cruxmelitensis</i>	Southern UK	No	No / No	2-4 (W)	ND	Solitary	Miranda et al. 2018

**FIGURE 7 |** Medusozoa fauna identified from 16S rRNA gene using FeDS. The table highlights morphological characteristics and residency in the Florida Keys sampling areas or closest geographic location. Line drawings to the left depict a representative taxon for each class, drawn in comparative scale. Arrows indicate species for which partially annotated genomes have been published (Ohdera et al., 2019). BH, bell height; BW, bell width; L, length of hydroid; W, width; ND, no data available; FLMNH, Florida Museum of Natural History; NMNH, National Museum of Natural History, Smithsonian Institution.

identity to the *T. cf. haplonema* rRNA gene from New Jersey. Furthermore, the tiny cubozoan, *Tripedalia cystophora*, was detected via eDNA as well (as a singleton). First described from Jamaica, *T. cystophora* has only recently been documented in Florida waters (Orellana and Collins, 2011; Lasley et al., 2016). Finally, a set of 17 reads corresponding to an unidentified species of *Carybdea* (closely matching sequences of the Caribbean species *Carybdea xaymacana*), suggest the presence of another yet-to-be described species of box jelly in the Florida Keys (Figure 7).

Although no species of the benthic stalked jellyfishes in the class Staurozoa were reported previously from Florida (Miranda et al., 2018), in this study we identified eDNA of the staurozoans *Calvadosia cruxmelitensis* and *Haliclystus cf. tenuis* (Figures 4–7). The former is of particular interest as its genome was recently published together with that of *C. xamachana* and *A. alata* (Ohdera et al., 2019). Staurozoans are relatively small medusozoans (Figure 7), and often cryptic and difficult to find in the field because they live on and blend in well with macroalgae. These species are exclusively benthic, so the presence of sequences corresponding to these taxa (*C. cruxmelitensis* being represented at every sampling location in this study) suggests that FeDS was able to detect eDNA of benthic species in addition to that of pelagic jellyfishes. *H. tenuis* was originally described from Japan (Kishinouye, 1910), but has recently been considered an introduced species in the north Atlantic (Holst and Laakmann, 2019); it has never been reported from the western Atlantic (Figure 7). *C. cruxmelitensis* is distributed throughout the British Isles, while congeners are the only known staurozoans to be distributed in warm tropical and

subtropical waters, including reports of *C. hawaiiensis* from Hawaii (Edmondson, 1930), an undetermined species from India (Panikkar, 1944), and *C. corbini* from Brazil (Grohmann et al., 1999), Puerto Rico (Capriles and Martinez, 1970; Larson, 1980), and the western Gulf of Mexico (Lechuga and Fernández-Álamo, 2005). While known geographic distributions of staurozoans (Miranda et al., 2018) would suggest that *C. corbini* is the most likely species to be encountered in Florida waters, our data unequivocally indicate that *C. cruxmelitensis* inhabits the Florida Keys (Figure 7). Nevertheless, this assertion should be confirmed through visual inspection of suitable coastal Florida habitats to assess a hypothetical introduction. Overall, these results suggest that extensive eDNA analysis could rapidly advance our understanding of the distribution of cryptic organisms.

We identified 36 Hydrozoa OTUs, despite only 15% of total reads mapping to hydrozoan sequences. Several of these taxa (e.g., species of *Aglaophenia*, *Eudendrium*, and *Halopteris*) lack a medusa stage, providing more evidence that our eDNA sampling captured benthic taxa (Figures 4, 7). Given the extensive hydrozoan diversity of over 3,500 known species, including hundreds described from the Caribbean, the more than 50% representation of all OTUs by hydrozoan taxa was not unexpected (Figures 4, 5).

## DISCUSSION

In this study, we have successfully demonstrated the efficacy of our FeDS kit which leverages the portable MinION sequencer to



enable rapid, onsite metabarcoding of eDNA corresponding to 53 medusozoan taxa in the Florida Keys. We executed all necessary steps, from collection to data generation, using accessible battery-operated equipment to conduct a multi-site biodiversity analysis of jellyfish in the Florida Keys. Despite the difficulty in visually identifying medusozoans that lack a pelagic swimming stage, our seawater eDNA analysis proved to be effective for detecting several species of hydroids and staurozoans (stalked jellyfish) lacking a swimming medusa stage. Although no single literature source exists that comprehensively documents the jellyfish fauna of Florida and the Caribbean, the results of our comparative evaluation of jellyfish biodiversity in these coastal habitats were generally consistent with the literature on medusozoans present in the region (Conant, 1897; Bigelow, 1900, 1918, 1938; Mayer, 1910; Kramp, 1961; Vervoort, 1967; Larson, 1976; Humann and Deloach, 2002; Holland et al., 2004; Calder, 2009, 2013; Orellana and Collins, 2011; Lasley et al., 2016; Cunha et al., 2017; Mendoza-Becerril et al., 2017; Miglietta et al., 2018; Miranda et al., 2018; Ohdera et al., 2018; NOAA, 2020) (summarized herein in **Figure 7**). Due to the large amount of sequence data generated, we were able to filter reads stringently and still recover a great deal of medusozoan biodiversity as a proof-of-concept that eDNA metabarcoding with FeDS identified higher overall biodiversity than could be detected with traditional survey methods alone, validating its utility for field applications.

Overall, FeDS-generated 16S rRNA gene sequences primarily corresponded to *Cassiopea* (up to 96% of sequences in Upper Keys sites and 64% in Lower Keys sites), with the majority of sequences corresponding to *C. xamachana*. In the case of *Cassiopea andromeda*, although we detected its eDNA in the Florida Keys some workers have suggested that *C. xamachana* and *C. andromeda* may be the same species (Holland et al., 2004). However, in our analysis, consensus sequences of putative *C. andromeda* and *C. xamachana* diverge by roughly 4%, raising the hypothesis that a separate species is present, which is corroborated by recent findings (Stampar et al., 2020). The fact that resident *Cassiopea* species, *C. xamachana* and *C. frondosa*, can be readily distinguished based on both morphology and genetics is evidence for two reproductively isolated species. *C. andromeda* was originally described from the Red Sea, from where it has recently spread throughout the world to warm, coastal waters, possibly introduced at the microscopic life stage in ballast water or as polyps on ship hulls (Holland et al., 2004; Stampar et al., 2020).

*Cassiopea xamachana* medusae are known to release large amounts of mucus that contains motile clusters of stinging cells called cassinosomes (Ames et al., 2020). Thought to be an important component of healthy mangrove ecosystems, both spawn and mucus likely contributed to our success in preferentially amplifying *Cassiopea* eDNA (representing 82% of all matched reads). Together with our recent publication of the reference genome of the upside-down jellyfish *C. xamachana* (Ohdera et al., 2019), recent works have brought attention to this model system as a viable biomonitor species with promising applications for coastal ecosystem management and conservation (Todd et al., 2006; Newkirk et al., 2020). At BC03, however, FeDS detected a diminutive eDNA signature for *Cassiopea*

(**Supplementary Figure 2C**). This low-level detection at this site may be related to the effects of the devastating Hurricane Irma (Dilling et al., 2017), which in September 2017 depleted the *Cassiopea* population at this site almost entirely (**Supplementary Figure 2D**). However, at that same location during the 3rd annual *Cassiopea* International Workshop (a year after deploying FeDS), coauthors of this study (WF and AO) verified that the *Cassiopea* medusa numbers had rebounded to pre-Irma abundances. While tentative, it appears that our FeDS kit was able to detect a small eDNA signal during the early stages of a population recovery. Like many jellyfishes, *Cassiopea* exhibits alternation of generations in its life cycle (**Supplementary Figure 1**); the advantage conferred by the persistence of the asexual polyp stage may be the key to their resilience, despite anthropogenic or natural pressures.

Our eDNA findings also indicated a significant presence of two species of venomous box jellyfish (*Tamoya* sp., *A. alata*) in the Upper Keys (up to 42% of sequences), and in the Lower Keys (up to 23% of sequences); the latter are in the vicinity of SFUWOS SCUBA diving drop-off sites. In the absence of visual confirmation of these relatively large medusae, it is conceivable that unseen minute stages (e.g., juvenile medusae) have been the cause of serious envenomation reports (Guest, 1950; Burnett and Gable, 1989; Grady and Burnett, 2003; Lawley et al., 2016).

Despite the inherent difficulty in visually identifying medusozoans that lack a pelagic swimming stage, FeDS was shown to be effective in detecting several species of hydroids and staurozoans (stalked jellyfish) lacking a swimming medusa stage. Therefore, given the proven applications of eDNA for rapid detection of cryptic, dangerous and/or introduced species in coastal environments (Berry et al., 2019; Holman et al., 2019), our FeDS kit could serve as a powerful tool to test whether jellyfish are resilient to global shifts toward warming oceans, or if changes in climate might drastically alter patterns of jellyfish proliferation [discussed in Purcell et al. (2007); Bayha and Graham (2013), Condon et al. (2013), Olguín-Jacobson et al. (2020)].

The speed of our FeDS protocol (sample-to-sequence) was in stark contrast to the time-lag involved in developing a suitable pipeline to analyze multi-site nanopore metabarcoding data (sequence-to-assessment) due to the limited availability of appropriate bioinformatic tools [for a review of computational challenges of nanopore data and potential software see Santos et al. (2020); Watsa et al. (2020)]. Despite initial data analysis setbacks, we are confident that the final custom pipeline we developed is a suitable, reliable bioinformatics approach for handling the data with ease of reproducibility for any study system. Recently, several third-party freeware options have been developed to analyze long read data generated by nanopore sequencing devices (Chang et al., 2020a; de Koning et al., 2020; Rodríguez-pérez et al., 2020), offering promise for a standardized pipeline in the near future. For our homology search, we used a subset of all metazoan sequences in GenBank with species level identifications, called the MIDORI database (Machida et al., 2017). While this public database is deemed trustworthy (Leray et al., 2019), it is far from an exhaustive repertoire of Florida Keys fauna. Future expansion of the initial medusozoan reference database generated in this study from

eDNA sequences will facilitate large-scale biodiversity studies of the region. Furthermore, once FeDS is equipped with the latest nanopore sequencing chemistry (R10.3 barcodes) researchers can achieve fieldable eDNA biodiversity studies with ~99.9% accuracy when compared with Illumina reference barcodes at an affordable price (Chang et al., 2020a,b). With a number of well-established regional databases becoming available to the public [e.g., Smithsonian Marine Global Earth Observatory (MarineGEO) monitoring site (Nguyen et al., 2020)], FeDS becomes a highly attractive option for timely and accurate eDNA detection in aquatic environments toward discovery of regional biodiversity patterns.

## CONCLUSION

Our FeDS workflow is easily adaptable for biodiversity assessments given its: (1) Low-complexity protocol with a relatively short “sample-to-sequence” timeframe; (2) Fieldable eDNA metabarcoding capabilities for austere environments through portable, manual and/or battery-powered equipment, ensuring a minimal environmental footprint; and (3) Multiplexing capabilities for the simultaneous evaluation of multiple collection sites and genetic markers. FeDS has surmounted the hurdles previously impeding rapid biodiversity assessments in the field, and has demonstrated the ability to perform effective identification assays under resource-limited, offline conditions. Our FeDS kit is poised as a practical molecular tool for both civilian and naval management to regularly and proactively analyze water samples for early detection of declining endemic species, as well as aquatic threats, such as venomous jellyfish. The equipment and other components of the mobile kit assembled for this study are affordable, readily available and can be optimized for any situation, eliminating the need for access to expensive, space- and energy-consuming laboratory equipment. While we suspect that the fieldable eDNA sequencing tools described herein can be deployed to conduct regular, real-time analysis of seawater samples for the purposes of sting mitigation, resource management and even predicting recovering populations following natural disasters, further assessments of that assertion are warranted. Finally, as nanopore chemistry has and will continue to improve, further enhancements to our FeDS kit, such as the integration of a device with remote communication capabilities, could eventually lead to the development of an autonomous environmental DNA sequencing system, important commercially, and for public safety and conservation.

## DATA AVAILABILITY STATEMENT

Filtered and trimmed 16S and COI MinION data sets have been made available at: [https://github.com/aohdera/Ames\\_et\\_al\\_2020](https://github.com/aohdera/Ames_et_al_2020). Nanopore sequences for medusozoans (16S; classes Scyphozoa, Cubozoa, and Staurozoa) have been separately accessioned into GenBank (see **Table 2**). All code and data sets used in this study are provided as **Supplementary Data Sheet 1**: [https://github.com/aohdera/Ames\\_et\\_al\\_2020](https://github.com/aohdera/Ames_et_al_2020).

## AUTHOR CONTRIBUTIONS

CA conceived, designed, and carried out sample collection, and all steps in the FeDS workflow in Key Largo and Fleming Key, conducted bioinformatic analyses and phylogenetic analyses, coauthored the first draft of the manuscript, and prepared figures and tables. AO carried out sample collection and MinION sequencing in Key Largo, conducted bioinformatic analyses, prepared figures and tables, and coauthored the first draft. SC helped to design the experiments, provided training in MinION technology, assisted with MinION read processing, and prepared figures and tables. AC conducted phylogenetic analyses and interpretation of results, historical data assessment and synopsis, prepared figures and tables, and coauthored the first draft. WF assisted with sample collection in Key Largo, provided ecological data related to pre- and post-Irma conditions in Key Largo, and conducted photo-documentation. ACM assisted with sample collection in Key Largo, species identification, and conducted photo-documentation. JE provided technical guidance during experimental design and developing equipment for portability. GV helped to conceive of the experiments, oversaw all aspects of the project from start to finish, assisted with FeDS kit design, and contributed reagents, materials, and analysis tools. All authors provided content for each manuscript draft and approved the final draft.

## FUNDING

This research was supported by the Office of Naval Research via Naval Research Laboratory core funds (work unit 6B84). CA and SC acknowledge postdoctoral fellowships through the National Research Council's Research Associateship Program. ACM was supported by FAPESP 2015/21007-9 and CNPq 309440/2019-0.

## ACKNOWLEDGMENTS

We are grateful to Mónica Medina, whose assistance in establishing the *Cassiopea* model meeting in Key Largo (FL, United States) allowed us to conduct this research, and the meeting attendees for their assistance with collecting. Additionally, we acknowledge technical support received from Vanessa Molina, NRL Key West, and CPT Brett Ambrosion, Diving Medical Officer, Special Forces Underwater Operations School, Key West, for logistical assistance in Fleming Key (FL, United States). Finally, we are grateful to two reviewers and the Editor for their constructive comments. This is a contribution of NP-BioMar USP. The opinions and assertions contained herein are those of the authors and are not to be construed as those of the U.S. Navy, military service at large or U.S. Government.

## SUPPLEMENTARY MATERIAL

The Supplementary Material for this article can be found online at: <https://www.frontiersin.org/articles/10.3389/fmars.2021.640527/full#supplementary-material>

## REFERENCES

- Ames, C. L., Klompen, A. M. L., Badhiwala, K., Muffett, K., Reft, A. J., Kumar, M., et al. (2020). Cassiosomes are stinging-cell structures in the mucus of the upside-down jellyfish *Cassiopea xamachana*. *Commun. Biol.* 3:67.
- Balachandran, P., Trevino, R., Wang, X., Standage-Beier, K., and Faucon, P. (2017). "High accuracy base calls in Nanopore sequencing," in *Proceedings of the 2017 6th International Conference on Bioinformatics and Biomedical Science, ICBBS 2017 Association for Computing Machinery*, New York, NY, 12–16.
- Barnes, J. H. (1964). Cause and effects of Irukandji stings. *Med. J. Aust.* 1, 897–904. doi: 10.5694/j.1326-5377.1964.tb114424.x
- Bayha, K. M., and Graham, W. M. (2013). "Nonindigenous marine jellyfish: invasiveness, invasibility and impacts," in *Jellyfish Blooms*, eds K. A. Pitt and C. H. Lucas (Dordrech: Springer).
- Berry, T. E., Saunders, B. J., Coghlan, M. L., Stat, M., Jarman, S., Richardson, A. J., et al. (2019). Marine environmental DNA biomonitoring reveals seasonal patterns in biodiversity and identifies ecosystem responses to anomalous climatic events. *PLoS Genet* 15:e1007943. doi: 10.1371/journal.pgen.1007943
- Bigelow, H. B. (1918). Some Medusae and Siphonophora from the western Atlantic. (Intergovernmental Panel on Climate Change, Ed). *Bull. Museum Comp. Zool. Harvard Coll.* 62, 363–442.
- Bigelow, H. B. (1938). Plankton of Bermuda oceanographic expeditions. VIII. Medusae taken during the Years 1929 and 1930. *Zool. Sci. Contrib. N. Y. Zool. Soc.* 23, 99–189.
- Bigelow, R. P. (1900). *The Anatomy and Development of Cassiopea xamachana*. Boston, MA: Boston Society of Natural History.
- Bolte, B., Goldsburly, J., Jerry, D., and Kingsford, M. (2021). Validation of eDNA as a viable method of detection for dangerous cubozoan jellyfish. *Environmental DNA* 1–11. doi: 10.1002/edn3.181
- Bolyen, E., Rideout, J. R., Dillon, M. R., Bokulich, N. A., Abnet, C. C., Al-Ghalith, G. A., et al. (2019). Reproducible, interactive, scalable and extensible microbiome data science using QIIME 2. *Nat. Biotechnol.* 37, 852–857.
- Bouyer-Monot, D., Pelczar, S., Ferracci, S., and Boucaud-Maitre, D. (2017). Retrospective study of jellyfish envenomation in emergency wards in Guadeloupe between 2010 and 2016: when to diagnose Irukandji syndrome? *Toxicon* 137, 73–77. doi: 10.1016/j.toxicon.2017.07.011
- Bucklin, A., Lindeque, P. K., Rodriguez-Ezpeleta, N., Albaina, A., and Lehtiniemi, M. (2016). Metabarcoding of marine zooplankton: prospects, progress and pitfalls. *J. Plankton Res.* 38, 393–400. doi: 10.1093/plankt/fbw023
- Burnett, J. W., and Gable, W. D. (1989). A fatal jellyfish envenomation by the Portuguese man-o'-war. *Toxicon* 27, 823–824. doi: 10.1016/0041-0101(89)90050-0
- Calder, D. R. (2009). Cubozoan and scyphozoan jellyfishes of the Carolinian biogeographic province, southeastern USA. *R. Ont. Mus. Contrib. Sci.* 3, 1–58. doi: 10.1007/978-94-007-6288-6\_67-1
- Calder, D. R. (2013). Some shallow-water hydroids (Cnidaria: Hydrozoa) from the central east coast of Florida, USA. *Zootaxa* 3648:1. doi: 10.11646/zootaxa.3648.1.1
- Capriles, V. A., and Martinez, H. (1970). First report of a Stauromedusae from Puerto Rico. *Caribb. J. Sci.* 10:106.
- Chang, J. J. M., Ip, Y. C. A., Bauman, A. G., and Huang, D. (2020a). MinION-in-ARMS: nanopore sequencing to expedite barcoding of specimen-rich macrofaunal samples from autonomous reef monitoring structures. *Front. Mar. Sci.* 7:448. doi: 10.3389/fmars.2020.00448
- Chang, J. J. M., Ip, Y. C. A., Ng, C. S. L., and Huang, D. (2020b). Takeaways from mobile DNA barcoding with BentoLab and MinION. *Genes (Basel)* 11:1121. doi: 10.3390/genes11101121
- Collins, A. G., Bentlage, B., Gillan, W., Lynn, T. H., Morandini, A. C., and Marques, A. C. (2011). Naming the Bonaire banded box jelly, *Tamoya ohbaya*, n. sp. (Cnidaria: Cubozoa: Carybdeida: Tamoyidae). *Zootaxa* 68, 53–68. doi: 10.11646/zootaxa.2753.1.3
- Conant, F. S. (1897). Notes on the Cubomedusae. *John Hopkins Univ. Circ* 132, 8–10.
- Condon, R. H., Duarte, C. M., Pitt, K. A., Robinson, K. L., Lucas, C. H., Sutherland, K. R., et al. (2013). Recurrent jellyfish blooms are a consequence of global oscillations. *Proc. Natl. Acad. Sci. U.S.A.* 110, 1000–1005.
- Cunha, A. F., Collins, A. G., and Marques, A. C. (2017). Phylogenetic relationships of Proboscoida Broch, 1910 (Cnidaria, Hydrozoa): are traditional morphological diagnostic characters relevant for the delimitation of lineages at the species, genus, and family levels? *Mol. Phylogenet. Evol.* 106, 118–135. doi: 10.1016/j.ympev.2016.09.012
- Dawson, M. N. (2003). Macro-morphological variation among cryptic species of the moon jellyfish, *Aurelia* (Cnidaria: Scyphozoa). *Mar. Biol.* 143, 369–379. doi: 10.1007/s00227-003-1070-3
- De Coster, W., D'Hert, S., Schultz, D. T., Cruts, M., and Van Broeckhoven, C. (2018). NanoPack: visualizing and processing long-read sequencing data. *Bioinformatics* 34, 2666–2669. doi: 10.1093/bioinformatics/bty149
- de Koning, W., Miladi, M., Hiltmann, S., Heikema, A., Hays, J. P., Flemming, S., et al. (2020). NanoGalaxy: nanopore long-read sequencing data analysis in Galaxy. *Gigascience* 9:giaa105.
- Dibattista, J. D., Reimer, J. D., Stat, M., Masucci, G. D., Biondi, P., De Brauer, M., et al. (2020). Environmental DNA can act as a biodiversity barometer of anthropogenic pressures in coastal ecosystems. *Sci. Rep.* 10:8365.
- Dilling, L., Morss, R., and Wilhelm, O. (2017). Learning to expect surprise: hurricanes Harvey, Irma, Maria, and beyond. *J. Extrem. Events* 04:1771001. doi: 10.1142/s2345737617710014
- Edmondson, C. H. (1930). New Hawaiian medusae. *Br. Mus. Occas. Pap.* 9, 1–16.
- Fitt, W. K., and Costley, K. (1998). The role of temperature in survival of the polyp stage of the tropical rhizostome jellyfish *Cassiopea xamachana*. *J. Exp. Mar. Biol. Ecol.* 222, 79–91. doi: 10.1016/s0022-0981(97)00139-1
- Fitt, W. K., and Trench, R. K. (1983). Endocytosis of the symbiotic dinoflagellate *Symbiodinium microdriaticum* Freudenthal by endodermal cells of the scyphistomae of *Cassiopea xamachana* and resistance of algae to host digestion. *J. Cell Sci.* 64, 195–212.
- Geller, J., Meyer, C., Parker, M., and Hawk, H. (2013). Redesign of PCR primers for mitochondrial cytochrome c oxidase subunit I for marine invertebrates and application in all-taxa biotic surveys. *Mol. Ecol. Resour.* 13, 851–861. doi: 10.1111/1755-0998.12138
- Goldberg, C. S., Turner, C. R., Deiner, K., Klymus, K. E., Thomsen, P. F., Murphy, M. A., et al. (2016). Critical considerations for the application of environmental DNA methods to detect aquatic species. *Methods Ecol. Evol.* 7, 1299–1307. doi: 10.1111/2041-210x.12595
- Grady, J. D., and Burnett, J. W. (2003). Irukandji-like syndrome in South Florida divers. *Ann. Emerg. Med.* 42, 763–766. doi: 10.1016/s0196-0644(03)00513-4
- Graham, M. (1998). Short papers and notes: first report of *Carybdea alata* var. *grandis* (Reynaud 1830) (Cnidaria: Cubozoa) from the Gulf of Mexico. *Gulf Mex. Sci.* 1, 28–30.
- Grohmann, P. A., Magalhaes, M. P., and Hirano, Y. M. (1999). First record of the order stauromedusae (Cnidaria, Scyphozoa) from the Tropical Southwestern Atlantic, with a review of the distribution of Stauromedusae in the Southern hemisphere. *Species Divers* 4, 381–388. doi: 10.12782/specdiv.4.381
- Guest, W. C. (1950). The occurrence of the jellyfish *Chiropsalmus quadrumanus* in Matagorda Bay, Texas. *Texas Game Fish Comm. Mar. Lab.* 9, 79–83.
- Hinlo, R., Gleeson, D., Lintermans, M., and Furlan, E. (2017). Methods to maximise recovery of environmental DNA from water samples (H Doi, Ed). *PLoS One* 12:e0179251. doi: 10.1371/journal.pone.0179251
- Hofmann, D. K., Fitt, W. K., and Fleck, J. (1996). Checkpoints in the life-cycle of *Cassiopea* spp.: control of metagenesis and metamorphosis in a tropical jellyfish. *Int. J. Dev. Biol.* 40, 331–338.
- Holland, B. S., Dawson, M. N., Crow, G. L., and Hofmann, D. K. (2004). Global phylogeography of *Cassiopea* (Scyphozoa: Rhizostomeae): molecular evidence for cryptic species and multiple invasions of the Hawaiian Islands. *Mar. Biol.* 145, 1119–1128. doi: 10.1007/s00227-004-1409-4
- Holman, L. E., de Bruyn, M., Creer, S., Carvalho, G., Robidart, J., and Rius, M. (2019). Detection of introduced and resident marine species using environmental DNA metabarcoding of sediment and water. *Sci. Rep.* 9:11559.
- Holst, S., and Laakmann, S. (2019). First record of the stalked jellyfish *Halicystus tenuis* Kishinouye, 1910 (Cnidaria: Staurozoa) in Atlantic waters. *Mar. Biodivers.* 49, 1061–1066. doi: 10.1007/s12526-018-0888-3
- Humann, P., and Deloach, N. (2002). *Reef Creature Identification: Florida, Caribbean, Bahamas*. Jacksonville, FL: New World Publications Inc.
- Jain, M., Olsen, H. E., Paten, B., and Akeson, M. (2016). Erratum to: the Oxford nanopore MinION: delivery of nanopore sequencing to the genomics community. *Genome Biol.* 17:256.



- Katoh, K., and Standley, D. M. (2013). MAFFT multiple sequence alignment software version 7: improvements in performance and usability. *Mol. Biol. Evol.* 30, 772–780. doi: 10.1093/molbev/mst010
- Kishinouye, K. (1910). Some medusae of Japanese waters. *J. Coll. Sci. Imp. Univ. Tokyo* 27, 1–35.
- Kramp, P. L. (1961). Synopsis of the medusae of the World. *J. Mar. Biol. Assoc. UK* 40, 1–149.
- Krehenwinkel, H., Pomerantz, A., and Prost, S. (2019). Genetic biomonitoring and biodiversity assessment using portable sequencing technologies: Current uses and future directions. *Genes (Basel)* 10:858. doi: 10.3390/genes10110858
- Laramie, M. B., Pilliod, D. S., Goldberg, C. S., and Strickler, K. M. (2015). Environmental DNA sampling protocol - filtering water to capture DNA from aquatic organisms. *US Geol. Surv. Tech. Methods Book* 2:15.
- Larson, R. J. (1976). *Marine Flora and Fauna of the Northeastern United States. Cnidaria: Scyphozoa*. Washington, DC: United States Government Printing Office.
- Larson, R. J. (1980). A new stauromedusa, *Kishinouyea corbini* (Scyphozoa, Stauromedusae) from the tropical western Atlantic. *Bull. Mar. Sci.* 30, 102–107.
- Lasley, R. M., Ames, C. L., Erdman, R., Parks, S., and Collins, A. G. (2016). First record of the box jellyfish *Tripedalia cystophora* (Cnidaria: Cubozoa: Tripedaliidae) in the Gulf of Mexico. *Proc. Biol. Soc. Washingt.* 129, 164–172. doi: 10.2988/0006-324x-129.q2.164
- Lawley, J. W., Ames, C. L., Bentlage, B., Yanagihara, A., Goodwill, R., Kayal, E., et al. (2016). Box jellyfish *Alatina alata* has a circumtropical distribution. *Biol. Bull.* 231, 152–169.
- Lechuga, G. R., and Fernández-Álamo, M. A. (2005). Primer registro de *Kishinouyea corbini* Larson, 1980 (Cnidaria: Scyphozoa, Stauromedusae) para México. *Rev. Soc. Mex. Hist. Nat.* 7, 107–110.
- Leray, M., Knowlton, N., Ho, S. L., Nguyen, B. N., and Machida, R. J. (2019). GenBank is a reliable resource for 21st century biodiversity research. *Proc Natl Acad Sci U.S.A.* 116, 22651–22656. doi: 10.1073/pnas.1911714116
- Lewis Ames, C., Ryan, J. F., Bely, A. E., Cartwright, P., and Collins, A. G. (2016). A new transcriptome and transcriptome profiling of adult and larval tissue in the box jellyfish *Alatina alata*, an emerging model for studying venom, vision and sex. *BMC Genomics* 17:650. doi: 10.1186/s12864-016-2944-3
- Lewis, C., Bentlage, B., Yanagihara, A. A., Gillan, W., van Blerk, J., Keil, D. P., et al. (2013). Redescription of *Alatina alata* (Reynaud, 1830) (Cnidaria: Cubozoa) from Bonaire, Dutch Caribbean. *Zootaxa* 3737, 473–487. doi: 10.11646/zootaxa.3737.4.8
- Machida, R. J., Leray, M., Ho, S.-L., and Knowlton, N. (2017). Metazoan mitochondrial gene sequence reference datasets for taxonomic assignment of environmental samples. *Sci. Data* 4:170027.
- Martin, M. (2011). Cutadapt removes adapter sequences from high-throughput sequencing reads. *EMBnet.Journal* 17, 10–12. doi: 10.14806/ej.17.1.200 (accessed March 29, 2021).
- Mayer, A. G. (1910). *Medusae of the World Volume III the Scyphomedusae*. Washington, DC: Carnegie Institution of Washington.
- Mendoza-Becerril, M. A., Simoes, N., and Genzano, G. (2017). Benthic hydroids (Cnidaria, Hydrozoa) from Alacranes. *Bull. Mar. Sci.* 94, 125–142. doi: 10.5343/bms.2017.1072
- Miglietta, M. P., Piraino, S., Pruski, S., Gonzalez, M. A., Iglesias, S. C., Jerónimo-Aguilar, S., et al. (2018). An integrative identification guide to the Hydrozoa (Cnidaria) of Bocas del Toro. *Panama. Neotrop. Biodivers.* 4, 103–113. doi: 10.1080/23766808.2018.1488656
- Minamoto, T., Naka, T., Moji, K., and Maruyama, A. (2016). Techniques for the practical collection of environmental DNA: filter selection, preservation, and extraction. *Limnology* 17, 23–32. doi: 10.1007/s10201-015-0457-4
- Miranda, L. S., Mills, C. E., Hirano, Y. M., Collins, A. G., and Marques, A. C. (2018). A review of the global diversity and natural history of stalked jellyfishes (Cnidaria, Staurozoa). *Mar. Biodivers.* 48, 1695–1714. doi: 10.1007/s12526-017-0721-4
- Nelson-Chorney, H. T., Davis, C. S., Poesch, M. S., Vinebrooke, R. D., Carli, C. M., and Taylor, M. K. (2019). Environmental DNA in lake sediment reveals biogeography of native genetic diversity. *Front. Ecol. Environ.* 17:313–318. doi: 10.1002/fee.2073
- Newkirk, C. R., Frazer, T. K., Martindale, M. Q., and Schnitzler, C. E. (2020). Adaptation to bleaching: are thermotolerant Symbiodiniaceae strains more successful than other strains under elevated temperatures in a model symbiotic cnidarian? *Front. Microbiol.* 11:822. doi: 10.3389/fmicb.2020.00822
- Nguyen, B. N., Shen, E. W., Seemann, J., Correa, A. M. S., O'Donnell, J. L., Altieri, A. H., et al. (2020). Environmental DNA survey captures patterns of fish and invertebrate diversity across a tropical seascape. *Sci. Rep.* 10:6729.
- NOAA (2020). *What are the Most Common Jellies in the Keys?*. Available online at: <https://floridakeys.noaa.gov/animals/commonkeysjellies.html> (accessed Aug 11, 2019).
- Ohdera, A. H., Abrams, M. J., Ames, C. L., Baker, D. M., Suescún-Bolívar, L. P., Collins, A. G., et al. (2018). Upside-down but headed in the right direction: Review of the highly versatile *Cassiopea xamachana* system. *Front. Ecol. Evol.* 6:35. doi: 10.3389/fevo.2018.00035
- Ohdera, A., Ames, C. L., Dikow, R. B., Kayal, E., Chiodin, M., Busby, B., et al. (2019). Box, stalked, and upside-down? Draft genomes from diverse jellyfish (Cnidaria, Acraspeda) lineages: *Alatina alata* (Cubozoa), *Calvadosia cruxmelitensis* (Staurozoa), and *Cassiopea xamachana* (Scyphozoa). *Gigascience* 8:giz069.
- Olguín-Jacobson, C., Pitt, K. A., Carroll, A. R., and Melvin, S. D. (2020). Polyps of the Jellyfish *Aurelia aurita* are unaffected by chronic exposure to a combination of pesticides. *Environ. Toxicol. Chem.* 39, 1685–1692. doi: 10.1002/etc.4750
- Ondov, B. D., Bergman, N. H., and Phillippy, A. M. (2011). Interactive metagenomic visualization in a Web browser. *BMC Bioinformatics* 12:385. doi: 10.1186/1471-2105-12-385
- Orellana, E. R., and Collins, A. G. (2011). First report of the box jellyfish *Tripedalia cystophora* (Cubozoa: Tripedaliidae) in the continental USA, from Lake Wyman, Boca Raton, Florida. *Mar. Biodivers. Rec.* 4:e54.
- Panikkar, N. K. (1944). Occurrence of a stauromedusa on the Indian coast. *Curr. Sci.* 13, 238–239.
- Parsons, K. M., Everett, M., Dahlheim, M., and Park, L. (2018). Water, water everywhere: environmental DNA can unlock population structure in elusive marine species. *R. Soc. Open Sci.* 5:180537. doi: 10.1098/rsos.180537
- Pomerantz, A., Peñafiel, N., Arteaga, A., Bustamante, L., Pichardo, F., Coloma, L. A., et al. (2018). Real-time DNA barcoding in a rainforest using nanopore sequencing: opportunities for rapid biodiversity assessments and local capacity building. *Gigascience* 7:giy033.
- Port, J. A., O'Donnell, J. L., Romero-Maraccini, O. C., Leary, P. R., Litvin, S. Y., Nickols, K. J., et al. (2016). Assessing vertebrate biodiversity in a kelp forest ecosystem using environmental DNA. *Mol. Ecol.* 25, 527–541. doi: 10.1111/mec.13481
- Price, M. N., Dehal, P. S., and Arkin, A. P. (2010). FastTree 2 Approximately maximum-likelihood trees for large alignments. *PLoS One* 5:e9490. doi: 10.1371/journal.pone.0009490
- Purcell, J. E., Uye, S. I., and Lo, W. T. (2007). Anthropogenic causes of jellyfish blooms and their direct consequences for humans: a review. *Mar. Ecol. Prog. Ser.* 350, 153–174. doi: 10.3354/meps07093
- Rodríguez-pérez, H., Ciuffreda, L., and Flores, C. (2020). NanoCLUST: a species-level analysis of 16S rRNA nanopore sequencing data. *bioRxiv* [Preprint]. doi: 10.1101/2020.05.14.087353
- Santos, A., van Aerle, R., Barrientos, L., and Martínez-Urtaza, J. (2020). Computational methods for 16S metabarcoding studies using Nanopore sequencing data. *Comput. Struct. Biotechnol. J.* 18, 296–305. doi: 10.1016/j.csbj.2020.01.005
- Sawaya, N. A., Djurhuus, A., Closek, C. J., Hepner, M., Olesin, E., Visser, L., et al. (2019). Assessing eukaryotic biodiversity in the Florida Keys National Marine Sanctuary through environmental DNA metabarcoding. *Ecol. Evol.* 9, 1029–1040. doi: 10.1002/ece3.4742
- Stampar, S. N., Gamero-Mora, E., Maronna, M. M., Fritscher, J. M., Oliveira, B. S. P., Sampaio, C. L. S., et al. (2020). The puzzling occurrence of the upside-down jellyfish *cassiopea* (Cnidaria: Scyphozoa) along the Brazilian coast: a result of several invasion events? *Zoologia* 37, 1–10. doi: 10.3897/zoologia.37.e50834
- Stoeckle, M. Y., Adolf, J., Charlop-powers, Z., Dunton, K. J., Hinks, G., and VanMorter, S. M. (2020). Trawl and eDNA assessment of marine fish diversity, seasonality, and relative abundance in coastal New Jersey, USA. *ICES J. Mar. Sci.* 78, 293–304. doi: 10.1093/icesjms/fsaa225



- Takasu, H., Inomata, H., Uchino, K., Tahara, S., Mori, K., Hirano, Y., et al. (2019). Spatio-temporal distribution of environmental DNA derived from Japanese sea nettle jellyfish *Chrysaora pacifica* in Omura Bay, Kyushu, Japan. *Plankt. Benthos Res.* 14, 320–323. doi: 10.3800/pbr.14.320
- Thomsen, P. F., and Willerslev, E. (2015). Environmental DNA - An emerging tool in conservation for monitoring past and present biodiversity. *Biol. Conserv.* 183, 4–18. doi: 10.1016/j.biocon.2014.11.019
- Thomsen, P. F., Kielgast, J., Iversen, L. L., Møller, P. R., Rasmussen, M., and Willerslev, E. (2012). Detection of a diverse marine fish fauna using environmental DNA from seawater samples (S Lin, Ed). *PLoS One* 7:e41732. doi: 10.1371/journal.pone.0041732
- Todd, B. D., Thornhill, D. J., and Fitt, W. K. (2006). Patterns of inorganic phosphate uptake in *Cassiopea xamachana*: a bioindicator species. *Mar. Pollut. Bull.* 52, 515–521. doi: 10.1016/j.marpolbul.2005.09.044
- Vervoort, W. (1967). Report on a collection of hydroids from the Caribbean Region, including an annotated checklist of caribbean hydroids. *Zool. Verh.* 92, 1–124. doi: 10.11646/zootaxa.3171.1.1
- Watsa, M., Erkenwick, G. A., Pomerantz, A., and Prost, S. (2020). Portable sequencing as a teaching tool in conservation and biodiversity research. *PLoS Biol.* 18:e3000667. doi: 10.1371/journal.pbio.3000667
- Wick, R. (2017). *Porechop*. Available online at: <https://github.com/rrwick/Porechop> (accessed March 29, 2021).
- Yamamoto, S., Minami, K., Fukaya, K., Takahashi, K., Sawada, H., Murakami, H., et al. (2016). Environmental DNA as a 'snapshot' of fish distribution: a case study of Japanese Jack Mackerel in Maizuru Bay, Sea of Japan. *PLoS One* 11:e0149786. doi: 10.1371/journal.pone.0149786
- Zapata, F., Goetz, F. E., Smith, S. A., Howison, M., Siebert, S., Church, S. H., et al. (2015). Phylogenomic analyses support traditional relationships within Cnidaria. *PLoS One* 10:e0139068. doi: 10.1371/journal.pone.0139068
- Zhou, X., Li, Y., Liu, S., Yang, Q., Su, X., Zhou, L., et al. (2013). Ultra-deep sequencing enables high-fidelity recovery of biodiversity for bulk arthropod samples without PCR amplification. *Gigascience* 2:4.
- Conflict of Interest:** The authors declare that the research was conducted in the absence of any commercial or financial relationships that could be construed as a potential conflict of interest.

Copyright © 2021 Ames, Ohdera, Colston, Collins, Fitt, Morandini, Erickson and Vora. This is an open-access article distributed under the terms of the Creative Commons Attribution License (CC BY). The use, distribution or reproduction in other forums is permitted, provided the original author(s) and the copyright owner(s) are credited and that the original publication in this journal is cited, in accordance with accepted academic practice. No use, distribution or reproduction is permitted which does not comply with these terms.



# Distribution, Temporal Change, and Conservation Status of Tropical Seagrass Beds in Southeast Asia: 2000–2020

Kenji Sudo<sup>1\*</sup>, T. E. Angela L. Quiros<sup>1</sup>, Anchana Pratthep<sup>2</sup>, Cao Van Luong<sup>3</sup>, Hsing-Juh Lin<sup>4,5</sup>, Japar Sidik Bujang<sup>6</sup>, Jillian Lean Sim Ooi<sup>7</sup>, Miguel D. Fortes<sup>8</sup>, Muta Harah Zakaria<sup>9,10</sup>, Siti Maryam Yaakub<sup>11</sup>, Yi Mei Tan<sup>12</sup>, Xiaoping Huang<sup>13</sup> and Masahiro Nakaoka<sup>1</sup>

<sup>1</sup> Akkeshi Marine Station, Field Science Center for Northern Biosphere, Hokkaido University, Hokkaido, Japan, <sup>2</sup> Seaweed and Seagrass Research Unit, Excellence Centre for Biodiversity of Peninsular Thailand, Division of Biological Science, Faculty of Science, Prince of Songkla University, Hat Yai, Thailand, <sup>3</sup> Institute of Marine Environment and Resources, Vietnam Academy of Science and Technology, Hai Phong, Vietnam, <sup>4</sup> Department of Life Sciences, National Chung Hsing University, Taichung, Taiwan, <sup>5</sup> Innovation and Development Center of Sustainable Agriculture, National Chung Hsing University, Taichung, Taiwan, <sup>6</sup> Department of Biology, Faculty of Science, Universiti Putra Malaysia, Serdang, Malaysia, <sup>7</sup> Department of Geography, Faculty of Arts and Social Sciences, Universiti Malaya, Kuala Lumpur, Malaysia, <sup>8</sup> Marine Science Institute CS, University of the Philippines, Quezon, Philippines, <sup>9</sup> Department of Aquaculture, Faculty of Agriculture, Universiti Putra Malaysia, Serdang, Malaysia, <sup>10</sup> The International Institute of Aquaculture and Aquatic Sciences, Port Dickson, Malaysia, <sup>11</sup> DHI Water & Environment (S) Pte Ltd., Singapore, Singapore, <sup>12</sup> Centre for Integrative Ecology, School of Life and Environmental Sciences, Deakin University, Geelong, VIC, Australia, <sup>13</sup> Key Laboratory of Tropical Marine Bio-Resources and Ecology, South China Sea Institute of Oceanology, Chinese Academy of Sciences, Guangzhou, China

## OPEN ACCESS

### Edited by:

Frank Edgar Muller-Karger,  
University of South Florida,  
United States

### Reviewed by:

Luis Lizcano-Sandoval,  
University of South Florida,  
United States

Inés Mazarrasa,  
Environmental Hydraulics Institute  
(IH Cantabria), Spain

### \*Correspondence:

Kenji Sudo  
ksudo.hokudai@gmail.com

### Specialty section:

This article was submitted to  
Marine Conservation  
and Sustainability,  
a section of the journal  
Frontiers in Marine Science

**Received:** 04 December 2020

**Accepted:** 31 May 2021

**Published:** 08 July 2021

### Citation:

Sudo K, Quiros TEAL, Pratthep A, Luong CV, Lin H-J, Bujang JS, Ooi JLS, Fortes MD, Zakaria MH, Yaakub SM, Tan YM, Huang X and Nakaoka M (2021) Distribution, Temporal Change, and Conservation Status of Tropical Seagrass Beds in Southeast Asia: 2000–2020. *Front. Mar. Sci.* 8:637722. doi: 10.3389/fmars.2021.637722

Although Southeast Asia is a hotspot of global seagrass diversity, there are considerable information gaps in the distribution of seagrass beds. Broad-scale seagrass distribution has not been updated in the global seagrass database by UNEP-WCMC since 2000, although studies on seagrasses have been undertaken intensively in each region. Here we analyze the recent distribution of tropical seagrass beds, their temporal changes, causes of decline and conservation status in Southeast Asia (plus southern mainland China, Taiwan and Ryukyu Island of Japan) using data collected after 2000. Based on the 195 literature published since 2000, we identified 1,259 point data and 1,461 polygon data showing the distribution of seagrass beds. A large discrepancy was found in the seagrass bed distribution between our updated data and the UNEP-WCMC database, mostly due to inaccurate and low resolution location information in the latter. Temporal changes in seagrass bed area analyzed for 68 sites in nine countries/regions demonstrated that more than 60% of seagrass beds declined at an average rate of 10.9% year<sup>-1</sup>, whereas 20% of beds increased at an average rate of 8.1% year<sup>-1</sup>, leading to an overall average decline of 4.7% year<sup>-1</sup>. Various types of human-induced threats were reported as causes for the decline, including coastal development, fisheries/aquaculture, and natural factors such as typhoons and tsunamis. The percentage of seagrass beds covered with existing marine protected areas (MPAs) varied greatly among countries/regions, from less than 1% in Brunei Darussalam and Singapore to 100% in southern Japan. However, the degree of

conservation regulation was not sufficient even in regions with higher MPA coverage. The percentage of seagrass beds within EBSAs (Ecologically and Biologically Significant Area determined by the Convention of Biological Diversity) was higher than that within MPAs because EBSAs cover a greater area than MPAs. Therefore, designating EBSAs as legally effective MPAs can greatly improve the conservation status of seagrass beds in Southeast Asia.

**Keywords:** broad-scale distribution, coastal ecosystem, GIS mapping, marine protected area, temporal trend

## INTRODUCTION

Seagrass beds consist of marine flowering plants and are one of the most important habitats in the coastal ecosystem of the world (Hemminga and Duarte, 2000; Short et al., 2007). Seagrass beds support numerous flora and fauna, including endangered and commercially important species (Kikuchi and Peres, 1977; Williams and Heck, 2001; Nakaoka, 2005). They provide many valuable ecosystem services to humans, such as seafood provision (Unsworth et al., 2019), water quality control (Nakaoka et al., 2014; Lamb et al., 2017), disaster resilience (Duarte et al., 2013), blue carbon stock (Fourqurean et al., 2012), disease control, climate regulation, and tourism (United Nations Environment Programme [UNEP], 2020). The total economic value of seagrass ecosystem services per area exceeds that of terrestrial ecosystems such as forests (Costanza et al., 1997, 2014; Dewsbury et al., 2016). Costanza et al. (2014) estimated values of seagrass/algae beds were \$28,916 ha<sup>-1</sup> year<sup>-1</sup>, while values of tropical forests were \$5,382 ha<sup>-1</sup> year<sup>-1</sup>.

Seagrass beds have been threatened by various types of human-induced stressors, including eutrophication, coastal development, and global climate change (Orth et al., 2006; Waycott et al., 2009; Japar Sidik et al., 2018; Muta Harah et al., 2019). Such multiple human-induced impacts cause rapid loss and deterioration of this important coastal habitat. Waycott et al. (2009) estimated that seagrass beds were disappearing at a rate of 7% year<sup>-1</sup> globally. However, their data did not contain those from Southeast Asia, where seagrass diversity is the highest in the world (Green and Short, 2003). The estimated global decline of seagrass beds may have been underestimated due to a lack of long-term quantitative scientific data from this region. Thus, it is urgently needed to collect more data and compile already existing data on the distribution of seagrass beds, and to conduct analyses of their recent status and temporal trends for promoting their effective conservation and management.

International efforts of seagrass researchers to understand the status of seagrass beds of the world have been continuing since the 1990s (Green and Short, 2003). One of the outputs is the global map of seagrass published as the “World Atlas of Seagrass” (Green and Short, 2003). The geographic information system (GIS) data on this map have been available from the database “Global Distribution of Seagrasses” (GDS) by UNEP-WCMC<sup>1</sup>. Developed countries in North America, Europe, and Australia have frequently updated data on seagrass beds after

2003. In contrast, they have not been updated for most Asian countries since 2001. Furthermore, the GIS data from these countries were mostly based on low-resolution spatial data with low accuracy. For example, some GDS data in Thailand was mapped at the resolution of maximum 10 km along the coast, which lead to an estimate 10 times larger than the area estimated by conducted by diving surveys (Department of Marine and Coastal Resources, 2012). Furthermore, some GDS points in Vietnam occurred 10–30 km offshore from the coastline, which is too deep for seagrass beds to occur. This may be ascribed to inaccurate GPS coordinates.

With the increasing awareness of the importance of seagrass beds in the coastal ecosystems of Southeast Asia, the amount of research by scientists and governmental managers to monitor and study seagrass beds has been increasing since the beginning of this century (e.g., Nakaoka et al., 2014). The accuracy of mapping seagrass distribution has also improved with the development of novel GIS and remote sensing techniques (Luong et al., 2012; Hossain et al., 2015; Chen et al., 2016; Koedsin et al., 2016; Huong et al., 2017). The development of a robust networked system of seagrass observations has recently been initiated (Duffy et al., 2019) including archiving of open-access data. However, most new data collected by local researchers and managers in Asia have been reported in their local literature (mostly in their native languages), which precludes more frequent updates to the global database. The situation ultimately limits planning effective conservation and management by decision makers based on the most recent information. Fortes et al. (2018) reviewed the distribution, extent, species diversity, and knowledge gaps of seagrasses in Southeast Asia, although they only presented summary data for each country with precise spatial information lacking in some regions.

The aim of this paper is to report the distribution of seagrass beds between 2000 and 2020, their temporal changes, and protection status in Southeast Asia, based on up-to-date information. To achieve this goal, we compiled data on seagrass beds published since 2000. We first analyzed the distribution of tropical seagrass beds in 13 countries/regions and compared them with the global database by GDS (version 6 in UNEP-WCMC and Short, 2018). Second, we analyzed temporal changes in areal distribution of seagrass beds. Finally, we examined the conservation status of these seagrass beds with marine protected areas (MPAs), and with Ecologically or Biologically Significant Marine Areas (EBSAs) that are candidates of future MPAs designated by the Convention on Biological Diversity<sup>2</sup>

<sup>1</sup><http://data.unep-wcmc.org/> (accessed on September 2020).

<sup>2</sup><https://www.cbd.int/ebsa/>

(Convention on Biological Diversity, 2010; Yamakita et al., 2017). The obtained results from our study will contribute to updating the global map of seagrass, and to facilitate effective management of seagrass habitat and associated marine biodiversity in Southeast Asia.

## MATERIALS AND METHODS

### Study Site

This study targeted the tropical region of Southeast Asia spanning 10 countries: Brunei Darussalam, Cambodia, Timor-Leste, Indonesia, Malaysia, Myanmar, Philippines, Singapore, Thailand, and Vietnam. We also included subtropical regions in southern mainland China, Taiwan, and the Ryukyu Islands of Japan. The northern boundary was set so that it covered the northern limit of tropical seagrass species; i.e., Fujian Province in China (26 °N), Taiwan (26 °N), and the southern part of Kagoshima in Japan (31 °N) (Zheng et al., 2013; Environment Agency and Marine Parks Center of Japan, 1994).

### Data Collection

We searched literature available online (peer-reviewed/non-peer-reviewed scientific papers, and reports) using the terms “seagrass” and target country/region name (e.g., “Brunei Darussalam”) through Web of Science, Google Scholar, and Google. From reference lists of collected literature, we also carried out a secondary survey for literature written in local languages. Some of these local literatures were available only as hard copies stored in offices and libraries of research institutions. We obtained these information as well as other sources by requesting them from researchers and governmental officials in these institutions. In total, we compiled more than 195 scientific papers and reports published after 2000. The data collected by 2018 were published as a data paper (Sudo and Nakaoka, 2020). In this paper, we added 88 literature and 719 data published by 2020 that was not included in the data paper (**Supplementary Table 1**). From these literatures, we obtained a total of 2,720 data on the distribution of seagrass beds (**Supplementary Tables 1, 2**).

### Data Analyses

The compiled seagrass bed distribution data were georeferenced using the ArcGIS georeference tool and classified into two formats to make the GIS database; point data ( $n = 1,259$ ) and polygon data ( $n = 1,461$ ). When seagrass meadow cartography was presented (such as a map in figures), we compiled it as a polygon datum by remapping manually from the published resource. When it was not available, we only used the record of the seagrass bed site information as a point datum. For each datum, areas of seagrass beds were recorded if given in the literature. Among 1,259 point data, 228 had area information written directly in the paper without further spatial information. Original data sources of 1,461 polygon data (from 42 literature) varied greatly. Among the 16 literature that used satellite images for areal estimation, 13 applied low-resolution products such as Landsats 5–8, ALOS (Advanced Land Observing Satellite), Sentinel 2 and SPOT 5 (Système Pour l’Observation de la Terre 5)

(ca 30 m/pixel resolution), whereas three literature applied more fine-resolution WorldView-2 imagery (ca 0.5 m/pixel resolution). Area estimation for the other polygon data were based on *in situ* field surveys (22 literature) and aerial photographs (two literature). The original sources of area estimation are given in our database (**Supplementary Table 1**). If the seagrass bed area was not available in the original sources, we directly calculated the area by GIS from the polygon data.

Temporal changes in seagrass bed area were analyzed for all the seagrass beds with multiple data (at least two data points), separated by at least 2 years. A total of 68 seagrass beds had such temporal data; 29 in Vietnam, 17 in Thailand, 11 in mainland China, 6 in Malaysia, 2 in the Ryukyu Islands, and one in Singapore, the Philippines, and Taiwan (**Supplementary Table 3**). The data taken before 2000 was included for this analysis if the area was estimated by the same method in each literature (see **Supplementary Table 3**). Among the 68 seagrass beds, 54 had only two data, two had three data, and 12 had more than 4 data for estimating trends in seagrass area cover. The rate of seagrass bed distribution change ( $\mu, \% \text{ year}^{-1}$ ) for each seagrass bed was calculated over a time interval,  $t$ , from the initial to final reported areas ( $A_0$  and  $A_t$ , respectively) as  $\mu = \ln(A_t/A_0)/t \times 100$  (Waycott et al., 2009). We calculated the overall trend in  $\mu$  as the median and mean rate of change, and standard errors (SEs). To avoid possible variation due to seasonal change, we used data on the same month or season if there were more than three temporal data and the month/season was known. According to Waycott et al. (2009), we defined seagrass bed area as increasing/declining when there was more than a 10% change in area detected between the initial and final time periods, whereas we defined no change if the change was less than 10%. The seagrass beds that had seriously declined during the monitoring period (with an area estimate of 0 in the final time, but seagrasses still present in a patchy manner) were excluded from the calculation of percentage rate of change (Waycott et al., 2009).

Threats against seagrass beds were recorded if the information was available. They were classified into the following 10 categories; coastal development (e.g., port construction, dredging, reclamation, etc.), sedimentation, aquaculture, destructive fishing, water quality (pollution), mangrove plantation, tourism, shipping, tsunami, and other natural factors.

The conservation status of seagrass beds in each country/region was analyzed by calculating the area of seagrass protected inside MPAs and EBSAs. The area of MPAs was obtained from Protected Planet (UNEP-WCMC and IUCN, 2020)<sup>3</sup>. For each MPA, the degree of protection level was classified following the IUCN protected areas categories as follows; Strict nature reserve (Ia), Wilderness area (Ib), National park (II), Natural monument or feature (III), Habitat/species management area (IV), Protected landscape/seascape/area (V), and Protected area with sustainable use of natural resources (VI) (Day et al., 2012; see **Supplementary Table 4**). In short, regulation is stricter with a lower category number. We obtained spatial data on EBSAs from the Clearing-House Mechanism of the Convention on Biological Diversity Information Submission

<sup>3</sup><https://www.protectedplanet.net/marine> (accessed September 11, 2020).



Services (Convention on Biological Diversity, 2018)<sup>4</sup>. EBSAs consist of coastal, pelagic and deep-sea areas. In this study we only used the coastal EBSAs for the analysis. The percentage of seagrass beds covered by MPAs and EBSAs was calculated as follows. For countries/regions which only have polygon data, the overlap between the area of seagrass beds and MPAs/EBSAs were directly calculated using GIS. For those only with point data, the number of point data found within each MPA or EBSA was counted and expressed as a percentage of the total number of seagrass point data in that particular country/region. For those with both point and polygon data, polygon data were first converted to point data by extracting the center of gravity. Then, the same calculation was made as in those only with point data.

## RESULTS

### Seagrass Bed Distribution

We mapped the distribution of 2,720 seagrass beds present between 2000 and 2020 in **Figure 1A**. Seagrass bed distribution data from the GDS collected before 2001 is shown in **Figure 1B**. Seagrass beds are present along most coastlines of our study areas. Regions with very few seagrass beds are also found in these two databases, such as in the southern part of Vietnam, the middle part of Myanmar, northern and southern Sumatra Island, the southeast part of Borneo Island and coastline of West Papua facing Arafura Sea (**Figure 1**).

The area of seagrass beds greatly differed between our database and GDS. Large discrepancies were found in some countries/regions in Vietnam, Myanmar, Cambodia, and Taiwan, whereas overlap is better for the Philippines, Singapore, and southern mainland China (**Supplementary Figure 5**). In the case of Vietnam, point data by GDS was located far offshore (deeper than 20 m sea bottom) compared to those used in our study. Distribution of seagrass beds in Myanmar by GDS data did not totally overlap with our data. In Cambodia and Taiwan, our database had more seagrass beds than GDS, and only one seagrass bed overlapped in both databases for each country/region.

### Temporal Changes in Seagrass Bed Area and Their Causes

Temporal changes were assessed for 68 seagrass beds in eight countries/regions, in which data from southern mainland China, Vietnam, and Thailand are dominant, but the time-series data were not available for any seagrass bed in Indonesia, Cambodia, Myanmar, Brunei Darussalam, Timor-Leste, and Indonesia. Forty-four sites (64.7%) experienced decline with the mean rate of  $10.9 \pm 2.6\%$  year<sup>-1</sup>. Ten sites (14.7%) showed no detectable change and 14 sites (20.6%) showed an increase in seagrass bed size with a mean rate of  $8.1 \pm 2.2\%$  year<sup>-1</sup> (**Table 1**). Overall, the mean percentage rate of change of all the seagrass beds (excluding the seven seriously-declined beds) was  $-4.7 \pm 2.0\%$  year<sup>-1</sup>. Median rate of change was somewhat smaller than mean in absolute values (**Table 1**). The declining beds were mostly located in the southern mainland China, Vietnam, but also found

in the Ryukyu Islands, the Philippines, Thailand, Malaysia, and Singapore (**Figure 2**). Beds with the increasing area were mostly found in Thailand and some in Vietnam.

Among the human-induced stressors, seagrass bed decline was mostly caused by coastal development, followed by aquaculture activities, destructive fishing, and water quality deterioration (**Table 2**). Tourism, shipping, and mangrove plantation were also reported as causes for the decline. Coastal development as a cause for the decline was reported from all countries/regions, and aquaculture from southern mainland China, Philippines, and Vietnam such as shrimp pond and fish cage. Destructive fishing was reported from southern mainland China, Philippines and Vietnam. In Thailand, threats against seagrass beds were classified as destructive fishing (6 cases), sedimentation (5), development (3), and aquaculture (2).

Natural factors such as large typhoons caused decline in seagrass beds in 16 sites. The tsunami caused by the 2004 Indian Ocean earthquake was a declining factor in Thailand (three sites).

### Protection Status

The percentage of seagrass beds located within existing MPAs and EBSAs varied greatly among countries/regions (**Table 3**). Among 4 countries/regions which have seagrass bed polygon data over their whole coastal area, more than 99% of seagrass beds are within MPAs in Ryukyu Islands of Japan, 50% in Timor-Leste, 33% in Indonesia, 20% in Thailand, and 13% in Cambodia. For countries/regions estimated by point data, more than 50% of seagrass beds are within MPAs in Taiwan and Vietnam, 43% in Myanmar, 15% in Malaysia, 9% in the Philippines, and only 6% in the southern mainland China (**Table 3**). Seagrass beds in Singapore and Brunei Darussalam were not covered by MPAs.

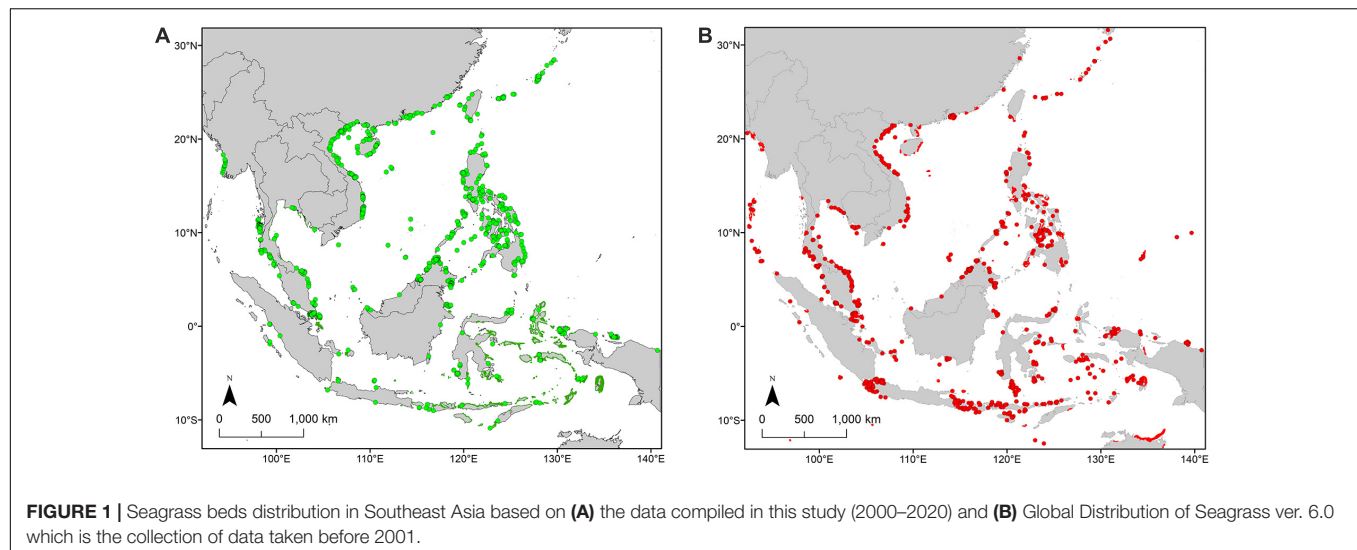
Among different categories of MPAs, only a small proportion of seagrass beds in Cambodia, Indonesia and Malaysia are included in the categories Ia and Ib (strict nature reserve and wilderness) (**Table 3**). Up to 43% of seagrass beds are included in the categories II (national parks), whereas those covered by the categories IV, V, and VI (habitat/species management area, protected landscape/seascape, and protected area with sustainable use of natural resources) are small except Ryukyu Islands (**Table 3**). Seagrass beds are not covered with the category III (natural monument or feature). Protection categories are not specified for >30% of seagrass beds in MPAs for Indonesia, Timor-Leste, and Vietnam (**Table 3**).

The proportion of seagrass beds in EBSAs greatly varies among countries/regions (**Table 3**). More than 50% of seagrass beds are within EBSAs for the Ryukyu Islands, Singapore, and Malaysia, whereas less than 10% for Cambodia, Vietnam, Indonesia, and southern mainland China. No seagrass beds are covered with EBSAs for Brunei Darussalam and Taiwan because EBSAs have not been set for these countries/regions.

## DISCUSSION

The present study updated the seagrass bed distribution in Southeast Asia where information in the global seagrass database had been stagnant. GIS analyses revealed large differences in the

<sup>4</sup><https://chm.cbd.int/database> (accessed February 17, 2018).



**TABLE 1 |** Percentage rate of change for seagrass beds.

Proportion in category (%)		Mean% rate of change		Median% rate of change	N
		$\mu$	$\pm SE$	$\mu$	
Declining	64.7	−10.9	2.6	−6.9	44
Increasing	20.6	8.1	2.2	4.9	14
No detectable change	14.7	0.0	0.1	0.0	10
Overall	100	−4.7	2.0	−2.5	68

location and area of seagrass beds compared with the GDS data collected before 2001. Analyses of temporal changes in seagrass bed size revealed that more than half of the seagrass beds are declining in most regions, and that seagrass beds located inside MPAs were less than 50%.

## Comparison of the Updated GIS Data With Previous Information

Our study compiled seagrass bed distribution data along the whole coastline of Southeast Asia. Compared to the GDS data, our study dramatically increased the information from Cambodia, Thailand, Timor-Leste, Singapore, Vietnam, southern mainland China, and the Ryukyu Islands of Japan. Before our data updates, Brunei Darussalam had no reports, and Myanmar and Taiwan had very few data. On the other hand, large regional gaps in seagrass bed information remain in the Philippines and Indonesia, which was also pointed out by a recent global estimation on seagrass bed distribution (McKenzie et al., 2020). In these regions, ongoing projects are trying to map habitats including seagrass beds and mangroves by satellite and lidar analysis (Republic of the Philippines, 2019), but as they are not yet open to the public, we did not use them in this paper.

We found great discrepancies in the areas of seagrass beds between the GDS information collected before 2001 and our updated data. The discrepancies could be due to either (1) the change (increase or decrease) in seagrass beds, (2) new discoveries in the previously unsurveyed areas, or (3) low

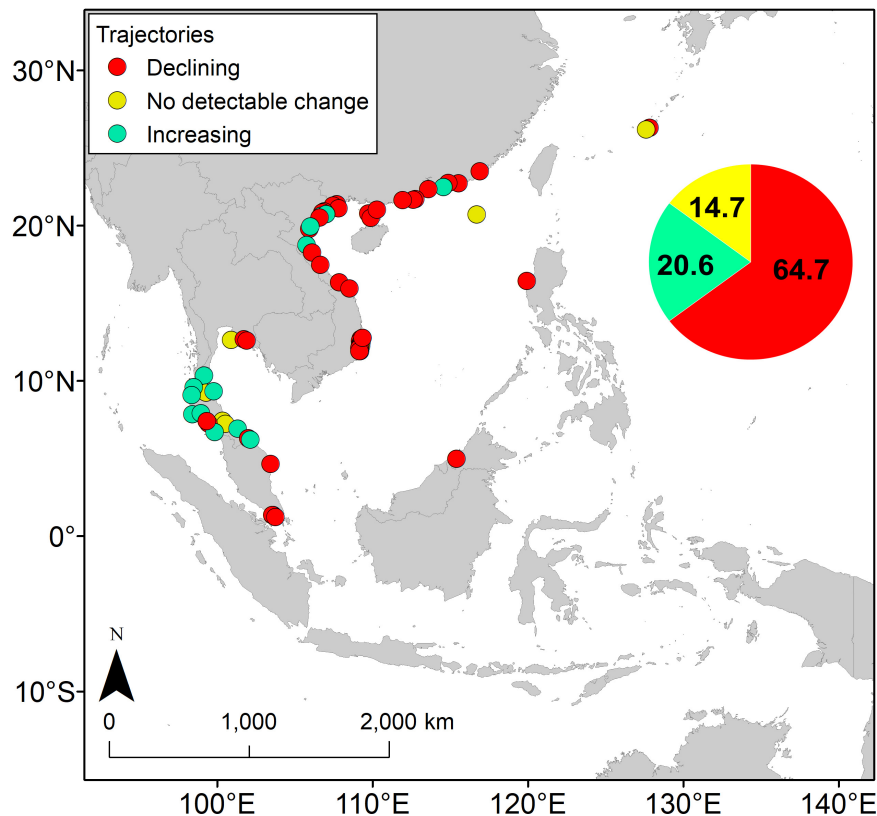
accuracy and low resolution in the data. Due to the second and third reasons, it is not plausible to examine long-term changes in seagrass bed areas by comparing data across the databases.

Low accuracy in the previous data can likely explain most discrepancies. For example, GDS seagrass beds in Vietnam occur far offshore from the coastline (**Supplementary Figure 5**). Water depth here is deeper than 20 m, which exceeds the major distributional zone of seagrass beds. Similar biases in seagrass bed distribution due to inaccurate GPS information were also found in Malaysia and Indonesia. Too coarse resolution of the previous GIS data is another source for the discrepancy among databases. For example, seagrass beds in Ranong, Phuket and Krabi Provinces in Thailand extend more than 5 km from the coastline in the GDS due to its coarse grain size. Actual distribution in these sites were less than 500 m from the coastline based on more recent analyses by the Thailand Government (Department of Marine and Coastal Resources, 2018)<sup>5,6</sup>, which is included in our database.

GIS-based image analyses of whole coastal areas using satellite images improved the seagrass bed distribution mapping, which had been difficult to estimate only by field surveys. In our dataset however, most of the satellite images were Landsat and similar satellite products, which had too low resolution for accurate discrimination of seagrass beds. Our database also contains area estimates for the point data where the area is written only

<sup>5</sup><http://marinegiscenter.dmcr.go.th/gis> (accessed April 9, 2018).

<sup>6</sup><https://datacenter.dmcr.go.th/> (accessed April 2, 2021).



**FIGURE 2 |** Trajectories of seagrass beds in the Southeast Asia.

**TABLE 2 |** The number of literature (peer-reviewed/non-peer-reviewed scientific papers and reports) reporting drivers that were responsible for the decline of seagrass beds.

	RIJ	SMC	MYS	PHL	SGP	THA	VNM	Total
Coastal development	2	4	3		1	6	3	19
Sedimentation						2	3	6
Aquaculture		6		1		2	6	14
Destructive fishing		1				6	3	10
Water quality		3			1	2	3	8
Tourism		1				1	2	4
Shipping					1		2	3
Mangrove plantation		1					0	1
Tsunami						2	1	3
Natural factor	1		3			10	2	16

RIJ, Ryukyu Island of Japan; SMC, Southern mainland China; MYS, Malaysia; PHL, Philippines; THA, Thailand; VNM, Vietnam.

in the text without explicate spatial information, so evaluation of accuracy was not possible. On the other hand, the massive effort of diving surveys in Cambodia, Thailand, and Taiwan highly improved accuracy in seagrass bed distribution estimation. Seagrass bed distribution in southern mainland China has also been reviewed and updated (Zheng et al., 2013; Jiang et al., 2020). All these efforts have led to more precise information on seagrass bed distribution in Southeast Asia.

Both our study and the GDS detected very few seagrass beds in some coastlines over several hundred kilometers. These regions

likely lack seagrass beds due to unsuitable habitat. Seagrass beds rarely develop on too muddy bottoms covered with turbid water, which may explain their absence in southern Vietnam and the central coast of Myanmar where great deltas are created by major river inputs of the Mekong and Irrawaddy, respectively. Likewise, coastlines of the northeast and south Borneo are dominated by mangroves and generally too sedimentary for seagrass beds. However, surveys may not be sufficiently conducted in some areas to understand overall seagrass bed distribution in Southeast Asia. More frequent data input and updates are required,

**TABLE 3** | Percentage of seagrass beds covered with MPAs and EBSAs.

	MPA area (km <sup>2</sup> )		% Covered with MPAs by IUCN categories								EBSA area (km <sup>2</sup> )		% Covered with EBSAs
	Total		Ia	Ib	II	III	IV	V	VI	NR			
Subtropical		6,823					6.1	15.8	77.9		8,980		86.6
Ryukyu Islands of Japan	100												
Southern mainland China	6.4	7						3.2		3.2	561		4.8
Taiwan	52.6	41			31.6		21.1				0		0
Tropical		0.1									0		0
Brunei Darussalam	0												
Cambodia	13.4	13	4.8		0.2		0.6	7.8			915		7.9
Indonesia	33.2	2,155	0.5	0.0	4.4	0.1	1.2	0.6	18.2	32.4	177,570		9.7
Malaysia	15.8	50	0.5		13.0					2.2	37,240		52.2
Myanmar	43.1	13			43.1						2,002		40.0
Philippines	9.4	293			0.7			8.0	0.7	0.5	181,316		25.8
Singapore	0	0.1									753		59.6
Thailand	20.3	70			20.3						28,009		38.1
Timor-Leste	50.2	18						13.8		36.4	1,458		16.5
Vietnam	54.1	258					0.5	1.9		51.7	3,071		1.4

Ia, Strict Nature Reserve; Ib, Wilderness Area; II, National Park; III, Natural Monument or Feature; IV, Habitat/Species Management Area; V, Protected Landscape/Seascape; VI, Protected area with sustainable use of natural resources; NR, Not reported.

especially for some key countries such as Indonesia, Malaysia, and the Philippines.

The data summarized for each country/region can be compared with the GDS and that of Fortes et al. (2018), where seagrass distribution data up to 2017 were used for 10 Southeast Asian countries (Table 4). Our data showed that Indonesia has the greatest seagrass bed area (2,934.6 km<sup>2</sup>), followed by Cambodia, Thailand, and Vietnam (>150 km<sup>2</sup>) although information on seagrass bed area was very scarce for the Philippines (Table 3). The estimated bed area was smaller than that of the GDS for all regions. The area estimated by our survey is less than 1% of the GDS for Myanmar and southern mainland China, and less than 10% for Taiwan, Malaysia, Philippines, Singapore, and Timor-Leste (Table 4). The differences are mostly due to overestimation of the GDS seagrass bed area due to low resolution images, as discussed earlier. In contrast, the estimates of seagrass bed area in most countries in our study are in close agreement with those reported by Fortes et al. (2018) because the two studies share many of the same original data sources. However, the addition of ca. 2,500 new data in our study increased the seagrass bed extent for Malaysia, Singapore, and Thailand, even within the short time difference between the two studies. In Cambodia, our estimate becomes smaller than Fortes et al. (2018) because we used more accurate data provided later by the Cambodian Government (Supkong and Bourne, 2014). However, our estimates are much smaller for the Philippines and Indonesia than Fortes et al. (2018) because the criteria for including data to our dataset are more strict (only published data taken on and after 2000).

## Temporal Changes in Seagrass Beds and Their Causes

To examine temporal changes in seagrass beds, we avoided using data from multiple sources due to large biases among different databases as mentioned above. This resulted in a relatively small amount of data on temporal change ( $n = 68$  meadows), and the data are spatially biased toward some countries like Vietnam and Thailand. Furthermore, most of these data had only two data points which may not reflect actual patterns of temporal fluctuation. Nevertheless, it contributes to information on the changes of seagrass beds, which were not included in the previous global assessment of seagrass beds (Waycott et al., 2009).

The percentage of declining seagrass beds (65%) was higher than that reported globally (58%) and that of *Zostera marina* in Europe (57%). Furthermore, the mean decline rate (11% year<sup>-1</sup>) was 1.6 times greater than the global average of 6.9% year<sup>-1</sup> and higher than the 9.5% year<sup>-1</sup> decline in Europe (Waycott et al., 2009; de los Santos et al., 2019). Our estimate seems reasonable considering the high economic growth rate of Southeast Asia, where the majority of people live along the coastal area (Neumann et al., 2015).

We observed geographical variation in the patterns of temporal change. More seagrass beds are declining in Vietnam and southern mainland China, whereas most seagrass beds are stable or even increasing along the coast of Thailand. The increase in many Thailand seagrass beds may be explained by the fact



**TABLE 4 |** Comparison of areal extent of seagrass beds (km<sup>2</sup>) by countries/regions.

		This study*	GDS (UNEP-WCMC)	Fortes et al., 2018
Subtropical	Ryukyu Islands of Japan	23.9	69	NA
	Southern mainland China	71.4	7,584	NA
	Taiwan	68.2	1,242	NA
Tropical	Brunei Darussalam	1.5	NA	1.5
	Cambodia	229.8	NA	324.9
	Indonesia	2934.6	17,597	8,812.9
	Malaysia	49.0	541	16.3
	Myanmar	4.3	2,942	4.3
	Philippines	82.1	14,923	27,262.2
	Singapore	2.0	127	0.3
	Thailand	189.9	1,813	148.5
	Timor-Leste	19.0	335	NA
	Vietnam	157.5	216	157.4

\*Methods of estimation is given in **Supplementary Table 1** (Sheet "5 Remarks").

that these data were collected after 2004 when the Andaman Sea Coast was hit by the 2004 Indian Ocean Earthquake and Tsunami. The tsunami heavily affected some seagrass beds in this region (Adulyanukosol and Poovachiranon, 2006; Whanpetch et al., 2010). The increase in seagrass beds in this region may reflect a natural recovery from the catastrophic disturbance. In contrast, decline in southern mainland China and Vietnam may be ascribed to coastal development, which reflects active economic development in these regions (Luong et al., 2012; Jiang et al., 2020). The data on temporal change in seagrass beds are still very scarce in other counties and regions, which preclude the general evaluation of seagrass bed trends in the whole Southeast Asia.

Various types of threats have been reported as causes for the decline or loss of seagrass beds around the world, such as coastal development, sedimentation, dredging, degraded water quality, and climate changes (Orth et al., 2006; Waycott et al., 2009; Japar Sidik et al., 2018; Muta Harah et al., 2019). In Europe, water quality degradation, wasting disease, coastal modification, mechanical damage, extreme events, and non-native macroalgae invasion was recently reported as major factors related to seagrass bed change (de los Santos et al., 2019). In our study, development, aquaculture and destructive fishing were reported as major anthropogenic factors for seagrass bed decline in Southeast Asia, which agrees with previous studies reviewing the status of seagrass beds in this region (Luong et al., 2012; Nakaoka et al., 2014; Chen et al., 2016; Fortes et al., 2018; Japar Sidik et al., 2018).

In addition to anthropogenic factors, it is worth to mention that natural factors such as floods, typhoons, tsunamis and El Niño-Southern Oscillation (ENSO) were reported as major causes for seagrass bed declines in this region (Adulyanukosol and Poovachiranon, 2006; Nakaoka et al., 2007; Whanpetch et al., 2010; Luong et al., 2012; Japar Sidik et al., 2018; Lin et al., 2018; Vo et al., 2020). For the typhoon damage however, it may also be related to human activities because of the recent storm intensification with ongoing climate change. Another unique case we found as cause of decline are mangrove plantations, which

suggests that improper restoration efforts without sound scientific knowledge can lead to deterioration of coastal ecosystems (Primavera and Esteban, 2008; Sharma et al., 2017; Mendoza et al., 2019).

## Conservation Status of Seagrass Beds

Marine protected areas can protect coastal ecosystems and resident organisms from various human activities such as coastal development and overexploitation (Short and Wyllie-Echeverria, 1996). Our analysis showed that percentage of seagrass beds within the existing MPAs are highly variable among countries/regions. Almost all the tropical seagrass beds are within MPAs in the Ryukyu Islands. In contrast, MPAs protect no seagrass beds in Singapore and Brunei Darussalam. However, even within MPAs, regulation levels for conservation also vary, which can be evaluated using the IUCN protected area management categories (Dudley, 2008). The categories Ia (strict nature reserve) and Ib (wilderness area) are considered highly effective to protect seagrass beds, but very few sites are in these categories. The category II (national parks) is also effective in preventing seagrass beds from coastal development and aquaculture activities, and less than 45% of seagrass beds in our study area are covered under this category. In contrast, a greater percentage of seagrass beds are covered by the categories V and VI, which allow fishing and aquaculture activities (Day et al., 2012), and thus have less conservation impact on seagrass beds and their biodiversity.

The Aichi Target of the CBD declared to protect more than 10% of the coastal and marine areas inside MPAs by 2020, and the CBD is preparing more ambitious targets to increase protected areas by 2030 (Convention on Biological Diversity, 2020). To attain these goals, EBSAs were determined as candidates for future MPAs (Dunn et al., 2014; Yamakita et al., 2017). Because the coverage of EBSAs is broader than most MPAs (see **Table 3**), the percentage of seagrass beds located within EBSAs is higher than that inside MPAs, except for Brunei Darussalam and Taiwan, which do not have any EBSAs. This indicates that efforts to designate EBSAs as legally effective MPAs to meet CBD

targets will be promising to improve the conservation status of seagrass beds and to prevent further loss of seagrass beds in Southeast Asia.

## CONCLUSION

This study clarified the recent distribution of tropical seagrass beds, their temporal changes and conservation status based on the updated information taken on and after 2000 in Southeast Asia, where information has been scattered among local literature. We found large differences in the estimation of seagrass bed areas between our updated information and the previous version of the seagrass database by GDS, which is mostly ascribed to inaccurate information and many remaining gaps. We also found that more than 60% of seagrass beds declined at an average rate of 11% year<sup>-1</sup>, whereas 20% of beds increased at an average rate of 8% year<sup>-1</sup>, leading to an overall average decline of 5% year<sup>-1</sup>. The proportion of seagrass beds included in MPAs is high in some countries/regions, although the level of actual regulation for conservation was not sufficient. Our updated information is still insufficient to understand the overall status of seagrass beds in Southeast Asia and more data input is required for some key countries such as Indonesia, Malaysia and the Philippines. Nevertheless, our fine-resolution, broad-scale information will contribute to updating global information on seagrass beds and facilitate effective conservation and management of seagrass beds in the Southeast Asia region, which is still under great threat by multiple human-induced stresses. Included in these stressors are unsound policies emanating from the failure of governments to link science, policy and practice (Fortes, 2018).

## DATA AVAILABILITY STATEMENT

The original contributions presented in the study are included in the article/Supplementary Material, further inquiries can be directed to the corresponding author.

## AUTHOR CONTRIBUTIONS

KS, TQ, and MN conceived the research, analyzed the data, and wrote the manuscript. AP, CL, H-JL, JB, JO, MF, MZ, SMY, YT,

and XH provided seagrass beds information and contributed to improve the quality of the manuscript. All authors contributed to the article and approved the submitted version.

## FUNDING

This study was supported by Environment Research and Technology Development Funds by Environmental Restoration and Conservation Agency, Japan (S-15: Predicting and Assessing Natural Capital and Ecosystem Services), the Belmont Forum fund by Japan Science and Technology Agency (TSUNAGARI), SATPREPS program by Japan Science and Technology Agency-Japan International Cooperation Agency (BlueCARES), Japan Society of the Promotion of Science-Kakenhi (No. 20KK0246), Core-to-Core Program by Japan Society for the Promotion of Science Program, B. Asia-Africa Science Platforms, project with coded 03/HD-SKHCN, and Vietnam Academy of Science and Technology project (VAST06.06/21-22).

## ACKNOWLEDGMENTS

This manuscript is a contribution to the Asia-Pacific Marine Biodiversity Observation Network (AP-MBON) of the Group on Earth Observations Biodiversity Observation Network (GEO BON). We are grateful to the members of Phuket Marine Biological Center in Thailand and the Vietnam Academy of Science and Technology for providing local literature and data on seagrass bed distribution. This paper is dedicated to Chittima Aryuthaka who contributed greatly to the development of marine biology and ecology in Asia during her lifetime.

## SUPPLEMENTARY MATERIAL

The Supplementary Material for this article can be found online at: <https://www.frontiersin.org/articles/10.3389/fmars.2021.637722/full#supplementary-material>

## REFERENCES

- Adulyanukosol, K., and Poovachiranon, S. (2006). "Dugong (*Dugong dugon*) and seagrass in Thailand: present status and future challenges," in *Proceedings of the 3rd International Symposium on SEASTAR2000 and Asian Bio-Logging Science (The 7th SEASTAR2000 Workshop) Graduate School of Informatics*, (Kyoto: Kyoto University), 41–50.
- Chen, C. F., Lau, V. K., Chang, N. B., Son, N. T., and Chiang, S. H. (2016). Multi-temporal change detection of seagrass beds using integrated Landsat TM/ETM+/OLI imageries in Cam Ranh Bay, Vietnam. *Ecol. Inform.* 35, 43–54. doi: 10.1016/j.ecoinf.2016.07.005
- Convention on Biological Diversity (2010). *Decision adopted by the Conference of the Parties to the Convention on Biological Diversity at its Tenth Meeting (UNEP/CBD/COP/DEC/X/29)*. Rio de Janeiro: Convention on Biological Diversity.
- Convention on Biological Diversity (2018). Clearing-House Mechanism of the Convention on Biological Diversity Information Submission Services. Available online at: <https://chm.cbd.int/database> (accessed February 17, 2018).
- Convention on Biological Diversity (2020). *Update of the Zero Draft of the Post-2020 Global Biodiversity Framework (CBD/POST2020/PREP/2/1)*. Rio de Janeiro: Convention on Biological Diversity.
- Costanza, R., d'Arge, R., De Groot, R., Farber, S., Grasso, M., Hannon, B., et al. (1997). The value of the world's ecosystem services and natural capital. *Nature* 387, 253–260. doi: 10.1038/387253a0
- Costanza, R., De Groot, R., Sutton, P., Van der Ploeg, S., Anderson, S. J., Kubiszewski, I., et al. (2014). Changes in the global value of ecosystem services. *Glob. Environ. Change* 26, 152–158. doi: 10.1016/j.gloenvcha.2014.04.002
- Day, J., Dudley, N., Hockings, M., Holmes, G., Laffoley, D. D. A., Stolton, S., et al. (2012). *Guidelines for Applying the IUCN Protected Area Management*

- Categories to Marine Protected Areas*. Available online at: <https://portals.iucn.org/library/node/10201> (accessed September 22, 2018).
- de los Santos, C. B., Krause-Jensen, D., Alcoverro, T., Marbà, N., Duarte, C. M., van Katwijk, M. M., et al. (2019). Recent trend reversal for declining European seagrass meadows. *Nat. Comm.* 10:3356. doi: 10.1038/s41467-019-11340-4
- Department of Marine and Coastal Resources (2012). *Status of Seagrass in Thailand*. Available online at: [https://km.dmcg.go.th/en/c\\_4/d\\_775](https://km.dmcg.go.th/en/c_4/d_775) (accessed March 31, 2021).
- Department of Marine and Coastal Resources (2018). *Thailand Central Database System and Data Standard for Marine and Coastal Resources*. Available online at: <http://marinegiscenter.dmcg.go.th/gis> <https://datacenter.dmcg.go.th/> (accessed April 9, 2018).
- Dewsbury, B. M., Bhat, M., and Fourqurean, J. W. (2016). A review of seagrass economic valuations: gaps and progress in valuation approaches. *Ecosyst. Serv.* 18, 68–77. doi: 10.1016/j.ecoser.2016.02.010
- Duarte, C. M., Kennedy, H., Marbà, N., and Hendriks, I. (2013). Assessing the capacity of seagrass meadows for carbon burial: current limitations and future strategies. *Ocean Coast. Manag.* 83, 32–38. doi: 10.1016/j.ocecoaman.2011.09.001
- Dudley, N. (2008). *Guidelines for Applying Protected Area Management Categories*. Gland, Switzerland: IUCN. x + 86pp. WITH Stolton, S., Shadie P. and Dudley N. (2013). IUCN WCPA Best Practice Guidance on Recognising Protected Areas and Assigning Management Categories and Governance Types, Best Practice Protected Area Guidelines Series No. 21. Gland: IUCN, 31.
- Duffy, J. E., Benedetti-Cecchi, L., Trinanes, J., Muller-Karger, F. E., Ambo-Rappe, R., Boström, C., et al. (2019). Toward a Coordinated global observing system for seagrasses and marine macroalgae. *Front. Mar. Sci.* 6:317. doi: 10.3389/fmars.2019.00317
- Dunn, D. C., Ardron, J., Bax, N., Bernal, P., Cleary, J., Cresswell, I., et al. (2014). The convention on biological diversity's ecologically or biologically significant areas: origins, development, and current status. *Mar. Policy* 49, 137–145. doi: 10.1016/j.marpol.2013.12.002
- Environment Agency and Marine Parks Center of Japan (1994). *The Report of the Marine Biotic Environment Survey in the 4th National Survey on the Natural Environment*. Algal and Sea-Grass Beds.
- Fortes, M. D. (2018). Seagrass ecosystem conservation in Southeast Asia needs to link science to policy and practice. *Ocean Coast. Manag.* 159, 51–56.
- Fortes, M. D., Ooi, J. L. S., Tan, Y. M., Prathep, A., Bujang, J. S., and Yaakub, S. M. (2018). Seagrass in Southeast Asia: a review of status and knowledge gaps, and a road map for conservation. *Botanica Marina* 61, 269–288. doi: 10.1515/bot-2018-0008
- Fourqurean, J. W., Duarte, C. M., Kennedy, H., Marbà, N., Holmer, M., Mateo, M. A., et al. (2012). Seagrass ecosystems as a globally significant carbon stock. *Nat. Geosci.* 5, 505–509. doi: 10.1038/ngeo1477
- Green, E. P., and Short, F. (2003). World atlas of seagrasses. Prepared by the UIMEP World Conservation Monitoring Centre. Berkeley, CA: University of California Press.
- Hemminga, M. A., and Duarte, C. M. (2000). *Seagrass Ecology*. Cambridge: Cambridge University Press, 312.
- Hossain, M. S., Japar Sidik, B., Muta Harah, Z., and Hashim, M. (2015). Application of landsat images to seagrass areal cover change analysis for Lawas, Terengganu and Kelantan of Malaysia. *Cont. Shelf Res.* 110, 124–148. doi: 10.1016/j.csr.2015.10.009
- Huong, N. T. T., Tuan, T. A., Thach, V. T., and Tin, H. C. (2017). A review of seagrass studies by using satellite remote sensing data in the southeast asia: status and potential. *Vietnam J. Sci. Technol.* 55:148.
- Japar Sidik, B., Muta Harah, Z., and Short, F. T. (2018). "Seagrass in Malaysia: issues and challenges," in *The Wetland Book II: Distribution, Description and Conservation*, eds C. Max Finlayson, G. Randy Milton, R. Crawford Prentice, and N. C. Davidson (Berlin: Springer), 1875–18839. doi: 10.1007/s13280-010-0067-7
- Jiang, Z., Cui, L., Liu, S., Zhao, C., Wu, Y., Chen, Q., et al. (2020). Historical changes in seagrass beds in a rapidly urbanizing area of Guangdong province: implications for conservation and management. *Glob. Ecol. Conserv.* 22:e01035. doi: 10.1016/j.gecco.2020.e01035
- Kikuchi, T., and Peres, J. M. (1977). "Consumer ecology of seagrass beds," in *Seagrass Ecosystems: A Scientific Perspective*, eds C. P. McRoy and C. Helfferich (New York, NY: Marcel Dekker Inc.).
- Koedsin, W., Intararuang, W., Ritchie, R. J., and Huete, A. (2016). An integrated field and remote sensing method for mapping seagrass species, cover, and biomass in southern Thailand. *Remote Sens.* 8:292.
- Lamb, J. B., van de Water, J. A. J. M., Bourne, D. G., Altier, C., Hein, M. Y., Fiorenza, E. A., et al. (2017). Seagrass ecosystems reduce exposure to bacterial pathogens of humans, fishes, and invertebrates. *Science* 355, 731–733. doi: 10.1126/science.aal1956
- Lin, H. J., Lee, C. L., Peng, S. E., Hung, M. C., Liu, P. J., and Mayfield, A. B. (2018). The effects of El Niño–Southern Oscillation events on intertidal seagrass beds over a long-term timescale. *Glob. Change Biol.* 24, 4566–4580. doi: 10.1111/gcb.14404
- Luong, C. V., Van Thao, N., Komatsu, T., Ve, N. D., and Tien, D. D. (2012). "Status and threats on seagrass beds using GIS in Vietnam," in *Proceedings of the Remote Sensing of the Marine Environment II*, Vol. 8525, (Bellingham: International Society for Optics and Photonics), 852512. doi: 10.1117/12.977277
- McKenzie, L., Nordlund, L. M., Jones, B. L., Cullen-Unsworth, L. C., Roelfsema, C. M., and Unsworth, R. (2020). The global distribution of seagrass meadows. *Environ. Res. Lett.* 15:074041. doi: 10.1088/1748-9326/ab7d06
- Mendoza, A. R., Patalinghug, J. M. R., and Divinagracia, J. Y. (2019). The benefit of one cannot replace the other: seagrass and mangrove ecosystems at Santa Fe, Bantayan Island. *J. Ecol. Environ.* 43:18. doi: 10.1186/s41610-019-0114-7
- Muta Harah, Z., Japar Sidik, B., Syed, N. N. F., Ramaiya, S. D., Emmclan, S. S. H. E., and Hayashizaki, K. (2019). Macroalgae associated with Tanjung Adang Laut seagrass meadow, Sungai Pulaui estuary, Johor, Malaysia, from 2015 to 2017. *Phil. J. of Nat. Sci.* 24, 66–79.
- Nakaoka, M. (2005). Plant–animal interactions in seagrass beds: ongoing and future challenges for understanding population and community dynamics. *Popul. Ecol.* 47, 167–177.
- Nakaoka, M., Lee, K.-S., Huang, X., Almonte, T., Bujang, J., Kiswara, W., et al. (2014). "Regional comparison of the ecosystem services from seagrass beds in Asia," in *Integrative Observations and Assessments. Ecological Research Monographs*, eds S. Nakano, T. Yahara, and T. Nakashizuka (Tokyo: Springer), doi: 10.1007/978-4-431-54783-9\_20
- Nakaoka, M., Tanaka, Y., Mukai, H., Suzuki, T., and Aryuthaka, C. (2007). *Tsunami Impacts on Biodiversity of Seagrass Communities in the Andaman Sea, Thailand: (1) Seagrass Abundance and Diversity*. Kyoto: Kyoto University.
- Neumann, B., Vafeidis, A. T., Zimmermann, J., and Nicholls, R. J. (2015). Future coastal population growth and exposure to sea-level rise and coastal flooding—a global assessment. *PLoS One* 10:e0118571. doi: 10.1371/journal.pone.0118571
- Orth, R. J., Carruthers, T. J., Dennison, W. C., Duarte, C. M., Fourqurean, J. W., Heck, K. L., et al. (2006). A global crisis for seagrass ecosystems. *Bioscience* 56, 987–996.
- Primavera, J. H., and Esteban, J. M. A. (2008). A review of mangrove rehabilitation in the Philippines: successes, failures and future prospects. *Wetl. Ecol. Manag.* 16, 345–358. doi: 10.1007/s11273-008-9101-y
- Republic of the Philippines (2019). *6th National Report for the Convention on Biological Diversity*. Available online at: <https://chm.cbd.int/database/record/9D0D456A-FAC1-9806-3B90-21B37D4DEE5B> (accessed April 2, 2020).
- Sharma, S., Nadaoka, K., Nakaoka, M., Uy, W. H., MacKenzie, R. A., Friess, D. A., et al. (2017). Growth performance and structure of a mangrove afforestation project on a former seagrass bed, Mindanao Island, Philippines. *Hydrobiologia* 803, 359–371. doi: 10.1007/s10750-017-3252-x
- Short, F. T., Carruthers, T., Dennison, W., and Waycott, M. (2007). Global seagrass distribution and diversity: a bioregional model. *J. Exp. Mar. Biol. Ecol.* 350, 3–20. doi: 10.1016/j.jembe.2007.06.012
- Short, F. T., and Wyllie-Echeverria, S. (1996). Natural and human-induced disturbance of seagrasses. *Environ. Conserv.* 27, 17–27.
- Sudo, K., and Nakaoka, M. (2020). Fine-scale distribution of tropical seagrass beds in Southeast Asia. *Ecol. Res.* 35, 994–1000. doi: 10.1111/1440-1703.12137
- Supkong, P., and Bourne, L. (2014). *A Survey of Seagrass Beds in Kampot, Cambodia*. Thailand: IUCN, 91.
- UNEP-WCMC and IUCN (2020). *Marine Protected Planet: [The World Database on Protected Areas (WDPA)]*. Cambridge: UNEP-WCMC.
- UNEP-WCMC and Short, F. T. (2018). *Global Distribution of Seagrasses (version 6.0). Sixth Update to the Data Layer used in Green and Short (2003)*. Cambridge: UN Environment World Conservation Monitoring Centre.

- United Nations Environment Programme [UNEP] (2020). *Out of the Blue: The Value of Seagrasses to the Environment and to People*. Nairobi: UNEP.
- Unsworth, R. K., Nordlund, L. M., and Cullen-Unsworth, L. C. (2019). Seagrass meadows support global fisheries production. *Conserv. Lett.* 12:e12566. doi: 10.1111/conl.12566
- Vo, T. T., Lau, K., Liao, L. M., and Nguyen, X. V. (2020). Satellite image analysis reveals changes in seagrass beds at Van Phong Bay, Vietnam during the last 30 years. *Aquat. Living Resour.* 33:4. doi: 10.1051/alr/2020005
- Waycott, M., Duarte, C. M., Carruthers, T. J. B., Orth, R. J., Dennison, W. C., Olyarnik, S., et al. (2009). Accelerating loss of seagrasses across the globe threatens coastal ecosystems. *Proc. Natl. Acad. Sci. U.S.A.* 106, 12377–12381. doi: 10.1073/pnas.0905620106
- Whanpetch, N., Nakaoka, M., Mukai, H., Suzuki, T., Nojima, S., Kawai, T., et al. (2010). Temporal changes in benthic communities of seagrass beds impacted by a tsunami in the Andaman Sea, Thailand. *Estuar. Coast. Shelf Sci.* 87, 246–252. doi: 10.1016/j.ecss.2010.01.001
- Williams, S. L., and Heck, K. L. Jr. (2001). Seagrass community ecology,” in *Marine Community Ecology* eds M. D. Bertness, S. D. Gaines, and M. E. Hay (Sunderland, MA: Sinauer Associates, Inc), 317–337.
- Yamakita, T., Sudo, K., Jintsu-Uchifune, Y., Yamamoto, H., and Shirayama, Y. (2017). Identification of important marine areas using ecologically or biologically significant areas (EBSAs) criteria in the East to Southeast Asia region and comparison with existing registered areas for the purpose of conservation. *Mar. Pol.* 81, 273–284. doi: 10.1016/j.marpol.2017.03.040
- Zheng, F., Qiu, G., Fan, H., and Zhang, W. (2013). Diversity, distribution and conservation of Chinese seagrass species. *Biodivers. Sci.* 21, 517–526. doi: 10.3724/SP.J.1003.2013.10038

**Conflict of Interest:** SMY was employed by the company DHI Water & Environment (S) Pte Ltd.

The remaining authors declare that the research was conducted in the absence of any commercial or financial relationships that could be construed as a potential conflict of interest.

Copyright © 2021 Sudo, Quiros, Prathep, Luong, Lin, Bujang, Ooi, Fortes, Zakaria, Yaakub, Tan, Huang and Nakaoka. This is an open-access article distributed under the terms of the Creative Commons Attribution License (CC BY). The use, distribution or reproduction in other forums is permitted, provided the original author(s) and the copyright owner(s) are credited and that the original publication in this journal is cited, in accordance with accepted academic practice. No use, distribution or reproduction is permitted which does not comply with these terms.





# A Standardized Workflow Based on the STAVIRO Unbaited Underwater Video System for Monitoring Fish and Habitat Essential Biodiversity Variables in Coastal Areas

## OPEN ACCESS

### Edited by:

Oscar Schofield,  
Rutgers, The State University  
of New Jersey, United States

### Reviewed by:

Thomas Marcellin Grothues,  
Rutgers, The State University  
of New Jersey, United States  
Antoine De Ramon N'Yeurt,  
University of the South Pacific, Fiji

### \*Correspondence:

Dominique Pelletier  
dominique.pelletier@ifremer.fr

### †ORCID:

Dominique Pelletier  
[orcid.org/0000-0003-2420-1942](https://orcid.org/0000-0003-2420-1942)  
David Roos  
[orcid.org/0000-0003-0273-3585](https://orcid.org/0000-0003-0273-3585)  
Jessica Garcia  
[orcid.org/0000-0002-1179-5692](https://orcid.org/0000-0002-1179-5692)  
Coline Royaux  
[orcid.org/0000-0003-4308-5617](https://orcid.org/0000-0003-4308-5617)  
Yvan Le Bras  
[orcid.org/0000-0002-8504-068X](https://orcid.org/0000-0002-8504-068X)  
Yves Reecht  
[orcid.org/0000-0003-3583-1843](https://orcid.org/0000-0003-3583-1843)

### Specialty section:

This article was submitted to  
Ocean Observation,  
a section of the journal  
Frontiers in Marine Science

**Received:** 31 March 2021

**Accepted:** 02 July 2021

**Published:** 29 July 2021

**Dominique Pelletier<sup>1,2\*†</sup>, David Roos<sup>3†</sup>, Marc Bouchoucha<sup>4</sup>, Thomas Schohn<sup>1</sup>, William Roman<sup>1</sup>, Charles Gonson<sup>1</sup>, Thomas Bockel<sup>1,5</sup>, Liliane Carpentier<sup>1</sup>, Bastien Preuss<sup>6</sup>, Abigail Powell<sup>1</sup>, Jessica Garcia<sup>1,7†</sup>, Matthias Gaboriau<sup>8</sup>, Florent Cadé<sup>9</sup>, Coline Royaux<sup>10†</sup>, Yvan Le Bras<sup>10†</sup> and Yves Reecht<sup>11,12†</sup>**

<sup>1</sup> Unité Lagons, Ecosystèmes et Aquaculture Durable en Nouvelle Calédonie, Département Ressources Biologiques et Environnement, Institut Français de Recherche pour l'Exploitation de la Mer, Nouméa, New Caledonia, <sup>2</sup> Unité Ecologie et Modèles pour l'Haliéutique, Département Ressources Biologiques et Environnement, Institut Français de Recherche pour l'Exploitation de la Mer, Nantes, France, <sup>3</sup> Délégation Océan Indien, Département Ressources Biologiques et Environnement, Institut Français de Recherche pour l'Exploitation de la Mer, Le Port, France, <sup>4</sup> Laboratoire Environnement Ressources, Département Océanographie et Dynamique des Ecosystèmes, La Seyne-sur-Mer, France, <sup>5</sup> Andromède Océanologie, Carnon Plage, France, <sup>6</sup> Bureau d'études SQUALE, Nouméa, New Caledonia, <sup>7</sup> UMS CNRS 3514 STELLA MARE, Université di Corsica Pasquale Paoli, Biguglia, France, <sup>8</sup> 18 Carrer Sant Jordi, Banyuls-sur-Mer, France, <sup>9</sup> OCEANS.mov, Nouméa, New Caledonia, <sup>10</sup> Pôle National de Données de Biodiversité, UMS 2006 PatriNat, Station Marine de Concarneau, Muséum National d'Histoire Naturelle, Concarneau, France, <sup>11</sup> Unité Sciences et Technologies Haliéutiques, Département Ressources Biologiques et Environnement, Institut Français de Recherche pour l'Exploitation de la Mer, Plouzané, France, <sup>12</sup> Institute of Marine Research/Havforskningsinstituttet, Bergen, Norway

Essential Biodiversity Variables (EBV) related to benthic habitats and high trophic levels such as fish communities must be measured at fine scale but monitored and assessed at spatial scales that are relevant for policy and management actions. Local scales are important for assessing anthropogenic impacts, and conservation-related and fisheries management actions, while reporting on the conservation status of biodiversity to formulate national and international policies requires much broader scales. Measurements must account for the fact that coastal habitats and fish communities are heterogeneously distributed locally and at larger scales. Assessments based on *in situ* monitoring generally suffer from poor spatial replication and limited geographical coverage, which is challenging for area-wide assessments. Requirements for appropriate monitoring comprise cost-efficient and standardized observation protocols and data formats, spatially scalable and versatile data workflows, data that comply with the FAIR (Findable, Accessible, Interoperable, and Reusable) principles, while minimizing the environmental impact of measurements. This paper describes a standardized workflow based on remote underwater video that aims to assess fishes

(at species and community levels) and habitat-related EBVs in coastal areas. This panoramic unbaited video technique was developed in 2007 to survey both fishes and benthic habitats in a cost-efficient manner, and with minimal effect on biodiversity. It can be deployed in areas where low underwater visibility is not a permanent or major limitation. The technique was consolidated and standardized and has been successfully used in varied settings over the last 12 years. We operationalized the EBV workflow by documenting the field protocol, survey design, image post-processing, EBV production and data curation. Applications of the workflow are illustrated here based on some 4,500 observations (fishes and benthic habitats) in the Pacific, Indian and Atlantic Oceans, and Mediterranean Sea. The STAVIRO's proven track-record of utility and cost-effectiveness indicates that it should be considered by other researchers for future applications.

**Keywords:** underwater video, essential biodiversity variables, monitoring, assessment, standardized workflow, FAIR principles, PAMPA

## INTRODUCTION

To track the progress of initiatives to conserve marine biodiversity and achieve sustainable development goals requires assessments at spatial scales that are relevant for management actions. Scales are multiple, ranging from locally managed areas (e.g., Locally Managed Marine Areas) to national networks of Marine Protected Areas (MPAs), up to global scale for reporting to international conventions and policies. Essential variables related to habitats and high trophic levels such as fish communities include fish abundance and distribution, biotic cover and composition for Essential Ocean Variables (EOVs) (Miloslavich et al., 2018), and species distribution, taxonomic diversity, population abundance and structure, habitat structure and ecosystem composition and function for Essential Biodiversity Variables (EBVs) (Muller-Karger et al., 2018). Assessing changes in these variables involves *in situ* monitoring to identify, count and measure both fish species and habitat cover.

Coastal biodiversity is heterogeneously distributed, locally and at larger scales, and is subject to anthropogenic pressures that are generally both intense and spatially heterogeneous. Monitoring-based assessments of fish communities and biotic habitats in coastal areas generally lack sufficient spatial replication to permit robust area-wide assessments of these key biological components. Requirements for appropriate monitoring comprise cost-efficient and standardized observation protocols, data formats and workflows that are spatially scalable and widely applicable, data that comply with the FAIR (Findable, Accessible, Interoperable, and Reusable) principles (Wilkinson et al., 2016), and methods that minimize environmental impact of measurements, particularly in MPAs.

Underwater optical imagery has been increasingly used as a non-obtrusive and non-extractive observation means for conspicuous biodiversity components (Mallet and Pelletier, 2014). Video-based protocols and tools for monitoring fishes include point-source Baited Remote Underwater Video (BRUV) landers (Whitmarsh et al., 2017; Langlois et al., 2020); transects conducted from Remotely Operated Vehicles

(ROV) (Sward et al., 2019) (particularly at depths beyond 30 m); and Diver-Operated Video (DOV) transects in shallow areas (Goetze et al., 2019). Benthic habitats may be observed from Autonomous Underwater Vehicle (AUV), towed video (see e.g., standard operating procedures in Przeslawski et al. (2019)), but also from ROV and DOV.

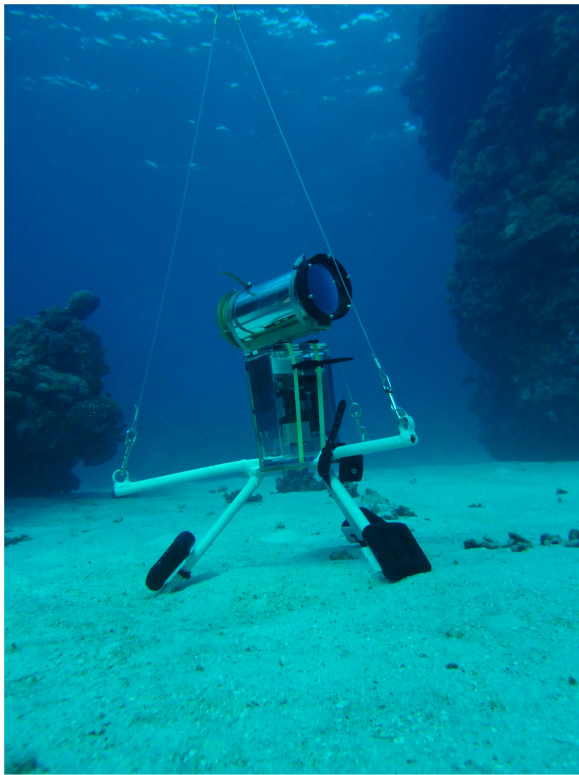
A remote panoramic unbaited video technique developed in 2007 and subsequently tested and improved (Pelletier et al., 2012) aimed to survey both fishes and habitats in a cost-efficient manner, and with minimal effect on biodiversity. The absence of bait removes issues such as effects of soak time, selective attraction and inter-specific effects, and the typically unknown characteristics of bait plumes. The panoramic video makes it possible to quantify both fish abundance and habitat cover over an extended field of view around the device.

After 12 years of successful use (more than 4,500 observations of fishes and benthic cover), the protocol was operationalized and standardized. It was implemented for research, and for a range of assessment needs including Marine Protected Areas management effectiveness, anthropogenic impacts and ecosystem health. With sufficient detail to enable interoperability and adoption by other users, this paper presents the four steps of this standardized procedure and data workflow from sampling to EBV assessment: data acquisition, data curation and management, image analysis, and products for end-users. Application examples are provided for illustration. The strengths and limitations of the observation protocol and its utility to address challenges in monitoring and assessment of biodiversity are discussed based on these experiences.

## MATERIALS AND EQUIPMENT

### STAVIRO Lander Description

The lander consists of two waterproof housings connected by a stainless steel axis (**Figure 1**). The upper housing contains the camera and its battery while the lower housing contains a motor and its battery. The upper housing is a plexiglass tube (3 mm



**FIGURE 1 |** The STAVIRO lander on a sandy bottom in New Caledonia. Credits: B. Preuss – Ifremer AMBIO project.

thick) with a flat window of 10 mm-thick crystal glass at one end, and an aluminum lid secured by stainless steel screws and bolts at the other end. It is made waterproof through double O-rings on each side. The lower housing is an Ikelite™ housing. The stainless steel axis crosses the lid of the housing with metallic seals and a watertight cable gland that enables the upper housing to rotate at programmed angles and timings. The camera housing rotates 60° every 30 s, yielding six contiguous 60° fixed frames per 360° rotation; the duration of a rotation is hence ~3 min. The angle, timing and duration of a given rotation follow from extensive testing in 2007 and 2008 in varied conditions. A 12 V lead-acid battery (e.g., PANASONIC LCR21R3) results in an autonomy of ~15 h for the motor.

The recommended features for the camera are High Definition (Full HD, i.e., 1,920 × 1,080 pixels), an approximate field of view of 60°, a large sensitive low-noise back-illuminated sensor (SONY™ CMOS Exmor R sensor) and a capture rate of at least 25 frames per second in progressive scanning system (25 p). Higher definitions or capture rates may improve identification but inflate file size. The last camera used is a SONY™ CX900E camera (1 inch sensor) equipped with an optical complement Raynox HD-7062, and a long lasting battery SONY NP-FV100 Li-Ion 3700 mAh (average autonomy 7 h, depending on the battery age). Images are saved on 64 or 128 Go Class 10 SD card inserted in the camera using the AVCHD™ format which is based on the MPEG-4 AVC/H.264 for image compression. The housing and

camera result in an approximate focal angle of 60°. The settings of the camera are as follows: (i) field of view: wide angle; (ii) fixed focus set to maximum; (iii) capture rate: 25 p. Once in the housing, the camera is switched on and off by a magnet activating a magnetic switch; therefore not requiring opening the housing. Note that the waterproof Paralenz™ cameras have also been successfully tested in the last years.

When the housings are assembled and set on their support (see section “Equipment for Deployment”), the camera records on a horizontal plane at an approximate height of 0.8 m, up to a 10 m distance depending on visibility. The blind spot is very limited due to the relatively wide angle of the camera.

## Equipment for Deployment

The device is fixed on an anodized aluminum support used to drop and retrieve the system. The support is rigged to an intermediate buoy that keeps the rigging tight, this buoy being itself fixed to a line connected to a large float at the surface that was used to spot the system and retrieve it when needed. Each of the three legs of the support is weighted with 2 kg of lead, and a depth meter is fixed on one leg to record the depth at the exact lander location. The housings with camera, motor and batteries are transported within protective cases such as Peli™ cases.

This relatively lightweight lander is dropped from the boat at the desired location and set horizontally on the sea bed. When underwater visibility is enough, an aquascope<sup>1</sup> is used to adjust the lander on the sea bed. In other cases, the depth sounder of the boat helps to visualize the descent of the lander and adjust its final position. Deployments may occur from diverse boat types such as a small rigid inflatable (including a tender to a large vessel), or an aluminum boat. Desirable boat features are a reduced draft for very shallow areas, good maneuverability, a reasonably low gunwale, and a deck large enough for the equipment and three crew including the pilot. A davit arm on the side of the boat may be helpful in deep areas or to simply reduce repeated handling efforts.

The cost of the equipment is relatively modest; it is sturdy and can be used for years. The large-sensor cameras used cost between 700 and 1200 euros each (including battery and SD card), and last at least 6 years. The two housings equipped with electronics and motor, and the tripod and rigging approximately amount to 3,300 euros. The rest of the equipment is relatively cheap.

## Hardware and Software for Image and Data Post-Processing

Images are downloaded using the PlayMemories Home™ free software from SONY™. The software also renames the videos with date and time information. However, other tools may be used. Two copies of each video are stored on external hard drives (capacity 1 or 2 To, format allowing for the transfer of large files). The typical size for a video is ~2 Go.

Image post-processing (extraction of features of interest from videos) is achieved using VLC media player (VideoLan, 2006) or an equivalent software, enabling zooming, speed control and

<sup>1</sup><https://www.plastimo.com/en/powerboat-engine-access/fishing-angling-equipment/fishing-angling-accessories/aquascope-demontable.html>

production of snapshots. A large Full HD monitor (preferably 27 inches) is desirable, but the enhanced contrast of a smaller screen (e.g., laptop) is sometimes useful. An additional monitor is needed to input the counts in a spreadsheet. Identification guides and bibliography about the species likely to be observed facilitate the analysis as well as web-based resources, e.g., FishBase (Froese and Pauly, 2019).

## Software for EO/EBV Production

Quantitative data resulting from post-processing are analyzed in various ways. Our routine assessments use the R-based PAMPA User Interface (UI) (Pelletier et al., 2014; Pelletier, 2020a) for producing and analyzing fish and habitat-related EBVs. Functionalities of the PAMPA UI include data import, computation of a wide range of ecological metrics based on species traits, versatile plotting of these metrics and their analysis through Generalized Linear Models (GLM). Metrics are exported to flat files for other analyses, e.g., GIS-based or other statistical modeling. The UI also provides guidance for model selection. The UI does not require a connection to run and may be installed from an installer freely downloadable at [https://github.com/yreecht/Plateforme\\_PAMPA/releases](https://github.com/yreecht/Plateforme_PAMPA/releases).

The PAMPA toolsuite has also been implemented on the Galaxy-E web-based platform<sup>2</sup>, for the most common metrics

<sup>2</sup><https://ecology.usegalaxy.eu/>

(abundance, species richness, and other diversity indices). It is freely accessible and with a tutorial<sup>3</sup>. This implementation also proposes guidance for evaluating the models<sup>4</sup>.

## IMPLEMENTATION, WORKFLOW AND OUTPUTS

The standardized workflow, developed and consolidated in many different settings and contexts (**Table 1**), covers survey design, field work, image post-processing, quantitative assessment, and dissemination. Each step of the workflow generates specific outputs and implies data curation activities (Pelletier et al., 2016).







### Survey Design

The survey design covers the entire area of interest with a systematic distribution of the observations stratified according to habitat and anthropogenic pressures or protection status. The definition of sampling strata relies on existing maps and knowledge gained from the end-users, e.g., MPA managers or local communities. Habitat may encompass here geomorphology,

<sup>3</sup><https://training.galaxyproject.org/training-material/topics/ecology/tutorials/PAMPA-toolsuite-tutorial/tutorial.html>

<sup>4</sup><https://ecology.usegalaxy.eu/datasets/11ac94870d0bb33a5383255468c716b2/display/>

**TABLE 1** | Steps of the workflow with corresponding outcomes and output data.

Step		Outcomes	Output data
Survey design		<ul style="list-style-type: none"> <li>Planned latitude and longitude for deployments</li> <li>Context information for deployments</li> </ul>	<ul style="list-style-type: none"> <li>GPX file</li> </ul>
Field work		<ul style="list-style-type: none"> <li>Videos</li> <li>Field information on deployments</li> </ul>	<ul style="list-style-type: none"> <li>Folders with valid footages</li> <li>Metadata for videos</li> </ul>
Image post-processing		<ul style="list-style-type: none"> <li>Description of benthic habitats</li> <li>Counts and identification of fish and other marine animals</li> </ul>	<ul style="list-style-type: none"> <li>Validated data sheet for habitat attributes</li> <li>Validated data sheet for counts of fish and other marine animals</li> </ul>
Data validation and formatting		<ul style="list-style-type: none"> <li>Fish and habitat data files for assessment and databasing</li> <li>Scalable habitat typology</li> </ul>	<ul style="list-style-type: none"> <li>Formatted files for the PAMPA user interface</li> <li>Input data for the habitat typology</li> </ul>
Assessment		<ul style="list-style-type: none"> <li>Habitat typology</li> <li>Baseline study</li> <li>Spatial variations</li> <li>Temporal changes</li> <li>Ecological status</li> <li>Impact of pressures</li> </ul>	<ul style="list-style-type: none"> <li>Data sets of ecological metrics (fish and habitats)</li> <li>GIS layers of ecological metrics (fish and habitats)</li> </ul>
Dissemination		<ul style="list-style-type: none"> <li>Reports, presentations and data for managers and decision-makers</li> <li>Data for research</li> <li>Images and data for the public</li> </ul>	<ul style="list-style-type: none"> <li>Accessible PDF files</li> <li>Metadata and data in databases</li> <li>Educational and memory video clips</li> </ul>

*Output data in a given step form inputs for the following step.*



benthic coverage types or exposure to waves and wind. Observations are distributed in each habitat with a higher sampling effort in habitats where biodiversity is more diverse and abundant, ensuring a better precision of derived estimators (Cochran, 1977). With respect to protection status, the survey design has multiple observations in each regulation zone of the MPA, and for anthropogenic pressures, in zones bearing distinct pressure levels. Baseline assessments typically involve a larger number of observations than follow-up surveys. The design is generated on a GIS (e.g., QGIS Development Team, 2021), and the resulting latitudes and longitudes are transferred to a portable GPS for field work. Establishing the sampling design for a baseline in a new area takes ca. two work days.

## Field Implementation

The STAVIRO lander is dropped from the boat at the desired location and set horizontally on the seabed. To minimize disturbances due to boat presence, engine noise and lander drop and retrieval, the lander is left *in situ* for approximately 15 min so that images are recorded over three complete undisturbed rotations. The duration of an observation and the number of rotations recorded follow from extensive testing in 2007 and 2008.

Two landers are used together at nearby places to optimize time at sea. The number of observations that can be achieved per hour depends on the distance between stations; we recommend that the two landers are not set too far apart to minimize traveling distances. In a given day, corresponding to ca. 6 h of field work, a pair of systems can achieve an average of 20–40 deployments, depending on traveling time between stations, bottom rugosity, depth and weather conditions. Deployments require a skilled pilot and two or three crew with technical roles, with at least one trained for deployments, the other crew helping with the drops/retrievals and with the field sheet. In shallow depths (down to 15 m) and under good weather conditions, a pilot and one crew are enough.

Practical operational steps and checklists have been developed and are used to avoid errors and facilitate the uptake of the protocol by new operators (**Supplementary Materials 1, 2**). Pre-field work tasks include checking batteries and camera settings and closing the housings, while post-field tasks consist in rinsing the equipment with freshwater, loading the batteries and taking care of the images. Hence, after each sampling day or trip, images are downloaded on a laptop, and checked through a rapid screening process (derushing). A video is deemed valid for image analysis when: (i) underwater visibility (estimated from reference images, see below) is at least 5 m; (ii) the field of view is not obstructed by any sea floor or benthos relief that would prevent image analysis within a 5 m radius around the lander; and (iii) three complete undisturbed rotations are recorded. If (i) and (ii) are met for at least a complete rotation, the video is only analyzed for habitat, or else it is used either for communication purposes only, or discarded. Information from the derushing and field metadata are input in a standardized Excel spreadsheet (**Supplementary Material 3**). These metadata are critically needed for the effective management and analysis

of large numbers of observations. The tasks inherent to pre- and post-field work each day, respectively take 1–2 and 3 h with two of the crew.

## Image Post-processing

For each valid video, habitat attributes (**Table 2**) are evaluated from a single rotation for an estimated 5 m radius around the lander, corresponding to an observed surface area of ca. 78.5 m<sup>2</sup>. Habitat attributes are evaluated in each frame of the rotation (**Supplementary Material 4**).

Fishes and other marine animals (termed herebelow macrofauna) are identified at the most precise taxonomic level based on a reference species list (see below), and counted on each frame and for each of three successive undisturbed rotations within a 5 m radius around the system (**Supplementary Material 5**). To minimize disturbance, counting starts once a complete rotation has been achieved after the lander is set on the bottom.

The species list is cross-referenced with WoRMS (Horton et al., 2021). In coral reef ecosystems, two reference lists were constructed. The most exhaustive list includes families that have at least one species that inhabits reef and lagoon areas in depths in the 0–50 m range, i.e., 56 families (**Table 3**), and excludes cryptic, nocturnal and buried species, as well as species with Lmax smaller than 18 cm as determined from FishBase (Froese and Pauly, 2019). The list comprises fishes, turtles and sea snakes (see Pelletier et al., 2016 for details). For species that may be confused, species complexes were defined

**TABLE 2** | Habitat attributes annotated on each frame of a footage for coral reef ecosystems.

Attribute	Definition
Depth (m)	Measured from a depth gauge on the STAVIRO
Topography	Scores the seabed steepness. If <i>h</i> denotes the largest altitude between troughs and elevations: <i>h</i> negligible, <i>h</i> < 1 m, 1 < <i>h</i> < 2 m, 2 < <i>h</i> < 3 m, <i>h</i> > 3 m
Complexity	Scores the number and diversity in size of potential refuges: none, low, medium, strong, outstanding
Substrate	% of five substrate categories: i) sand; ii) debris (< 0.3 m); iii) boulder (between 0.3 m and 1 m); iv) rock (> 1 m); and v) slab
Live coral	% of live coral
Dead coral	% of recently dead coral
Macroalgae	% of macroalgae
Seagrass	% of seagrass
Coral form	% of morphotype: branch, massive, digitate, foliate, table, others (relative to live coral cover)
Macroalgae	% of erect algae, % of turf and % of other algae (relative to macroalgae cover)
Seagrass height	% of elevated and % of short seagrass (relative to seagrass cover)
Seagrass density	% of dense seagrass, % of semi-dense seagrass, % of sparse seagrass (relative to seagrass cover)

*Percent covers (%) refer to the observed surface area on the frame for main attributes. For secondary attributes, % refers to the surface area of the corresponding main attribute. "Macroalgae" does not include encrusting algae. "Other algae" mostly includes algal turf, i.e., typically low-lying (mm to cm tall) layer of algae (Connell et al., 2014). "Dead coral" still retains a coral shape.*

**TABLE 3 |** Species lists considered for counts in image analysis.

Fish families		
<i>Acanthuridae</i>	<i>Haemulidae</i>	<i>Pentacerotidae</i>
<i>Albulidae</i>	<i>Hemiramphidae</i>	<i>Pinguipedidae</i>
<i>Aulostomidae</i>	<i>Kuhliidae</i>	<i>Plotosidae</i>
<i>Balistidae</i>	<i>Kyphosidae</i>	<i>Polynemidae</i>
<i>Belonidae</i>	<i>Labridae</i>	<i>Pomacanthidae</i>
<i>Caesionidae</i>	<i>Lamnidae</i>	<i>Priacanthidae</i>
<i>Carangidae</i>	<i>Leiognathidae</i>	<i>Rhinchodontidae</i>
<i>Carcharinidae</i>	<i>Lethrinidae</i>	<i>Rhinobatidae</i>
<i>Chaetodontidae</i>	<i>Lobotidae</i>	<i>Scaridae</i>
<i>Chanidae</i>	<i>Lutjanidae</i>	<i>Scombridae</i>
<i>Chirocentridae</i>	<i>Malacanthidae</i>	<i>Serranidae</i>
<i>Dasyatidae</i>	<i>Megalopidae</i>	<i>Siganidae</i>
<i>Diodontidae</i>	<i>Monacanthidae</i>	<i>Sphyrnidae</i>
<i>Echeneidae</i>	<i>Mugilidae</i>	<i>Sphyrnidae</i>
<i>Ephippidae</i>	<i>Mullidae</i>	<i>Stegostomatidae</i>
<i>Fistulariidae</i>	<i>Myliobatidae</i>	<i>Tetraodontidae</i>
<i>Gerreidae</i>	<i>Nemipteridae</i>	<i>Zanclidae</i>
<i>Ginglymostomatidae</i>	<i>Ostraciidae</i>	
Other animals		
<i>Elapidae</i>	<i>Cheloniidae</i>	<i>Dugongidae</i>

Species with *L*<sub>max</sub> smaller than 20 cm are not counted, except for *Chaetodontidae*. "Other animals" include families that do not belong to *Pisces*, but have an iconic interest and are easily observed with the STAVIRO technique. The most complete list comprises the 56 taxonomic families. The second list only comprises the 42 families with species that are either iconic, fished or of particular ecological significance (IEHE list) (*italics*).

jointly with Underwater Visual Census (UVC) fish experts. From this first "complete" list, a second reference list focuses on species that are either fished, iconic, protected, or of particular ecological significance. This second list is used for instance when the assessment is focused on fishing resources. In temperate ecosystems, all species that are not cryptic, nocturnal or buried are identified and counted.

Animals are identified to species level or alternatively at genus or family level. A snapshot or short video clip is sent to experts, or to collaborative tools such as iNaturalist<sup>5</sup>, if identification needs confirmation. Quality assurance for image analysis relies on the training of analysts. Each analyst conducts joint annotations with an expert. For fish counts in coral reef ecosystems, training takes up to 1 month. Training is validated after successful joint analyses of a set of videos. In parallel, 5% of the videos are independently reviewed by an expert analyst. If identifications and counts differ by more than 10%, the video must be reanalyzed. Attention is paid to species that may be potentially confused with one another. Estimation of visibility and 5 m radius followed training of annotators with calibrated reference images comprising bright and dark fish silhouettes of several sizes filmed at a range of distances and in several visibility conditions. The template file for animal counts comprises several fields to record the time code and the position of the animal on the frame, in order to ease quality control and to anticipate the future making of annotated image databases for machine learning (ML) algorithms

<sup>5</sup><https://www.inaturalist.org/>

(see section "Information Gained from Images"). Finally, once the set of videos has been analyzed and controlled for quality, the data are checked for inconsistencies using R scripts developed for this purpose.

Analyzing a video requires 10–90 min for identifying and counting macrofauna depending on diversity and abundance, and 15 min for habitat description. This is achieved by a trained person and facilitated when a second person inputs the data.

## EBV Production and Analyses

The data tables resulting from the macrofauna counts and the field metadata are then, respectively formatted following the PAMPA template into a file for counts and a file with the metadata per observation unit. The abundance per taxon is computed by the PAMPA UI for each observation as the mean count over three rotations (within 5 m around the camera), which averages out the variability between rotations. Abundance is expressed in densities (numbers of individuals per 100 m<sup>2</sup>, ind/100 m<sup>2</sup>). Species richness is the total number of species observed within 5 m around the camera during the three rotations. The interface also computes other diversity indices such as Shannon's, Pielou's, Simpson's, and Hill's (Hill, 1973). A wide array of abundance and diversity metrics may be easily calculated based on a range of species-specific taxonomy, trait and use-related criteria. Habitat-related metrics such as biotic covers may also be analyzed through the UI. Biotic cover per observation unit is defined as the mean percent cover of the biotic category (i.e., macroalgae, sea grass, or live coral) averaged over the six frames of the analyzed rotation.

Habitat data are moreover formatted in a data table to construct a habitat typology based on clustering and classification (Pelletier et al., 2020). This typology defines the local habitat to each observation unit as a covariate for spatial and temporal differences e.g., in fish abundance and diversity. This is important because observation units are collected in various habitats, and the distribution of mobile macrofauna is strongly linked to habitat distribution.

Metrics are efficiently computed, plotted and analyzed with GLMs using the PAMPA UI, and now with the Galaxy-E web platform (**Supplementary Material 6**). GLMs test for the effect of either protection status or anthropogenic pressure, while accounting for local habitat derived from the typology. Where several years of data are available, temporal changes are tested too.

## EBV Products for End-Users

Several EBVs and EOVs are documented by this protocol (**Table 4**) and their spatial replication enables the distribution of variables inherent to both EOVs and EBVs to also be assessed.

Applications for the STAVIRO protocol first include assessments linked to human activities and interventions: (i) MPA effectiveness, i.e., tracking progress toward biodiversity conservation and sustainable fishing goals; and (ii) assessment of the impact of anthropogenic pressures, among which recreational and commercial uses of coastal areas, industrial projects, urbanization and marine renewable energies. In each use case, a baseline survey is conducted to establish the spatial distribution of EBVs and test the differences between zones with distinct protection levels, regulations of uses, and

**TABLE 4 |** Link between EOVs and EBVs, and the indicators derived from STAVIRO data.

Indicators derived from STAVIRO data	Related EOVs	Related EBVs
Mobile macrofauna abundance and occurrences List of species Diversity indices	Fish, marine turtles and sea snake abundance and distribution	Taxonomic diversity Species distribution Population abundance Population structure by size class Phenology
Macroalgal cover Seagrass cover	Macroalgal canopy cover and composition Seagrass cover and composition	Habitat structure Ecosystem extent/fragmentation Ecosystem composition/functional type
Live coral and hard coral covers	Hard coral cover and composition	

*Indicators are computed at each observation unit and their spatial distribution may be analyzed.*

anthropogenic pressures. Follow-up assessments involve testing both spatial and temporal variations of EBVs according to the same factors.

The second application type deals with assessing ecosystem health or biodiversity status against conservation objectives at the scale of territories or wide areas. With numerous data collected in varied habitats subject to contrasted anthropogenic and environmental pressures, the distribution of EBVs is representative and may be mapped at the scale of the site, area or territory. EBVs may be scored and assigned color codes per observation unit; five scores are used from red (bad) to blue (excellent). For each EBV, scores are then averaged at the scale of each surveyed site and organized into aggregated radarplots. Such concise displays enable straightforward comparison of ecological status across sites within a given region.

In both applications, the conservation goals considered follow from previous projects with MPA managers (Pelletier, 2020a): (i) sustainable exploitation of resources and (ii) conservation of biodiversity with four objectives targeting: communities and species representative of the ecosystem, ecosystem functions, species of particular significance, and representative habitats. Indicators are selected according to their relevance to the conservation objectives, and analyzed depending on habitat, local anthropogenic pressures and protection status following a template (Supplementary Material 7). EBV maps are obtained by exporting georeferenced metrics from the PAMPA UI toward GIS layers. In addition to the indicators, the list of species and the relative frequencies of dominant families document the Taxonomic Diversity EBV. Lastly, each baseline assessment includes a recommended sampling design for follow-up surveys. Additional information reported with the assessment for quality assurance and transparency comprise the percentage of valid drops, the percentage of individuals identified at species, genus and family levels, and the time spent for image analysis.

The third application of the STAVIRO data lies in a variety of research studies, including biogeographic studies, socio-ecosystems analysis and modeling, as well as studies of

fish behavior and interspecific relationships enabled by the unobtrusiveness of the lander.

## Dissemination of Outcomes and Data Management

The STAVIRO protocol generates spatially replicated EBV and a large number of observations. GIS-layers of EBVs are hosted on an institutional Open Access map serve<sup>6</sup>. Quantitative data issued from image analysis are uploaded on institutional databases and/or shared to other initiatives for data sharing. Assessment reports are systematically posted on the Open archive <https://archimer.ifremer.fr/search>. Image data are safeguarded through archives on institutional databases servers and duplicated on local hard drives.

Two types of image-based outcomes are produced: (i) a video clip assembling short sequences recorded at a subset of representative stations, yielding a memory of the ecological status of the area at the time of the survey; (ii) a compilation of outstanding images that either depict the biodiversity assets inherent to the area, in order to provide end-users with a better knowledge of the values to be protected in the area; or display areas under critical anthropogenic pressure. Image-based outcomes of interest to a broader audience or helpful to complement assessments or research outcomes are posted on the image portal <https://image.ifremer.fr/>.

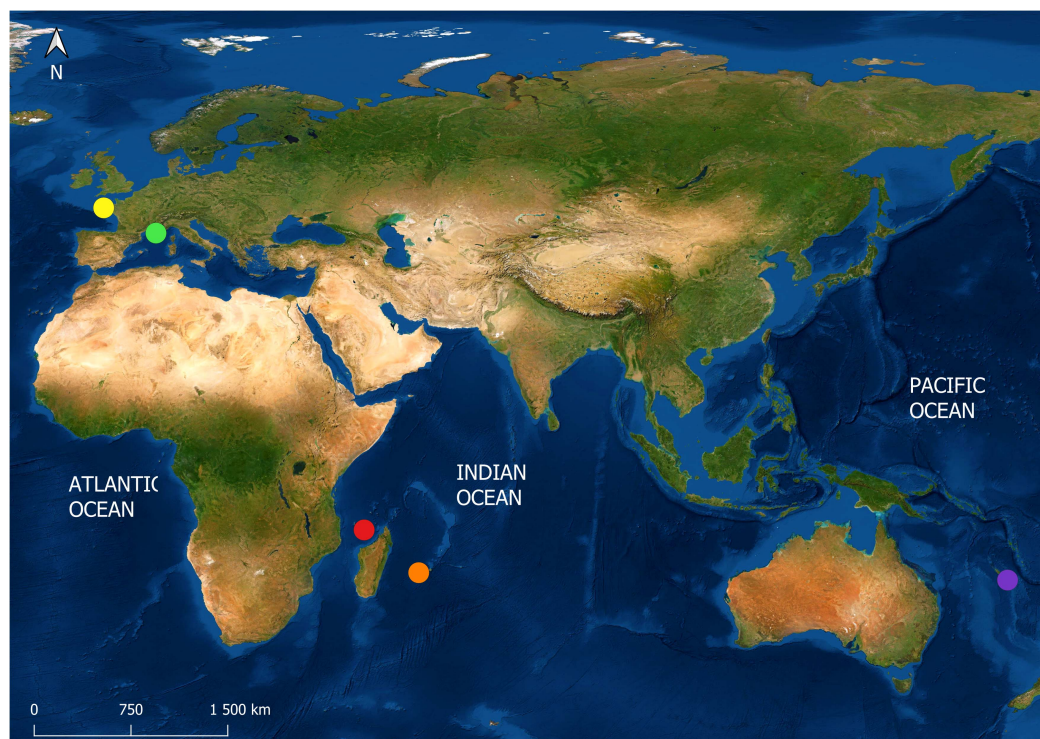
## APPLICATIONS

The wide range of applications of the STAVIRO protocol—four ecosystems located in three oceanic regions: the Southwest Pacific (New Caledonia), the Indian Ocean (Reunion and Mayotte Is.), the Northwestern Mediterranean Sea and the Atlantic Ocean—is illustrated in Figure 2 and Table 5. Between 2007 and 2020, more than 4500 observations were collected to assess fish and habitats to inform a range of conservation-related questions occurring at different spatial scales (Table 5) in a variety of ecosystems, habitats and depths (Table 6 and Supplementary Material 8). In New Caledonia and in the Indian Ocean, vast areas were sampled intensively over relatively short period of time, e.g., the Geyser Bank (230 obs., 7 days, Figure 3), Chesterfield and Bellona reefs and atolls (202 obs., 10 days), and the complex Corne Sud reefs (143 obs., 6 days) (Figure 4). 900 observations were sampled in the Mediterranean Sea along the French coast and in Corsica (Figure 5). Overall, the proportion of valid observations per survey lied between 80 and 95%, depending on weather conditions and water clarity. Example imagery is given in Figure 6.

EBV products and dissemination are illustrated by outcomes from New Caledonian data. A first EBV product for monitoring and assessment is habitat structure per observation unit, through (i) five main types of habitat (Sea grass beds, Macroalgae, Sandy bottoms, Live coral and Debris) and (ii) within each habitat type, rules describing heterogeneities at finer scale (Pelletier et al., 2020). Habitat structure is representative of the

<sup>6</sup><https://sextant.ifremer.fr/>





**FIGURE 2 |** Regions where the STAVIRO protocol was implemented: New Caledonia (purple), Reunion Island (orange), Mayotte Island (red), Mediterranean Sea (green) and Atlantic Ocean (yellow).

**TABLE 5 |** Assessments conducted using the protocol.

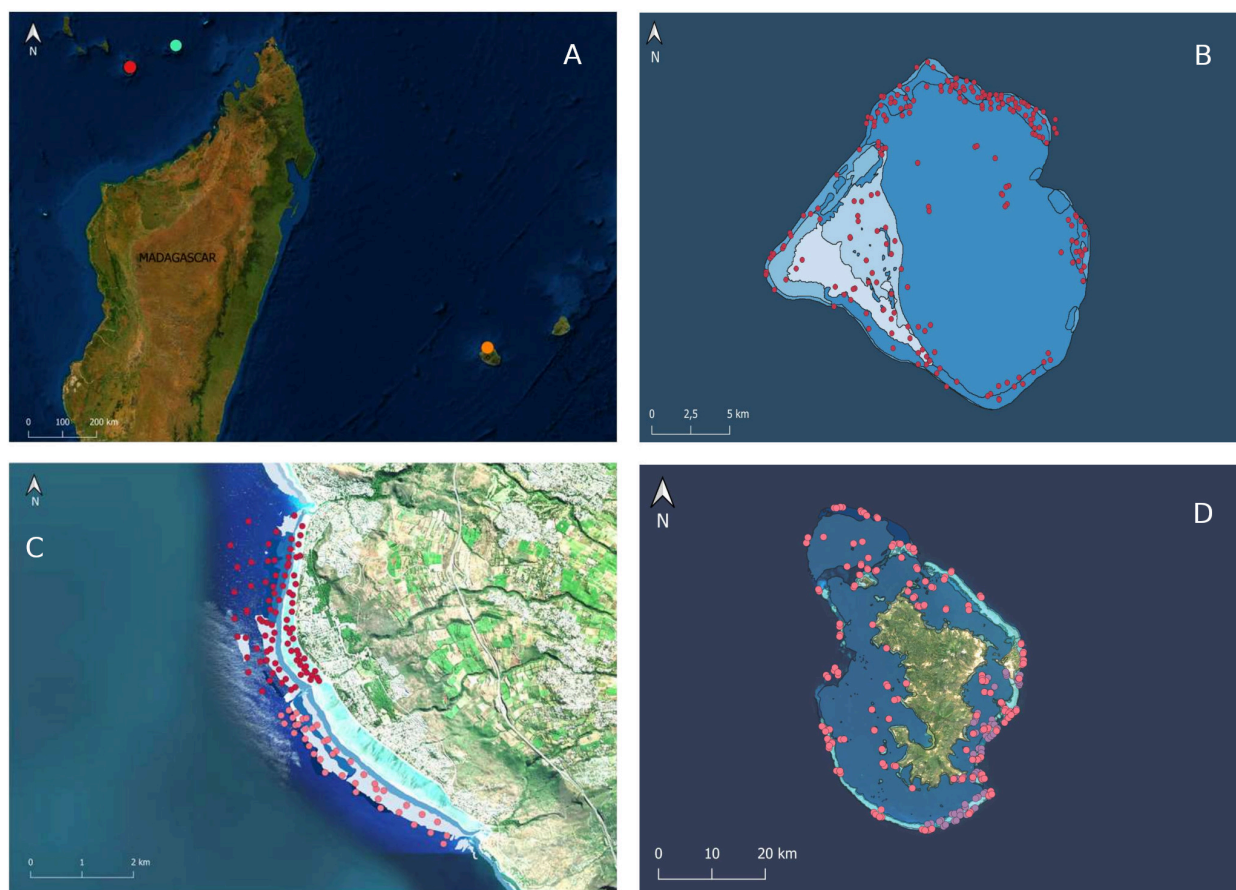
Use case	Region	Spatial extent	Status(es)	Anthropogenic pressures	Objectives of the assessment
Coral Sea Marine Park	SPAC	1,292,967 km <sup>2</sup>	Marine Park, World Heritage (WH), Marine Reserve	Fishing	Baseline: ecological status and fishing resources Impact of illegal fishing
New Caledonian lagoons	SPAC	15,743 km <sup>2</sup>	WH Marine Reserves	Mining industry, urbanization, coastal uses, fishing, cruiseships	Baseline: ecological status and fish resources Effect of MPA protection Impact of anthropogenic pressures
Mayotte Is. Lagoon Iris Bank	IND	1,100 km <sup>2</sup> 235 km <sup>2</sup>	Mayotte Natural Marine Park (Mayotte EEZ, 68,381 km <sup>2</sup> )	Urbanization, coastal uses, fishing	Baseline: ecological status and fish resources Effect of MPA protection
Reunion Island	IND	135 km <sup>2</sup> (depth < 90 m)	Reunion Natural Reserve (35 km <sup>2</sup> )	Urbanization, coastal uses, fishing	Baseline: ecological status and fish resources Effect of MPA protection
Geyser Oceanic Bank	IND	268 km <sup>2</sup>	The Glorieuses Islands Natural Marine Park	Illegal fishing	Baseline: ecological status and fish resources Effect of MPA protection
Cerbère-Banyuls Natural Reserve	MED	6,5 km <sup>2</sup> core integral reserve (64 ha)	Natural Reserve IUCN Green List in 2015, global ocean refuge system in 2018	Urbanization, coastal uses, fishing	Baseline: ecological status and fish resources Effect of MPA protection
Côte Bleue Marine Park	MED	188.64 km <sup>2</sup> Two no-take reserves (295 ha)	Marine Park with two no-take reserves, IUCN Green List in 2014	Urbanization, coastal uses, fishing	Baseline: ecological status and fish resources Effect of MPA protection
Var Corsica	MED	Not measured, several areas	No protection	Urbanization, coastal uses, fishing	Baseline: ecological status and anthropogenic pressures (WFD)
Concarneau-Les Glénan	ATL	220 km <sup>2</sup>	Natura 2000 (Habitat Directive, MPA)	Urbanization, coastal uses, fishing	Baseline: ecological status and fish resources

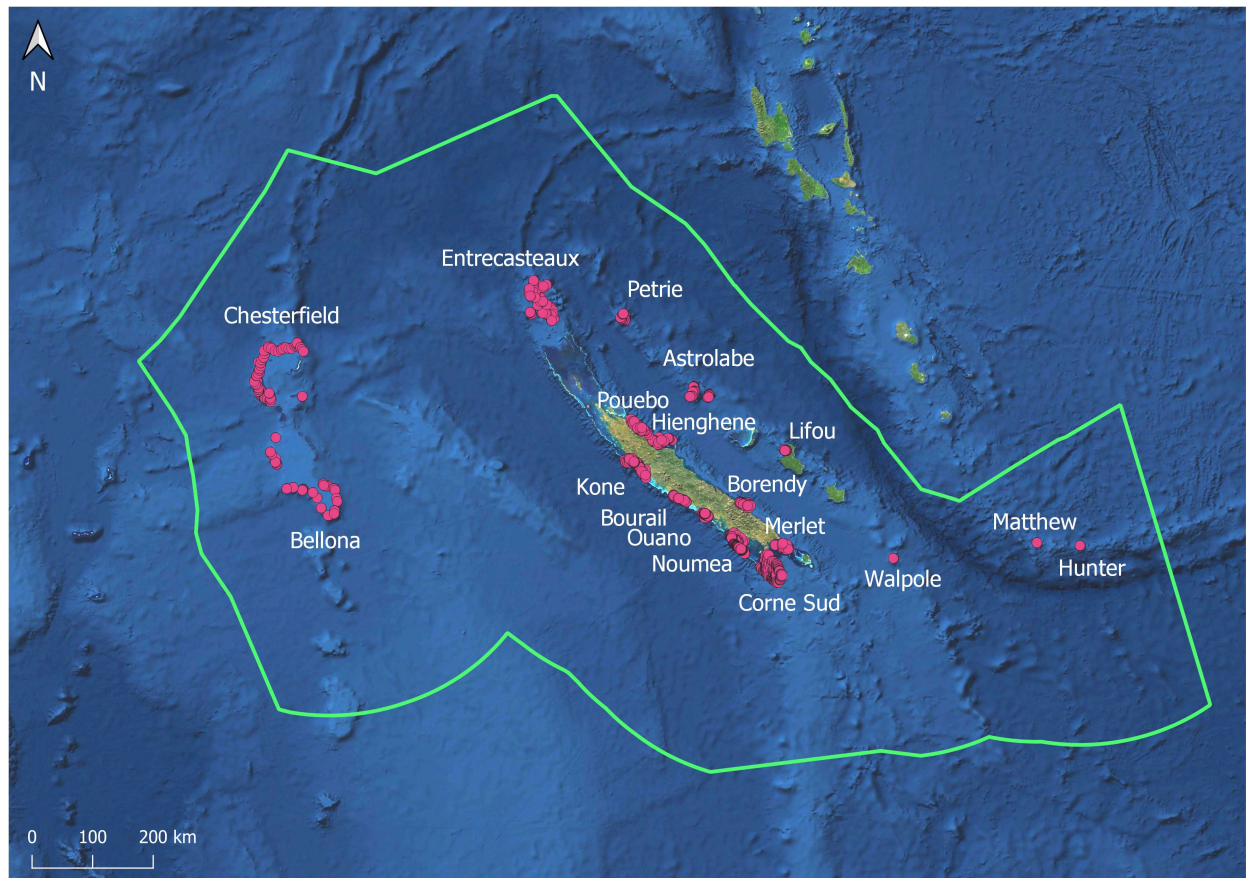
WFD stands for Water Framework Directive (EU 2000). Baseline stands for Baseline assessment. SPAC, Southwest Pacific Ocean; IND, Indian Ocean; MED, Northwestern Mediterranean Sea; ATL, Northeast Atlantic Ocean.



**TABLE 6 |** Main features of samples for the use cases.

Use case	Sampling years	Sample size (# obs.)	Depth range (m)	Sampled habitats	Sampled geomorphologies
Coral Sea Marine Park	2013–2017	498	1–36	Live coral, Sandy bottoms, debris	Lagoon and reef patches, External and internal slopes of barrier reef, reef passes
New Caledonian lagoons	2007–2008 and 2013	2,209	1–49	Live coral, Sandy bottoms, debris, sea grass beds, Algal beds	Lagoon and reef patches, external and internal slopes of barrier reef, Intermediate and fringing reefs, reef passes
Mayotte Is. Lagoon and Iris Bank	2014–2017	351	1–60	Live coral, sandy bottoms, debris, sea grass beds, algal beds	Same as above
Reunion Island	2016–2017 2019–2020	153 331	1–90	Live coral, sandy bottoms, debris, sea grass beds, algal beds	Same as above
Geyser Oceanic Bank	2016	230	1–45	Live coral, sandy bottoms, debris, sea grass beds, algal beds	Lagoon and reef patches, external and internal slopes of barrier reef
Cerbère-Banyuls Natural Reserve	2011, 2012 and 2013	202	1–26	Rock, boulders, debris, sea grass beds, coralligenous	Shoreline
Côte Bleue Marine Park	2010, 2011 and 2019	186	1–32	Rocky habitats, debris, sea grass beds, coralligenous	Shoreline, flat bottoms, and reefs
French Riviera and Corsica	2010–2019	15	1–40	Rocky habitats, debris, sea grass beds, coralligenous	Shoreline
Concarneau—Les Glénan	2019–2020	127	1–17	Sea grass beds, <i>Laminaria</i> beds, sandy bottoms, rocky habitats, debris	Shoreline, archipelago lagoon, and reefs

**FIGURE 3 |** Sampled sites in the Indian Ocean **(A)** [Geyser Bank (light blue); Mayotte (red) and Réunion Island (orange)], and sampled stations in Geyser Bank **(B)**, Réunion Natural Reserve **(C)** and Mayotte **(D)**. At the Réunion Natural Reserve **(C)**, sampling corresponds to 2016 (red) and 2017 (pink).



**FIGURE 4 |** Sampled sites in New Caledonia. The Economic Exclusive Zone (EEZ) (green) also delineates the outer boundary of the Coral Sea Marine Park (CSMP) (Table 5). The CSMP inner boundary is the barrier reef surrounding the main island and the three islands of the Loyalty archipelago, (among which Lifou Island) located between Astrolabe and Walpole. Boundaries of the World Heritage property are in orange.

reef and lagoon habitats of New Caledonia's EEZ (Figure 4) and was mapped at site (Figure 7) and region scale. In assessments of ecological status, habitat types better explained habitat-related variations of biotic covers, fish communities, and other marine animals, than e.g., geomorphological maps (Supplementary Material 8). As a second EBV product, 27 indicators for fishes and other animals, and four indicators for habitat-related EBVs form the basis for the assessments at each surveyed site (Table 7, link with EBVs and EOVs in Table 4). In addition, the main indicators were scored from ~2,400 observations and used to compare the ecological status of reefs across the World Heritage sites, and within the Coral Sea Marine Park (CSMP) and (Figure 8 and Table 5). In the CSMP, our assessments contributed to update site-specific species inventories and revise the status of potential target species, e.g., in the Chesterfield and Bellona atolls and reefs (Supplementary Material 8). They also showed the exceptional health of Astrolabe's reefs, which are now a fully protected integral reserve. The presence of iconic and keystone species was quantified, in particular in the CSMP where frequent occurrences and large abundances of sharks were observed in the absence of any bait. During presentations to stakeholders, managers or to the public, screenshots and short

clips illustrated scores and figures in a simple way. Lastly, the New Caledonian habitat data were part of the reference samples used in ML-based mapping of coral habitats for the Allen Coral Atlas<sup>7</sup>.

Many research opportunities are supported by the wealth of data provided by STAVIRO, in particular, statistical modeling requiring spatially distributed and replicated data, for example, species distribution modeling, spatial patterns of habitats (Pelletier et al., 2020) and relationships between species and environmental variables (Powell et al., 2016; Garcia et al., 2018). The programmable version of the STAVIRO, the MICADO, is suited for longitudinal studies, e.g., of short-term variations of fish abundance (Mallet et al., 2016) and phenological processes such as spawning aggregations (Pelletier D., unpublished data).

Lastly, our work has resulted in the production of communication and outreach material: image sets (Pelletier, 2020b), educational conferences and video clips that are freely available on YouTube, at <https://www.seanoe.org/> and at <https://image.ifremer.fr/search>.

<sup>7</sup><https://allencoralatlas.org/>





**FIGURE 5 |** Main sampled sites in the Mediterranean Sea **(A)** (Cerbère-Banyuls Natural Marine Reserve (green), and Côte Bleue Marine Park (light blue), and Sicié Cape (orange) and sampled stations at the two coastal MPAs surveyed with the protocol: **(B)** Cerbère-Banyuls Natural Marine Reserve and **(C)** Côte Bleue Marine Park.

## DISCUSSION

The STAVIRO protocol—all steps from data collection to knowledge production and dissemination—has been applied in various settings over a period of 12 years. This enabled the different steps of the workflow to be adapted to the final goal of EBV and EOv production. The protocol has both advantages and limitations relative to other observation protocols, and these are discussed below, as well as perspectives.

### Non-obtrusive Observation

Like all video-based observation techniques, the STAVIRO is non-extractive which is an advantage for assessments, particularly in areas that are protected or host vulnerable biodiversity. As a lightweight lander, it has no impact on benthic habitat, is inconspicuous, and is unbaited, resulting in a minimal effect on the behavior of fishes and other mobile macrofauna. This is an advantage compared to diver-operated observation techniques like UVC and DOV that may be prone to differences between observers (for UVC), and to diver avoidance by some species (Kulbicki et al., 2010; Dickens et al., 2011). In a paired experiment, the STAVIRO observed more individuals from large species and target species than UVC (Mallet et al., 2014). This

minimal disturbance is also an advantage for studying animal behavior and interspecific relationships, and the automatic version of the STAVIRO has been used for this purpose (Mallet et al., 2016; Pelletier, unpublished data).

### Easy and Fast Deployments

This lightweight lander is easily deployed from diverse boat types, which has fostered the participation of diverse operators, e.g., in New Caledonia, people from the management committees, commercial fishers and rangers. Hence, field work can be realized by non-expert staff entailing (i) reduced personnel costs on the field (no need of expert divers or researchers); and (ii) the potential to engage into participative and citizen-based approaches, and encouraging knowledge exchange and capacity building.

Another strength of the STAVIRO protocol is its ability to survey large areas and obtain spatially replicated data for statistical analyses, as many observations can be collected per day at sea. Most habitats may be surveyed and depth is hardly a limitation (within the euphotic zone) when compared to diver-operated techniques which are constrained by both depth and time taken per observation. Shallow water BRUVs also typically have a deployment time of 1 h.



**FIGURE 6** | Example of images recorded by the STAVIRO. Top: Chesterfield reef, CSMP, New Caledonia. Bottom: Concarneau Bay, Atlantic Ocean.

Yet, the fine-scale positioning of the STAVIRO system requires training for the crew and pilot, as the lander must be horizontal with no obstacles around, sometimes in deep water and navigating in wind and waves. To date, just a single camera housing was damaged during thousands of stations. The lander is very stable and the entanglement of the rigging during the observation, generally due to currents, is quite rare and is completely avoided by a rigid rigging.

### Field of View and Panoramic Video

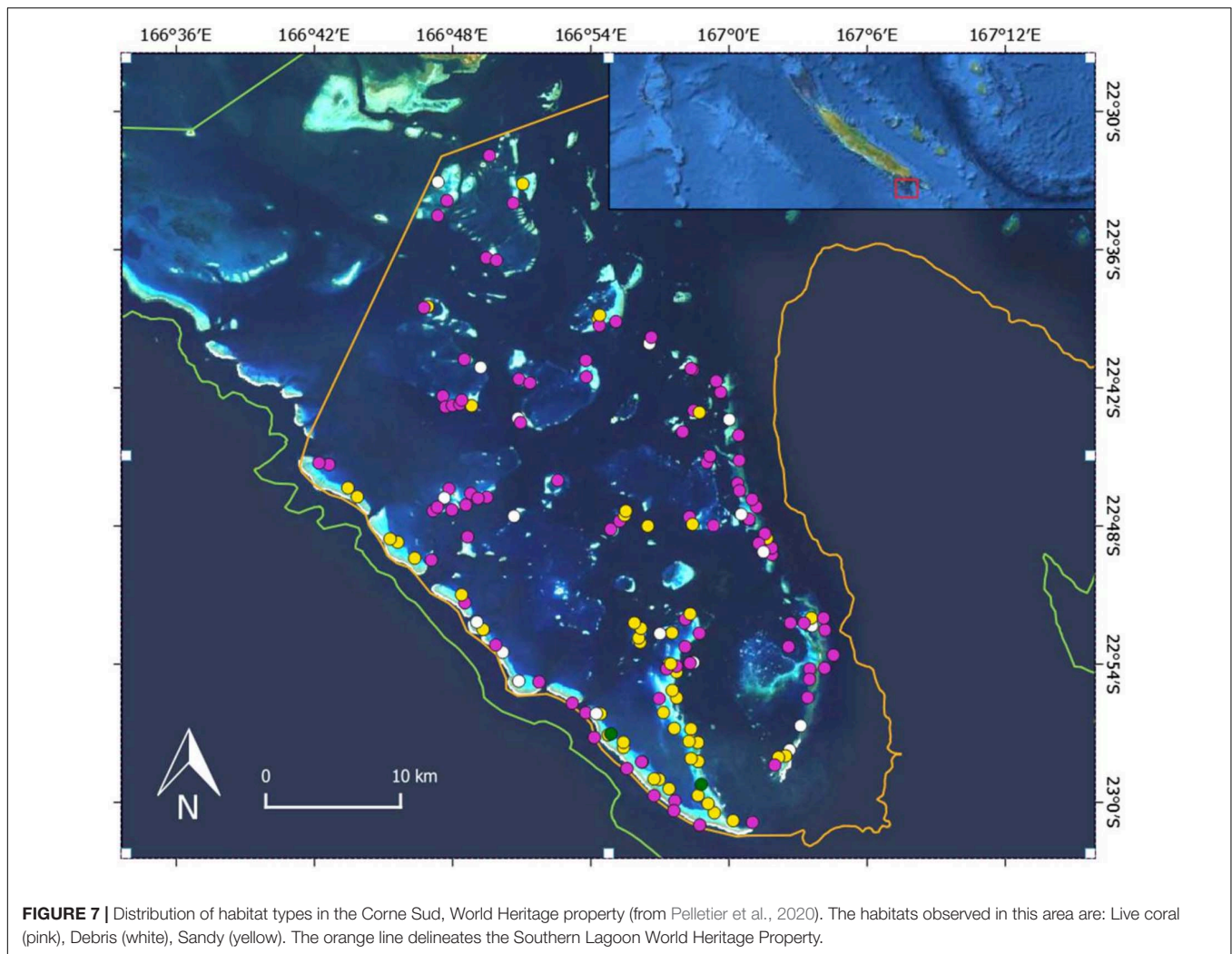
The frames recorded by the rotating camera are similar to the field of view of human eyes, thereby minimizing image distortion entailed by wider angles of view. This feature and the horizontal view facilitate image analysis for both mobile animals and benthic covers. The panoramic view together with the 60° angle of view enables to characterize habitat and count animals at a distance of at least 5 m and to compute abundance densities (and not only relative abundance indices). We acknowledge that the estimation of the 5 m distance is subject to some uncertainty, as the STAVIRO does not use stereo video (but see section “Information

Gained From Images”); however, this uncertainty is minimized by the training of analysts and the reliance on reference images.

### Information Gained From Images

Image post-processing has, to date, been carried out manually by trained analysts. This step of the workflow is time consuming due to the large number of videos collected and the substantial processing time per video. Double counting and missed animals are possible for any observation technique where the entire seascape is not simultaneously observed over a 360° field of view, but were minimized at each step of the workflow: (i) in early deployments, the duration of each fixed frame, the angle and speed of rotation were adjusted to the movements of the observed fauna; (ii) during image analysis, attention is paid to the direction of the moving animals and any animal potentially *déjà vu* is not counted; and (iii) animal abundance computed as a mean count over three rotations smoothes out variability due to moving animals. This estimate is analogous to the MeanCount statistic sometimes used instead of MaxN for BRUV (Campbell et al., 2015; Stobart et al., 2015).





An acknowledged drawback is that our protocol provides coarse and visually estimated size classes, not precise size information. To circumvent this, a stereo version of the system was trialed, but it is bulkier on board and deployments were relatively slow. A second stereo version is currently being developed. A mixed protocol could be implemented in which spatial cover and replication is achieved via the current lander, and a subset of the observations using a stereo version provides size-based information and distance measurements.

Video imagery enables annotators to work collaboratively to ensure that identifications are consistent and relies on an iterative and somewhat time-consuming process (Langlois et al., 2020). Our current procedure for image post-processing, both collaborative and iterative, is effective. Possible differences between analysts as well as uncertainties about size class and surface estimation are handled in a conservative and prudent manner, during post-processing and in the choice of indicators, e.g., most of the indicators used in assessments are not at species level.

In terms of observed taxa, the STAVIRO cannot capture cryptic and nocturnal species, just like UVC or other video-based

protocols. In addition, the panoramic video differs from BRUV or UVCs which recording animals at close distances: small species are not observed in a consistent way up to a 5 m distance. These species are thus either excluded from the counts in diversified coral reef ecosystems, or from data analyses in other ecosystems. In addition to the two species lists for coral reef ecosystems (section “Image Post-processing”), a simpler list was devised based on the species groups considered in the participative Reef Check protocol<sup>8</sup>. This list enables citizen involvement in image analysis, but was not used in our assessments. Web-based tools are also currently being developed for citizen-based image annotation (Matabos et al., 2016).

The next improvement in our protocol lies in the use of annotation tools for direct annotation, and for constructing databases of images for ML algorithms. We have successfully used the EventMeasure software (seagis.com.au) and are investigating adapting BIIGLE (Langenkämper et al., 2017) for video imagery. Our archived data enable to build training data sets to implement ML-based approaches in future applications.

<sup>8</sup><https://www.reefcheck.org/>

**TABLE 7 |** Indicators derived from STAVIRO data collected in New Caledonia to document EBV related to mobile macrofauna in the light of tracking progress toward conservation objectives.

Indicator used in the assessment	Conservation objective				
	Diversity	Functions	Iconic	Habitat	Resources
List of species and occurrences for dominant families	•				
Overall species richness	•				
Species richness of <i>Chaetodontidae</i>	•				
Overall abundance density	•				•
Abundance density per family ( <i>Acanthuridae</i> , <i>Scaridae</i> , <i>Labridae</i> , <i>Chaetodontidae</i> , <i>Serranidae</i> , <i>Lethrinidae</i> , <i>Siganidae</i> , <i>Mullidae</i> )					
Abundance density per trophic group (carnivores, herbivores, piscivore, plankton feeders)		•			
Occurrence of iconic species (sharks, rays, turtles, Napoleon wrasse, sea snake)			•		
Abundance density of fished species (commercial species, species caught by non-professional fishers)					•
Abundance density of target species per fishing gear (spearfishing, line, net)					•
Occurrence of important target species ( <i>Plectropomus leopardus</i> , <i>Lethrinus nebulosus</i> , <i>Naso unicornis</i> , jacks, <i>picot kanak</i> )	•				•
Live coral cover (overall and branch coral)				•	
Sea grass cover				•	
Macroalgae cover				•	

Indicators are computed at the scale of each observation (see section “EBV Products for End-Users”). “Diversity” corresponds to “Maintaining communities and species representative of the ecosystem,” “Functions” corresponds to “Maintaining ecosystem functions,” “Iconic” corresponds to “Conservation of species of particular significance,” “Habitat” corresponds to “Maintaining representative habitats” and “Resources” corresponds to “Sustainable exploitation of resources.” *picot kanak* includes *Acanthurus blochii*, *A. dussumieri*, *A. xanthopterus*, and *A. nigricauda*.

## Lander Reproducibility

One drawback in the light of long-term monitoring is the lander’s dependence on commercial cameras which evolve over years and are replaced by different models, thus requiring the housing or electronics to be adapted and incurring undesirable costs. Because this may be an obstacle to the adoption of the system by other workers, the KOSMOS project was commenced in 2020 to re-develop the STAVIRO (and the MICADO), as a fully Open Source, reasonably costed tool that provides images compatible with the previous version. KOSMOS focuses on the assembly of essential parts, i.e., lens, sensor, housing, electronics and processor, in a more compact system and bypasses the irrelevant features of commercial cameras. Its design and fabrication is a collaborative project<sup>9</sup> implemented with a French FabLab, i.e., a digital fabrication laboratory providing access to the environment, skills, materials and technology to allow volunteers to create, learn and innovate<sup>10</sup>. A prototype was

recently successfully tested. The cost of the complete system will range between 1000 and 1,500 euros, and will make the entire STAVIRO protocol become Open Source and reproducible by a wide audience.

## EOV/EBV Data Products and Dissemination

Through simultaneous observations of fishes, habitats and some other marine animals such as turtles and sea snakes, the STAVIRO protocol documents several EBVs: taxonomic diversity, population abundance (with additional information per size-class), habitat structure, ecosystem composition (and functional type) and phenology. Medium to large size mobile animals are well observed (section “Non-obtrusive Observation”). Relationships between habitat and macrofauna may be studied through paired information. However, the STAVIRO protocol is not the most appropriate protocol for counting small species and semi-cryptic species concealed in coral, crevasses or under rocks. It may thus be used in combination with a complementary monitoring protocol, in which case protocols should be intercalibrated. For instance, participative UVC sampling schemes deployed over large areas such as Reef Life Survey (Edgar et al., 2020) offer opportunities for spatial coverage. BRUVs are another avenue to reveal some cryptic species that may be attracted by bait.

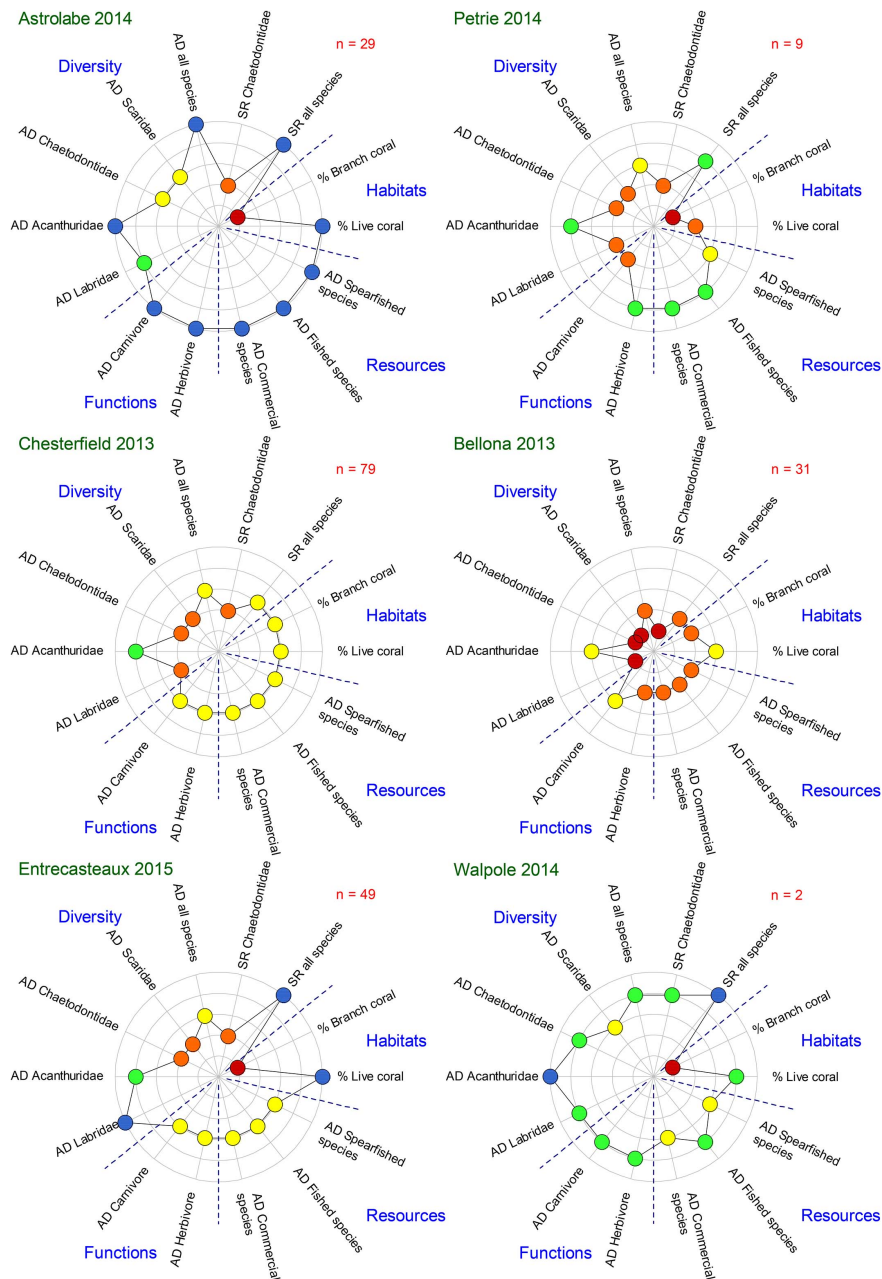
By collecting many deployments per day at sea with only two STAVIRO units, the protocol provides replicated data over large areas, thereby informing distributional EBVs such as species distribution, ecosystem extent and fragmentation. Standardization is indispensable not only for data quality and reproducibility, but also for effective management and analysis of these big datasets. The PAMPA UI was central for operationalizing the production and analysis of EBVs, and coding the PAMPA workflow on Galaxy-E (section “Software for EOV/EBV Production”) facilitates data re-use.

Our video-based assessments provide unique baseline studies for areas that had been poorly surveyed before, either because they were remote, too deep, or too vast. Designs that encompass the main habitats encountered in the surveyed area enable the distributions of species to be characterized according to habitat and geomorphology. In combination with replicated observations across areas subject to distinct pressures and protection status, a comprehensive and statistically robust assessment can be obtained. Because of both high sampling effort, large coverage and sampling in all habitats, the assessments provide a holistic view of the surveyed area. In addition, the standardized protocol makes these assessments scalable to large territories and comparable across sites.

A central motivation is to make the protocol, workflow and data visible, traceable and accessible for scalable assessment and research. With imaging, raw (images) and annotated data (counts and habitat description) may be archived, shared, and re-analyzed for similar or different objectives. Given the efforts invested in data acquisition and image post-processing, sharing the resulting data is an obvious necessity.

<sup>9</sup><https://wikifactory.com/@gheleguen/kosmos-20-r%C3%A9alisation>

<sup>10</sup><https://fabfoundation.org/>



**FIGURE 8 |** Cross-site comparison of ecological status of the main reef areas in the Coral Sea Marine Park, New Caledonia. The locations of the reefs are showed on **Figure 4**. AD and SR stands for abundance density and species richness, respectively.

To satisfy the principles of Open Science (Kissling et al., 2018), each step of the workflow can be achieved from freeware, data are progressively made FAIR, data management links raw data, processed data and outcomes including dissemination, and data will be eventually uploaded to international biodiversity archives, e.g., OBIS<sup>11</sup>.

Equally important to promote the use of the protocol to scientists and other end-users for monitoring and assessment

are the dissemination and capacity building activities. Our end-users included environmental managers and agencies (e.g., MPA staff), participatory management committees, fishers and private operators. In addition to staff from academia and environmental agencies, a number of people were trained in the four regions sampled and became private operators for monitoring and for research.

A final and important aspect of dissemination lies in outreach. Image-based products proved useful for communicating results to most audiences for several reasons: (i) they conveniently

<sup>11</sup><https://obis.org/>



illustrate numerical and graphical outcomes; (ii) imagery-based evidence facilitates knowledge exchange with local management committees and the public, who discover or revisit “their” marine biodiversity and resources (Pelletier, 2020a), and (iii) from an educational standpoint, images provide a sense of pride and custodianship about “their” territory, with positive consequences for caring about the environment. In our protocol, fishes and animals behave in a natural way and show undisturbed behaviors which have raised the interest of many viewers.

## CONCLUSION

The standardized STAVIRO protocol and workflow have been fully operationalized through extensive and successful implementation in a variety of contexts, including at the scale of vast managed areas. The imagery, annotation and the derived EBV products and outcomes support assessments of coastal fish assemblages and habitats in a robust and effective way according to procedures that are evolving toward meeting FAIR principles. In future years, the protocol will support: (i) additional technology to optimize collection of imagery, (ii) software developments, especially machine learning, to facilitate image post-processing and annotation; and (iii) enhanced interoperability with other researchers and stakeholders.

This paper aims to help using the protocol by sharing our extensive experience, the data collected and the savoir-faire gained since 2007. As a versatile and accessible protocol, it can be applied in diverse contexts for monitoring, research and educative needs. The STAVIRO’s proven track-record of utility and cost-effectiveness indicates that it should be considered more broadly for future applications.

## DATA AVAILABILITY STATEMENT

The original contributions presented in the study are included in the article/**Supplementary Material**, further inquiries can be directed to the corresponding author/s.

## AUTHOR CONTRIBUTIONS

DP conceived the STAVIRO protocol, the workflow and the manuscript. DP, DR, and MB led extensive surveys and assessments in the different regions and they tested and consolidated the protocol with the help of WR, CG, TB, LC, TS, BP, AP, JG, MG, and FC. YR developed and maintain the PAMPA user interface. CR and YL developed the Galaxy-E PAMPA application for STAVIRO data. DP wrote the manuscript. All authors have contributed to the writing and editing of the manuscript.

## FUNDING

New Caledonia data were collected during (i) the PAMPA project with the support of the Research Institute for Development;

and (ii) the AMBIO project funded by both IFREMER, New Caledonia Government and Provinces, the Conservatoire des Espaces Naturels of New Caledonia, and the French Ministry of Ecology, the French Initiative for Coral Reefs (IFRECOR), and the French Marine Protected Area Agency. Mediterranean data were collected with the support of IFREMER, the Cerbère-Banyuls Natural Marine Reserve, the Côte Bleue Marine Park and the French Water Agency. In the Indian Ocean, data collection was co-funded by Ifremer and by (i) the Reunion Marine Natural Reserve (PECHTRAD project), (ii) the Mayotte Marine Natural Park (Staviro Mayotte project), (iii) the 10th European Development Fund (FED), the Departmental Collectivity of Mayotte, the French Southern and Antarctic Lands and the University Center of Mayotte (EPICURE project), (iv) the European Fund for Maritime Affairs and Fisheries (FEAMP) and the French government (IPERDMX project).

## ACKNOWLEDGMENTS

We thanks to the numerous collaborators who helped with field work, image analysis, managing and analyzing the data collected since 2007 among which: in New Caledonia: Kévin Leleu, Delphine Mallet, Charlotte Giraud-Carrier, Fanny Witkowski, Cyrielle Jac; in la Réunion: Johanna Herfaut and Paul Giannasi from the Mayotte Natural Marine Park; in the Mediterranean Sea: Gilles Hervé, Jérémy Pastor, Eric Charbonnel; and in the Atlantic Ocean: Claude Merrien and Aouregan Terre-Terrillon. We thank Eric Charbonnel, Jérôme Payrot, Jérémy Pastor, and Philippe Lenfant for facilitating the survey in the Banyuls and Côte Bleue MPAs. We thank Eric Charbonnel, Jérôme Payrot, Jérémy Pastor and Philippe Lenfant for their great help during the survey in the Banyuls and Côte Bleue MPAs.

## SUPPLEMENTARY MATERIAL

The Supplementary Material for this article can be found online at: <https://www.frontiersin.org/articles/10.3389/fmars.2021.689280/full#supplementary-material>

**Supplementary Table 1** | Checklist for field work and naming convention for the video files.

**Supplementary Table 2** | Datasheet for field work.

**Supplementary Table 3** | Metadata for each deployment and video.

**Supplementary Table 4** | Datasheet for habitat (coral reefs).

**Supplementary Table 5** | Datasheet for fish counts.

**Supplementary Table 6** | Galaxy-E workflow implementing part of the PAMPA UI.

**Supplementary Table 7** | Standardized template for indicator analysis.

**Supplementary Table 8** | List of assessment reports in New Caledonia and Indian Ocean.



## REFERENCES

- Campbell, M. D., Pollack, A. G., Gledhill, C. T., Switzer, T. S., and DeVries, D. A. (2015). Comparison of relative abundance indices calculated from two methods of generating video count data. *Fish. Res.* 170, 125–133. doi: 10.1016/j.fishres.2015.05.011
- Cochran, W. G. (1977). *Sampling Techniques*, 3rd Edn. New York, NY: Wiley.
- Dickens, L. C., Goatley, C. H. R., Tanner, J. K., and Bellwood, D. R. (2011). Quantifying relative diver effects in underwater visual censuses. *PLoS One* 6:e18965. doi: 10.1371/journal.pone.0018965
- Edgar, G. J., Cooper, A., Baker, S. C., Barker, W., Barrett, N. S., Becerro, M. A., et al. (2020). Reef Life Survey: establishing the ecological basis for conservation of shallow marine life. *Biol. Conserv.* 252:108855. doi: 10.1016/j.biocon.2020.108855
- Froese, R., and Pauly, D. (2019). *FishBase. World Wide Web Electronic Publication*. Available online at: [www.fishbase.org](http://www.fishbase.org) (accessed January 30, 2020).
- Garcia, J., Pelletier, D., Carpentier, L., Roman, W., and Bockel, T. (2018). Scale-dependency of the environmental influence on fish  $\beta$ -diversity: implications for ecoregionalization and conservation. *J. Biogeogr.* 45, 1818–1832. doi: 10.1111/jbi.13381
- Goetze, J. S., Bond, T., McLean, D. L., Saunders, B. J., Langlois, T. J., Lindfield, S., et al. (2019). A field and video analysis guide for diver operated stereo-video. *Methods Ecol. Evol.* 10, 1083–1090. doi: 10.1111/2041-210X.13189
- Hill, M. O. (1973). Diversity and evenness: a unifying notation and its consequences. *Ecology* 54, 427–432. doi: 10.2307/1934352
- Horton, T., Kroh, A., Ah Yong, S., Bailly, N., Boyko, C. B., Brandão, S. N., et al. (2021). *World Register of Marine Species (WoRMS)*. Available online at: <https://www.marinespecies.org> (accessed March 8, 2021).
- Kissling, W. D., Ahumada, J. A., Bowser, A., Fernandez, M., Fernández, N., García, E. A., et al. (2018). Building essential biodiversity variables (EBVs) of species distribution and abundance at a global scale. *Biol. Rev.* 93, 600–625. doi: 10.1111/brv.12359
- Kulbicki, M., Cornuet, N., Vigliola, L., Wantiez, L., Moutham, G., and Chabanet, P. (2010). Counting coral reef fishes: interaction between fish life-history traits and transect design. *J. Exp. Mar. Biol. Ecol.* 387, 15–23. doi: 10.1016/j.jembe.2010.03.003
- Langenkämper, D., Zuurwilt, M., Schoening, T., and Nattkemper, T. W. (2017). BIIGLE 2.0 - browsing and annotating large marine image collections. *Front. Mar. Sci.* 4:83. doi: 10.3389/fmars.2017.00083
- Langlois, T., Goetze, J., Bond, T., Monk, J., Abesamis, R. A., Asher, J., et al. (2020). A field and video annotation guide for baited remote underwater stereo-video surveys of demersal fish assemblages. *Methods Ecol. Evol.* 11, 1401–1409. doi: 10.1111/2041-210X.13470
- Mallet, D., and Pelletier, D. (2014). Underwater video techniques for observing coastal marine biodiversity: a review of sixty years of publications (1952–2012). *Fish. Res.* 154, 44–62. doi: 10.1016/j.fishres.2014.01.019
- Mallet, D., Vigliola, L., Wantiez, L., and Pelletier, D. (2016). Diurnal temporal patterns of the diversity and the abundance of reef fishes in a branching coral patch in New Caledonia. *Austral Ecol.* 41, 733–744. doi: 10.1111/aec.12360
- Mallet, D., Wantiez, L., Lemouellic, S., Vigliola, L., and Pelletier, D. (2014). Complementarity of rotating video and underwater visual census for assessing species richness, frequency and density of reef fish on coral reef slopes. *PLoS One* 9:e84344. doi: 10.1371/journal.pone.0084344
- Matabos, M., Borremans, C., Tourolle, J., and Decker, C. (2016). *Prototype of a Web-Based Annotation Tool Ready for User Testing. D14.1 of the ENVRI+ Project Funded Under the European Union's Horizon 2020 Research and Innovation Programme GA No 654182*. Available online at: <http://www.envriplus.eu/wp-content/uploads/2015/08/D14.1.pdf> (accessed March 16, 2021).
- Miloslavich, P., Bax, N. J., Simmons, S. E., Klein, E., Appeltans, W., Aburto-Oropeza, O., et al. (2018). Essential ocean variables for global sustained observations of biodiversity and ecosystem changes. *Glob. Change Biol.* 24, 2416–2433. doi: 10.1111/gcb.14108
- Muller-Karger, F. E., Miloslavich, P., Bax, N. J., Simmons, S., Costello, M. J., Sousa Pinto, I., et al. (2018). Advancing Marine Biological Observations and Data Requirements of the Complementary Essential Ocean Variables (EOVs) and Essential Biodiversity Variables (EBVs) Frameworks. *Front. Mar. Sci.* 5:211. doi: 10.3389/fmars.2018.00211
- Pelletier, D. (2020a). Assessing the effectiveness of coastal marine protected area management: four learned lessons for science uptake and Upscaling. *Front. Mar. Sci.* 7:978. doi: 10.3389/fmars.2020.545930
- Pelletier, D. (2020b). The diversity of shallow habitats in new caledonia reefs and lagoons. *SEANOE*. doi: 10.17882/73937
- Pelletier, D., Bissery, C., and Gonson, C. (2014). *User Guide for the PAMPA Software*. V2. Brest: IFREMER.
- Pelletier, D., Carpentier, L., Roman, W., and Bockel, T. (2016). *Unbaited Rotating Video for Observing Coastal Habitats and Macrofauna. Methodological Guide for STAVIRO and MICADO Systems*. Nouméa: Ifremer. doi: 10.13155/46859
- Pelletier, D., Leleu, K., Mallet, D., Mou-Tham, G., Hervé, G., Boureau, M., et al. (2012). Remote high-definition rotating video enables fast spatial survey of marine underwater macrofauna and habitats. *PLoS One* 7:e30536. doi: 10.1371/journal.pone.0030536
- Pelletier, D., Selmaoui-Folcher, N., Bockel, T., and Schohn, T. (2020). A regionally scalable habitat typology for assessing benthic habitats and fish communities: application to New Caledonia reefs and lagoons. *Ecol. Evol.* 10, 7021–7049. doi: 10.1002/ece3.6405
- Powell, A., Pelletier, D., Jones, T., and Mallet, D. (2016). The impacts of short-term temporal factors on the magnitude and direction of marine protected area effects detected in reef fish monitoring. *Glob. Ecol. Conserv.* 8, 263–276. doi: 10.1016/j.gecco.2016.09.006
- Przeslawski, R., Foster, S., Monk, J., Barrett, N., Bouchet, P., Carroll, A., et al. (2019). A suite of field manuals for marine sampling to monitor Australian waters. *Front. Mar. Sci.* 6:177. doi: 10.3389/fmars.2019.00177
- QGIS Development Team (2021). *QGIS Geographic Information System. Open Source Geospatial Foundation Project*. Available at: <http://qgis.osgeo.org> (accessed February 9, 2021).
- Stobart, B., Diaz, D., Alvarez, F., Alonso, C., Mallol, S., and Goñi, R. (2015). Performance of baited underwater video: Does it underestimate abundance at high population densities? *PLoS One* 10:e0127559. doi: 10.1371/journal.pone.0127559
- Sward, D., Monk, J., and Barrett, N. (2019). A systematic review of remotely operated vehicle surveys for visually assessing fish assemblages. *Front. Mar. Sci.* 6:134. doi: 10.3389/fmars.2019.00134
- VideoLan (2006). *VLC Media Player*. Available online at: <https://www.videolan.org/vlc/index.html> (accessed March 30, 2021).
- Whitmarsh, S. K., Fairweather, P. G., and Huveneers, C. (2017). What is Big BRUVver up to? Methods and uses of baited underwater video. *Rev. Fish Biol. Fish.* 27, 53–73.
- Wilkinson, M. D., Dumontier, M., Aalbersberg, I. J. J., Appleton, G., Axton, M., Baak, A., et al. (2016). Comment: the FAIR Guiding principles for scientific data management and stewardship. *Sci. Data* 3:160018. doi: 10.1038/sdata.2016.18

**Conflict of Interest:** The authors declare that the research was conducted in the absence of any commercial or financial relationships that could be construed as a potential conflict of interest.

**Publisher's Note:** All claims expressed in this article are solely those of the authors and do not necessarily represent those of their affiliated organizations, or those of the publisher, the editors and the reviewers. Any product that may be evaluated in this article, or claim that may be made by its manufacturer, is not guaranteed or endorsed by the publisher.

**Citation:** Pelletier D, Roos D, Bouchoucha M, Schohn T, Roman W, Gonson C, Bockel T, Carpentier L, Preuss B, Powell A, Garcia J, Gaboriau M, Cadé F, Royaux C, Le Bras Y and Reece Y (2021) A Standardized Workflow Based on the STAVIRO Unbaited Underwater Video System for Monitoring Fish and Habitat Essential Biodiversity Variables in Coastal Areas. *Front. Mar. Sci.* 8:689280. doi: 10.3389/fmars.2021.689280

Copyright © 2021 Pelletier, Roos, Bouchoucha, Schohn, Roman, Gonson, Bockel, Carpentier, Preuss, Powell, Garcia, Gaboriau, Cadé, Royaux, Le Bras and Reece. This is an open-access article distributed under the terms of the Creative Commons Attribution License (CC BY). The use, distribution or reproduction in other forums is permitted, provided the original author(s) and the copyright owner(s) are credited and that the original publication in this journal is cited, in accordance with accepted academic practice. No use, distribution or reproduction is permitted which does not comply with these terms.



# Robots Versus Humans: Automated Annotation Accurately Quantifies Essential Ocean Variables of Rocky Intertidal Functional Groups and Habitat State

Gonzalo Bravo<sup>1\*</sup>, Nicolas Moity<sup>2</sup>, Edgardo Londoño-Cruz<sup>3</sup>, Frank Muller-Karger<sup>4</sup>, Gregorio Bigatti<sup>1,5</sup>, Eduardo Klein<sup>6</sup>, Francis Choi<sup>7</sup>, Lark Parmalee<sup>7</sup>, Brian Helmuth<sup>7</sup> and Enrique Montes<sup>4\*</sup>

## OPEN ACCESS

### Edited by:

Tim Wilhelm Nattkemper,  
Bielefeld University, Germany

### Reviewed by:

Boguslaw Cyganek,  
AGH University of Science  
and Technology, Poland  
Frederico Tapajós De Souza  
Tâmega,  
Federal University of Rio Grande,  
Brazil  
Aiko Iwasaki,  
Tohoku University, Japan

### \*Correspondence:

Gonzalo Bravo  
gonzalobravoargentina@gmail.com  
Enrique Montes  
emontesh@usf.edu

### Specialty section:

This article was submitted to  
Ocean Observation,  
a section of the journal  
Frontiers in Marine Science

**Received:** 06 April 2021

**Accepted:** 31 August 2021

**Published:** 23 September 2021

### Citation:

Bravo G, Moity N,  
Londoño-Cruz E, Muller-Karger F,  
Bigatti G, Klein E, Choi F, Parmalee L,  
Helmuth B and Montes E (2021)  
Robots Versus Humans: Automated  
Annotation Accurately Quantifies  
Essential Ocean Variables of Rocky  
Intertidal Functional Groups  
and Habitat State.  
Front. Mar. Sci. 8:691313.  
doi: 10.3389/fmars.2021.691313

<sup>1</sup> Instituto de Biología de Organismos Marinos, IBIOMAR-CONICET, Puerto Madryn, Argentina, <sup>2</sup> Charles Darwin Research Station, Charles Darwin Foundation, Puerto Ayora, Ecuador, <sup>3</sup> Departamento de Biología, Universidad del Valle, Cali, Colombia, <sup>4</sup> College of Marine Science, University of South Florida St. Petersburg, St. Petersburg, FL, United States, <sup>5</sup> Centro de Investigaciones, Universidad Espíritu Santo, Samborombón, Ecuador, <sup>6</sup> Departamento de Estudios Ambientales, Universidad Simón Bolívar, Caracas, Venezuela, <sup>7</sup> Coastal Sustainability Institute, Northeastern University, Boston, MA, United States

Standardized methods for effectively and rapidly monitoring changes in the biodiversity of marine ecosystems are critical to assess status and trends in ways that are comparable between locations and over time. In intertidal and subtidal habitats, estimates of fractional cover and abundance of organisms are typically obtained with traditional quadrat-based methods, and collection of photoquadrat imagery is a standard practice. However, visual analysis of quadrats, either in the field or from photographs, can be very time-consuming. Cutting-edge machine learning tools are now being used to annotate species records from photoquadrat imagery automatically, significantly reducing processing time of image collections. However, it is not always clear whether information is lost, and if so to what degree, using automated approaches. In this study, we compared results from visual quadrats versus automated photoquadrat assessments of macroalgae and sessile organisms on rocky shores across the American continent, from Patagonia (Argentina), Galapagos Islands (Ecuador), Gorgona Island (Colombian Pacific), and the northeast coast of the United States (Gulf of Maine) using the automated software CoralNet. Photoquadrat imagery was collected at the same time as visual surveys following a protocol implemented across the Americas by the Marine Biodiversity Observation Network (MBON) Pole to Pole of the Americas program. Our results show that photoquadrat machine learning annotations can estimate percent cover levels of intertidal benthic cover categories and functional groups (algae, bare substrate, and invertebrate cover) nearly identical to those from visual quadrat analysis. We found no statistical differences of cover estimations of dominant groups in photoquadrat images annotated by humans and those processed in CoralNet (binomial generalized linear mixed model or GLMM). Differences between these analyses were not significant, resulting in a Bray-Curtis average distance of 0.13 (sd 0.11) for the

full label set, and 0.12 (sd 0.14) for functional groups. This is the first time that CoralNet automated annotation software has been used to monitor “Invertebrate Abundance and Distribution” and “Macroalgal Canopy Cover and Composition” Essential Ocean Variables (EOVs) in intertidal habitats. We recommend its use for rapid, continuous surveys over expanded geographical scales and monitoring of intertidal areas globally.

**Keywords:** Americas, biodiversity monitoring, machine learning, marine biodiversity, Essential Ocean Variables (EOVs), photoquadrats, rocky intertidal zone, CoralNet

## INTRODUCTION

Sustained monitoring of the coastal zone is fundamental for the assessment, management, and conservation of living resources over scales ranging from local to global (Miloslavich et al., 2018; Canonico et al., 2019). There still exist major observational gaps across the world. Many protocols available for sampling of marine biota may not be easily implemented, and are time consuming and expensive, limiting their deployment (Titley et al., 2017; Muller-Karger et al., 2018). This has led to a pervasive absence of biodiversity surveys in much of the global coastal zones and ocean, and especially in the global south where resources can be especially limited (Barber et al., 2014).

Machine learning for automated analysis of photoquadrat images can accelerate the flow of information from monitoring programs to decision makers. This facilitates early detection of changes in biological communities and rapid responses to mitigate habitat degradation (González-Rivero et al., 2020). Over the past two decades, the availability of tools that extract taxonomic information from digital imagery of benthic communities has grown. Automated image annotations have already been used successfully in machine learning applications for rapid assessments of the health of coastal and marine habitats, such as in coral reefs (Marcos et al., 2005; Stokes and Deane, 2009; Shihavuddin et al., 2013; Beijbom et al., 2015; González-Rivero et al., 2016; Griffin et al., 2017; Williams et al., 2019; Raphael et al., 2020). Point annotations are typically performed using manual annotation software like pointCount99 (Porter et al., 2002), Coral Point Count with Excel Extensions (Kohler and Gill, 2006), photoQuad (Trygonis and Sini, 2012), or Biigle (Langenkämper et al., 2017). These facilitate the annotation process through graphical user interfaces and tools for the export of occurrence observations in various digital formats. The CoralNet software<sup>1</sup> is one of these tools, which also serves as a collaborative research platform that allows multiple users to interact and analyze large common data sets simultaneously.

The use of images to identify benthic organisms and compare analyses between different locations requires standardized annotation, labels, and metadata. Categories for benthic substrates and biota have been proposed by the Collaborative and Automated Tools for Analysis of Marine Imagery (CATAMI; Althaus et al., 2015). The CATAMI categories include several of the biological and ecological Essential Ocean Variables (EOVs; Miloslavich et al., 2018), and thus provide opportunities

for conducting standardized global assessment of benthic ecosystems using common indicators with relevance to societal needs. EOVs are being implemented by the Global Ocean Observing System (GOOS; Intergovernmental Oceanographic Commission of UNESCO), who define EOVs as “...those sustained measurements that are necessary to assess the state and change of marine ecosystems, address scientific and societal questions and needs, and positively impact society by providing data that will help mitigate pressures on ecosystems at local, regional and global scales.”

In this study, we specifically use machine learning to quantify the “Invertebrate Abundance and Distribution” and “Macroalgal Canopy Cover and Composition” EOVs in the rocky intertidal zones of four countries in the Americas participating in the Marine Biodiversity Observation Network Pole to Pole of the Americas (MBON Pole to Pole; Canonico et al., 2019). We evaluate the accuracy of the automated analysis done with the CoralNet software to quantify benthic cover of CATAMI categories. This leads to several recommendations for the implementation of image-based biodiversity surveys of macro-algal and sessile macro-invertebrate coastal communities.

## MATERIALS AND METHODS

Intertidal rocky shore localities in Argentina, Galapagos Islands, Colombia, and the northeastern United States (Gulf of Maine) were surveyed during 2018 and 2019. This was part of a large-scale MBON Pole to Pole collaboration. Five localities were sampled across these four countries (Table 1). At each locality, three sites separated by 1–10 km from each other were selected for sampling (Figure 1). At all sites, the rocky intertidal zone was divided into three strata (low, mid, and high tide level), based on the presence of indicator species in each stratum and tidal height. Due to logistical challenges at the United States sites, particularly of working in areas with very large tidal ranges, only two strata were sampled at these sites. At each level, ten 0.5 m × 0.5 m quadrats with a regular 100-point grid (except United States where quadrats were 0.25 m × 0.25 m) were laid at random locations over the substrate in a stretch of rocky shore that goes along the water for a distance of at least 50 m (ideally 100 m). The taxonomic identity and substrate below each grid intersection were registered *in situ*. These observations were used to quantify the fractional coverage of sessile fauna, macro-algae, and bare substrate. In this study we call these observations visual

<sup>1</sup><https://coralnet.ucsd.edu/>

**TABLE 1** | Summary of sampling sites.

	Argentina	Ecuador	Colombia	United States
Investigator	Gregorio Bigatti	Nicolas Moity	Edgardo Londoño-Cruz	Brian Helmuth
Sampling year	2018	2019	2018	2018–2019
Locality	Puerto Madryn	Santa Cruz	Gorgona Island	Massachusetts Maine
Sites	Punta Cuevas Punta Este Punta Loma	Charles Darwin Foundation Ratonera Tortuga Bay	La Mancora La Ventana Playa Verde	Marblehead Pumphouse Chamberlain Grindstone
Camera type	Nikon AW130	Canon S120	Canon G16	Nikon D5100
Image cover (m)	0.5 × 0.5	0.5 × 0.5	0.5 × 0.5	0.25 × 0.25
# Quadrats	90	90	90	92

quadrats (VQ). A detailed field protocol is available on the Ocean Best Practices System<sup>2</sup>.

Photos of the same quadrats (photoquadrats – PQ) were taken with a digital compact camera fixed to a rigid structure to ensure a focal distance of 60 cm with respect to the substrate (**Figure 1**). At each site, ten photoquadrats were collected per tidal level for a cumulative total of 362 photoquadrats across all sampled sites. All images were uploaded to CoralNet and are publicly available on the CoralNet website at MBON\_AR\_CO\_EC\_US\_Human<sup>3</sup>. A 100-point regular grid was digitally overlaid on each PQ and the identity of the item at each intersection was annotated by the observer (PQ.human). The percent cover for each photoquadrat was determined and the average percent cover was computed per country and tidal level for each category. The same sets of images were manually annotated by an observer, focusing on an independent set of 100 points randomly distributed on each image grid. This was done to train CoralNet automated annotator using EfficientNet-b0 (Tan and Le, 2019) as a feature extractor, and Multi-Layer Perceptron for a classifier. Randomly annotated photoquadrats by human observation, and automated annotation were stored in a different public source in CoralNet<sup>4</sup>. Photoquadrats were uploaded as an independent set of images to this CoralNet source for fully automated points-annotations (PQ.robot). We aimed to extract three types of percentage cover estimations from each quadrat (VQ, PQ.human, and PQ.robot), with the exception of the United States sites where VQ were not performed in the exact same area as PQ.

## Statistical Analyses

We used the confusion matrix provided by CoralNet to evaluate the performance of the classifier. The accuracy metric is calculated by training the robot with 7/8 of the provided annotations ( $n = 31,853$ ) and using the remaining data points

as a test set ( $n = 4,347$ ). Detailed accuracy for each of the benthic categories was also calculated using the R package “Caret” (Kuhn, 2009).

With the trained classifier, the percent cover estimates for each benthic category were compared between robot and human annotations, and robot versus visual annotations using a generalized (binomial) linear mixed model (GLMM) to detect effects of annotation methods (i.e., human vs. robot). As field percent cover estimates do not record the exact coordinate where the organism occurs below each intersect point in the gridded quadrat, it was not possible to match point annotations produced by the robot. Thus, we compared sets of taxa annotations derived from human observations with those from the automated annotations by the robot [i.e., PQ.robot vs. VQ, and PQ.robot vs. PQ.human] using Bray-Curtis (BC) distance with a generalized (binomial) nested model. BC distances were computed from paired community matrices derived from each of the methods for each of the quadrats. This metric is typically used to quantify differences in community composition between samples (beta diversity), and is adequate to these type of data (counts). Therefore, the analysis will determine the effect of the factors “stratum” and “country” on BC distances and allow to calculate how different estimates of community composition (in terms of percentage of similarity) are between methods. As photoquadrats in the United States were not taken at the exact location as those analyzed visually in the field, data from this country were not included in the comparison with visual observations.

To avoid performance problems of automated annotations due to a low set of training points, we used categories that accumulate up to 95% of all the points present in the quadrats (SC, MAF, MOB, MAEN, and MAA) (see **Supplementary Table 1**).

All statistical analyses and plots were performed in R (R Core Team, 2020); the GLMM was modeled with lme4 R package version 1.1-23 (Bates et al., 2015).

## Study Locations Patagonia, Argentina

Biodiversity data were collected at three Atlantic Patagonia sites: Punta Cuevas in the city of Puerto Madryn, Punta Este, and the Marine Protected Area Punta Loma (**Figure 1**). The three sites are located in Golfo Nuevo at  $\sim 42.5^\circ\text{S}$ ,  $65^\circ\text{W}$ . Sea surface temperature ranges from 8 to  $18^\circ\text{C}$  at all sites. The Patagonian rocky intertidal zone is often exposed to extreme physical conditions, with air temperature variations of up to  $\sim 40^\circ\text{C}$  during the year, maximum wind speeds of  $\sim 90$  km/h, semidiurnal tides (Rechimont et al., 2013), high solar radiation, and exposure to prolonged desiccation.

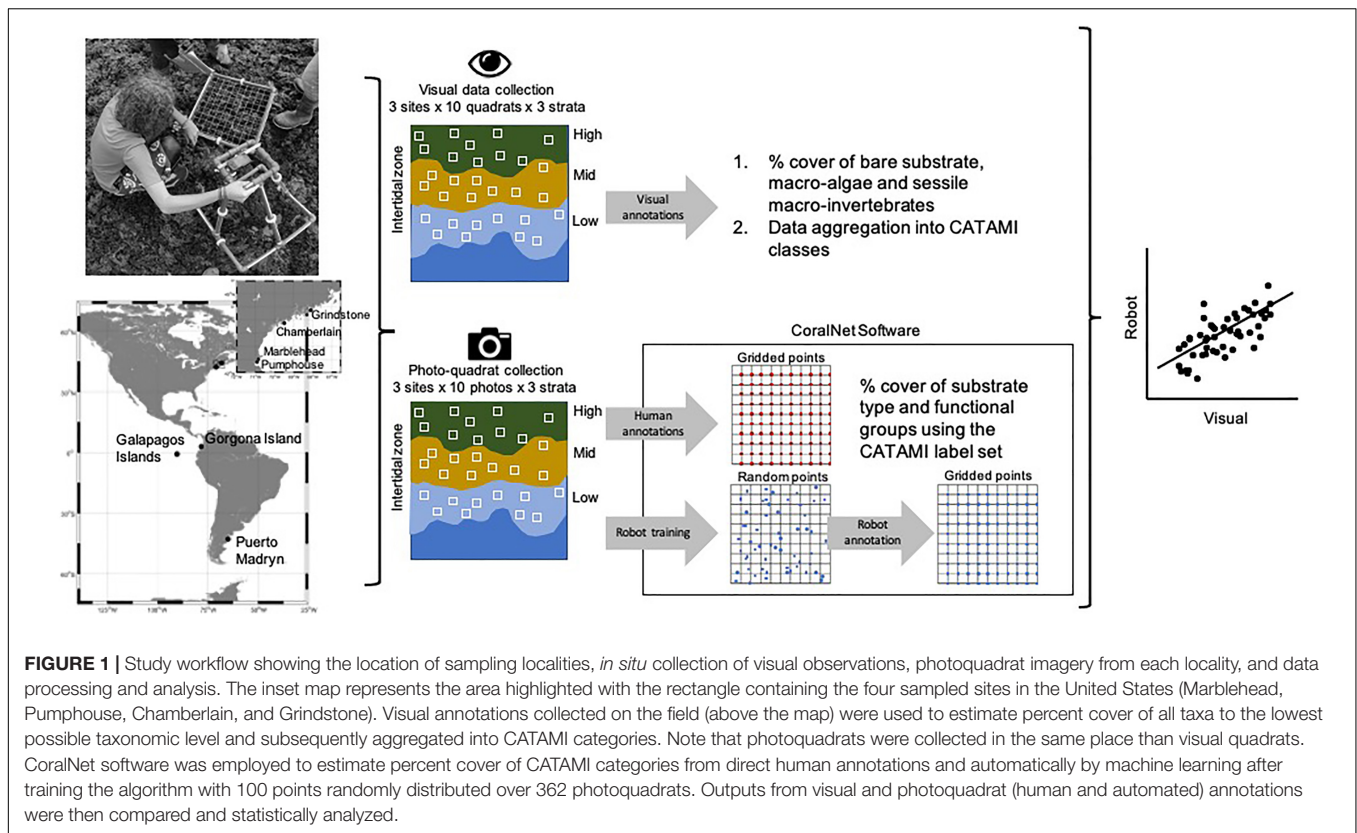
Biological zonation at the low tide level of this rocky intertidal site is characterized by macro-algae assemblages of *Corallina officinalis*, *Ulva* sp., *Ceramium* sp., the invasive *Undaria pinnatifida*, and mobile invertebrates (Miloslavich et al., 2011). The mid tide level is typically dominated by mussel beds composed of two small species *Brachidontes rodriguezii* and *Brachidontes (Perumytilus) purpuratus*, and its predator *Trophon geversianus*. The high tide level is represented by large areas

<sup>2</sup><https://repository.oceanbestpractices.org/handle/11329/1143>

<sup>3</sup><https://coralnet.ucsd.edu/source/2268/>

<sup>4</sup><https://coralnet.ucsd.edu/source/2048/>





of bare substrate and partial cover of *Ulva prolifera*, *Balanus glandula*, encrusting algae of the *Ralfsia* genus, and the presence of the pulmonate false limpet *Siphonaria lessonii*.

### Gorgona, Colombia

The Gorgona National Natural Park, which is part of the Tropical Eastern Pacific Marine Corridor, is a protected area located about 30 km off the Colombian Pacific coast (Figure 1). This island, along with Gorgonilla, is the largest insular territory on the Pacific coast of Colombia (Giraldo, 2012; Cardona-Gutiérrez and Londoño-Cruz, 2020). Tides range 4–5 m and the horizontal extent of the intertidal zone can range from a few centimeters to hundreds of meters depending on the slope of the coastal zone. The sea surface temperature varies between 26 and 29°C, although it can occasionally descend below 19°C during upwelling events at the beginning of the year (Diaz et al., 2001; Zapata, 2001).

Three sites were sampled: La Ventana, Playa Verde, and La Camaronera. The slope at sampled sites is gentle, hence, the intertidal is approximately 100–150 m wide during low tide. The high intertidal zone normally has a steeper slope producing a narrow band. This band is typically devoid of organisms likely due to high temperatures of rocks during daytime. Most inhabitants are mobile or well-adapted to these conditions, like littorinids and *Nerita scabricosta*. The mid-intertidal is wider, and the lichen *Verrucaria* sp. is common along with calcareous coralline algae such as *Lithophyllum* sp. and the green algae *Cladophoropsis adhaerens*. Snails like *Vasula melones*, *Nerita*

*funiculata*, *Parvanachis pygmaea*, and the bivalve *Isognomon janus* are common. Chitons like *Ischnochiton dispar* and *Chiton stokesii* are relatively common in this zone. The low intertidal is similar in algal composition to the mid-intertidal but with higher coverage. Here, the red algae *Ceramium* sp. is common. In addition to the mollusks mentioned above, *Fissurella virescens* normally occupies this zone. Different species of ophiuroids are also present in this stratum.

### Galápagos, Ecuador

We repeatedly sampled three sites in the south of Santa Cruz island, in the central part of the Galapagos archipelago near 0.74°S (Figure 1). The sites are Ratonera, the Charles Darwin Foundation (both located within Academy Bay in Puerto Ayora), and Tortuga Bay (located 5 km to the southwest). This area is seasonally influenced by the North Equatorial Counter Current the South Equatorial Current, and the Humboldt Current (Edgar et al., 2004; Palacios, 2004). Sea surface temperature in the study sites ranges from an average low of ~22°C in the cold season to ~25°C in the warm season; mean air temperature range from ~21 to ~27°C in the cold and warm season, respectively, with high solar radiation conditions all year round due to the proximity to the Equator. The rocky intertidal shores of Santa Cruz are characterized by a black, basaltic substratum of volcanic origin (Geist, 1996; Vinuesa et al., 2014). The tides are semidiurnal, spanning 1.8–2.4 m (Wellington, 1975). Low tide level cover is characterized by the presence of *Ulva* spp. and *Zoanthus* spp. This is the only stratum where the slate pencil

sea urchin *Eucidaris galapagensis* can be found. The mid-tide stratum has the highest abundance of the endemic thatched-roof barnacle (*Tetraclita milleporosa*) and the mobile invertebrate *Thais* sp. The high tide layer is almost entirely composed of bare black lava rock sparsely covered with biofilm (algae-bacterial mat), with macro algae only occurring in crevices and between boulders that retain humidity and are protected from direct sunlight exposure. Mobile invertebrates here are characterized by *Plicopurpura* sp. The intertidal shores are home to the only marine iguana in the world (*Amblyrhynchus cristatus*) and the abundant sally lightfoot crabs (*Grapsus grapsus*), which are important consumers of the macro-algae present in these habitats (Vinueza et al., 2006).

## United States

The rocky intertidal zone in the northeast of the United States, specifically the Gulf of Maine (GOM), covers a vast area of the coast. Sea surface temperature in the GOM ranges from an average low of  $\sim 5^{\circ}\text{C}$  in winter to  $\sim 18^{\circ}\text{C}$  in summer, although recent years have seen considerably warmer temperatures in both winter ( $7^{\circ}\text{C}$ ) and summer ( $20^{\circ}\text{C}$ ). The region is among the fastest warming on the planet, with an increasing number of marine heat waves (Pershing et al., 2015). Tidal amplitude can be as large as 16 m in parts of the Bay of Fundy in the northern Gulf of Maine (Fautin et al., 2010); however, at the sites sampled the tidal range was between 4 and 5 m (Figure 1). Two localities in the GOM were used, the north shore of Massachusetts (MA) and the mid coast of Maine (ME) (Figure 1). Two sites at each locality were used, namely Pumphouse (Nahant) and Marblehead in MA; and Chamberlain and Grindstone in ME. We defined the “high zone” for this study as that corresponding to the upper half of the band defined by the presence of the sessile invertebrates *Mytilus edulis* and *Semibalanus balanoides*. The “mid zone” was defined as the lower half of the *Mytilus*-dominated zone. Moving lower in the intertidal, sessile invertebrates are gradually replaced by macroalgae, specifically *Ascophyllum nodosum*, and *Fucus* spp. Mobile invertebrates, such as *Littorina littorea*, *Littorina obtusata*, and *Nucella lapillus*, are usually associated with these macroalgal habitats.

## Collaborative and Automated Tools for Analysis of Marine Imagery Label-Set

PQ.human and VQ were annotated using categories developed under CATAMI. The consensus label-set (Table 2) was defined by the same experts that performed VQ annotations.

## RESULTS

A total of 18 CATAMI categories were included (Table 2), four of which were common to all the countries (barnacles, encrusting algae, filamentous algae, and hard substrate). Of these, eight categories found are presented in Figure 2. Rocky intertidal sites in Argentina presented more variability of CATAMI groups, with a marked dominance of the consolidated substrate class in the high tide zone, bivalves in the mid tide zone, and algae in the low tide zone. In Colombia and Ecuador, all tidal

strata (low-, mid-, and high) presented low cover of algae and invertebrates, resulting in high cover of consolidated substrate. For the United States sites (Maine and Massachusetts) the erect coarse branching macroalgae covered most of the substrate, followed by barnacles (CRB).

Training of the automatic classifier resulted in an average accuracy of 87% (Supplementary Table 2 and Supplementary Figure 1). As expected, the classifier performed better with CATAMI labels that were well represented in the training set (SC, MAEC, MOB, MAF, CRB, MAS, MAA, accuracy between  $\sim 90$  and  $98\%$ ). The accuracy of the classification of rare or less frequent labels was lower (e.g., MOG, WPOT, accuracy between  $\sim 78\%$ ). For example, the Encrusting Macroalgae category (MAEN) presented a high number of training annotations (Table 2), but had a low detection rate resulting in a low accuracy ( $\sim 78\%$ , Supplementary Table 2). Mollusk bivalves (MOB) had a similar training number to MAEN, but this category was clearly distinguished by humans in the photos and therefore resulted in a higher detection rate than the robot (accuracy  $\sim 98\%$ , Supplementary Table 2). The total accuracy of the classifier improved to  $\sim 89\%$  after classifying groups that aggregate CATAMI labels into broader categories that we refer to as “functional” groups, specifically “hard substrate,” “algae,” “invertebrates,” and “other” (Supplementary Table 3).

Comparisons between the CATAMI labels percent cover estimates from robot and human annotations resulted in non-significant differences in a fully nested GLMM model (Supplementary Table 4), using both the quadrats and sites as random factors. However, high variability was observed in less frequent groups of organisms in both robot and human estimates (Figures 2A,B).

Comparisons of percent cover estimates between PQ.human and PQ.robot revealed that the CoralNet algorithm reliably quantifies relative abundances of the most representative CATAMI categories (Figure 2). In some cases, the PQ.robot indicated presence of MAEC or MAF categories in countries or tidal levels where they were not present. In Argentina, for example, MALCB was misidentified as MAEC in four of the resulting classifications. Disparities between VQ records and PQ.robot annotations were more evident in areas with low percent cover values (Figure 2). Encrusting macroalgae (MAEN) was generally underestimated by the automated annotation in Ecuador and Colombia. Furthermore, percent cover of articulated calcareous macroalgae (MAA) was underestimated by the robot in Argentina whereas it was overestimated in Colombia. The opposite was observed with filamentous macroalgae (MAF), with overestimated percent cover values in Argentina and underestimated ones in Colombia and Ecuador.

Average percent cover of broad classes including algae, invertebrates, and substrate in each tidal level and country were computed by aggregating percent cover values of corresponding CATAMI categories (Figures 3A,B and Supplementary Table 5). Using these broad groups, PQ.human and automated PQ.robot percent cover also presented almost equal estimations, with the exception of algae cover in the high tide level in Colombia and Ecuador because of the misclassifications of the automated annotations. Comparison of VQ versus PQ.robot for the

**TABLE 2 |** Collaborative and Automated Tools for Analysis of Marine Imagery (CATAMI) classification scheme used in this study.

Name	Label	# Training annotations	Countries	ID CoralNet	ID CATAMI
Substrate: Consolidated (hard)	SC	17814	AR, CO, EC, US	4114	82001001
Macroalgae: Erect coarse branching	MAEC	4766	US	317	80300903
Macroalgae: Filamentous/filiform	MAF	2931	AR, CO, EC, US	309	80300930
Macroalgae: Encrusting	MAEN	2891	AR, CO, EC, US	321	80300926
Mollusks: Bivalves	MOB	2753	AR, US	355	23199000
Crustacea: Barnacles	CRB	2196	AR, CO, EC, US	357	27500000
Macroalgae: Sheet-like / membranous	MAS	1418	AR, CO, US	294	80300922
Macroalgae: Articulated calcareous	MAA	612	AR, CO	325	80300911
Worms: Polychaetes: Tube worms	WPOT	283	AR, CO, EC	361	22000901
Unscorable	Unc	179	AR, CO, EC, US	118	00000001
Mollusks: Gastropods	MOG	145	CO, US	353	24000000
Macroalgae: Large canopy-forming: brown	MALCB	73	AR	299	80300902
Bryozoan	BRY	66	US	1853	20000000
Macroalgae: Laminate	MALA	55	US	301	80300918
Macroalgae: Erect fine branching	MAEF	9	US	313	80300907
Cnidaria: True anemones	CNTR	4	EC, US	4774	11229000
Cnidaria: Colonial anemones	CNCA	3	EC	4773	11500901
Macroalgae: Globose / saccate	MAG	2	AR	305	80300914

Country codes: AR, Argentina; US, United States; EC, Ecuador; CO, Colombia.

functional groups (hard substrate, algae, invertebrates, and other) showed similar results to PQ.human versus PQ.robot. However, percent cover of invertebrates detected by the robot in Ecuador was slightly lower than that estimated by VQ. Also, a slightly lower cover was estimated by the robot with algae cover in the high tide level of Ecuador and invertebrates in the low tide level of Colombia than that estimated by VQ.

To compare the performance of the classifier at community level, we computed the Bray-Curtis (BC) distance between the percent cover of the dominant CATAMI categories and results from the CoralNet classifier (PQ.robot) and PQ annotated by human (PQ.human). We also computed BC distance between functional groups estimated using field annotations (VQ) and the PQ.robot and PQ.human. A BC value close to zero denotes no significant differences between the communities estimated by the two methods.

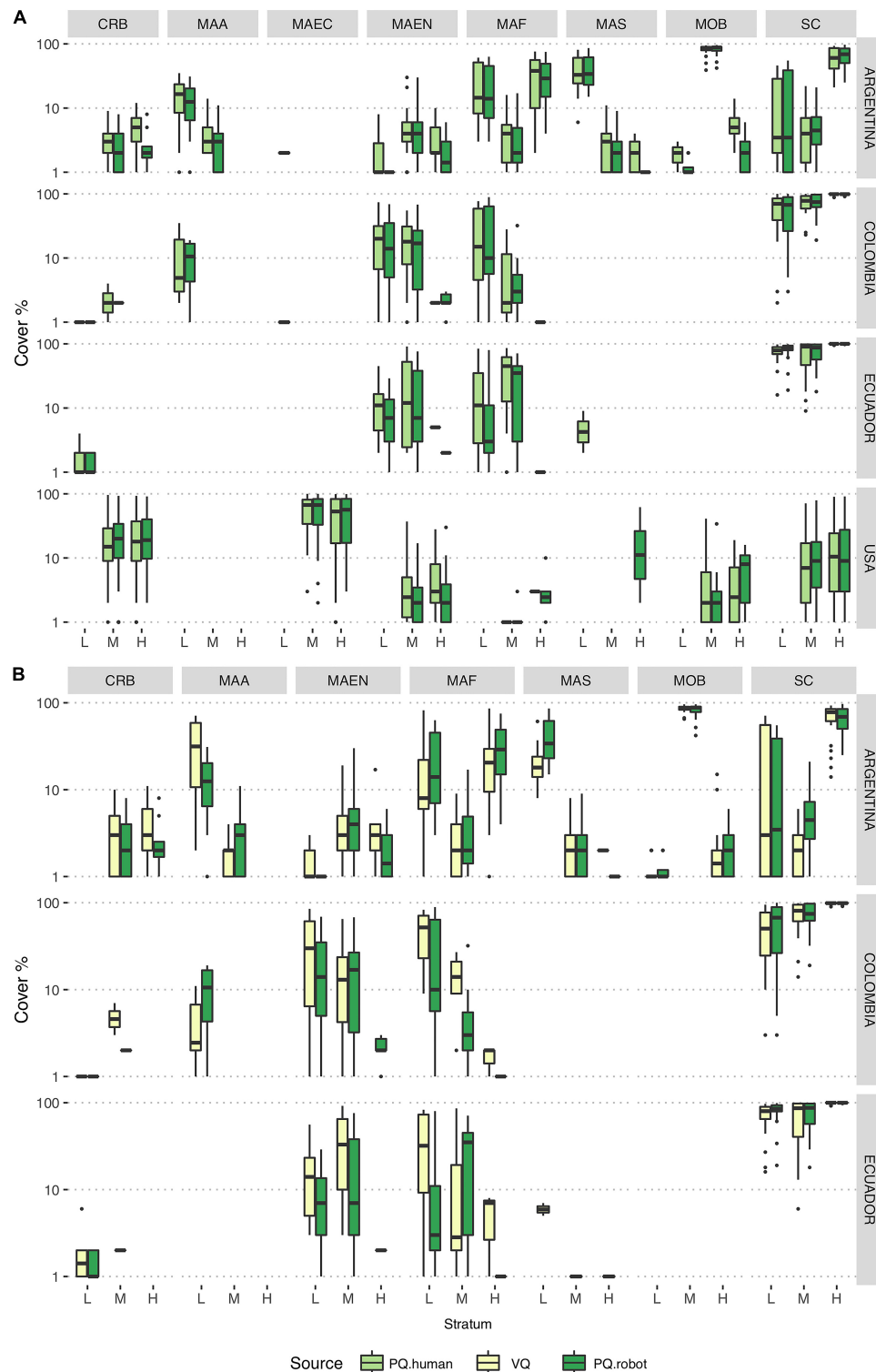
Functional groups were identified with more accuracy by the CoralNet classifier, thus yielding lower BC distances compared to those based on CATAMI categories (**Figures 4A,B** versus **C,D**). High tide strata in Colombia and Ecuador exhibited the lowest BC distances for both CATAMI and functional groups. In general, the largest BC distances were observed at the low tide level at all locations. However, no statistically significant differences were detected when tested with a GLMM nested model (**Supplementary Tables 6, 7**).

## DISCUSSION

Standardized field methods and machine learning allowed to assess changes in Essential Ocean Variables of percent cover of intertidal rocky shore and benthic biodiversity in different locations of the Americas. Intertidal zones, like coral reefs, are

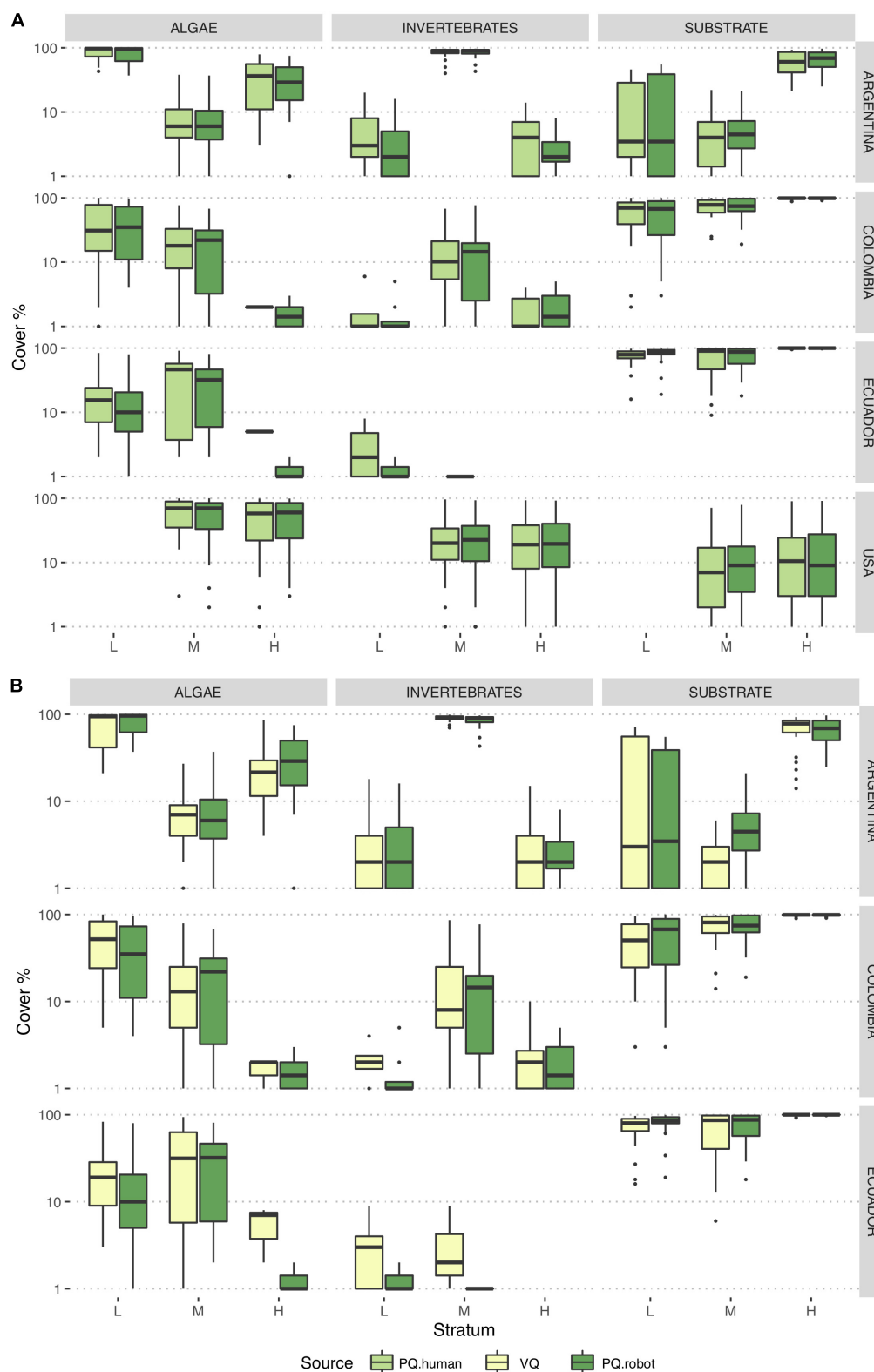
potential bellwethers for the ongoing impacts of global climate change (Helmuth et al., 2006). Intertidal invertebrates and algae are exposed to extreme weather and climate variability with large fluctuations in temperature, salinity, and water availability (Madeira et al., 2012). Mass mortality events have been reported from intertidal sites across the globe (e.g., Harley, 2008; Mendez et al., 2021), and the incidence of marine heat waves is increasing (Hobday et al., 2016). It is not clear yet what the potential consequences of these mortality events are for patterns of species distribution, biodiversity, and ecosystem services (Román et al., 2020; Vye et al., 2020).

Using imagery from diverse rocky intertidal habitats we demonstrate that the CoralNet machine learning system can estimate nearly identical fractional abundances of functional groups (i.e., aggregates of CATAMI categories) as those derived from manual photoquadrat annotation. In most cases, results based on automated annotations were comparable to those obtained from *in situ* visual observations. This approach opens avenues for collecting biodiversity data to monitor rapid changes in marine coastal environments to inform management. Documenting changes in biodiversity using time series has proven incredibly valuable, but such efforts have occurred in only a few locations (e.g., Vye et al., 2020). Long-term records from the global south are rare. The use of artificial intelligence to facilitate analysis of photos, which can be accomplished rapidly by a few people and with relatively few resources, can play a valuable role in the creation of much-needed monitoring networks. They play an important role in locations where access to sites is limited, dangerous, or otherwise restricted. For example, in the Gulf of Maine, visual surveys were not conducted in the lowest part of the intertidal zone because of the extreme tidal range, which can cause very rapid rates of tidal return; coupled with large waves, this makes sampling in this zone for extensive time periods very difficult. The adoption of standardized methods, such as

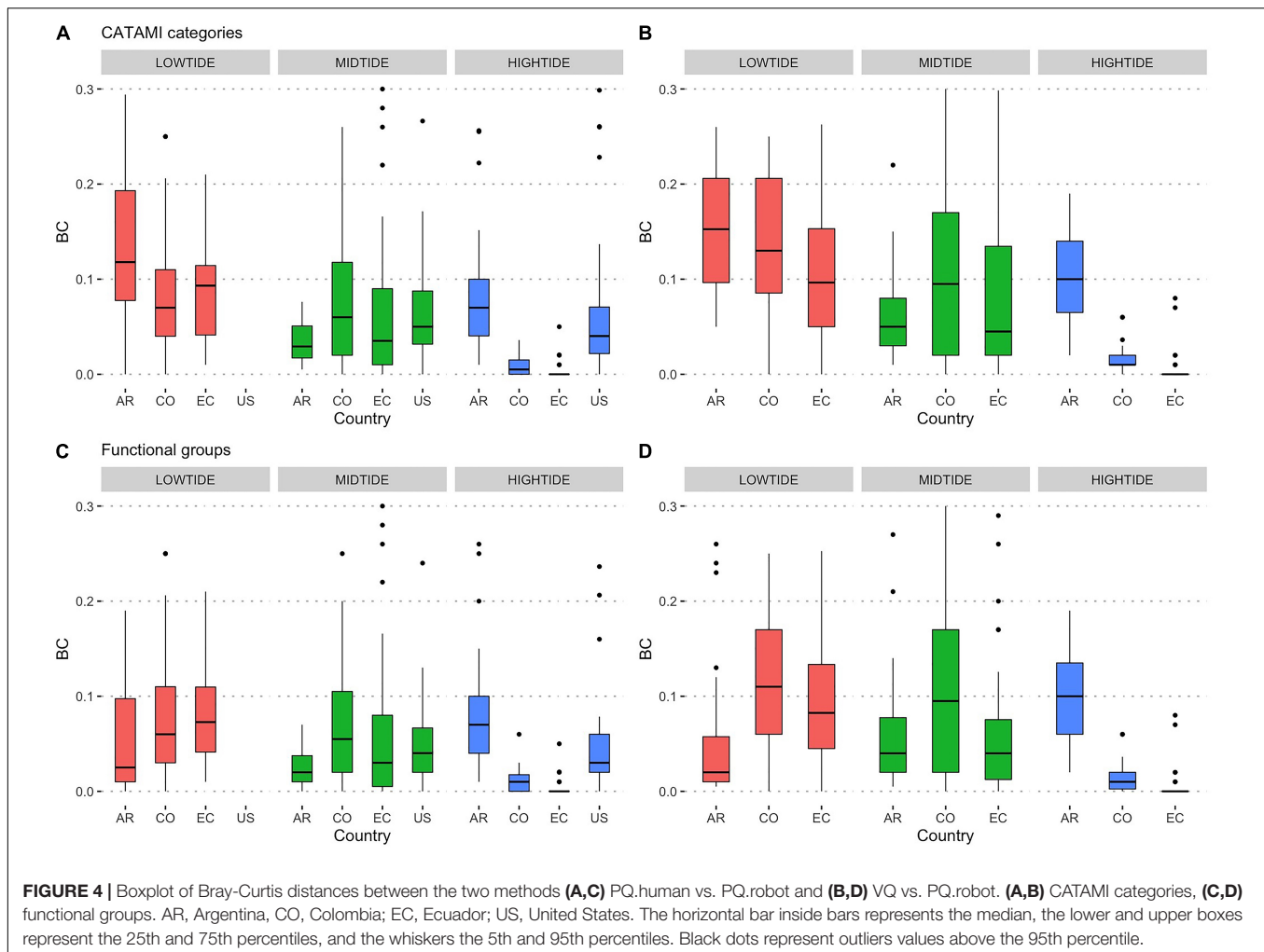


**FIGURE 2 |** Boxplots showing percentage cover estimates of most abundant CATAMI categories [CRB, Crustacea: Barnacles; MOB, Mollusks: Bivalves; SC, Substrate: Consolidated (hard); MAF, Macroalgae: Filamentous/filiform; MAEN, Macroalgae: Encrusting; MAA, Macroalgae: Articulated calcareous; MAS, Macroalgae: Sheet-like/membranous; MAEC, Macroalgae: Erect coarse branching] in each country and tidal strata as determined by different annotation methods. The horizontal bar within boxes represents the median, the lower and upper boxes represent the 25th and 75th percentiles, respectively, and the whiskers the 5th and 95th percentiles. Black dots represent outliers above the 95th percentile. **(A)** PQ.human vs. PQ.robot, **(B)** VQ vs. PQ.robot. L, low tide level; M, mid tide level; H, high tide level.





**FIGURE 3 |** Boxplots showing percentage cover by tidal level in each country for algae, substrate, and invertebrates. The horizontal bar within boxes represents the median, the lower and upper boxes represent the 25th and 75th percentiles, and the whiskers the 5th and 95th percentiles. Black dots represent outliers values above the 95th percentile. **(A)** PQ.human vs. PQ.robot, **(B)** VQ vs. PQ.robot. L, low tide level; M, mid tide level; H, high tide level.



those used here, facilitates collaborative efforts that span wide geographic ranges.

The accuracy of automatic annotation of intertidal image collections depends on many factors. This includes imaging conditions (e.g., light level, angle of view, camera quality, and resolution), the number of training annotations and the variability of taxa sampled. Photos used in this study had similar lighting, camera quality, resolution, angle of view, and focal distances. This provided homogeneity among image sets. Nonetheless, we observed that shadows can affect portions of the photos and rendered them not suitable for automated classifications. We observed poor robot classification capacity in dark shadows or in overexposed areas of the photographs, as well as in areas with water, bubbles, and wind that moves these around. These areas, present in some photoquadrats, lowered the accuracy of the automated results. To provide a more uniform light to the area to be photographed, the target can be illuminated with lights or strobes. Also, shading the area where imagery will be captured with a sun cover over the frame (e.g., using an umbrella) to provide uniform illumination is another option to increase image quality.

By using 100 points per photoquadrat we trained the robot with more than 36,000 annotations. Nonetheless, we often had less than the 1,000 minimum training annotations recommended by CoralNet developers<sup>5</sup>. A solution to avoid misinterpretation is to use a semi-automated mode (known as “alleviate” mode) that uses classification scores to decide when to register automated annotations and when to leave annotations to be manually registered by humans. For example, Beijbom et al. (2015) showed that by using a level of alleviate of 50%, the quality of the percent cover estimation was not notably affected. In this study, the alleviate mode was not tested. Based on the machine confidence of our data, a 50% threshold would require a manual annotation of only ~2% of the points (i.e., 724 points).

*In situ* visual surveys are often more effective than photoquadrats for species-level taxonomic identification and especially for counting rare species and mobile fauna that may be hidden in crevices and under the algal cover. However, we found instances when using photographs was advantageous. For example, we observed that differences between visual

<sup>5</sup><https://coralnet.ucsd.edu/blog/a-new-deep-learning-engine-for-coralnet/>

quadrat versus photoquadrat-based annotations of sessile (or semi-sessile, such as gastropods) species were likely due to parallax error in visual quadrat observations. The 100-point intersection grid in the visual quadrat is usually placed in the middle of the frame leaving some space between the intersections and the substrate. If the observer is not looking exactly above the quadrat (i.e.,  $\sim 0^\circ$  zenith angle), incorrect annotations may be attributed to parallax (Hill and Wilkinson, 2004; Leujak and Ormond, 2007). Nevertheless, errors due to parallax are difficult to quantify and beyond the scope of this study. We tried to minimize its effect by always looking at the quadrat directly from above.

In addition, we noted that observers often identified rare species when they were located near, but not necessarily exactly on, a grid intersection. This resulted in the recording of rare species as the minimum cover percentage, which might better describe the richness of the site while introducing errors due to differences among observers when comparing sites. Such errors are not reproduced with photoquadrat methods, which use digitally gridded intersections that do not yield parallax errors and minimize the overestimation of rare species that do not fall exactly on the digital grid.

In this study, while the same observer performed visual annotations and photoquadrats analyses, there was a time gap between observations. Therefore, some differences can be expected in the classification of the same quadrat. One of the key benefits of CoralNet automated annotations is that the analysis is consistent across all the images and parallax, and inter-annotation errors will not interfere in the analysis performance (Beijbom et al., 2015). In this sense, typical human errors associated with manual annotations and data entry are minimized by this method, helping to standardize the protocol used. This methodology could be used in regional monitoring programs involving a great amount of samples in different sampling sites/countries.

In Colombia and Ecuador, it was difficult to discriminate among encrusting algae and hard substrate by direct human annotations. This impacted the robot classification performance for the MAEN category. In the field, investigators were able to touch the rock in order to detect the encrusting algae and this resulted in a higher cover estimation on the VQ. In such cases, where a category is difficult to detect in photoquadrats, we expected to find low accuracy in the automated classifier. Manual annotations can diminish this bias, but such errors are a problem for the machine learning tool.

CoralNet is a collaborative platform that can be adopted more widely to help large-scale, collaborative networks and communities of practice such as the MBON Pole to Pole to enhance the spatial coverage and sampling frequency of their biodiversity monitoring programs. This can augment the quality and interoperability of annotations by using a common label-set amongst multiple observers, while training the robot or new users that may use previous annotations for verification. We showed that 36,000 manual point annotations were enough to properly train the most dominant benthic cover categories over four distinctive locations along the American continent. However, combining several countries on the same CoralNet

source may lead to confusion among similar categories from different locations. The creation of separate training sets for each country or even for each site should be investigated to avoid confusion among similar categories from different sites. The protocol used in our work gives the capacity to rapidly process a large set of new photos to obtain robust percent cover estimated within hours. Such estimates can then be used to detect rapid changes in biological and ecosystem EOVs resulting, for example, from massive mortality events, macroalgae blooms or the loss of benthic coverage. The protocol performed in our work helps advance ecological studies and can be applied for the detection of rapid changes in benthic coverage which could serve as an early warning of the impacts of contamination events or global climate change.

## CONCLUSION

Image-based biodiversity surveys using automated annotations from CoralNet software were sufficiently robust to characterize the relative abundance of benthic cover categories and functional groups, specifically for “Invertebrate Abundance and Distribution” and “Macroalgal Canopy Cover and Composition” EOVs in rocky intertidal habitat in four countries of the Americas with very different environmental regimes and spanning more than  $80^\circ$  of latitude. We found no statistical differences in percent cover estimates of the dominant functional groups annotated visually by observers and automatically by CoralNet using photoquadrats. Differences between visual quadrats annotated in the field and automated annotations by CoralNet on photoquadrats based on the analysis of community matrices were not significant, resulting in a Bray-Curtis average distance of 0.13 (sd 0.11) for the full label set and 0.12 (sd 0.14) for functional groups set. Our results indicate that automated image-based annotations are a practical source of information for biodiversity monitoring in intertidal benthic habitats to detect rapid changes over large geographic domains, and can optimize sampling effort in the field to expand the area of monitoring sites and sampling frequency minimizing human errors while increasing field safety.

## DATA AVAILABILITY STATEMENT

The original contributions presented in the study are included in the article/**Supplementary Material**, further inquiries can be directed to the corresponding author/s.

## AUTHOR CONTRIBUTIONS

NM, EL-C, GBi, FC, LP, and BH performed field work and visual surveys on intertidal areas. GBi analyzed photoquadrats from Argentina, EL-C from Colombia, NM from Galápagos and FC from United States. GBi and EK coordinated the photoquadrats analysis in CoralNet software and performed statistical analyses. All authors designed the study and wrote the manuscript.

## FUNDING

This project was supported by the NASA award titled “Laying the foundations of the Marine Biodiversity Observation Network Pole to Pole of the Americas” (grant number: 80NSSC18K0318), NASA grants NNX14AP62A and 80NSSC20K0017; NOAA U.S. Integrated Ocean Observing System (IOOS grant NA19NOS0120199); ANPCyT-FONCyT (PICT 2018-0969); United States National Science Foundation OCE-1635989; and the United States National Oceanographic Partnership Program (NOPP).

## ACKNOWLEDGMENTS

The Charles Darwin Foundation (CDF) author would like to thank the Gordon and Betty Moore Foundation for funding the staff time, and Sofia Green for her help in the field. This study was conducted under the research permit of the Galapagos National Park Directorate No. PC-41-20. The authors from

Argentina thank Juan Pablo Livore, María Marta Mendez, and María Eugenia Segade for field work and technical support. EL-C is deeply indebted to Maria Fernanda Cardona-Gutiérrez and Kevin Stiven Mendoza for field assistance and to Gorgona National Natural Park personnel, particularly Ximena Zorrilla and Luis Payán for logistic support. The authors from the United States thank Tim Briggs, Jaxon Derow, Sophia Ly, Sahana Simonetti, and Jessica Torossian for their help in the field. This publication is contribution number 2392 of the Charles Darwin Foundation for the Galápagos Islands and 154 of the Laboratorio de Reproducción y Biología Integrativa de Invertebrados Marinos (LARBIM).

## SUPPLEMENTARY MATERIAL

The Supplementary Material for this article can be found online at: <https://www.frontiersin.org/articles/10.3389/fmars.2021.691313/full#supplementary-material>

## REFERENCES

- Althaus, F., Hill, N., Ferrari, R., Edwards, L., Przeslawski, R., Schönberg, C. H. L., et al. (2015). A standardised vocabulary for identifying benthic biota and substrata from underwater imagery: the CATAMI classification scheme. *PLoS One* 10:e0141039. doi: 10.1371/journal.pone.0141039
- Barber, P. H., Ablan-Lagman, M. C. A., Ambariyanto, A., Berlinck, R. G. S., Cahyani, D., Crandall, E. D., et al. (2014). Advancing biodiversity research in developing countries: the need for changing paradigms. *Bull. Mar. Sci.* 90, 187–210. doi: 10.5343/bms.2012.1108
- Bates, D., Mächler, M., Bolker, B. M., and Walker, S. C. (2015). Fitting linear mixed-effects models using lme4. *J. Stat. Softw.* 67, 1–48. doi: 10.18637/jss.v067.i01
- Beijbom, O., Edmunds, P. J., Roelfsema, C., Smith, J., Kline, D. I., Neal, B. P., et al. (2015). Towards Automated Annotation of Benthic Survey Images: variability of Human Experts and Operational Modes of Automation. *PLoS One* 10:e0130312. doi: 10.1371/journal.pone.0130312
- Canonica, G., Buttigieg, P. L., Montes, E., Muller-Karger, F. E., Stepien, C., Wright, D., et al. (2019). Global observational needs and resources for marine biodiversity. *Front. Mar. Sci.* 6:367. doi: 10.3389/fmars.2019.00367
- Cardona-Gutiérrez, M. F., and Londoño-Cruz, E. (2020). Boring worms (Sipuncula and Annelida: Polychaeta): their early impact on Eastern Tropical Pacific coral reefs. *Mar. Ecol. Prog. Ser.* 641, 101–110. doi: 10.3354/meps13298
- Diaz, J., Pinzón, C. J., Perdomo, A., María, L., and López-Victoria, M. (2001). “Gorgona marina: contribución al conocimiento de una isla única,” in *Edition: Serie Publicaciones Especiales 7Chapter: Generalidades*, eds L. M. Barrios and M. L. ópez-Victoria (Santa Marta, Colombia: INVEMAR), 17–26.
- Edgar, G. J., Banks, S., Fariña, J. M., Calvopiña, M., and Martínez, C. (2004). Regional biogeography of shallow reef fish and macro-invertebrate communities in the Galapagos archipelago. *J. Biogeogr.* 31, 1107–1124. doi: 10.1111/j.1365-2699.2004.01055.x
- Fautin, D., Dalton, P., Incze, L. S., Leong, J. A. C., Pautzke, C., Rosenberg, A., et al. (2010). An overview of marine biodiversity in United States waters. *PLoS One* 5:e11914. doi: 10.1371/journal.pone.0011914
- Geist, D. (1996). On the emergence and submergence of the Galapagos Islands. *Not. Galapagos* 56, 5–9.
- Giraldo, A. (2012). “Geomorfología e hidroclimatología de isla Gorgona,” in *Gorgona: paraíso de biodiversidad y ciencia*, eds A. Giraldo and B. Valencia (Cali: Universidad del Valle), 226.
- González-Rivero, M., Beijbom, O., Rodríguez-Ramírez, A., Bryant, D. E. P., Ganase, A., González-Marrero, Y., et al. (2020). Monitoring of coral reefs using artificial intelligence: a feasible and cost-effective approach. *Remote Sens.* 12, 1–22. doi: 10.3390/rs12030489
- González-Rivero, M., Beijbom, O., Rodríguez-Ramírez, A., Holtrop, T., González-Marrero, Y., Ganase, A., et al. (2016). Scaling up Ecological Measurements of Coral Reefs Using Semi-Automated Field Image Collection and Analysis. *Remote Sens.* 8:30. doi: 10.3390/rs8010030
- Griffin, K. J., Hedge, L. H., González-Rivero, M., Hoegh-Guldberg, O. I., and Johnston, E. L. (2017). An evaluation of semi-automated methods for collecting ecosystem-level data in temperate marine systems. *Ecol. Evol.* 7, 4640–4650. doi: 10.1002/ece3.3041
- Harley, C. D. G. (2008). Tidal dynamics, topographic orientation, and temperature-mediated mass mortalities on rocky shores. *Mar. Ecol. Prog. Ser.* 371, 37–46.
- Helmuth, B., Mieszkowska, N., Moore, P., and Hawkins, S. J. (2006). Living on the Edge of Two Worlds: forecasting the Responses of Rocky Intertidal Ecosystems to Climate Change. *Annu. Rev. Ecol. Syst.* 37, 373–404. doi: 10.2307/annurev.ecolsys.37.091305.30000015
- Hill, J., and Wilkinson, C. (2004). *Methods for ecological monitoring of coral reefs*. Townsville: Australian Institute of Marine Science (AIMS).
- Hobday, A. J., Alexander, L. V., Perkins, S. E., Smale, D. A., Straub, S. C., Oliver, E. C. J., et al. (2016). A hierarchical approach to defining marine heatwaves. *Prog. Oceanogr.* 141, 227–238. doi: 10.1016/j.pocean.2015.12.014
- Kohler, K. E., and Gill, S. M. (2006). Coral Point Count with Excel extensions (CPCe): a Visual Basic program for the determination of coral and substrate coverage using random point count methodology. *Comput. Geosci.* 32, 1259–1269. doi: 10.1016/j.cageo.2005.11.009
- Kuhn, M. (2009). The caret package. *J. Stat. Softw.* 28, 1–26.
- Langenkämper, D., Zuurwilt, M., Schoening, T., and Nattkemper, T. W. (2017). BIIGLE 2.0 - Browsing and Annotating Large Marine Image Collections. *Front. Mar. Sci.* 4:83. doi: 10.3389/fmars.2017.00083
- Leujak, W., and Ormond, R. F. G. (2007). Comparative accuracy and efficiency of six coral community survey methods. *J. Exp. Mar. Bio. Ecol.* 351, 168–187. doi: 10.1016/j.jembe.2007.06.028
- Madeira, D., Narciso, L., Cabral, H. N., and Vinagre, C. (2012). Thermal tolerance and potential impacts of climate change on coastal and estuarine organisms. *J. Sea Res.* 70, 32–41.
- Marcos, M. S. A. C., Soriano, M. N., and Saloma, C. A. (2005). Classification of coral reef images from underwater video using neural networks. *Opt. Express* 13:8766. doi: 10.1364/oe.13.008766
- Mendez, M. M., Livore, J. P., Márquez, F., and Bigatti, G. (2021). Mass Mortality of Foundation Species on Rocky Shores: testing a Methodology for a Continental Monitoring Program. *Front. Mar. Sci.* 8:620866. doi: 10.3389/fmars.2021.620866
- Miloslavich, P., Bax, N. J., Simmons, S. E., Klein, E., Appeltans, W., Aburto-Oropeza, O., et al. (2018). Essential ocean variables for global sustained



- observations of biodiversity and ecosystem changes. *Glob. Chang. Biol.* 24, 2416–2433. doi: 10.1111/gcb.14108
- Miloslavich, P., Klein, E., Díaz, J. M., Hernández, C. E., Bigatti, G., Campos, L., et al. (2011). Marine biodiversity in the Atlantic and Pacific coasts of South America: knowledge and gaps. *PLoS One* 6:e14631. doi: 10.1371/journal.pone.0014631
- Muller-Karger, F. E., Miloslavich, P., Bax, N. J., Simmons, S., Costello, M. J., Pinto, I. S., et al. (2018). Advancing marine biological observations and data requirements of the complementary Essential Ocean Variables (EOVs) and Essential Biodiversity Variables (EBVs) frameworks. *Front. Mar. Sci.* 5:211. doi: 10.3389/fmars.2018.00211
- Palacios, D. M. (2004). Seasonal patterns of sea-surface temperature and ocean color around the Galápagos: regional and local influences. *Deep Res. II Top. Stud. Oceanogr.* 51, 43–57. doi: 10.1016/j.dsr2.2003.08.001
- Pershing, A. J., Alexander, M. A., Hernandez, C. M., Kerr, L. A., Le Bris, A., Mills, K. E., et al. (2015). Slow adaptation in the face of rapid warming leads to collapse of the Gulf of Maine cod fishery. *Science* 350, 809–812. doi: 10.1126/science.aac9819
- Porter, J. W., Kosmynin, V., Patterson, K. L., Porter, K. G., Jaap, W. C., Wheaton, J. L., et al. (2002). Detection of coral reef change by the Florida Keys coral reef monitoring project. *The Everglades, Florida Bay, and Coral Reefs of the Florida Keys: An Ecosystem Sourcebook*. 749–769. doi: 10.1201/9781420039412-32
- R Core Team (2020). *R: A language and environment for statistical computing*. Austria: R Foundation for Statistical Computing.
- Raphael, A., Dubinsky, Z., Iluz, D., Benichou, J. I. C., and Netanyahu, N. S. (2020). Deep neural network recognition of shallow water corals in the Gulf of Eilat (Aqaba). *Sci. Rep.* 10:12959. doi: 10.1038/s41598-020-69201-w
- Rechimont, M. E., Galván, D. E., Sueiro, M. C., Casas, G., Piriz, M. L., Diez, M. E., et al. (2013). Benthic diversity and assemblage structure of a north Patagonian rocky shore: a monitoring legacy of the NaGISA project. *J. Mar. Biol. Assoc. U. K.* 93, 2049–2058. doi: 10.1017/S0025315413001069
- Román, M., Román, S., Vázquez, E., Troncoso, J., and Olabarria, C. (2020). Heatwaves during low tide are critical for the physiological performance of intertidal macroalgae under global warming scenarios. *Sci. Rep.* 10:21408.
- Shihavuddin, A. S. M., Gracias, N., Garcia, R., Gleason, A. C. R., and Gintert, B. (2013). Image-based coral reef classification and thematic mapping. *Remote Sens.* 5, 1809–1841. doi: 10.3390/rs5041809
- Stokes, M. D., and Deane, G. B. (2009). Automated processing of coral reef benthic images. *Limnol. Oceanogr. Methods* 7, 157–168. doi: 10.4319/lom.2009.7.157
- Tan, M., and Le, Q. V. (2019). “EfficientNet: rethinking model scaling for convolutional neural networks,” in *Proceedings of the 36th International Conference on Machine Learning*, (Long Beach: ICML), 6105–6114.
- Titlye, M. A., Snaddon, J. L., and Turner, E. C. (2017). Scientific research on animal biodiversity is systematically biased towards vertebrates and temperate regions. *PLoS One* 12:e0189577. doi: 10.1371/journal.pone.0189577
- Trygonis, V., and Sini, M. (2012). PhotoQuad: a dedicated seabed image processing software, and a comparative error analysis of four photoquadrat methods. *J. Exp. Mar. Bio. Ecol.* 424–425, 99–108. doi: 10.1016/j.jembe.2012.04.018
- Vinueza, L. R., Branch, G. M., Branch, M. L., and Bustamante, R. H. (2006). Top-down herbivory and bottom-up el niño effects on galápagos rocky-shore communities. *Ecol. Monogr.* 76, 111–131. doi: 10.1890/04-1957
- Vinueza, L. R., Menge, B. A., Ruiz, D., and Palacios, D. M. (2014). Oceanographic and climatic variation drive top-down/bottom-up coupling in the Galápagos intertidal meta-ecosystem. *Ecol. Monogr.* 84, 411–434. doi: 10.1890/13-0169.1
- Vye, S. R., Dickens, S., Adams, L., Bohn, K., Chenery, J., Dobson, N., et al. (2020). Patterns of abundance across geographical ranges as a predictor for responses to climate change: evidence from UK rocky shores. *Divers. Distrib.* 26, 1357–1365.
- Wellington, G. M. (1975). *Medio Ambientes Marinos Costeros de Galápagos*. Quito: Un informe de recursos al Departamento de Parques Nacionales y Vida Silvestre.
- Williams, I. D., Couch, C. S., Beijbom, O., Oliver, T. A., Vargas-angel, B., Schumacher, B. D., et al. (2019). Leveraging Automated Image Analysis Tools to Transform Our Capacity to Assess Status and Trends of Coral Reefs. *Front. Mar. Sci.* 6:222. doi: 10.3389/fmars.2019.00222
- Zapata, F. (2001). “Formaciones coralinas de isla Gorgona,” in *Gorgona marina: contribución al conocimiento de una isla única*, eds M. López-Victoria and L. M. Barrios (Santa Marta: INVEMAR), 27–40.

**Conflict of Interest:** The authors declare that the research was conducted in the absence of any commercial or financial relationships that could be construed as a potential conflict of interest.

**Publisher’s Note:** All claims expressed in this article are solely those of the authors and do not necessarily represent those of their affiliated organizations, or those of the publisher, the editors and the reviewers. Any product that may be evaluated in this article, or claim that may be made by its manufacturer, is not guaranteed or endorsed by the publisher.

Copyright © 2021 Bravo, Moity, Londoño-Cruz, Muller-Karger, Bigatti, Klein, Choi, Parmalee, Helmuth and Montes. This is an open-access article distributed under the terms of the Creative Commons Attribution License (CC BY). The use, distribution or reproduction in other forums is permitted, provided the original author(s) and the copyright owner(s) are credited and that the original publication in this journal is cited, in accordance with accepted academic practice. No use, distribution or reproduction is permitted which does not comply with these terms.

# Advantages of publishing in Frontiers



## OPEN ACCESS

Articles are free to read  
for greatest visibility  
and readership



## FAST PUBLICATION

Around 90 days  
from submission  
to decision



## HIGH QUALITY PEER-REVIEW

Rigorous, collaborative,  
and constructive  
peer-review



## TRANSPARENT PEER-REVIEW

Editors and reviewers  
acknowledged by name  
on published articles

## Frontiers

Avenue du Tribunal-Fédéral 34  
1005 Lausanne | Switzerland

**Visit us:** [www.frontiersin.org](http://www.frontiersin.org)

**Contact us:** [frontiersin.org/about/contact](http://frontiersin.org/about/contact)



## REPRODUCIBILITY OF RESEARCH

Support open data  
and methods to enhance  
research reproducibility



## DIGITAL PUBLISHING

Articles designed  
for optimal readership  
across devices



## FOLLOW US

@frontiersin



## IMPACT METRICS

Advanced article metrics  
track visibility across  
digital media



## EXTENSIVE PROMOTION

Marketing  
and promotion  
of impactful research



## LOOP RESEARCH NETWORK

Our network  
increases your  
article's readership